8

Plane Electromagnetic Waves

8–1 Introduction

In Chapter 7 we showed that in a source-free nonconducting simple medium, Maxwell's equations (Eqs. 7–79a, b, c, and d) can be combined to yield homogeneous vector wave equations in **E** and in **H**. These two equations, Eqs. (7–81) and (7–82), have exactly the same form. In free space the source-free wave equation for **E** is

$$\nabla^2\mathbf{E} - \frac{1}{c^2}\frac{\partial^2\mathbf{E}}{\partial t^2} = 0, \tag{8–1}$$

where

$$c = \frac{1}{\sqrt{\mu_0\epsilon_0}} \cong 3 \times 10^8 \text{ (m/s)} = 300 \quad \text{(Mm/s)} \tag{8–2}$$

is the velocity of wave propagation (the speed of light) in free space. The solutions of Eq. (8–1) represent waves. The study of the behavior of waves that have a one-dimensional spatial dependence (***plane waves***) is the main concern of this chapter.

We begin the chapter with a study of the propagation of time-harmonic plane-wave fields in an unbounded homogeneous medium. Medium parameters such as intrinsic impedance, attenuation constant, and phase constant will be introduced. The meaning of ***skin depth***, the depth of wave penetration into a good conductor, will be explained. Electromagnetic waves carry with them electromagnetic power. The concept of ***Poynting vector***, a power flux density, will be discussed.

We will examine the behavior of a plane wave incident normally on a plane boundary. The laws governing the reflection and refraction of plane waves incident obliquely on a plane boundary will then be discussed, and the conditions for no reflection and for total reflection will be examined.

A ***uniform plane wave*** is a particular solution of Maxwell's equations with **E** assuming the same direction, same magnitude, and same phase in infinite planes perpendicular to the direction of propagation (similarly for **H**). Strictly speaking, a uni-

form plane wave does not exist in practice because a source infinite in extent would be required to creat it, and practical wave sources are always finite in extent. But, if we are far enough away from a source, the ***wavefront*** (surface of constant phase) becomes almost spherical; and a very small portion of the surface of a giant sphere is very nearly a plane. The characteristics of uniform plane waves are particularly simple, and their study is of fundamental theoretical, as well as practical, importance.

8–2 Plane Waves in Lossless Media

In this and future chapters we focus our attention on wave behavior in the sinusoidal steady state, using phasors to great advantage. The source-free wave equation, Eq. (8–1), for free space becomes a homogeneous vector Helmholtz's equation (see Eq. 7–105):

$$\boxed{\nabla^2\mathbf{E} + k_0^2\mathbf{E} = 0,} \tag{8–3}$$

where k_0 is the ***free-space wavenumber***

$$\boxed{k_0 = \omega\sqrt{\mu_0\epsilon_0} = \frac{\omega}{c} \quad \text{(rad/m).}} \tag{8–4}$$

In Cartesian coordinates, Eq. (8–3) is equivalent to three scalar Helmholtz's equations, one each in the components E_x, E_y, and E_z. Writing it for the component E_x, we have

$$\left(\frac{\partial^2}{\partial x^2} + \frac{\partial^2}{\partial y^2} + \frac{\partial^2}{\partial z^2} + k_0^2\right)E_x = 0. \tag{8–5}$$

Consider a uniform plane wave characterized by a uniform E_x (uniform magnitude and constant phase) over plane surfaces perpendicular to z; that is,

$$\partial^2 E_x/\partial x^2 = 0 \qquad \text{and} \qquad \partial^2 E_x/\partial y^2 = 0.$$

Equation (8–5) simplifies to

$$\frac{d^2E_x}{dz^2} + k_0^2 E_x = 0, \tag{8–6}$$

which is an ordinary differential equation because E_x, a phasor, depends only on z.

The solution of Eq. (8–6) is readily seen to be

$$\begin{aligned} E_x(z) &= E_x^+(z) + E_x^-(z) \\ &= E_0^+ e^{-jk_0z} + E_0^- e^{jk_0z}, \end{aligned} \tag{8–7}$$

where E_0^+ and E_0^- are arbitrary (and, in general, complex) constants that must be determined by boundary conditions. Note that since Eq. (8–6) is a second-order equation, its general solution in Eq. (8–7) contains two integration constants.

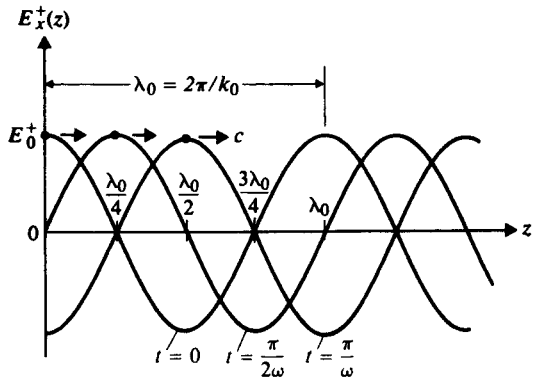

FIGURE 8–1
Wave traveling in positive z direction $E_x^+(z, t) = E_0^+ \cos(\omega t - k_0 z)$, for several values of t.

Now let us examine what the first phasor term on the right side of Eq. (8–7) represents in real time. Using $\cos \omega t$ as the reference and assuming E_0^+ to be a real constant (zero reference phase at $z = 0$), we have

$$\begin{aligned} E_x^+(z, t) &= \mathscr{R}e[E_x^+(z)e^{j\omega t}] \\ &= \mathscr{R}e[E_0^+ e^{j(\omega t - k_0 z)}] \\ &= E_0^+ \cos(\omega t - k_0 z) \qquad \text{(V/m)}. \end{aligned} \tag{8–8}$$

Equation (8–8) has been plotted in Fig. 8–1 for several values of t. At $t = 0$, $E_x^+(z, 0) = E_0^+ \cos k_0 z$ is a cosine curve with an amplitude E_0^+. At successive times the curve effectively travels in the positive z direction. We have, then, a ***traveling wave***. If we fix our attention on a particular point (a point of a particular phase) on the wave, we set $\cos(\omega t - k_0 z) =$ a constant or

$$\omega t - k_0 z = \text{A constant phase},$$

from which we obtain

$$u_p = \frac{dz}{dt} = \frac{\omega}{k_0} = \frac{1}{\sqrt{\mu_0 \epsilon_0}} = c. \tag{8–9}$$

Equation (8–9) assures us that the velocity of propagation of an equiphase front (the ***phase velocity***) in free space is equal to the velocity of light, which is approximately 3×10^8 (m/s) in free space.

Wavenumber k_0 bears a definite relation to the wavelength. From Eq. (8–4), $k_0 = 2\pi f/c$ or

$$\boxed{k_0 = \frac{2\pi}{\lambda_0} \qquad \text{(rad/m)},} \tag{8–10}$$

which measures the number of wavelengths in a complete cycle, hence its name. An inverse relation of Eq. (8-10) is

$$\boxed{\lambda_0 = \frac{2\pi}{k_0} \quad \text{(m)}.} \tag{8-11}$$

Equations (8-10) and (8-11) are valid without the subscript 0 if the medium is a lossless material such as a perfect dielectric, instead of free space.

It is obvious without replotting that the second phasor term on the right side of Eq. (8-7), $E_0^- e^{jk_0 z}$, represents a cosinusoidal wave traveling in the $-z$ direction with the same velocity c. If we are concerned only with the wave traveling in the $+z$ direction, $E_0^- = 0$. However, if there are discontinuities in the medium, reflected waves traveling in the opposite direction must also be considered, as we will see later in this chapter.

The associated magnetic field **H** can be found from Eq. (7-104a)

$$\nabla \times \mathbf{E} = \begin{vmatrix} \mathbf{a}_x & \mathbf{a}_y & \mathbf{a}_z \\ 0 & 0 & \dfrac{\partial}{\partial z} \\ E_x^+(z) & 0 & 0 \end{vmatrix} = -j\omega\mu_0(\mathbf{a}_x H_x^+ + \mathbf{a}_y H_y^+ + \mathbf{a}_z H_z^+),$$

which leads to

$$H_x^+ = 0, \tag{8-12a}$$

$$H_y^+ = \frac{1}{-j\omega\mu_0}\frac{\partial E_x^+(z)}{\partial z}, \tag{8-12b}$$

$$H_z^+ = 0. \tag{8-12c}$$

Thus H_y^+ is the only nonzero component of **H**; and since

$$\frac{\partial E_x^+(z)}{\partial z} = \frac{\partial}{\partial z}(E_0^+ e^{-jk_0 z}) = -jk_0 E_x^+(z),$$

Eq. (8-12b) yields

$$H_y^+(z) = \frac{k_0}{\omega\mu_0} E_x^+(z) = \frac{1}{\eta_0} E_x^+(z) \qquad \text{(A/m)}. \tag{8-13}^\dagger$$

We have introduced a new quantity, η_0, in Eq. (8-13):

$$\boxed{\eta_0 = \sqrt{\frac{\mu_0}{\epsilon_0}} \cong 120\pi \cong 377 \qquad (\Omega),} \tag{8-14}$$

---

† If we had started with $E_x^-(z) = E_0^- e^{jk_0 z}$, we would obtain $H_y^-(z) = -\dfrac{1}{\eta_0} E_x^-(z)$.

which is called the ***intrinsic impedance of the free space***. Because η_0 is a real number, $H_y^+(z)$ is in phase with $E_x^+(z)$, and we can write the instantaneous expression for $\mathbf{H}$ as

$$\begin{aligned}\mathbf{H}(z, t) &= \mathbf{a}_y H_y^+(z, t) = \mathbf{a}_y \mathscr{R}e[H_y^+(z)e^{j\omega t}] \\ &= \mathbf{a}_y \frac{E_0^+}{\eta_0} \cos(\omega t - k_0 z) \qquad \text{(A/m)}.\end{aligned} \tag{8-15}$$

Hence, for a uniform plane wave the ratio of the magnitudes of $\mathbf{E}$ and $\mathbf{H}$ is the intrinsic impedance of the medium. We also note that $\mathbf{H}$ is perpendicular to $\mathbf{E}$ and that both are normal to the direction of propagation. The fact that we specified $\mathbf{E} = \mathbf{a}_x E_x$ is not as restrictive as it appears, inasmuch as we are free to designate the direction of $\mathbf{E}$ as the $+x$-direction, which is normal to the direction of propagation $\mathbf{a}_z$.

EXAMPLE 8–1 A uniform plane wave with $\mathbf{E} = \mathbf{a}_x E_x$ propagates in a lossless simple medium ($\epsilon_r = 4$, $\mu_r = 1$, $\sigma = 0$) in the $+z$-direction. Assume that E_x is sinusoidal with a frequency 100 (MHz) and has a maximum value of $+10^{-4}$ (V/m) at $t = 0$ and $z = \frac{1}{8}$ (m).

a) Write the instantaneous expression for $\mathbf{E}$ for any t and z.

b) Write the instantaneous expression for $\mathbf{H}$.

c) Determine the locations where E_x is a positive maximum when $t = 10^{-8}$ (s).

Solution First we find k:

$$\begin{aligned}k = \omega\sqrt{\mu\epsilon} &= \frac{\omega}{c}\sqrt{\mu_r\epsilon_r} \\ &= \frac{2\pi 10^8}{3 \times 10^8}\sqrt{4} = \frac{4\pi}{3} \quad \text{(rad/m)}.\end{aligned}$$

a) Using $\cos \omega t$ as the reference, we find the instantaneous expression for $\mathbf{E}$ to be

$$\mathbf{E}(z, t) = \mathbf{a}_x E_x = \mathbf{a}_x 10^{-4} \cos(2\pi 10^8 t - kz + \psi).$$

Since E_x equals $+10^{-4}$ when the argument of the cosine function equals zero—that is, when

$$2\pi 10^8 t - kz + \psi = 0,$$

we have, at $t = 0$ and $z = \frac{1}{8}$,

$$\psi = kz = \left(\frac{4\pi}{3}\right)\left(\frac{1}{8}\right) = \frac{\pi}{6} \quad \text{(rad)}.$$

Thus,

$$\begin{aligned}\mathbf{E}(z, t) &= \mathbf{a}_x 10^{-4} \cos\left(2\pi 10^8 t - \frac{4\pi}{3} z + \frac{\pi}{6}\right) \\ &= \mathbf{a}_x 10^{-4} \cos\left[2\pi 10^8 t - \frac{4\pi}{3}\left(z - \frac{1}{8}\right)\right] \quad \text{(V/m)}.\end{aligned}$$

This expression shows a shift of $\frac{1}{8}$ (m) in the $+z$-direction and could have been written down directly from the statement of the problem.

b) The phasor expression for **H** is

$$\mathbf{H} = \mathbf{a}_y H_y = \mathbf{a}_y \frac{E_x}{\eta},$$

where

$$\eta = \sqrt{\frac{\mu}{\epsilon}} = \frac{\eta_0}{\sqrt{\epsilon_r}} = 60\pi \quad (\Omega).$$

Hence,

$$\mathbf{H}(z, t) = \mathbf{a}_y \frac{10^{-4}}{60\pi} \cos\left[2\pi 10^8 t - \frac{4\pi}{3}\left(z - \frac{1}{8}\right)\right] \quad (\text{A/m}).$$

c) At $t = 10^{-8}$, we equate the argument of the cosine function to $+2n\pi$ in order to make E_x a positive maximum:

$$2\pi 10^8 (10^{-8}) - \frac{4\pi}{3}\left(z_m - \frac{1}{8}\right) = \pm 2n\pi,$$

from which we get

$$z_m = \frac{13}{8} \pm \frac{3}{2} n \quad (\text{m}), \qquad n = 0, 1, 2, \ldots; \qquad z_m > 0.$$

Examining this result more closely, we note that the wavelength in the given medium is

$$\lambda = \frac{2\pi}{k} = \frac{3}{2} \quad (\text{m}).$$

Hence the positive maximum value of E_x occurs at

$$z_m = \frac{13}{8} \pm n\lambda \quad (\text{m}).$$

The **E** and **H** fields are shown in Fig. 8–2 as functions of z for the reference time $t = 0$. ■

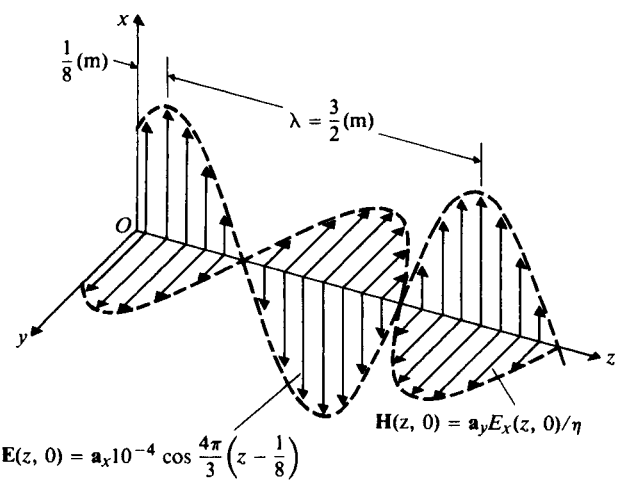

FIGURE 8–2
E and **H** fields of a uniform plane wave at $t = 0$ (Example 8–1).

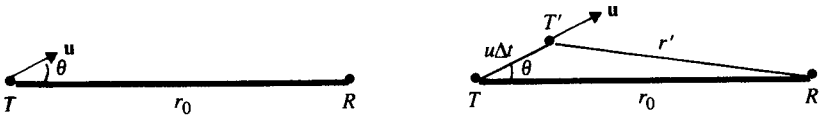

(a) At t = 0. (b) At t = Δt.

FIGURE 8–3
Illustrating the Doppler effect.

8–2.1 DOPPLER EFFECT

When there is relative motion between a time-harmonic source and a receiver, the frequency of the wave detected by the receiver tends to be different from that emitted by the source. This phenomenon is known as the ***Doppler effect.***† The Doppler effect manifests itself in acoustics as well as in electromagnetics. Perhaps you have experienced the changes in the pitch of a fast-moving locomotive whistle. In the following we give an explanation of the Doppler effect.

Let us assume that the source (transmitter) T of a time-harmonic wave of a frequency f moves with a velocity $\mathbf{u}$ at an angle θ relative to the direct line to a stationary receiver R, as illustrated in Fig. 8–3(a). The electromagnetic wave emitted by T at a reference time $t = 0$ will reach R at

$$t_1 = \frac{r_0}{c}. \tag{8-16}$$

At a later time $t = \Delta t$, T has moved to the new position T', and the wave emitted by T' at that time will reach R at

$$\begin{aligned} t_2 &= \Delta t + \frac{r'}{c} \\ &= \Delta t + \frac{1}{c}[r_0^2 - 2r_0(u\,\Delta t)\cos\theta + (u\,\Delta t)^2]^{1/2}. \end{aligned} \tag{8-17}$$

If $(u\,\Delta t)^2 \ll r_0^2$, Eq. (8–17) becomes

$$t_2 \cong \Delta t + \frac{r_0}{c}\left(1 - \frac{u\,\Delta t}{r_0}\cos\theta\right). \tag{8-18}$$

Hence the time elapsed at R, $\Delta t'$, corresponding to Δt at T is

$$\begin{aligned} \Delta t' &= t_2 - t_1 \\ &= \Delta t\left(1 - \frac{u}{c}\cos\theta\right), \end{aligned} \tag{8-19}$$

which is not equal to Δt.

† C. Doppler (1803–1853).

If Δt represents a period of the time-harmonic source—that is, if $\Delta t = 1/f$—then the frequency of the received wave at R is

$$f' = \frac{1}{\Delta t'} = \frac{f}{\left(1 - \frac{u}{c}\cos\theta\right)} \cong f\left(1 + \frac{u}{c}\cos\theta\right) \tag{8–20}$$

for the usual case of $(u/c)^2 \ll 1$. Equation (8–20) is an approximate formula and does not hold when θ is close to $\pi/2$. (Do you know why?) For $\theta = 0$, Eq. (8–20) clearly indicates that the frequency perceived at R is higher than the transmitted frequency when T moves toward R. Conversely, the perceived frequency is lower than the transmitted frequency when T moves away from R ($\theta = \pi$). It is obvious that similar results are obtained if R moves and T is stationary.

The Doppler effect is the basis of operation of the (Doppler) radar used by police to check the speed of a moving vehicle. The frequency shift of the received wave reflected by a moving vehicle is proportional to the speed of the vehicle and can be detected and displayed on a hand-held unit. (See Problem P.8–3). The Doppler effect is also the cause of the so-called ***red shift*** of the light spectrum emitted by a receding distant star in astronomy. As the star *moves away* at a high speed from an observer on earth, the received frequency shifts toward the *lower frequency* (*red*) end of the spectrum.

8–2.2 TRANSVERSE ELECTROMAGNETIC WAVES

We have seen that a uniform plane wave characterized by $\mathbf{E} = \mathbf{a}_x E_x$ propagating in the $+z$-direction has associated with it a magnetic field $\mathbf{H} = \mathbf{a}_y H_y$. Thus $\mathbf{E}$ and $\mathbf{H}$ are perpendicular to each other, and both are transverse to the direction of propagation. It is a particular case of a ***transverse electromagnetic (TEM) wave***. The phasor field quantities are functions of only the distance z along a single coordinate axis. We now consider the propagation of a uniform plane wave along an arbitrary direction that does not necessarily coincide with a coordinate axis.

The phasor electric field intensity for a uniform plane wave propagating in the $+z$-direction is

$$\mathbf{E}(z) = \mathbf{E}_0 e^{-jkz}, \tag{8–21}$$

where $\mathbf{E}_0$ is a constant vector. A more general form of Eq. (8–21) is

$$\mathbf{E}(x, y, z) = \mathbf{E}_0 e^{-jk_x x - jk_y y - jk_z z}. \tag{8–22}$$

It can be easily proved by direct substitution that this expression satisfies the homogeneous Helmholtz's equation, provided that

$$k_x^2 + k_y^2 + k_z^2 = \omega^2 \mu\epsilon. \tag{8–23}$$

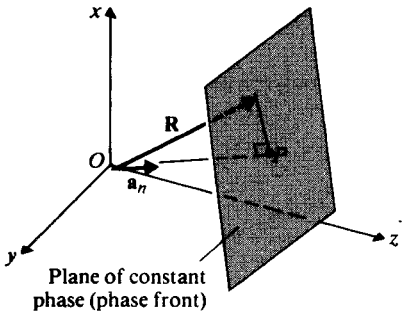

FIGURE 8–4
Radius vector and wave normal to a phase front of a uniform plane wave.

If we define a ***wavenumber vector*** as

$$\mathbf{k} = \mathbf{a}_x k_x + \mathbf{a}_y k_y + \mathbf{a}_z k_z = k\mathbf{a}_n \tag{8-24}$$

and a radius vector from the origin

$$\mathbf{R} = \mathbf{a}_x x + \mathbf{a}_y y + \mathbf{a}_z z, \tag{8-25}$$

then Eq. (8–22) can be written compactly as

$$\boxed{\mathbf{E}(\mathbf{R}) = \mathbf{E}_0 e^{-j\mathbf{k}\cdot\mathbf{R}} = \mathbf{E}_0 e^{-jk\mathbf{a}_n\cdot\mathbf{R}} \quad \text{(V/m)},} \tag{8-26}$$

where $\mathbf{a}_n$ is a unit vector in the direction of propagation. From Eq. (8–24) it is clear that

$$k_x = \mathbf{k}\cdot\mathbf{a}_x = k\mathbf{a}_n\cdot\mathbf{a}_x, \tag{8-27a}$$

$$k_y = \mathbf{k}\cdot\mathbf{a}_y = k\mathbf{a}_n\cdot\mathbf{a}_y, \tag{8-27b}$$

$$k_z = \mathbf{k}\cdot\mathbf{a}_z = k\mathbf{a}_n\cdot\mathbf{a}_z, \tag{8-27c}$$

and that $\mathbf{a}_n\cdot\mathbf{a}_x$, $\mathbf{a}_n\cdot\mathbf{a}_y$ and $\mathbf{a}_n\cdot\mathbf{a}_z$ are direction cosines of $\mathbf{a}_n$.

The geometrical relations of $\mathbf{a}_n$ and $\mathbf{R}$ are illustrated in Fig. 8–4, from which we see that

$$\mathbf{a}_n\cdot\mathbf{R} = \text{Length } \overline{OP} \quad \text{(a constant)}$$

is the equation of a plane normal to $\mathbf{a}_n$, the direction of propagation. Just as $z =$ Constant denotes a plane of constant phase and uniform amplitude for the wave in Eq. (8–21), $\mathbf{a}_n\cdot\mathbf{R} =$ Constant is a plane of constant phase and uniform amplitude for the wave in Eq. (8–26). In a charge-free region, $\nabla\cdot\mathbf{E} = 0$. As a result,

$$\mathbf{E}_0\cdot\nabla(e^{-jk\mathbf{a}_n\cdot\mathbf{R}}) = 0. \tag{8-28a}^{\dagger}$$

† This is a consequence of the fact that $\nabla\cdot\mathbf{E}_0 = 0$, where $\mathbf{E}_0$ is a constant vector (see Problem P.2–28).

But

$$\nabla(e^{-jk\mathbf{a}_n\cdot\mathbf{R}}) = \left(\mathbf{a}_x\frac{\partial}{\partial x} + \mathbf{a}_y\frac{\partial}{\partial y} + \mathbf{a}_z\frac{\partial}{\partial z}\right)e^{-j(k_x x + k_y y + k_z z)}$$
$$= -j(\mathbf{a}_x k_x + \mathbf{a}_y k_y + \mathbf{a}_z k_z)e^{-j(k_x x + k_y y + k_z z)}$$
$$= -jk\mathbf{a}_n e^{-jk\mathbf{a}_n\cdot\mathbf{R}},$$

hence Eq. (8–28a) can be written as

$$-jk(\mathbf{E}_0\cdot\mathbf{a}_n)e^{-jk\mathbf{a}_n\cdot\mathbf{R}} = 0,$$

which requires

$$\mathbf{a}_n\cdot\mathbf{E}_0 = 0. \tag{8–28b}$$

Thus the plane-wave solution in Eq. (8–26) imples that $\mathbf{E}_0$ is transverse to the direction of propagation.

The magnetic field associated with $\mathbf{E}(\mathbf{R})$ in Eq. (8–26) may be obtained from Eq. (7–104a) as

$$\mathbf{H}(\mathbf{R}) = -\frac{1}{j\omega\mu}\nabla\times\mathbf{E}(\mathbf{R})$$

or

$$\boxed{\mathbf{H}(\mathbf{R}) = \frac{1}{\eta}\mathbf{a}_n\times\mathbf{E}(\mathbf{R}) \quad \text{(A/m)},} \tag{8–29}$$

where

$$\boxed{\eta = \frac{\omega\mu}{k} = \sqrt{\frac{\mu}{\epsilon}} \quad (\Omega)} \tag{8–30}$$

is the ***intrinsic impedance***† of the medium. Substitution of Eq. (8–26) in Eq. (8–29) yields

$$\boxed{\mathbf{H}(\mathbf{R}) = \frac{1}{\eta}(\mathbf{a}_n\times\mathbf{E}_0)e^{-jk\mathbf{a}_n\cdot\mathbf{R}} \quad \text{(A/m)}.} \tag{8–31}$$

It is now clear that a uniform plane wave propagating in an arbitrary direction, $\mathbf{a}_n$, is a TEM wave with $\mathbf{E}\perp\mathbf{H}$ and that both $\mathbf{E}$ and $\mathbf{H}$ are normal to $\mathbf{a}_n$.

EXAMPLE 8–2 If $\mathbf{E}(\mathbf{R})$ of a TEM wave is given, as in Eq. (8–26), $\mathbf{H}(\mathbf{R})$ can be found by using Eq. (8–29). Obtain a relation expressing $\mathbf{E}(\mathbf{R})$ in terms of $\mathbf{H}(\mathbf{R})$.

Solution Assuming $\mathbf{H}(\mathbf{R})$ to have the form

$$\mathbf{H}(\mathbf{R}) = \mathbf{H}_0 e^{-jk\mathbf{a}_n\cdot\mathbf{R}}, \tag{8–32}$$

† Also called ***wave impedance.***

we obtain from Eq. (7–104b)

$$\mathbf{E}(\mathbf{R}) = \frac{1}{j\omega\epsilon}\nabla \times \mathbf{H}(\mathbf{R})$$
$$= \frac{1}{j\omega\epsilon}(-jk)\mathbf{a}_n \times \mathbf{H}(\mathbf{R})$$

or

$$\boxed{\mathbf{E}(\mathbf{R}) = -\eta\mathbf{a}_n \times \mathbf{H}(\mathbf{R}) \qquad (\text{V/m}).} \tag{8–33}$$

Alternatively, we can obtain the same result by cross-multiplying both sides of Eq. (8–29) by $\mathbf{a}_n$ and using the back-cab rule in Eq. (2–20). ■

8–2.3 POLARIZATION OF PLANE WAVES

The ***polarization*** of a uniform plane wave describes the time-varying behavior of the electric field intensity vector at a given point in space. Since the **E** vector of the plane wave in Example 8–1 is fixed in the x direction ($\mathbf{E} = \mathbf{a}_x E_x$, where E_x may be positive or negative), the wave is said to be ***linearly polarized*** in the x-direction. A separate description of magnetic-field behavior is not necessary, inasmuch as the direction of **H** is definitely related to that of **E**.

In some cases the direction of **E** of a plane wave at a given point may change with time. Consider the superposition of two linearly polarized waves: one polarized in the x-direction, and the other polarized in the y-direction and lagging 90° (or $\pi/2$ rad) in time phase. In phasor notation we have

$$\begin{aligned}\mathbf{E}(z) &= \mathbf{a}_x E_1(z) + \mathbf{a}_y E_2(z)\\ &= \mathbf{a}_x E_{10} e^{-jkz} - \mathbf{a}_y j E_{20} e^{-jkz},\end{aligned} \tag{8–34}$$

where E_{10} and E_{20} are real numbers denoting the amplitudes of the two linearly polarized waves.

The instantaneous expression for **E** is

$$\begin{aligned}\mathbf{E}(z, t) &= \mathcal{R}e\{[\mathbf{a}_x E_1(z) + \mathbf{a}_y E_2(z)]e^{j\omega t}\}\\ &= \mathbf{a}_x E_{10}\cos(\omega t - kz) + \mathbf{a}_y E_{20}\cos\left(\omega t - kz - \frac{\pi}{2}\right).\end{aligned}$$

In examining the direction change of **E** at a given point as t changes, it is convenient to set $z = 0$. We have

$$\begin{aligned}\mathbf{E}(0, t) &= \mathbf{a}_x E_1(0, t) + \mathbf{a}_y E_2(0, t)\\ &= \mathbf{a}_x E_{10}\cos\omega t + \mathbf{a}_y E_{20}\sin\omega t.\end{aligned} \tag{8–35}$$

As ωt increases from 0 through $\pi/2$, π, and $3\pi/2$—completing the cycle at 2π—the tip of the vector $\mathbf{E}(0, t)$ will traverse an elliptical locus in the counterclockwise

direction. Analytically, we have

$$\cos \omega t = \frac{E_1(0, t)}{E_{10}}$$

and

$$\sin \omega t = \frac{E_2(0, t)}{E_{20}}$$
$$= \sqrt{1 - \cos^2 \omega t} = \sqrt{1 - \left[\frac{E_1(0, t)}{E_{10}}\right]^2},$$

which leads to the following equation for an ellipse:

$$\left[\frac{E_2(0, t)}{E_{20}}\right]^2 + \left[\frac{E_1(0, t)}{E_{10}}\right]^2 = 1. \tag{8–36}$$

Hence **E**, which is the sum of two linearly polarized waves in both space and time quadrature, is ***elliptically polarized*** if $E_{20} \neq E_{10}$, and is ***circularly polarized*** if $E_{20} = E_{10}$. A typical polarization circle is shown in Fig. 8–5(a).

When $E_{20} = E_{10}$, the instantaneous angle α that **E** makes with the x-axis at $z = 0$ is

$$\alpha = \tan^{-1} \frac{E_2(0, t)}{E_1(0, t)} = \omega t, \tag{8–37}$$

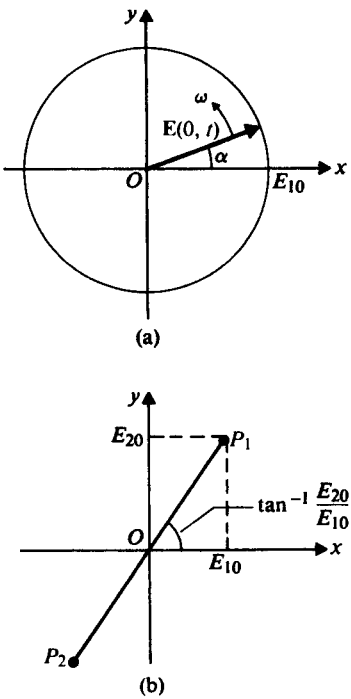

FIGURE 8–5
Polarization diagrams for sum of two linearly polarized waves in space quadrature at $z = 0$: (a) circular polarization, $E(0, t) = E_{10}(\mathbf{a}_x \cos \omega t + \mathbf{a}_y \sin \omega t)$; (b) linear polarization, $\mathbf{E}(0, t) = (\mathbf{a}_x E_{10} + \mathbf{a}_y E_{20}) \cos \omega t$.

which indicates that **E** rotates at a uniform rate with an angular velocity ω in a *counterclockwise* direction. When the fingers of the right hand follow the direction of the rotation of **E**, the thumb points to the direction of propagation of the wave. This is a ***right-hand*** or ***positive circularly polarized wave.***

If we start with an $E_2(z)$, which *leads* $E_1(z)$ by 90° ($\pi/2$ rad) in time phase, Eqs. (8–34) and (8–35) will be, respectively,

$$\mathbf{E}(z) = \mathbf{a}_x E_{10} e^{-jkz} + \mathbf{a}_y j E_{20} e^{-jkz} \tag{8–38}$$

and

$$\mathbf{E}(0, t) = \mathbf{a}_x E_{10} \cos \omega t - \mathbf{a}_y E_{20} \sin \omega t. \tag{8–39}$$

Comparing Eq. (8–39) with Eq. (8–35), we see that **E** will still be elliptically polarized. If $E_{20} = E_{10}$, **E** will be circularly polarized, and its angle measured from the x-axis at $z = 0$ will now be $-\omega t$, indicating that **E** will rotate with an angular velocity ω in a *clockwise* direction; this is a ***left-hand*** or ***negative circularly polarized wave.***

If $E_2(z)$ and $E_1(z)$ are in space quadrature but in time phase, their sum **E** will be linearly polarized along a line that makes an angle $\tan^{-1}(E_{20}/E_{10})$ with the x-axis, as depicted in Fig. 8–5(b). The instantaneous expression for **E** at $z = 0$ is

$$\mathbf{E}(0, t) = (\mathbf{a}_x E_{10} + \mathbf{a}_y E_{20}) \cos \omega t. \tag{8–40}$$

The tip of the $\mathbf{E}(0, t)$ will be at the point P_1 when $\omega t = 0$. Its magnitude will decrease toward zero as ωt increases toward $\pi/2$. After that, $\mathbf{E}(0, t)$ starts to increase again, in the opposite direction, toward the point P_2 where $\omega t = \pi$.

In the general case, $E_2(z)$ and $E_1(z)$, which are in space quadrature, can have unequal amplitudes ($E_{20} \neq E_{10}$) and can differ in phase by an arbitrary amount (not zero or an integral multiple of $\pi/2$). Their sum **E** will be elliptically polarized, and the principal axes of the polarization ellipse will not coincide with the axes of the coordinates (see Problem P.8–7).

We note here that the electromagnetic waves radiated by AM broadcast stations from their antenna towers are linearly polarized with the **E**-field perpendicular to the ground. For maximum reception the receiving antenna should be parallel to the **E**-field—that is, vertical. Television signals, on the other hand, are linearly polarized in the horizontal direction. This is why the wires of rooftop TV receiving antennas are horizontal. The waves radiated by FM broadcast stations are generally circularly polarized; hence the orientation of an FM receiving antenna is not critical as long as it lies in a plane normal to the direction of the signal.

EXAMPLE 8–3 Prove that a linearly polarized plane wave can be resolved into a right-hand circularly polarized wave and a left-hand circularly polarized wave of equal amplitude.

Solution Consider a linearly polarized plane wave propagating in the $+z$-direction. We can assume, with no loss of generality, that **E** is polarized in the x-direction. In

phasor notation we have

$$\mathbf{E}(z) = \mathbf{a}_x E_0 e^{-jkz}.$$

But this can be written as

$$\mathbf{E}(z) = \mathbf{E}_{rc}(z) + \mathbf{E}_{lc}(z),$$

where

$$\mathbf{E}_{rc}(z) = \frac{E_0}{2}(\mathbf{a}_x - j\mathbf{a}_y)e^{-jkz} \tag{8–41a}$$

and

$$\mathbf{E}_{lc}(z) = \frac{E_0}{2}(\mathbf{a}_x + j\mathbf{a}_y)e^{-jkz}. \tag{8–41b}$$

From previous discussions we recognize that $\mathbf{E}_{rc}(z)$ in Eq. (8–41a) and $\mathbf{E}_{lc}(z)$ in Eq. (8–41b) represent right-hand and left-hand circularly polarized waves, respectively, each having an amplitude $E_0/2$. The statement of this problem is therefore proved. The converse statement that the sum of two oppositely rotating circularly polarized waves of equal amplitude is a linearly polarized wave is, of course, also true. ■

8–3 Plane Waves in Lossy Media

In a source-free lossy medium the homogeneous vector Helmholtz's equation to be solved is

$$\nabla^2\mathbf{E} + k_c^2\mathbf{E} = 0, \tag{8–42}$$

where the wavenumber $k_c = \omega\sqrt{\mu\epsilon_c}$ is a complex number, as given in Eq. (7–114). The derivations and discussions pertaining to plane waves in a lossless medium in Section 8–2 can be modified to apply to wave propagation in a lossy medium by simply replacing k with k_c. However, in an effort to conform with the conventional notation used in transmission-line theory, it is customary to define a propagation constant, γ, such that

$$\boxed{\gamma = jk_c = j\omega\sqrt{\mu\epsilon_c} \qquad (\text{m}^{-1}).} \tag{8–43}$$

Since γ is complex, we write, with the help of Eq. (7–110),

$$\gamma = \alpha + j\beta = j\omega\sqrt{\mu\epsilon}\left(1 + \frac{\sigma}{j\omega\epsilon}\right)^{1/2}, \tag{8–44}$$

or, from Eq. (7–114),

$$\gamma = \alpha + j\beta = j\omega\sqrt{\mu\epsilon'}\left(1 - j\frac{\epsilon''}{\epsilon'}\right)^{1/2}, \tag{8–45}$$

where α and β are the real and imaginary parts of γ, respectively. Their physical significance will be explained presently. For a lossless medium, $\sigma = 0$ ($\epsilon'' = 0$, $\epsilon = \epsilon'$), $\alpha = 0$, and $\beta = k = \omega\sqrt{\mu\epsilon}$.

The Helmholtz's equation, Eq. (8–42), becomes

$$\nabla^2\mathbf{E} - \gamma^2\mathbf{E} = 0. \tag{8–46}$$

The solution of Eq. (8–46), representing a uniform plane wave propagating in the $+z$-direction, is

$$\mathbf{E} = \mathbf{a}_x E_x = \mathbf{a}_x E_0 e^{-\gamma z}, \tag{8–47}$$

where we have assumed that the wave is linearly polarized in the x-direction. The propagation factor $e^{-\gamma z}$ can be written as a product of two factors:

$$E_x = E_0 e^{-\alpha z} e^{-j\beta z}.$$

As we shall see, both α and β are positive quantities. The first factor, $e^{-\alpha z}$, decreases as z increases and thus is an attenuation factor, and α is called an ***attenuation constant***. The SI unit of the attenuation constant is neper per meter (Np/m).† The second factor, $e^{-j\beta z}$, is a phase factor; β is called a ***phase constant*** and is expressed in radians per meter (rad/m). The phase constant expresses the amount of phase shift that occurs as the wave travels one meter.

General expressions of α and β in terms of ω and the constitutive parameters—ϵ, μ, and σ—of the medium are rather involved (see Problem P.8–9). In the following paragraphs we examine the approximate expressions for low-loss dielectrics, good conductors, and ionized gases.

8–3.1 LOW-LOSS DIELECTRICS

A low-loss dielectric is a good but imperfect insulator with a nonzero equivalent conductivity, such that $\epsilon'' \ll \epsilon'$ or $\sigma/\omega\epsilon \ll 1$. Under this condition, γ in Eq. (8–45) can be approximated by using the binomial expansion:

$$\gamma = \alpha + j\beta \cong j\omega\sqrt{\mu\epsilon'}\left[1 - j\frac{\epsilon''}{2\epsilon'} + \frac{1}{8}\left(\frac{\epsilon''}{\epsilon'}\right)^2\right],$$

from which we obtain the attenuation constant

$$\alpha \cong \frac{\omega\epsilon''}{2}\sqrt{\frac{\mu}{\epsilon'}} \quad \text{(Np/m)} \tag{8–48}$$

and the phase constant

$$\beta \cong \omega\sqrt{\mu\epsilon'}\left[1 + \frac{1}{8}\left(\frac{\epsilon''}{\epsilon'}\right)^2\right] \quad \text{(rad/m)}. \tag{8–49}$$

It is seen from Eq. (8–48) that the attenuation constant of a low-loss dielectric is a positive quantity and is approximately directly proportional to the frequency. The phase constant in Eq. (8–49) deviates only very slightly from the value $\omega\sqrt{\mu\epsilon}$ for a perfect (lossless) dielectric.

---

† Neper is a dimensionless quantity. If $\alpha = 1$ (Np/m), then a unit wave amplitude decreases to a magnitude e^{-1} $(=0.368)$ as it travels a distance of 1 (m). An attenuation of 1 (Np/m) equals 20 $\log_{10} e =$ 8.69 (dB/m).

The intrinsic impedance of a low-loss dielectric is a complex quantity.

$$\eta_c = \sqrt{\frac{\mu}{\epsilon'}}\left(1 - j\frac{\epsilon''}{\epsilon'}\right)^{-1/2} \cong \sqrt{\frac{\mu}{\epsilon'}}\left(1 + j\frac{\epsilon''}{2\epsilon'}\right) \quad (\Omega). \tag{8–50}$$

Since the intrinsic impedance is the ratio of E_x and H_y for a uniform plane wave, the electric and magnetic field intensities in a lossy dielectric are thus not in time phase, as they are in a lossless medium.

The phase velocity u_p is obtained from the ratio ω/β in a manner similar to that in Eq. (8–9). Using Eq. (8–49), we have

$$u_p = \frac{\omega}{\beta} \cong \frac{1}{\sqrt{\mu\epsilon'}}\left[1 - \frac{1}{8}\left(\frac{\epsilon''}{\epsilon'}\right)^2\right] \quad \text{(m/s)}. \tag{8–51}$$

8–3.2 GOOD CONDUCTORS

A good conductor is a medium for which $\sigma/\omega\epsilon \gg 1$. Under this condition it is convenient to use Eq. (8–44) and neglect 1 in comparison with the term $\sigma/j\omega\epsilon$. We write

$$\gamma \cong j\omega\sqrt{\mu\epsilon}\sqrt{\frac{\sigma}{j\omega\epsilon}} = \sqrt{j}\sqrt{\omega\mu\sigma} = \frac{1+j}{\sqrt{2}}\sqrt{\omega\mu\sigma}$$

or

$$\gamma = \alpha + j\beta \cong (1+j)\sqrt{\pi f\mu\sigma}, \tag{8–52}$$

where we have used the relations

$$\sqrt{j} = (e^{j\pi/2})^{1/2} = e^{j\pi/4} = (1+j)/\sqrt{2}$$

and $\omega = 2\pi f$. Equation (8–52) indicates that α and β for a good conductor are approximately equal and both increase as $\sqrt{f}$ and $\sqrt{\sigma}$. For a good conductor,

$$\boxed{\alpha = \beta = \sqrt{\pi f\mu\sigma}.} \tag{8–53}$$

The intrinsic impedance of a good conductor is

$$\eta_c = \sqrt{\frac{\mu}{\epsilon_c}} \cong \sqrt{\frac{j\omega\mu}{\sigma}} = (1+j)\sqrt{\frac{\pi f\mu}{\sigma}} = (1+j)\frac{\alpha}{\sigma} \quad (\Omega), \tag{8–54}$$

which has a phase angle of 45°. Hence the magnetic field intensity lags behind the electric field intensity by 45°.

The phase velocity in a good conductor is

$$u_p = \frac{\omega}{\beta} \cong \sqrt{\frac{2\omega}{\mu\sigma}} \quad \text{(m/s)}, \tag{8–55}$$

which is proportional to $\sqrt{f}$ and $1/\sqrt{\sigma}$. Consider copper as an example:

$$\sigma = 5.80 \times 10^7 \quad \text{(S/m)},$$
$$\mu = 4\pi \times 10^{-7} \quad \text{(H/m)},$$
$$u_p = 720 \text{ (m/s)} \quad \text{at} \quad 3 \text{ (MHz)},$$

which is about twice the velocity of sound in air and is many orders of magnitude slower than the velocity of light in air. The wavelength of a plane wave in a good conductor is

$$\lambda = \frac{2\pi}{\beta} = \frac{u_p}{f} = 2\sqrt{\frac{\pi}{f\mu\sigma}} \quad \text{(m)}. \tag{8-56}$$

For copper at 3 (MHz), $\lambda = 0.24$ (mm). As a comparison, a 3 (MHz) electromagnetic wave in air has a wavelength of 100 (m).

At very high frequencies the attenuation constant α for a good conductor, as given by Eq. (8–53), tends to be very large. For copper at 3 (MHz),

$$\alpha = \sqrt{\pi(3 \times 10^6)(4\pi \times 10^{-7})(5.80 \times 10^7)} = 2.62 \times 10^4 \quad \text{(Np/m)}.$$

Since the attenuation factor is $e^{-\alpha z}$, the amplitude of a wave will be attenuated by a factor of $e^{-1} = 0.368$ when it travels a distance $\delta = 1/\alpha$. For copper at 3 (MHz) this distance is $(1/2.62) \times 10^{-4}$ (m), or 0.038 (mm). At 10 (GHz) it is only 0.66 (μm)—a very small distance indeed. Thus a high-frequency electromagnetic wave is attenuated very rapidly as it propagates in a good conductor. The distance δ through which the amplitude of a traveling plane wave decreases by a factor of e^{-1} or 0.368 is called the ***skin depth*** or the ***depth of penetration*** of a conductor:

$$\boxed{\delta = \frac{1}{\alpha} = \frac{1}{\sqrt{\pi f\mu\sigma}} \quad \text{(m)}.} \tag{8-57}$$

Since $\alpha = \beta$ for a good conductor, δ can also be written as

$$\boxed{\delta = \frac{1}{\beta} = \frac{\lambda}{2\pi} \quad \text{(m)}.} \tag{8-58}$$

At microwave frequencies the skin depth or depth of penetration of a good conductor is so small that fields and currents can be considered as, for all practical purposes, confined in a very thin layer (that is, in the skin) of the conductor surface.

Table 8–1 lists the skin depths of several types of materials at various frequencies.

EXAMPLE 8–4 The electric field intensity of a linearly polarized uniform plane wave propagating in the $+z$-direction in seawater is $\mathbf{E} = \mathbf{a}_x 100 \cos(10^7 \pi t)$ (V/m) at $z = 0$. The constitutive parameters of seawater are $\epsilon_r = 72$, $\mu_r = 1$, and $\sigma = 4$ (S/m). (a) De-

TABLE 8–1
Skin Depths, δ in (mm), of Various Materials

Material	σ (S/m)	$f = 60$ (Hz)	1 (MHz)	1 (GHz)
Silver	6.17×10^7	8.27 (mm)	0.064 (mm)	0.0020 (mm)
Copper	5.80×10^7	8.53	0.066	0.0021
Gold	4.10×10^7	10.14	0.079	0.0025
Aluminum	3.54×10^7	10.92	0.084	0.0027
Iron ($\mu_r \cong 10^3$)	1.00×10^7	0.65	0.005	0.00016
Seawater	4	32 (m)	0.25 (m)	†

† The ϵ of seawater is approximately $72\epsilon_0$. At $f = 1$ (GHz), $\sigma/\omega\epsilon \cong 1$ (not $\gg 1$). Under these conditions, seawater is not a good conductor, and Eq. (8–57) is no longer applicable.

termine the attenuation constant, phase constant, intrinsic impedance, phase velocity, wavelength, and skin depth. (b) Find the distance at which the amplitude of **E** is 1% of its value at $z = 0$. (c) Write the expressions for $\mathbf{E}(z, t)$ and $\mathbf{H}(z, t)$ at $z = 0.8$ (m) as functions of t.

Solution

$$\omega = 10^7\pi \quad \text{(rad/s)},$$

$$f = \frac{\omega}{2\pi} = 5 \times 10^6 \quad \text{(Hz)},$$

$$\frac{\sigma}{\omega\epsilon} = \frac{\sigma}{\omega\epsilon_0\epsilon_r} = \frac{4}{10^7\pi\left(\frac{1}{36\pi} \times 10^{-9}\right)72} = 200 \gg 1.$$

Hence we can use the formulas for good conductors.

a) Attenuation constant:

$$\alpha = \sqrt{\pi f\mu\sigma} = \sqrt{5\pi 10^6(4\pi 10^{-7})4} = 8.89 \quad \text{(Np/m)}.$$

Phase constant:

$$\beta = \sqrt{\pi f\mu\sigma} = 8.89 \quad \text{(rad/m)}.$$

Intrinsic impedance:

$$\eta_c = (1 + j)\sqrt{\frac{\pi f\mu}{\sigma}}$$

$$= (1 + j)\sqrt{\frac{\pi(5 \times 10^6)(4\pi \times 10^{-7})}{4}} = \pi e^{j\pi/4} \quad (\Omega).$$

Phase velocity:

$$u_p = \frac{\omega}{\beta} = \frac{10^7\pi}{8.89} = 3.53 \times 10^6 \quad \text{(m/s)}.$$

Wavelength:

$$\lambda = \frac{2\pi}{\beta} = \frac{2\pi}{8.89} = 0.707 \quad \text{(m)}.$$

Skin depth:

$$\delta = \frac{1}{\alpha} = \frac{1}{8.89} = 0.112 \quad \text{(m)}.$$

b) Distance z_1 at which the amplitude of wave decreases to 1% of its value at $z = 0$:

$$e^{-\alpha z_1} = 0.01 \qquad \text{or} \qquad e^{\alpha z_1} = \frac{1}{0.01} = 100,$$

$$z_1 = \frac{1}{\alpha} \ln 100 = \frac{4.605}{8.89} = 0.518 \quad \text{(m)}.$$

c) In phasor notation,

$$\mathbf{E}(z) = \mathbf{a}_x 100 e^{-\alpha z} e^{-j\beta z}.$$

The instantaneous expression for $\mathbf{E}$ is

$$\begin{aligned}\mathbf{E}(z, t) &= \mathscr{R}e[\mathbf{E}(z)e^{j\omega t}] \\ &= \mathscr{R}e[\mathbf{a}_x 100 e^{-\alpha z} e^{j(\omega t - \beta z)}] = \mathbf{a}_x 100 e^{-\alpha z} \cos(\omega t - \beta z).\end{aligned}$$

At $z = 0.8$ (m) we have

$$\begin{aligned}\mathbf{E}(0.8, t) &= \mathbf{a}_x 100 e^{-0.8\alpha} \cos(10^7 \pi t - 0.8\beta) \\ &= \mathbf{a}_x 0.082 \cos(10^7 \pi t - 7.11) \quad \text{(V/m)}.\end{aligned}$$

We know that a uniform plane wave is a TEM wave with $\mathbf{E} \perp \mathbf{H}$ and that both are normal to the direction of wave propagation $\mathbf{a}_z$. Thus $\mathbf{H} = \mathbf{a}_y H_y$. To find $\mathbf{H}(z, t)$, the instantaneous expression of $\mathbf{H}$ as a function of t, *we must not make the mistake of writing* $H_y(z, t) = E_x(z, t)/\eta_c$ because this would be mixing real time functions $E_x(z, t)$ and $H_z(z, t)$ with a complex quantity η_c. Phasor quantities $E_x(z)$ and $H_y(z)$ must be used. That is,

$$H_y(z) = \frac{E_x(z)}{\eta_c},$$

from which we obtain the relation between instantaneous quantities

$$H_y(z, t) = \mathscr{R}e\left[\frac{E_x(z)}{\eta_c} e^{j\omega t}\right].$$

For the present problem we have, in phasors,

$$H_y(0.8) = \frac{100 e^{-0.8\alpha} e^{-j0.8\beta}}{\pi e^{j\pi/4}} = \frac{0.082 e^{-j7.11}}{\pi e^{j\pi/4}} = 0.026 e^{-j1.61}.$$

Note that *both* angles must be in radians before combining. The instantaneous expression for $\mathbf{H}$ at $z = 0.8$ (m) is then

$$\mathbf{H}(0.8, t) = \mathbf{a}_y 0.026 \cos(10^7 \pi t - 1.61) \quad \text{(A/m)}.$$

We can see that a 5 (MHz) plane wave attenuates very rapidly in seawater and becomes negligibly weak a very short distance from the source. Even at very low

frequencies, long-distance radio communication with a submerged submarine is very difficult. ■

8–3.3 IONIZED GASES

In the earth's upper atmosphere, roughly from 50 to 500 (km) in altitude, there exist layers of ionized gases called the ***ionosphere***. The ionosphere consists of free electrons and positive ions that are produced when the ultraviolet radiation from the sun is absorbed by the atoms and molecules in the upper atmosphere. The charged particles tend to be trapped by the earth's magnetic field. The altitude and character of the ionized layers depend both on the nature of the solar radiation and on the composition of the atmosphere. They change with the sunspot cycle, the season, and the hour of the day in a very complicated way. The electron and ion densities in the individual ionized layers are essentially equal. Ionized gases with equal electron and ion densities are called ***plasmas***.

The ionosphere plays an important role in the propagation of electromagnetic waves and affects telecommunication. Because the electrons are much lighter than the positive ions, they are accelerated more by the electric fields of electromagnetic waves passing through the ionosphere. In our analysis we shall ignore the motion of the ions and regard the ionosphere as a free electron gas. Furthermore, we shall neglect the collisions between the electrons and the gas atoms and molecules.†

An electron of charge $-e$ and mass m in a time-harmonic electric field $\mathbf{E}$ in the x-direction at an angular frequency ω experiences a force $-eE$, which displaces it from a positive ion by a distance $\mathbf{x}$ such that

$$-e\mathbf{E} = m\frac{d^2\mathbf{x}}{dt^2} = -m\omega^2\mathbf{x} \tag{8–59}$$

or

$$\mathbf{x} = \frac{e}{m\omega^2}\mathbf{E}, \tag{8–60}$$

where $\mathbf{E}$ and $\mathbf{x}$ are phasors. Such a displacement gives rise to an electric dipole moment:

$$\mathbf{p} = -e\mathbf{x}. \tag{8–61}$$

If there are N electrons per unit volume, we have a volume density of electric dipole moment or polarization vector

$$\mathbf{P} = N\mathbf{p} = -\frac{Ne^2}{m\omega^2}\mathbf{E}. \tag{8–62}$$

In writing Eq. (8–62) we have implicitly neglected the mutual effect of the induced dipole moments of the electrons on one another. From Eqs. (3–97) and (8–62) we

† This is not a good assumption in the lowest regions of the ionosphere where the atmospheric pressure is high.

obtain

$$\mathbf{D} = \epsilon_0 \mathbf{E} + \mathbf{P} = \epsilon_0 \left(1 - \frac{Ne^2}{m\omega^2 \epsilon_0}\right) \mathbf{E}$$
$$= \epsilon_0 \left(1 - \frac{\omega_p^2}{\omega^2}\right) \mathbf{E}, \tag{8-63}$$

where

$$\omega_p = \sqrt{\frac{Ne^2}{m\epsilon_0}} \quad \text{(rad/s)} \tag{8-64}$$

is called the ***plasma angular frequency***, a characteristic of the ionized medium. The corresponding ***plasma frequency*** is

$$f_p = \frac{\omega_p}{2\pi} = \frac{1}{2\pi} \sqrt{\frac{Ne^2}{m\epsilon_0}} \quad \text{(Hz)}. \tag{8-65}$$

Thus the equivalent permittivity of the ionosphere or plasma is

$$\boxed{\begin{aligned} \epsilon_p &= \epsilon_0 \left(1 - \frac{\omega_p^2}{\omega^2}\right) \\ &= \epsilon_0 \left(1 - \frac{f_p^2}{f^2}\right) \quad \text{(F/m)}. \end{aligned}} \tag{8-66}$$

On the basis of Eq. (8–66) we obtain the propagation constant as

$$\gamma = j\omega \sqrt{\mu\epsilon_0} \sqrt{1 - \left(\frac{f_p}{f}\right)^2}, \tag{8–67}$$

and the intrinsic impedance as

$$\eta_p = \frac{\eta_0}{\sqrt{1 - \left(\frac{f_p}{f}\right)^2}}, \tag{8-68}$$

where $\eta_0 = \sqrt{\mu_0/\epsilon_0} = 120\pi\ (\Omega)$.

From Eq. (8–66) we note the peculiar phenomenon of a vanishing ϵ as f approaches f_p. When ϵ becomes zero, electric displacement $\mathbf{D}$ (which depends on free charges only) is zero even when electric field intensity $\mathbf{E}$ (which depends on both free and polarization charges) is not. In that case it would be possible for an oscillating $\mathbf{E}$ to exist in the plasma in the absence of free charges, leading to a so-called ***plasma oscillation.***

When $f < f_p$, γ becomes purely real, indicating an attenuation without propagation; at the same time, η_p becomes purely imaginary, indicating a reactive load with no transmission of power. Thus f_p is also referred to as the ***cutoff frequency***. We will discuss wave reflection and transmission under various conditions later in this chapter. When $f > f_p$, γ is purely imaginary, and electromagnetic waves propagate unattenuated in the plasma (assuming negligible collision losses).

If the value of e, m, and ϵ_0 are substituted into Eq. (8–65), we find a very simple formula for the plasma (cutoff) frequency:

$$f_p \cong 9\sqrt{N} \qquad \text{(Hz)}. \tag{8–69}$$

As we have mentioned before, N at a given altitude is not a constant; it varies with the time of the day, the season, and other factors. The electron density of the ionosphere ranges from about $10^{10}/m^3$ in the lowest layer to $10^{12}/m^3$ in the highest layer. Using these values for N in Eq. (8–69), we find f_p to vary from 0.9 to 9 (MHz). Hence, for communication with a satellite or a space station beyond the ionosphere we must use frequencies much higher than 9 (MHz) to ensure wave penetration through the layer with the largest N at any angle of incidence (see Problem P.8–14). Signals with frequencies lower than 0.9 (MHz) cannot penetrate into even the lowest layer of the ionosphere but may propagate very far around the earth by way of multiple reflections at the ionosphere's boundary and the earth's surface. Signals having frequencies between 0.9 and 9 (MHz) will penetrate partially into the lower ionospheric layers but will eventually be turned back where N is large. We have given here only a very simplified picture of wave propagation in the ionosphere. The actual situation is complicated by the lack of distinct layers of constant electron densities and by the presence of the earth's magnetic field.

EXAMPLE 8–5 When a spacecraft reenters the earth's atmosphere, its speed and temperature ionize the surrounding atoms and molecules and create a plasma. It has been estimated that the electron density is in the neighborhood of 2×10^8 per (cm^3). Discuss the plasma's effect on frequency usage in radio communication between the spacecraft and the mission controllers on earth.

Solution For

$$N = 2 \times 10^8 \text{ per (cm}^3\text{)}$$
$$= 2 \times 10^{14} \text{ per (m}^3\text{)},$$

Eq. (8–69) gives $f_p = 9 \times \sqrt{2 \times 10^{14}} = 12.7 \times 10^7$ (Hz), or 127 (MHz). Thus, radio communication cannot be established for frequencies below 127 (MHz). ■

8–4 Group Velocity

In Section 8–2 we defined the phase velocity, u_p, of a single-frequency plane wave as the velocity of propagation of an equiphase wavefront. The relation between u_p and the phase constant, β, is

$$\boxed{u_p = \frac{\omega}{\beta} \qquad \text{(m/s)}.} \tag{8–70}$$

For plane waves in a lossless medium, $\beta = \omega\sqrt{\mu\epsilon}$ is a linear function of ω. As a consequence, the phase velocity $u_p = 1/\sqrt{\mu\epsilon}$ is a constant that is independent of frequency. However, in some cases (such as wave propagation in a lossy dielectric, as discussed previously, or along a transmission line, or in a waveguide to be discussed

in later chapters) the phase constant is not a linear function of ω; waves of different frequencies will propagate with different phase velocities. Inasmuch as all information-bearing signals consist of a band of frequencies, waves of the component frequencies travel with different phase velocities, causing a distortion in the signal wave shape. The signal "disperses." The phenomenon of signal distortion caused by a dependence of the phase velocity on frequency is called ***dispersion***. In view of Eqs. (8–51) and (7–115), we conclude that a lossy dielectric is obviously a ***dispersive medium***.

An information-bearing signal normally has a small spread of frequencies (sidebands) around a high carrier frequency. Such a signal comprises a "group" of frequencies and forms a wave packet. A ***group velocity*** is the velocity of propagation of the wave-packet envelope (of a group of frequencies).

Consider the simplest case of a wave packet that consists of two traveling waves having equal amplitude and slightly different angular frequencies $\omega_0 + \Delta\omega$ and $\omega_0 - \Delta\omega$ ($\Delta\omega \ll \omega_0$). The phase constants, being functions of frequency, will also be slightly different. Let the phase constants corresponding to the two frequencies be $\beta_0 + \Delta\beta$ and $\beta_0 - \Delta\beta$. We have

$$\begin{aligned} E(z, t) &= E_0 \cos\left[(\omega_0 + \Delta\omega)t - (\beta_0 + \Delta\beta)z\right] \\ &\quad + E_0 \cos\left[(\omega_0 - \Delta\omega)t - (\beta_0 - \Delta\beta)z\right] \\ &= 2E_0 \cos(t\,\Delta\omega - z\,\Delta\beta) \cos(\omega_0 t - \beta_0 z). \end{aligned} \tag{8–71}$$

Since $\Delta\omega \ll \omega_0$, the expression in Eq. (8–71) represents a rapidly oscillating wave having an angular frequency ω_0 and an amplitude that varies slowly with an angular frequency $\Delta\omega$. This is depicted in Fig. 8–6.

The wave inside the envelope propagates with a phase velocity found by setting $\omega_0 t - \beta_0 z = \text{Constant}$:

$$u_p = \frac{dz}{dt} = \frac{\omega_0}{\beta_0}.$$

The velocity of the envelope (the ***group velocity*** u_g) can be determined by setting the argument of the first cosine factor in Eq. (8–71) equal to a constant:

$$t\,\Delta\omega - z\,\Delta\beta = \text{Constant},$$

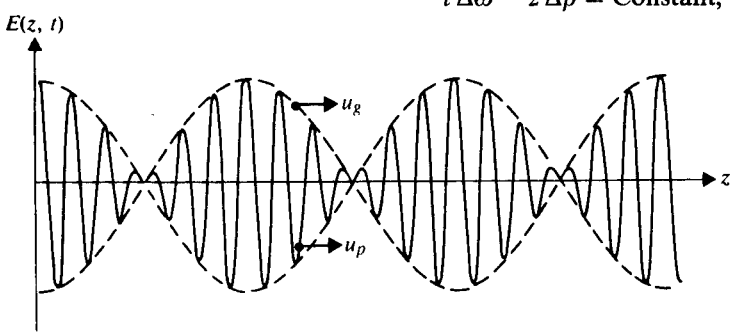

FIGURE 8–6
Sum of two time-harmonic traveling waves of equal amplitude and slightly different frequencies at a given t.

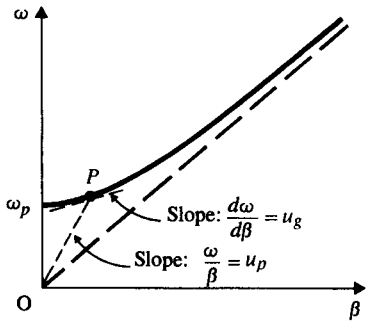

FIGURE 8–7
ω–β graph for ionized gas.

from which we obtain

$$u_g = \frac{dz}{dt} = \frac{\Delta\omega}{\Delta\beta} = \frac{1}{\Delta\beta/\Delta\omega}.$$

In the limit that $\Delta\omega \to 0$, we have the formula for computing the group velocity in a dispersive medium:

$$\boxed{u_g = \frac{1}{d\beta/d\omega} \quad \text{(m/s)}.} \tag{8–72}$$

This is the velocity of a point on the envelope of the wave packet, as shown in Fig. 8–6, and is identified as the velocity of the narrow-band signal.† As we saw in Subsection 8–3.3, β is a function of ω. If ω is plotted versus β, an ω–β graph is obtained. The slope of the straight line drawn from the origin to a point on the graph gives the phase velocity, ω/β, and the local slope of the tangent to the graph at the point is the group velocity, $d\omega/d\beta$.

In Fig. 8–7 an ω–β graph for wave propagation in an ionized medium is plotted, based on Eq. (8–67):

$$\begin{aligned}\beta &= \omega\sqrt{\mu\epsilon_0}\sqrt{1-\left(\frac{f_p}{f}\right)^2} \\ &= \frac{\omega}{c}\sqrt{1-\left(\frac{\omega_p}{\omega}\right)^2}.\end{aligned} \tag{8–73}$$

At $\omega = \omega_p$ (the cutoff angular frequency), $\beta = 0$. For $\omega > \omega_p$, wave propagation is possible, and

$$u_p = \frac{\omega}{\beta} = \frac{c}{\sqrt{1-\left(\frac{\omega_p}{\omega}\right)^2}}. \tag{8–74}$$

† The concept of group velocity is not applicable to wide-band signals in a dispersive medium (see Subsection 10–3.2).

Substituting Eq. (8–73) in Eq. (8–72), we have

$$u_g = c\sqrt{1 - \left(\frac{\omega_p}{\omega}\right)^2}. \tag{8–75}$$

We note that $u_p \geq c$ and $u_g \leq c$, and for wave propagation in an ionized medium, $u_p u_g = c^2$. A similar situation exists in waveguides (Section 10–2).

A general relation between the group and phase velocities may be obtained by combining Eqs. (8–70) and (8–72). From Eq. (8–70) we have

$$\frac{d\beta}{d\omega} = \frac{d}{d\omega}\left(\frac{\omega}{u_p}\right) = \frac{1}{u_p} - \frac{\omega}{u_p^2}\frac{du_p}{d\omega}.$$

Substitution of the above in Eq. (8–72) yields

$$u_g = \frac{u_p}{1 - \dfrac{\omega}{u_p}\dfrac{du_p}{d\omega}}. \tag{8–76}$$

From Eq. (8–76) we see three possible cases:

a) No dispersion:

$$\frac{du_p}{d\omega} = 0 \qquad (u_p \text{ independent of } \omega,\ \beta \text{ a linear function of } \omega),$$

$$u_g = u_p.$$

b) Normal dispersion:

$$\frac{du_p}{d\omega} < 0 \qquad (u_p \text{ decreasing with } \omega),$$

$$u_g < u_p.$$

c) Anomalous dispersion:

$$\frac{du_p}{d\omega} > 0 \qquad (u_p \text{ increasing with } \omega),$$

$$u_g > u_p.$$

EXAMPLE 8–6 A narrow-band signal propagates in a lossy dielectric medium which has a loss tangent 0.2 at 550 (kHz), the carrier frequency of the signal. The dielectric constant of the medium is 2.5. (a) Determine α and β. (b) Determine u_p and u_g. Is the medium dispersive?

Solution

a) Since the loss tangent $\epsilon''/\epsilon' = 0.2$ and $\epsilon''^2/8\epsilon'^2 \ll 1$, Eqs. (8–48) and (8–49) can be used to determine α and β respectively. But first we find ϵ'' from the loss tangent:

$$\epsilon'' = 0.2\,\epsilon' = 0.2 \times 2.5\,\epsilon_0$$
$$= 4.42 \times 10^{-12} \quad \text{(F/m)}.$$

Thus,

$$\alpha = \frac{\omega\epsilon''}{2}\sqrt{\frac{\mu}{\epsilon'}} = \pi(550 \times 10^3) \times (4.42 \times 10^{-12}) \times \frac{377}{\sqrt{2.5}} = 1.82 \times 10^{-3} \quad \text{(Np/m)};$$

$$\beta = \omega\sqrt{\mu\epsilon'}\left[1 + \frac{1}{8}\left(\frac{\epsilon''}{\epsilon'}\right)^2\right]$$

$$= 2\pi(550 \times 10^3)\frac{\sqrt{2.5}}{3 \times 10^8}\left[1 + \frac{1}{8}(0.2)^2\right]$$

$$= 0.0182 \times 1.005 = 0.0183 \quad \text{(rad/m)}.$$

b) Phase velocity (from Eq. 8–51):

$$u_p = \frac{\omega}{\beta} = \frac{1}{\sqrt{\mu\epsilon'}\left[1 + \frac{1}{8}\left(\frac{\epsilon''}{\epsilon'}\right)^2\right]} \cong \frac{1}{\sqrt{\mu\epsilon'}}\left[1 - \frac{1}{8}\left(\frac{\epsilon''}{\epsilon'}\right)^2\right]$$

$$= \frac{3 \times 10^8}{\sqrt{2.5}}\left[1 - \frac{1}{8}(0.2)^2\right] = 1.888 \times 10^8 \quad \text{(m/s)}.$$

c) Group velocity (from Eq. 8–49):

$$\frac{d\beta}{d\omega} = \sqrt{\mu\epsilon'}\left[1 + \frac{1}{8}\left(\frac{\epsilon''}{\epsilon'}\right)^2\right].$$

$$u_g = \frac{1}{(d\beta/d\omega)} \cong \frac{1}{\sqrt{\mu\epsilon'}} \cong u_p.$$

Thus a low-loss dielectric is nearly nondispersive. Here we have assumed ϵ'' to be independent of frequency. For a high-loss dielectric, ϵ'' will be a function of ω and may have a magnitude comparable to ϵ'. The approximation in Eq. (8–49) will no longer hold, and the medium will be dispersive. ■

8–5 Flow of Electromagnetic Power and the Poynting Vector

Electromagnetic waves carry with them electromagnetic power. Energy is transported through space to distant receiving points by electromagnetic waves. We will now derive a relation between the rate of such energy transfer and the electric and magnetic field intensities associated with a traveling electromagnetic wave.

We begin with the curl equations:

$$\nabla \times \mathbf{E} = -\frac{\partial \mathbf{B}}{\partial t}, \qquad \text{(7–53a)} \quad \text{(8–77)}$$

$$\nabla \times \mathbf{H} = \mathbf{J} + \frac{\partial \mathbf{D}}{\partial t}. \qquad \text{(7–53b)} \quad \text{(8–78)}$$

The verification of the following identity of vector operations (see Problem P.2–33) is straightforward:

$$\nabla \cdot (\mathbf{E} \times \mathbf{H}) = \mathbf{H} \cdot (\nabla \times \mathbf{E}) - \mathbf{E} \cdot (\nabla \times \mathbf{H}). \tag{8–79}$$

Substitution of Eqs. (8–77) and (8–78) in Eq. (8–79) yields

$$\nabla \cdot (\mathbf{E} \times \mathbf{H}) = -\mathbf{H} \cdot \frac{\partial \mathbf{B}}{\partial t} - \mathbf{E} \cdot \frac{\partial \mathbf{D}}{\partial t} - \mathbf{E} \cdot \mathbf{J}. \tag{8–80}$$

In a simple medium, whose constitutive parameters ϵ, μ, and σ do not change with time, we have

$$\mathbf{H} \cdot \frac{\partial \mathbf{B}}{\partial t} = \mathbf{H} \cdot \frac{\partial(\mu \mathbf{H})}{\partial t} = \frac{1}{2} \frac{\partial(\mu \mathbf{H} \cdot \mathbf{H})}{\partial t} = \frac{\partial}{\partial t}\left(\frac{1}{2} \mu H^2\right),$$

$$\mathbf{E} \cdot \frac{\partial \mathbf{D}}{\partial t} = \mathbf{E} \cdot \frac{\partial(\epsilon \mathbf{E})}{\partial t} = \frac{1}{2} \frac{\partial(\epsilon \mathbf{E} \cdot \mathbf{E})}{\partial t} = \frac{\partial}{\partial t}\left(\frac{1}{2} \epsilon E^2\right),$$

$$\mathbf{E} \cdot \mathbf{J} = \mathbf{E} \cdot (\sigma \mathbf{E}) = \sigma E^2.$$

Equation (8–80) can then be written as

$$\nabla \cdot (\mathbf{E} \times \mathbf{H}) = -\frac{\partial}{\partial t}\left(\frac{1}{2} \epsilon E^2 + \frac{1}{2} \mu H^2\right) - \sigma E^2, \tag{8–81}$$

which is a point-function relationship. An integral form of Eq. (8–81) is obtained by integrating both sides over the volume of concern:

$$\oint_S (\mathbf{E} \times \mathbf{H}) \cdot d\mathbf{s} = -\frac{\partial}{\partial t} \int_V \left(\frac{1}{2} \epsilon E^2 + \frac{1}{2} \mu H^2\right) dv - \int_V \sigma E^2 \, dv, \tag{8–82}$$

where the divergence theorem has been applied to convert the volume integral of $\nabla \cdot (\mathbf{E} \times \mathbf{H})$ to the closed surface integral of $(\mathbf{E} \times \mathbf{H})$.

We recognize that the first and second terms on the right side of Eq. (8–82) represent the time-rate of change of the energy stored in the electric and magnetic fields, respectively. [Compare with Eqs. (3–176b) and (6–172c).] The last term is the ohmic power dissipated in the volume as a result of the flow of conduction current density $\sigma \mathbf{E}$ in the presence of the electric field $\mathbf{E}$. Hence we may interpret the right side of Eq. (8–82) as the *rate of decrease* of the electric and magnetic energies stored, subtracted by the ohmic power dissipated as heat in the volume V. To be consistent with the law of conservation of energy, this must equal the power (rate of energy) *leaving* the volume through its surface. Thus the quantity $(\mathbf{E} \times \mathbf{H})$ is a vector representing the power flow per unit area. Define

$$\boxed{\mathscr{P} = \mathbf{E} \times \mathbf{H} \qquad (\mathrm{W/m^2}).} \tag{8–83}$$

Quantity $\mathscr{P}$ is known as the ***Poynting vector***, which is a power density vector associated with an electromagnetic field. The assertion that the surface integral of $\mathscr{P}$ over a closed surface, as given by the left side of Eq. (8–82), equals the power leaving

the enclosed volume is referred to as ***Poynting's theorem.*** This assertion is not limited to plane waves.

Equation (8–82) may be written in another form:

$$-\oint_S \mathcal{P} \cdot d\mathbf{s} = \frac{\partial}{\partial t} \int_V (w_e + w_m)\, dv + \int_V p_\sigma\, dv, \tag{8–84}$$

where

$$w_e = \tfrac{1}{2}\epsilon E^2 = \tfrac{1}{2}\epsilon \mathbf{E} \cdot \mathbf{E}^* = \text{Electric energy density}, \tag{8–85}$$

$$w_m = \tfrac{1}{2}\mu H^2 = \tfrac{1}{2}\mu \mathbf{H} \cdot \mathbf{H}^* = \text{Magnetic energy density}, \tag{8–86}$$

$$p_\sigma = \sigma E^2 = J^2/\sigma = \sigma \mathbf{E} \cdot \mathbf{E}^* = \mathbf{J} \cdot \mathbf{J}^*/\sigma = \text{Ohmic power density}. \tag{8–87}$$

In words, Eq. (8–84) states that the total power flowing *into* a closed surface at any instant equals the sum of the rates of increase of the stored electric and magnetic energies and the ohmic power dissipated within the enclosed volume.

Two points concerning the Poynting vector are worthy of note. First, the power relations given in Eqs. (8–82) and (8–84) pertain to the total power flow across a closed surface obtained by the surface integral of $(\mathbf{E} \times \mathbf{H})$. The definition of the Poynting vector in Eq. (8–83) as the power density vector at *every point* on the surface is an *arbitrary*, albeit useful, *concept*. Second, the Poynting vector $\mathcal{P}$ is in a direction normal to both $\mathbf{E}$ and $\mathbf{H}$.

If the region of concern is lossless ($\sigma = 0$), then the last term in Eq. (8–84) vanishes, and the total power flowing into a closed surface is equal to the rate of increase of the stored electric and magnetic energies in the enclosed volume. In a static situation, the first two terms on the right side of Eq. (8–84) vanish, and the total power flowing into a closed surface is equal to the ohmic power dissipated in the enclosed volume.

EXAMPLE 8–7 Find the Poynting vector on the surface of a long, straight conducting wire (of radius b and conductivity σ) that carries a direct current I. Verify Poynting's theorem.

Solution Since we have a d-c situation, the current in the wire is uniformly distributed over its cross-sectional area. Let us assume that the axis of the wire coincides with the z-axis. Figure 8–8 shows a segment of length ℓ of the long wire. We have

$$\mathbf{J} = \mathbf{a}_z \frac{I}{\pi b^2}$$

and

$$\mathbf{E} = \frac{\mathbf{J}}{\sigma} = \mathbf{a}_z \frac{I}{\sigma \pi b^2}.$$

On the surface of the wire,

$$\mathbf{H} = \mathbf{a}_\phi \frac{I}{2\pi b}.$$

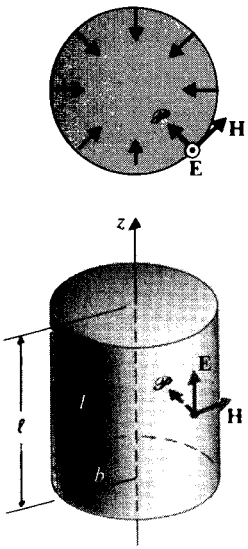

FIGURE 8–8
Illustrating Poynting's theorem (Example 8–7).

Thus the Poynting vector at the surface of the wire is

$$\mathscr{P} = \mathbf{E} \times \mathbf{H} = (\mathbf{a}_z \times \mathbf{a}_\phi) \frac{I^2}{2\sigma\pi^2 b^3}$$
$$= -\mathbf{a}_r \frac{I^2}{2\sigma\pi^2 b^3},$$

which is directed everywhere into the wire surface.

To verify Poynting's theorem, we integrate $\mathscr{P}$ over the wall of the wire segment in Fig. 8–8:

$$-\oint_S \mathscr{P} \cdot d\mathbf{s} = -\oint_S \mathscr{P} \cdot \mathbf{a}_r \, ds = \left(\frac{I^2}{2\sigma\pi^2 b^3}\right) 2\pi b\ell$$
$$= I^2\left(\frac{\ell}{\sigma\pi b^2}\right) = I^2 R,$$

where the formula for the resistance of a straight wire in Eq. (5–27), $R = \ell/\sigma S$, has been used. The above result affirms that the negative surface integral of the Poynting vector is exactly equal to the I^2R ohmic power loss in the conducting wire. Hence Poynting's theorem is verified. ■

8–5.1 INSTANTANEOUS AND AVERAGE POWER DENSITIES

In dealing with time-harmonic electromagnetic waves we have found it convenient to use phasor notation. The instantaneous value of a quantity is then the real part

of the product of the phasor quantity and $e^{j\omega t}$ when $\cos \omega t$ is used as the reference. For example, for the phasor

$$\mathbf{E}(z) = \mathbf{a}_x E_x(z) = \mathbf{a}_x E_0 e^{-(\alpha + j\beta)z}, \tag{8-88}$$

the instantaneous expression is

$$\begin{aligned} \mathbf{E}(z, t) &= \mathscr{R}e[\mathbf{E}(z)e^{j\omega t}] = \mathbf{a}_x E_0 e^{-\alpha z}\, \mathscr{R}e[e^{j(\omega t - \beta z)}] \\ &= \mathbf{a}_x E_0 e^{-\alpha z} \cos(\omega t - \beta z). \end{aligned} \tag{8-89}$$

For a uniform plane wave propagating in a lossy medium in the $+z$-direction, the associated magnetic field intensity phasor is

$$\mathbf{H}(z) = \mathbf{a}_y H_y(z) = \mathbf{a}_y \frac{E_0}{|\eta|} e^{-\alpha z} e^{-j(\beta z + \theta_\eta)}, \tag{8-90}$$

where θ_η is the phase angle of the intrinsic impedance $\eta = |\eta| e^{j\theta_\eta}$ of the medium. The corresponding instantaneous expression for $\mathbf{H}(z)$ is

$$\mathbf{H}(z, t) = \mathscr{R}e[\mathbf{H}(z)e^{j\omega t}] = \mathbf{a}_y \frac{E_0}{|\eta|} e^{-\alpha z} \cos(\omega t - \beta z - \theta_\eta). \tag{8-91}$$

This procedure is permissible as long as the operations and/or the equations involving the quantities with sinusoidal time dependence are *linear*. Erroneous results will be obtained if this procedure is applied to such nonlinear operations as a product of two sinusoidal quantities. (A Poynting vector, being the cross product of **E** and **H**, falls in this category.) The reason is that

$$\mathscr{R}e[\mathbf{E}(z)e^{j\omega t}] \times \mathscr{R}e[\mathbf{H}(z)e^{j\omega t}] \neq \mathscr{R}e[\mathbf{E}(z) \times \mathbf{H}(z)e^{j\omega t}].$$

The instantaneous expression for the Poynting vector or power density vector, from Eqs. (8–88) and (8–90), is

$$\begin{aligned} \mathscr{P}(z, t) &= \mathbf{E}(z, t) \times \mathbf{H}(z, t) = \mathscr{R}e[\mathbf{E}(z)e^{j\omega t}] \times \mathscr{R}e[\mathbf{H}(z)e^{j\omega t}] \\ &= \mathbf{a}_z \frac{E_0^2}{|\eta|} e^{-2\alpha z} \cos(\omega t - \beta z) \cos(\omega t - \beta z - \theta_\eta) \\ &= \mathbf{a}_z \frac{E_0^2}{2|\eta|} e^{-2\alpha z}[\cos\theta_\eta + \cos(2\omega t - 2\beta z - \theta_\eta)]. \end{aligned} \tag{8-92}$$

† Consider two general complex vectors **A** and **B**. We know that

$$\mathscr{R}e(\mathbf{A}) = \tfrac{1}{2}(\mathbf{A} + \mathbf{A}^*) \quad \text{and} \quad \mathscr{R}e(\mathbf{B}) = \tfrac{1}{2}(\mathbf{B} + \mathbf{B}^*),$$

where the asterisk denotes "the complex conjugate of." Thus

$$\begin{aligned} \mathscr{R}e(\mathbf{A}) \times \mathscr{R}e(\mathbf{B}) &= \tfrac{1}{2}(\mathbf{A} + \mathbf{A}^*) \times \tfrac{1}{2}(\mathbf{B} + \mathbf{B}^*) \\ &= \tfrac{1}{4}[(\mathbf{A} \times \mathbf{B}^* + \mathbf{A}^* \times \mathbf{B}) + (\mathbf{A} \times \mathbf{B} + \mathbf{A}^* \times \mathbf{B}^*)] \\ &= \tfrac{1}{2}\mathscr{R}e(\mathbf{A} \times \mathbf{B}^* + \mathbf{A} \times \mathbf{B}). \end{aligned} \tag{8-93}$$

This relation holds also for dot products of vector functions and for products of two complex scalar functions. It is a straightforward exercise to obtain the result in Eq. (8–92) by identifying the vectors **A** and **B** in Eq. (8–93) with $\mathbf{E}(z)e^{j\omega t}$ and $\mathbf{H}(z)e^{j\omega t}$, respectively.

On the other hand,

$$\mathscr{R}e[\mathbf{E}(z) \times \mathbf{H}(z)e^{j\omega t}] = \mathbf{a}_z \frac{E_0^2}{|\eta|} e^{-2\alpha z} \cos(\omega t - 2\beta z - \theta_\eta),$$

which is obviously not the same as the expression in Eq. (8–92).

As far as the power transmitted by an electromagnetic wave is concerned, its average value is a more significant quantity than its instantaneous value. From Eq. (8–92), we obtain the time-average Poynting vector, $\mathscr{P}_{av}(z)$:

$$\boxed{\mathscr{P}_{av}(z) = \frac{1}{T}\int_0^T \mathscr{P}(z, t)\,dt = \mathbf{a}_z \frac{E_0^2}{2|\eta|} e^{-2\alpha z} \cos\theta_\eta \qquad (\text{W/m}^2),} \tag{8–94}^\dagger$$

where $T = 2\pi/\omega$ is the time period of the wave. The second term on the right side of Eq. (8–92) is a cosine function of a double frequency whose average is zero over a fundamental period.

Using Eq. (8–93), we can express the instantaneous Poynting vector in Eq. (8–92) as the real part of the sum of two terms, instead of the product of the real parts of two complex vectors:

$$\begin{aligned}\mathscr{P}(z, t) &= \mathscr{R}e[\mathbf{E}(z)e^{j\omega t}] \times \mathscr{R}e[\mathbf{H}(z)e^{j\omega t}] \\ &= \tfrac{1}{2}\mathscr{R}e[\mathbf{E}(z) \times \mathbf{H}^*(z) + \mathbf{E}(z) \times \mathbf{H}(z)e^{j2\omega t}].\end{aligned} \tag{8–95}$$

The average power density, $\mathscr{P}_{av}(z)$, can be obtained by integrating $\mathscr{P}(z, t)$ over a fundamental period T. Since the average of the last (second-harmonic) term in Eq. (8–95) vanishes, we have

$$\mathscr{P}_{av}(z) = \tfrac{1}{2}\mathscr{R}e[\mathbf{E}(z) \times \mathbf{H}^*(z)].$$

---

† Equation (8–94) is quite similar to the formula for computing the power dissipated in an impedance $Z = |Z|e^{j\theta_z}$ when a sinusoidal voltage $v(t) = V_0 \cos\omega t$ appears across its terminals. The instantaneous expression for the current $i(t)$ through the impedance is

$$i(t) = \frac{V_0}{|Z|}\cos(\omega t - \theta_z).$$

From the theory of a-c circuits we know that the average power dissipated in Z is

$$P_{av} = \frac{1}{T}\int_0^T v(t)i(t)\,dt = \frac{V_0^2}{2|Z|}\cos\theta_z,$$

where $\cos\theta_z$ is the power factor of the load impedance. The $\cos\theta_\eta$ factor in Eq. (8–94) can be considered as the power factor of the intrinsic impedance of the medium.

In the general case we may not be dealing with a wave propagating in the z-direction. We write

$$\boxed{\mathcal{P}_{av} = \tfrac{1}{2}\mathcal{R}e(\mathbf{E} \times \mathbf{H}^*) \qquad (\text{W/m}^2),} \tag{8-96}^{\dagger}$$

which is a general formula for computing the average power density in a propagating wave.

EXAMPLE 8–8 The far field of a short vertical current element $I\,d\ell$ located at the origin of a spherical coordinate system in free space is

$$\mathbf{E}(R, \theta) = \mathbf{a}_\theta E_\theta(R, \theta) = \mathbf{a}_\theta\left(j\frac{60\pi I\,d\ell}{\lambda R}\sin\theta\right)e^{-j\beta R} \qquad (\text{V/m})$$

and

$$\mathbf{H}(R, \theta) = \mathbf{a}_\phi\frac{E_\theta(R, \theta)}{\eta_0} = \mathbf{a}_\phi\left(j\frac{I\,d\ell}{2\lambda R}\sin\theta\right)e^{-j\beta R} \qquad (\text{A/m}),$$

where $\lambda = 2\pi/\beta$ is the wavelength.

a) Write the expression for instantaneous Poynting vector.

b) Find the total average power radiated by the current element.

Solution

a) We note that $E_\theta/H_\phi = \eta_0 = 120\,\pi\ (\Omega)$. The instantaneous Poynting vector is

$$\begin{aligned}\mathcal{P}(R, \theta; t) &= \mathcal{R}e[\mathbf{E}(R, \theta)e^{j\omega t}] \times \mathcal{R}e[\mathbf{H}(R, \theta)e^{j\omega t}] \\ &= (\mathbf{a}_\theta \times \mathbf{a}_\phi)30\pi\left(\frac{I\,d\ell}{\lambda R}\right)^2 \sin^2\theta\sin^2(\omega t - \beta R) \\ &= \mathbf{a}_R 15\pi\left(\frac{I\,d\ell}{\lambda R}\right)^2 \sin^2\theta[1 - \cos 2(\omega t - \beta R)] \qquad (\text{W/m}^2).\end{aligned}$$

b) The average power density vector is, from Eq. (8–96),

$$\mathcal{P}_{av}(R, \theta) = \mathbf{a}_R 15\pi\left(\frac{I\,d\ell}{\lambda R}\right)^2 \sin^2\theta,$$

which is seen to equal the time-average value of $\mathcal{P}(R, \theta; t)$ given in part (a) of this solution. The total average power radiated is obtained by integrating $\mathcal{P}_{av}(R, \theta)$

---

† We are reminded that in circuit theory if a voltage $v(t) = V_0\cos(\omega t + \phi) = \mathcal{R}e[V_0 e^{j(\omega t + \phi)}]$ produces a current $i(t) = I_0\cos(\omega t + \phi - \theta_z) = \mathcal{R}e[I_0 e^{j(\omega t + \phi - \theta_z)}]$ in an impedance, the average power dissipated is $P_{av} = (V_0 I_0/2)\cos\theta_z$. In terms of phasors we have $V = V_0 e^{j\phi}$, $I = I_0 e^{j(\phi - \theta_z)}$, and

$$P_{av} = \tfrac{1}{2}V_0 I_0\cos\theta_z = \tfrac{1}{2}\mathcal{R}e(VI^*) \qquad (\text{W}), \tag{8-97}$$

which is analogous to Eq. (8–96).

over the surface of the sphere of radius R:

$$\text{Total } P_{\text{av}} = \oint_S \mathcal{P}_{\text{av}}(R, \theta) \cdot d\mathbf{s} = \int_0^{2\pi} \int_0^{\pi} \left[15\pi \left(\frac{I\, d\ell}{\lambda R} \right)^2 \sin^2 \theta \right] R^2 \sin \theta \, d\theta \, d\phi$$

$$= 40\pi^2 \left(\frac{d\ell}{\lambda} \right)^2 I^2 \qquad \text{(W)},$$

where I is the amplitude ($\sqrt{2}$ times the effective value) of the sinusoidal current in $d\ell$. ■

8–6 Normal Incidence at a Plane Conducting Boundary

Up to this point we have discussed the propagation of uniform plane waves in an unbounded homogeneous medium. In practice, waves often propagate in bounded regions where several media with different constitutive parameters are present. When an electromagnetic wave traveling in one medium impinges on another medium with a different intrinsic impedance, it experiences a reflection. In Sections 8–6 and 8–7 we examine the behavior of a plane wave when it is incident upon a plane conducting boundary. Wave behavior at an interface between two dielectric media will be discussed in Sections 8–8, 8–9, and 8–10.

For simplicity we shall assume that the incident wave ($\mathbf{E}_i$, $\mathbf{H}_i$) travels in a lossless medium (medium 1: $\sigma_1 = 0$) and that the boundary is an interface with a perfect conductor (medium 2: $\sigma_2 = \infty$). Two cases will be considered: normal incidence and oblique incidence. In this section we study the field behavior of a uniform plane wave incident normally on a plane conducting boundary.

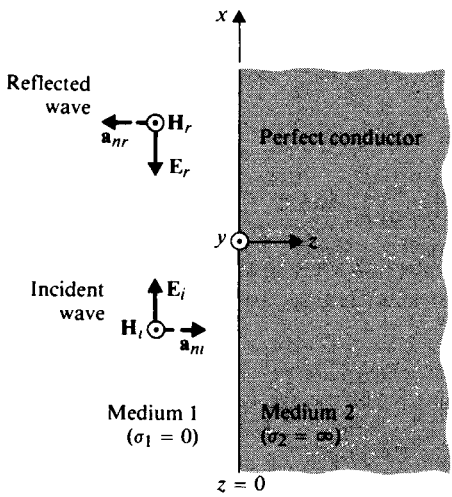

FIGURE 8–9
Plane wave incident normally on a plane conducting boundary.

Consider the situation in Fig. 8–9 where the incident wave travels in the $+z$-direction, and the boundary surface is the plane $z = 0$. The incident electric and magnetic field intensity phasors are

$$\mathbf{E}_i(z) = \mathbf{a}_x E_{i0} e^{-j\beta_1 z}, \tag{8–98}$$

$$\mathbf{H}_i(z) = \mathbf{a}_y \frac{E_{i0}}{\eta_1} e^{-j\beta_1 z}, \tag{8–99}$$

where E_{i0} is the magnitude of $\mathbf{E}_i$ at $z = 0$, and β_1 and η_1 are the phase constant and the intrinsic impedance, respectively, of medium 1. It is noted that the Poynting vector of the incident wave, $\mathscr{P}_i(z) = \mathbf{E}_i(z) \times \mathbf{H}_i(z)$, is in the $\mathbf{a}_z$ direction, which is the direction of energy propagation. The variable z is negative in medium 1.

Inside medium 2 (a perfect conductor), both electric and magnetic fields vanish, $\mathbf{E}_2 = 0$, $\mathbf{H}_2 = 0$; hence no wave is transmitted across the boundary into the $z > 0$ region. The incident wave is reflected, giving rise to a reflected wave ($\mathbf{E}_r$, $\mathbf{H}_r$). The reflected electric field intensity can be written as

$$\mathbf{E}_r(z) = \mathbf{a}_x E_{r0} e^{+j\beta_1 z}, \tag{8–100}$$

where the positive sign in the exponent signifies that the reflected wave travels in the $-z$-direction, as discussed in Section 8–2. The total electric field intensity in medium 1 is the sum of $\mathbf{E}_i$ and $\mathbf{E}_r$:

$$\mathbf{E}_1(z) = \mathbf{E}_i(z) + \mathbf{E}_r(z) = \mathbf{a}_x(E_{i0} e^{-j\beta_1 z} + E_{r0} e^{+j\beta_1 z}). \tag{8–101}$$

Continuity of the tangential component of the **E**-field at the boundary $z = 0$ demands that

$$\mathbf{E}_1(0) = \mathbf{a}_x(E_{i0} + E_{r0}) = \mathbf{E}_2(0) = 0,$$

which yields $E_{r0} = -E_{i0}$. Thus, Eq. (8–101) becomes

$$\begin{aligned} \mathbf{E}_1(z) &= \mathbf{a}_x E_{i0}(e^{-j\beta_1 z} - e^{+j\beta_1 z}) \\ &= -\mathbf{a}_x j2E_{i0} \sin \beta_1 z. \end{aligned} \tag{8–102}$$

The magnetic field intensity $\mathbf{H}_r$ of the reflected wave is related to $\mathbf{E}_r$ by Eq. (8–29):

$$\begin{aligned} \mathbf{H}_r(z) &= \frac{1}{\eta_1} \mathbf{a}_{nr} \times \mathbf{E}_r(z) = \frac{1}{\eta_1}(-\mathbf{a}_z) \times \mathbf{E}_r(z) \\ &= -\mathbf{a}_y \frac{1}{\eta_1} E_{r0} e^{+j\beta_1 z} = \mathbf{a}_y \frac{E_{i0}}{\eta_1} e^{+j\beta_1 z}. \end{aligned}$$

Combining $\mathbf{H}_r(z)$ with $\mathbf{H}_i(z)$ in Eq. (8–99), we obtain the total magnetic field intensity in medium 1:

$$\mathbf{H}_1(z) = \mathbf{H}_i(z) + \mathbf{H}_r(z) = \mathbf{a}_y 2 \frac{E_{i0}}{\eta_1} \cos \beta_1 z. \tag{8–103}$$

It is clear from Eqs. (8–102), (8–103), and (8–96) that no average power is associated with the total electromagnetic wave in medium 1, since $\mathbf{E}_1(z)$ and $\mathbf{H}_1(z)$ are in phase quadrature.

In order to examine the space-time behavior of the total field in medium 1, we first write the instantaneous expressions corresponding to the electric and magnetic field intensity phasors obtained in Eqs. (8–102) and (8–103):

$$\mathbf{E}_1(z, t) = \mathcal{R}e[\mathbf{E}_1(z)e^{j\omega t}] = \mathbf{a}_x 2E_{i0} \sin \beta_1 z \sin \omega t, \tag{8–104}$$

$$\mathbf{H}_1(z, t) = \mathcal{R}e[\mathbf{H}_1(z)e^{j\omega t}] = \mathbf{a}_y 2\frac{E_{i0}}{\eta_1} \cos \beta_1 z \cos \omega t. \tag{8–105}$$

Both $\mathbf{E}_1(z, t)$ and $\mathbf{H}_1(z, t)$ possess zeros and maxima at fixed distances from the conducting boundary for all t, as follows:

$$\left.\begin{matrix}\text{Zeros of } \mathbf{E}_1(z, t) \\ \text{Maxima of } \mathbf{H}_1(z, t)\end{matrix}\right\} \text{occur at } \beta_1 z = -n\pi, \quad \text{or } z = -n\frac{\lambda}{2}, \qquad n = 0, 1, 2, \ldots$$

$$\left.\begin{matrix}\text{Maxima of } \mathbf{E}_1(z, t) \\ \text{Zeros of } \mathbf{H}_1(z, t)\end{matrix}\right\} \text{occur at } \beta_1 z = -(2n+1)\frac{\pi}{2}, \quad \text{or } z = -(2n+1)\frac{\lambda}{4}, \qquad n = 0, 1, 2, \ldots$$

The total wave in medium 1 is not a traveling wave. It is a ***standing wave***, resulting from the superposition of two waves traveling in opposite directions. For a given t, both $\mathbf{E}_1$ and $\mathbf{H}_1$ vary sinusoidally with the distance measured from the boundary plane. The standing waves of $\mathbf{E}_1 = \mathbf{a}_x E_1$ and $\mathbf{H}_1 = \mathbf{a}_y H_1$ are shown in Fig. 8–10 for

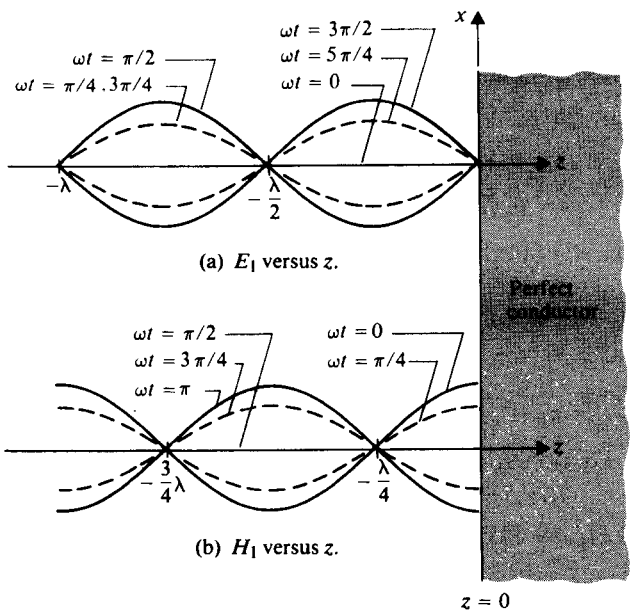

FIGURE 8–10
Standing waves of $\mathbf{E}_1 = \mathbf{a}_x E_1$ and $\mathbf{H}_1 = \mathbf{a}_y H_1$ for several values of ωt.

several values of ωt. Note the following three points: (1) $\mathbf{E}_1$ vanishes on the conducting boundary ($E_{r0} = -E_{i0}$) as well as at points that are multiples of $\lambda/2$ from the boundary; (2) $\mathbf{H}_1$ is a maximum on the conducting boundary ($H_{r0} = H_{i0} = E_{i0}/\eta_1$); (3) the standing waves of $\mathbf{E}_1$ and $\mathbf{H}_1$ are in time quadrature (90° phase difference) and are shifted in space by a quarter wavelength.

EXAMPLE 8–9 A y-polarized uniform plane wave ($\mathbf{E}_i$, $\mathbf{H}_i$) with a frequency 100 (MHz) propagates in air in the $+x$ direction and impinges normally on a perfectly conducting plane at $x = 0$. Assuming the amplitude of $\mathbf{E}_i$ to be 6 (mV/m), write the phasor and instantaneous expressions for (a) $\mathbf{E}_i$ and $\mathbf{H}_i$ of the incident wave; (b) $\mathbf{E}_r$ and $\mathbf{H}_r$ of the reflected wave; and (c) $\mathbf{E}_1$ and $\mathbf{H}_1$ of the total wave in air. (d) Determine the location nearest to the conducting plane where E_1 is zero.

Solution At the given frequency 100 (MHz),

$$\omega = 2\pi f = 2\pi \times 10^8 \qquad \text{(rad/s)},$$

$$\beta_1 = k_0 = \frac{\omega}{c} = \frac{2\pi \times 10^8}{3 \times 10^8} = \frac{2\pi}{3} \qquad \text{(rad/m)},$$

$$\eta_1 = \eta_0 = \sqrt{\frac{\mu_0}{\epsilon_0}} = 120\pi \qquad (\Omega).$$

a) *For the incident wave (a traveling wave):*

i) Phasor expressions:

$$\mathbf{E}_i(x) = \mathbf{a}_y 6 \times 10^{-3} e^{-j2\pi x/3} \qquad \text{(V/m)},$$

$$\mathbf{H}_i(x) = \frac{1}{\eta_1}\mathbf{a}_x \times \mathbf{E}_i(x) = \mathbf{a}_z \frac{10^{-4}}{2\pi} e^{-j2\pi x/3} \qquad \text{(A/m)}.$$

ii) Instantaneous expressions:

$$\mathbf{E}_i(x, t) = \mathscr{R}e[\mathbf{E}_i(x)e^{j\omega t}]$$

$$= \mathbf{a}_y 6 \times 10^{-3} \cos\left(2\pi \times 10^8 t - \frac{2\pi}{3}x\right) \qquad \text{(V/m)},$$

$$\mathbf{H}_i(x, t) = \mathbf{a}_z \frac{10^{-4}}{2\pi} \cos\left(2\pi \times 10^8 t - \frac{2\pi}{3}x\right) \qquad \text{(A/m)}.$$

b) *For the reflected wave (a traveling wave):*

i) Phasor expressions:

$$\mathbf{E}_r(x) = -\mathbf{a}_y 6 \times 10^{-3} e^{j2\pi x/3} \qquad \text{(V/m)},$$

$$\mathbf{H}_r(x) = \frac{1}{\eta_1}(-\mathbf{a}_x) \times \mathbf{E}_r(x) = \mathbf{a}_z \frac{10^{-4}}{2\pi} e^{j2\pi x/3} \qquad \text{(A/m)}.$$

ii) Instantaneous expressions:

$$\mathbf{E}_r(x, t) = \mathcal{R}e[\mathbf{E}_r(x)e^{j\omega t}] = -\mathbf{a}_y 6 \times 10^{-3} \cos\left(2\pi \times 10^8 t + \frac{2\pi}{3}x\right) \quad \text{(V/m)},$$

$$\mathbf{H}_r(x, t) = \mathbf{a}_z \frac{10^{-4}}{2\pi} \cos\left(2\pi \times 10^8 t + \frac{2\pi}{3}x\right) \quad \text{(A/m)}.$$

c) *For the total wave (a standing wave)*:

i) Phasor expressions:

$$\mathbf{E}_1(x) = \mathbf{E}_i(x) + \mathbf{E}_r(x) = -\mathbf{a}_y j12 \times 10^{-3} \sin\left(\frac{2\pi}{3}x\right) \quad \text{(V/m)},$$

$$\mathbf{H}_1(x) = \mathbf{H}_i(x) + \mathbf{H}_r(x) = \mathbf{a}_z \frac{10^{-4}}{\pi} \cos\left(\frac{2\pi}{3}x\right) \quad \text{(A/m)}.$$

ii) Instantaneous expressions:

$$\mathbf{E}_1(x, t) = \mathcal{R}e[\mathbf{E}_1(x)e^{j\omega t}] = \mathbf{a}_y 12 \times 10^{-3} \sin\left(\frac{2\pi}{3}x\right) \sin(2\pi \times 10^8 t) \quad \text{(V/m)},$$

$$\mathbf{H}_1(x, t) = \mathbf{a}_z \frac{10^{-4}}{\pi} \cos\left(\frac{2\pi}{3}x\right) \cos(2\pi \times 10^8 t) \quad \text{(A/m)}.$$

d) The electric field vanishes at the surface of the conducting plane at $x = 0$. In medium 1 the first null occurs at

$$x = -\frac{\lambda_1}{2} = -\frac{\pi}{\beta_1} = -\frac{3}{2} \quad \text{(m)}. \qquad \blacksquare$$

8–7 Oblique Incidence at a Plane Conducting Boundary

When a uniform plane wave is incident on a plane conducting surface obliquely, the behavior of the reflected wave depends on the polarization of the incident wave. In order to be specific about the direction of $\mathbf{E}_i$ we define a ***plane of incidence*** as the plane containing the vector indicating the direction of propagation of the incident wave and the normal to the boundary surface. Since an $\mathbf{E}_i$ polarized in an arbitrary direction can always be decomposed into two components—one perpendicular and the other parallel to the plane of incidence—we consider these two cases separately. The general case is obtained by superposing the results of the two component cases.

8–7.1 PERPENDICULAR POLARIZATION†

In the case of ***perpendicular polarization***, $\mathbf{E}_i$ is perpendicular to the plane of incidence, as illustrated in Fig. 8–11. Noting that

$$\mathbf{a}_{ni} = \mathbf{a}_x \sin\theta_i + \mathbf{a}_z \cos\theta_i, \tag{8–106}$$

† Also referred to as ***horizontal polarization*** or ***E-polarization***.

where θ_i is the ***angle of incidence*** measured from the normal to the boundary surface, we obtain, using Eqs. (8–26) and (8–29),

$$\mathbf{E}_i(x, z) = \mathbf{a}_y E_{i0} e^{-j\beta_1 \mathbf{a}_{ni} \cdot \mathbf{R}} = \mathbf{a}_y E_{i0} e^{-j\beta_1 (x \sin\theta_i + z \cos\theta_i)}, \tag{8–107}$$

$$\begin{aligned} \mathbf{H}_i(x, z) &= \frac{1}{\eta_1} [\mathbf{a}_{ni} \times \mathbf{E}_i(x, z)] \\ &= \frac{E_{i0}}{\eta_1} (-\mathbf{a}_x \cos\theta_i + \mathbf{a}_z \sin\theta_i) e^{-j\beta_1 (x \sin\theta_i + z \cos\theta_i)}. \end{aligned} \tag{8–108}$$

For the reflected wave,

$$\mathbf{a}_{nr} = \mathbf{a}_x \sin\theta_r - \mathbf{a}_z \cos\theta_r, \tag{8–109}$$

where θ_r is the ***angle of reflection***, we have

$$\mathbf{E}_r(x, z) = \mathbf{a}_y E_{r0} e^{-j\beta_1 (x \sin\theta_r - z \cos\theta_r)}. \tag{8–110}$$

At the boundary surface, $z = 0$, the total electric field intensity must vanish. Thus,

$$\begin{aligned} \mathbf{E}_1(x, 0) &= \mathbf{E}_i(x, 0) + \mathbf{E}_r(x, 0) \\ &= \mathbf{a}_y (E_{i0} e^{-j\beta_1 x \sin\theta_i} + E_{r0} e^{-j\beta_1 x \sin\theta_r}) = 0. \end{aligned}$$

In order for this relation to hold for all values of x, we must have $E_{r0} = -E_{i0}$ and matched phase terms, that is, $\theta_r = \theta_i$. The latter relation, asserting that ***the angle of reflection equals the angle of incidence***, is referred to as ***Snell's law of reflection***. Thus, Eq. (8–110) becomes

$$\mathbf{E}_r(x, z) = -\mathbf{a}_y E_{i0} e^{-j\beta_1 (x \sin\theta_i - z \cos\theta_i)}. \tag{8–111}$$

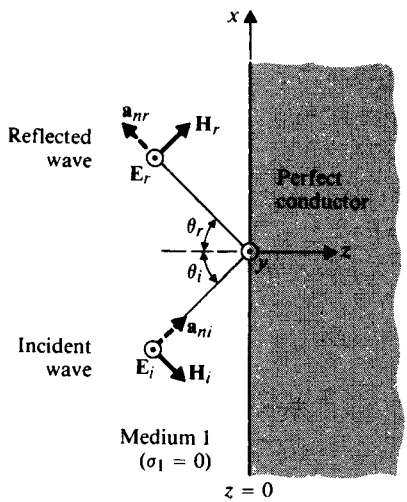

FIGURE 8–11
Plane wave incident obliquely on a plane conducting boundary (perpendicular polarization).

The corresponding $\mathbf{H}_r(x, z)$ is

$$\begin{aligned}\mathbf{H}_r(x, z) &= \frac{1}{\eta_1}[\mathbf{a}_{nr} \times \mathbf{E}_r(x, z)] \\ &= \frac{E_{i0}}{\eta_1}(-\mathbf{a}_x \cos\theta_i - \mathbf{a}_z \sin\theta_i)e^{-j\beta_1(x \sin\theta_i - z\cos\theta_i)}.\end{aligned} \tag{8-112}$$

The total field is obtained by adding the incident and reflected fields. From Eqs. (8–107) and (8–111) we have

$$\begin{aligned}\mathbf{E}_1(x, z) &= \mathbf{E}_i(x, z) + \mathbf{E}_r(x, z) \\ &= \mathbf{a}_y E_{i0}(e^{-j\beta_1 z\cos\theta_i} - e^{j\beta_1 z\cos\theta_i})e^{-j\beta_1 x\sin\theta_i} \\ &= -\mathbf{a}_y j2E_{i0}\sin(\beta_1 z\cos\theta_i)e^{-j\beta_1 x\sin\theta_i}.\end{aligned} \tag{8-113}$$

Adding the results in Eqs. (8–108) and (8–112), we get

$$\begin{aligned}\mathbf{H}_1(x, z) = -2\frac{E_{i0}}{\eta_1}[&\mathbf{a}_x \cos\theta_i \cos(\beta_1 z\cos\theta_i)e^{-j\beta_1 x\sin\theta_i} \\ &+ \mathbf{a}_z j\sin\theta_i \sin(\beta_1 z\cos\theta_i)e^{-j\beta_1 x\sin\theta_i}].\end{aligned} \tag{8-114}$$

Equations (8–113) and (8–114) are rather complicated expressions, but we can make the following observations about the oblique incidence of a uniform plane wave with perpendicular polarization on a plane conducting boundary:

1. In the direction (z-direction) normal to the boundary, E_{1y} and H_{1x} maintain standing-wave patterns according to $\sin\beta_{1z}z$ and $\cos\beta_{1z}z$, respectively, where $\beta_{1z} = \beta_1\cos\theta_i$. No average power is propagated in this direction since E_{1y} and H_{1x} are 90° out of time phase.
2. In the direction (x-direction) parallel to the boundary, E_{1y} and H_{1z} are in both time and space phase and propagate with a phase velocity

$$u_{1x} = \frac{\omega}{\beta_{1x}} = \frac{\omega}{\beta_1\sin\theta_i} = \frac{u_1}{\sin\theta_i}. \tag{8-115}$$

The wavelength in this direction is

$$\lambda_{1x} = \frac{2\pi}{\beta_{1x}} = \frac{\lambda_1}{\sin\theta_i}. \tag{8-116}$$

3. The propagating wave in the x direction is a ***nonuniform plane wave*** because its amplitude varies with z.
4. Since $\mathbf{E}_1 = 0$ for all x when $\sin(\beta_1 z\cos\theta_i) = 0$ or when

$$\beta_1 z\cos\theta_i = \frac{2\pi}{\lambda_1}z\cos\theta_i = -m\pi, \qquad m = 1, 2, 3, \ldots,$$

a conducting plate could be inserted at

$$z = -\frac{m\lambda_1}{2\cos\theta_i}, \qquad m = 1, 2, 3, \ldots, \tag{8-117}$$

without changing the field pattern that exists between the conducting plate and the conducting boundary at $z = 0$. A ***transverse electric* (TE) *wave*** ($E_{1x} = 0$) would bounce back and forth between the conducting planes and propagate in the x-direction. We would have, in effect, a parallel-plate waveguide.

An illustration of the bouncing waves and the interference pattern between a conducting plate inserted at $z = -\lambda_1/2 \cos \theta_i$ and the conducting boundary at $z = 0$ is given in Fig. 8–12. The long (thick) dashed lines represent the plane-wave crests with the **E**-vector out of the page, and the short (thin) dashed lines represent wave troughs with the **E**-vector into the page. At the conducting surfaces the reflected **E**-vector has a 180° phase change, cancelling the incident **E**-vector; hence the intersections of the long and short dashed lines (such as points O, A, and A'') are locations of zero electric intensity. The intersections of two long dashed lines (such as B) are locations of maximum electric field intensity directed out of the page, and the intersections of two short dashed lines (such as B') are locations of maximum electric field intensity into the page. The intersections of the two plane waves (incident and reflected) travel in the x-direction with a phase velocity given by Eq. (8–115). From Fig. 8–12 we have

$$\overline{OA'} = \frac{\lambda_1}{2} = \frac{\pi}{\beta_1}, \tag{8–118}$$

$$\overline{OA} = b = \frac{\lambda_1}{2 \cos \theta_i}. \tag{8–119}$$

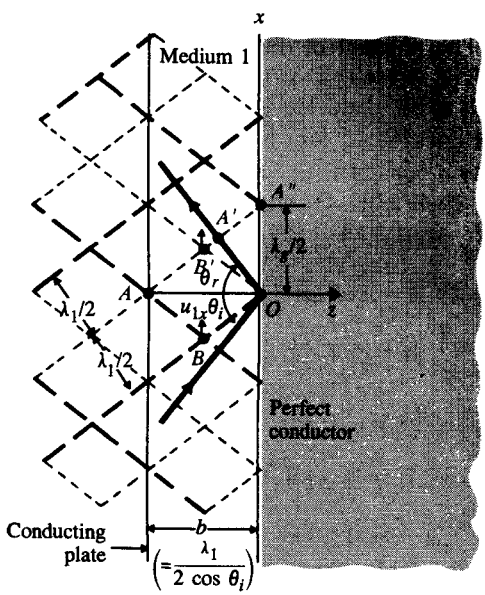

FIGURE 8–12
Illustrating bouncing waves and interference patterns of oblique incidence at a plane conducting boundary (perpendicular polarization).

The traveling wave in the parallel-plate waveguide has a guide wavelength equal to $2\overline{OA}''$, or

$$\lambda_g = 2\overline{OA}'' = 2\frac{\overline{OA}'}{\sin\theta_i} = \frac{\lambda_1}{\sin\theta_i} > \lambda_1. \tag{8-120}$$

At $\theta_i = 0$ there would be no propagating wave in the x-direction. The properties of TE waves between parallel plates will be discussed in Subsection 10–3.2.

EXAMPLE 8–10 A uniform plane wave ($\mathbf{E}_i$, $\mathbf{H}_i$) of an angular frequency ω is incident from air on a very large, perfectly conducting wall at an angle of incidence θ_i with perpendicular polarization. Find (a) the current induced on the wall surface, and (b) the time-average Poynting vector in medium 1.

Solution

a) The conditions of this problem are exactly those we have just discussed; hence we could use the formulas directly. Let $z = 0$ be the plane representing the surface of the perfectly conducting wall, and let $\mathbf{E}_i$ be polarized in the y direction, as was shown in Fig. 8–11. At $z = 0$, $\mathbf{E}_1(x, 0) = 0$, and $\mathbf{H}_1(x, 0)$ can be obtained from Eq. (8–114):

$$\mathbf{H}_1(x, 0) = -\frac{E_{i0}}{\eta_0}(\mathbf{a}_x 2\cos\theta_i)e^{-j\beta_0 x\sin\theta_i}. \tag{8-121}$$

Inside the perfectly conducting wall, both $\mathbf{E}_2$ and $\mathbf{H}_2$ must vanish. There is then a discontinuity in the magnetic field. The amount of discontinuity is equal to

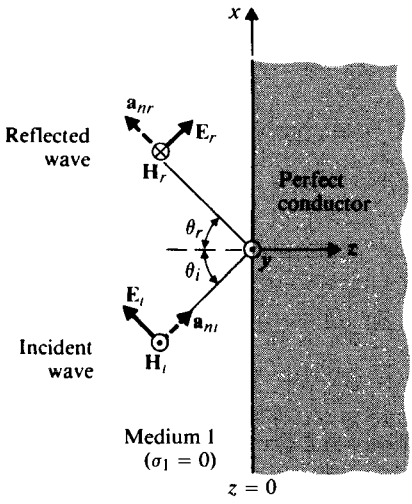

FIGURE 8–13
Plane wave incident obliquely on a plane conducting boundary (parallel polarization).

the surface current. From Eq. (7–68b) we have

$$\begin{aligned}\mathbf{J}_s(x) &= \mathbf{a}_{n2} \times \mathbf{H}_1(x, 0)\\ &= (-\mathbf{a}_z) \times (-\mathbf{a}_x)\frac{E_{i0}}{\eta_0}(2\cos\theta_i)e^{-j\beta_0 x \sin\theta_i}\\ &= \mathbf{a}_y \frac{E_{i0}}{60\pi}(\cos\theta_i)e^{-j(\omega/c)x\sin\theta_i}.\end{aligned}$$

The instantaneous expression for the surface current is

$$\mathbf{J}_s(x, t) = \mathbf{a}_y \frac{E_{i0}}{60\pi}\cos\theta_i \cos\omega\left(t - \frac{x}{c}\sin\theta_i\right) \quad \text{(A/m)}. \tag{8–122}$$

It is this induced current on the wall surface that gives rise to the reflected wave in medium 1 and cancels the incident wave in the conducting wall.

b) The time-average Poynting vector in medium 1 is found by using Eqs. (8–113) and (8–114) in Eq. (8–96). Since E_{1y} and H_{1x} are in time quadrature, $\mathscr{P}_{\text{av}}$ will only have a nonvanishing x-component arising from E_{1y} and H_{1z}:

$$\begin{aligned}\mathscr{P}_{\text{av}_1} &= \tfrac{1}{2}\mathscr{R}e[\mathbf{E}_1(x, z) \times \mathbf{H}_1^*(x, z)]\\ &= \mathbf{a}_x 2\frac{E_{i0}^2}{\eta_1}\sin\theta_i \sin^2\beta_{1z}z,\end{aligned} \tag{8–123}$$

where $\beta_{1z} = \beta_1 \cos\theta_i$. The time-average Poynting vector in medium 2 (a perfect conductor) is, of course, zero. ■

8–7.2 PARALLEL POLARIZATION†

We now consider the case of $\mathbf{E}_i$ lying in the plane of incidence while a uniform plane wave impinges obliquely on a perfectly conducting plane boundary, as depicted in Fig. 8–13. The unit vectors $\mathbf{a}_{ni}$ and $\mathbf{a}_{nr}$, representing the directions of propagation of the incident and reflected waves, respectively, remain the same as those given in Eqs. (8–106) and (8–109). Both $\mathbf{E}_i$ and $\mathbf{E}_r$ now have components in x- and z-directions, whereas $\mathbf{H}_i$ and $\mathbf{H}_r$ have only a y-component. We have, for the incident wave,

$$\mathbf{E}_i(x, z) = E_{i0}(\mathbf{a}_x \cos\theta_i - \mathbf{a}_z \sin\theta_i)e^{-j\beta_1(x\sin\theta_i + z\cos\theta_i)}, \tag{8–124}$$

$$\mathbf{H}_i(x, z) = \mathbf{a}_y \frac{E_{i0}}{\eta_1} e^{-j\beta_1(x\sin\theta_i + z\cos\theta_i)}. \tag{8–125}$$

The reflected wave ($\mathbf{E}_r$, $\mathbf{H}_r$) have the following phasor expressions:

$$\mathbf{E}_r(x, z) = E_{r0}(\mathbf{a}_x \cos\theta_r + \mathbf{a}_z \sin\theta_r)e^{-j\beta_1(x\sin\theta_r - z\cos\theta_r)}, \tag{8–126}$$

$$\mathbf{H}_r(x, z) = -\mathbf{a}_y \frac{E_{r0}}{\eta_1} e^{-j\beta_1(x\sin\theta_r - z\cos\theta_r)}. \tag{8–127}$$

† Also referred to as ***vertical polarization*** or **H-*polarization***.

At the surface of the perfect conductor, $z = 0$, the tangential component (the x-component) of the total electric field intensity must vanish for all x, or $E_{ix}(x, 0) + E_{rx}(x, 0) = 0$. From Eqs. (8–124) and (8–126) we have

$$(E_{i0} \cos \theta_i)e^{-j\beta_1 x \sin \theta_i} + (E_{r0} \cos \theta_r)e^{-j\beta_1 x \sin \theta_r} = 0,$$

which requires $E_{r0} = -E_{i0}$ and $\theta_r = \theta_i$. The total electric field intensity in medium 1 is the sum of Eqs. (8–124) and (8–126):

$$\begin{aligned}\mathbf{E}_1(x, z) &= \mathbf{E}_i(x, z) + \mathbf{E}_r(x, z) \\ &= \mathbf{a}_x E_{i0} \cos \theta_i (e^{-j\beta_1 z \cos \theta_i} - e^{j\beta_1 z \cos \theta_i})e^{-j\beta_1 x \sin \theta_i} \\ &\quad - \mathbf{a}_z E_{i0} \sin \theta_i (e^{-j\beta_1 z \cos \theta_i} + e^{j\beta_1 z \cos \theta_i})e^{-j\beta_1 x \sin \theta_i}\end{aligned}$$

or

$$\begin{aligned}\mathbf{E}_1(x, z) = -2E_{i0}[&\mathbf{a}_x j \cos \theta_i \sin (\beta_1 z \cos \theta_i) \\ &+ \mathbf{a}_z \sin \theta_i \cos (\beta_1 z \cos \theta_i)]e^{-j\beta_1 x \sin \theta_i}.\end{aligned} \tag{8–128}$$

Adding Eqs. (8–125) and (8–127), we obtain the total magnetic field intensity in medium 1:

$$\begin{aligned}\mathbf{H}_1(x, z) &= \mathbf{H}_i(x, z) + \mathbf{H}_r(x, z) \\ &= \mathbf{a}_y 2 \frac{E_{i0}}{\eta_1} \cos (\beta_1 z \cos \theta_i)e^{-j\beta_1 x \sin \theta_i}.\end{aligned} \tag{8–129}$$

The interpretation of Eqs. (8–128) and (8–129) is similar to that of Eqs. (8–113) and (8–114) for the perpendicular-polarization case, except that $\mathbf{E}_1(x, z)$, instead of $\mathbf{H}_1(x, z)$, now has both an x- and a z-component. We conclude, therefore:

1. In the direction (z-direction) normal to the boundary, E_{1x} and H_{1y} maintain standing-wave patterns according to $\sin \beta_{1z} z$ and $\cos \beta_{1z} z$, respectively, where $\beta_{1z} = \beta_1 \cos \theta_i$. No average power is propagated in this direction, since E_{1x} and H_{1y} are 90° out of time phase.
2. In the x-direction parallel to the boundary, E_{1z} and H_{1y} are in both time and space phase and propagate with a phase velocity $u_{1x} = u_1/\sin \theta_i$, which is the same as that in the perpendicular polarization.
3. As in the case of perpendicular polarization, the propagating wave in the x-direction is a nonuniform plane wave.
4. The insertion of a conducting plate at $z = -m\lambda_1/2 \cos \theta_i$ ($m = 1, 2, 3, \ldots$) where $E_{1x} = 0$ for all x would not affect the field pattern that exists between the conducting plate and the conducting boundary at $z = 0$; we would then have a parallel-plate waveguide. A ***tranverse magnetic* (TM) *wave*** ($H_{1x} = 0$) will propagate in the x-direction. (TM waves between parallel plates will be discussed in Subsection 10–3.1.)

We note here that the $\mathbf{E}_1$ and $\mathbf{H}_1$ expressions for oblique incidence in Eqs. (8–113), (8–114), (8–128), and (8–129) are the sums of the fields of incident and reflected waves. They represent interference patterns. If the incident wave is confined in a narrow beam, the reflected waves will also be a narrow beam propagating in a

different direction. There will then be no interference except for a very small region near the conducting surface. Thus, the reflectors on microwave relay towers receive, amplify, and retransmit the original incident wave, not the interference pattern.

8–8 Normal Incidence at a Plane Dielectric Boundary

When an electromagnetic wave is incident on the surface of a dielectric medium that has an intrinsic impedance different from that of the medium in which the wave is originated, part of the incident power is reflected and part is transmitted. We may think of the situation as being like an impedance mismatch in circuits. The case of wave incidence on a perfectly conducting boundary discussed in the two previous sections is like terminating a generator that has a certain internal impedance with a short circuit; no power is transmitted into the conducting region.

As before, we will consider separately the two cases of the normal incidence and the oblique incidence of a uniform plane wave on a plane dielectric medium. Both media are assumed to be dissipationless ($\sigma_1 = \sigma_2 = 0$). We will discuss the wave behavior for normal incidence in this section. The case of oblique incidence will be taken up in Section 8–9.

Consider the situation in Fig. 8–14, where the incident wave travels in the $+z$-direction and the boundary surface is the plane $z = 0$. The incident electric and magnetic field intensity phasors are

$$\mathbf{E}_i(z) = \mathbf{a}_x E_{i0} e^{-j\beta_1 z}, \tag{8–130}$$

$$\mathbf{H}_i(z) = \mathbf{a}_y \frac{E_{i0}}{\eta_1} e^{-j\beta_1 z}. \tag{8–131}$$

These are the same expressions as those given in Eqs. (8–98) and (8–99). Note that z is negative in medium 1.

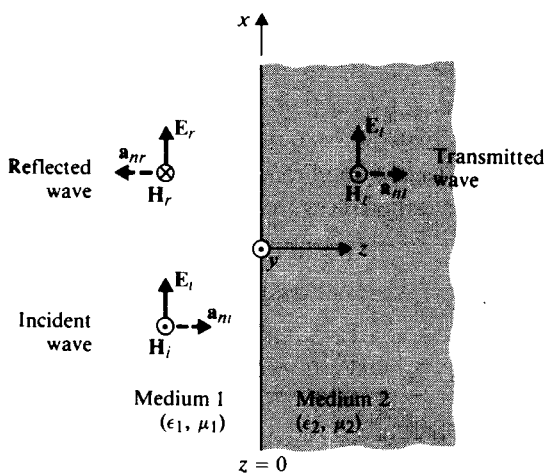

FIGURE 8–14
Plane wave incident normally on a plane dielectric boundary.

Because of the medium discontinuity at $z = 0$, the incident wave is partly reflected back into medium 1 and partly transmitted into medium 2. We have

a) *For the reflected wave* ($\mathbf{E}_r$, $\mathbf{H}_r$):

$$\mathbf{E}_r(z) = \mathbf{a}_x E_{r0} e^{j\beta_1 z}, \tag{8-132}$$

$$\mathbf{H}_r(z) = (-\mathbf{a}_z) \times \frac{1}{\eta_1} \mathbf{E}_r(z) = -\mathbf{a}_y \frac{E_{r0}}{\eta_1} e^{j\beta_1 z}. \tag{8-133}$$

b) *For the transmitted wave* ($\mathbf{E}_t$, $\mathbf{H}_t$):

$$\mathbf{E}_t(z) = \mathbf{a}_x E_{t0} e^{-j\beta_2 z}, \tag{8-134}$$

$$\mathbf{H}_t(z) = \mathbf{a}_z \times \frac{1}{\eta_2} \mathbf{E}_t(z) = \mathbf{a}_y \frac{E_{t0}}{\eta_2} e^{-j\beta_2 z}, \tag{8-135}$$

where E_{t0} is the magnitude of $\mathbf{E}_t$ at $z = 0$, and β_2 and η_2 are the phase constant and the intrinsic impedance, respectively, of medium 2.

Note that the directions of the arrows for $\mathbf{E}_r$ and $\mathbf{E}_t$ in Fig. 8–14 are arbitrarily drawn because E_{r0} and E_{t0} may themselves be positive or negative, depending on the relative magnitudes of the constitutive parameters of the two media.

Two equations are needed for determining the two unknown magnitudes E_{r0} and E_{t0}. These equations are supplied by the boundary conditions that must be satisfied by the electric and magnetic fields. At the dielectric interface $z = 0$ the tangential components (the x-components) of the electric and magnetic field intensities must be continuous. We have

$$\mathbf{E}_i(0) + \mathbf{E}_r(0) = \mathbf{E}_t(0) \quad \text{or} \quad E_{i0} + E_{r0} = E_{t0} \tag{8-136}$$

and

$$\mathbf{H}_i(0) + \mathbf{H}_r(0) = \mathbf{H}_t(0) \quad \text{or} \quad \frac{1}{\eta_1}(E_{i0} - E_{r0}) = \frac{E_{t0}}{\eta_2}. \tag{8-137}$$

Solving Eqs. (8–136) and (8–137), we obtain

$$E_{r0} = \frac{\eta_2 - \eta_1}{\eta_2 + \eta_1} E_{i0}, \tag{8-138}$$

$$E_{t0} = \frac{2\eta_2}{\eta_2 + \eta_1} E_{i0}. \tag{8-139}$$

The ratios E_{r0}/E_{i0} and E_{t0}/E_{i0} are called ***reflection coefficient*** and ***transmission coefficient***, respectively. In terms of the intrinsic impedances they are

$$\boxed{\Gamma = \frac{E_{r0}}{E_{i0}} = \frac{\eta_2 - \eta_1}{\eta_2 + \eta_1} \quad \text{(Dimensionless)}} \tag{8-140}$$

and

$$\boxed{\tau = \frac{E_{t0}}{E_{i0}} = \frac{2\eta_2}{\eta_2 + \eta_1} \quad \text{(Dimensionless).}} \tag{8-141}$$

Note that the reflection coefficient Γ in Eq. (8–140) can be positive or negative, depending on whether η_2 is greater or less than η_1. The transmission coefficient τ, however, is always positive.

The definitions for Γ and τ in Eqs. (8–140) and (8–141) apply even when the media are dissipative—that is, even when η_1 and/or η_2 are complex. Thus Γ and τ may themselves be complex in the general case. A complex Γ (or τ) simply means that a phase shift is introduced at the interface upon reflection (or transmission). Reflection and transmission coefficients are related by the following equation:

$$\boxed{1 + \Gamma = \tau \qquad \text{(Dimensionless).}} \tag{8–142}$$

If medium 2 is a perfect conductor, $\eta_2 = 0$, Eqs. (8–140) and (8–141) yield $\Gamma = -1$ and $\tau = 0$. Consequently, $E_{r0} = -E_{i0}$, and $E_{t0} = 0$. The incident wave will be totally reflected, and a standing wave will be produced in medium 1. The standing wave will have zero and maximum points, as discussed in Section 8–6.

If medium 2 is not a perfect conductor, partial reflection will result. The total electric field in medium 1 can be written as

$$\begin{aligned}\mathbf{E}_1(z) &= \mathbf{E}_i(z) + \mathbf{E}_r(z) = \mathbf{a}_x E_{i0}(e^{-j\beta_1 z} + \Gamma e^{j\beta_1 z}) \\ &= \mathbf{a}_x E_{i0}[(1 + \Gamma)e^{-j\beta_1 z} + \Gamma(e^{j\beta_1 z} - e^{-j\beta_1 z})] \\ &= \mathbf{a}_x E_{i0}[(1 + \Gamma)e^{-j\beta_1 z} + \Gamma(j2 \sin \beta_1 z)]\end{aligned}$$

or, in view of Eq. (8–142),

$$\mathbf{E}_1(z) = \mathbf{a}_x E_{i0}[\tau e^{-j\beta_1 z} + \Gamma(j2 \sin \beta_1 z)]. \tag{8–143}$$

We see in Eq. (8–143) that $\mathbf{E}_1(z)$ is composed of two parts: a traveling wave with an amplitude $\tau \mathbf{E}_{i0}$ and a standing wave with an amplitude $2\Gamma \mathbf{E}_{i0}$. Because of the existence of the traveling wave, $\mathbf{E}_1(z)$ does not go to zero at fixed distances from the interface; it merely has locations of maximum and minimum values.

The locations of maximum and minimum $|\mathbf{E}_1(z)|$ are conveniently found by rewriting $\mathbf{E}_1(z)$ as

$$\mathbf{E}_1(z) = \mathbf{a}_x E_{i0} e^{-j\beta_1 z}(1 + \Gamma e^{j2\beta_1 z}). \tag{8–144}$$

For dissipationless media, η_1 and η_2 are real, making both Γ and τ also real. However, Γ can be positive or negative. Consider the following two cases.

1. $\Gamma > 0$ $(\eta_2 > \eta_1)$.

The maximum value of $|\mathbf{E}_1(z)|$ is $E_{i0}(1 + \Gamma)$, which occurs when $2\beta_1 z_{\max} = -2n\pi$ $(n = 0, 1, 2, \ldots)$, or at

$$z_{\max} = -\frac{n\pi}{\beta_1} = -\frac{n\lambda_1}{2}, \qquad n = 0, 1, 2, \ldots \tag{8–145}$$

The minimum value of $|\mathbf{E}_1(z)|$ is $E_{i0}(1 - \Gamma)$, which occurs when $2\beta_1 z_{\min} = -(2n + 1)\pi$, or at

$$z_{\min} = -\frac{(2n + 1)\pi}{2\beta_1} = -\frac{(2n + 1)\lambda_1}{4}, \qquad n = 0, 1, 2, \ldots \tag{8–146}$$

2. $\Gamma < 0$ ($\eta_2 < \eta_1$).

The maximum value of $|\mathbf{E}_1(z)|$ is $E_{i0}(1 - \Gamma)$, which occurs at $z_{\min}$ given in Eq. (8–146); and the minimum value of $|\mathbf{E}_1(z)|$ is $E_{i0}(1 + \Gamma)$, which occurs at $z_{\max}$ given in Eq. (8–145). In other words, the locations for $|E_1(z)|_{\max}$ and $|E_1(z)|_{\min}$ when $\Gamma > 0$ and when $\Gamma < 0$ are interchanged.

The ratio of the maximum value to the minimum value of the electric field intensity of a standing wave is called the ***standing-wave ratio*** **(SWR)**, S.

$$\boxed{S = \frac{|E|_{\max}}{|E|_{\min}} = \frac{1 + |\Gamma|}{1 - |\Gamma|} \qquad \text{(Dimensionless).}} \tag{8–147}$$

An inverse relation of Eq. (8–147) is

$$\boxed{|\Gamma| = \frac{S - 1}{S + 1} \qquad \text{(Dimensionless).}} \tag{8–148}$$

While the value of Γ ranges from -1 to $+1$, the value of S ranges from 1 to ∞. It is customary to express S on a logarithmic scale. The standing-wave ratio in decibels is $20 \log_{10} S$. Thus $S = 2$ corresponds to a standing-wave ratio of $20 \log_{10} 2 = 6.02$ dB and $|\Gamma| = (2 - 1)/(2 + 1) = \frac{1}{3}$. A standing-wave ratio of 2 dB is equivalent to $S = 1.26$ and $|\Gamma| = 0.115$.

The magnetic field intensity in medium 1 is obtained by combining $\mathbf{H}_i(z)$ and $\mathbf{H}_r(z)$ in Eqs. (8–131) and (8–133), respectively:

$$\begin{aligned} \mathbf{H}_1(z) &= \mathbf{a}_y \frac{E_{i0}}{\eta_1} (e^{-j\beta_1 z} - \Gamma e^{j\beta_1 z}) \\ &= \mathbf{a}_y \frac{E_{i0}}{\eta_1} e^{-j\beta_1 z}(1 - \Gamma e^{j2\beta_1 z}). \end{aligned} \tag{8–149}$$

This should be compared with $\mathbf{E}_1(z)$ in Eq. (8–144). In a dissipationless medium, Γ is real; and $|\mathbf{H}_1(z)|$ will be a minimum at locations where $|\mathbf{E}_1(z)|$ is a maximum, and vice versa.

In medium 2, $(\mathbf{E}_t, \mathbf{H}_t)$ constitute the transmitted wave propagating in $+z$-direction. From Eqs. (8–134) and (8–141) we have

$$\mathbf{E}_t(z) = \mathbf{a}_x \tau E_{i0} e^{-j\beta_2 z}. \tag{8–150}$$

And from Eq. (8–135) we obtain

$$\mathbf{H}_t(z) = \mathbf{a}_y \frac{\tau}{\eta_2} E_{i0} e^{-j\beta_2 z}. \tag{8–151}$$

EXAMPLE 8–11 A uniform plane wave in a lossless medium with intrinsic impedance η_1 is incident normally onto another lossless medium with intrinsic impedance

η_2 through a plane boundary. Obtain the expressions for the time-average power densities in both media.

Solution Equation (8–96) provides the formula for computing the time-average power density, or time-average Poynting vector:

$$\mathscr{P}_{av} = \tfrac{1}{2}\mathscr{R}e(\mathbf{E} \times \mathbf{H}^*).$$

In medium 1 we use Eqs. (8–144) and (8–149):

$$\begin{aligned}(\mathscr{P}_{av})_1 &= \mathbf{a}_z \frac{E_{i0}^2}{2\eta_1} \mathscr{R}e[(1 + \Gamma e^{j2\beta_1 z})(1 - \Gamma e^{-j2\beta_1 z})] \\ &= \mathbf{a}_z \frac{E_{i0}^2}{2\eta_1} \mathscr{R}e[(1 - \Gamma^2) + \Gamma(e^{j2\beta_1 z} - e^{-j2\beta_1 z})] \\ &= \mathbf{a}_z \frac{E_{i0}^2}{2\eta_1} \mathscr{R}e[(1 - \Gamma^2) + j2\Gamma \sin 2\beta_1 z] \\ &= \mathbf{a}_z \frac{E_{i0}^2}{2\eta_1} (1 - \Gamma^2),\end{aligned} \tag{8–152}$$

where Γ is a real number because both media are lossless.

In medium 2 we use Eqs. (8–150) and (8–151) to obtain

$$(\mathscr{P}_{av})_2 = \mathbf{a}_z \frac{E_{i0}^2}{2\eta_2} \tau^2. \tag{8–153}$$

Since we are dealing with lossless media, the power flow in medium 1 must equal that in medium 2; that is,

$$(\mathscr{P}_{av})_1 = (\mathscr{P}_{av})_2, \tag{8–154}$$

or

$$\boxed{1 - \Gamma^2 = \frac{\eta_1}{\eta_2} \tau^2.} \tag{8–155}$$

That Eq. (8–155) is true can be readily verified by using Eqs. (8–140) and (8–141).

■

8–9 Normal Incidence at Multiple Dielectric Interfaces

In certain practical situations a wave may be incident on several layers of dielectric media with different constitutive parameters. One such situation is the use of a dielectric coating on glass to reduce glare from sunlight. Another is a ***radome***, which is a dome-shaped enclosure designed not only to protect radar installations from inclement weather but to permit the propagation of electromagnetic waves through

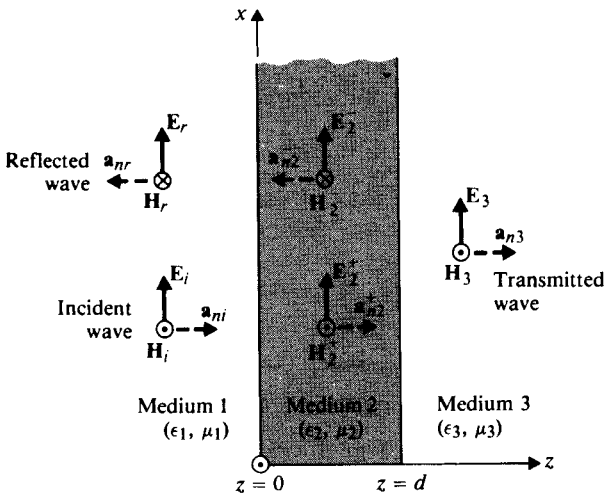

FIGURE 8–15
Normal incidence at multiple dielectric interfaces.

the enclosure with as little reflection as possible. In both situations, determining the proper dielectric material and its thickness is an important design problem.

We now consider the three-region situation depicted in Fig. 8–15. A uniform plane wave traveling in the $+z$-direction in medium 1 (ϵ_1, μ_1) impinges normally at a plane boundary with medium 2 (ϵ_2, μ_2), at $z = 0$. Medium 2 has a finite thickness and interfaces with medium 3 (ϵ_3, μ_3) at $z = d$. Reflection occurs at both $z = 0$ and $z = d$. Assuming an x-polarized incident field, the total electric field intensity in medium 1 can always be written as the sum of the incident component $\mathbf{a}_x E_{i0} e^{-j\beta_1 z}$ and a reflected component $\mathbf{a}_x E_{r0} e^{j\beta_1 z}$:

$$\mathbf{E}_1 = \mathbf{a}_x (E_{i0} e^{-j\beta_1 z} + E_{r0} e^{j\beta_1 z}). \tag{8–156}$$

However, owing to the existence of a second discontinuity at $z = d$, E_{r0} is no longer related to E_{i0} by Eq. (8–138) or Eq. (8–140). Within medium 2, parts of waves bounce back and forth between the two bounding surfaces, some penetrating into media 1 and 3. The reflected field in medium 1 is the sum of (a) the field reflected from the interface at $z = 0$ as the incident wave impinges on it, (b) the field transmitted back into medium 1 from medium 2 after a first reflection from the interface at $z = d$, (c) the field transmitted back into medium 1 from medium 2 after a second reflection at $z = d$, and so on. The total reflected wave is, in fact, the resultant of the initial reflected component and an infinite sequence of multiply reflected contributions within medium 2 that are transmitted back into medium 1. Since all of the contributions propagate in the $-z$-direction in medium 1 and contain the propagation factor $e^{j\beta_1 z}$, they can be combined into a single term with a coefficient E_{r0}. But how do we determine the relation between E_{r0} and E_{i0} now?

One way to find E_{r0} is to write down the electric and magnetic field intensity vectors in all three regions and apply the boundary conditions. The $\mathbf{H}_1$ in region 1

that corresponds to the $\mathbf{E}_1$ in Eq. (8–156) is, from Eqs. (8–131) and (8–133),

$$\mathbf{H}_1 = \mathbf{a}_y \frac{1}{\eta_1}(E_{i0}e^{-j\beta_1 z} - E_{r0}e^{j\beta_1 z}). \tag{8–157}$$

The electric and magnetic fields in region 2 can also be represented by combinations of forward and backward waves:

$$\mathbf{E}_2 = \mathbf{a}_x(E_2^+ e^{-j\beta_2 z} + E_2^- e^{j\beta_2 z}), \tag{8–158}$$

$$\mathbf{H}_2 = \mathbf{a}_y \frac{1}{\eta_2}(E_2^+ e^{-j\beta_2 z} - E_2^- e^{j\beta_2 z}). \tag{8–159}$$

In region 3, only a forward wave traveling in $+z$-direction exists. Thus,

$$\mathbf{E}_3 = \mathbf{a}_x E_3^+ e^{-j\beta_3 z}, \tag{8–160}$$

$$\mathbf{H}_3 = \mathbf{a}_y \frac{E_3^+}{\eta_3} e^{-j\beta_3 z}. \tag{8–161}$$

On the right side of Eqs. (8–156) through (8–161) there are a total of four unknown amplitudes: E_{r0}, E_2^+, E_2^-, and E_3^+. They can be determined by solving the four boundary-condition equations required by the continuity of the tangential components of the electric and magnetic fields.

At $z = 0$:

$$\mathbf{E}_1(0) = \mathbf{E}_2(0), \tag{8–162}$$

$$\mathbf{H}_1(0) = \mathbf{H}_2(0). \tag{8–163}$$

At $z = d$:

$$\mathbf{E}_2(d) = \mathbf{E}_3(d), \tag{8–164}$$

$$\mathbf{H}_2(d) = \mathbf{H}_3(d). \tag{8–165}$$

The procedure is straightforward and purely algebraic (Problem P.8–29). In the following subsections we introduce the concept of wave impedance and use it in an alternative approach for studying the problem of multiple reflections at normal incidence.

8–9.1 WAVE IMPEDANCE OF THE TOTAL FIELD

We define the ***wave impedance of the total field*** at any plane parallel to the plane boundary as the ratio of the total electric field intensity to the total magnetic field intensity. With a z-dependent uniform plane wave, as was shown in Fig. 8–15, we write, in general,

$$Z(z) = \frac{\text{Total } E_x(z)}{\text{Total } H_y(z)} \quad (\Omega). \tag{8–166}$$

For a single wave propagating in the $+z$-direction in an unbounded medium, the wave impedance equals the intrinsic impedance, η, of the medium; for a single wave traveling in the $-z$-direction, it is $-\eta$ for all z.

In the case of a uniform plane wave incident from medium 1 normally on a plane boundary with an infinite medium 2, such as that illustrated in Fig. 8–14 and discussed in Section 8–8, the magnitudes of the total electric and magnetic field intensities in medium 1 are, from Eqs. (8–144) and (8–149),

$$E_{1x}(z) = E_{i0}(e^{-j\beta_1 z} + \Gamma e^{j\beta_1 z}), \tag{8–167}$$

$$H_{1y}(z) = \frac{E_{i0}}{\eta_1}(e^{-j\beta_1 z} - \Gamma e^{j\beta_1 z}). \tag{8–168}$$

Their ratio defines the wave impedance of the total field in medium 1 at a distance z from the boundary plane:

$$Z_1(z) = \frac{E_{1x}(z)}{H_{1y}(z)} = \eta_1 \frac{e^{-j\beta_1 z} + \Gamma e^{j\beta_1 z}}{e^{-j\beta_1 z} - \Gamma e^{j\beta_1 z}}, \tag{8–169}$$

which is obviously a function of z.

A distance $z = -\ell$ to the left of the boundary plane,

$$Z_1(-\ell) = \frac{E_{1x}(-\ell)}{H_{1y}(-\ell)} = \eta_1 \frac{e^{j\beta_1 \ell} + \Gamma e^{-j\beta_1 \ell}}{e^{j\beta_1 \ell} - \Gamma e^{-j\beta_1 \ell}}. \tag{8–170}$$

Using the definition of $\Gamma = (\eta_2 - \eta_1)/(\eta_2 + \eta_1)$ in Eq. (8–170), we obtain

$$Z_1(-\ell) = \eta_1 \frac{\eta_2 \cos \beta_1 \ell + j\eta_1 \sin \beta_1 \ell}{\eta_1 \cos \beta_1 \ell + j\eta_2 \sin \beta_1 \ell}, \tag{8–171}$$

which correctly reduces to η_1 when $\eta_2 = \eta_1$. In that case there is no discontinuity at $z = 0$; hence there is no reflected wave and the total-field wave impedance is the same as the intrinsic impedance of the medium.

When we study transmission lines in the next chapter, we will find that Eqs. (8–170) and (8–171) are similar to the formulas for the input impedance of a transmission line of length ℓ that has a characteristic impedance η_1 and terminates in an impedance η_2. There is a close similarity between the behavior of the propagation of uniform plane waves at normal incidence and the behavior of transmission lines.

If the plane boundary is perfectly conducting, $\eta_2 = 0$ and $\Gamma = -1$, and Eq. (8–171) becomes

$$Z_1(-\ell) = j\eta_1 \tan \beta_1 \ell, \tag{8–172}$$

which is the same as the input impedance of a transmission line of length ℓ that has a characteristic impedance η_1 and terminates in a short circuit.

8–9.2 IMPEDANCE TRANSFORMATION WITH MULTIPLE DIELECTRICS

The concept of total-field wave impedance is very useful in solving problems with multiple dielectric interfaces such as the situation shown in Fig. 8–15. The total field in medium 2 is the result of multiple reflections of the two boundary planes at $z = 0$ and $z = d$; but it can be grouped into a wave traveling in the $+z$-direction and another traveling in the $-z$-direction. The wave impedance of the total field in medium

2 at the left-hand interface $z = 0$ can be found from the right side of Eq. (8–171) by replacing η_2 by η_3, η_1 by η_2, β_1 by β_2, and ℓ by d. Thus,

$$Z_2(0) = \eta_2 \frac{\eta_3 \cos \beta_2 d + j\eta_2 \sin \beta_2 d}{\eta_2 \cos \beta_2 d + j\eta_3 \sin \beta_2 d}. \tag{8–173}$$

As far as the wave in medium 1 is concerned, it encounters a discontinuity at $z = 0$ and the discontinuity can be characterized by an infinite medium with an intrinsic impedance $Z_2(0)$ as given in Eq. (8–173). The effective reflection coefficient at $z = 0$ for the incident wave in medium 1 is

$$\Gamma_0 = \frac{E_{r0}}{E_{i0}} = -\frac{H_{r0}}{H_{i0}} = \frac{Z_2(0) - \eta_1}{Z_2(0) + \eta_1}. \tag{8–174}$$

We note that Γ_0 differs from Γ only in that η_2 has been replaced by $Z_2(0)$. Hence the insertion of a dielectric layer of thickness d and intrinsic impedance η_2 in front of medium 3, which has intrinsic impedance η_3, has the effect of transforming η_3 to $Z_2(0)$. Given η_1 and η_3, Γ_0 can be adjusted by suitable choices of η_2 and d.

Once Γ_0 has been found from Eq. (8–174), E_{r0} of the reflected wave in medium 1 can be calculated: $E_{r0} = \Gamma_0 E_{i0}$. In many applications, Γ_0 and E_{r0} are the only quantities of interest; hence this impedance-transformation approach is conceptually simple and yields the desired answers in a direct manner. If the fields E_2^+, E_2^-, and E_t in media 2 and 3 are also desired, they can be determined from the boundary conditions at $z = 0$ and $z = d$, as indicated in Eqs. (8–162) through (8–165).

EXAMPLE 8–12 A dielectric layer of thickness d and intrinsic impedance η_2 is placed between media 1 and 3 having intrinsic impedances η_1 and η_3, respectively. Determine d and η_2 such that no reflection occurs when a uniform plane wave in medium 1 impinges normally on the interface with medium 2.

Solution With the dielectric layer interposed between media 1 and 3 as shown in Fig. 8–15, the condition of no reflection at interface $z = 0$ requires $\Gamma_0 = 0$, or $Z_2(0) = \eta_1$. From Eq. (8–173) we have

$$\eta_2(\eta_3 \cos \beta_2 d + j\eta_2 \sin \beta_2 d) = \eta_1(\eta_2 \cos \beta_2 d + j\eta_3 \sin \beta_2 d). \tag{8–175}$$

Equating the real and imaginary parts separately, we require

$$\eta_3 \cos \beta_2 d = \eta_1 \cos \beta_2 d \tag{8–176}$$

and

$$\eta_2^2 \sin \beta_2 d = \eta_1 \eta_3 \sin \beta_2 d. \tag{8–177}$$

Equation (8–176) is satisfied if *either*

$$\eta_3 = \eta_1 \tag{8–178}$$

or

$$\cos \beta_2 d = 0, \tag{8–179}$$

which implies that

$$\beta_2 d = (2n + 1)\frac{\pi}{2},$$

or

$$d = (2n + 1)\frac{\lambda_2}{4}, \qquad n = 0, 1, 2, \ldots \tag{8-180}$$

On the one hand, if condition (8–178) holds, Eq. (8–177) can be satisfied when either (a) $\eta_2 = \eta_3 = \eta_1$, which is the trivial case of no discontinuities at all, or (b) $\sin \beta_2 d = 0$, or $d = n\lambda_2/2$.

On the other hand, if relation (8–179) or (8–180) holds, $\sin \beta_2 d$ does not vanish, and Eq. (8–177) can be satisfied when $\eta_2 = \sqrt{\eta_1 \eta_3}$. We have then two possibilities for the condition of no reflection.

1. *When $\eta_3 = \eta_1$, we require*

$$d = n\frac{\lambda_2}{2}, \qquad n = 0, 1, 2, \ldots, \tag{8-181}$$

that is, that the thickness of the dielectric layer be a multiple of a half-wavelength in the dielectric at the operating frequency. Such a dielectric layer is referred to as a ***half-wave dielectric window***. Since $\lambda_2 = u_{p2}/f = 1/f\sqrt{\mu_2 \epsilon_2}$, where f is the operating frequency, a half-wave dielectric window is a narrow-band device.

2. *When $\eta_3 \neq \eta_1$, we require*

$$\eta_2 = \sqrt{\eta_1 \eta_3} \tag{8-182a}$$

and

$$d = (2n + 1)\frac{\lambda_2}{4}, \qquad n = 0, 1, 2, \ldots. \tag{8-182b}$$

When media 1 and 3 are different, η_2 should be the geometric mean of η_1 and η_3, and d should be an odd multiple of a quarter wavelength in the dielectric layer at the operating frequency in order to eliminate reflection. Under these conditions the dielectric layer (medium 2) acts like a ***quarter-wave impedance transformer***. We will refer to this term again when we study analogous transmission-line problems in Chapter 9. ■

We see from the above that if a radome is to be constructed around a radar installation ($\eta_1 = \eta_3 = \eta_0$), it should be a half-wave window in order to minimize reflection; that is, it should be a multiple of $\lambda_2/2\,(= 1/2f_2\sqrt{\mu_2 \epsilon_2})$ thick at the operating radar frequency f_2, where μ_2 and ϵ_2 are the permeability and permittivity, respectively, of the radome material.

8–10 Oblique Incidence at a Plane Dielectric Boundary

We now consider the case of a plane wave that is incident obliquely at an arbitrary angle of incidence θ_i on a plane interface between two dielectric media. The media are assumed to be lossless and to have different constitutive parameters (ϵ_1, μ_1) and

(ϵ_2, μ_2), as indicated in Fig. 8–16. Because of the medium's discontinuity at the interface, a part of the incident wave is reflected and a part is transmitted. Lines AO, $O'A'$, and $O'B$ are the intersections of the wavefronts (surfaces of constant phase) of the incident, reflected, and transmitted waves respectively, with the plane of incidence. Since both the incident and the reflected waves propagate in medium 1 with the same phase velocity u_{p1}, the distances $\overline{OA'}$ and $\overline{AO'}$ must be equal. Thus,

$$\overline{OO'} \sin \theta_r = \overline{OO'} \sin \theta_i$$

or

$$\boxed{\theta_r = \theta_i.} \tag{8–183}$$

Equation (8–183) assures us that ***the angle of reflection is equal to the angle of incidence***, which is ***Snell's law of reflection.***

In medium 2 the time it takes for the transmitted wave to travel from O to B equals the time for the incident wave to travel from A to O'. We have

$$\frac{\overline{OB}}{u_{p2}} = \frac{\overline{AO'}}{u_{p1}},$$

$$\frac{\overline{OB}}{\overline{AO'}} = \frac{\overline{OO'} \sin \theta_t}{\overline{OO'} \sin \theta_i} = \frac{u_{p2}}{u_{p1}},$$

from which we obtain

$$\boxed{\frac{\sin \theta_t}{\sin \theta_i} = \frac{u_{p2}}{u_{p1}} = \frac{\beta_1}{\beta_2} = \frac{n_1}{n_2},} \tag{8–184}$$

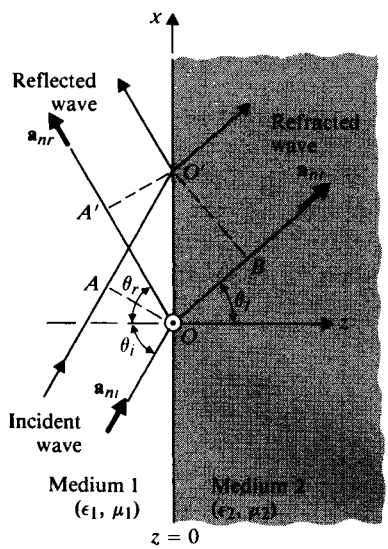

FIGURE 8–16
Uniform plane wave incident obliquely on a plane dielectric boundary.

where n_1 and n_2 are the indices of refraction for media 1 and 2, respectively. The ***index of refraction*** of a medium is the ratio of the speed of light (electromagnetic wave) in free space to that in the medium; that is, $n = c/u_p$. The relation in Eq. (8–184) is known as ***Snell's law of refraction.*** It states that ***at an interface between two dielectric media, the ratio of the sine of the angle of refraction (transmission) in medium 2 to the sine of the angle of incidence in medium 1 is equal to the inverse ratio of indices of refraction n_1/n_2.***

For *nonmagnetic media*, $\mu_1 = \mu_2 = \mu_0$, Eq. (8–184) becomes

$$\boxed{\frac{\sin\theta_t}{\sin\theta_i} = \sqrt{\frac{\epsilon_1}{\epsilon_2}} = \sqrt{\frac{\epsilon_{r1}}{\epsilon_{r2}}} = \frac{n_1}{n_2} = \frac{\eta_2}{\eta_1},} \tag{8–185}$$

where η_1 and η_2 are the intrinsic impedances of the media. Furthermore, if medium 1 is free space such that $\epsilon_{r1} = 1$ and $n_1 = 1$, Eq. (8–185) reduces to

$$\boxed{\frac{\sin\theta_t}{\sin\theta_i} = \frac{1}{\sqrt{\epsilon_{r2}}} = \frac{1}{n_2} = \frac{\eta_2}{120\pi}.} \tag{8–186}$$

Since $n_2 \geq 1$, it is clear that a plane wave incident obliquely at an interface with a denser medium will be bent toward the normal.

We have derived here Snell's law of reflection and Snell's law of refraction from a consideration of the ray paths of the incident, reflected, and refracted waves. No mention has been made of the polarization of the waves. Thus Snell's laws are independent of wave polarization. These laws can also be derived by matching the phases of the various propagating waves at the boundary surface $z = 0$, as we shall see when we take up the cases of perpendicular polarization (Subsection 8–10.2) and parallel polarization (Subsection 8–10.3).

8–10.1 TOTAL REFLECTION

Let us now examine Snell's law in Eq. (8–185) for $\epsilon_1 > \epsilon_2$—that is, when the wave in medium 1 is incident on a less dense medium 2. In that case, $\theta_t > \theta_i$. Since θ_t increases with θ_i, an interesting situation airses when $\theta_t = \pi/2$, at which angle the refracted wave will glaze along the interface; a further increase in θ_i would result in no refracted wave, and the incident wave is then said to be totally reflected. The angle of incidence θ_c (which corresponds to the threshold of ***total reflection*** $\theta_t = \pi/2$) is called the ***critical angle.*** We have, by setting $\theta_t = \pi/2$ in Eq. (8–185),

$$\sin\theta_c = \sqrt{\frac{\epsilon_2}{\epsilon_1}} \tag{8–187}$$

or

$$\boxed{\theta_c = \sin^{-1}\sqrt{\frac{\epsilon_2}{\epsilon_1}} = \sin^{-1}\left(\frac{n_2}{n_1}\right).} \tag{8–188}$$

This situation is illustrated in Fig. 8–17, where $\mathbf{a}_{ni}$, $\mathbf{a}_{nr}$, and $\mathbf{a}_{nt}$ are unit vectors denoting the directions of propagation of the incident, reflected, and transmitted waves, respectively.

What happens mathematically if θ_i is larger than the critical angle θ_c ($\sin\theta_i > \sin\theta_c = \sqrt{\epsilon_2/\epsilon_1}$)? From Eq. (8–185) we have

$$\sin\theta_t = \sqrt{\frac{\epsilon_1}{\epsilon_2}}\sin\theta_i > 1, \tag{8–189}$$

which does not yield a real solution for θ_t. Although $\sin\theta_t$ in Eq. (8–189) is still real, $\cos\theta_t$ becomes imaginary when $\sin\theta_t > 1$:

$$\cos\theta_t = \sqrt{1-\sin^2\theta_t} = \pm j\sqrt{\frac{\epsilon_1}{\epsilon_2}\sin^2\theta_i - 1}. \tag{8–190}$$

In medium 2 the unit vector $\mathbf{a}_{nt}$ in the direction of propagation of a typical transmitted (refracted) wave, as shown in Fig. 8–16, is

$$\mathbf{a}_{nt} = \mathbf{a}_x\sin\theta_t + \mathbf{a}_z\cos\theta_t. \tag{8–191}$$

Both $\mathbf{E}_t$ and $\mathbf{H}_t$ vary spatially in accordance with the following factor:

$$e^{-j\beta_2\mathbf{a}_{nt}\cdot\mathbf{R}} = e^{-j\beta_2(x\sin\theta_t + z\cos\theta_t)},$$

which, when Eqs. (8–189) and (8–190) for $\theta_i > \theta_c$ are used, becomes

$$e^{-\alpha_2 z}e^{-j\beta_{2x}x}, \tag{8–192}$$

where

$$\alpha_2 = \beta_2\sqrt{(\epsilon_1/\epsilon_2)\sin^2\theta_i - 1}$$

and

$$\beta_{2x} = \beta_2\sqrt{\epsilon_1/\epsilon_2}\sin\theta_i.$$

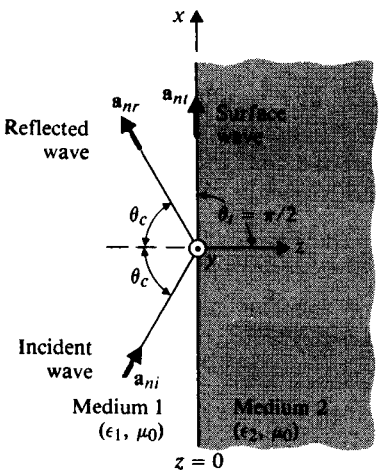

FIGURE 8–17
Plane wave incident at critical angle, $\epsilon_1 > \epsilon_2$.

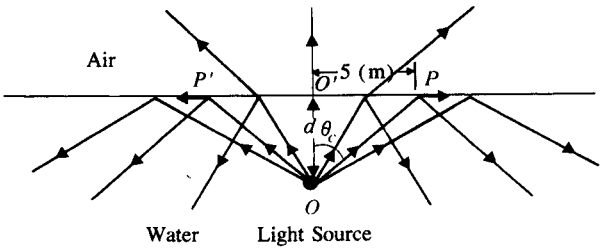

FIGURE 8–18
An underwater light source (Example 8–13).

The upper sign in Eq. (8–190) has been abandoned because it would lead to the impossible result of an increasing field as z increases. We can conclude from (8–192) that for $\theta_i > \theta_c$ an ***evanescent wave*** exists *along* the interface (in the x-direction), which is attenuated exponentially (rapidly) in medium 2 in the normal direction (z-direction). This wave is tightly bound to the interface and is called a ***surface wave***. It is illustrated in Fig. 8–17. Obviously, it is a nonuniform plane wave. No power is transmitted into medium 2 under these conditions. (See Problem P.8–37.)

EXAMPLE 8–13 The permittivity of water at optical frequencies is $1.75\epsilon_0$. It is found that an isotropic light source at a distance d under water yields an illuminated circular area of a radius 5 (m). Determine d.

Solution The index of refraction of water is $n_w = \sqrt{1.75} = 1.32$. Refer to Fig. 8–18. The radius of illuminated area, $O'P = 5$ (m), corresponds to the critical angle

$$\theta_c = \sin^{-1}\left(\frac{1}{n_w}\right) = \sin^{-1}\left(\frac{1}{1.32}\right) = 49.2°.$$

Hence,

$$d = \frac{\overline{O'P}}{\tan\theta_c} = \frac{5}{\tan 49.2°} = 4.32 \quad \text{(m)}.$$

As illustrated in Fig. 8–18, an incident ray with $\theta_i = \theta_c$ at P results in a reflected ray and a tangential refracted ray. Incident waves for $\theta_i < \theta_c$ are partially reflected back into the water and partially refracted into the air above, and those for $\theta_i > \theta_c$ are totally reflected (the evanescent surface waves are not shown).

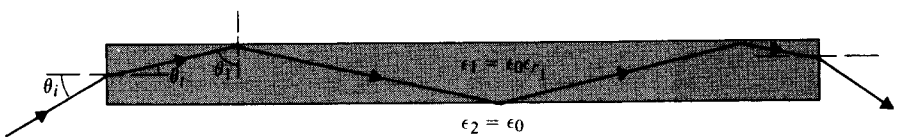

FIGURE 8–19
Dielectric rod or fiber guiding electromagnetic wave by total internal reflection.

EXAMPLE 8–14 A dielectric rod or fiber of a transparent material can be used to guide light or an electromagnetic wave under the conditions of total internal reflection. Determine the minimum dielectric constant of the guiding medium so that a wave incident on one end at any angle will be confined within the rod until it emerges from the other end.

Solution Refer to Fig. 8–19. For total internal reflection, θ_1 must be greater than or equal to θ_c for the guiding dielectric medium; that is,

$$\sin \theta_1 \geq \sin \theta_c$$

or, since $\theta_1 = \pi/2 - \theta_t$,

$$\cos \theta_t \geq \sin \theta_c. \tag{8–193}$$

From Snell's law of refraction, Eq. (8–186), we have

$$\sin \theta_t = \frac{1}{\sqrt{\epsilon_{r1}}} \sin \theta_i. \tag{8–194}$$

It is important to note here that the dielectric medium has been designated as medium 1 (the denser medium) in order to be consistent with the notation of this subsection. Combining Eqs. (8–193), (8–194), and (8–187), we obtain

$$\sqrt{1 - \frac{1}{\epsilon_{r1}} \sin^2 \theta_i} \geq \sqrt{\frac{\epsilon_0}{\epsilon_1}} = \frac{1}{\sqrt{\epsilon_{r1}}},$$

which requires

$$\epsilon_{r1} \geq 1 + \sin^2 \theta_i. \tag{8–195}$$

Since the largest value of the right side of (8–195) is reached when $\theta_i = \pi/2$, we require the dielectric constant of the guiding medium to be at least 2, which corresponds to an index of refraction $n_1 = \sqrt{2}$. This requirement is satisfied by glass and quartz.

We observe that Snell's law of refraction in Eq. (8–185) and the critical angle for total reflection in Eq. (8–188) are independent of the polarization of the incident electric field. The formulas for the reflection and transmission coefficients, however, are polarization-dependent. In the following two subsections we discuss perpendicular polarization and parallel polarization separately.

8–10.2 PERPENDICULAR POLARIZATION

For oblique incidence with perpendicular polarization we refer to Fig. 8–20. The incident electric and magnetic field intensity phasors in medium 1 are, from Eqs. (8–107) and (8–108),

$$\mathbf{E}_i(x, z) = \mathbf{a}_y E_{i0} e^{-j\beta_1(x \sin \theta_i + z \cos \theta_i)} \tag{8–196}$$

$$\mathbf{H}_i(x, z) = \frac{E_{i0}}{\eta_1} (-\mathbf{a}_x \cos \theta_i + \mathbf{a}_z \sin \theta_i) e^{-j\beta_1(x \sin \theta_i + z \cos \theta_i)}. \tag{8–197}$$

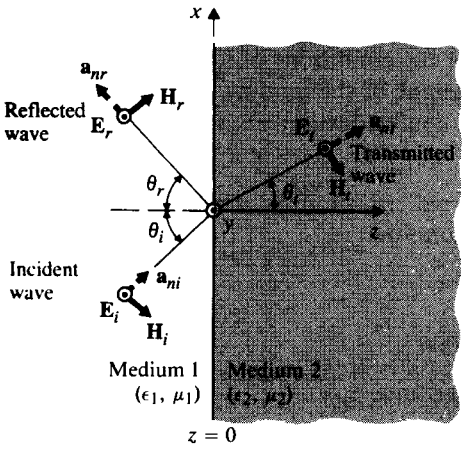

FIGURE 8–20
Plane wave incident on a plane dielectric boundary (perpendicular polarization).

The reflected electric and magnetic fields can be obtained from Eqs. (8–110) and (8–112), but remember that E_{r0} is no longer equal to $-E_{i0}$:

$$\mathbf{E}_r(x, z) = \mathbf{a}_y E_{r0} e^{-j\beta_1(x \sin\theta_r - z\cos\theta_r)} \tag{8–198}$$

$$\mathbf{H}_r(x, z) = \frac{E_{r0}}{\eta_1}(\mathbf{a}_x \cos\theta_r + \mathbf{a}_z \sin\theta_r) e^{-j\beta_1(x\sin\theta_r - z\cos\theta_r)}. \tag{8–199}$$

In medium 2 the transmitted electric and magnetic field intensity phasors can be similarly written as

$$\mathbf{E}_t(x, z) = \mathbf{a}_y E_{t0} e^{-j\beta_2(x\sin\theta_t + z\cos\theta_t)} \tag{8–200}$$

$$\mathbf{H}_t(x, z) = \frac{E_{t0}}{\eta_2}(-\mathbf{a}_x \cos\theta_t + \mathbf{a}_z \sin\theta_t) e^{-j\beta_2(x\sin\theta_t + z\cos\theta_t)}. \tag{8–201}$$

There are four unknown quantities in Eqs. (8–196) through (8–201), namely, E_{r0}, E_{t0}, θ_r, and θ_t. Their determination follows from the requirements that the tangential components of **E** and **H** be continuous at the boundary $z = 0$. From $E_{iy}(x, 0) + E_{ry}(x, 0) = E_{ty}(x, 0)$ we have

$$E_{i0} e^{-j\beta_1 x\sin\theta_i} + E_{r0} e^{-j\beta_1 x\sin\theta_r} = E_{t0} e^{-j\beta_2 x\sin\theta_t}. \tag{8–202}$$

Similarly, from $H_{ix}(x, 0) + H_{rx}(x, 0) = H_{tx}(x, 0)$ we require

$$\frac{1}{\eta_1}(-E_{i0}\cos\theta_i e^{-j\beta_1 x\sin\theta_i} + E_{r0}\cos\theta_r e^{-j\beta_1 x\sin\theta_r}) = -\frac{E_{t0}}{\eta_2}\cos\theta_t e^{-j\beta_2 x\sin\theta_t}. \tag{8–203}$$

Because Eqs. (8–202) and (8–203) are to be satisfied *for all* x, all three exponential factors that are functions of x must be equal ("phase-matching"). Thus,

$$\beta_1 x\sin\theta_i = \beta_1 x\sin\theta_r = \beta_2 x\sin\theta_t,$$

which leads to Snell's law of reflection ($\theta_r = \theta_i$) and Snell's law of refraction ($\sin \theta_t / \sin \theta_i = \beta_1/\beta_2 = n_1/n_2$). Equations (8–202) and (8–203) can now be written simply as

$$E_{i0} + E_{r0} = E_{t0} \tag{8–204}$$

and

$$\frac{1}{\eta_1}(E_{i0} - E_{r0}) \cos \theta_i = \frac{E_{t0}}{\eta_2} \cos \theta_t, \tag{8–205}$$

from which E_{r0} and E_{t0} can be found in terms of E_{i0}. We have

$$\begin{aligned} \Gamma_\perp = \frac{E_{r0}}{E_{i0}} &= \frac{\eta_2 \cos \theta_i - \eta_1 \cos \theta_t}{\eta_2 \cos \theta_i + \eta_1 \cos \theta_t} \\ &= \frac{(\eta_2/\cos \theta_t) - (\eta_1/\cos \theta_i)}{(\eta_2/\cos \theta_t) + (\eta_1/\cos \theta_i)} \end{aligned} \tag{8–206}^\dagger$$

and

$$\begin{aligned} \tau_\perp = \frac{E_{t0}}{E_{i0}} &= \frac{2\eta_2 \cos \theta_i}{\eta_2 \cos \theta_i + \eta_1 \cos \theta_t} \\ &= \frac{2(\eta_2/\cos \theta_t)}{(\eta_2/\cos \theta_t) + (\eta_1/\cos \theta_i)}. \end{aligned} \tag{8–207}^\dagger$$

Comparing these expressions with the formulas for the reflection and transmission coefficients at normal incidence, Eqs. (8–140) and (8–141), we see that the same formulas apply if η_1 and η_2 are changed to $(\eta_1/\cos \theta_i)$ and $(\eta_2/\cos \theta_t)$, respectively. When $\theta_i = 0$, making $\theta_r = \theta_t = 0$, these expressions reduce to those for normal incidence, as they should. Furthermore, $\Gamma_\perp$ and $\tau_\perp$ are related in the following way:

$$\boxed{1 + \Gamma_\perp = \tau_\perp,} \tag{8–208}$$

which is similar to Eq. (8–142) for normal incidence.

If medium 2 is a perfect conductor, $\eta_2 = 0$. We have $\Gamma_\perp = -1$ ($E_{r0} = -E_{i0}$) and $\tau_\perp = 0$ ($E_{t0} = 0$). The tangential **E** field on the surface of the conductor vanishes, and no energy is transmitted across a perfectly conducting boundary, as we have noted in Sections 8–6 and 8–7.

Noting that the numerator for the reflection coefficient in Eq. (8–206) is in the form of a difference of two terms, we inquire whether there is a combination of η_1, η_2, and θ_i, which makes $\Gamma_\perp = 0$ for no reflection. Denoting this particular θ_i by $\theta_{B\perp}$, we require

$$\eta_2 \cos \theta_{B\perp} = \eta_1 \cos \theta_t. \tag{8–209}$$

Using Snell's law of refraction, we have

$$\cos \theta_t = \sqrt{1 - \sin^2 \theta_t} = \sqrt{1 - \frac{n_1^2}{n_2^2} \sin^2 \theta_i} \tag{8–210}$$

---

† These are sometimes referred to as ***Fresnel's equations***.

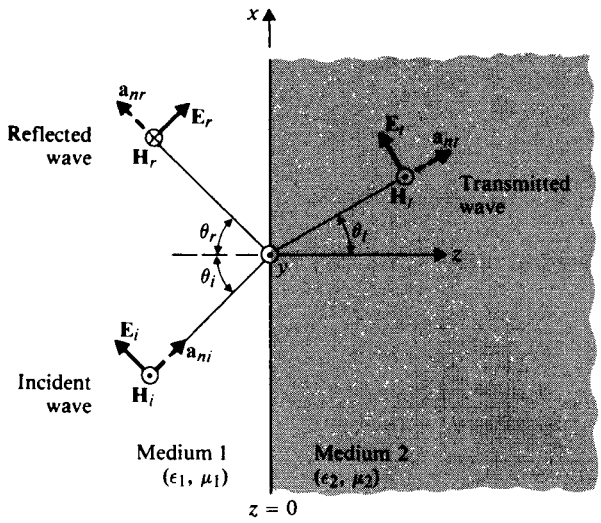

FIGURE 8–21
Plane wave incident obliquely on a plane dielectric boundary (parallel polarization).

and obtain from Eq. (8–209)

$$\sin^2 \theta_{B\perp} = \frac{1 - \mu_1\epsilon_2/\mu_2\epsilon_1}{1 - (\mu_1/\mu_2)^2}. \tag{8–211}$$

The angle $\theta_{B\perp}$ is called the ***Brewster angle*** of no reflection for the case of perpendicular polarization. For *nonmagnetic media*, $\mu_1 = \mu_2 = \mu_0$, the right side of Eq. (8–211) becomes infinite, and $\theta_{B\perp}$ *does not exist*. In the case of $\epsilon_1 = \epsilon_2$ and $\mu_1 \neq \mu_2$, Eq. (8–211) reduces to

$$\sin \theta_{B\perp} = \frac{1}{\sqrt{1 + (\mu_1/\mu_2)}}, \tag{8–212}$$

which does have a solution whether μ_1/μ_2 is greater or less than unity. However, it is a very rare situation in electromagnetics that two contiguous media have the same permittivity but different permeabilities.

8–10.3 PARALLEL POLARIZATION

When a uniform plane wave with parallel polarization is incident obliquely on a plane boundary, as illustrated in Fig. 8–21, the incident and reflected electric and magnetic field intensity phasors in medium 1 are, from Eqs. (8–124) through (8–127):

$$\mathbf{E}_i(x, z) = E_{i0}(\mathbf{a}_x \cos \theta_i - \mathbf{a}_z \sin \theta_i)e^{-j\beta_1(x \sin \theta_i + z \cos \theta_i)} \tag{8–213}$$

$$\mathbf{H}_i(x, z) = \mathbf{a}_y \frac{E_{i0}}{\eta_1} e^{-j\beta_1(x \sin \theta_i + z \cos \theta_i)} \tag{8–214}$$

$$\mathbf{E}_r(x, z) = E_{r0}(\mathbf{a}_x \cos\theta_r + \mathbf{a}_z \sin\theta_r)e^{-j\beta_1(x\sin\theta_r - z\cos\theta_r)}, \tag{8–215}$$

$$\mathbf{H}_r(x, z) = -\mathbf{a}_y \frac{E_{r0}}{\eta_1} e^{-j\beta_1(x\sin\theta_r - z\cos\theta_r)}. \tag{8–216}$$

The transmitted electric and magnetic field intensity phasors in medium 2 are

$$\mathbf{E}_t(x, z) = E_{t0}(\mathbf{a}_x \cos\theta_t - \mathbf{a}_z \sin\theta_t)e^{-j\beta_2(x\sin\theta_t + z\cos\theta_t)}, \tag{8–217}$$

$$\mathbf{H}_t(x, z) = \mathbf{a}_y \frac{E_{t0}}{\eta_2} e^{-j\beta_2(x\sin\theta_t + z\cos\theta_t)}. \tag{8–218}$$

Continuity requirements for the tangential components of $\mathbf{E}$ and $\mathbf{H}$ at $z = 0$ lead again to Snell's laws of reflection and refraction, as well as to the following two equations:

$$(E_{i0} + E_{r0})\cos\theta_i = E_{t0}\cos\theta_t, \tag{8–219}$$

$$\frac{1}{\eta_1}(E_{i0} - E_{r0}) = \frac{1}{\eta_2} E_{t0}. \tag{8–220}$$

Solving for E_{r0} and E_{t0} in terms of E_{i0}, we obtain

$$\Gamma_{||} = \frac{E_{r0}}{E_{i0}} = \frac{\eta_2\cos\theta_t - \eta_1\cos\theta_i}{\eta_2\cos\theta_t + \eta_1\cos\theta_i} \tag{8–221}^{\dagger}$$

and

$$\tau_{||} = \frac{E_{t0}}{E_{i0}} = \frac{2\eta_2\cos\theta_i}{\eta_2\cos\theta_t + \eta_1\cos\theta_i}. \tag{8–222}^{\dagger}$$

It is easy to verify that

$$\boxed{1 + \Gamma_{||} = \tau_{||}\left(\frac{\cos\theta_t}{\cos\theta_i}\right).} \tag{8–223}$$

Equation (8–223) is seen to be different from Eq. (8–208) for perpendicular polarization except when $\theta_i = \theta_t = 0$, which is the case for normal incidence. At normal incidence, $\Gamma_{||}$ and $\tau_{||}$ reduce to Γ and τ given in Eqs. (8–140) and (8–141), respectively, as did $\Gamma_\perp$ and $\tau_\perp$.

If medium 2 is a perfect conductor ($\eta_2 = 0$), Eqs. (8–221) and (8–222) simplify to $\Gamma_{||} = -1$ and $\tau_{||} = 0$, respectively, making the tangential component of the total $\mathbf{E}$ field on the surface of the conductor vanish, as expected. We note here that the choices of the reference directions of $\mathbf{E}_r$ and $\mathbf{H}_r$ in Figs. 8–11, 8–13, 8–20, and 8–21 are all arbitrary. The actual directions of $\mathbf{E}_r$ and $\mathbf{H}_r$ in Figs. 8–11 and 8–13 are opposite to those chosen because $E_{r0} = -E_{i0}$. In Figs. 8–20 and 8–21 the actual directions of $\mathbf{E}_r$ and $\mathbf{H}_r$ may or may not be the same as those shown, depending on whether $\Gamma_\perp$ in Eq. (8–206) and $\Gamma_{||}$ in Eq. (8–221) is positive or negative, respectively.

If we plot $|\Gamma_\perp|^2$ and $|\Gamma_{||}|^2$ versus θ_i, we will find the former always greater than

---

† These are also referred to as ***Fresnel's equations.***

the latter except for $\theta_i = 0$. This means that when an unpolarized wave strikes a plane dielectric interface, the reflected wave will contain more power in the component with perpendicular polarization than that with parallel polarization. A popular application of this fact is the design of Polaroid sunglasses to reduce sun glare. Much of the sunlight received by the eye has been reflected from horizontal surfaces on earth. Because $|\Gamma_\perp|^2 > |\Gamma_{||}|^2$, the light reaching the eye is predominantly perpendicular to the plane of reflection (same as the plane of incidence), and hence the electric field is parallel to the earth's surface. Polaroid sunglasses are designed to filter out this component.

From Eq. (8–221) we find that $\Gamma_{||}$ goes to zero when the angle of incidence θ_i equals $\theta_{B||}$, such that

$$\eta_2 \cos \theta_t = \eta_1 \cos \theta_{B||}, \tag{8–224}$$

which, together with Eq. (8–210), requires that

$$\boxed{\sin^2 \theta_{B||} = \frac{1 - \mu_2\epsilon_1/\mu_1\epsilon_2}{1 - (\epsilon_1/\epsilon_2)^2}.} \quad (\mu_1 = \mu_2) \tag{8–225}$$

The angle $\theta_{B||}$ is known as the ***Brewster angle*** of no reflection for the case of parallel polarization. A solution for Eq. (8–225) always exists for two contiguous nonmagnetic media. Thus if $\mu_1 = \mu_2$, a reflection-free condition is obtained when the angle of incidence in medium 1 equals the Brewster angle $\theta_{B||}$, such that

$$\boxed{\sin \theta_{B||} = \frac{1}{\sqrt{1 + (\epsilon_1/\epsilon_2)}}.} \quad (\mu_1 = \mu_2) \tag{8–226}$$

An alternative form for Eq. (8–226) is

$$\boxed{\theta_{B||} = \tan^{-1} \sqrt{\frac{\epsilon_2}{\epsilon_1}} = \tan^{-1}\left(\frac{n_2}{n_1}\right).} \quad (\mu_1 = \mu_2) \tag{8–227}$$

Because of the difference in the formulas for Brewster angles for perpendicular and parallel polarizations, it is possible to separate these two types of polarization in an unpolarized wave. When an unpolarized wave such as random light is incident upon a boundary at the Brewster angle $\theta_{B||}$ given by Eq. (8–225), only the component with perpendicular polarization will be reflected. Thus a Brewster angle is also referred to as a ***polarizing angle***. Based on this principle, quartz windows set at the Brewster angle at the ends of a laser tube are used to control the polarization of an emitted light beam.

EXAMPLE 8–15 The dielectric constant of pure water is 80. (a) Determine the Brewster angle for parallel polarization, $\theta_{B||}$, and the corresponding angle of trans-

mission. (b) A plane wave with perpendicular polarization is incident from air on water surface at $\theta_i = \theta_{B\|}$. Find the reflection and transmission coefficients.

Solution

a) The Brewster angle of no reflection for parallel polarization can be obtained directly from Eq. (8–226):

$$\theta_{B\|} = \sin^{-1} \frac{1}{\sqrt{1 + (1/\epsilon_{r2})}}$$

$$= \sin^{-1} \frac{1}{\sqrt{1 + (1/80)}} = 81.0°.$$

The corresponding angle of transmission is, from Eq. (8–186),

$$\theta_t = \sin^{-1} \left(\frac{\sin \theta_{B\|}}{\sqrt{\epsilon_{r2}}} \right) = \sin^{-1} \left(\frac{1}{\sqrt{\epsilon_{r2} + 1}} \right)$$

$$= \sin^{-1} \left(\frac{1}{\sqrt{81}} \right) = 6.38°.$$

b) For an incident wave with perpendicular polarization, we use Eqs. (8–206) and (8–207) to find $\Gamma_\perp$ and $\tau_\perp$ at $\theta_i = 81.0°$ and $\theta_t = 6.38°$:

$$\eta_1 = 377 \quad (\Omega), \qquad \eta_1/\cos \theta_i = 2410 \quad (\Omega),$$

$$\eta_2 = \frac{377}{\sqrt{\epsilon_{r2}}} = 40.1 \quad (\Omega), \qquad \eta_2/\cos \theta_t = 40.4 \quad (\Omega).$$

Thus,

$$\Gamma_\perp = \frac{40.4 - 2410}{40.4 + 2410} = -0.967,$$

$$\tau_\perp = \frac{2 \times 40.4}{40.4 + 2410} = 0.033.$$

We note that the relation between $\Gamma_\perp$ and $\tau_\perp$ given in Eq. (8–208) is satisfied. ■

Review Questions

R.8–1 Define *uniform plane wave.*

R.8–2 What is a *wavefront*?

R.8–3 Write the homogeneous vector Helmholtz's equation for **E** in free space.

R.8–4 Define *wavenumber.* How is wavenumber related to wavelength?

R.8–5 Define *phase velocity.*

R.8–6 Define *intrinsic impedance* of a medium. What is the value of the intrinsic impedance of free space?

R.8–7 What is *Doppler effect*?

R.8–8 What is a TEM wave?

R.8–9 Write the phasor expressions for the electric and magnetic field intensity vectors of an x-polarized uniform plane wave propagating in the $+z$-direction.

R.8–10 What is meant by the *polarization* of a wave? When is a wave linearly polarized? Circularly polarized?

R.8–11 Two orthogonal linearly polarized waves are combined. State the conditions under which the resultant will be (a) another linearly polarized wave, (b) a circularly polarized wave, and (c) an elliptically polarized wave.

R.8–12 How is the E-field from AM broadcast stations polarized? From television stations? From FM broadcast stations?

R.8–13 Define (a) *propagation constant*, (b) *attenuation constant*, and (c) *phase constant*.

R.8–14 What is meant by the *skin depth* of a conductor? How is it related to the attenuation constant? How does it depend on σ? On f?

R.8–15 What is the constitution of the ionosphere?

R.8–16 What is a *plasma*?

R.8–17 What is the significance of *plasma frequency*?

R.8–18 When does the equivalent permittivity of the ionosphere become negative? What is the significance of a negative permittivity in terms of wave propagation?

R.8–19 What is meant by the *dispersion* of a signal? Give an example of a dispersive medium.

R.8–20 Define *group velocity*. In what ways is group velocity different from phase velocity?

R.8–21 Define *Poynting vector*. What is the SI unit for this vector?

R.8–22 State Poynting's theorem.

R.8–23 For a time-harmonic electromagnetic field, write the expressions in terms of electric and magnetic field intensity vectors for (a) instantaneous Poynting vector, and (b) time-average Poynting vector.

R.8–24 What is a *standing wave*?

R.8–25 What do we know about the magnitude of the tangential components of **E** and **H** at the interface when a wave impinges normally on a perfectly conducting plane boundary?

R.8–26 Define *plane of incidence*.

R.8–27 What do we mean when we say that an incident wave has (a) perpendicular polarization, and (b) parallel polarization?

R.8–28 Define *reflection coefficient* and *transmission coefficient*. What is the relationship between them?

R.8–29 Under what conditions will reflection and transmission coefficients be real?

R.8–30 What are the values of the reflection and transmission coefficients at an interface with a perfectly conducting boundary?

R.8–31 A plane wave originating in medium 1 (ϵ_1, $\mu_1 = \mu_0$, $\sigma_1 = 0$) is incident normally on a plane interface with medium 2 ($\epsilon_2 \neq \epsilon_1$, $\mu_2 = \mu_0$, $\sigma_2 = 0$). Under what condition will the electric field at the interface be a maximum? A minimum?

R.8–32 Define *standing-wave ratio*. What is its relationship with reflection coefficient?

R.8–33 What is meant by the wave impedance of the total field. When is this impedance equal to the intrinsic impedance of the medium?

R.8–34 A thin dielectric coating is sprayed on optical instruments to reduce glare. What factors determine the thickness of the coating?

R.8–35 How should the thickness of the radome in a radar installation be chosen?

R.8–36 State *Snell's law of reflection.*

R.8–37 State *Snell's law of refraction.*

R.8–38 Define *critical angle.* When does it exist at an interface of two nonmagnetic media?

R.8–39 Define *Brewster angle.* When does it exist at an interface of two nonmagnetic media?

R.8–40 Why is a Brewster angle also called a *polarizing angle*?

R.8–41 Under what conditions will the reflection and transmission coefficients for perpendicular polarization be the same as those for parallel polarization?

Problems

P.8–1 Obtain the wave equations governing the **E** and **H** fields in a source-free conducting medium with constitutive parameters ϵ, μ, and σ.

P.8–2 Prove that the electric field intensity in Eq. (8–22) satisfies the homogeneous Helmholtz's equation provided that the condition in Eq. (8–23) is satisfied.

P.8–3 A Doppler radar is used to determine the speed of a moving vehicle by measuring the frequency shift of the wave reflected from the vehicle.

a) Assuming that the reflecting surface of the vehicle can be represented by a perfectly conducting plane and that the transmitted signal is a time-harmonic uniform plane wave of a frequency f incident normally on the reflecting surface, find the relation between the frequency shift Δf and the speed u of the vehicle.

b) Determine u both in (km/hr) and in (miles/hr) if $\Delta f = 2.33$ (kHz) with $f = 10.5$ (GHz).

P.8–4 For a harmonic uniform plane wave propagating in a simple medium, both **E** and **H** vary in accordance with the factor $\exp(-j\mathbf{k}\cdot\mathbf{R})$ as indicated in Eq. (8–26). Show that the four Maxwell's equations for uniform plane wave in a source-free region reduce to the following:

$$\mathbf{k}\times\mathbf{E} = \omega\mu\mathbf{H},$$
$$\mathbf{k}\times\mathbf{H} = -\omega\epsilon\mathbf{E},$$
$$\mathbf{k}\cdot\mathbf{E} = 0,$$
$$\mathbf{k}\cdot\mathbf{H} = 0.$$

P.8–5 The instantaneous expression for the magnetic field intensity of a uniform plane wave propagating in the $+y$ direction in air is given by

$$\mathbf{H} = \mathbf{a}_z 4\times 10^{-6}\cos\left(10^7\pi t - k_0 y + \frac{\pi}{4}\right) \quad \text{(A/m)}.$$

a) Determine k_0 and the location where H_z vanishes at $t = 3$ (ms).

b) Write the instantaneous expression for **E**.

P.8–6 The E-field of a uniform plane wave propagating in a dielectric medium is given by

$$E(t, z) = \mathbf{a}_x 2\cos(10^8 t - z/\sqrt{3}) - \mathbf{a}_y \sin(10^8 t - z/\sqrt{3}) \quad \text{(V/m)}.$$

a) Determine the frequency and wavelength of the wave.
b) What is the dielectric constant of the medium?
c) Describe the polarization of the wave.
d) Find the corresponding H-field.

P.8–7 Show that a plane wave with an instantaneous expression for the electric field

$$\mathbf{E}(z, t) = \mathbf{a}_x E_{10} \sin(\omega t - kz) + \mathbf{a}_y E_{20} \sin(\omega t - kz + \psi)$$

is elliptically polarized. Find the polarization ellipse.

P.8–8 Prove the following:
a) An elliptically polarized plane wave can be resolved into right-hand and left-hand circularly polarized waves.
b) A circularly polarized plane wave can be obtained from a superposition of two oppositely directed elliptically polarized waves.

P.8–9 Derive the following general expressions of the attenuation and phase constants for conducting media:

$$\alpha = \omega \sqrt{\frac{\mu\epsilon}{2}} \left[\sqrt{1 + \left(\frac{\sigma}{\omega\epsilon}\right)^2} - 1 \right]^{1/2} \quad \text{(Np/m)}.$$

$$\beta = \omega \sqrt{\frac{\mu\epsilon}{2}} \left[\sqrt{1 + \left(\frac{\sigma}{\omega\epsilon}\right)^2} + 1 \right]^{1/2} \quad \text{(rad/m)}.$$

P.8–10 Determine and compare the intrinsic impedance, attentuation constant (in both Np/m and dB/m), and skin depth of copper [$\sigma_{cu} = 5.80 \times 10^7$ (S/m)], silver [$\sigma_{ag} = 6.15 \times 10^7$ (S/m)], and brass [$\sigma_{br} = 1.59 \times 10^7$ (S/m)] at the following frequencies: (a) 60 (Hz), (b) 1 (MHz), and (c) 1 (GHz).

P.8–11 A 3 (GHz), y-polarized uniform plane wave propagates in the $+x$-direction in a nonmagnetic medium having a dielectric constant 2.5 and a loss tangent 10^{-2}.
a) Determine the distance over which the amplitude of the propagating wave will be cut in half.
b) Determine the intrinsic impedance, the wavelength, the phase velocity, and the group velocity of the wave in the medium.
c) Assuming $\mathbf{E} = \mathbf{a}_y 50 \sin(6\pi 10^9 t + \pi/3)$(V/m) at $x = 0$, write the instantaneous expression for $\mathbf{H}$ for all t and x.

P.8–12 The magnetic field intensity of a linearly polarized uniform plane wave propagating in the $+y$-direction in seawater [$\epsilon_r = 80$, $\mu_r = 1$, $\sigma = 4$ (S/m)] is

$$\mathbf{H} = \mathbf{a}_x 0.1 \sin(10^{10}\pi t - \pi/3) \quad \text{(A/m)}$$

at $y = 0$.
a) Determine the attenuation constant, the phase constant, the intrinsic impedance, the phase velocity, the wavelength, and the skin depth.
b) Find the location at which the amplitude of $\mathbf{H}$ is 0.01 (A/m).
c) Write the expressions for $\mathbf{E}(y, t)$ and $\mathbf{H}(y, t)$ at $y = 0.5$ (m) as functions of t.

P.8–13 Given that the skin depth for graphite at 100 (MHz) is 0.16 (mm), determine (a) the conductivity of graphite, and (b) the distance that a 1 (GHz) wave travels in graphite such that its field intensity is reduced by 30 (dB).

P.8–14 Assume the ionosphere to be modeled by a plasma region with an electron density that increases with altitude from a low value at the lower boundary toward a value N_{max}

and decreases again as the altitude gets higher. A plane electromagnetic wave impinges on the lower boundary at an angle θ_i with the normal. Determine the highest frequency of the wave that will be turned back toward the earth. (*Hint:* Imagine the ionosphere to be stratified into layers of successively decreasing constant permittivities until the layer containing N_{max}. The frequency to be determined corresponds to that for an emerging angle of $\pi/2$.)

P.8–15 Prove the following relations between group velocity u_g and phase velocity u_p in a dispersive medium:

a) $u_g = u_p + \beta \dfrac{du_p}{d\beta}$ **b)** $u_g = u_p - \lambda \dfrac{du_p}{d\lambda}$.

P.8–16 There is a continuing discussion on radiation hazards to human health. The following calculations will provide a rough comparison.

a) The U.S. standard for personal safety in a microwave environment is that the power density be less than 10 (mW/cm^2). Calculate the corresponding standard in terms of electric field intensity. In terms of magnetic field intensity.

b) It is estimated that the earth receives radiant energy from the sun at a rate of about 1.3 (kW/m^2) on a sunny day. Assuming a monochromatic plane wave (which it is not), calculate the equivalent amplitudes of the electric and magnetic field intensity vectors.

P.8–17 Show that the instantaneous Poynting vector of a circularly polarized plane wave propagating in a lossless medium is a constant that is independent of time and distance.

P.8–18 Assuming that the radiation electric field intensity of an antenna system is

$$\mathbf{E} = \mathbf{a}_\theta E_\theta + \mathbf{a}_\phi E_\phi,$$

find the expression for the average outward power flow per unit area.

P.8–19 From the point of view of electromagnetics, the power transmitted by a lossless coaxial cable can be considered in terms of the Poynting vector inside the dielectric medium between the inner conductor and the outer sheath. Assuming that a d-c voltage V_0 applied between the inner conductor (of radius a) and the outer sheath (of inner radius b) causes a current I to flow to a load resistance, verify that the integration of the Poynting vector over the cross-sectional area of the dielectric medium equals the power $V_0 I$ that is transmitted to the load.

P.8–20 A uniform plane electromagnetic wave propagates in the $+z$- (downward) direction and impinges normally at $z = 0$ on an ocean surface. Let the magnetic field at $z = 0$ be $\mathbf{H}(0, t) = \mathbf{a}_y H_0 \cos 10^4 t$ (A/m).

a) Determine the skin depth. (For the ocean: Conductivity = σ, permeability = μ_0.)

b) Find the expressions for $\mathbf{H}(z, t)$ and $\mathbf{E}(z, t)$.

c) Find the power loss per unit area (in terms of H_0) into the ocean.

P.8–21 A right-hand circularly polarized plane wave represented by the phasor

$$\mathbf{E}(z) = E_0(\mathbf{a}_x - j\mathbf{a}_y)e^{-j\beta z}$$

impinges normally on a perfectly conducting wall at $z = 0$.

a) Determine the polarization of the reflected wave.

b) Find the induced current on the conducting wall.

c) Obtain the instantaneous expression of the total electric intensity based on a cosine time reference.

P.8–22 A uniform sinusoidal plane wave in air with the following phasor expression for electric intensity

$$\mathbf{E}_i(x, z) = \mathbf{a}_y 10e^{-j(6x+8z)} \qquad \text{(V/m)}$$

is incident on a perfectly conducting plane at $z = 0$.

a) Find the frequency and wavelength of the wave.
b) Write the instantaneous expressions for $\mathbf{E}_i(x, z; t)$ and $\mathbf{H}_i(x, z; t)$, using a cosine reference.
c) Determine the angle of incidence.
d) Find $\mathbf{E}_r(x, z)$ and $\mathbf{H}_r(x, z)$ of the reflected wave.
e) Find $\mathbf{E}_1(x, z)$ and $\mathbf{H}_1(x, z)$ of the total field.

P.8–23 Repeat Problem P.8–22 for $\mathbf{E}_i(y, z) = 5(\mathbf{a}_y + \mathbf{a}_z\sqrt{3})e^{j6(\sqrt{3}y-z)}$ (V/m).

P.8–24 For the case of oblique incidence of a uniform plane wave with perpendicular polarization on a perfectly conducting plane boundary as shown in Fig. 8–11, write (a) the instantaneous expressions

$$\mathbf{E}_1(x, z; t) \qquad \text{and} \qquad \mathbf{H}_1(x, z; t)$$

for the total field in medium 1, using a cosine reference, and (b) the time-average Poynting vector.

P.8–25 For the case of oblique incidence of a uniform plane wave with parallel polarization on a perfectly conducting plane boundary as shown in Fig. 8–13, write (a) the instantaneous expressions

$$\mathbf{E}_1(x, z; t) \qquad \text{and} \qquad \mathbf{H}_1(x, z; t)$$

for the total field in medium 1, using a sine reference, and (b) the time-average Poynting vector.

P.8–26 Determine the condition under which the magnitude of the reflection coefficient equals that of the transmission coefficient for a uniform plane wave at normal incidence on an interface between two lossless dielectric media. What is the standing-wave ratio in dB under this condition?

P.8–27 A uniform plane wave in air with $\mathbf{E}_i(z) = \mathbf{a}_x 10e^{-j6z}$ (V/m) is incident normally on an interface at $z = 0$ with a lossy medium having a dielectric constant 2.5 and a loss tangent 0.5. Find the following:

a) The instantaneous expressions for $\mathbf{E}_r(z, t)$, $\mathbf{H}_r(z, t)$, $\mathbf{E}_t(z, t)$, and $\mathbf{H}_t(z, t)$, using a cosine reference.
b) The expressions for time-average Poynting vectors in air and in the lossy medium.

P.8–28 A uniform plane wave in air with $\mathbf{E}_i(z) = \mathbf{a}_x E_0 \exp(-j\beta_0 z)$ impinges normally onto the surface at $z = 0$ of a highly conducting medium having constitutive parameters ϵ_0, μ, and σ ($\sigma/\omega\epsilon_0 \gg 1$).

a) Find the reflection coefficient.
b) Derive the expression for the fraction of the incident power absorbed by the conducting medium.
c) Obtain the fraction of the power absorbed at 1 (MHz) if the medium is iron.

P.8–29 Consider the situation of normal incidence at a lossless dielectric slab of thickness d in air, as shown in Fig. 8–15 with

$$\epsilon_1 = \epsilon_3 = \epsilon_0 \qquad \text{and} \qquad \mu_1 = \mu_3 = \mu_0.$$

a) Find E_{r0}, E_2^+, E_2^-, and E_{t0} in terms of E_{i0}, d, ϵ_2, and μ_2.
b) Will there be reflection at interface $z = 0$ if $d = \lambda_2/4$? If $d = \lambda_2/2$? Explain.

P.8–30 A transparent dielectric coating is applied to glass ($\epsilon_r = 4$, $\mu_r = 1$) to eliminate the reflection of red light [$\lambda_0 = 0.75$ (μm)].
a) Determine the required dielectric constant and thickness of the coating.
b) If violet light [$\lambda_0 = 0.42$ (μm)] is shone normally on the coated glass, what percentage of the incident power will be reflected?

P.8–31 Refer to Fig. 8–15, which depicts three different dielectric media with two parallel interfaces. A uniform plane wave in medium 1 propagates in the $+z$-direction. Let Γ_{12} and Γ_{23} denote the reflection coefficients between media 1 and 2 and between media 2 and 3, respectively. Express the effective reflection coefficient, Γ_0, at $z = 0$ for the incident wave in terms of Γ_{12}, Γ_{23}, and $\beta_2 d$.

P.8–32 A uniform plane wave with

$$\mathbf{E}_i(z, t) = \mathbf{a}_x E_{i0} \cos \omega\left(t - \frac{z}{u_p}\right)$$

in medium 1 (ϵ_1, μ_1) is incident normally onto a lossless dielectric slab (ϵ_2, μ_2) of a thickness d backed by a perfectly conducting plane, as shown in Fig. 8–22. Find
a) $\mathbf{E}_r(z, t)$ **b)** $\mathbf{E}_1(z, t)$ **c)** $\mathbf{E}_2(z, t)$ **d)** $(\mathscr{P}_{av})_1$ **e)** $(\mathscr{P}_{av})_2$
f) Determine the thickness d that makes $\mathbf{E}_1(z, t)$ the same as if the dielectric slab were absent.

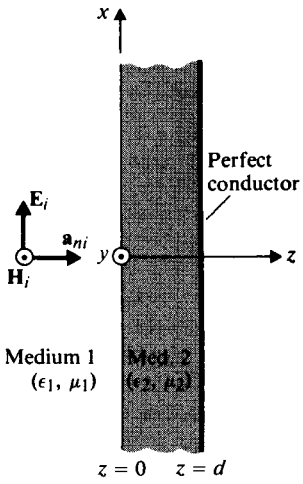

FIGURE 8–22
Plane wave incident normally onto a dielectric slab backed by a perfectly conducting plane (Problem P.8–32).

P.8–33 A uniform plane wave with $\mathbf{E}_i(z) = \mathbf{a}_x E_{i0} e^{-j\beta_0 z}$ in air propagates normally through a thin copper sheet of thickness d, as shown in Fig. 8–23. Neglecting multiple reflections within the copper sheets, find
a) E_2^+, H_2^+ **b)** E_2^-, H_2^- **c)** E_{30}, H_{30} **d)** $(\mathscr{P}_{av})_3/(\mathscr{P}_{av})_i$
Calculate $(\mathscr{P}_{av})_3/(\mathscr{P}_{av})_i$ for a thickness d that equals one skin depth at 10 (MHz). (Note that this pertains to the shielding effectiveness of the thin copper sheet.)

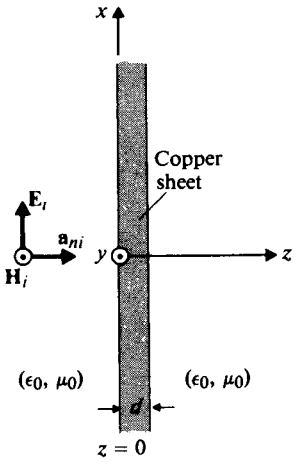

FIGURE 8–23
Plane wave propagating through a thin copper sheet (Problem P.8–33).

P.8–34 A uniform plane wave is incident on the ionosphere at an angle of incidence $\theta_i = 60°$. Assuming a constant electron density and a wave frequency equal to one-half of the plasma frequency of the ionosphere, determine

a) $\Gamma_\perp$ and $\tau_\perp$,

b) $\Gamma_{||}$ and $\tau_{||}$.

Interpret the significance of these complex quantities.

P.8–35 A 10 (kHz) parallelly polarized electromagnetic wave in air is incident obliquely on an ocean surface at a near-grazing angle $\theta_i = 88°$. Using $\epsilon_r = 81$, $\mu_r = 1$, and $\sigma = 4$ (S/m) for seawater, find (a) the angle of refraction θ_t, (b) the transmission coefficient $\tau_{||}$, (c) $(\mathscr{P}_{av})_t/(\mathscr{P}_{av})_i$, and (d) the distance below the ocean surface where the field intensity has been diminished by 30 (dB).

P.8–36 A light ray is incident from air obliquely on a transparent sheet of thickness d with an index of refraction n, as shown in Fig. 8–24. The angle of incidence is θ_i. Find (a) θ_t, (b) the distance ℓ_1 at the point of exit, and (c) the amount of the lateral displacement ℓ_2 of the emerging ray.

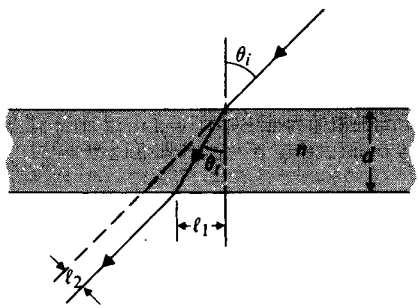

FIGURE 8–24
Light-ray impinging obliquely on a transparent sheet of refraction index n (Problem P.8–36).

P.8–37 A uniform plane wave with perpendicular polarization represented by Eqs. (8–196) and (8–197) is incident on a plane interface at $z = 0$, as shown in Fig. 8–16. Assuming

$\epsilon_2 < \epsilon_1$ and $\theta_i > \theta_c$, (a) obtain the phasor expressions for the transmitted field ($\mathbf{E}_t$, $\mathbf{H}_t$), and (b) verify that the average power transmitted into medium 2 vanishes.

P.8–38 A uniform plane wave of angular frequency ω in medium 1 having a refractive index n_1 is incident on a plane interface at $z = 0$ with medium 2 having a refractive index n_2 ($< n_1$) at the critical angle. Let E_{i0} and E_{t0} denote the amplitudes of the incident and refracted electric field intensities, respectively.

a) Find the ratio E_{t0}/E_{i0} for perpendicular polarization.

b) Find the ratio E_{t0}/E_{i0} for parallel polarization.

c) Write the instantaneous expressions of $\mathbf{E}_i(x, z; t)$ and $\mathbf{E}_t(x, z; t)$ for perpendicular polarization in terms of the parameters ω, n_1, n_2, θ_i, and E_{i0}.

P.8–39 An electromagnetic wave from an underwater source with perpendicular polarization is incident on a water–air interface at $\theta_i = 20°$. Using $\epsilon_r = 81$ and $\mu_r = 1$ for fresh water, find (a) critical angle θ_c, (b) reflection coefficient $\Gamma_\perp$, (c) transmission coefficient $\tau_\perp$, and (d) attenuation in dB for each wavelength into the air.

P.8–40 Glass isosceles triangular prisms shown in Fig. 8–25 are used in optical instruments. Assuming $\epsilon_r = 4$ for glass, calculate the percentage of the incident light power reflected back by the prism.

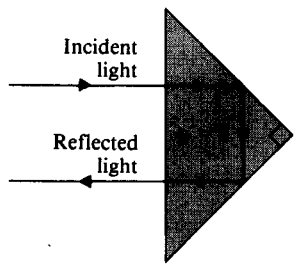

FIGURE 8–25
Light reflection by a right isosceles triangular prism (Problem P.8–40).

P.8–41 For preventing interference of waves in neighboring fibers and for mechanical protection, individual optical fibers are usually cladded by a material of a lower refractive index, as shown in Fig. 8–26, where $n_2 < n_1$.

a) Express the maximum angle of incidence θ_a in terms of n_0, n_1, and n_2 for meridional rays incident on the core's end face to be trapped inside the core by total internal reflection. (***Meridional rays*** are those that pass through the fiber axis. The angle θ_a is called the ***acceptance angle***, and $\sin \theta_a$ the ***numerical aperture*** (N.A.) of the fiber.)

b) Find θ_a and N.A. if $n_1 = 2$, $n_2 = 1.74$, and $n_0 = 1$.

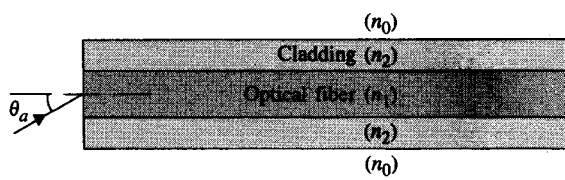

FIGURE 8–26
A cladded-core optical fiber (Problem P.8–41).

P.8–42 An electromagnetic wave in dielectric medium 1 (ϵ_1, μ_0) impinges obliquely on a boundary plane with dielectric medium 2 (ϵ_2, μ_0). Let θ_i and θ_t denote the incident and refraction angles, respectively, and prove the following:

a) For perpendicular polarization:

$$\Gamma_\perp = \frac{\sin(\theta_t - \theta_i)}{\sin(\theta_t + \theta_i)}, \qquad \tau_\perp = \frac{2 \sin\theta_t \cos\theta_i}{\sin(\theta_t + \theta_i)}.$$

b) For parallel polarization:

$$\Gamma_{||} = \frac{\sin 2\theta_t - \sin 2\theta_i}{\sin 2\theta_t + \sin 2\theta_i}, \qquad \tau_{||} = \frac{4 \sin\theta_t \cos\theta_i}{\sin 2\theta_t + \sin 2\theta_i}.$$

(These four relations are known as ***Fresnel formulas.***)

P.8–43 Prove that, under the condition of no reflection at an interface, the sum of the Brewster angle and the angle of refraction is $\pi/2$ for:

a) perpendicular polarization ($\mu_1 \neq \mu_2$),

b) parallel polarization ($\epsilon_1 \neq \epsilon_2$).

P.8–44 For an incident wave with parallel polarization:

a) Find the relation between the critical angle θ_c and the Brewster angle $\theta_{B||}$ for nonmagnetic media.

b) Plot θ_c and $\theta_{B||}$ versus the ratio ϵ_1/ϵ_2.

P.8–45 By using Snell's law of refraction, (a) express Γ and τ in terms of ϵ_{r1}, ϵ_{r2}, and θ_i; and (b) plot Γ and τ versus θ_i for $\epsilon_{r1}/\epsilon_{r2} = 2.25$ for both perpendicular and parallel polarizations.

P.8–46 A perpendicularly polarized uniform plane wave in air of frequency f is incident obliquely at an angle of incidence θ_i on a plane boundary with a lossy dielectric medium that is characterized by a complex permittivity $\epsilon_2 = \epsilon' - j\epsilon''$. Let the incident electric field be

$$\mathbf{E}_i(x, z) = \mathbf{a}_y E_{i0} e^{-jk_0(x \sin\theta_i - z\cos\theta_i)}.$$

a) Find the expressions of the transmitted electric and magnetic field intensity phasors in terms of the given parameters.

b) Show that the angle of refraction is complex and that $\mathbf{H}_t$ is elliptically polarized.

P.8–47 In some books the reflection and transmission coefficients for parallel polarization are defined as the ratios of the amplitude of the tangential components of the reflected and transmitted **E** fields, respectively, to the amplitude of the tangential component of the incident **E** field. Let the coefficients defined in this manner be designated $\Gamma'_{||}$ and $\tau'_{||}$, respectively.

a) Find $\Gamma'_{||}$ and $\tau'_{||}$ in terms of η_1, η_2, θ_i, and θ_t; and compare them with $\Gamma_{||}$ and $\tau_{||}$ in Eqs. (8–221) and (8–222).

b) Find the relation between $\Gamma'_{||}$ and $\tau'_{||}$, and compare it with Eq. (8–223).

9

Theory and Applications of Transmission Lines

9–1 Introduction

We have now developed an electromagnetic model with which we can analyze electromagnetic actions that occur at a distance and are caused by time-varying charges and currents. These actions are explained in terms of electromagnetic fields and waves. An isotropic or omnidirectional electromagnetic source radiates waves equally in all directions. Even when the source radiates through a highly directive antenna, its energy spreads over a wide area at large distances. This radiated energy is not guided, and the transmission of power and information from the source to a receiver is inefficient. This is especially true at lower frequencies for which directive antennas would have huge dimensions and therefore would be excessively expensive. For instance, at AM broadcast frequencies a single half-wavelength antenna (which is only mildly directive[†]) would be over a hundred meters long. At the 60 (Hz) power frequency a wavelength is 5 million meters or 5 (Mm)!

For efficient point-to-point transmission of power and information the source energy must be directed or guided. In this chapter we study transverse electromagnetic (TEM) waves guided by transmission lines. The TEM mode of guided waves is one in which **E** and **H** are perpendicular to each other and both are transverse to the direction of propagation along the guiding line. We discussed the propagation of unguided TEM plane waves in the last chapter. We will show in this chapter that many of the characteristics of TEM waves guided by transmission lines are the same as those for a uniform plane wave propagating in an unbounded dielectric medium.

The three most common types of guiding structures that support TEM waves are:

a) *Parallel-plate transmission line.* This type of transmission line consists of two parallel conducting plates separated by a dielectric slab of a uniform thickness.

[†] Principles of antennas and radiating systems will be discussed in Chapter 11.

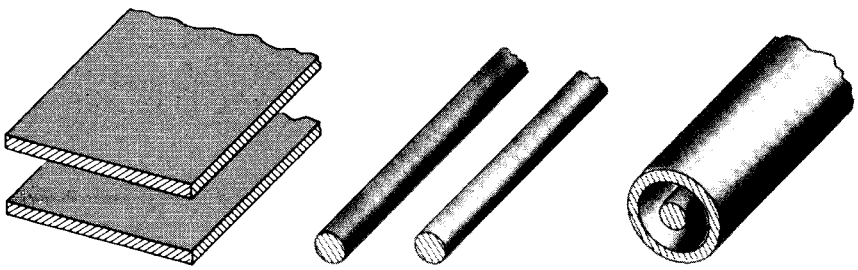

(a) Parallel-plate transmission line. (b) Two-wire transmission line. (c) Coaxial transmission line.

FIGURE 9–1
Common types of transmission lines.

[See Fig. 9–1(a).] At microwave frequencies, parallel-plate transmission lines can be fabricated inexpensively on a dielectric substrate using printed-circuit technology. They are often called ***striplines***.

b) *Two-wire transmission line.* This transmission line consists of a pair of parallel conducting wires separated by a uniform distance. [See Fig. 9–1(b).] Examples are the ubiquitous overhead power and telephone lines seen in rural areas and the flat lead-in lines from a rooftop antenna to a television receiver.

c) *Coaxial transmission line.* This consists of an inner conductor and a coaxial outer conducting sheath separated by a dielectric medium. [See Fig. 9–1(c).] This structure has the important advantage of confining the electric and magnetic fields entirely within the dielectric region. No stray fields are generated by a coaxial transmission line, and little external interference is coupled into the line. Examples are telephone and TV cables and the input cables to high-frequency precision measuring instruments.

We should note that other wave modes more complicated than the TEM mode can propagate on all three of these types of transmission lines when the separation between the conductors is greater than certain fractions of the operating wavelength. These other transmission modes will be considered in the next chapter.

We will show that the TEM wave solution of Maxwell's equations for the parallel-plate guiding structure in Fig. 9–1(a) leads directly to a pair of transmission-line equations. The general transmission-line equations can also be derived from a circuit model in terms of the resistance, inductance, conductance, and capacitance per unit length of a line. The transition from the circuit model to the electromagnetic model is effected from a network with lumped-parameter elements (discrete resistors, inductors, and capacitors) to one with distributed parameters (continuous distributions of R, L, G, and C along the line). From the transmission-line equations, all the characteristics of wave propagation along a given line can be derived and studied.

The study of time-harmonic steady-state properties of transmission lines is greatly facilitated by the use of graphical charts, which avert the necessity of repeated calculations with complex numbers. The best known and most widely used graphical chart is the ***Smith chart***. The use of Smith chart for determining wave characteristics on a transmission line and for impedance matching will be discussed.

9–2 Transverse Electromagnetic Wave along a Parallel-Plate Transmission Line

Let us consider a y-polarized TEM wave propagating in the $+z$-direction along a uniform parallel-plate transmission line. Figure 9–2 shows the cross-sectional dimensions of such a line and the chosen coordinate system. For time-harmonic fields the wave equation to be satisfied in the sourceless dielectric region becomes the homogeneous Helmholtz's equation, Eq. (8–46). In the present case the appropriate phasor solution for the wave propagating in the $+z$-direction is

$$\mathbf{E} = \mathbf{a}_y E_y = \mathbf{a}_y E_0 e^{-\gamma z}. \tag{9–1a}$$

The associated **H** field is, from Eq. (8–31),

$$\mathbf{H} = \mathbf{a}_x H_x = -\mathbf{a}_x \frac{E_0}{\eta} e^{-\gamma z}, \tag{9–1b}$$

where γ and η are the propagation constant and the intrinsic impedance, respectively, of the dielectric medium. Fringe fields at the edges of the plates are neglected. Assuming perfectly conducting plates and a lossless dielectric, we have, from Chapter 8,

$$\gamma = j\beta = j\omega\sqrt{\mu\epsilon} \tag{9–2}$$

and

$$\eta = \sqrt{\frac{\mu}{\epsilon}}. \tag{9–3}$$

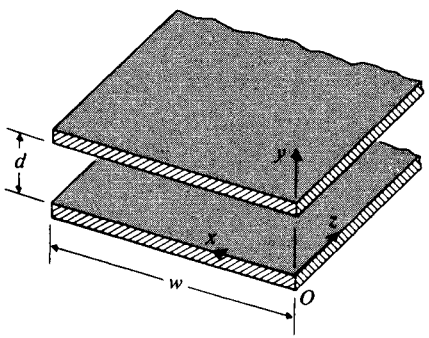

FIGURE 9–2
Parallel-plate transmission line.

The boundary conditions to be satisfied at the interfaces of the dielectric and the perfectly conducting planes are, from Eqs. (7–68a, b, c, and d), as follows:

At both $y = 0$ and $y = d$:

$$E_t = 0 \tag{9-4}$$

and

$$H_n = 0, \tag{9-5}$$

which are obviously satisfied because $E_x = E_z = 0$ and $H_y = 0$.

At $y = 0$ (lower plate), $\mathbf{a}_n = \mathbf{a}_y$:

$$\mathbf{a}_y \cdot \mathbf{D} = \rho_{s\ell} \quad \text{or} \quad \rho_{s\ell} = \epsilon E_y = \epsilon E_0 e^{-j\beta z}; \tag{9-6a}$$

$$\mathbf{a}_y \times \mathbf{H} = \mathbf{J}_{s\ell} \quad \text{or} \quad \mathbf{J}_{s\ell} = -\mathbf{a}_z H_x = \mathbf{a}_z \frac{E_0}{\eta} e^{-j\beta z}. \tag{9-7a}$$

At $y = d$ (upper plate), $\mathbf{a}_n = -\mathbf{a}_y$:

$$-\mathbf{a}_y \cdot \mathbf{D} = \rho_{su} \quad \text{or} \quad \rho_{su} = -\epsilon E_y = -\epsilon E_0 e^{-j\beta z}; \tag{9-6b}$$

$$-\mathbf{a}_y \times \mathbf{H} = \mathbf{J}_{su} \quad \text{or} \quad \mathbf{J}_{su} = \mathbf{a}_z H_x = -\mathbf{a}_z \frac{E_0}{\eta} e^{-j\beta z}. \tag{9-7b}$$

Equations (9–6) and (9–7) indicate that surface charges and surface currents on the conducting planes vary sinusoidally with z, as do E_y and H_x. This is illustrated schematically in Fig. 9–3.

Field phasors $\mathbf{E}$ and $\mathbf{H}$ in Eqs. (9–1a) and (9–1b) satisfy the two Maxwell's curl equations:

$$\nabla \times \mathbf{E} = -j\omega\mu\mathbf{H} \tag{9-8}$$

and

$$\nabla \times \mathbf{H} = j\omega\epsilon\mathbf{E}. \tag{9-9}$$

Since $\mathbf{E} = \mathbf{a}_y E_y$ and $\mathbf{H} = \mathbf{a}_x H_x$, Eqs. (9–8) and (9–9) become

$$\frac{dE_y}{dz} = j\omega\mu H_x \tag{9-10}$$

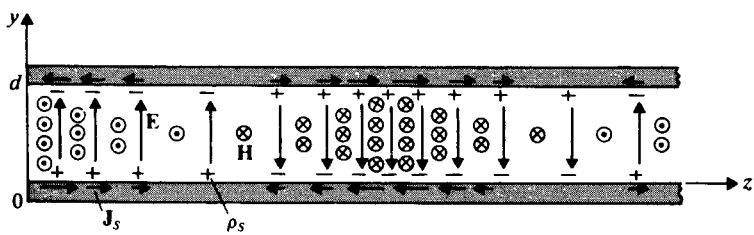

FIGURE 9–3
Field, charge, and current distributions along a parallel-plate transmission line.

and

$$\frac{dH_x}{dz} = j\omega\epsilon E_y. \tag{9–11}$$

Ordinary derivatives appear above because phasors E_y and H_x are functions of z only.

Integrating Eq. (9–10) over y from 0 to d, we have

$$\frac{d}{dz}\int_0^d E_y\,dy = j\omega\mu\int_0^d H_x\,dy$$

or

$$-\frac{dV(z)}{dz} = j\omega\mu J_{su}(z)d = j\omega\left(\mu\frac{d}{w}\right)[J_{su}(z)w] = j\omega LI(z), \tag{9–12}$$

where

$$V(z) = -\int_0^d E_y\,dy = -E_y(z)d$$

is the potential difference or voltage between the upper and lower plates,

$$I(z) = J_{su}(z)w$$

is the total current flowing in the $+z$ direction in the upper plate (w = plate width), and

$$\boxed{L = \mu\frac{d}{w} \quad \text{(H/m)}} \tag{9–13}$$

is the inductance per unit length of the parallel-plate transmission line. The dependence of phasors $V(z)$ and $I(z)$ on z is noted explicitly in Eq. (9–12) for emphasis.

Similarly, we integrate Eq. (9–11) over x from 0 to w to obtain

$$\frac{d}{dz}\int_0^w H_x\,dx = j\omega\epsilon\int_0^w E_y\,dx$$

or

$$-\frac{dI(z)}{dz} = -j\omega\epsilon E_y(z)w = j\omega\left(\epsilon\frac{w}{d}\right)[-E_y(z)d] = j\omega CV(z), \tag{9–14}$$

where

$$\boxed{C = \epsilon\frac{w}{d} \quad \text{(F/m)}} \tag{9–15}$$

is the capacitance per unit length of the parallel-plate transmission line.

Equations (9–12) and (9–14) constitute a pair of ***time-harmonic transmission-line equations*** for phasors $V(z)$ and $I(z)$. They may be combined to yield second-order

differential equations for $V(z)$ and for $I(z)$:

$$\frac{d^2V(z)}{dz^2} = -\omega^2 LCV(z), \tag{9-16a}$$

$$\frac{d^2I(z)}{dz^2} = -\omega^2 LCI(z). \tag{9-16b}$$

The solutions of Eqs. (9–16a) and (9–16b) are, for waves propagating in the $+z$-direction,

$$V(z) = V_0 e^{-j\beta z} \tag{9-17a}$$

and

$$I(z) = I_0 e^{-j\beta z}, \tag{9-17b}$$

where the phase constant

$$\boxed{\beta = \omega\sqrt{LC} = \omega\sqrt{\mu\epsilon} \quad \text{(rad/m)}} \tag{9-18}$$

is the same as that given in Eq. (9–2). The relation between V_0 and I_0 can be found by using either Eq. (9–12) or Eq. (9–14):

$$\boxed{Z_0 = \frac{V(z)}{I(z)} = \frac{V_0}{I_0} = \sqrt{\frac{L}{C}} \quad (\Omega),} \tag{9-19}$$

which becomes, in view of the results of Eqs. (9–13) and (9–15),

$$\boxed{Z_0 = \frac{d}{w}\sqrt{\frac{\mu}{\epsilon}} = \frac{d}{w}\eta \quad (\Omega).} \tag{9-20}$$

The quantity Z_0 is the impedance at any location that looks toward an infinitely long (no reflections) transmission line. It is called the ***characteristic impedance*** of the line. The ratio of $V(z)$ and $I(z)$ at any point on a finite line of any length terminated in Z_0 is Z_0.† For a parallel-plate transmission line with perfectly conducting plates of width w and separated by a lossless dielectric slab of thickness d, the characteristic impedance Z_0 is (d/w) times the intrinsic impedance η of the dielectric medium.

The velocity of propagation along the line is

$$\boxed{u_p = \frac{\omega}{\beta} = \frac{1}{\sqrt{LC}} = \frac{1}{\sqrt{\mu\epsilon}} \quad \text{(m/s),}} \tag{9-21}$$

which is the same as the phase velocity of a TEM plane wave in the dielectric medium.

† This statement will be proved in Section 9–4 (see Eq. 9–107).

9–2.1 LOSSY PARALLEL-PLATE TRANSMISSION LINES

We have so far assumed the parallel-plate transmission line to be lossless. In actual situations, loss may arise from two causes. First, the dielectric medium may have a nonvanishing loss tangent; second, the plates may not be perfectly conducting. To characterize these two effects, we define two new parameters: G, the conductance per unit length across the two plates; and R, the resistance per unit length of the *two* plate conductors.

The conductance between two conductors separated by a dielectric medium having a permittivity ϵ and an equivalent conductivity σ can be determined readily by using Eq. (5–81) when the capacitance between the two conductors is known. We have

$$G = \frac{\sigma}{\epsilon} C. \tag{9–22}$$

Use of Eq. (9–15) directly yields

$$\boxed{G = \sigma \frac{w}{d} \quad \text{(S/m)}.} \tag{9–23}$$

If the parallel-plate conductors have a very large but finite conductivity σ_c (which must not be confused with the conductivity σ of the dielectric medium), ohmic power will be dissipated in the plates. This necessitates the presence of a nonvanishing axial electric field $\mathbf{a}_z E_z$ at the plate surfaces, such that the average Poynting vector

$$\mathscr{P}_{\text{av}} = \mathbf{a}_y p_\sigma = \tfrac{1}{2}\mathscr{R}e(\mathbf{a}_z E_z \times \mathbf{a}_x H_x^*) \tag{9–24}$$

has a y-component and equals the average power per unit area dissipated in each of the conducting plates. (Obviously the cross product of $\mathbf{a}_y E_y$ and $\mathbf{a}_x H_x$ does not result in a y-component.)

Consider the upper plate where the surface current density is $J_{su} = H_x$. It is convenient to define a ***surface impedance*** of an imperfect conductor, Z_s, as the ratio of the tangential component of the electric field to the surface current density at the conductor surface.

$$\boxed{Z_s = \frac{E_t}{J_s} \quad (\Omega).} \tag{9–25}$$

For the upper plate we have

$$Z_s = \frac{E_z}{J_{su}} = \frac{E_z}{H_x} = \eta_c, \tag{9–26a}$$

where η_c is the intrinsic impedance of the plate conductor. Here we assume that both the conductivity σ_c of the plate conductor and the operating frequency are sufficiently high that the current flows in a very thin surface layer and can be represented by

the surface current J_{su}. The intrinsic impedance of a good conductor has been given in Eq. (8–54). We have

$$Z_s = R_s + jX_s = (1+j)\sqrt{\frac{\pi f \mu_c}{\sigma_c}} \quad (\Omega), \tag{9–26b}$$

where the subscript c is used to indicate the properties of the conductor.

Substitution of Eq. (9–26a) in Eq. (9–24) gives

$$\begin{aligned} p_\sigma &= \tfrac{1}{2}\mathscr{R}e(|J_{su}|^2 Z_s) \\ &= \tfrac{1}{2}|J_{su}|^2 R_s \quad (\text{W/m}^2). \end{aligned} \tag{9–27}$$

The ohmic power dissipated in a unit length of the plate having a width w is wp_σ, which can be expressed in terms of the total surface current, $I = wJ_{su}$, as

$$P_\sigma = wp_\sigma = \frac{1}{2} I^2 \left(\frac{R_s}{w}\right) \quad (\text{W/m}). \tag{9–28}$$

Equation (9–28) is the power dissipated when a sinusoidal current of amplitude I flows through a resistance R_s/w. Thus, the effective series resistance per unit length for *both* plates of a parallel-plate transmission line of width w is

$$\boxed{R = 2\left(\frac{R_s}{w}\right) = \frac{2}{w}\sqrt{\frac{\pi f \mu_c}{\sigma_c}} \quad (\Omega/\text{m}).} \tag{9–29}$$

Table 9–1 lists the expressions for the four *distributed parameters* (R, L, G, and C per unit length) of a parallel-plate transmission line of width w and separation d.

TABLE 9–1
Distributed Parameters of Parallel-Plate Transmission Line (Width = w, Separation = d)

Parameter	Formula	Unit
R	$\frac{2}{w}\sqrt{\frac{\pi f \mu_c}{\sigma_c}}$	Ω/m
L	$\mu \frac{d}{w}$	H/m
G	$\sigma \frac{w}{d}$	S/m
C	$\epsilon \frac{w}{d}$	F/m

We note from Eq. (9–26b) that surface impedance Z_s has a positive reactance term X_s that is numerically equal to R_s. If the total complex power (instead of its real part, the ohmic power P_σ, only) associated with a unit length of the plate is considered, X_s will lead to an ***internal series inductance*** per unit length $L_i = X_s/\omega = R_s/\omega$. At high frequencies, L_i is negligible in comparison with the external inductance L.

We note in the calculation of the power loss in the plate conductors of a finite conductivity σ_c that a nonvanishing electric field $\mathbf{a}_z E_z$ must exist. The very existence of this axial electric field makes the wave along a lossy transmission line strictly not TEM. However, this axial component is ordinarily very small in comparison to the transverse component E_y. An estimate of their relative magnitudes can be made as follows:

$$\frac{|E_z|}{|E_y|} = \frac{|\eta_c H_x|}{|\eta H_x|} = \sqrt{\frac{\epsilon}{\mu}}\,|\eta_c| = \sqrt{\frac{\omega\epsilon\mu_c}{\mu\sigma_c}} = \sqrt{\frac{\omega\epsilon}{\sigma_c}},$$

where Eq. (8–54) has been used. For copper plates [$\sigma_c = 5.80 \times 10^7$ (S/m)] in air [$\epsilon = \epsilon_0 = 10^{-9}/36\pi$ (F/m)] at a frequency of 3 (GHz),

$$|E_z| \cong 5.3 \times 10^{-5}|E_y| \ll |E_y|.$$

Hence we retain the designation TEM as well as all its consequences. The introduction of a small E_z in the calculation of p_σ and R is considered a slight perturbation.

9–2.2 MICROSTRIP LINES

The development of solid-state microwave devices and systems has led to the widespread use of a form of parallel-plate transmission lines called microstrip lines or simply ***striplines***. A stripline usually consists of a dielectric substrate sitting on a grounded conducting plane with a thin narrow metal strip on top of the substrate, as shown in Fig. 9–4(a). Since the advent of printed-circuit techniques, striplines can be easily fabricated and integrated with other circuit components. However, because the results that we have derived in this section were based on the assumption of two wide

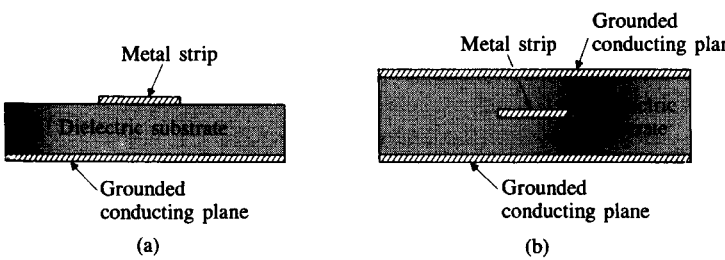

FIGURE 9–4
Two types of microstrip lines.

conducting plates (with negligible fringing effect) of equal width, they are not expected to apply here exactly. The approximation is closer if the width of the metal strip is much greater than the substrate thickness.

When the substrate has a high dielectric constant, a TEM approximation is found to be reasonably satisfactory. An exact analytical solution of the stripline in Fig. 9–4(a) satisfying all the boundary conditions is a difficult problem. Not all the fields will be confined in the dielectric substrate; some will stray from the top strip into the region outside of the strip, thus causing interference in the neighboring circuits. Semiempirical modifications to the formulas for the distributed parameters and the characteristic impedance are necessary for more accurate calculations.† All of these quantities tend to be frequency-dependent, and striplines are dispersive.

One method for reducing the stray fields of striplines is to have a grounded conducting plane on both sides of the dielectric substrate and to put the thin metal strip in the middle as in Fig. 9–4(b). This arrangement is known as a ***triplate line***. We can appreciate that triplate lines are more difficult and costly to fabricate and that the characteristic impedance of a triplate line is one-half of that of a corresponding stripline.

EXAMPLE 9–1 Neglecting losses and fringe effects and assuming the substrate of a stripline to have a thickness 0.4 (mm) and a dielectric constant 2.25, (a) determine the required width w of the metal strip in order for the stripline to have a characteristic resistance of 50 (Ω); (b) determine L and C of the line; and (c) determine u_p along the line. (d) Repeat parts (a), (b), and (c) for a characteristic resistance of 75 (Ω).

Solution

a) We use Eq. (9–20) directly to find w:

$$w = \frac{d}{Z_0}\sqrt{\frac{\mu}{\epsilon}} = \frac{0.4 \times 10^{-3}}{50}\frac{\eta_0}{\sqrt{\epsilon_r}}$$

$$= \frac{0.4 \times 10^{-3} \times 377}{50\sqrt{2.25}} = 2 \times 10^{-3} \quad \text{(m)}, \quad \text{or } 2 \quad \text{(mm)}.$$

b) $L = \mu\frac{d}{w} = 4\pi 10^{-7} \times \frac{0.4}{2} = 2.51 \times 10^{-7}$ (H/m), or 0.251 (μH/m).

$$C = \epsilon_0\epsilon_r\frac{w}{d} = \frac{10^{-9}}{36\pi} \times 2.25 \times \frac{2}{0.4} = 99.5 \times 10^{-12} \quad \text{(F/m)}, \quad \text{or } 99.5 \quad \text{(pF/m)}.$$

c) $u_p = \frac{1}{\sqrt{\mu\epsilon}} = \frac{c}{\sqrt{\epsilon_r}} = \frac{c}{\sqrt{2.25}} = \frac{c}{1.5} = 2 \times 10^8$ (m/s).

† See, for instance, K. F. Sander and G. A. L. Reed, *Transmission and Propagation of Electromagnetic Waves*, 2nd edition, Sec. 6.5.6, Cambridge University Press, New York, 1986.

d) Since w is inversely proportional to Z_0, we have, for $Z_0' = 75\ (\Omega)$,

$$w' = \left(\frac{Z_0}{Z_0'}\right)w = \frac{50}{75} \times 2 = 1.33 \quad \text{(mm)}.$$

$$L' = \left(\frac{w}{w'}\right)L = \left(\frac{2}{1.33}\right) \times 0.251 = 0.377 \quad (\mu\text{H/m}).$$

$$C' = \left(\frac{w'}{w}\right)C = \left(\frac{1.33}{2}\right) \times 99.5 = 66.2 \quad \text{(pF/m)}.$$

$$u_p' = u_p = 2 \times 10^8 \quad \text{(m/s)}.$$

9–3 General Transmission-Line Equations

We will now derive the equations that govern general two-conductor uniform transmission lines that include parallel-plate, two-wire, and coaxial lines. Transmission lines differ from ordinary electric networks in one essential feature. Whereas the physical dimensions of electric networks are very much smaller than the operating wavelength, transmission lines are usually a considerable fraction of a wavelength and may even be many wavelengths long. The circuit elements in an ordinary electric network can be considered discrete and as such may be described by lumped parameters. It is assumed that currents flowing in lumped-circuit elements do not vary spatially over the elements, and that no standing waves exist. A transmission line, on the other hand, is a distributed-parameter network and must be described by circuit parameters that are distributed throughout its length. Except under matched conditions, standing waves exist in a transmission line.

Consider a differential length Δz of a transmission line that is described by the following four parameters:

R, resistance per unit length (both conductors), in Ω/m.

L, inductance per unit length (both conductors), in H/m.

G, conductance per unit length, in S/m.

C, capacitance per unit length, in F/m.

Note that R and L are series elements and G and C are shunt elements. Figure 9–5 shows the equivalent electric circuit of such a line segment. The quantities $v(z, t)$ and $v(z + \Delta z, t)$ denote the instantaneous voltages at z and $z + \Delta z$, respectively. Similarly, $i(z, t)$ and $i(z + \Delta z, t)$ denote the instantaneous currents at z and $z + \Delta z$, respectively. Applying Kirchhoff's voltage law, we obtain

$$v(z, t) - R\,\Delta z i(z, t) - L\,\Delta z \frac{\partial i(z, t)}{\partial t} - v(z + \Delta z, t) = 0, \tag{9–30}$$

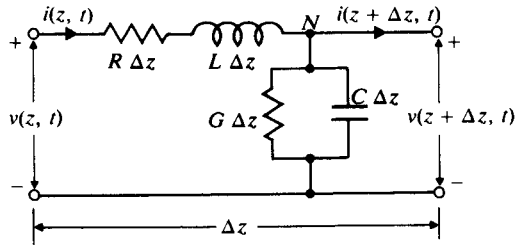

FIGURE 9–5
Equivalent circuit of a differential length Δz of a two-conductor transmission line.

which leads to

$$-\frac{v(z + \Delta z, t) - v(z, t)}{\Delta z} = Ri(z, t) + L\frac{\partial i(z, t)}{\partial t}. \tag{9–30a}$$

In the limit as $\Delta z \to 0$, Eq. (9–30a) becomes

$$\boxed{-\frac{\partial v(z, t)}{\partial z} = Ri(z, t) + L\frac{\partial i(z, t)}{\partial t}.} \tag{9–31}$$

Similarly, applying Kirchhoff's current law to the node N in Fig. 9–5, we have

$$i(z, t) - G\,\Delta z v(z + \Delta z, t) - C\,\Delta z\frac{\partial v(z + \Delta z, t)}{\partial t} - i(z + \Delta z, t) = 0. \tag{9–32}$$

On dividing by Δz and letting Δz approach zero, Eq. (9–32) becomes

$$\boxed{-\frac{\partial i(z, t)}{\partial z} = Gv(z, t) + C\frac{\partial v(z, t)}{\partial t}.} \tag{9–33}$$

Equations (9–31) and (9–33) are a pair of first-order partial differential equations in $v(z, t)$ and $i(z, t)$. They are the ***general transmission-line equations.***†

For harmonic time dependence the use of phasors simplifies the transmission-line equations to ordinary differential equations. For a cosine reference we write

$$v(z, t) = \mathcal{R}e[V(z)e^{j\omega t}], \tag{9–34a}$$

$$i(z, t) = \mathcal{R}e[I(z)e^{j\omega t}], \tag{9–34b}$$

where $V(z)$ and $I(z)$ are functions of the space coordinate z only and both may be complex. Substitution of Eqs. (9–34a) and (9–34b) in Eqs. (9–31) and (9–33) yields

† Sometimes referred to as the ***telegraphist's equations*** or ***telegrapher's equations.***

the following ordinary differential equations for phasors $V(z)$ and $I(z)$:

$$-\frac{dV(z)}{dz} = (R + j\omega L)I(z), \tag{9–35a}$$

$$-\frac{dI(z)}{dz} = (G + j\omega C)V(z). \tag{9–35b}$$

Equations (9–35a) and (9–35b) are ***time-harmonic transmission-line equations***, which reduce to Eqs. (9–12) and (9–14) under lossless conditions ($R = 0$, $G = 0$).

9–3.1 WAVE CHARACTERISTICS ON AN INFINITE TRANSMISSION LINE

The coupled time-harmonic transmission-line equations, Eqs. (9–35a) and (9–35b), can be combined to solve for $V(z)$ and $I(z)$. We obtain

$$\frac{d^2V(z)}{dz^2} = \gamma^2 V(z) \tag{9–36a}$$

and

$$\frac{d^2I(z)}{dz^2} = \gamma^2 I(z), \tag{9–36b}$$

where

$$\gamma = \alpha + j\beta = \sqrt{(R + j\omega L)(G + j\omega C)} \quad (m^{-1}) \tag{9–37}$$

is the ***propagation constant*** whose real and imaginary parts, α and β, are the ***attenuation constant*** (Np/m) and ***phase constant*** (rad/m) of the line, respectively. The nomenclature here is similar to that for plane-wave propagation in lossy media as defined in Section 8–3. These quantities are not really constants because, in general, they depend on ω in a complicated way.

The solutions of Eqs. (9–36a) and (9–36b) are

$$\begin{aligned} V(z) &= V^+(z) + V^-(z) \\ &= V_0^+ e^{-\gamma z} + V_0^- e^{\gamma z}, \end{aligned} \tag{9–38a}$$

$$\begin{aligned} I(z) &= I^+(z) + I^-(z) \\ &= I_0^+ e^{-\gamma z} + I_0^- e^{\gamma z}, \end{aligned} \tag{9–38b}$$

where the plus and minus superscripts denote waves traveling in the $+z$- and $-z$-directions, respectively. Wave amplitudes (V_0^+, I_0^+) and (V_0^-, I_0^-) are related by Eqs. (9–35a) and (9–35b), and it is easy to verify (Problem P.9–5) that

$$\frac{V_0^+}{I_0^+} = -\frac{V_0^-}{I_0^-} = \frac{R + j\omega L}{\gamma}. \tag{9–39}$$

For an infinite line (actually a semi-infinite line with the source at the left end) the terms containing the $e^{\gamma z}$ factor must vanish. There are no reflected waves; only the waves traveling in the $+z$-direction exist. We have

$$V(z) = V^+(z) = V_0^+ e^{-\gamma z}, \tag{9-40a}$$

$$I(z) = I^+(z) = I_0^+ e^{-\gamma z}. \tag{9-40b}$$

The ratio of the voltage and the current at any z for an infinitely long line is independent of z and is called the ***characteristic impedance*** of the line.

$$\boxed{Z_0 = \frac{R + j\omega L}{\gamma} = \frac{\gamma}{G + j\omega C} = \sqrt{\frac{R + j\omega L}{G + j\omega C}} \quad (\Omega).} \tag{9-41}$$

Note that γ and Z_0 are characteristic properties of a transmission line whether or not the line is infinitely long. They depend on R, L, G, C, and ω—not on the length of the line. An infinite line simply implies that there are no reflected waves.

There is a close analogy between the general governing equations and the wave characteristics of a transmission line and those of uniform plane waves in a lossy medium. This analogy will be discussed in the following example.

EXAMPLE 9–2 Demonstrate the analogy between the wave characteristics on a transmission line and uniform plane waves in a lossy medium.

Solution In a lossy medium with a complex permittivity $\epsilon_c = \epsilon' - j\epsilon''$ and a complex permeability $\mu = \mu' - j\mu''$ the Maxwell's curl equations (7–104a) and (7–104b) become

$$\nabla \times \mathbf{E} = -j\omega(\mu' - j\mu'')\mathbf{H}, \tag{9-42a}$$

$$\nabla \times \mathbf{H} = j\omega(\epsilon' - j\epsilon'')\mathbf{E}. \tag{9-42b}$$

If we assume a uniform plane wave characterized by an E_x that varies only with z, Eq. (9–42a) reduces to (see Eq. 8–12b)

$$-\frac{dE_x(z)}{dz} = j\omega(\mu' - j\mu'')H_y = (\omega\mu'' + j\omega\mu')H_y. \tag{9-43a}$$

Similarly, we obtain from Eq. (9–42b) the following relation:

$$-\frac{dH_y(z)}{dz} = (\omega\epsilon'' + j\omega\epsilon')E_x. \tag{9-43b}$$

Comparing Eqs. (9–43a) and (9–43b) with Eqs. (9–35a) and (9–35b), respectively, we recognize immediately the analogy of the governing equations for E_x and H_y of a uniform plane wave and those for V and I on a transmission line.

Equations (9–43a) and (9–43b) can be combined to give

$$\frac{d^2E_x(z)}{dz^2} = \gamma^2 E_x(z) \tag{9–44a}$$

and

$$\frac{d^2H_y(z)}{dz^2} = \gamma^2 H_y(z), \tag{9–44b}$$

which are entirely similar to Eqs. (9–36a) and (9–36b). The propagation constant of the uniform plane wave is

$$\gamma = \alpha + j\beta = \sqrt{(\omega\mu'' + j\omega\mu')(\omega\epsilon'' + j\omega\epsilon')}, \tag{9–45}$$

which should be compared with Eq. (9–37) for the transmission line. The intrinsic impedance of the lossy medium (the wave impedance of the plane wave traveling in the $+z$-direction) is (see Eq. 8–30)

$$\eta_c = \sqrt{\frac{\mu'' + j\mu'}{\epsilon'' + j\epsilon'}}, \tag{9–46}$$

which is analogous to the expression for the characteristic impedance of a transmission line in Eq. (9–41).

Because of the above analogies, many of the results obtained for normal incidence of uniform plane waves can be adapted to transmission-line problems, and vice versa. ■

The general expressions for the characteristic impedance in Eq. (9–41) and the propagation constant in Eq. (9–37) are relatively complicated. The following three limiting cases have special significance.

1. *Lossless Line* ($R = 0, G = 0$).

   a) Propagation constant:

$$\gamma = \alpha + j\beta = j\omega\sqrt{LC}; \tag{9–47}$$

$$\alpha = 0, \tag{9–48}$$

$$\beta = \omega\sqrt{LC} \qquad \text{(a linear function of } \omega\text{)}. \tag{9–49}$$

   b) Phase velocity:

$$u_p = \frac{\omega}{\beta} = \frac{1}{\sqrt{LC}} \qquad \text{(constant)}. \tag{9–50}$$

   c) Characteristic impedance:

$$Z_0 = R_0 + jX_0 = \sqrt{\frac{L}{C}}; \tag{9–51}$$

$$R_0 = \sqrt{\frac{L}{C}} \qquad \text{(constant)}, \tag{9–52}$$

$$X_0 = 0. \tag{9–53}$$

2. *Low-Loss Line* ($R \ll \omega L$, $G \ll \omega C$). The low-loss conditions are more easily satisfied at very high frequencies.

a) Propagation constant:

$$\gamma = \alpha + j\beta = j\omega\sqrt{LC}\left(1 + \frac{R}{j\omega L}\right)^{1/2}\left(1 + \frac{G}{j\omega C}\right)^{1/2}$$

$$\cong j\omega\sqrt{LC}\left(1 + \frac{R}{2j\omega L}\right)\left(1 + \frac{G}{2j\omega C}\right) \tag{9-54}$$

$$\cong j\omega\sqrt{LC}\left[1 + \frac{1}{2j\omega}\left(\frac{R}{L} + \frac{G}{C}\right)\right];$$

$$\alpha \cong \frac{1}{2}\left(R\sqrt{\frac{C}{L}} + G\sqrt{\frac{L}{C}}\right), \tag{9-55}$$

$$\beta \cong \omega\sqrt{LC} \qquad \text{(approximately a linear function of } \omega\text{)}. \tag{9-56}$$

b) Phase velocity:

$$u_p = \frac{\omega}{\beta} \cong \frac{1}{\sqrt{LC}} \qquad \text{(approximately constant)}. \tag{9-57}$$

c) Characteristic impedance:

$$Z_0 = R_0 + jX_0 = \sqrt{\frac{L}{C}}\left(1 + \frac{R}{j\omega L}\right)^{1/2}\left(1 + \frac{G}{j\omega C}\right)^{-1/2}$$

$$\cong \sqrt{\frac{L}{C}}\left[1 + \frac{1}{2j\omega}\left(\frac{R}{L} - \frac{G}{C}\right)\right]; \tag{9-58}$$

$$R_0 \cong \sqrt{\frac{L}{C}}, \tag{9-59}$$

$$X_0 \cong -\sqrt{\frac{L}{C}}\frac{1}{2\omega}\left(\frac{R}{L} - \frac{G}{C}\right) \cong 0. \tag{9-60}$$

3. *Distortionless Line* ($R/L = G/C$). If the condition

$$\frac{R}{L} = \frac{G}{C} \tag{9-61}$$

is satisfied, the expressions for both γ and Z_0 simplify.

a) Propagation constant:

$$\gamma = \alpha + j\beta = \sqrt{(R + j\omega L)\left(\frac{RC}{L} + j\omega C\right)}$$

$$= \sqrt{\frac{C}{L}}\,(R + j\omega L); \tag{9-62}$$

$$\alpha = R\sqrt{\frac{C}{L}}, \tag{9-63}$$

$$\beta = \omega\sqrt{LC} \qquad \text{(a linear function of } \omega\text{)}. \tag{9-64}$$

b) Phase velocity:

$$u_p = \frac{\omega}{\beta} = \frac{1}{\sqrt{LC}} \qquad \text{(constant)}. \tag{9–65}$$

c) Characteristic impedance:

$$Z_0 = R_0 + jX_0 = \sqrt{\frac{R + j\omega L}{(RC/L) + j\omega C}} = \sqrt{\frac{L}{C}}; \tag{9–66}$$

$$R_0 = \sqrt{\frac{L}{C}} \qquad \text{(constant)}, \tag{9–67}$$

$$X_0 = 0. \tag{9–68}$$

Thus, except for a nonvanishing attenuation constant, the characteristics of a distortionless line are the same as those of a lossless line—namely, a constant phase velocity ($u_p = 1/\sqrt{LC}$) and a constant real characteristic impedance ($Z_0 = R_0 = \sqrt{L/C}$).

A constant phase velocity is a direct consequence of the linear dependence of the phase constant β on ω. Since a signal usually consists of a band of frequencies, it is essential that the different frequency components travel along a transmission line at the same velocity in order to avoid distortion. This condition is satisfied by a lossless line and is approximated by a line with very low losses. For a lossy line, wave amplitudes will be attentuated, and distortion will result when different frequency components attenuate differently, even when they travel with the same velocity. The condition specified in Eq. (9–61) leads to both a constant α and a constant u_p—thus the name ***distortionless line***.

The phase constant of a lossy transmission line is determined by expanding the expression for γ in Eq. (9–37). In general, the phase constant is not a linear function of ω; thus it will lead to a u_p, which depends on frequency. As the different frequency components of a signal propagate along the line with different velocities, the signal suffers ***dispersion***. A general, lossy, transmission line is therefore *dispersive*, as is a lossy dielectric.

EXAMPLE 9–3 It is found that the attenuation on a 50 (Ω) distortionless transmission line is 0.01 (dB/m). The line has a capacitance of 0.1 (nF/m).

a) Find the resistance, inductance, and conductance per meter of the line.

b) Find the velocity of wave propagation.

c) Determine the percentage to which the amplitude of a voltage traveling wave decreases in 1 (km) and in 5 (km).

Solution

a) For a distortionless line,

$$\frac{R}{L} = \frac{G}{C}.$$

The given quantities are

$$R_0 = \sqrt{\frac{L}{C}} = 50 \quad (\Omega),$$

$$\alpha = R\sqrt{\frac{C}{L}} = 0.01 \quad (\text{dB/m})$$

$$= \frac{0.01}{8.69}\,(\text{Np/m}) = 1.15 \times 10^{-3} \quad (\text{Np/m}).$$

The three relations above are sufficient to solve for the three unknowns R, L, and G in terms of the given $C = 10^{-10}$ (F/m):

$$R = \alpha R_0 = (1.15 \times 10^{-3}) \times 50 = 0.057 \quad (\Omega/\text{m});$$

$$L = CR_0^2 = 10^{-10} \times 50^2 = 0.25 \quad (\mu\text{H/m});$$

$$G = \frac{RC}{L} = \frac{R}{R_0^2} = \frac{0.057}{50^2} = 22.8 \quad (\mu\text{S/m}).$$

b) The velocity of wave propagation on a distortionless line is the phase velocity given by Eq. (9–65).

$$u_p = \frac{1}{\sqrt{LC}} = \frac{1}{\sqrt{(0.25 \times 10^{-6} \times 10^{-10}}} = 2 \times 10^8 \quad (\text{m/s}).$$

c) The ratio of two voltages a distance z apart along the line is

$$\frac{V_2}{V_1} = e^{-\alpha z}.$$

After 1 (km), $(V_2/V_1) = e^{-1000\alpha} = e^{-1.15} = 0.317$, or 31.7%.

After 5 (km), $(V_2/V_1) = e^{-5000\alpha} = e^{-5.75} = 0.0032$, or 0.32%. ■

9–3.2 TRANSMISSION-LINE PARAMETERS

The electrical properties of a transmission line at a given frequency are completely characterized by its four distributed parameters R, L, G, and C. These parameters for a parallel-plate transmission line are listed in Table 9–1. We will now obtain them for two-wire and coaxial transmission lines.

Our basic premise is that the conductivity of the conductors in a transmission line is usually so high that the effect of the series resistance on the computation of the propagation constant is negligible, the implication being that the waves on the line are approximately TEM. We may write, in dropping R from Eq. (9–37),

$$\gamma = j\omega\sqrt{LC}\left(1 + \frac{G}{j\omega C}\right)^{1/2}. \tag{9–69}$$

From Eq. (8–44) we know that the propagation constant for a TEM wave in a medium with constitutive parameters (μ, ϵ, σ) is

$$\gamma = j\omega\sqrt{\mu\epsilon}\left(1 + \frac{\sigma}{j\omega\epsilon}\right)^{1/2}. \tag{9–70}$$

But

$$\frac{G}{C} = \frac{\sigma}{\epsilon} \tag{9–71}$$

in accordance with Eq. (5–81); hence comparison of Eqs. (9–69) and (9–70) yields

$$\boxed{LC = \mu\epsilon.} \tag{9–72}$$

Equation (9–72) is a very useful relation, because if L is known for a line with a given medium, C can be determined, and vice versa. Knowing C, we can find G from Eq. (9–71). Series resistance R is determined by introducing a small axial E_z as a slight perturbation of the TEM wave and by finding the ohmic power dissipated in a unit length of the line, as was done in Subsection 9–2.1.

Equation (9–72), of course, also holds for a lossless line. ***The velocity of wave propagation on a lossless transmission line, $u_p = 1/\sqrt{LC}$, therefore, is equal to the velocity of propagation, $1/\sqrt{\mu\epsilon}$, of unguided plane wave in the dielectric of the line.*** This fact has been pointed out in connection with Eq. (9–21) for parallel-plate lines.

1. *Two-wire transmission line.* The capacitance per unit length of a two-wire transmission line, whose wires have a radius a and are separated by a distance D, has been found in Eq. (4–47). We have

$$\boxed{C = \frac{\pi\epsilon}{\cosh^{-1}(D/2a)} \quad \text{(F/m).}} \tag{9–73}^{\dagger}$$

From Eqs. (9–72) and (9–71) we obtain

$$\boxed{L = \frac{\mu}{\pi}\cosh^{-1}\left(\frac{D}{2a}\right) \quad \text{(H/m)}} \tag{9–74}^{\dagger}$$

and

$$\boxed{G = \frac{\pi\sigma}{\cosh^{-1}(D/2a)} \quad \text{(S/m).}} \tag{9–75}^{\dagger}$$

---

† $\cosh^{-1}(D/2a) \cong \ln(D/a)$ if $(D/2a)^2 \gg 1$.

To determine R, we go back to Eq. (9–28) and express the ohmic power dissipated per unit length of both wires in terms of p_σ. Assuming the current J_s (A/m) to flow in a very thin surface layer, the current in each wire is $I = 2\pi a J_s$, and

$$P_\sigma = 2\pi a p_\sigma = \frac{1}{2} I^2 \left(\frac{R_s}{2\pi a}\right) \quad \text{(W/m)}. \tag{9–76}$$

Hence the series resistance per unit length for both wires is

$$\boxed{R = 2\left(\frac{R_s}{2\pi a}\right) = \frac{1}{\pi a}\sqrt{\frac{\pi f \mu_c}{\sigma_c}} \quad (\Omega/\text{m}).} \tag{9–77}$$

In deriving Eqs. (9–76) and (9–77), we have assumed the surface current J_s to be uniform over the circumference of both wires. This is an approximation, inasmuch as the proximity of the two wires tends to make the surface current nonuniform.

2. *Coaxial transmission line.* The external inductance per unit length of a coaxial transmission line with a center conductor of radius a and an outer conductor of inner radius b has been found in Eq. (6–140):

$$\boxed{L = \frac{\mu}{2\pi} \ln \frac{b}{a} \quad \text{(H/m)}.} \tag{9–78}$$

From Eq. (9–72) we obtain

$$\boxed{C = \frac{2\pi\epsilon}{\ln (b/a)} \quad \text{(F/m)},} \tag{9–79}$$

and from Eq. (9–71),

$$\boxed{G = \frac{2\pi\sigma}{\ln (b/a)} \quad \text{(S/m)},} \tag{9–80}$$

where σ is the equivalent conductivity of the lossy dielectric. If one prefers, σ could be replaced by $\omega\epsilon''$ as in Eq. (7–112).

To determine R, we again return to Eq. (9–27), where J_{si} on the surface of the center conductor is different from J_{so} on the inner surface of the outer conductor. We must have

$$I = 2\pi a J_{si} = 2\pi b J_{so}. \tag{9–81}$$

The power dissipated in a unit length of the center and outer conductors are, respectively,

$$P_{\sigma i} = 2\pi a p_{\sigma i} = \frac{1}{2} I^2 \left(\frac{R_s}{2\pi a}\right), \tag{9–82}$$

TABLE 9–2
Distributed Parameters of Two-Wire and Coaxial Transmission Lines

Parameter	Two-Wire Line	Coaxial Line	Unit
R	$\frac{R_s}{\pi a}$	$\frac{R_s}{2\pi}\left(\frac{1}{a}+\frac{1}{b}\right)$	Ω/m
L	$\frac{\mu}{\pi}\cosh^{-1}\left(\frac{D}{2a}\right)$	$\frac{\mu}{2\pi}\ln\frac{b}{a}$	H/m
G	$\frac{\pi\sigma}{\cosh^{-1}(D/2a)}$	$\frac{2\pi\sigma}{\ln(b/a)}$	S/m
C	$\frac{\pi\epsilon}{\cosh^{-1}(D/2a)}$	$\frac{2\pi\epsilon}{\ln(b/a)}$	F/m

Note: $R_s = \sqrt{\pi f \mu_c/\sigma_c}$; $\cosh^{-1}(D/2a) \cong \ln(D/a)$ if $(D/2a)^2 \gg 1$. Internal inductance is not included.

$$P_{\sigma o} = 2\pi b p_{\sigma o} = \frac{1}{2} I^2 \left(\frac{R_s}{2\pi b}\right). \tag{9–83}$$

From Eqs. (9–82) and (9–83), we obtain the resistance per unit length:

$$\boxed{R = \frac{R_s}{2\pi}\left(\frac{1}{a}+\frac{1}{b}\right) = \frac{1}{2\pi}\sqrt{\frac{\pi f \mu_c}{\sigma_c}}\left(\frac{1}{a}+\frac{1}{b}\right) \quad (\Omega/\text{m}).} \tag{9–84}$$

The R, L, G, C parameters for two-wire and coaxial transmission lines are listed in Table 9–2.

9–3.3 ATTENUATION CONSTANT FROM POWER RELATIONS

The attenuation constant of a traveling wave on a transmission line is the real part of the propagation constant; it can be determined from the basic definition in Eq. (9–37):

$$\alpha = \mathcal{R}e(\gamma) = \mathcal{R}e[\sqrt{(R + j\omega L)(G + j\omega C)}]. \tag{9–85}$$

The attenuation constant can also be found from a power relationship. The phasor voltage and phasor current distributions on an infinitely long transmission line (no reflections) may be written as (Eqs. (9–40a) and (9–40b) with the plus superscript dropped for simplicity):

$$V(z) = V_0 e^{-(\alpha + j\beta)z}, \tag{9–86a}$$

$$I(z) = \frac{V_0}{Z_0} e^{-(\alpha + j\beta)z}. \tag{9–86b}$$

The time-average power propagated along the line at any z is

$$\begin{aligned} P(z) &= \tfrac{1}{2}\mathscr{R}e[V(z)I^*(z)] \\ &= \frac{V_0^2}{2|Z_0|^2} R_0 e^{-2\alpha z}. \end{aligned} \tag{9-87}$$

The law of conservation of energy requires that the rate of decrease of $P(z)$ with distance along the line equals the time-average power loss P_L per unit length. Thus,

$$\begin{aligned} -\frac{\partial P(z)}{\partial z} &= P_L(z) \\ &= 2\alpha P(z), \end{aligned}$$

from which we obtain the following formula:

$$\boxed{\alpha = \frac{P_L(z)}{2P(z)} \quad \text{(Np/m)}.} \tag{9-88}$$

EXAMPLE 9–4

a) Use Eq. (9–88) to find the attenuation constant of a lossy transmission line with distributed parameters R, L, G, and C.

b) Specialize the result in part (a) to obtain the attenuation constants of a low-loss line and of a distortionless line.

Solution

a) For a lossy transmission line the time-average power loss per unit length is

$$\begin{aligned} P_L(z) &= \tfrac{1}{2}[|I(z)|^2 R + |V(z)|^2 G] \\ &= \frac{V_0^2}{2|Z_0|^2}(R + G|Z_0|^2)e^{-2\alpha z}. \end{aligned} \tag{9-89}$$

Substitution of Eqs. (9–87) and (9–89) in Eq. (9–88) gives

$$\boxed{\alpha = \frac{1}{2R_0}(R + G|Z_0|^2) \quad \text{(Np/m)}.} \tag{9-90}$$

b) For a low-loss line, $Z_0 \cong R_0 = \sqrt{L/C}$, Eq. (9–90) becomes

$$\begin{aligned} \alpha &\cong \frac{1}{2}\left(\frac{R}{R_0} + GR_0\right) \\ &= \frac{1}{2}\left(R\sqrt{\frac{C}{L}} + G\sqrt{\frac{L}{C}}\right), \end{aligned} \tag{9-91}$$

which checks with Eq. (9–55). For a distortionless line, $Z_0 = R_0 = \sqrt{L/C}$, Eq. (9–91) applies, and

$$\alpha = \frac{1}{2} R \sqrt{\frac{C}{L}} \left(1 + \frac{G}{R}\frac{L}{C}\right),$$

which, in view of the condition in Eq. (9–61), reduces to

$$\alpha = R\sqrt{\frac{C}{L}}. \tag{9–92}$$

Equation (9–92) is the same as Eq. (9–63). ■

9–4 Wave Characteristics on Finite Transmission Lines

In Subsection 9–3.1 we indicated that the general solutions for the time-harmonic one-dimensional Helmholtz equations, Eqs. (9–36a) and (9–36b), for transmission lines are

$$V(z) = V_0^+ e^{-\gamma z} + V_0^- e^{\gamma z} \tag{9–93a}$$

and

$$I(z) = I_0^+ e^{-\gamma z} + I_0^- e^{\gamma z}, \tag{9–93b}$$

where

$$\frac{V_0^+}{I_0^+} = -\frac{V_0^-}{I_0^-} = Z_0. \tag{9–94}$$

For waves launched on an infinitely long line at $z = 0$ there can be only forward waves traveling in the $+z$-direction, and the second terms on the right side of Eqs. (9–93a) and (9–93b), representing reflected waves, vanish. This is also true for finite lines terminated in a characteristic impedance; that is, when the lines are ***matched.*** From circuit theory we know that *a maximum transfer of power from a given voltage source to a load occurs under "matched conditions" when the load impedance is the complex conjugate of the source impedance* (Problem P.9–11). In transmission line terminology, ***a line is matched when the load impedance is equal to the characteristic impedance (not the complex conjugate of the characteristic impedance) of the line.***

Let us now consider the general case of a finite transmission line having a characteristic impedance Z_0 terminated in an arbitrary load impedance Z_L, as depicted in Fig. 9–6. The length of the line is ℓ. A *sinusoidal* voltage source $V_g\underline{/0°}$ with an internal impedance Z_g is connected to the line at $z = 0$. In such a case,

$$\left(\frac{V}{I}\right)_{z=\ell} = \frac{V_L}{I_L} = Z_L, \tag{9–95}$$

which obviously cannot be satisfied without the second terms on the right side of Eqs. (9–93a) and (9–93b) unless $Z_L = Z_0$. Thus reflected waves exist on unmatched lines.

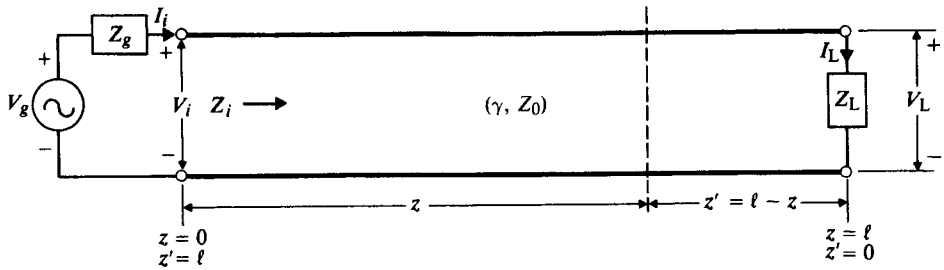

FIGURE 9–6
Finite transmission line terminated with load impedance Z_L.

Given the characteristic γ and Z_0 of the line and its length ℓ, there are four unknowns V_0^+, V_0^-, I_0^+, and I_0^- in Eqs. (9–93a) and (9–93b). These four unknowns are not all independent because they are constrained by the relations at $z = 0$ and at $z = \ell$. Both $V(z)$ and $I(z)$ can be expressed either in terms of V_i and I_i at the input end (Problem P.9–12), or in terms of the conditions at the load end. Consider the latter case.

Let $z = \ell$ in Eqs. (9–93a) and (9–93b). We have

$$V_L = V_0^+ e^{-\gamma\ell} + V_0^- e^{\gamma\ell}, \tag{9–96a}$$

$$I_L = \frac{V_0^+}{Z_0} e^{-\gamma\ell} - \frac{V_0^-}{Z_0} e^{\gamma\ell}. \tag{9–96b}$$

Solving Eqs. (9–96a) and (9–96b) for V_0^+ and V_0^-, we have

$$V_0^+ = \tfrac{1}{2}(V_L + I_L Z_0) e^{\gamma\ell}, \tag{9–97a}$$

$$V_0^- = \tfrac{1}{2}(V_L - I_L Z_0) e^{-\gamma\ell}. \tag{9–97b}$$

Substituting Eq. (9–95) in Eqs. (9–97a) and (9–97b), and using the results in Eqs. (9–93a) and (9–93b), we obtain

$$V(z) = \frac{I_L}{2}[(Z_L + Z_0)e^{\gamma(\ell - z)} + (Z_L - Z_0)e^{-\gamma(\ell - z)}], \tag{9–98a}$$

$$I(z) = \frac{I_L}{2Z_0}[(Z_L + Z_0)e^{\gamma(\ell - z)} - (Z_L - Z_0)e^{-\gamma(\ell - z)}]. \tag{9–98b}$$

Since ℓ and z appear together in the combination $(\ell - z)$, it is expedient to introduce a new variable $z' = \ell - z$, which is the distance measured backward from the load. Equations (9–98a) and (9–98b) then become

$$V(z') = \frac{I_L}{2}[(Z_L + Z_0)e^{\gamma z'} + (Z_L - Z_0)e^{-\gamma z'}], \tag{9–99a}$$

$$I(z') = \frac{I_L}{2Z_0}[(Z_L + Z_0)e^{\gamma z'} - (Z_L - Z_0)e^{-\gamma z'}]. \tag{9–99b}$$

We note here that although the same symbols V and I are used in Eqs. (9–99a) and (9–99b) as in Eqs. (9–98a) and (9–98b), the dependence of $V(z')$ and $I(z')$ on z' is different from the dependence of $V(z)$ and $I(z)$ on z.

The use of hyperbolic functions simplifies the equations above. Recalling the relations

$$e^{\gamma z'} + e^{-\gamma z'} = 2\cosh \gamma z' \qquad \text{and} \qquad e^{\gamma z'} - e^{-\gamma z'} = 2\sinh \gamma z',$$

we may write Eqs. (9–99a) and (9–99b) as

$$V(z') = I_L(Z_L \cosh \gamma z' + Z_0 \sinh \gamma z'), \tag{9–100a}$$

$$I(z') = \frac{I_L}{Z_0}(Z_L \sinh \gamma z' + Z_0 \cosh \gamma z'), \tag{9–100b}$$

which can be used to find the voltage and current at any point along a transmission line in terms of I_L, Z_L, γ, and Z_0.

The ratio $V(z')/I(z')$ is the impedance when we look toward the load end of the line at a distance z' from the load.

$$Z(z') = \frac{V(z')}{I(z')} = Z_0 \frac{Z_L \cosh \gamma z' + Z_0 \sinh \gamma z'}{Z_L \sinh \gamma z' + Z_0 \cosh \gamma z'} \tag{9–101}$$

or

$$Z(z') = Z_0 \frac{Z_L + Z_0 \tanh \gamma z'}{Z_0 + Z_L \tanh \gamma z'} \quad (\Omega). \tag{9–102}$$

At the source end of the line, $z' = \ell$, the generator looking into the line sees an ***input impedance*** Z_i.

$$Z_i = (Z)_{\substack{z=0 \\ z'=\ell}} = Z_0 \frac{Z_L + Z_0 \tanh \gamma \ell}{Z_0 + Z_L \tanh \gamma \ell} \quad (\Omega). \tag{9–103}$$

As far as the conditions at the generator are concerned, the terminated finite transmission line can be replaced by Z_i, as shown in Fig. 9–7. The input voltage V_i and input current I_i in Fig. 9–6 are found easily from the equivalent circuit in Fig. 9–7.

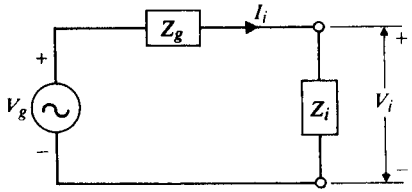

FIGURE 9–7
Equivalent circuit for finite transmission line in Figure 9–6 at generator end.

They are

$$V_i = \frac{Z_i}{Z_g + Z_i} V_g, \tag{9-104a}$$

$$I_i = \frac{V_g}{Z_g + Z_i}. \tag{9-104b}$$

Of course, the voltage and current at any other location on line cannot be determined by using the equivalent circuit in Fig. 9–7.

The average power delivered by the generator to the input terminals of the line is

$$(P_{av})_i = \tfrac{1}{2}\mathscr{R}e[V_i I_i^*]_{z=0,\, z'=\ell}. \tag{9-105}$$

The average power delivered to the load is

$$\begin{aligned}(P_{av})_L &= \tfrac{1}{2}\mathscr{R}e[V_L I_L^*]_{z=\ell,\, z'=0} \\ &= \frac{1}{2}\left|\frac{V_L}{Z_L}\right|^2 R_L = \frac{1}{2}|I_L|^2 R_L.\end{aligned} \tag{9-106}$$

For a lossless line, conservation of power requires that $(P_{av})_i = (P_{av})_L$.

A particularly important special case is when a line is terminated with its characteristic impedance—that is, when $Z_L = Z_0$. The input impedance, Z_i in Eq. (9–103), is seen to be equal to Z_0. As a matter of fact, the impedance of the line looking toward the load at any distance z' from the load is, from Eq. (9–102),

$$Z(z') = Z_0 \qquad (\text{for } Z_L = Z_0). \tag{9-107}$$

The voltage and current equations in Eqs. (9–98a) and (9–98b) reduce to

$$V(z) = (I_L Z_0 e^{\gamma\ell})e^{-\gamma z} = V_i e^{-\gamma z}, \tag{9-108a}$$

$$I(z) = (I_L e^{\gamma\ell})e^{-\gamma z} = I_i e^{-\gamma z}. \tag{9-108b}$$

Equations (9–108a) and (9–108b) correspond to the pair of voltage and current equations—Eqs. (9–40a) and (9–40b)—representing waves traveling in $+z$-direction, and there are no reflected waves. Hence, ***when a finite transmission line is terminated with its own characteristic impedance (when a finite transmission line is matched), the voltage and current distributions on the line are exactly the same as though the line has been extended to infinity.***

EXAMPLE 9–5 A signal generator having an internal resistance 1 (Ω) and an open-circuit voltage $v_g(t) = 0.3 \cos 2\pi 10^8 t$ (V) is connected to a 50 (Ω) lossless transmission line. The line is 4 (m) long, and the velocity of wave propagation on the line is 2.5×10^8 (m/s). For a matched load, find (a) the instantaneous expressions for the voltage and current at an arbitrary location on the line, (b) the instantaneous expressions for the voltage and current at the load, and (c) the average power transmitted to the load.

Solution

a) In order to find the voltage and current at an arbitrary location on the line, it is first necessary to obtain those at the input end ($z = 0$, $z' = \ell$). The given quantities are as follows:

$$\begin{aligned} V_g &= 0.3\underline{/0^\circ} \quad \text{(V)}, \qquad \text{a phasor with a cosine reference,} \\ Z_g &= R_g = 1 \quad (\Omega), \\ Z_0 &= R_0 = 50 \quad (\Omega), \\ \omega &= 2\pi \times 10^8 \quad \text{(rad/s)}, \\ u_p &= 2.5 \times 10^8 \quad \text{(m/s)}, \\ \ell &= 4 \quad \text{(m)}. \end{aligned}$$

Since the line is terminated with a matched load, $Z_i = Z_0 = 50\ (\Omega)$. The voltage and current at the input terminals can be evaluated from the equivalent circuit in Fig. 9–7. From Eqs. (9–104a) and (9–104b) we have

$$V_i = \frac{50}{1 + 50} \times 0.3\underline{/0^\circ} = 0.294\underline{/0^\circ} \quad \text{(V)},$$

$$I_i = \frac{0.3\underline{/0^\circ}}{1 + 50} = 0.0059\underline{/0^\circ} \quad \text{(A)}.$$

Since only forward-traveling waves exist on a matched line, we use Eqs. (9–86a) and (9–86b) for the voltage and current, respectively, at an arbitrary location. For the given line, $\alpha = 0$ and

$$\beta = \frac{\omega}{u_p} = \frac{2\pi \times 10^8}{2.5 \times 10^8} = 0.8\pi \quad \text{(rad/m)}.$$

Thus,

$$\begin{aligned} V(z) &= 0.294e^{-j0.8\pi z} \quad \text{(V)}, \\ I(z) &= 0.0059e^{-j0.8\pi z} \quad \text{(A)}. \end{aligned}$$

These are phasors. The corresponding instantaneous expressions are, from Eqs. (9–34a) and (9–34b),

$$\begin{aligned} v(z, t) &= \mathscr{R}e[0.294e^{j(2\pi 10^8 t - 0.8\pi z)}] \\ &= 0.294 \cos (2\pi 10^8 t - 0.8\pi z) \quad \text{(V)}, \\ i(z, t) &= \mathscr{R}e[0.0059e^{j(2\pi 10^8 t - 0.8\pi z)}] \\ &= 0.0059 \cos (2\pi 10^8 t - 0.8\pi z) \quad \text{(A)}. \end{aligned}$$

b) At the load, $z = \ell = 4$ (m),

$$\begin{aligned} v(4, t) &= 0.294 \cos (2\pi 10^8 t - 3.2\pi) \quad \text{(V)}, \\ i(4, t) &= 0.0059 \cos (2\pi 10^8 t - 3.2\pi) \quad \text{(A)}. \end{aligned}$$

c) The average power transmitted to the load on a lossless line is equal to that at the input terminals.

$$\begin{aligned} (P_{av})_L &= (P_{av})_i = \tfrac{1}{2}\mathscr{R}e[V(z)I^*(z)] \\ &= \tfrac{1}{2}(0.294 \times 0.0059) = 8.7 \times 10^{-4}\ \text{(W)} = 0.87 \quad \text{(mW)}. \end{aligned}$$

9-4.1 TRANSMISSION LINES AS CIRCUIT ELEMENTS

Not only can transmission lines be used as wave-guiding structures for transferring power and information from one point to another, but at ultrahigh frequencies—UHF: frequency from 300 (MHz) to 3 (GHz), wavelength from 1 (m) to 0.1 (m)—they may serve as circuit elements. At these frequencies, ordinary lumped-circuit elements are difficult to make, and stray fields become important. Sections of transmission lines can be designed to give an inductive or capacitive impedance and are used to match an arbitrary load to the internal impedance of a generator for maximum power transfer. The required length of such lines as circuit elements becomes practical in the UHF range. At frequencies much lower than 300 (MHz) the required lines tend to be too long, whereas at frequencies higher than 3 (GHz) the physical dimensions become inconveniently small, and it would be advantageous to use waveguide components.

In most cases, transmission-line segments can be considered lossless: $\gamma = j\beta$, $Z_0 = R_0$, and $\tanh \gamma\ell = \tanh(j\beta\ell) = j \tan \beta\ell$. The formula in Eq. (9–103) for the input impedance Z_i of a lossless line of length ℓ terminated in Z_L becomes

$$\boxed{Z_i = R_0 \frac{Z_L + jR_0 \tan \beta\ell}{R_0 + jZ_L \tan \beta\ell} \quad (\Omega).} \qquad (9\text{–}109)$$

(Lossless line)

Comparison of Eq. (9–109) with Eq. (8–171) again confirms the similarity between normal incidence of a uniform plane wave on a plane interface and wave propagation along a terminated transmission line.

We now consider several important special cases.

1. *Open-circuit termination* ($Z_L \to \infty$). We have, from Eq. (9–109),

$$Z_{io} = jX_{io} = -\frac{jR_0}{\tan \beta\ell} = -jR_0 \cot \beta\ell. \qquad (9\text{–}110)$$

Equation (9–110) shows that the input impedance of an open-circuited lossless line is purely reactive. The line can, however, be either capacitive or inductive because the function cot $\beta\ell$ can be either positive or negative, depending on the value of $\beta\ell$ ($= 2\pi\ell/\lambda$). Figure 9–8 is a plot of $X_{io} = -R_0 \cot \beta\ell$ versus ℓ. We see that X_{io} can assume all values from $-\infty$ to $+\infty$.

When the length of an open-circuited line is very short in comparison with a wavelength, $\beta\ell \ll 1$, we can obtain a very simple formula for its capacitive reactance by noting that $\tan \beta\ell \cong \beta\ell$. From Eq. (9–110) we have

$$Z_{io} = jX_{io} \cong -j\frac{R_0}{\beta\ell} = -j\frac{\sqrt{L/C}}{\omega\sqrt{LC}\ell} = -j\frac{1}{\omega C\ell}, \qquad (9\text{–}111)$$

which is the impedance of a capacitance of $C\ell$ farads.

In practice, it is not possible to obtain an infinite load impedance at the end of a transmission line, especially at high frequencies, because of coupling to nearby objects and because of radiation from the open end.

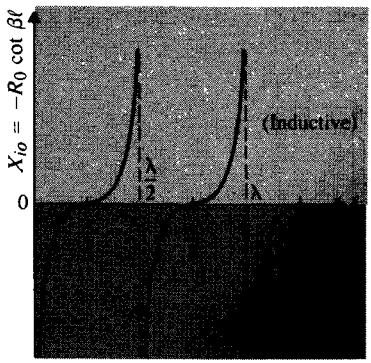

FIGURE 9–8
Input reactance of open-circuited transmission line.

2. *Short-circuit termination* ($Z_L = 0$). In this case, Eq. (9–109) reduces to

$$Z_{is} = jX_{is} = jR_0 \tan \beta\ell. \tag{9–112}$$

Since tan $\beta\ell$ can range from $-\infty$ to $+\infty$, the input impedance of a short-circuited lossless line can also be either purely inductive or purely capacitive, depending on the value of $\beta\ell$. Figure 9–9 is a graph of X_{is} versus ℓ. We note that Eq. (9–112) has exactly the same form as that—Eq. (8–172)—of the wave impedance of the total field at a distance ℓ from a perfectly conducting plane boundary.

Comparing Figs. 9–8 and 9–9, we see that in the range where X_{io} is capacitive X_{is} is inductive, and vice versa. The input reactances of open-circuited and short-circuited lossless transmission lines are the same if their lengths differ by an odd multiple of $\lambda/4$.

When the length of a short-circuited line is very short in comparison with a wavelength, $\beta\ell \ll 1$, Eq. (9–112) becomes approximately

$$Z_{is} = jX_{is} \cong jR_0\beta\ell = j\sqrt{\frac{L}{C}}\,\omega\sqrt{LC}\ell = j\omega L\ell, \tag{9–113}$$

which is the impedance of an inductance of $L\ell$ henries.

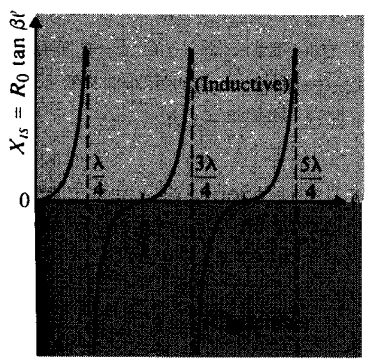

FIGURE 9–9
Input reactance of short-circuited transmission line.

3. *Quarter-wave section* ($\ell = \lambda/4$, $\beta\ell = \pi/2$). When the length of a line is an odd multiple of $\lambda/4$, $\ell = (2n-1)\lambda/4$, $(n = 1, 2, 3, \ldots)$,

$$\beta\ell = \frac{2\pi}{\lambda}(2n-1)\frac{\lambda}{4} = (2n-1)\frac{\pi}{2},$$

$$\tan\beta\ell = \tan\left[(2n-1)\frac{\pi}{2}\right] \to \pm\infty,$$

and Eq. (9–109) becomes

$$\boxed{Z_i = \frac{R_0^2}{Z_L} \qquad \text{(Quarter-wave line).}} \tag{9–114}$$

Hence, ***a quarter-wave lossless line transforms the load impedance to the input terminals as its inverse multiplied by the square of the characteristic resistance.*** It acts as an impedance inverter and is often referred to as a ***quarter-wave transformer.*** An open-circuited, quarter-wave line appears as a short circuit at the input terminals, and a short-circuited quarter-wave line appears as an open circuit. Actually, if the series resistance of the line itself is not neglected, the input impedance of a short-circuited, quarter-wave line is an impedance of a very high value similar to that of a parallel resonant circuit. It is interesting to compare Eq. (9–114) with the formula for quarter-wave impedance transformation with multiple dielectrics, Eq. (8–182a).

4. *Half-wave section* ($\ell = \lambda/2$, $\beta\ell = \pi$). When the length of a line is an integral multiple of $\lambda/2$, $\ell = n\lambda/2$ $(n = 1, 2, 3, \ldots)$,

$$\beta\ell = \frac{2\pi}{\lambda}\left(\frac{n\lambda}{2}\right) = n\pi,$$

$$\tan\beta\ell = 0,$$

and Eq. (9–109) reduces to

$$\boxed{Z_i = Z_L \qquad \text{(Half-wave line).}} \tag{9–115}$$

Equation (9–115) states that ***a half-wave lossless line transfers the load impedance to the input terminals without change.*** From Eq. (9–103) we observe that a half-wave line with loss does not have this property unless $Z_L = Z_0$.

By measuring the input impedance of a line section under open- and short-circuit conditions, we can determine the characteristic impedance and the propagation constant of the line. The following expressions follow directly from Eq. (9–103).

Open-circuited line, $Z_L \to \infty$: $\quad Z_{io} = Z_0 \coth\gamma\ell.$ (9–116)

Short-circuited line, $Z_L = 0$: $\quad Z_{is} = Z_0 \tanh\gamma\ell.$ (9–117)

From Eqs. (9–116) and (9–117) we have

$$\boxed{Z_0 = \sqrt{Z_{io}Z_{is}} \quad (\Omega)} \tag{9–118}$$

and

$$\boxed{\gamma = \frac{1}{\ell}\tanh^{-1}\sqrt{\frac{Z_{is}}{Z_{io}}} \quad (\text{m}^{-1}).} \tag{9–119}$$

Equations (9–118) and (9–119) apply whether or not the line is lossy.

EXAMPLE 9–6 The open-circuit and short-circuit impedances measured at the input terminals of a lossless transmission line of length 1.5 (m), which is less than a quarter wavelength, are $-j54.6$ (Ω) and $j103$ (Ω), respectively. (a) Find Z_0 and γ of the line. (b) Without changing the operating frequency, find the input impedance of a short-circuited line that is twice the given length. (c) How long should the short-circuited line be in order for it to appear as an open circuit at the input terminals?

Solution The given quantities are

$$Z_{io} = -j54.6, \qquad Z_{is} = j103, \qquad \ell = 1.5.$$

a) Using Eqs. (9–118) and (9–119), we find

$$Z_0 = \sqrt{-j54.6(j103)} = 75 \quad (\Omega)$$

$$\gamma = \frac{1}{1.5}\tanh^{-1}\sqrt{\frac{j103}{-j54.6}} = \frac{j}{1.5}\tan^{-1}1.373 = j0.628 \quad (\text{rad/m}).$$

b) For a short-circuited line twice as long, $\ell = 3.0$ (m),

$$\gamma\ell = j0.628 \times 3.0 = j1.884 \quad (\text{rad}).$$

The input impedance is, from Eq. (9–117),

$$Z_{is} = 75\tanh(j1.884) = j75\tan 108°$$
$$= j75(-3.08) = -j231 \quad (\Omega).$$

Note that Z_{is} for the 3 (m) line is now a capacitive reactance, whereas that for the 1.5 (m) line in part (a) is an inductive reactance. We may conclude from Fig. 9–9 that $1.5\ (\text{m}) < \lambda/4 < 3.0\ (\text{m})$.

c) In order for a short-circuited line to appear as an open circuit at the input terminals, it should be an odd multiple of a quarter-wavelength long:

$$\lambda = \frac{2\pi}{\beta} = \frac{2\pi}{0.628} = 10 \quad (\text{m}).$$

Hence the required line length is

$$\ell = \frac{\lambda}{4} + (n-1)\frac{\lambda}{2}$$
$$= 2.5 + 5(n-1) \quad (\text{m}), \qquad n = 1, 2, 3, \ldots.$$

So far in this subsection we have considered only open- and short-circuited lossless lines as circuit elements. We have seen in Figs. 9–8 and 9–9 that, depending on the length of the line, the input impedance of an open- or short-circuited lossless line can be either purely inductive or purely capacitive. Let us now examine the input impedance of a lossy line with a short-circuit termination. When the line length is a multiple of $\lambda/2$, the input impedance will not vanish as in Fig. 9–9. Instead, we have, from Eq. (9–117),

$$\begin{aligned} Z_{is} &= Z_0 \tanh \gamma\ell = Z_0 \frac{\sinh (\alpha + j\beta)\ell}{\cosh (\alpha + j\beta)\ell} \\ &= Z_0 \frac{\sinh \alpha\ell \cos \beta\ell + j \cosh \alpha\ell \sin \beta\ell}{\cosh \alpha\ell \cos \beta\ell + j \sinh \alpha\ell \sin \beta\ell}. \end{aligned} \tag{9–120}$$

For $\ell = n\lambda/2$, $\beta\ell = n\pi$, $\sin \beta\ell = 0$, Eq. (9–120) reduces to

$$Z_{is} = Z_0 \tanh \alpha\ell \cong Z_0(\alpha\ell), \tag{9–121}$$

where we have assumed a low-loss line: $\alpha\ell \ll 1$ and $\tanh \alpha\ell \cong \alpha\ell$. The quantity Z_{is} in Eq. (9–121) is small but not zero. At $\ell = n\lambda/2$ we have the condition of a series-resonant circuit.

When the length of a shorted lossy line is an odd multiple of $\lambda/4$, the input impedance will not go to infinity as indicated in Fig. 9–9. For $\ell = n\lambda/4$, $\beta\ell = n\pi/2$ (n = odd), $\cos \beta\ell = 0$, and Eq. (9–120) becomes

$$Z_{is} = \frac{Z_0}{\tanh \alpha\ell} \cong \frac{Z_0}{\alpha\ell}, \tag{9–122}$$

which is large but not infinite. We have the condition of a parallel-resonant circuit. It is a frequency-selective circuit, and we can determine the ***quality factor***, or Q, of such a circuit by first finding its ***half-power bandwidth***, or simply the ***bandwidth***. The bandwidth of a parallel-resonant circuit is the frequency range $\Delta f = f_2 - f_1$ around the resonant frequency f_0, where $f_2 = f_0 + \Delta f/2$ and $f_1 = f_0 - \Delta f/2$ are half-power frequencies at which the voltage across the parallel circuit is $1/\sqrt{2}$ or 70.7% of its maximum value at f_0 (assuming a constant-current source). Hence the associated power, which is proportional to $|Z_{is}|^2$ and is maximum at f_0, is one-half of its value at f_1 and f_2.

Let $f = f_0 + \delta f$, where δf is a small frequency shift from the resonant frequency. We have

$$\begin{aligned} \beta\ell &= \frac{2\pi f}{u_p}\ell = \frac{2\pi(f_0 + \delta f)}{u_p}\ell \\ &= \frac{n\pi}{2} + \frac{n\pi}{2}\left(\frac{\delta f}{f_0}\right), \qquad n = \text{odd}, \end{aligned} \tag{9–123}$$

$$\cos \beta\ell = -\sin\left[\frac{n\pi}{2}\left(\frac{\delta f}{f_0}\right)\right] \cong -\frac{n\pi}{2}\left(\frac{\delta f}{f_0}\right), \tag{9–124}$$

$$\sin \beta\ell = \cos\left[\frac{n\pi}{2}\left(\frac{\delta f}{f_0}\right)\right] \cong 1, \tag{9–125}$$

where we have assumed $(n\pi/2)(\delta f/f_0) \ll 1$. Substituting Eqs. (9–123), (9–124), and (9–125) in Eq. (9–120), noting that $\alpha\ell \ll 1$, and retaining only small terms of the first order, we obtain

$$Z_{is} = \frac{Z_0}{\alpha\ell + j\dfrac{n\pi}{2}\left(\dfrac{\delta f}{f_0}\right)} \tag{9–126}$$

and

$$|Z_{is}|^2 = \frac{|Z_0|^2}{(\alpha\ell)^2 + \left[\dfrac{n\pi}{2}\left(\dfrac{\delta f}{f_0}\right)\right]^2}. \tag{9–127}$$

At $f = f_0$, $\delta f = 0$, $|Z_{is}|^2$ is a maximum and equals $|Z_{is}|^2_{\max} = |Z_0|^2/(\alpha\ell)^2$. Thus,

$$\frac{|Z_{is}|^2}{|Z_{is}|^2_{\max}} = \frac{1}{1 + \left[\dfrac{n\pi}{2\alpha\ell}\left(\dfrac{\delta f}{f_0}\right)\right]^2}. \tag{9–128}$$

When $\delta f = \pm\Delta f/2$, we have the half-power frequencies f_2 and f_1, at which the ratio in Eq. (9–128) equals $\frac{1}{2}$, or

$$\frac{n\pi}{2\alpha\ell}\left(\frac{\Delta f}{2f_0}\right) = \frac{\beta}{2\alpha}\left(\frac{\Delta f}{f_0}\right) = 1, \qquad n = \text{odd}. \tag{9–129}$$

Therefore, the Q of the parallel-resonant circuit (a shorted lossy line having a length equal to an odd multiple of $\lambda/4$) is

$$\boxed{Q = \frac{f_0}{\Delta f} = \frac{\beta}{2\alpha}.} \tag{9–130}$$

Using the expressions of α and β for a low-loss line in Eqs. (9–55) and (9–56), we obtain

$$Q = \frac{\omega L}{R + GL/C} = \frac{1}{[(R/\omega L) + (G/\omega C)]}. \tag{9–131}$$

For a well-insulated line, $GL/C \ll R$, and Eq. (9–131) reduces to the familiar expression for the Q of a parallel-resonant circuit:

$$Q = \frac{\omega L}{R}. \tag{9–132}$$

In a similar manner an analysis can be made for the resonant behavior of an open-circuited low-loss transmission line whose length is an odd multiple of $\lambda/4$ (series resonance) or a multiple of $\lambda/2$ (parallel resonance). (See Problem P.9–21.)

EXAMPLE 9–7 The measured attenuation of an air-dielectric coaxial transmission line at 400 (MHz) is 0.01 (dB/m). Determine the Q and the half-power bandwidth of a quarter-wavelength section of the line with a short-circuit termination.

Solution At $f = 4 \times 10^8$ (Hz),

$$\lambda = \frac{c}{f} = \frac{3 \times 10^8}{4 \times 10^8} = 0.75 \quad \text{(m)},$$

$$\beta = \frac{2\pi}{\lambda} = \frac{2\pi}{0.75} = 8.38 \quad \text{(rad/m)},$$

$$\alpha = 0.01 \text{ (dB/m)} = \frac{0.01}{8.69} \quad \text{(Np/m)}.$$

Therefore,

$$Q = \frac{\beta}{2\alpha} = \frac{8.38 \times 8.69}{2 \times 0.01} = 3641,$$

which is much higher than the Q obtainable from any lumped-element parallel-resonant circuit at 400 (MHz). The half-power bandwidth is

$$\Delta f = \frac{f_0}{Q} = \frac{4 \times 10^8}{3641} = 0.11 \times 10^6 \quad \text{(Hz)}$$
$$= 0.11 \quad \text{(MHz)}, \quad \text{or } 110 \quad \text{(kHz)}. \qquad \blacksquare$$

9–4.2 LINES WITH RESISTIVE TERMINATION

When a transmission line is terminated in a load impedance Z_L different from the characteristic impedance Z_0, both an incident wave (from the generator) and a reflected wave (from the load) exist. Equation (9–99a) gives the phasor expression for the voltage at any distance $z' = \ell - z$ from the load end. Note that in Eq. (9–99a), the term with $e^{\gamma z'}$ represents the incident voltage wave and the term with $e^{-\gamma z'}$ represents the reflected voltage wave. We may write

$$V(z') = \frac{I_L}{2}(Z_L + Z_0)e^{\gamma z'}\left[1 + \frac{Z_L - Z_0}{Z_L + Z_0}e^{-2\gamma z'}\right]$$
$$= \frac{I_L}{2}(Z_L + Z_0)e^{\gamma z'}[1 + \Gamma e^{-2\gamma z'}], \qquad (9\text{–}133a)$$

where

$$\boxed{\Gamma = \frac{Z_L - Z_0}{Z_L + Z_0} = |\Gamma|e^{j\theta_\Gamma} \quad \text{(Dimensionless)}} \qquad (9\text{–}134)$$

is the ratio of the complex amplitudes of the reflected and incident voltage waves at the load ($z' = 0$) and is called the ***voltage reflection coefficient*** of the load impedance Z_L. It is of the same form as the definition of the reflection coefficient in Eq. (8–140) for a plane wave incident normally on a plane interface between two dielectric media. It is, in general, a complex quantity with a magnitude $|\Gamma| \leq 1$. The current equation

corresponding to $V(z')$ in Eq. (9–133a) is, from Eq. (9–99b),

$$I(z') = \frac{I_L}{2Z_0}(Z_L + Z_0)e^{\gamma z'}[1 - \Gamma e^{-2\gamma z'}]. \tag{9–133b}$$

The current reflection coefficient defined as the ratio of the complex amplitudes of the reflected and incident current waves, I_0^-/I_0^+, is different from the voltage reflection coefficient. As a matter of fact, the former is the negative of the latter, inasmuch as $I_0^-/I_0^+ = -V_0^-/V_0^+$, as is evident from Eq. (9–94). In what follows we shall refer only to the voltage reflection coefficient.

For a *lossless* transmission line, $\gamma = j\beta$, Eqs. (9–133a) and (9–133b) become

$$\begin{aligned} V(z') &= \frac{I_L}{2}(Z_L + R_0)e^{j\beta z'}[1 + \Gamma e^{-j2\beta z'}] \\ &= \frac{I_L}{2}(Z_L + R_0)e^{j\beta z'}[1 + |\Gamma|e^{j(\theta_\Gamma - 2\beta z')}] \end{aligned} \tag{9–135a}$$

and

$$I(z') = \frac{I_L}{2R_0}(Z_L + R_0)e^{j\beta z'}[1 - |\Gamma|e^{j(\theta_\Gamma - 2\beta z')}]. \tag{9–135b}$$

The voltage and current phasors on a lossless line are more easily visualized from Eqs. (9–100a) and (9–100b) by setting $\gamma = j\beta$ and $V_L = I_L Z_L$. Noting that $\cosh j\theta = \cos\theta$, and $\sinh j\theta = j\sin\theta$, we obtain

$$\boxed{\begin{aligned} V(z') &= V_L \cos\beta z' + jI_L R_0 \sin\beta z', \qquad (9–136a) \\ I(z') &= I_L \cos\beta z' + j\frac{V_L}{R_0}\sin\beta z'. \qquad (9–136b) \end{aligned}}$$

(Lossless line)

If the terminating impedance is purely resistive, $Z_L = R_L$, $V_L = I_L R_L$, the voltage and current magnitudes are given by

$$|V(z')| = V_L\sqrt{\cos^2\beta z' + (R_0/R_L)^2\sin^2\beta z'}, \tag{9–137a}$$

$$|I(z')| = I_L\sqrt{\cos^2\beta z' + (R_L/R_0)^2\sin^2\beta z'}, \tag{9–137b}$$

where $R_0 = \sqrt{L/C}$. Plots of $|V(z')|$ and $|I(z')|$ as functions of z' are standing waves with their maxima and minima occurring at fixed locations along the line.

Analogously to the plane-wave case in Eq. (8–147), we define the ratio of the maximum to the minimum voltages along a finite, terminated line as the ***standing-wave ratio*** **(SWR)**, S:

$$\boxed{S = \frac{|V_{max}|}{|V_{min}|} = \frac{1 + |\Gamma|}{1 - |\Gamma|} \qquad \text{(Dimensionless).}} \tag{9–138}$$

The inverse relation of Eq. (9–138) is

$$\boxed{|\Gamma| = \frac{S-1}{S+1} \qquad \text{(Dimensionless).}} \tag{9–139}$$

It is clear from Eqs. (9–138) and (9–139) that on a lossless transmission line

$$\Gamma = 0, \qquad S = 1 \qquad \text{when } Z_L = Z_0 \text{ (Matched load);}$$
$$\Gamma = -1, \qquad S \to \infty \qquad \text{when } Z_L = 0 \text{ (Short circuit);}$$
$$\Gamma = +1, \qquad S \to \infty \qquad \text{when } Z_L \to \infty \text{ (Open circuit).}$$

Because of the wide range of S, it is customary to express it on a logarithmic scale: $20 \log_{10} S$ in (dB). Standing-wave ratio S defined in terms of $|I_{max}|/|I_{min}|$ results in the same expression as that defined in terms of $|V_{max}|/|V_{min}|$ in Eq. (9–138). A high standing-wave ratio on a line is undesirable because it results in a large power loss.

Examination of Eqs. (9–135a) and (9–135b) reveals that $|V_{max}|$ and $|I_{min}|$ occur together when

$$\theta_\Gamma - 2\beta z'_M = -2n\pi, \qquad n = 0, 1, 2, \ldots. \tag{9–140}$$

On the other hand, $|V_{min}|$ and $|I_{max}|$ occur together when

$$\theta_\Gamma - 2\beta z'_m = -(2n+1)\pi, \qquad n = 0, 1, 2, \ldots. \tag{9–141}$$

For resistive terminations on a lossless line, $Z_L = R_L$, $Z_0 = R_0$, and Eq. (9–134) simplifies to

$$\Gamma = \frac{R_L - R_0}{R_L + R_0} \qquad \text{(Resistive load).} \tag{9–142}$$

The voltage reflection coefficient is therefore purely real. Two cases are possible.

1. $R_L > R_0$. In this case, Γ is positive real and $\theta_\Gamma = 0$. At the termination, $z' = 0$, and condition (9–140) is satisfied (for $n = 0$). This means that a voltage maximum (current minimum) will occur at the terminating resistance. Other maxima of the voltage standing wave (minima of the current standing wave) will be located at $2\beta z' = 2n\pi$, or $z' = n\lambda/2$ ($n = 1, 2, \ldots$) from the load.
2. $R_L < R_0$. Equation (9–142) shows that Γ will be negative real and $\theta_\Gamma = -\pi$. At the termination, $z' = 0$, and condition (9–141) is satisfied (for $n = 0$). A voltage minimum (current maximum) will occur at the terminating resistance. Other minima of the voltage standing wave (maxima of the current standing wave) will be located at $z' = n\lambda/2$ ($n = 1, 2, \ldots$) from the load. The roles of the voltage and current standing waves are interchanged from those for the case of $R_L > R_0$.

Figure 9–10 illustrates some typical standing waves for a lossless line with resistive termination.

The standing waves on an open-circuited line are similar to those on a resistance-terminated line with $R_L > R_0$, except that the $|V(z')|$ and $|I(z')|$ curves are now magnitudes of sinusoidal functions of the distance z' from the load. This is seen from

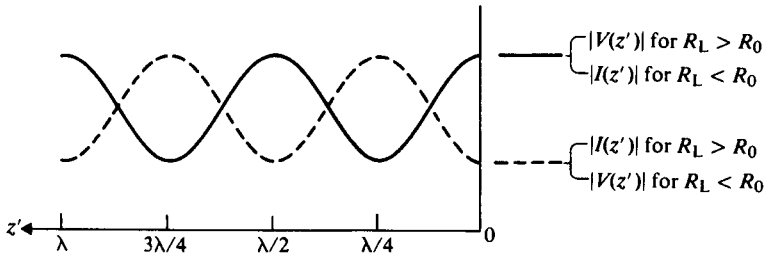

FIGURE 9–10
Voltage and current standing waves on resistance-terminated lossless lines.

Eqs. (9–137a) and (9–137b), by letting $R_L \to \infty$. Of course, $I_L = 0$, but V_L is finite. We have

$$|V(z')| = V_L|\cos \beta z'|, \tag{9–143a}$$

$$|I(z')| = \frac{V_L}{R_0}|\sin \beta z'|. \tag{9–143b}$$

All the minima go to zero. For an open-circuited line, $\Gamma = 1$ and $S \to \infty$.

On the other hand, the standing waves on a short-circuited line are similar to those on a resistance-terminated line with $R_L < R_0$. Here $R_L = 0$, $V_L = 0$, but I_L is finite. Equations (9–137a) and (9–137b) reduce to

$$|V(z')| = I_L R_0|\sin \beta z'|, \tag{9–144a}$$

$$|I(z')| = I_L|\cos \beta z'|. \tag{9–144b}$$

Typical standing waves for open- and short-circuited lossless lines are shown in Fig. 9–11.

EXAMPLE 9–8 The standing-wave ratio S on a transmission line is an easily measurable quantity. (a) Show how the value of a terminating resistance on a lossless line of known characteristic impedance R_0 can be determined by measuring S. (b) What

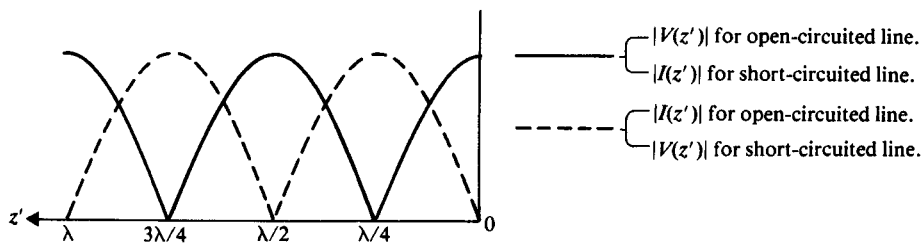

FIGURE 9–11
Voltage and current standing waves on open- and short-circuited lossless lines.

is the impedance of the line looking toward the load at a distance equal to one quarter of the operating wavelength?

Solution

a) Since the terminating impedance is purely resistive, $Z_L = R_L$, we can determine whether R_L is greater than R_0 (if there are voltage maxima at $z' = 0, \lambda/2, \lambda$, etc.) or whether R_L is less than R_0 (if there are voltage minima at $z' = 0, \lambda/2, \lambda$, etc.). This can be easily ascertained by measurements.

First, if $R_L > R_0$, $\theta_\Gamma = 0$. Both $|V_{max}|$ and $|I_{min}|$ occur at $\beta z' = 0$; and $|V_{min}|$ and $|I_{max}|$ occur at $\beta z' = \pi/2$. We have, from Eqs. (9–136a) and (9–136b),

$$|V_{max}| = V_L, \qquad |V_{min}| = V_L \frac{R_0}{R_L};$$

$$|I_{min}| = I_L, \qquad |I_{max}| = I_L \frac{R_L}{R_0}.$$

Thus,

$$\frac{|V_{max}|}{|V_{min}|} = \frac{|I_{max}|}{|I_{min}|} = S = \frac{R_L}{R_0}$$

or

$$R_L = SR_0. \tag{9–145}$$

Second, if $R_L < R_0$, $\theta_\Gamma = -\pi$. Both $|V_{min}|$ and $|I_{max}|$ occur at $\beta z' = 0$; and $|V_{max}|$ and $|I_{min}|$ occur at $\beta z' = \pi/2$. We have

$$|V_{min}| = V_L, \qquad |V_{max}| = V_L \frac{R_0}{R_L};$$

$$|I_{max}| = I_L, \qquad |I_{min}| = I_L \frac{R_L}{R_0}.$$

Therefore,

$$\frac{|V_{max}|}{|V_{min}|} = \frac{|I_{max}|}{|I_{min}|} = S = \frac{R_0}{R_L}$$

or

$$R_L = \frac{R_0}{S}. \tag{9–146}$$

b) The operating wavelength, λ, can be determined from twice the distance between two neighboring voltage (or current) maxima or minima. At $z' = \lambda/4$, $\beta z' = \pi/2$, $\cos \beta z' = 0$, and $\sin \beta z' = 1$. Equations (9–136a) and (9–136b) become

$$V(\lambda/4) = jI_L R_0,$$

$$I(\lambda/4) = j \frac{V_L}{R_0}.$$

(*Question:* What is the significance of the j in these equations?) The ratio of $V(\lambda/4)$ to $I(\lambda/4)$ is the input impedance of a quarter-wavelength, resistively terminated,

lossless line.

$$Z_i(z' = \lambda/4) = R_i = \frac{V(\lambda/4)}{I(\lambda/4)} = \frac{R_0^2}{R_L}.$$

This result is anticipated because of the impedance-transformation property of a quarter-wave line given in Eq. (9–114). ■

9–4.3 LINES WITH ARBITRARY TERMINATION

In the preceding subsection we noted that the standing wave on a *resistively terminated* lossless transmission line is such that a voltage maximum (a current minimum) occurs at the termination where $z' = 0$ if $R_L > R_0$, and a voltage minimum (a current maximum) occurs there if $R_L < R_0$. What will happen if the terminating impedance is not a pure resistance? It is intuitively correct to expect that a voltage maximum or minimum will not occur at the termination and that both will be shifted away from the termination. In this subsection we will show that information on the direction and amount of this shift can be used to determine the terminating impedance.

Let the terminating (or load) impedance be $Z_L = R_L + jX_L$, and assume the voltage standing wave on the line to look like that depicted in Fig. 9–12. We note that neither a voltage maximum nor a voltage minimum appears at the load at $z' = 0$. If we let the standing wave continue, say, by an extra distance ℓ_m, it will reach a minimum. The voltage minimum is where it should be if the original terminating impedance Z_L is replaced by a line section of length ℓ_m terminated by a pure resistance

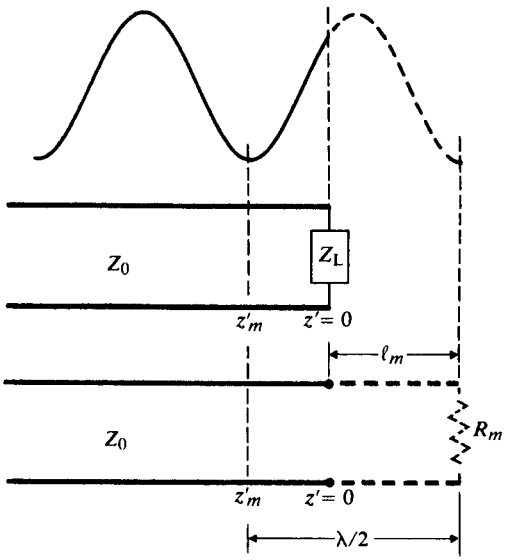

FIGURE 9–12
Voltage standing wave on a line terminated by an arbitrary impedance, and equivalent line section with pure resistive load.

$R_m < R_0$, as shown in the figure. The voltage distribution on the line to the left of the actual termination (where $z' > 0$) is not changed by this replacement.

The fact that any complex impedance can be obtained as the input impedance of a section of lossless line terminated in a resistive load can be seen from Eq. (9–109). Using R_m for Z_L and ℓ_m for ℓ, we have

$$R_i + jX_i = R_0 \frac{R_m + jR_0 \tan \beta\ell_m}{R_0 + jR_m \tan \beta\ell_m}. \tag{9–147}$$

The real and imaginary parts of Eq. (9–147) form two equations, from which the two unknowns, R_m and ℓ_m, can be solved (see Problem P.9–28).

The load impedance Z_L can be determined experimentally by measuring the standing-wave ratio S and the distance z'_m in Fig. 9–12. (Remember that $z'_m + \ell_m = \lambda/2$.) The procedure is as follows:

1. Find $|\Gamma|$ from S. Use $|\Gamma| = \dfrac{S-1}{S+1}$ from Eq. (9–139).
2. Find θ_Γ from z'_m. Use $\theta_\Gamma = 2\beta z'_m - \pi$ for $n = 0$ from Eq. (9–141).
3. Find Z_L, which is the ratio of Eqs. (9–135a) and (9–135b) at $z' = 0$:

$$Z_L = R_L + jX_L = R_0 \frac{1 + |\Gamma| e^{j\theta_\Gamma}}{1 - |\Gamma| e^{j\theta_\Gamma}}. \tag{9–148}$$

The value of R_m that, if terminated on a line of length ℓ_m, will yield an input impedance Z_L can be found easily from Eq. (9–147). Since $R_m < R_0$, $R_m = R_0/S$.

The procedure leading to Eq. (9–148) is used to determine Z_L from a measurement of S and of z'_m, the distance from the termination to the first voltage minimum. Of course, the distance from the termination to a voltage maximum, z'_M, could be used instead of z'_m. In that case, Eq. (9–140) should be used to find θ_Γ in Step 2 above.

EXAMPLE 9–9 The standing-wave ratio on a lossless 50 (Ω) transmission line terminated in an unknown load impedance is found to be 3.0. The distance between successive voltage minima is 20 (cm), and the first minimum is located at 5 (cm) from the load. Determine (a) the reflection coefficient Γ, and (b) the load impedance Z_L. In addition, find (c) the equivalent length and terminating resistance of a line such that the input impedance is equal to Z_L.

Solution

a) The distance between successive voltage minima is half a wavelength.

$$\lambda = 2 \times 0.2 = 0.4 \quad \text{(m)}, \qquad \beta = \frac{2\pi}{\lambda} = \frac{2\pi}{0.4} = 5\pi \quad \text{(rad/m)}.$$

Step 1: We find the magnitude of the reflection coefficient, $|\Gamma|$, from the standing-wave ratio $S = 3$.

$$|\Gamma| = \frac{S-1}{S+1} = \frac{3-1}{3+1} = 0.5.$$

Step 2: Find the angle of the reflection coefficient, θ_Γ, from

$$\theta_\Gamma = 2\beta z'_m - \pi = 2 \times 5\pi \times 0.05 - \pi = -0.5\pi \quad \text{(rad)},$$
$$\Gamma = |\Gamma| e^{j\theta_\Gamma} = 0.5e^{-j0.5\pi} = -j0.5.$$

b) The load impedance Z_L is determined from Eq. (9–148):

$$Z_L = 50\left(\frac{1 - j0.5}{1 + j0.5}\right) = 50(0.60 - j0.80) = 30 - j40 \quad (\Omega).$$

c) Now we find R_m and ℓ_m in Fig. 9–12. We may use Eq. (9–147),

$$30 - j40 = 50\left(\frac{R_m + j50 \tan \beta\ell_m}{50 + jR_m \tan \beta\ell_m}\right),$$

and solve the simultaneous equations obtained from the real and imaginary parts for R_m and $\beta\ell_m$. Actually, we know $z'_m + \ell_m = \lambda/2$ and $R_m = R_0/S$. Hence,†

$$\ell_m = \frac{\lambda}{2} - z'_m = 0.2 - 0.05 = 0.15 \quad \text{(m)}$$

and

$$R_m = \frac{50}{3} = 16.7 \quad (\Omega).$$

9–4.4 TRANSMISSION-LINE CIRCUITS

Our discussions on the properties of transmission lines so far have been restricted primarily to the effects of the load on the input impedance and on the characteristics of voltage and current waves. No attention has been paid to the generator at the "other end," which is the source of the waves. Just as the constraint (the boundary condition), $V_L = I_L Z_L$, which the voltage V_L and the current I_L must satisfy at the load end ($z = \ell$, $z' = 0$), a constraint exists at the generator end where $z = 0$ and $z' = \ell$. Let a voltage generator V_g with an internal impedance Z_g represent the source connected to a finite transmission line of length ℓ that is terminated in a load impedance Z_L, as shown in Fig. 9–6. The additional constraint at $z = 0$ will enable the voltage and current anywhere on the line to be expressed in terms of the source characteristics (V_g, Z_g), the line characteristics (γ, Z_0, ℓ), and the load impedance (Z_L).

The constraint at $z = 0$ is

$$V_i = V_g - I_i Z_g. \tag{9–149}$$

But, from Eqs. (9–133a) and (9–133b),

$$V_i = \frac{I_L}{2}(Z_L + Z_0)e^{\gamma\ell}[1 + \Gamma e^{-2\gamma\ell}] \tag{9–150a}$$

and

$$I_i = \frac{I_L}{2Z_0}(Z_L + Z_0)e^{\gamma\ell}[1 - \Gamma e^{-2\gamma\ell}]. \tag{9–150b}$$

† Another set of solutions to part (c) is $\ell'_m = \ell_m - \lambda/4 = 0.05$ (m) and $R'_m = SR_0 = 150$ (Ω). Do you see why?

Substitution of Eqs. (9–150a) and (9–150b) in Eq. (9–149) enables us to find

$$\frac{I_L}{2}(Z_L + Z_0)e^{\gamma\ell} = \frac{Z_0 V_g}{Z_0 + Z_g}\frac{1}{[1 - \Gamma_g \Gamma e^{-2\gamma\ell}]}, \tag{9–151}$$

where

$$\Gamma_g = \frac{Z_g - Z_0}{Z_g + Z_0} \tag{9–152}$$

is the ***voltage reflection coefficient*** at the generator end. Using Eq. (9–151) in Eqs. (9–133a) and (9–133b), we obtain

$$\boxed{V(z') = \frac{Z_0 V_g}{Z_0 + Z_g} e^{-\gamma z}\left(\frac{1 + \Gamma e^{-2\gamma z'}}{1 - \Gamma_g \Gamma e^{-2\gamma\ell}}\right).} \tag{9–153a}$$

Similarly,

$$\boxed{I(z') = \frac{V_g}{Z_0 + Z_g} e^{-\gamma z}\left(\frac{1 - \Gamma e^{-2\gamma z'}}{1 - \Gamma_g \Gamma e^{-2\gamma\ell}}\right).} \tag{9–153b}$$

Equations (9–153a) and (9–153b) are analytical phasor expressions for the voltage and current at any point on a finite line fed by a sinusoidal voltage source V_g. These are rather complicated expressions, but their significance can be interpreted in the following way. Let us concentrate our attention on the voltage equation (9–153a); obviously, the interpretation of the current equation (9–153b) is quite similar. We expand Eq. (9–153a) as follows:

$$\begin{aligned} V(z') &= \frac{Z_0 V_g}{Z_0 + Z_g} e^{-\gamma z}(1 + \Gamma e^{-2\gamma z'})(1 - \Gamma_g \Gamma e^{-2\gamma\ell})^{-1} \\ &= \frac{Z_0 V_g}{Z_0 + Z_g} e^{-\gamma z}(1 + \Gamma e^{-2\gamma z'})(1 + \Gamma_g \Gamma e^{-2\gamma\ell} + \Gamma_g^2 \Gamma^2 e^{-4\gamma\ell} + \cdots) \\ &= \frac{Z_0 V_g}{Z_0 + Z_g}[e^{-\gamma z} + (\Gamma e^{-\gamma\ell})e^{-\gamma z'} + \Gamma_g(\Gamma e^{-2\gamma\ell})e^{-\gamma z} + \cdots] \\ &= V_1^+ + V_1^- + V_2^+ + V_2^- + \cdots, \end{aligned} \tag{9–154}$$

where

$$V_1^+ = \frac{V_g Z_0}{Z_0 + Z_g} e^{-\gamma z} = V_M e^{-\gamma z}, \tag{9–154a}$$

$$V_1^- = \Gamma(V_M e^{-\gamma\ell})e^{-\gamma z'}, \tag{9–154b}$$

$$V_2^+ = \Gamma_g(\Gamma V_M e^{-2\gamma\ell})e^{-\gamma z}. \tag{9–154c}$$

$$\vdots$$

The quantity

$$V_M = \frac{Z_0 V_g}{Z_0 + Z_g} \tag{9–155}$$

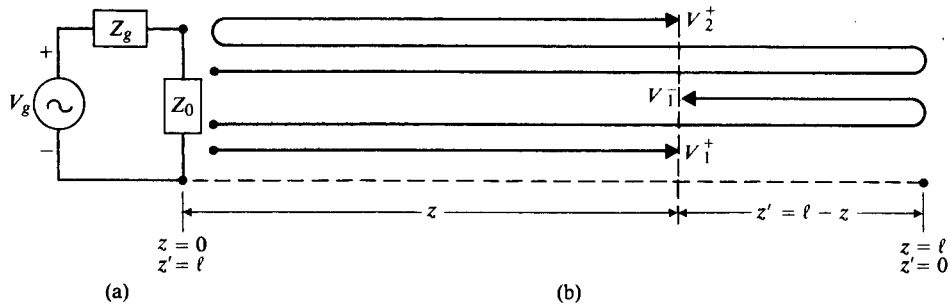

FIGURE 9–13
A transmission-line circuit and traveling waves.

is the complex amplitude of the voltage wave initially sent down the transmission line from the generator. It is obtained directly from the simple circuit shown in Fig. 9–13(a). The phasor V_1^+ in Eq. (9–154a) represents the initial wave traveling in the $+z$-direction. Before this wave reaches the load impedance Z_L, it sees Z_0 of the line as if the line were infinitely long.

When the first wave $V_1^+ = V_M e^{-\gamma z}$ reaches Z_L at $z = \ell$, it is reflected because of mismatch, resulting in a wave V_1^- with a complex amplitude $\Gamma(V_M e^{-\gamma \ell})$ traveling in the $-z$-direction. As the wave V_1^- returns to the generator at $z = 0$, it is again reflected for $Z_g \neq Z_0$, giving rise to a second wave V_2^+ with a complex amplitude $\Gamma_g(\Gamma V_M e^{-2\gamma \ell})$ traveling in $+z$-direction. This process continues indefinitely with reflections at both ends, and the resulting standing wave $V(z')$ is the sum of all the waves traveling in both directions. This is illustrated schematically in Fig. 9–13(b). In practice, $\gamma = \alpha + j\beta$ has a real part, and the attenuation effect of $e^{-\alpha \ell}$ diminishes the amplitude of a reflected wave each time the wave transverses the length of the line.

When the line is terminated with a matched load, $Z_L = Z_0$, $\Gamma = 0$, only V_1^+ exists, and it stops at the matched load with no reflections. If $Z_L \neq Z_0$ but $Z_g = Z_0$ (if the internal impedance of the generator is matched to the line), then $\Gamma \neq 0$ and $\Gamma_g = 0$. As a consequence, both V_1^+ and V_1^- exist, and V_2^+, V_2^- and all higher-order reflections vanish.

EXAMPLE 9–10 A 100 (MHz) generator with $V_g = 10\underline{/0°}$ (V) and internal resistance 50 (Ω) is connected to a lossless 50 (Ω) air line that is 3.6 (m) long and terminated in a $25 + j25$ (Ω) load. Find (a) $V(z)$ at a location z from the generator, (b) V_i at the input terminals and V_L at the load, (c) the voltage standing-wave ratio on the line, and (d) the average power delivered to the load.

Solution Referring to Fig. 9–6, the given quantities are

$$V_g = 10\underline{/0°} \quad (\text{V}), \qquad Z_g = 50 \quad (\Omega), \qquad f = 10^8 \quad (\text{Hz}),$$
$$R_0 = 50 \quad (\Omega), \qquad Z_L = 25 + j25 = 35.36\underline{/45°} \quad (\Omega), \qquad \ell = 3.6 \quad (\text{m}).$$

Thus,

$$\beta = \frac{\omega}{c} = \frac{2\pi 10^8}{3 \times 10^8} = \frac{2\pi}{3} \quad \text{(rad/m)}, \qquad \beta\ell = 2.4\pi \quad \text{(rad)},$$

$$\Gamma = \frac{Z_L - Z_0}{Z_L + Z_0} = \frac{(25 + j25) - 50}{(25 + j25) + 50} = \frac{-25 + j25}{75 + j25} = \frac{35.36/\underline{135°}}{79.1/\underline{18.4°}}$$

$$= 0.447/\underline{116.6°} = 0.447/\underline{0.648\pi},$$

$$\Gamma_g = 0.$$

a) From Eq. (9–153a) we have

$$V(z) = \frac{Z_0 V_g}{Z_0 + Z_g} e^{-j\beta z}[1 + \Gamma e^{-j2\beta(\ell - z)}]$$

$$= \frac{50(10)}{100} e^{-j2\pi z/3}[1 + 0.447e^{j(0.648 - 4.8)\pi} e^{j4\pi z/3}]$$

$$= 5[e^{-j2\pi z/3} + 0.447e^{j(2z/3 - 0.152)\pi}] \quad \text{(V)}.$$

We see that, because $\Gamma_g = 0$, $V(z)$ is the superposition of only two traveling waves, V_1^+ and V_1^-, as defined in Eq. (9–154).

b) At the input terminals,

$$V_i = V(0) = 5(1 + 0.447e^{-j0.152\pi})$$

$$= 5(1.396 - j0.207)$$

$$= 7.06/\underline{-8.43°} \quad \text{(V)}.$$

At the load,

$$V_L = V(3.6) = 5[e^{-j0.4\pi} + 0.447e^{j0.248\pi}]$$

$$= 5(0.627 - j0.637) = 4.47/\underline{-45.5°} \quad \text{(V)}.$$

c) The voltage standing-wave ratio (VSWR) is

$$S = \frac{1 + |\Gamma|}{1 - |\Gamma|} = \frac{1 + 0.447}{1 - 0.447} = 2.62.$$

d) The average power delivered to the load is

$$P_{av} = \frac{1}{2}\left|\frac{V_L}{Z_L}\right|^2 R_L = \frac{1}{2}\left(\frac{4.47}{35.36}\right)^2 \times 25 = 0.200 \quad \text{(W)}.$$

It is interesting to compare this result with the case of a matched load when $Z_L = Z_0 = 50 + j0\ (\Omega)$. In that case, $\Gamma = 0$,

$$|V_L| = |V_i| = \frac{V_g}{2} = 5 \quad \text{(V)},$$

and a maximum average power is delivered to the load:

$$\text{Maximum } P_{av} = \frac{V_L^2}{2R_L} = \frac{5^2}{2 \times 50} = 0.25 \quad \text{(W)},$$

which is larger than the P_{av} calculated for the unmatched load in part (d) by an amount equal to the power reflected, $|\Gamma|^2 \times 0.25 = 0.05$ (W). ■

9–5 Transients on Transmission Lines

The discussion of the wave characteristics on transmission lines in the previous section was based on steady-state, single-frequency, time-harmonic sources and signals. We worked with voltage and current phasors. Quantities such as reactances (X), wavelength (λ), wavenumber (k), and phase constant (β) would lose their meaning under transient conditions. However, there are important practical situations in which the sources and signals are not time-harmonic and the conditions are not steady-state. Examples are digital (pulse) signals in computer networks and sudden surges in power and telephone lines. In this section we will consider the transient behavior of lossless transmission lines. For such lines ($R = 0$, $G = 0$), characteristic impedance becomes characteristic resistance $R_0 = 1/\sqrt{LC}$, and voltage and current waves propagate along the line with a velocity $u = 1/\sqrt{LC}$.

The simplest case is shown in Fig. 9–14(a), where a d-c voltage source V_0 is applied through a series (internal) resistance R_g at $t = 0$ to the input terminals of a lossless line terminated in a characteristic resistance R_0. Since the impedance looking into the terminated line is R_0, a voltage wave of magnitude

$$V_1^+ = \frac{R_0}{R_0 + R_g} V_0 \tag{9-156}$$

travels down the line in the $+z$-direction with a velocity $u = 1/\sqrt{LC}$. The corresponding magnitude, I_1^+, of the current wave is

$$I_1^+ = \frac{V_1^+}{R_0} = \frac{V_0}{R_0 + R_g}. \tag{9-157}$$

If we plot the voltage across the line at $z = z_1$ as a function of time, we obtain a delayed step function at $t = z_1/u$ as in Fig. 9–14(b). The current in the line at $z = z_1$

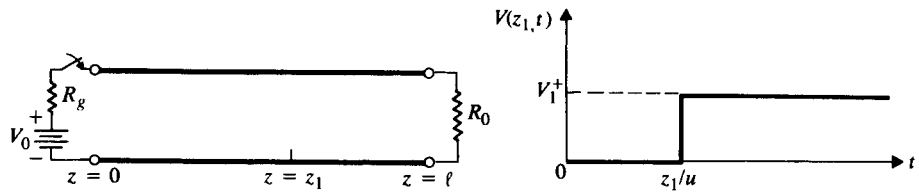

(a) Switch closed at $t = 0$. (b) Voltage at $z = z_1$.

FIGURE 9–14
A d-c source applied to a line terminated in characteristic resistance R_0 through a series resistance R_g.

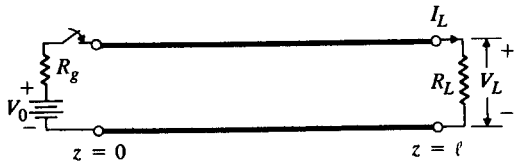

FIGURE 9–15
A d-c source applied to a terminated lossless line at $t = 0$ (general case).

has the same shape with a magnitude I_1^+ given in Eq. (9–157). When the voltage and current waves reach the termination at $z = \ell$, there are no reflected waves because $\Gamma = 0$. A steady state is established, and the entire line is charged to a voltage equal to V_1^+.

If both the series resistance R_g and the load resistance R_L are not equal to R_0, as in Fig. 9–15, the situation is more complicated. When the switch is closed at $t = 0$, the d-c source sends a voltage wave of magnitude

$$V_1^+ = \frac{R_0}{R_0 + R_g} V_0 \tag{9–158}$$

in the $+z$-direction with a velocity $u = 1/\sqrt{LC}$ as before because the V_1^+ wave has no knowledge of the length of the line or the nature of the load at the other end; it proceeds as if the line were infinitely long. At $t = T = \ell/u$ this wave reaches the load end $z = \ell$. Since $R_L \neq R_0$, a reflected wave will travel in the $-z$-direction with a magnitude

$$V_1^- = \Gamma_L V_1^+, \tag{9–159}$$

where

$$\Gamma_L = \frac{R_L - R_0}{R_L + R_0} \tag{9–160}$$

is the reflection coefficient of the load resistance R_L. This reflected wave arrives at the input end at $t = 2T$, where it is reflected by $R_g \neq R_0$. A new voltage wave having a magnitude V_2^+ then travels down the line, where

$$V_2^+ = \Gamma_g V_1^- = \Gamma_g \Gamma_L V_1^+. \tag{9–161}$$

In Eq. (9–161),

$$\Gamma_g = \frac{R_g - R_0}{R_g + R_0} \tag{9–162}$$

is the reflection coefficient of the series resistance R_g. This process will go on indefinitely with waves traveling back and forth, being reflected at each end at $t = nT$ ($n = 1, 2, 3, \ldots$).

Two points are worth noting here. First, some of the reflected waves traveling in either direction may have a negative amplitude, since Γ_L or Γ_g (or both) may be negative. Second, except for an open circuit or a short circuit, Γ_L and Γ_g are less than unity. Thus the magnitude of the successive reflected waves becomes smaller

and smaller, leading to a convergent process. The progression of the transient voltage waves on the lossless line in Fig. 9–15 for $R_L = 3R_0$ ($\Gamma_L = \frac{1}{2}$) and $R_g = 2R_0$ ($\Gamma_g = \frac{1}{3}$) is illustrated in Figs. 9–16(a), 9–16(b), and 9–16(c) for three different time intervals. The corresponding current waves are given in Figs. 9–16(d), 9–16(e), and 9–16(f), which are self-explanatory. The voltage and current at any particular location on the line in any particular time interval are just the *algebraic sums* $(V_1^+ + V_1^- + V_2^+ + V_2^- + \ldots)$ and $(I_1^+ + I_1^- + I_2^+ + I_2^- + \ldots)$, respectively.

It is interesting to check the ultimate value of the voltage across the load, $V_L = V(\ell)$, as t increases indefinitely. We have

$$\begin{aligned} V_L &= V_1^+ + V_1^- + V_2^+ + V_2^- + V_3^+ + V_3^- + \cdots \\ &= V_1^+(1 + \Gamma_L + \Gamma_g\Gamma_L + \Gamma_g\Gamma_L^2 + \Gamma_g^2\Gamma_L^2 + \Gamma_g^2\Gamma_L^3 + \cdots) \\ &= V_1^+[(1 + \Gamma_g\Gamma_L + \Gamma_g^2\Gamma_L^2 + \cdots) + \Gamma_L(1 + \Gamma_g\Gamma_L + \Gamma_g^2\Gamma_L^2 + \cdots)] \\ &= V_1^+\left[\left(\frac{1}{1 - \Gamma_g\Gamma_L}\right) + \left(\frac{\Gamma_L}{1 - \Gamma_g\Gamma_L}\right)\right] \\ &= V_1^+\left(\frac{1 + \Gamma_L}{1 - \Gamma_g\Gamma_L}\right). \end{aligned} \tag{9–163}$$

For the present case, $V_1^+ = V_0/3$, $\Gamma_L = \frac{1}{2}$, and $\Gamma_g = 1/3$, Eq. (9–163) gives

$$V_L = \tfrac{9}{5}V_1^+ = \tfrac{3}{5}V_0 \tag{9–163a}$$

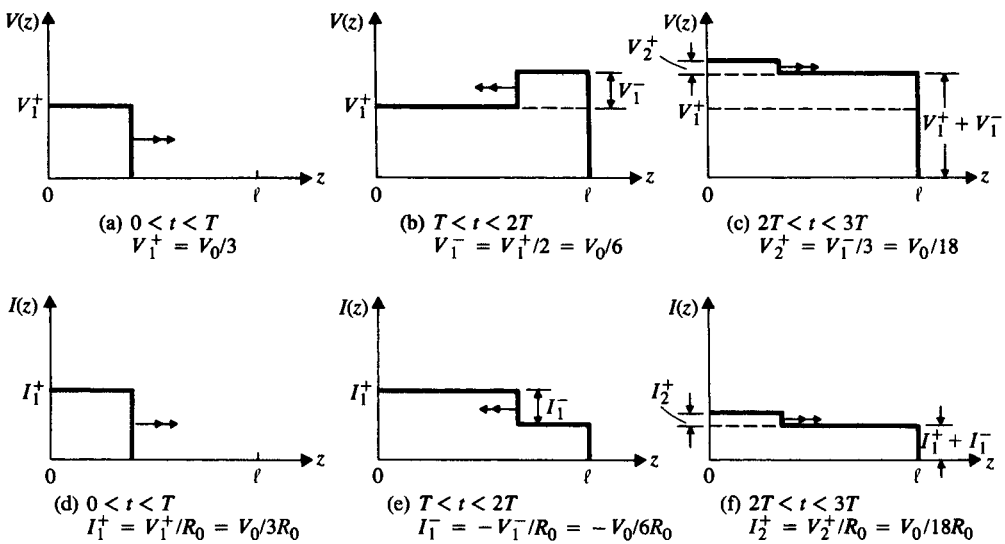

FIGURE 9–16
Transient voltage and current waves on transmission line in Fig. 9–15 for $R_L = 3R_0$ and $R_g = 2R_0$.

as $t \to \infty$. This result is obviously correct because, in the steady state, V_0 is divided between R_L and R_g in a ratio of 3 to 2. Similarly, we find

$$I_L = \left(\frac{1 - \Gamma_L}{1 - \Gamma_g \Gamma_L}\right)\frac{V_1^+}{R_0},$$

which yields

$$I_L = \frac{3}{5}\left(\frac{V_1^+}{R_0}\right) = \frac{V_0}{5R_0}, \tag{9-164}$$

as expected.

9-5.1 REFLECTION DIAGRAMS

The preceding step-by-step construction and calculation procedure of the voltage and current at a particular time and location on a transmission line with arbitrary resistive terminations tends to be tedious and difficult to visualize when it is necessary to consider many reflected waves. In such cases the graphical construction of a reflection diagram is very helpful. Let us first construct a ***voltage reflection diagram. A reflection diagram*** plots the time elapsed after the change of circuit conditions versus the distance z from the source end. The voltage reflection diagram for the transmission-line circuit in Fig. 9–15 is given in Fig. 9–17. It starts with a wave V_1^+ at $t = 0$ traveling from the source end ($z = 0$) in the $+z$-direction with a velocity $u = 1/\sqrt{LC}$. This wave is represented by the directed straight line marked V_1^+ from the origin. This line has a positive slope equal to $1/u$. When the V_1^+ wave reaches the load at $z = \ell$, a reflected wave $V_1^- = \Gamma_L V_1^+$ is created if $R_L \neq R_0$. The V_1^- wave travels in the $-z$-direction and is represented by the directed line marked $\Gamma_L V_1^+$ with a negative slope equal to $-1/u$.

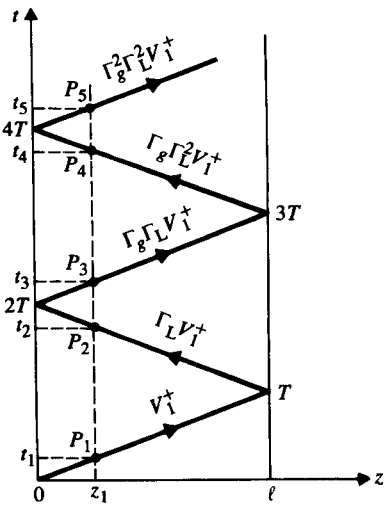

FIGURE 9–17
Voltage reflection diagram for transmission-line circuit in Fig. 9–15.

The V_1^- wave returns to the source end at $t = 2T$ and gives rise to a reflected wave $V_2^+ = \Gamma_g V_1^- = \Gamma_g \Gamma_L V_1^+$, which is represented by a second directed line with a positive slope. This process continues back and forth indefinitely. The voltage reflection diagram can be used conveniently to determine the voltage distribution along the transmission line at a given time as well as the variation of the voltage as a function of time at an arbitrary point on the line.

Suppose we wish to know the voltage distribution along the line at $t = t_4$ ($3T < t_4 < 4T$). We proceed as follows:

1. Mark t_4 on the vertical t-axis of the voltage reflection diagram.
2. Draw a horizontal line from t_4, intersecting the directed line marked $\Gamma_g \Gamma_L^2 V_1^+$ at P_4. (All directed lines above P_4 are irrelevant to our problem because they pertain to $t > t_4$.)
3. Draw a vertical line through P_4, intersecting the horizontal z-axis at z_1. The significance of z_1 is that in the range $0 < z < z_1$ (to the left of the vertical line) the voltage has a value equal to $V_1^+ + V_1^- + V_2^+ = V_1^+(1 + \Gamma_L + \Gamma_g \Gamma_L)$; and in the range $z_1 < z < \ell$ (to the right of the vertical line) the voltage is $V_1^+ + V_1^- + V_2^+ + V_2^- = V_1^+(1 + \Gamma_L + \Gamma_g \Gamma_L + \Gamma_g \Gamma_L^2)$. There is a voltage discontinuity equal to $\Gamma_g \Gamma_L^2 V_1^+$ at $z = z_1$.
4. The voltage distribution along the line at $t = t_4$, $V(z, t_4)$, is then as shown in Fig. 9–18(a), plotted for $R_L = 3R_0$ ($\Gamma_L = \frac{1}{2}$) and $R_g = 2R_0$ ($\Gamma_g = \frac{1}{3}$).

Next let us find the variation of the voltage as a function of time at the point $z = z_1$. We use the following procedure:

1. Draw a vertical line at z_1, intersecting the directed lines at points P_1, P_2, P_3, P_4, P_5, and so on. (There would be an infinite number of such intersection points if $R_L \neq R_0$ and $R_g \neq R_0$, as there would be an infinite number of directed lines if $\Gamma_L \neq 0$ and $\Gamma_g \neq 0$.)
2. From these intersection points, draw horizontal lines intersecting the vertical t-axis at t_1, t_2, t_3, t_4, t_5, and so on. These are the instants at which a new voltage wave arrives and abruptly changes the voltage at $z = z_1$.
3. The voltage at $z = z_1$ as a function of t can be read from the voltage reflection diagram as follows:

Time Range	Voltage	Voltage Discontinuity
$0 \leq t < t_1$ ($t_1 = z_1/u$)	0	0
$t_1 \leq t < t_2$ ($t_2 = 2T - t_1$)	V_1^+	V_1^+ at t_1
$t_2 \leq t < t_3$ ($t_3 = 2T + t_1$)	$V_1^+(1 + \Gamma_L)$	$\Gamma_L V_1^+$ at t_2
$t_3 \leq t < t_4$ ($t_4 = 4T - t_1$)	$V_1^+(1 + \Gamma_L + \Gamma_g \Gamma_L)$	$\Gamma_g \Gamma_L V_1^+$ at t_3
$t_4 \leq t < t_5$ ($t_5 = 4T + t_1$)	$V_1^+(1 + \Gamma_L + \Gamma_g \Gamma_L + \Gamma_g \Gamma_L^2)$	$\Gamma_g \Gamma_L^2 V_1^+$ at t_4
⋮	⋮	⋮

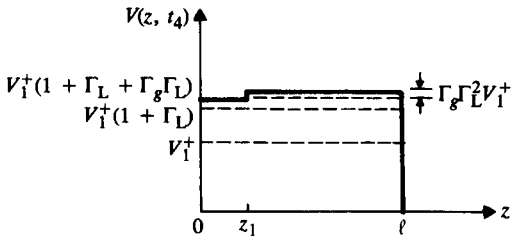

(a) $V(z, t_4)$ versus z;
$\Gamma_L = \frac{1}{2}$, $\Gamma_g = \frac{1}{3}$, $V_1^+ = V_0/3$.

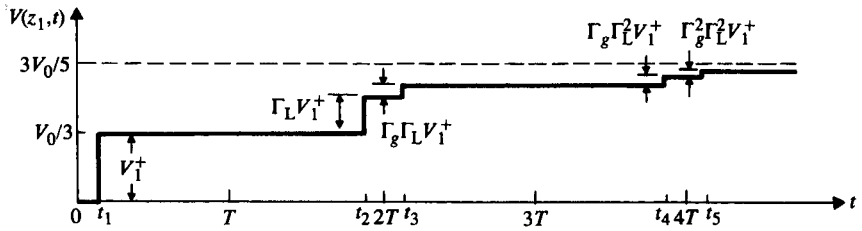

(b) $V(z_1,t)$ versus t; $V(z_1, \infty) = 3V_0/5$.

FIGURE 9–18
Transient voltage on lossless transmission line for $R_L = 3R_0$ and $R_g = 2R_0$.

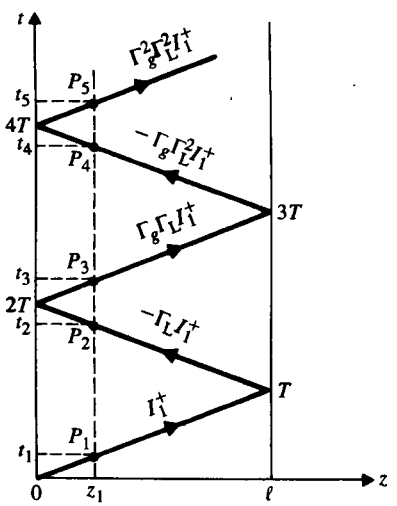

FIGURE 9–19
Current reflection diagram for transmission-line circuit in Fig. 9–15.

4. The graph of $V(z_1, t)$ is plotted in Fig. 9–18(b) for $\Gamma_L = \frac{1}{2}$ and $\Gamma_g = \frac{1}{3}$. When t increases indefinitely, the voltage at z_1 (and at all other points along the lossless line) will assume the value $3V_0/5$, as given in Eq. (9–163a).

Similar to the voltage reflection diagram in Fig. 9–17, a ***current reflection diagram*** for the transmission-line circuit of Fig. 9–15 can be constructed. This is shown in Fig. 9–19. Here we draw directed lines representing current waves. The essential difference between the voltage and current reflection diagrams is in the negative sign associated with the current waves traveling in the $-z$-direction on account of Eq. (9–94). The current reflection diagram can be used to determine the current distribution along the transmission line at a given time as well as the variation of the current as a function of time at a particular point on the line, following the same procedures outlined previously for voltage. For example, we can determine the current at $z = z_1$ by drawing a vertical line through z_1 in Fig. 9–19, intersecting the directed lines at points P_1, P_2, P_3, P_4, P_5, and so on, and by finding the corresponding times t_1, t_2, t_3, t_4, t_5, and so on, as before. Figure 9–20 is a plot of $I(z_1, t)$ versus t, which accompanies the $V(z_1, t)$ graph in Fig. 9–18(b). We see that they are quite dissimilar. The current along the line oscillates around the steady-state value of $V_0/5R_0$ (see Eq. 9–164) with successively smaller discontinuous jumps at t_1, t_2, t_3, t_4, t_5, etc.

We note two special cases here.

1. When $R_L = R_0$ (matched load, $\Gamma_L = 0$), the voltage and current reflection diagrams will each have only a single directed line, existing in the interval $0 < t < T$, irrespective of what R_g is.
2. When $R_g = R_0$ (matched source, $\Gamma_g = 0$) and $R_L \neq R_0$, the voltage and current reflection diagrams will each have only two directed lines, existing in the intervals $0 < t < T$ and $T < t < 2T$.

In both cases the determination of the transient behavior on the transmission line is much simplified.

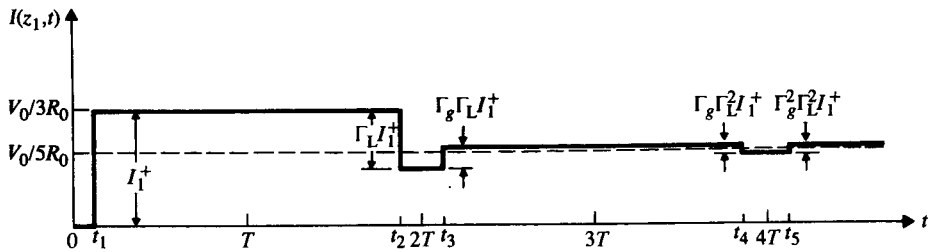

FIGURE 9–20
Transient current on lossless transmission line for $R_L = 3R_0$ and $R_g = 2R_0$.

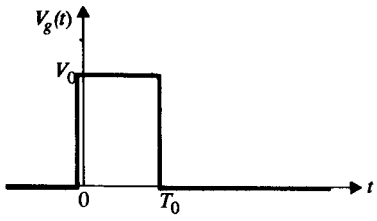

FIGURE 9–21
A rectangular pulse.

9–5.2 PULSE EXCITATION

So far, we have discussed the transient behavior of lossless transmission lines when the source is a sudden voltage surge in the form of a step function; that is,

$$v_g(t) = V_0 U(t), \tag{9–165}$$

where $U(t)$ denotes the unit step function

$$U(t) = \begin{cases} 0, & t < 0, \\ 1, & t > 0. \end{cases} \tag{9–166}$$

In many instances, such as in computer networks and pulse-modulation systems, the excitation may be in the form of pulses. The analysis of the transient behavior of a line with pulse excitation, however, does not present special difficulties because a rectangular pulse can be decomposed into two step functions. For example, the pulse of an amplitude V_0 lasting from $t = 0$ to $t = T_0$ shown in Fig. 9–21 can be written as

$$v_g(t) = V_0[U(t) - U(t - T_0)]. \tag{9–166a}$$

If $v_g(t)$ in Eq. (9–166a) is applied to a transmission line, the transient response is simply the superposition of the result obtained from a d-c voltage V_0 applied at $t = 0$ and that obtained from another d-c voltage $-V_0$ applied at $t = T_0$. We will illustrate this process by an example.

EXAMPLE 9–11 A rectangular pulse of an amplitude 15 (V) and a duration 1 (μs) is applied through a series resistance of 25 (Ω) to the input terminals of a 50 (Ω) lossless coaxial transmission line. The line is 400 (m) long and is short-circuited at the far end. Determine the voltage response at the midpoint of the line as a fuction of time up to 8 (μs). The dielectric constant of the insulating material in the cable is 2.25.

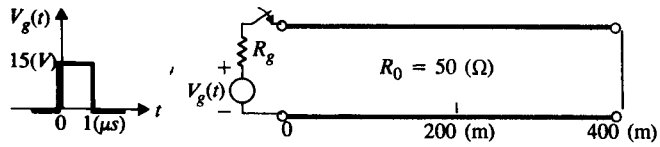

FIGURE 9–22
A pulse applied to a short-circuited line.

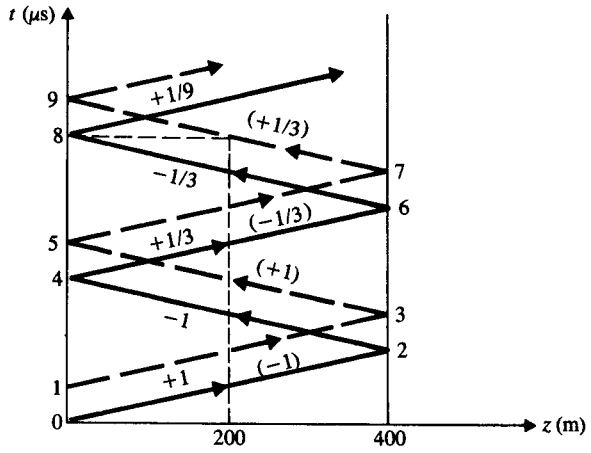

FIGURE 9–23
Voltage reflection diagram for Example 9–11.

Solution We have a situation as given in Fig. 9–22, where $R_g = 25\ (\Omega)$ and $R_L = 0$. Also,

$$\Gamma_L = -1, \qquad \Gamma_g = \frac{25 - 50}{25 + 50} = -\frac{1}{3},$$

$$v_g(t) = 10[U(t) - U(t - 10^{-6})],$$

$$u = \frac{c}{\sqrt{\epsilon_r}} = \frac{3 \times 10^8}{\sqrt{2.25}} = 2 \times 10^8 \quad \text{(m/s)},$$

$$T = \frac{\ell}{u} = \frac{400}{2 \times 10^8} = 2 \times 10^{-6}\ \text{(s)} = 2 \quad (\mu\text{s}),$$

$$V_1^+ = \frac{15R_0}{R_0 + R_g} = \frac{15 \times 50}{50 + 25} = 10 \quad \text{(V)}.$$

A voltage reflection diagram is constructed in Fig. 9–23 for this problem. There are two sets of directed lines: The solid lines are for $+15$ (V) applied at $t = 0$, and the dashed lines are for -15 (V) applied at $t = 1$ (μs). Along each directed line is marked the amplitude of the wave (with the appropriate sign) normalized with respect to $V_1^+ = 10$ (V). The markings for the applied voltage $-15U(t - 10^{-6})$ are enclosed in brackets for easy reference. To obtain the voltage variation at the line's midpoint for the interval $0 < t \leq 8$ (μs), we draw a vertical line at $z = 200$ (m) and a horizontal line at $t = 8$ (μs). The voltage function due to $15U(t)$ can be read from the intersections of the vertical line with the solid directed lines. This is sketched as v_a in Fig. 9–24(a). Similarly, the voltage function due to $-15U(t - 10^{-6})$ is read from the intersections of the vertical line with the dashed directed lines; it is sketched as v_b in Fig. 9–24(b). The required response $v(200, t)$ for $0 < t \leq 8$ (μs) is then the sum of the responses, $v_a + v_b$, and is given in Fig. 9–24(c). ■

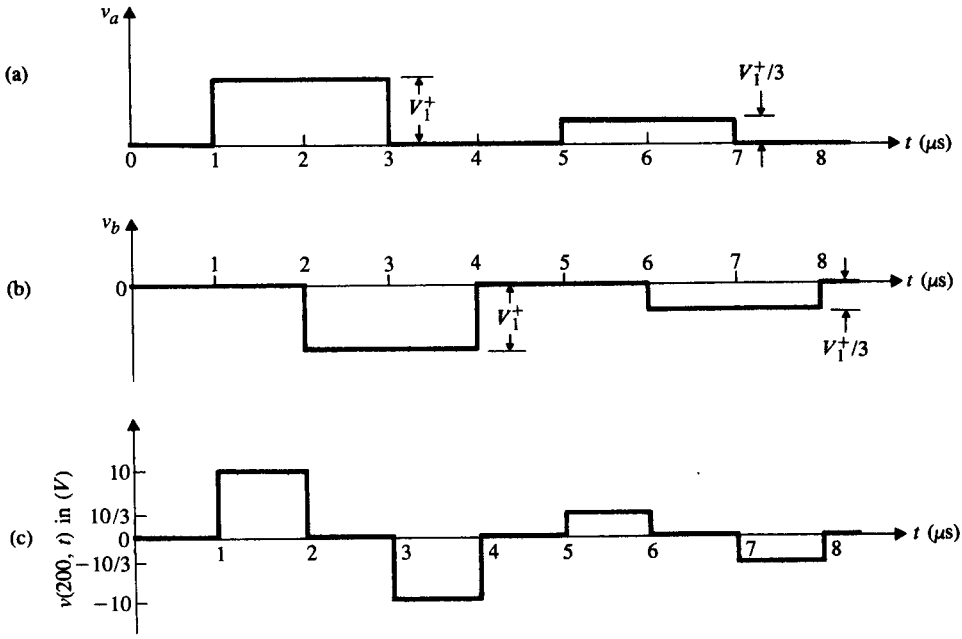

FIGURE 9–24
Voltage responses at the midpoint of the short-circuited line in Fig. 9–22 (Example 9–11).

9–5.3 INITIALLY CHARGED LINE

In our discussion of transients on transmission lines we have assumed that the lines themselves have no initial voltages or currents when an external source is applied. Actually, any disturbance or change in a transmission-line circuit will start transients along the line even without an external source if initial voltages and/or currents exist. We examine in this subsection a situation involving an initially charged line and develop a method of analysis.

Consider the following example.

EXAMPLE 9–12 A lossless, air-dielectric, open-circuited transmission line of characteristic resistance R_0 and length ℓ is initially charged to a voltage V_0. At $t = 0$ the line is connected to a resistance R. Determine the voltage across and the current in R as functions of time. Assume that $R = R_0$.

Solution This problem, as depicted in Fig. 9–25(a), can be analyzed by examining the circuits in Figs. 9–25(b), 9–25(c), and 9–25(d). The circuit in Fig. 9–25(b) is equivalent to that in Fig. 9–25(a). After the switch is closed, the conditions in the circuit in Fig. 9–25(b) are the same as the superposition of those shown in Figs. 9–25(c) and 9–25(d). But the circuit in Fig. 9–25(c) does not give rise to transients because of the opposing voltages; hence we use the circuit in Fig. 9–25(d) to study

the transient behavior of the original circuit in Fig. 9–25(a). The line in the circuit in Fig. 9–25(d) is uncharged, and our problem has then been reduced to one with which we are already familiar.

When the switch is closed, a voltage wave of amplitude V_1^+ will be sent down the line in the $+z$-direction, where

$$V_1^+ = -\frac{R_0}{R + R_0} V_0 = -\frac{V_0}{2}.$$

At $t = \ell/c$, the V_1^+ wave reaches the open end, having reduced the voltage along the whole line from V_0 to $V_0/2$. At the open end, $\Gamma = 1$, and a reflected V_1^- wave is sent back in the $-z$-direction with $V_1^- = V_1^+ = -V_0/2$. This reflected wave returns to the sending end at $t = 2\ell/c$, reducing the voltage on the line to zero.

From Fig. 9–25(d),

where

$$I_R = -I_1,$$

$$I_1 = I_1^+ = \frac{V_1^+}{R_0} = -\frac{V_0}{2R_0} \quad \text{for} \quad 0 \le t < 2\ell/c.$$

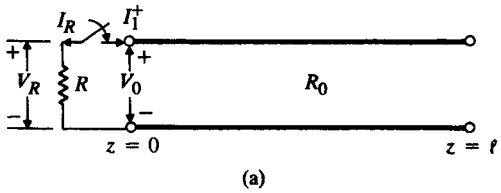

(a)

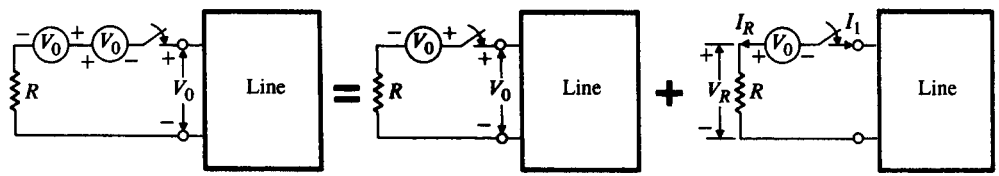

(b) (c) (d)

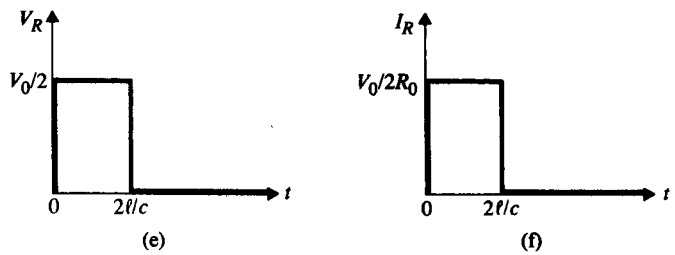

(e) (f)

FIGURE 9–25
Transient problem of an open-circuited, initially charged line, $R = R_0$ (Example 9–12).

At $t = \ell/c$, I_1^+ reaches the open end, and the reflected I_1^- must make the total current there zero. Hence,

$$I_1^- = -I_1^+ = \frac{V_0}{2R_0},$$

which reaches the sending end at $t = 2\ell/c$ and reduces both I_1 and I_R to zero. Since $R = R_0$, there is no further reflection, and the transient state ends. As shown in Figs. 9–25(e) and 9–25(f), both V_R and I_R are a pulse of duration $2\ell/c$. We then have a way of generating a pulse by discharging a charged open-circuited transmission line, the width of the pulse being adjustable by changing ℓ. ■

9–5.4 LINE WITH REACTIVE LOAD

When the termination on a transmission line is a resistance different from the characteristic resistance, an incident voltage or current wave will produce a reflected wave of the same time dependence. The ratio of the amplitudes of the reflected and incident waves is a constant, which is defined as the reflection coefficient. If, however, the termination is a reactive element such as an inductance or a capacitance, the reflected wave will no longer have the same time dependence (no longer be of the same shape) as the incident wave. The use of a constant reflection coefficient is not feasible in such cases, and it is necessary to solve a differential equation at the termination in order to study the transient behavior. We shall consider the effect on the reflected wave of an inductive termination and a capacitive termination separately in this subsection.

Figure 9–26(a) shows a lossless line with a characteristic resistance R_0, terminated at $z = \ell$ with an inductance L_L. A d-c voltage V_0 is applied to the line at $z = 0$ through a series resistance R_0. When the switch is closed at $t = 0$, a voltage wave of an amplitude

$$V_1^+ = \frac{V_0}{2} \tag{9–167}$$

travels toward the load. Upon reaching the load at $t = \ell/u = T$, a reflected wave $V_1^-(t)$ is produced because of mismatch. It is the relation between $V_1^-(t)$ and V_1^+ that we wish to find. At $z = \ell$, the following relations hold for all $t \geq T$:

$$v_L(t) = V_1^+ + V_1^-(t), \tag{9–168}$$

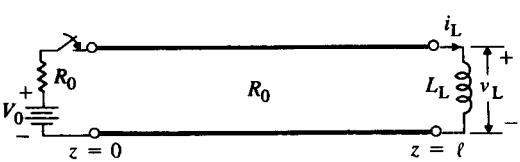

(a) Transmission-line circuit with inductive termination

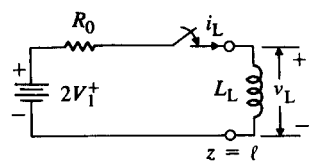

(b) Equivalent circuit for the load end, $t \geq T$

FIGURE 9–26
Transient calculations for a lossless line with an inductive termination.

$$i_L(t) = \frac{1}{R_0}[V_1^+ - V_1^-(t)], \tag{9–169}$$

$$v_L(t) = L_L \frac{di_L(t)}{dt}. \tag{9–170}$$

Eliminating $V_1^-(t)$ from Eqs. (9–168) and (9–169), we obtain

$$v_L(t) = 2V_1^+ - R_0 i_L(t). \tag{9–171}$$

It is seen that Eq. (9–171) describes the application of Kirchhoff's voltage law to the circuit in Fig. 9–26(b), which is then the equivalent circuit at the load end for $t \geq T$. In view of Eq. (9–170), Eq, (9–171) leads to a first-order differential equation with constant coefficients:

$$L_L \frac{di_L(t)}{dt} + R_0 i_L(t) = 2V_1^+, \qquad t \geq T. \tag{9–172}$$

The solution of Eq. (9–172) is

$$i_L(t) = \frac{2V_1^+}{R_0}[1 - e^{-(t-T)R_0/L_L}], \qquad t \geq T, \tag{9–173}$$

which correctly gives $i_L(T) = 0$ and $i_L(\infty) = 2V_1^+/R_0$. The voltage across the inductive load is

$$v_L(t) = L_L \frac{di_L(t)}{dt} = 2V_1^+ \cdot e^{-(t-T)R_0/L_L}, \qquad t \geq T. \tag{9–174}$$

The amplitude of the reflected wave, $V_1^-(t)$, can be found from Eq. (9–168):

$$\begin{aligned} V_1^-(t) &= v_L(t) - V_1^+ \\ &= 2V_1^+[e^{-(t-T)R_0/L_L} - \tfrac{1}{2}], \qquad t > T. \end{aligned} \tag{9–175}$$

This reflected wave travels in the $-z$-direction. The voltage at any point $z = z_1$ along the line is V_1^+ before the reflected wave from the load end reaches that point, $(t - T) < (\ell - z_1)/u$, and equals $V_1^+ + V_1^-(t - T)$ after that.

In Figs. 9–27(a), 9–27(b), and 9–27(c) are plotted $i_L(t)$, $v_L(t)$, and $V_1^-(t)$ at $z = \ell$ using Eqs. (9–173), (9–174), and (9–175). The voltage distribution along the line for $T < t_1 < 2T$ is shown in Fig. 9–27(d). Obviously, the transient behavior on a transmission line with a reactive termination is more complicated than that with a resistive termination.

We follow a similar procedure in examining the transient behavior of a lossless line with a capacitive termination, shown in Fig. 9–28(a). The same Eqs. (9–167), (9–168), (9–169), and (9–171) apply at $z = \ell$, but Eq. (9–170) relating the load current $i_L(t)$ and load voltage $v_L(t)$ must now be changed to

$$i_L(t) = C_L \frac{dv_L(t)}{dt}. \tag{9–176}^\dagger$$

---

† The subscript roman L denotes load; it has nothing to do with inductance.

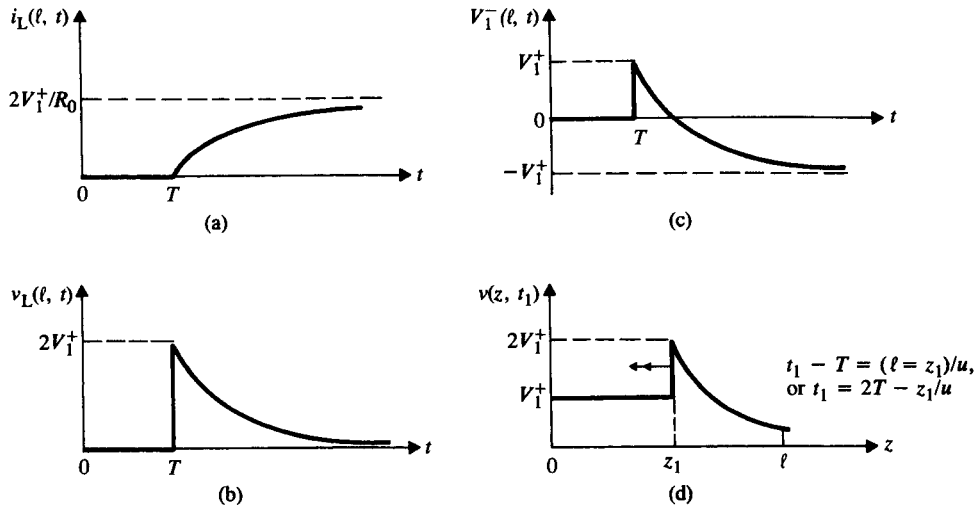

FIGURE 9–27
Transient responses of a lossless line with an inductive termination.

The differential equation to be solved at the load end is, by substituting Eq. (9–176) in Eq. (9–171),

$$C_L \frac{dv_L(t)}{dt} + \frac{1}{R_0} v_L(t) = \frac{2}{R_0} V_1^+, \qquad t \geq T, \tag{9–177}$$

where $V_1^+ = V_0/2$, as given in Eq. (9–167). The solution of Eq. (9–177) is

$$v_L(t) = 2V_1^+ [1 - e^{-(t-T)/R_0 C_L}], \qquad t \geq T. \tag{9–178}$$

The current in the load capacitance is obtained from Eq. (9–176):

$$i_L(t) = \frac{2V_1}{R_0} e^{-(t-T)/R_0 C_L}, \qquad t \geq T. \tag{9–179}$$

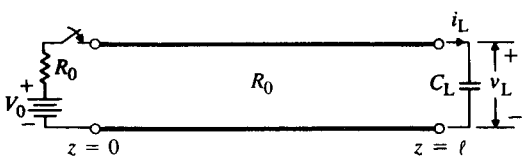

(a) Transmission-line circuit with capacitive termination. (b) Equivalent circuit for the load end, $t \geq T$.

FIGURE 9–28
Transient calculations for a lossless line with a capacitive termination.

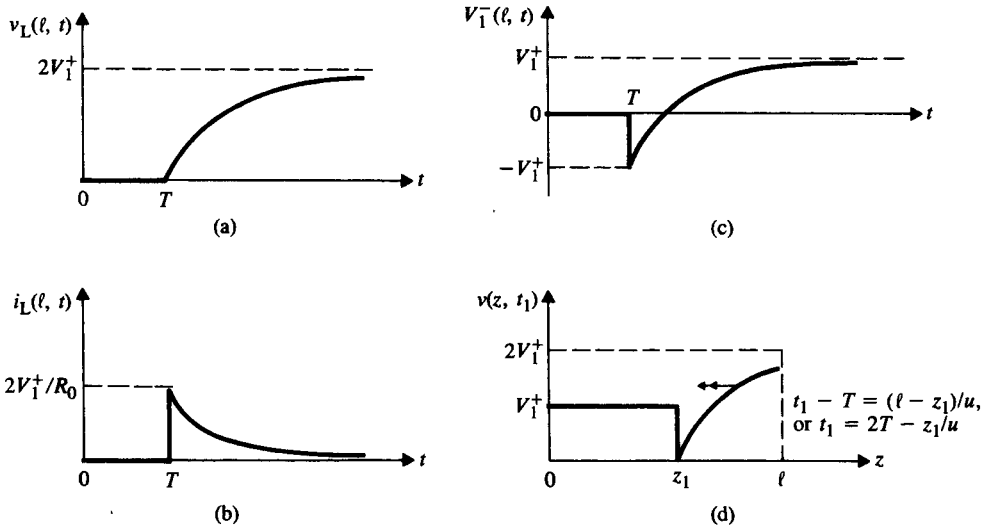

FIGURE 9–29
Transient responses of a lossless line with a capacitive termination.

Using Eq. (9–178) in Eq. (9–168), we find the amplitude of the reflected wave as a function of t:

$$V_1^-(t) = 2V_1^+[\tfrac{1}{2} - e^{-(t-T)/R_0C_L}], \qquad t \geq T. \tag{9–180}$$

The graphs of $v_L(t)$, $i_L(t)$, and $V_1^-(t)$ at $z = \ell$ are plotted in Figs. 9–29(a), 9–29(b), and 9–29(c) using Eqs. (9–178), (9–179), and (9–180), respectively. The voltage distribution along the line for $T < t_1 < 2T$ is shown in Fig. 9–29(d).

In this section we have discussed the transient behavior of only lossless transmission lines. For lossy lines, both the voltage and the current waves traveling in either direction will be attenuated as they proceed. This situation introduces additional complication in numerical computation, but the basic concept remains the same.

9–6 The Smith Chart

Transmission-line calculations—such as the determination of input impedance by Eq. (9–109), reflection coefficient by Eq. (9–134), and load impedance by Eq. (9–148)—often involve tedious manipulations of complex numbers. This tedium can be alleviated by using a graphical method of solution. The best known and most widely used graphical chart is the ***Smith chart*** devised by P. H. Smith.† Stated

† P H. Smith, "Transmission-line calculator," *Electronics*, vol. 12, p. 29, January 1939; and "An improved transmission-line calculator," *Electronics*, vol. 17, p. 130, January 1944.

succinctly, a Smith chart is a graphical plot of normalized resistance and reactance functions in the reflection-coefficient plane.

To understand how the Smith chart for a *lossless* transmission line is constructed, let us examine the voltage reflection coefficient of the load impedance defined in Eq. (9–134):

$$\Gamma = \frac{Z_L - R_0}{Z_L + R_0} = |\Gamma| e^{j\theta_\Gamma}. \tag{9–181}$$

Let the load impedance Z_L be normalized with respect to the characteristic impedance $R_0 = \sqrt{L/C}$ of the line.

$$z_L = \frac{Z_L}{R_0} = \frac{R_L}{R_0} + j\frac{X_L}{R_0} = r + jx \qquad \text{(Dimensionless)}, \tag{9–182}$$

where r and x are the normalized resistance and normalized reactance, respectively. Equation (9–181) can be rewritten as

$$\Gamma = \Gamma_r + j\Gamma_i = \frac{z_L - 1}{z_L + 1}, \tag{9–183}$$

where Γ_r and Γ_i are the real and imaginary parts, respectively, of the voltage reflection coefficient Γ. The inverse relation of Eq. (9–183) is

$$z_L = \frac{1 + \Gamma}{1 - \Gamma} = \frac{1 + |\Gamma| e^{j\theta_\Gamma}}{1 - |\Gamma| e^{j\theta_\Gamma}} \tag{9–184}$$

or

$$r + jx = \frac{(1 + \Gamma_r) + j\Gamma_i}{(1 - \Gamma_r) - j\Gamma_i}. \tag{9–185}$$

Multiplying both the numerator and the denominator of Eq. (9–185) by the complex conjugate of the denominator and separating the real and imaginary parts, we obtain

$$r = \frac{1 - \Gamma_r^2 - \Gamma_i^2}{(1 - \Gamma_r)^2 + \Gamma_i^2} \tag{9–186}$$

and

$$x = \frac{2\Gamma_i}{(1 - \Gamma_r)^2 + \Gamma_i^2}. \tag{9–187}$$

If Eq. (9–186) is plotted in the $\Gamma_r - \Gamma_i$ plane for a given value of r, the resulting graph is the locus for this r. The locus can be recognized when the equation is rearranged as

$$\left(\Gamma_r - \frac{r}{1 + r}\right)^2 + \Gamma_i^2 = \left(\frac{1}{1 + r}\right)^2. \tag{9–188}$$

It is the equation for a circle having a radius $1/(1 + r)$ and centered at $\Gamma_r = r/(1 + r)$ and $\Gamma_i = 0$. Different values of r yield circles of different radii with centers at different positions on the Γ_r-axis. A family of r-circles are shown in solid lines in Fig. 9–30. Since $|\Gamma| \leq 1$ for a lossless line, only that part of the graph lying within the unit circle on the $\Gamma_r - \Gamma_i$ plane is meaningful; everything outside can be disregarded.

Several salient properties of the r-circles are noted as follows:

1. The centers of all r-circles lie on the Γ_r-axis.
2. The $r = 0$ circle, having a unity radius and centered at the origin, is the largest.
3. The r-circles become progressively smaller as r increases from 0 toward ∞, ending at the ($\Gamma_r = 1$, $\Gamma_i = 0$) point for open-circuit.
4. All r-circles pass through the ($\Gamma_r = 1$, $\Gamma_i = 0$) point.

Similarly, Eq. (9–187) may be rearranged as

$$(\Gamma_r - 1)^2 + \left(\Gamma_i - \frac{1}{x}\right)^2 = \left(\frac{1}{x}\right)^2. \tag{9–189}$$

This is the equation for a circle having a radius $1/|x|$ and centered at $\Gamma_r = 1$ and $\Gamma_i = 1/x$. Different values of x yield circles of different radii with centers at different positions on the $\Gamma_r = 1$ line. A family of the portions of x-circles lying inside the $|\Gamma| = 1$ boundary are shown in dashed lines in Fig. 9–30. The following is a list of several salient properties of the x-circles.

1. The centers of all x-circles lie on the $\Gamma_r = 1$ line; those for $x > 0$ (inductive reactance) lie above the Γ_r-axis, and those for $x < 0$ (capacitive reactance) lie below the Γ_r-axis.
2. The $x = 0$ circle becomes the Γ_r-axis.

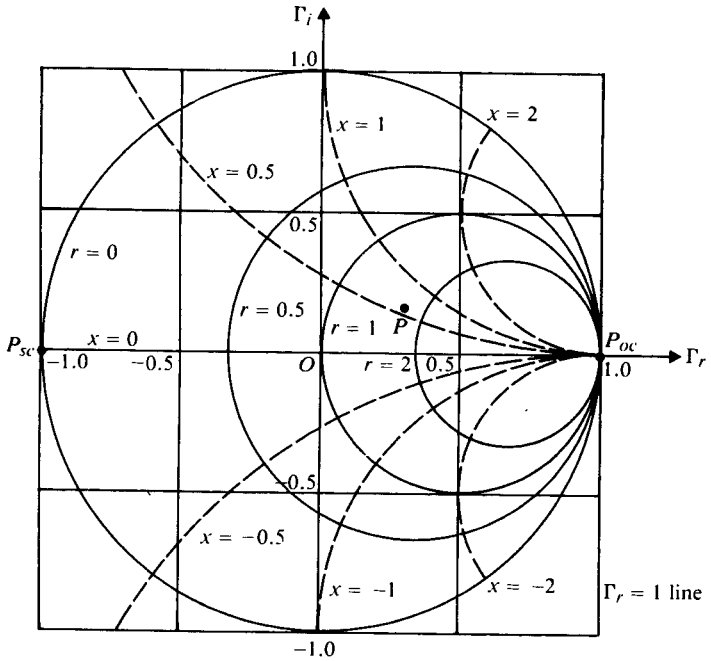

FIGURE 9–30
Smith chart with rectangular coordinates.

3. The x-circle becomes progressively smaller as $|x|$ increases from 0 toward ∞, ending at the $(\Gamma_r = 1, \Gamma_i = 0)$ point for open-circuit.
4. All x-circles pass through the $(\Gamma_r = 1, \Gamma_i = 0)$ point.

A Smith chart is a chart of r- and x-circles in the $\Gamma_r - \Gamma_i$ plane for $|\Gamma| \leq 1$. It can be proved that the r- and x-circles are everywhere orthogonal to one another. The intersection of an r-circle and an x-circle defines a point that represents a normalized load impedance $z_L = r + jx$. The actual load impedance is $Z_L = R_0(r + jx)$. Since a Simith chart plots the normalized impedance, it can be used for calculations concerning a lossless transmission line with an arbitrary characteristic impedance (resistance).

As an illustration, point P in Fig. 9–30 is the intersection of the $r = 1.7$ circle and the $x = 0.6$ circle. Hence it represents $z_L = 1.7 + j0.6$. The point P_{sc} at $(\Gamma_r = -1, \Gamma_i = 0)$ corresponds to $r = 0$ and $x = 0$ and therefore represents a short-circuit. The point P_{oc} at $(\Gamma_r = 1, \Gamma_i = 0)$ corresponds to an infinite impedance and represents an open-circuit.

The Smith chart in Fig. 9–30 is marked with Γ_r and Γ_i rectangular coordinates. The same chart can be marked with polar coordinates, such that every point in the Γ-plane is specified by a magnitude $|\Gamma|$ and a phase angle θ_Γ. This is illustrated in Fig. 9–31, where several $|\Gamma|$-circles are shown in dashed lines and some θ_Γ-angles are marked around the $|\Gamma| = 1$ circle. The $|\Gamma|$-circles are normally not shown on commercially available Smith charts; but once the point representing a certain $z_L = r + jx$ is located, it is a simple matter to draw a circle centered at the origin through the

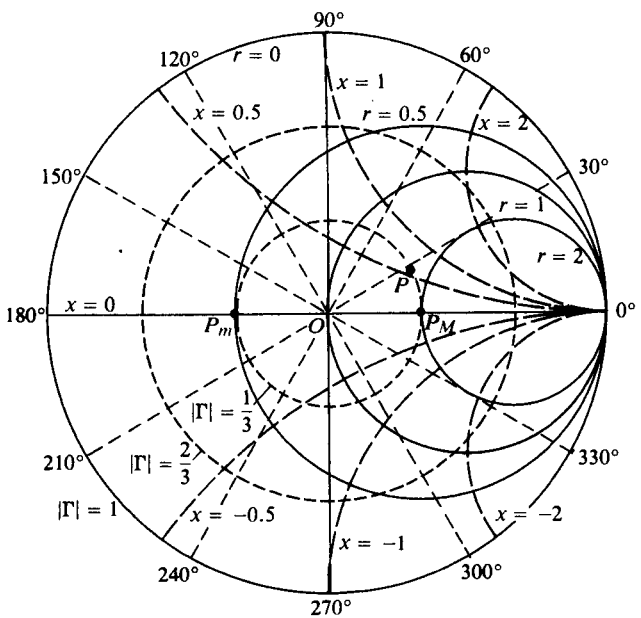

FIGURE 9–31
Smith chart with polar coordinates.

point. The fractional distance from the center to the point (compared with the unity radius to the edge of the chart) is equal to the magnitude $|\Gamma|$ of the load reflection coefficient; and the angle that the line to the point makes with the real axis is θ_Γ. This graphical determination circumvents the need for computing Γ by Eq. (9–183).

Each $|\Gamma|$-circle intersects the real axis at two points. In Fig. 9–31 we designate the point on the positive-real axis (OP_{oc}) as P_M and the point on the negative-real axis (OP_{sc}) as P_m. Since $x = 0$ along the real axis, P_M and P_m both represent situations with a purely resistive load, $Z_L = R_L$. Obviously, $R_L > R_0$ at P_M, where $r > 1$; and $R_L < R_0$ at P_m, where $r < 1$. In Eq. (9–145) we found that $S = R_L/R_0 = r$ for $R_L > R_0$. This relation enables us to say immediately, without using Eq. (9–138), that *the value of the r-circle passing through the point P_M is numerically equal to the standing-wave ratio.* Similarly, we conclude from Eq. (9–146) that *the value of the r-circle passing through the point P_m on the negative-real axis is numerically equal to* $1/S$. For the $z_L = 1.7 + j0.6$ point, marked P in Fig. 9–31, we find $|\Gamma| = \frac{1}{3}$ and $\theta_\Gamma = 28°$. At P_M, $r = S = 2.0$. These results can be verified analytically.

In summary, we note the following:

1. All $|\Gamma|$-circles are centered at the origin, and their radii vary uniformly from 0 to 1.
2. The angle, measured from the positive real axis, of the line drawn from the origin through the point representing z_L equals θ_Γ.
3. The value of the r-circle passing through the intersection of the $|\Gamma|$-circle and the positive-real axis equals the standing-wave ratio S.

So far we have based the construction of the Smith chart on the definition of the voltage reflection coefficient of the load impedance, as given in Eq. (9–134). The input impedance looking toward the load at a distance z' from the load is the ratio of $V(z')$ and $I(z')$. From Eqs. (9–133a) and (9–133b) we have, by writing $j\beta$ for γ for a lossless line,

$$Z_i(z') = \frac{V(z')}{I(z')} = Z_0\left[\frac{1 + \Gamma e^{-j2\beta z'}}{1 - \Gamma e^{-j2\beta z'}}\right]. \tag{9–190}$$

The normalized input impedance is

$$z_i = \frac{Z_i}{Z_0} = \frac{1 + \Gamma e^{-j2\beta z'}}{1 - \Gamma e^{-j2\beta z'}} = \frac{1 + |\Gamma| e^{j\phi}}{1 - |\Gamma| e^{j\phi}}, \tag{9–191}$$

where

$$\phi = \theta_\Gamma - 2\beta z'. \tag{9–192}$$

We note that Eq. (9–191) relating z_i and $\Gamma e^{-j2\beta z'} = |\Gamma| e^{j\phi}$ is of exactly the same form as Eq. (9–184) relating z_L and $\Gamma = |\Gamma| e^{j\theta_\Gamma}$. In fact, the latter is a special case of the former for $z' = 0$ ($\phi = \theta_\Gamma$). The magnitude, $|\Gamma|$, of the reflection coefficient and therefore the standing-wave ratio S, are not changed by the additional line length z'. Thus,

just as we can use the Smith chart to find $|\Gamma|$ and θ_Γ for a given z_L at the load, we can keep $|\Gamma|$ constant and *subtract* (rotate in the *clockwise* direction) from θ_Γ an angle equal to $2\beta z' = 4\pi z'/\lambda$. This will locate the point for $|\Gamma|e^{j\phi}$, which determines z_i, the normalized input impedance looking into a lossless line of characteristic impedance R_0, length z', and a normalized load impedance z_L. Two additional scales in $\Delta z'/\lambda$ are usually provided along the perimeter of the $|\Gamma| = 1$ circle for easy reading of the

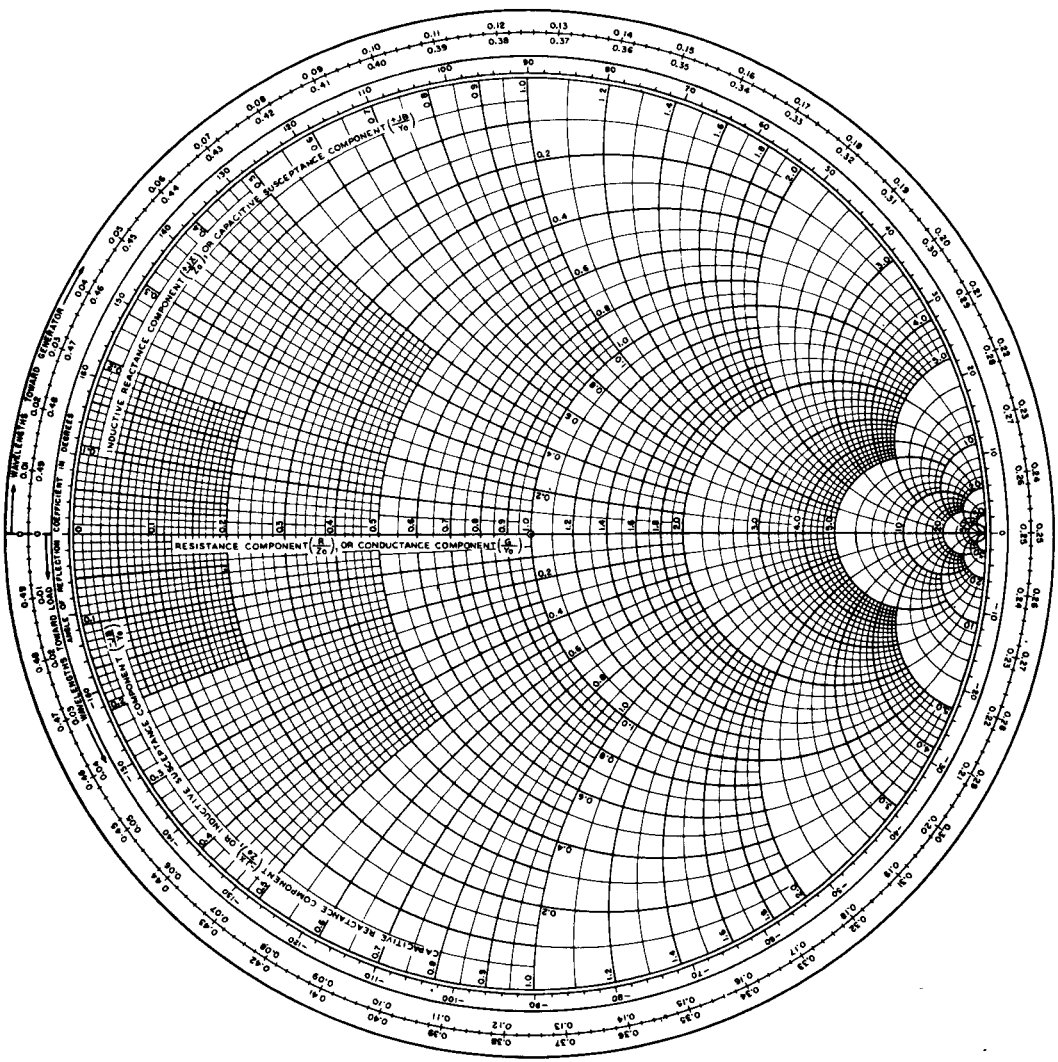

FIGURE 9–32
The Smith chart.

phase change $2\beta(\Delta z')$ due to a change in line length $\Delta z'$: The outer scale is marked "wavelengths toward generator" in the clockwise direction (increasing z'); and the inner scale is marked "wavelengths toward load" in the counterclockwise direction (decreasing z'). Figure 9–32 is a typical Smith chart, which is commercially available.† It has a complicated appearance, but it actually consists merely of constant-r and constant-x circles. We note that a change of half a wavelength in line length ($\Delta z' = \lambda/2$) corresponds to a $2\beta(\Delta z') = 2\pi$ change in ϕ. A complete revolution around a $|\Gamma|$-circle returns to the same point and results in no change in impedance, as was asserted in Eq. (9–115).

We shall illustrate the use of the Smith chart for solving some typical transmission-line problems by several examples.

EXAMPLE 9–13 Use the Smith chart to find the input impedance of a section of a 50 (Ω) lossless transmission line that is 0.1 wavelength long and is terminated in a short-circuit.

Solution Given

$$z_L = 0,$$
$$R_0 = 50 \quad (\Omega),$$
$$z' = 0.1\lambda.$$

1. Enter the Smith chart at the intersection of $r = 0$ and $x = 0$ (point P_{sc} on the extreme left of chart; see Fig. 9–33).
2. Move along the perimeter of the chart ($|\Gamma| = 1$) by 0.1 "wavelengths toward generator" in a clockwise direction to P_1.
3. At P_1, read $r = 0$ and $x \cong 0.725$, or $z_i = j0.725$. Thus, $Z_i = R_0 z_i = 50(j0.725) = j36.3$ (Ω). (The input impedance is purely inductive.)

This result can be checked readily by using Eq. (9–112):

$$Z_i = jR_0 \tan \beta\ell = j50 \tan\left(\frac{2\pi}{\lambda}\right)0.1\lambda$$
$$= j50 \tan 36° = j36.3 \quad (\Omega).$$

EXAMPLE 9–14 A lossless transmission line of length 0.434λ and characteristic impedance 100 (Ω) is terminated in an impedance $260 + j180$ (Ω). Find (a) the voltage reflection coefficient, (b) the standing-wave ratio, (c) the input impedance, and (d) the location of a voltage maximum on the line.

† All of the Smith charts used in this book are reprinted with permission of Emeloid Industries, Inc., New Jersey.

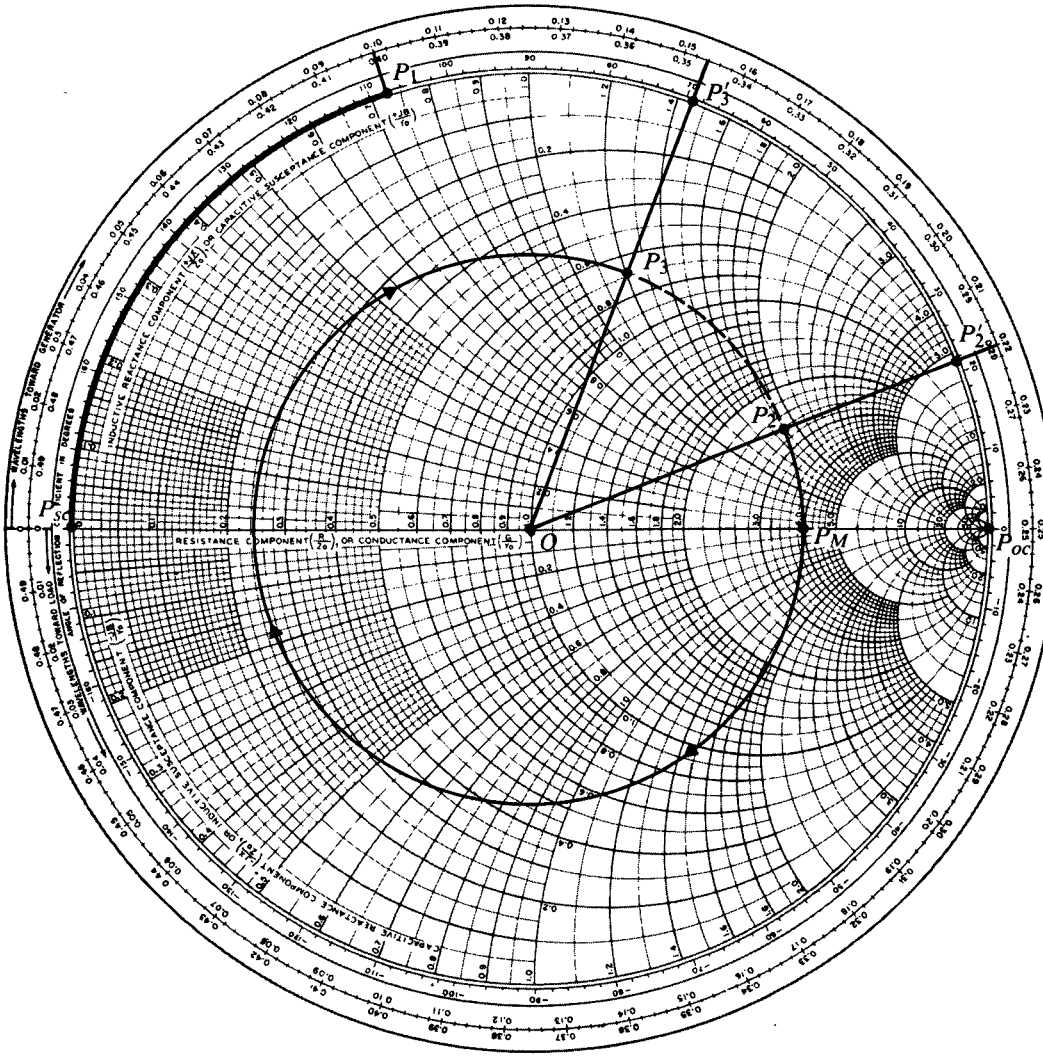

FIGURE 9–33
Smith-chart calculations for Examples 9–13 and 9–14.

Solution Given

$$z' = 0.434\lambda,$$
$$R_0 = 100 \quad (\Omega),$$
$$Z_L = 260 + j180 \quad (\Omega).$$

a) We find the voltage reflection coefficient in several steps:

1. Enter the Smith chart at $z_L = Z_L/R_0 = 2.6 + j1.8$ (point P_2 in Fig. 9–33).

2. With the center at the origin, draw a circle of radius $\overline{OP}_2 = |\Gamma| = 0.60$. (The radius of the chart $\overline{OP}_{sc}$ equals unity.)
3. Draw the straight line OP_2 and extend it to P'_2 on the periphery. Read 0.220 on "wavelengths toward generator" scale. The phase angle θ_Γ of the reflection coefficient is $(0.250 - 0.220) \times 4\pi = 0.12\pi$ (rad) or 21°. (We multiply the change in wavelengths by 4π because angles on the Smith chart are measured in $2\beta z'$ or $4\pi z'/\lambda$. A half-wavelength change in line length corresponds to a complete revolution on the Smith chart.) The answer to part (a) is then

$$\Gamma = |\Gamma| e^{j\theta_\Gamma} = 0.60 \underline{/21°}.$$

b) The $|\Gamma| = 0.60$ circle intersects with the positive-real axis OP_{oc} at $r = S = 4$. Thus the voltage standing-wave ratio is 4.

c) To find the input impedance, we proceed as follows:

1. Move P'_2 at 0.220 by a total of 0.434 "wavelengths toward generator," first to 0.500 (same as 0.000) and then further to 0.154[$(0.500 - 0.220) + 0.154 = 0.434$] to P'_3.
2. Join O and P'_3 by a straight line which intersects the $|\Gamma| = 0.60$ circle at P_3.
3. Read $r = 0.69$ and $x = 1.2$ at P_3. Hence,

$$Z_i = R_0 z_i = 100(0.69 + j1.2) = 69 + j120 \quad (\Omega).$$

d) In going from P_2 to P_3, the $|\Gamma| = 0.60$ circle intersects the positive-real axis OP_{oc} at P_M where the voltage is a maximum. Thus a voltage maximum appears at $(0.250 - 0.220)\lambda$ or 0.030λ from the load. ■

EXAMPLE 9–15 Solve Example 9–9 by using the Smith chart. Given

$$R_0 = 50 \quad (\Omega),$$
$$S = 3.0,$$
$$\lambda = 2 \times 0.2 = 0.4 \quad (\text{m}),$$
$$\text{First voltage minimum at } z'_m = 0.05 \text{ (m)},$$

find (a) Γ, (b) Z_L, (c) ℓ_m, and R_m (Fig. 9–12).

Solution

a) On the positive-real axis OP_{oc}, locate the point P_M at which $r = S = 3.0$ (see Fig. 9–34). Then $\overline{OP}_M = |\Gamma| = 0.5$ ($\overline{OP}_{oc} = 1.0$). We cannot find θ_Γ until we have located the point that represents the normalized load impedance.

b) We use the following procedure to find the load impedance on the Smith chart:

1. Draw a circle centered at the origin with radius $\overline{OP}_M$, which intersects with the negative-real axis OP_{sc} at P_m where there will be a voltage minimum.
2. Since $z'_m/\lambda = 0.05/0.4 = 0.125$, move from P_{sc} 0.125 "wavelengths toward load" in the counterclockwise direction to P'_L.
3. Join O and P'_L by a straight line, intersecting the $|\Gamma| = 0.5$ circle at P_L. This is the point representing the normalized load impedance.

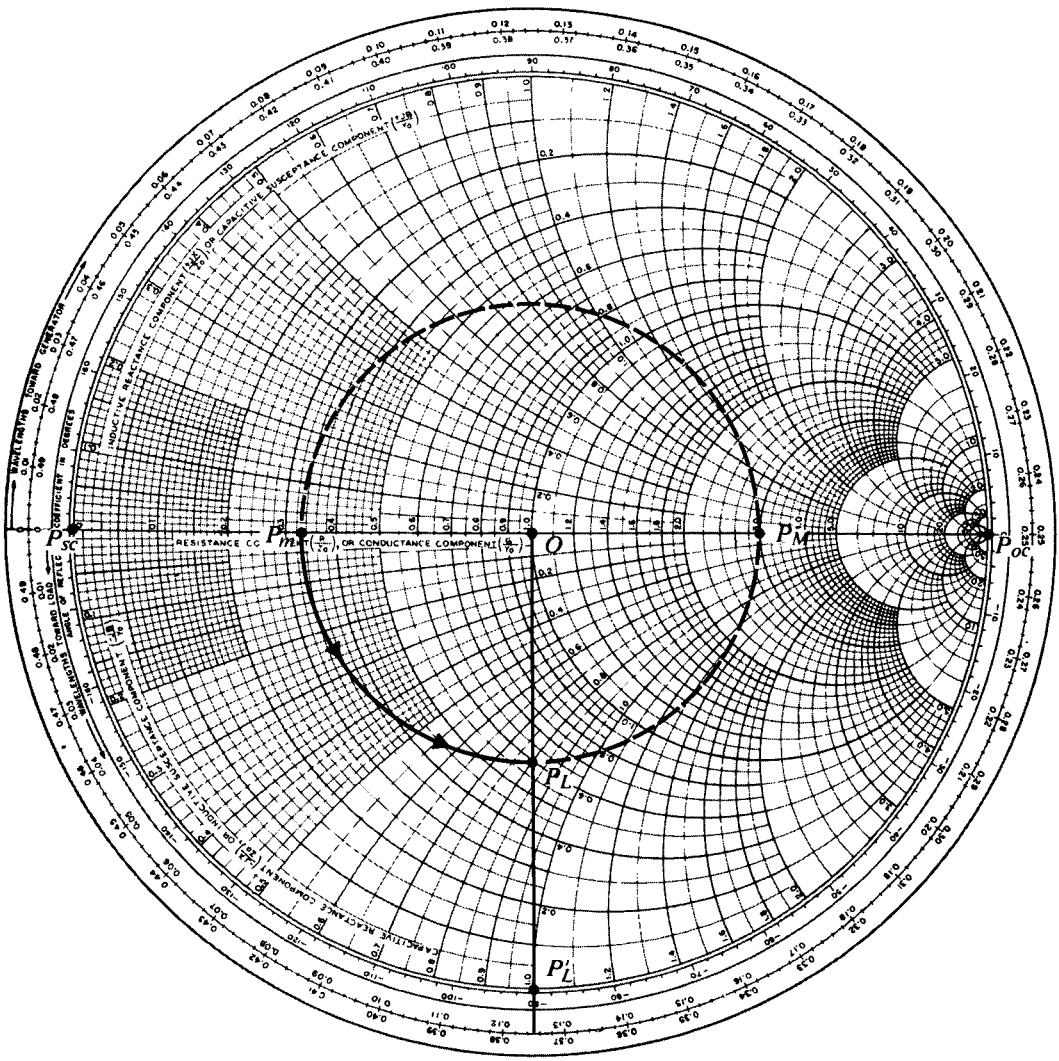

FIGURE 9–34
Smith-chart calculations for Example 9–15.

4. Read the angle $\angle P_{oc}OP'_L = 90° = \pi/2$ (rad). There is no need to use a protractor because $\angle P_{oc}OP'_L = 4\pi(0.250 - 0.125) = \pi/2$. Hence $\theta_\Gamma = -\pi/2$ (rad), or $\Gamma = 0.5\underline{/-90°} = -j0.5$.
5. Read at P_L, $z_L = 0.60 - j0.80$, which gives

$$Z_L = 50(0.60 - j0.80) = 30 - j40 \quad (\Omega).$$

c) The equivalent line length and the terminating resistance can be found easily:

$$\ell_m = \frac{\lambda}{2} - z'_m = 0.2 - 0.05 = 0.15 \quad \text{(m)},$$

$$R_m = \frac{R_0}{S} = \frac{50}{3} = 16.7 \quad (\Omega).$$

All the above results are the same as those obtained in Example 9–9, but no calculations with complex numbers are needed in using the Smith chart. ■

9–6.1 SMITH-CHART CALCULATIONS FOR LOSSY LINES

In discussing the use of the Smith chart for transmission-line calculations we have assumed the line to be lossless. This is normally a satisfactory approximation, since we generally deal with relatively short sections of low-loss lines. The lossless assumption enables us to say, following Eq. (9–191), that the magnitude of the $\Gamma e^{-j2\beta z'}$ term does not change with line length z' and that we can find z_i from z_L, and vice versa, by moving along the $|\Gamma|$-circle by an angle equal to $2\beta z'$.

For a lossy line of a sufficient length ℓ, such that $2\alpha\ell$ is not negligible in comparison to unity, Eq. (9–191) must be amended to read

$$\begin{aligned} z_i &= \frac{1 + \Gamma e^{-2\alpha z'} e^{-j2\beta z'}}{1 - \Gamma e^{-2\alpha z'} e^{-j2\beta z'}} \\ &= \frac{1 + |\Gamma| e^{-2\alpha z'} e^{j\phi}}{1 - |\Gamma| e^{-2\alpha z'} e^{j\phi}}, \qquad \phi = \theta_\Gamma - 2\beta z'. \end{aligned} \tag{9–193}$$

Hence, to find z_i from z_L, we cannot simply move along the $|\Gamma|$-circle; auxiliary calculations are necessary to account for the $e^{-2\alpha z'}$ factor. The following example illustrates what has to be done.

EXAMPLE 9–16 The input impedance of a short-circuited lossy transmission line of length 2 (m) and characteristic impedance 75 (Ω) (approximately real) is $45 + j225$ (Ω). (a) Find α and β of the line. (b) Determine the input impedance if the short-circuit is replaced by a load impedance $Z_L = 67.5 - j45$ (Ω).

Solution

a) The short-circuit load is represented by the point P_{sc} on the extreme left of the Smith impedance chart.

1. Enter $z_{i1} = (45 + j225)/75 = 0.60 + j3.0$ in the chart as P_1 (Fig. 9–35).
2. Draw a straight line from the origin O through P_1 to P'_1.
3. Measure $\overline{OP}_1/\overline{OP}'_1 = 0.89 = e^{-2\alpha\ell}$. It follows that

$$\alpha = \frac{1}{2\ell} \ln\left(\frac{1}{0.89}\right) = \frac{1}{4} \ln 1.124 = 0.029 \quad \text{(Np/m)}.$$

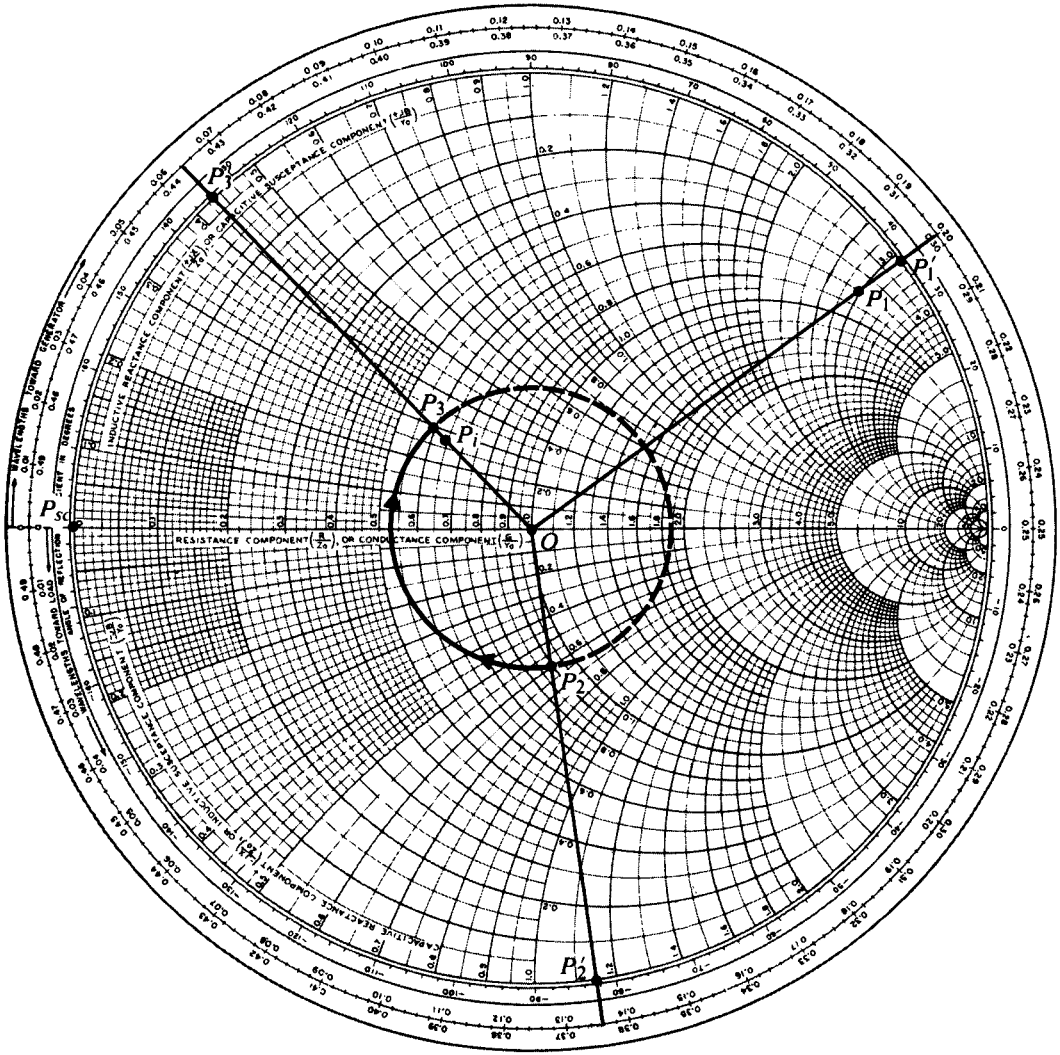

FIGURE 9–35
Smith-chart calculations for a lossy transmission line (Example 9–16).

4. Record that the arc $P_{sc}P_1'$ is 0.20 "wavelengths toward generator." We have $\ell/\lambda = 0.20$ and $2\beta\ell = 4\pi\ell/\lambda = 0.8\pi$. Thus,

$$\beta = \frac{0.8\pi}{2\ell} = \frac{0.8\pi}{4} = 0.2\pi \quad \text{(rad/m)}.$$

b) To find the input impedance for $Z_L = 67.5 - j45\ (\Omega)$:

1. Enter $z_L = Z_L/Z_0 = (67.5 - j45)/75 = 0.9 - j0.6$ on the Smith chart as P_2.

2. Draw a straight line from O through P_2 to P_2' where the "wavelengths toward generator" reading is 0.364.
3. Draw a $|\Gamma|$-circle centered at O with radius $\overline{OP}_2$.
4. Move P_2' along the perimeter by 0.20 "wavelengths toward generator" to P_3' at $0.364 + 0.20 = 0.564$ or 0.064.
5. Join P_3' and O by a straight line, intersecting the $|\Gamma|$-circle at P_3.
6. Mark on line OP_3 a point P_i such that $\overline{OP}_i/\overline{OP}_3 = e^{-2\alpha\ell} = 0.89$.
7. At P_i, read $z_i = 0.64 + j0.27$. Hence,

$$Z_i = 75(0.64 + j0.27) = 48.0 + j20.3 \quad (\Omega).$$

9–7 Transmission-Line Impedance Matching

Transmission lines are used for the transmission of power and information. For radio-frequency power transmission it is highly desirable that as much power as possible is transmitted from the generator to the load and as little power as possible is lost on the line itself. This will require that the load be matched to the characteristic impedance of the line so that the standing-wave ratio on the line is as close to unity as possible. For information transmission it is essential that the lines be matched because reflections from mismatched loads and junctions will result in echoes and will distort the information-carrying signal. In this section we discuss several methods for impedance-matching on lossless transmission lines. We note parenthetically that the methods we develop will be of little consequence to power transmission by 60 (Hz) lines inasmuch as these lines are generally very short in comparison to the 5 (Mm) wavelength and the line losses are appreciable. Sixty-hertz power-line circuits are usually analyzed in terms of equivalent lumped electrical networks.

9–7.1 IMPEDANCE MATCHING BY QUARTER-WAVE TRANSFORMER

A simple method for matching a resistive load R_L to a lossless transmission line of a characteristic impedance R_0 is to insert a quarter-wave transformer with a characteristic impedance R_0' such that

$$R_0' = \sqrt{R_0 R_L}. \tag{9–194}$$

Since the length of the quarter-wave line depends on wavelength, this matching method is frequency-sensitive, as are all the other methods to be discussed.

EXAMPLE 9–17 A signal generator is to feed equal power through a lossless air transmission line with a characteristic impedance 50 (Ω) to two separate resistive loads, 64 (Ω) and 25 (Ω). Quarter-wave transformers are used to match the loads to the 50 (Ω) line, as shown in Fig. 9–36. (a) Determine the required characteristic impedances of the quarter-wave lines. (b) Find the standing-wave ratios on the matching line sections.

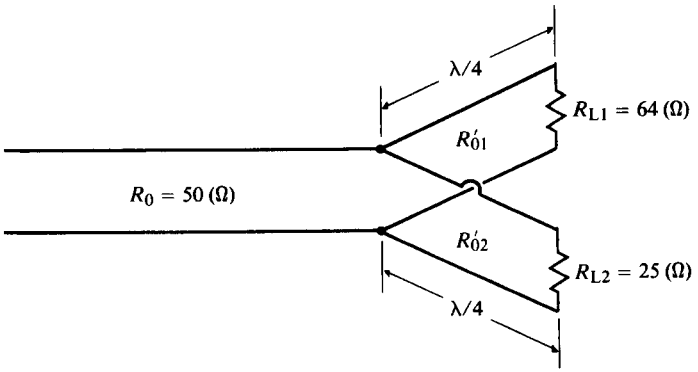

FIGURE 9–36
Impedance matching by quarter-wave lines (Example 9–17).

Solution

a) To feed equal power to the two loads, the input resistance at the junction with the main line looking toward each load must be equal to $2R_0$. $R_{i1} = R_{i2} = 2R_0 = 100\ (\Omega)$:

$$R'_{01} = \sqrt{R_{i1}R_{L1}} = \sqrt{100 \times 64} = 80 \quad (\Omega),$$
$$R'_{02} = \sqrt{R_{i2}R_{L2}} = \sqrt{100 \times 25} = 50 \quad (\Omega).$$

b) Under matched conditions there are no standing waves on the main transmission line ($S = 1$). The standing-wave ratios on the two matching line sections are as follows.

Matching section No. 1:

$$\Gamma_1 = \frac{R_{L1} - R'_{01}}{R_{L1} + R'_{01}} = \frac{64 - 80}{64 + 80} = -0.11,$$
$$S_1 = \frac{1 + |\Gamma_1|}{1 - |\Gamma_1|} = \frac{1 + 0.11}{1 - 0.11} = 1.25.$$

Matching section No. 2:

$$\Gamma_2 = \frac{R_{L2} - R'_{02}}{R_{L2} + R'_{02}} = \frac{25 - 50}{25 + 50} = -0.33,$$
$$S_2 = \frac{1 + |\Gamma_2|}{1 - |\Gamma_2|} = \frac{1 + 0.33}{1 - 0.33} = 1.99.$$

Ordinarily, the main transmission line and the matching line sections are essentially lossless. In that case, both R_0 and R'_0 are purely real, and Eq. (9–194) will have no solution if R_L is replaced by a complex Z_L. Hence quarter-wave transformers are not useful for matching a complex load impedance to a low-loss line.

In the following subsection we will discuss a method for matching an arbitrary load impedance to a line by using a single open- or short-circuited line section (a

single stub) in parallel with the main line and at an appropriate distance from the load. Since it is more convenient to use admittances instead of impedances for parallel connections, we first examine how the Smith chart can be used to make admittance calculations.

Let $Y_L = 1/Z_L$ denote the load admittance. The normalized load impedance is

$$z_L = \frac{Z_L}{R_0} = \frac{1}{R_0 Y_L} = \frac{1}{y_L}, \tag{9–195}$$

where

$$\begin{aligned} y_L &= Y_L/Y_0 = Y_L/G_0 \\ &= R_0 Y_L = g + jb \qquad \text{(Dimensionless)} \end{aligned} \tag{9–196}$$

is the normalized load admittance having normalized conductance g and normalized susceptance b as its real and imaginary parts, respectively. Equation (9–195) suggests that a quarter-wave line with a unity normalized characteristic impedance will transform z_L to y_L, and vice versa. On the Smith chart we need only move the point representing z_L along the $|\Gamma|$-circle by a quarter-wavelength to locate the point representing y_L. Since a $\lambda/4$-change in line length ($\Delta z'/\lambda = \frac{1}{4}$) corresponds to a change of π radians ($2\beta\,\Delta z' = \pi$) on the Smith chart, ***the points representing z_L and y_L are*** then ***diametrically opposite to each other on the $|\Gamma|$-circle.*** This observation enables us to find y_L from z_L, and z_L from y_L, on the Smith chart in a very simple manner.

EXAMPLE 9–18 Given $Z_L = 95 + j20$ (Ω), find Y_L.

Solution This problem has nothing to do with any transmission line. In order to use the Smith chart we can choose an arbitrary normalizing constant; for instance, $R_0 = 50$ (Ω). Thus,

$$z_L = \tfrac{1}{50}(95 + j20) = 1.9 + j0.4.$$

Enter z_L as point P_1 on the Smith chart in Fig. 9–37. The point P_2 on the other side of the line joining P_1 and O represents y_L: $\overline{OP}_2 = \overline{OP}_1$.

$$Y_L = \frac{1}{R_0} y_L = \frac{1}{50}(0.5 - j0.1) = 10 - j2 \quad \text{(mS)}.$$

EXAMPLE 9–19 Find the input admittance of an open-circuited line of characteristic impedance 300 (Ω) and length 0.04λ.

Solution

1. For an open-circuited line we start from the point P_{oc} on the extreme right of the impedance Smith chart, at 0.25 in Fig. 9–38.
2. Move along the perimeter of the chart by 0.04 "wavelengths toward generator" to P_3 (at 0.29).
3. Draw a straight line from P_3 through O, intersecting at P'_3 on the opposite side.

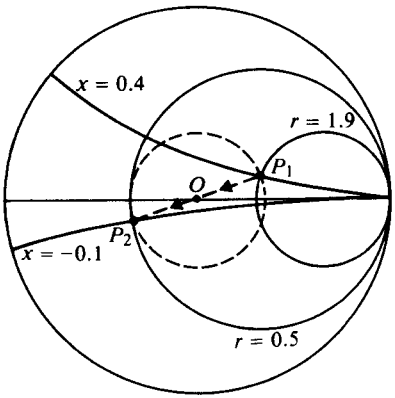

FIGURE 9–37
Finding admittance from impedance (Example 9–18).

4. Read at P'_3

$$y_i = 0 + j0.26.$$

Thus,

$$Y_i = \frac{1}{300}(0 + j0.26) = j0.87 \quad \text{(mS)}.$$

In the preceding two examples we have made admittance calculations by using the Smith chart as an impedance chart. The Smith chart can also be used as an admittance chart, in which case the r- and x-circles would be g- and b-circles. The points representing an open- and a short-circuit termination would be the points on the extreme left and the extreme right, respectively, on an admittance chart. For Example 9–19, we could then start from extreme left point on the chart, at 0.00 in Fig. 9–38, and move 0.04 "wavelengths toward generator" to P'_3 directly.

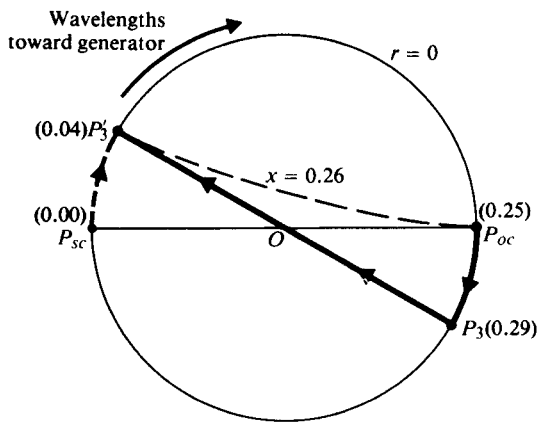

FIGURE 9–38
Finding input admittance of open-circuited line (Example 9–19).

9–7.2 SINGLE-STUB MATCHING

We now tackle the problem of matching a load impedance Z_L to a lossless line that has a characteristic impedance R_0 by placing a single short-circuited stub in parallel with the line, as shown in Fig. 9–39. This is the ***single-stub method*** for impedance matching. We need to determine the length of the stub, ℓ, and the distance from the load, d, such that the impedance of the parallel combination to the right of points B–B' equals R_0. Short-circuited stubs are usually used in preference to open-circuited stubs because an infinite terminating impedance is more difficult to realize than a zero terminating impedance for reasons of radiation from an open end and coupling effects with neighboring objects. Moreover, a short-circuited stub of an adjustable length and a constant characteristic resistance is much easier to construct than an open-circuited one. Of course, the difference in the required length for an open-circuited stub and that for a short-circuited stub is an odd multiple of a quarter-wavelength.

The parallel combination of a line terminated in Z_L and a stub at points B–B' in Fig. 9–39 suggest that it is advantageous to analyze the matching requirements in terms of admittances. The basic requirement is

$$\begin{aligned} Y_i &= Y_B + Y_s \\ &= Y_0 = \frac{1}{R_0}. \end{aligned} \tag{9–197}$$

In terms of normalized admittances, Eq. (9–197) becomes

$$1 = y_B + y_s, \tag{9–198}$$

where $y_B = R_0 Y_B$ is for the load section and $y_s = R_0 Y_s$ is for the short-circuited stub. However, since the input admittance of a short-circuited stub is purely susceptive, y_s is purely imaginary. As a consequence, Eq. (9–198) can be satisfied only if

$$y_B = 1 + jb_B \tag{9–199}$$

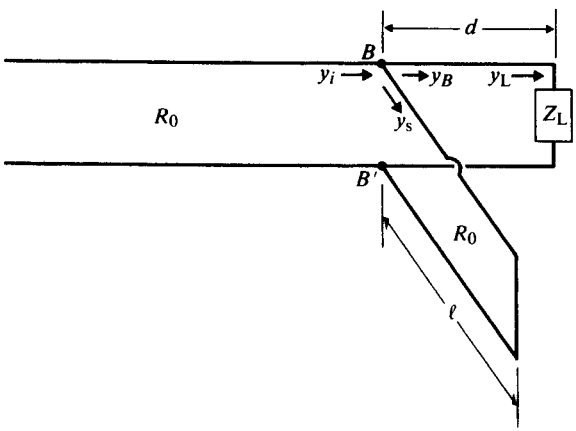

FIGURE 9–39
Impedance matching by single-stub method.

and

$$y_s = -jb_B, \tag{9-200}$$

where b_B can be either positive or negative. Our objectives, then, are to find the length d such that the admittance, y_B, of the load section looking to the right of terminals B–B' has a *unity real part* and to find the length ℓ_B of the stub required to *cancel the imaginary part.*

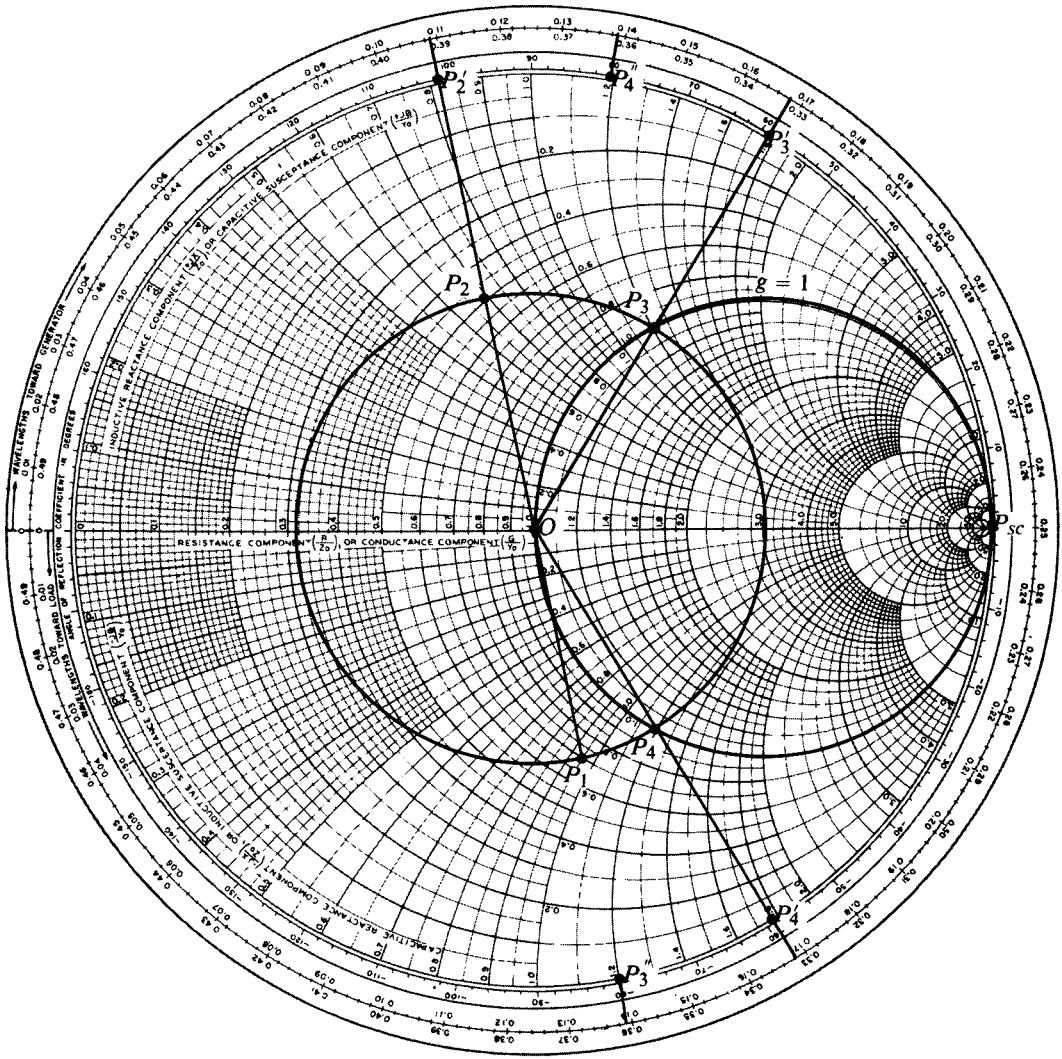

FIGURE 9–40
Construction for single-stub matching on Smith admittance chart (Example 9–20).

Using the Smith chart as an admittance chart, we proceed as follows for single-stub matching:

1. Enter the point representing the normalized load admittance y_L.
2. Draw the $|\Gamma|$-circle for y_L, which will intersect the $g = 1$ circle at two points. At these points, $y_{B1} = 1 + jb_{B1}$ and $y_{B2} = 1 + jb_{B2}$. Both are possible solutions.
3. Determine load-section lengths d_1 and d_2 from the angles between the point representing y_L and the points representing y_{B1} and y_{B2}.
4. Determine stub lengths ℓ_{B1} and ℓ_{B2} from the angles between the short-circuit point on the extreme right of the chart to the points representing $-jb_{B1}$ and $-jb_{B2}$, respectively.

The following example will illustrate the necessary steps.

EXAMPLE 9–20 A 50 (Ω) transmission line is connected to a load impedance $Z_L = 35 - j47.5$ (Ω). Find the position and length of a short-circuited stub required to match the line.

Solution Given

$$R_0 = 50\ (\Omega)$$
$$Z_L = 35 - j47.5\ (\Omega)$$
$$z_L = Z_L/R_0 = 0.70 - j0.95.$$

1. Enter z_L on the Smith chart as P_1 (Fig. 9–40).
2. Draw a $|\Gamma|$-circle centered at O with radius $\overline{OP}_1$.
3. Draw a straight line from P_1 through O to point P_2' on the perimeter, intersecting the $|\Gamma|$-circle at P_2, which represents y_L. Note 0.109 at P_2' on the "wavelengths toward generator" scale.
4. Note the two points of intersection of the $|\Gamma|$-circle with the $g = 1$ circle.

$$\text{At } P_3\text{:}\quad y_{B1} = 1 + j1.2 = 1 + jb_{B1};$$
$$\text{At } P_4\text{:}\quad y_{B2} = 1 - j1.2 = 1 + jb_{B2}.$$

5. Solutions for the position of the stub:

$$\text{For } P_3 \text{ (from } P_2' \text{ to } P_3')\text{:}\quad d_1 = (0.168 - 0.109)\lambda = 0.059\lambda;$$
$$\text{For } P_4 \text{ (from } P_2' \text{ to } P_4')\text{:}\quad d_2 = (0.332 - 0.109)\lambda = 0.223\lambda.$$

6. Solutions for the length of short-circuited stub to provide $y_s = -jb_B$:

   For P_3 (from P_{sc} on the extreme right of chart to P_3'', which represents $-jb_{B1} = -j1.2$):

$$\ell_{B1} = (0.361 - 0.250)\lambda = 0.111\lambda;$$

   For P_4 (from P_{sc} to P_4'', which represents $-jb_{B2} = j1.2$):

$$\ell_{B2} = (0.139 + 0.250)\lambda = 0.389\lambda.$$

In general, the solution with the shorter lengths is preferred unless there are other practical constraints. The exact length, ℓ_B, of the short-circuited stub may require fine adjustments in the actual matching procedure; hence the shorted matching sections are sometimes called ***stub tuners.*** ■

The use of Smith chart in solving impedance-matching problems avoids the manipulation of complex numbers and the computation of tangent and arc-tangent functions; but graphical constructions are needed, and graphical methods have limited accuracy. Actually, the analytical solutions of impedance-matching problems are relatively simple, and easy access to a computer may diminish the reliance on the Smith chart and, at the same time, yield more accurate results.

For the single-stub matching problem illustrated in Fig. 9–39 we have, from Eq. (9–109).

$$z_B = \frac{(r_L + jx_L) + jt}{1 + j(r_L + jx_L)t}, \tag{9–201}$$

where

$$t = \tan \beta d. \tag{9–202}$$

The normalized input admittance to the right of points B–B' is

$$y_B = \frac{1}{z_B} = g_B + jb_B, \tag{9–203}$$

where

$$g_B = \frac{r_L(1 - x_L t) + r_L t(x_L + t)}{r_L^2 + (x_L + t)^2} \tag{9–204}$$

and

$$b_B = \frac{r_L^2 t - (1 - x_L t)(x_L + t)}{r_L + (x_L + t)^2}. \tag{9–205}$$

A perfect match requires the simultaneous satisfaction of Eqs. (9–199) and (9–200). Equating g_B in Eq. (9–204) to unity, we have

$$(r_L - 1)t^2 - 2x_L t + (r_L - r_L^2 - x_L^2) = 0. \tag{9–206}$$

Solving Eq. (9–206), we obtain

$$t = \begin{cases} \dfrac{1}{r_L - 1}\{x_L \pm \sqrt{r_L[(1 - r_L)^2 + x_L^2]}\}, & r_L \neq 1, \quad \text{(9–207a)} \\ -\dfrac{x_L}{2}, & r_L = 1. \quad \text{(9–207b)} \end{cases}$$

The required length d can be found from Eqs. (9–202), (9–207a), and (9–207b):

$$\frac{d}{\lambda} = \begin{cases} \dfrac{1}{2\pi} \tan^{-1} t, & t \geq 0, \quad \text{(9–208a)} \\ \dfrac{1}{2\pi}(\pi + \tan^{-1} t), & t < 0. \quad \text{(9–208b)} \end{cases}$$

Similarly, from Eqs. (9–200) and (9–205), we obtain

$$\frac{\ell}{\lambda} = \begin{cases} \dfrac{1}{2\pi}\tan^{-1}\left(\dfrac{1}{b_B}\right), & b_B \geq 0, \qquad (9\text{–}209a) \\ \dfrac{1}{2\pi}\left[\pi + \tan^{-1}\left(\dfrac{1}{b_B}\right)\right], & b_B < 0. \qquad (9\text{–}209b) \end{cases}$$

For a given load impedance, both d/λ and ℓ/λ can be determined easily on a scientific calculator. It is also a simple matter to write a general computer program for the single-stub matching problem. More accurate answers to the problem in Example 9–20 ($r_L = 0.70$ and $x_L = -0.95$) are

$$d_1 = 0.05894469\lambda, \qquad \ell_{B1} = 0.11117792\lambda,$$
$$d_2 = 0.22347730\lambda, \qquad \ell_{B2} = 0.38882208\lambda.$$

Of course, such accuracies are seldom needed in an actual problem; but these answers have been obtained easily without a Smith chart.

9–7.3 DOUBLE-STUB MATCHING

The method of impedance matching by means of a single stub described in the preceding subsection can be used to match any arbitrary, nonzero, finite load impedance to the characteristic resistance of a line. However, the single-stub method requires that the stub be attached to the main line at a specific point, which varies as the load impedance or the operating frequency is changed. This requirement often presents practical difficulties because the specified junction point may occur at an undesirable location from a mechanical viewpoint. Furthermore, it is very difficult to build a variable-length coaxial line with a constant characteristic impedance. In such cases an alternative method for impedance-matching is to use two short-circuited stubs attached to the main line at fixed positions, as shown in Fig. 9–41. Here, the distance d_o is fixed and arbitrarily chosen (such as $\lambda/16$, $\lambda/8$, $3\lambda/16$, $3\lambda/8$, etc.), and the lengths of the two stub tuners are adjusted to match a given load impedance Z_L to the main line. This scheme is the ***double-stub method*** for impedance matching.

In the arrangement in Fig. 9–41 a stub of length ℓ_A is connected directly in parallel with the load impedance Z_L at terminals A–A', and a second stub of length ℓ_B is attached at terminals B–B' at a fixed distance d_o away. For impedance matching with a main line that has a characteristic resistance R_0, we demand the total input admittance at terminals B–B', looking toward the load, to equal the characteristic conductance of the line; that is,

$$\begin{aligned} Y_i &= Y_B + Y_{sB} \\ &= Y_0 = \frac{1}{R_0}. \end{aligned} \qquad (9\text{–}210)$$

In terms of normalized admittances, Eq. (9–210) becomes

$$1 = y_B + y_{sB}. \qquad (9\text{–}211)$$

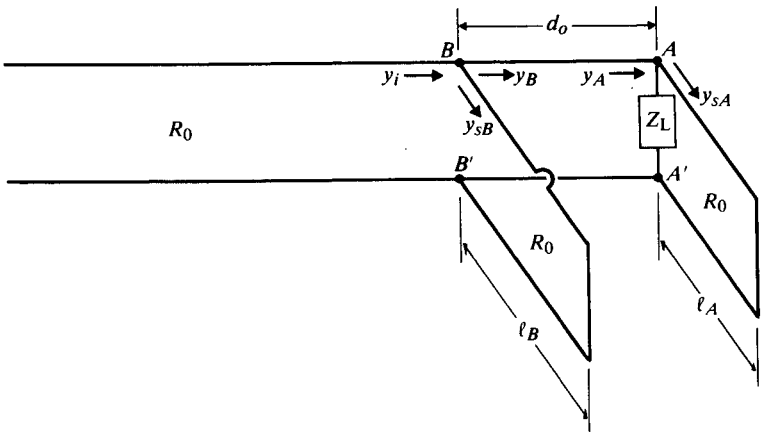

FIGURE 9–41
Impedance matching by double-stub method.

Now, since the input admittance y_{sB} of a short-circuited stub is purely imaginary, Eq. (9–211) can be satisfied only if

$$y_B = 1 + jb_B \tag{9–212}$$

and

$$y_{sB} = -jb_B. \tag{9–213}$$

Note that these requirements are exactly the same as those for single-stub matching.

On the Smith admittance chart the point representing y_B must lie on the $g = 1$ circle. This requirement must be translated by a distance d_o/λ "wavelengths toward load"; that is, y_A at terminals A–A' must lie on the $g = 1$ circle rotated by an angle $4\pi d_o/\lambda$ in the counterclockwise direction. Again, since the input admittance y_{sA} of the short-circuited stub is purely imaginary, the real part of y_A must be solely contributed by the real part of the normalized load admittance, g_L. The solution (or solutions) of the double-stub matching problem is then determined by the intersection (or intersections) of the g_L-circle with the rotated $g = 1$ circle. The procedure for solving a double-stub matching problem on the Smith admittance chart is as follows.

1. Draw the $g = 1$ circle. This is where the point representing y_B should be located.
2. Draw this circle rotated in the counterclockwise direction by d_o/λ "wavelengths toward load." This is where the point representing y_A should be located.
3. Enter the $y_L = g_L + jb_L$ point.
4. Draw the $g = g_L$ circle, intersecting the rotated $g = 1$ circle at one or two points where $y_A = g_L + jb_A$.
5. Mark the corresponding y_B-points on the $g = 1$ circle: $y_B = 1 + jb_B$.
6. Determine stub length ℓ_A from the angle between the point representing y_A and the point representing y_L.

7. Determine stub length ℓ_B from the angle between the point representing $-jb_B$ and P_{sc} on the extreme right.

EXAMPLE 9–21 A 50 (Ω) transmission line is connected to a load impedance $Z_L = 60 + j80$ (Ω). A double-stub tuner spaced an eighth of a wavelength apart is used to match the load to the line, as shown in Fig. 9–41. Find the required lengths of the short-circuited stubs.

Solution Given $R_0 = 50$ (Ω) and $Z_L = 60 + j80$ (Ω), it is easy to calculate

$$y_L = \frac{1}{z_L} = \frac{R_0}{Z_L} = \frac{50}{60 + j80} = 0.30 - j0.40.$$

(We could find y_L on the Smith chart by locating the point diametrically opposite to $z_L = (60 + j80)/50 = 1.20 + j1.60$, but this would clutter up the chart too much.) We follow the procedure outlined above, using a Smith admittance chart.

1. Draw the $g = 1$ circle (Fig. 9–42).
2. Rotate this $g = 1$ circle by $\frac{1}{8}$ "wavelengths toward load" in the counterclockwise direction. The angle of rotation is $4\pi/8$ (rad) or 90°.
3. Enter $y_L = 0.30 - j0.40$ as P_L.
4. Mark the two points of intersection, P_{A1} and P_{A2}, of the $g_L = 0.30$ circle with the rotated $g = 1$ circle.

   At P_{A1}, read $y_{A1} = 0.30 + j0.29$;
   At P_{A2}, read $y_{A2} = 0.30 + j1.75$.

5. Use a compass centered at the origin O to mark the points P_{B1} and P_{B2} on the $g = 1$ circle corresponding to the points P_{A1} and P_{A2}, respectively.

   At P_{B1}, read $y_{B1} = 1 + j1.38$;
   At P_{B2}, read $y_{B2} = 1 - j3.5$.

6. Determine the required stub lengths ℓ_{A1} and ℓ_{A2} from

   $(y_{sA})_1 = y_{A1} - y_L = j0.69$, $\ell_{A1} = (0.096 + 0.250)\lambda = 0.346\lambda$ (Point A_1),
   $(y_{sA})_2 = y_{A2} - y_L = j2.15$, $\ell_{A2} = (0.181 + 0.250)\lambda = 0.431\lambda$ (Point A_2).

7. Determine the required stub lengths ℓ_{B1} and ℓ_{B2} from

   $(y_{sB})_1 = -j1.38$, $\ell_{B1} = (0.350 - 0.250)\lambda = 0.100\lambda$ (Point B_1),
   $(y_{sB})_2 = j3.5$, $\ell_{B2} = (0.206 + 0.250)\lambda = 0.456\lambda$ (Point B_2).

Examination of the construction in Fig. 9–42 reveals that if the point P_L, representing the normalized load admittance $y_L = g_L + jb_L$, lies within the $g = 2$ circle (if $g_L > 2$), then the $g = g_L$ circle does not intersect with the rotated $g = 1$ circle, and no solution exists for double-stub matching with $d_o = \lambda/8$. This region for no solution varies with the chosen distance d_o between the stubs (Problem P.9–52). In such cases,

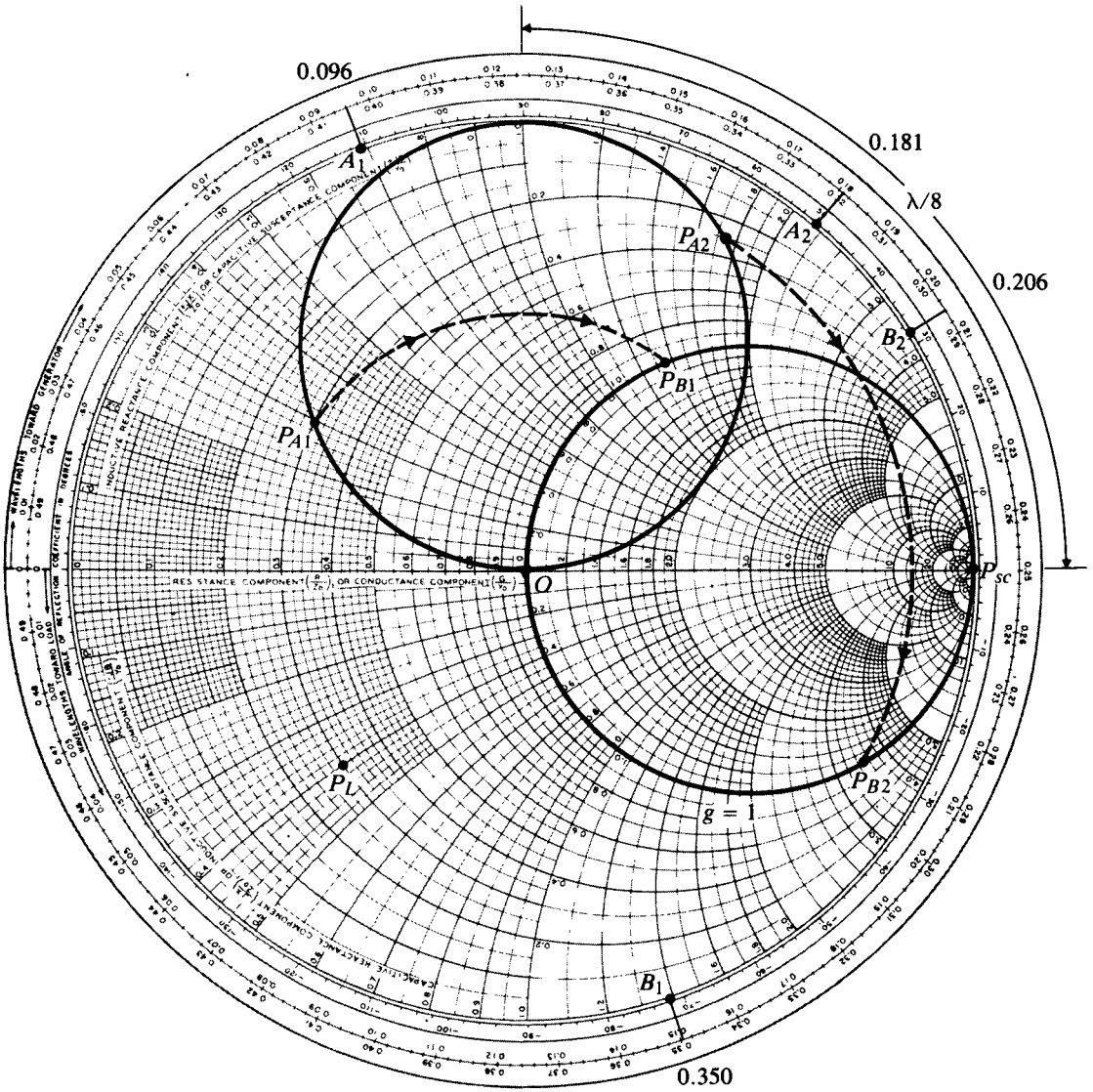

FIGURE 9–42
Construction for double-stub matching on Smith admittance chart.

impedance matching by the double-stub method can be achieved by adding an appropriate line section between Z_L and terminals A–A', as illustrated in Fig. 9–43 (Problem P.9–51).

An analytical solution of the double-stub impedance matching problem is, of course, also possible, albeit more involved than that of the single-stub problem devel-

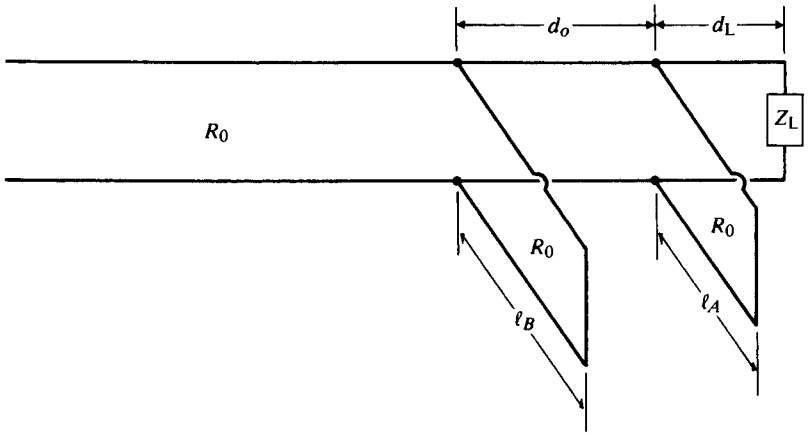

FIGURE 9–43
Double-stub impedance matching with added load-line section.

oped in the preceding subsection. The more ambitious reader may wish to obtain such an analytical solution and write a computer program for determining d_L/λ, ℓ_A/λ, and ℓ_B/λ in terms of z_L and d_o/λ.†

Review Questions

R.9–1 Discuss the similarities and dissimilarities of uniform plane waves in an unbounded media and TEM waves along transmission lines.

R.9–2 What are the three most common types of guiding structures that support TEM waves?

R.9–3 Compare the advantages and disadvantages of coaxial cables and two-wire transmission lines.

R.9–4 Write the transmission-line equations for a lossless parallel-plate line supporting TEM waves.

R.9–5 What are *striplines*?

R.9–6 Describe how the characteristic impedance of a parallel-plate transmission line depends on plate width and dielectric thickness.

R.9–7 Compare the velocity of TEM-wave propagation along a parallel-plate transmission line with that in an unbounded medium.

R.9–8 Define *surface impedance*. How is surface impedance related to the power dissipated in a plate conductor?

† D. K. Cheng and C. H. Liang, "Computer solution of double-stub impedance-matching problems," *IEEE Transactions on Education*, vol. E-25, pp. 120–123, November 1982.

R.9–9 State the difference between the surface resistance and the resistance per unit length of a parallel-plate transmission line.

R.9–10 What is the essential difference between a transmission line and an ordinary electric network?

R.9–11 Explain why waves along a lossy transmission line cannot be purely TEM.

R.9–12 What is a *triplate line*? How does the characteristic impedance of a triplate line compare with that of a corresponding stripline? Explain.

R.9–13 Write the general transmission-line equations for arbitrary time dependence and for time-harmonic time dependence.

R.9–14 Define *propagation constant* and *characteristic impedance* of a transmission line. Write their general expressions in terms of R, L, G, and C for sinusoidal excitation.

R.9–15 What is the phase relationship between the voltage and current waves on an infinitely long transmission line?

R.9–16 What is meant by a "distortionless line"? What relation must the distributed parameters of a line satisfy in order for the line to be distortionless?

R.9–17 Is a distortionless line lossless? Is a lossy transmission line dispersive? Explain.

R.9–18 Outline a procedure for determining the distributed parameters of a transmission line.

R.9–19 Show how the attenuation constant of a transmission line is determined from the propagated power and the power lost in the line per unit length.

R.9–20 What does "matched transmission line" mean?

R.9–21 On what factors does the input impedance of a transmission line depend?

R.9–22 What is the input impedance of an open-circuited lossless transmission line if the length of the line is (a) $\lambda/4$, (b) $\lambda/2$, and (c) $3\lambda/4$?

R.9–23 What is the input impedance of a short-circuited lossless transmission line if the length of the line is (a) $\lambda/4$, (b) $\lambda/2$, and (c) $3\lambda/4$?

R.9–24 Is the input reactance of a transmission line $\lambda/8$ long inductive or capacitive if it is (a) open-circuited, and (b) short-circuited?

R.9–25 On a line of length ℓ, what is the relation between the line's characteristic impedance and propagation constant and its open- and short-circuit input impedances?

R.9–26 What is a "quarter-wave transformer"? Why is it not useful for matching a complex load impedance to a low-loss line?

R.9–27 What is the input impedance of a lossless transmission line of length ℓ that is terminated in a load impedance Z_L if (a) $\ell = \lambda/2$, and (b) $\ell = \lambda$?

R.9–28 Discuss how a section of an open-circuited or short-circuited low-loss transmission line can be used to provide a parallel-resonant circuit.

R.9–29 Define the *bandwidth* and the *quality factor*, Q, of a parallel resonant circuit.

R.9–30 Define *voltage reflection coefficient*. Is it the same as "current reflection coefficient"? Explain.

R.9–31 Define *standing-wave ratio*. How is it related to voltage and current reflection coefficients?

R.9–32 What are Γ and S for a line with an open-circuit termination? A short-circuit termination?

R.9–33 Where do the minima of the voltage standing wave on a lossless line with a resistive termination occur (a) if $R_L > R_0$ and (b) if $R_L < R_0$?

R.9–34 Explain how the value of a terminating resistance can be determined by measuring the standing-wave ratio on a lossless transmission line.

R.9–35 Explain how the value of an arbitrary terminating impedance on a lossless transmission line can be determined by standing-wave measurements on the line.

R.9–36 A voltage generator having an internal impedance Z_g is connected at $t = 0$ to the input terminals of a lossless transmission line of length ℓ. The line has a characteristic impedance Z_0 and is terminated with a load impedance Z_L. At what time will a steady state on the line be reached if (a) $Z_g = Z_0$ and $Z_L = Z_0$, (b) $Z_L = Z_0$ but $Z_g \neq Z_0$, (c) $Z_g = Z_0$ but $Z_L \neq Z_0$, and (d) $Z_g \neq Z_0$ and $Z_L \neq Z_0$?

R.9–37 A battery of voltage V_0 is applied through a series resistance R_g to the input terminals of a lossless transmission line having a characteristic resistance R_0 and a load resistance R_L at the far end. What is the amplitude of the first transient voltage wave traveling from the battery to the load? What is the amplitude of the first reflected voltage wave from the load to the battery?

R.9–38 In Question R.9–37, what are the amplitudes of the first current wave traveling from the battery to the load and the first reflected current wave from the load to the battery?

R.9–39 What are *reflection diagrams* of transmission lines? For what purposes are they useful?

R.9–40 How do the voltage and current reflection diagrams of a terminated line differ?

R.9–41 A d-c voltage is applied to a lossless transmission line. Under what conditions will the transient voltage and current distributions along the line have different shapes? Under what conditions will they have the same shape?

R.9–42 Why is the concept of reflection coefficients not useful in analyzing the transient behavior of a transmission line terminated in a reactive load?

R.9–43 What is a Smith chart and why is it useful in making transmission-line calculations?

R.9–44 Where is the point representing a matched load on a Smith chart?

R.9–45 For a given load impedance Z_L on a lossless line of characteristic impedance Z_0, how do we use a Smith chart to determine (a) the reflection coefficient, and (b) the standing-wave ratio?

R.9–46 Why does a change of half a wavelength in line length correspond to a complete revolution on a Smith chart?

R.9–47 Given an impedance $Z = R + jX$, what procedure do we follow to find the admittance $Y = 1/Z$ on a Smith chart?

R.9–48 Given an admittance $Y = G + jB$, how do we use a Smith chart to find the impedance $Z = 1/Y$?

R.9–49 Where is the point representing a short-circuit on a Smith admittance chart?

R.9–50 Is the standing-wave ratio constant on a transmission line even when the line is lossy? Explain.

R.9–51 Can a Smith chart be used for impedance calculations on a lossy transmission line? Explain.

R.9–52 Why is it more convenient to use a Smith chart as an admittance chart for solving impedance-matching problems than to use it as an impedance chart?

R.9–53 Why is it desirable to achieve an impedance match in a transmission line?

R.9–54 Explain the single-stub method for impedance matching on a transmission line.

R.9–55 Explain the double-stub method for impedance matching on a transmission line.

R.9–56 Compare the relative advantages and disadvantages of the single-stub and the double-stub methods of impedance matching.

R.9–57 Why are the stubs used in impedance matching usually of the short-circuited type instead of the open-circuited type?

Problems

P.9–1 Neglecting fringe fields, prove analytically that a y-polarized TEM wave that propagates along a parallel-plate transmission line in $+z$-direction has the following properties: $\partial E_y/\partial x = 0$ and $\partial H_x/\partial y = 0$.

P.9–2 The electric and magnetic fields of a general TEM wave traveling in the $+z$-direction along a transmission line may have both x- and y-components, and both components may be functions of the transverse dimensions.

a) Find the relations among $E_x(x, y)$, $E_y(x, y)$, $H_x(x, y)$, and $H_y(x, y)$.

b) Verify that all the four field components in part (a) satisfy the two-dimensional Laplace's equation for static fields.

P.9–3 Consider lossless stripline designs for a given characteristic impedance.

a) How should the dielectric thickness, d, be changed for a given plate width, w, if the dielectric constant, ϵ_r, is doubled?

b) How should w be changed for a given d if ϵ_r is doubled?

c) How should w be changed for a given ϵ_r if d is doubled?

d) Will the velocity of propagation remain the same as that for the original line after the changes specified in parts (a), (b), and (c)? Explain.

P.9–4 Consider a transmission line made of two parallel brass strips—$\sigma_c = 1.6 \times 10^7$ (S/m)—of width 20 (mm) and separated by a lossy dielectric slab—$\mu = \mu_0$, $\epsilon_r = 3$, $\sigma = 10^{-3}$ (S/m)—of thickness 2.5 (mm). The operating frequency is 500 MHz.

a) Calculate the R, L, G, and C per unit length.

b) Compare the magnitudes of the axial and transverse components of the electric field.

c) Find γ and Z_0.

P.9–5 Verify Eq. (9–39).

P.9–6 Show that the attenuation and phase constants for a transmission line with perfect conductors separated by a lossy dielectric that has a complex permittivity $\epsilon = \epsilon' - j\epsilon''$ are, respectively,

$$\alpha = \omega\sqrt{\frac{\mu\epsilon'}{2}}\left[\sqrt{1+\left(\frac{\epsilon''}{\epsilon'}\right)^2} - 1\right]^{1/2} \quad \text{(Np/m)}, \tag{9–214}$$

$$\beta = \omega\sqrt{\frac{\mu\epsilon'}{2}}\left[\sqrt{1+\left(\frac{\epsilon''}{\epsilon'}\right)^2} + 1\right]^{1/2} \quad \text{(rad/m)}. \tag{9–215}$$

P.9–7 In the derivation of the approximate formulas of γ and Z_0 for low-loss lines in Subsection 9–3.1, all terms containing the second and higher powers of $(R/\omega L)$ and $(G/\omega C)$

were neglected in comparison with unity. At lower frequencies, better approximations than those given in Eqs. (9–54) and (9–58) may be required. Find new formulas for γ and Z_0 for low-loss lines that retain terms containing $(R/\omega L)^2$ and $(G/\omega C)^2$. Obtain the corresponding expression for phase velocity.

P.9–8 Obtain approximate expressions for γ and Z_0 for a lossy transmission line at very low frequencies such that $\omega L \ll R$ and $\omega C \ll G$.

P.9–9 The following characteristics have been measured on a lossy transmission line at 100 MHz:

$$Z_0 = 50 + j0 \quad (\Omega),$$
$$\alpha = 0.01 \quad (\text{dB/m}),$$
$$\beta = 0.8\pi \quad (\text{rad/m}).$$

Determine R, L, G, and C for the line.

P.9–10 It is desired to construct uniform transmission lines using polyethylene ($\epsilon_r = 2.25$) as the dielectric medium. Assuming negligible losses, (a) find the distance of separation for a 300 (Ω) two-wire line, where the radius of the conducting wires is 0.6 (mm); and (b) find the inner radius of the outer conductor for a 75 (Ω) coaxial line, where the radius of the center conductor is 0.6 (mm).

P.9–11 Prove that a maximum power is transferred from a voltage source with an internal impedance Z_g to a load impedance Z_L over a lossless transmission line when $Z_i = Z_g^*$, where Z_i is the impedance looking into the loaded line. What is the maximum power-transfer efficiency?

P.9–12 Express $V(z)$ and $I(z)$ in terms of the voltage V_i and current I_i at the input end and γ and Z_0 of a transmission line (a) in exponential form, and (b) in hyperbolic form.

P.9–13 Consider a section of a uniform transmission line of length ℓ, characteristic impedance Z_0, and propagation constant γ between terminal pairs 1–1′ and 2–2′ shown in Fig. 9–44(a). Let (V_1, I_1) and (V_2, I_2) be the phasor voltages and phasor currents at terminals 1–1′ and 2–2′, respectively.

a) Use Eqs. (9–100a) and (9–100b) to write the equations relating (V_1, I_1) and (V_2, I_2) in the form

$$\begin{bmatrix} V_1 \\ I_1 \end{bmatrix} = \begin{bmatrix} A & B \\ C & D \end{bmatrix} \begin{bmatrix} V_2 \\ I_2 \end{bmatrix}. \tag{9–216}$$

Determine A, B, C, and D, and note the following relations:

$$A = D \tag{9–217}$$

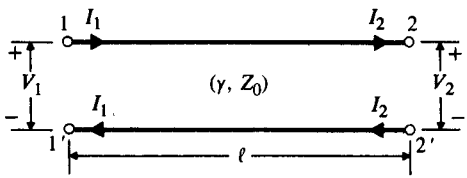

(a) A line section of length ℓ.

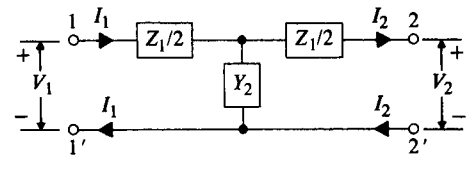

(b) An equivalent two-port symmetrical T-network.

FIGURE 9–44
Equivalence of a line section and a symmetrical two-port network.

and

$$AD - BC = 1. \tag{9-218}$$

b) Because of Eqs. (9–216), (9–217), and (9–218), the line section in Fig. 9–44(a) can be replaced by an equivalent two-port symmetrical T-network shown in Fig. 9–44(b). Prove that

$$Z_1 = \frac{2}{C}(A - 1) = 2Z_0 \tanh \frac{\gamma \ell}{2} \tag{9-219}$$

and

$$Y_2 = C = \frac{1}{Z_0} \sinh \gamma \ell. \tag{9-220}$$

P.9–14 A d-c generator of voltage V_g and internal resistance R_g is connected to a lossy transmission line characterized by a resistance per unit length R and a conductance per unit length G.

a) Write the governing voltage and current transmission-line equations.
b) Find the general solutions for $V(z)$ and $I(z)$.
c) Specialize the solutions in part (b) to those for an infinite line.
d) Specialize the solutions in part (b) to those for a finite line of length ℓ that is terminated in a load resistance R_L.

P.9–15 A generator with an open-circuit voltage $v_g(t) = 10 \sin 8000\pi t$ (V) and internal impedance $Z_g = 40 + j30$ (Ω) is connected to a 50 (Ω) distortionless line. The line has a resistance of 0.5 (Ω/m), and its lossy dielectric medium has a loss tangent of 0.18%. The line is 50 (m) long and is terminated in a matched load. Find (a) the instantaneous expressions for the voltage and current at an arbitrary location on the line, (b) the instantaneous expressions for the voltage and current at the load, and (c) the average power transmitted to the load.

P.9–16 The input impedance of an open- or short-circuited *lossy* transmission line has both a resistive and a reactive component. Prove that the input impedance of a very short section ℓ of a slightly lossy line ($\alpha\ell \ll 1$ and $\beta\ell \ll 1$) is approximately

a) $Z_{in} = (R + j\omega L)\ell$ with a short-circuit termination.
b) $Z_{in} = (G - j\omega C)/[G^2 + (\omega C)^2]\ell$ with an open-circuit termination.

P.9–17 Find the input impedance of a low-loss quarter-wavelength line ($\alpha\lambda \ll 1$)

a) terminated in a short circuit.
b) terminated in an open circuit.

P.9–18 A 2 (m) lossless air-spaced transmission line having a characteristic impedance 50 (Ω) is terminated with an impedance $40 + j30$ (Ω) at an operating frequency of 200 (MHz). Find the input impedance.

P.9–19 The open-circuit and short-circuit impedances measured at the input terminals of an air-spaced transmission line 4 (m) long are $250/\underline{-50°}$ (Ω) and $360/\underline{20°}$ (Ω), respectively.

a) Determine Z_0, α, and β of the line.
b) Determine R, L, G, and C.

P.9–20 Measurements on a 0.6 (m) lossless coaxial cable at 100 (kHz) show a capacitance of 54 (pF) when the cable is open-circuited and an inductance of 0.30 (μH) when it is short-circuited.

a) Determine Z_0 and the dielectric constant of its insulating medium.
b) Calculate the X_{io} and X_{is} at 10 (MHz).

P.9–21 Starting from the input impedance of an open-circuited lossy transmission line in Eq. (9–116), find the expressions for the half-power bandwidth and the Q of a low-loss line with $\ell = n\lambda/2$.

P.9–22 A lossless quarter-wave line section of characteristic impedance R_0 is terminated with an inductive load impedance $Z_L = R_L + jX_L$.

a) Prove that the input impedance is effectively a resistance R_i in parallel with a capacitive reactance X_i. Determine R_i and X_i in terms of R_0, R_L, and X_L.

b) Find the ratio of the magnitude of the voltage at the input to that at the load (*voltage transformation ratio*, $|V_{in}|/|V_L|$) in terms of R_0 and Z_L.

P.9–23 A 75 (Ω) lossless line is terminated in a load impedance $Z_L = R_L + jX_L$.

a) What must be the relation between R_L and X_L in order that the standing-wave ratio on the line be 3?

b) Find X_L, if $R_L = 150$ (Ω).

c) Where does the voltage minimum nearest to the load occur on the line for part (b)?

P.9–24 Consider a lossless transmission line.

a) Determine the line's characteristic resistance so that it will have a minimum possible standing-wave ratio for a load impedance $40 + j30$ (Ω).

b) Find this minimum standing-wave ratio and the corresponding voltage reflection coefficient.

c) Find the location of the voltage minimum nearest to the load.

P.9–25 A lossy transmission line with characteristic impedance Z_0 is terminated in an arbitrary load impedance Z_L.

a) Express the standing-wave ratio S on the line in terms of Z_0 and Z_L.

b) Find in terms of S and Z_0 the impedance looking toward the load at the location of a voltage maximum.

c) Find the impedance looking toward the load at a location of a voltage minimum.

P.9–26 A transmission line of characteristic impedance $R_0 = 50$ (Ω) is to be matched to a load impedance $Z_L = 40 + j10$ (Ω) through a length ℓ' of another transmission line of characteristic impedance R_0'. Find the required ℓ' and R_0' for matching.

P.9–27 The standing-wave ratio on a lossless 300 (Ω) transmission line terminated in an unknown load impedance is 2.0, and the nearest voltage minimum is at a distance 0.3λ from the load. Determine (a) the reflection coefficient Γ of the load, (b) the unknown load impedance Z_L, and (c) the equivalent length and terminating resistance of a line, such that the input impedance is equal to Z_L.

P.9–28 Obtain from Eq. (9–147) the formulas for finding the length ℓ_m and the terminating resistance R_m of a lossless line having a characteristic impedance R_0 such that the input impedance equals $Z_i = R_i + jX_i$.

P.9–29 Obtain an analytical expression for the load impedance Z_L connected to a line of characteristic impedance Z_0 in terms of standing-wave ratio S and the distance, z_m'/λ, of the voltage minimum closest to the load.

P.9–30 A sinusoidal voltage generator with $V_g = 0.1\underline{/0°}$ (V) and internal impedance $Z_g = R_0$ is connected to a lossless transmission line having a characteristic impedance $R_0 = 50$ (Ω). The line is ℓ meters long and is terminated in a load resistance $R_L = 25$ (Ω). Find (a) V_i, I_i, V_L, and I_L; (b) the standing-wave ratio on the line; and (c) the average power delivered to the load. Compare the result in part (c) with the case where $R_L = 50$ (Ω).

P.9–31 Consider a lossless transmission line of a characteristic impedance R_0. A time-harmonic voltage source of an amplitude V_g and an internal impedance $R_g = R_0$ is connected to the input terminals of the line, which is terminated with a load impedance $Z_L = R_L + jX_L$. Let P_{inc} be the average incident power associated with the wave traveling in the $+z$-direction.

a) Find the expression for P_{inc} in terms of V_g and R_0.
b) Find the expression for the average power P_L delivered to the load in terms of V_g and the reflection coefficient Γ.
c) Express the ratio P_L/P_{inc} in terms of the standing-wave ratio S.
d) For $V_g = 100$ (V), $R_g = R_0 = 50$ (Ω), $Z_L = 50 - j25$ (Ω) determine P_{inc}, Γ, S, P_L, $|V_L|$, and $|I_L|$.

P.9–32 A sinusoidal voltage generator $v_g = 110 \sin \omega t$ (V) and internal impedance $Z_g = 50$ (Ω) is connected to a quarter-wave lossless line having a characteristic impedance $R_0 = 50$ (Ω) that is terminated in a purely reactive load $Z_L = j50$ (Ω).

a) Obtain the voltage and current phasor expressions $V(z')$ and $I(z')$.
b) Write the instantaneous voltage and current expressions $v(z', t)$ and $i(z', t)$.
c) Obtain the instantaneous power and the average power delivered to the load.

P.9–33 A d-c voltage V_0 is applied at $t = 0$ directly to the input terminals of an open-circuited lossless transmission line of length ℓ as in Fig. 9–45. Sketch the voltage and current waves on the line (in the manner of Fig. 9–16) for the following time intervals:

a) $0 < t < T\ (= \ell/u)$
b) $T < t < 2T$
c) $2T < t < 3T$
d) $3T < t < 4T$

What happens after $t = 4T$?

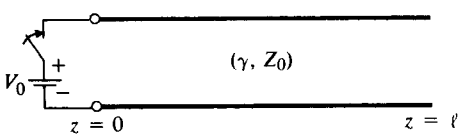

FIGURE 9–45
A d-c voltage applied to an open-circuited line (Problem P.9–33).

P.9–34 A 100 (V) d-c voltage is applied at $t = 0$ to the input terminals of a lossless coaxial cable ($R_{01} = 50$ (Ω), dielectric constant of insulation $\epsilon_{r1} = 2.25$) through an internal resistance $R_g = R_{01}$. The cable is 200 (m) long and is connected to a lossless two-wire line ($R_{02} = 200$ (Ω), $\epsilon_{r2} = 1$), which is 400 (m) long and is terminated in its characteristic resistance.

a) Describe the transient behavior of the system and find the amplitudes of all reflected and transmitted voltage and current waves.
b) Sketch the voltage and current as functions of t at the midpoint of the coaxial cable.
c) Repeat part (b) at the midpoint of the two-wire line.

P.9–35 A d-c voltage V_0 is applied at $t = 0$ to the input terminals of an open-circuited air-dielectric line of a length ℓ through a series resistance equal to $R_0/2$, where R_0 is the characteristic resistance of the line.

a) Draw the voltage and current reflection diagrams.
b) Sketch $V(0, t)$ and and $I(0, t)$.
c) Sketch $V(\ell/2, t)$ and $I(\ell/2, t)$.

P.9–36 A d-c voltage V_0 is applied at $t = 0$ directly to the input terminals of a lossless air-dielectric transmission line of a length ℓ. The line has a characteristic resistance R_0 and is terminated in a load resistance $R_L = 2R_0$.
a) Draw the voltage and currrent reflection diagrams.
b) Sketch $V(\ell, t)$ and $I(\ell, t)$.
c) Sketch $V(z, 2.5T)$ and $I(z, 2.5T)$, where $T = \ell/u$.

P.9–37 For the problem in Example 9–11, determine and sketch $i(200, t)$.

P.9–38 A lossless, air-dielectric, open-circuited transmission line of characteristic resistance R_0 and length ℓ is initially charged to a voltage V_0. At $t = 0$ the line is connected to a resistance R, as shown in Fig. 9–46. Determine $V_R(t)$ and $I_R(t)$ for $0 < t < 5\ell/c$:
a) if $R = 2R_0$,
b) if $R = R_0/2$.

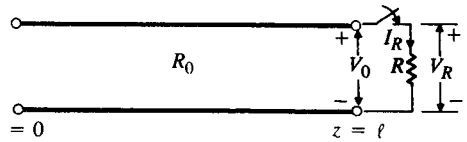

FIGURE 9–46
An initially charged line connected to a resistance (Problem 9–38).

P.9–39 Refer to Fig. 9–26(a) but change the load from a pure inductance to a series combination of $R_L = 10\ (\Omega)$ and $L_L = 48\ (\mu H)$. Assume that $V_0 = 100\ (V)$, $R_0 = 50\ (\Omega)$, $\ell = 900\ (m)$, and $u = c$.
a) Find the expressions for the current in and the voltage across the load as functions of t.
b) Sketch the current and voltage distributions along the transmission line at $t_1 = 4\ (\mu s)$.

P.9–40 Refer to Fig. 9–28(a) but change the load from a pure capacitance to a parallel combination of $C_L = 14\ (nF)$ and $R_L = 1000\ (\Omega)$. Assume that $V_0 = 100\ (V)$, $R_0 = 50\ (\Omega)$, $\ell = 900\ (m)$, and $u = c$.
a) Find the expressions for the current in and the voltage across the load as functions of t.
b) Sketch the current and voltage distributions along the transmission line at $t_1 = 4\ (\mu s)$.

P.9–41 The Smith chart, constructed on the basis of Eqs. (9–188) and (9–189) for a lossless transmission line, is restricted to a unit circle because $|\Gamma| \leq 1$. In the case of a lossy line, Z_0 is a complex quantity, and so, in general, is the normalized load impedance $z_L = Z_L/Z_0$.
a) Show that the phase angle of z_L, θ_L, lies between $\pm 3\pi/4$.
b) Show that $|\Gamma|$ may be greater than unity.
c) Prove that max. $|\Gamma| = 2.414$.

P.9–42 The characteristic impedance of a given lossless transmission line is 75 (Ω). Use a Smith chart to find the input impedance at 200 (MHz) of such a line that is (a) 1 (m) long

and open-circuited, and (b) 0.8 (m) long and short-circuited. Then (c) determine the corresponding input admittances for the lines in parts (a) and (b).

P.9–43 A load impedance $30 + j10$ (Ω) is connected to a lossless transmission line of length 0.101λ and characteristic impedance 50 (Ω). Use a Smith chart to find (a) the standing-wave ratio, (b) the voltage reflection coefficient, (c) the input impedance, (d) the input admittance, and (e) the location of the voltage minimum on the line.

P.9–44 Repeat Problem P.9–43 for a load impedance $30 - j10$ (Ω).

P.9–45 In a laboratory experiment conducted on a 50 (Ω) lossless transmission line terminated in an unknown load impedance, it is found that the standing-wave ratio is 2.0. The successive voltage minima are 25 (cm) apart, and the first minimum occurs at 5 (cm) from the load. Find (a) the load impedance, and (b) the reflection coefficient of the load. (c) Where would the first voltage minimum be located if the load were replaced by a short-circuit?

P.9–46 The input impedance of a short-circuited lossy transmission line of length 1.5 (m) ($< \lambda/2$) and characteristic impedance 100 (Ω) (approximately real) is $40 - j280$ (Ω).

a) Find α and β of the line.

b) Determine the input impedance if the short-circuit is replaced by a load impedance $Z_L = 50 + j50$ (Ω).

c) Find the input impedance of the short-circuited line for a line length 0.15λ.

P.9–47 A dipole antenna having an input impedance of 73 (Ω) is fed by a 200 (MHz) source through a 300 (Ω) two-wire transmission line. Design a quarter-wave two-wire air line with a 2 (cm) spacing to match the antenna to the 300 (Ω) line.

P.9–48 The single-stub method is used to match a load impedance $25 + j25$ (Ω) to a 50 (Ω) transmission line.

a) Find the required length and position of a short-circuited stub made of a section of the same 50 (Ω) line.

b) Repeat part (a) assuming that the short-circuited stub is made of a section of a line that has a characteristic impedance of 75 (Ω).

P.9–49 A load impedance can be matched to a transmission line also by using a single stub placed in series with the load at an appropriate location, as shown in Fig. 9–47. Assuming that $Z_L = 25 + j25$ (Ω), $R_0 = 50$ (Ω), and $R_0' = 35$ (Ω), find d and ℓ required for matching.

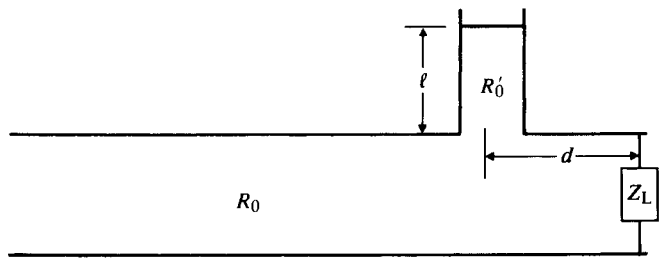

FIGURE 9–47
Impedance matching by a series stub (Problem P.9–49).

P.9–50 The double-stub method is used to match a load impedance $100 + j100$ (Ω) to a lossless transmission line of characteristic impedance 300 (Ω). The spacing between the stubs is $3\lambda/8$,

with one stub connected directly in parallel with the load. Determine the lengths of the stub tuners (a) if they are both short-circuited, and (b) if they are both open-circuited.

P.9–51 If the load impedance in Problem P.9–50 is changed to $100 + j50\ (\Omega)$, one discovers that a perfect match using the double-stub method with $d_0 = 3\lambda/8$ and one stub connected directly across the load is not possible. However, the modified arrangement shown in Fig. 9–43 can be used to match this load with the line.

a) Find the minimum required additional line length d_L.

b) Find the required lengths of the short-circuited stub tuners, using the minimum d_L found in part (a).

P.9–52 The double-stub method shown in Fig. 9–41 cannot be used to match certain loads to a line with a given characteristic impedance. Determine the regions of load admittances on a Smith admittance chart for which the double-stub arrangement in Fig. 9–41 cannot lead to a match for $d_o = \lambda/16$, $\lambda/4$, $3\lambda/8$, and $7\lambda/16$.

10

Waveguides and Cavity Resonators

10–1 Introduction

In the preceding chapter we studied the characteristic properties of transverse electromagnetic (TEM) waves guided by transmission lines. The TEM mode of guided waves is one in which the electric and magnetic fields are perpendicular to each other and both are transverse to the direction of propagation along the guiding line. One of the salient properties of TEM waves guided by conducting lines of negligible resistance is that the velocity of propagation of a wave of any frequency is the same as that in an unbounded dielectric medium. This was pointed out in connection with Eq. (9–21) and was reinforced by Eq. (9–72).

TEM waves, however, are not the only mode of guided waves that can propagate on transmission lines; nor are the three types of transmission lines (parallel-plate, two-wire, and coaxial) mentioned in Section 9–1 the only possible wave-guiding structures. As a matter of fact, we see from Eqs. (9–55) and (9–63) that the attenuation constant resulting from the finite conductivity of the lines increases with R, the resistance per unit line length, which, in turn, is proportional to $\sqrt{f}$ in accordance with Tables 9–1 and 9–2. Hence the attenuation of TEM waves tends to increase monotonically with frequency and would be prohibitively high in the microwave range.

In this chapter we first present a general analysis of the characteristics of the waves propagating along uniform guiding structures. Waveguiding structures are called ***waveguides***, of which the three types of transmission lines are special cases. The basic governing equations will be examined. We will see that, in addition to ***transverse electromagnetic (TEM) waves***, which have no field components in the direction of propagation, both ***transverse magnetic (TM) waves*** with a longitudinal electric-field component and ***transverse electric (TE) waves*** with a longitudinal magnetic-field component can also exist. Both TM and TE modes have characteristic ***cutoff frequencies***. Waves of frequencies below the cutoff frequency of a particular mode cannot propagate, and power and signal transmission at that mode is possible

only for frequencies higher than the cutoff frequency. Thus waveguides operating in TM and TE modes are like high-pass filters.

Also in this chapter we will reexamine the field and wave characteristics of parallel-plate waveguides with emphasis on TM and TE modes and show that all transverse field components can be expressed in terms of E_z (z being the direction of propagation) for TM waves and in terms of H_z for TE waves. The attenuation constants resulting from imperfectly conducting walls will be determined for TM and TE waves, and we will find that the attenuation constant depends, in a complicated way, on the mode of the propagating wave, as well as on frequency. For some modes the attenuation may decrease as the frequency increases; for other modes the attenuation may reach a minimum as the frequency exceeds the cutoff frequency by a certain amount.

Electromagnetic waves can propagate through hollow metal pipes of an arbitrary cross section. Without electromagnetic theory it would not be possible to explain the properties of hollow waveguides. We will see that single-conductor waveguides cannot support TEM waves. We will examine in detail the fields, the current and charge distributions, and the propagation and attenuation characteristics of rectangular and circular cylindrical waveguides. Both TM and TE modes will be discussed.

Electromagnetic waves can also be guided by an open dielectric-slab waveguide. The fields are essentially confined within the dielectric region and decay rapidly away from the slab surface in the transverse plane. For this reason the waves supported by a dielectric-slab waveguide are called ***surface waves***. Both TM and TE modes are possible. We will examine the field characteristics and cutoff frequencies of those surface waves. Cylindrical optical fibers will also be discussed.

At microwave frequencies, ordinary lumped-parameter elements (such as inductances and capacitances) connected by wires are no longer practical as circuit elements or as resonant circuits because the dimensions of the elements would have to be extremely small, because the resistance of the wire circuits becomes very high as a result of the skin effect, and because of radiation. We will briefly discuss irises and posts as waveguide reactive elements. A hollow conducting box with proper dimensions can be used as a resonant device. The box walls provide large areas for current flow, and losses are extremely small. Consequently, an enclosed conducting box can be a resonator of a very high Q. Such a box, which is essentially a segment of a waveguide with closed end faces, is called a ***cavity resonator***. We will discuss the different mode patterns of the fields inside rectangular as well as circular cylindrical cavity resonators.

10–2 General Wave Behaviors along Uniform Guiding Structures

In this section we examine some general characteristics for waves propagating along straight guiding structures with a uniform cross section. We will assume that the waves propagate in the $+z$-direction with a propagation constant $\gamma = \alpha + j\beta$ that is yet to be determined. For harmonic time dependence with an angular frequency ω, the dependence on z and t for all field components can be described by the exponential

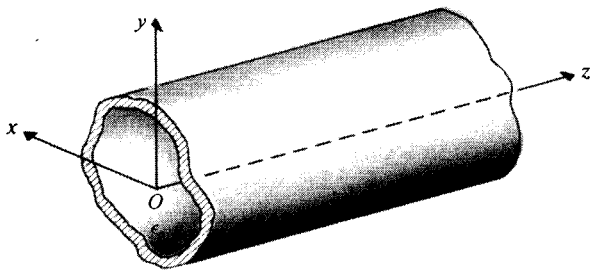

FIGURE 10–1
A uniform waveguide with an arbitrary cross section.

factor

$$e^{-\gamma z}e^{j\omega t} = e^{(j\omega t - \gamma z)} = e^{-\alpha z}e^{j(\omega t - \beta z)}. \tag{10–1}$$

As an example, for a cosine reference we may write the instantaneous expression for the **E** field in Cartesian coordinates as

$$\mathbf{E}(x, y, z; t) = \mathscr{R}e[\mathbf{E}^0(x, y)e^{(j\omega t - \gamma z)}], \tag{10–2}$$

where $\mathbf{E}^0(x, y)$ is a two-dimensional vector phasor that depends only on the cross-sectional coordinates. The instantaneous expression for the **H** field can be written in a similar way. Hence, in using a phasor representation in equations relating field quantities we may replace partial derivatives with respect to t and z simply by products with $(j\omega)$ and $(-\gamma)$, respectively; the common factor $e^{(j\omega t - \gamma z)}$ can be dropped.

We consider a straight waveguide in the form of a dielectric-filled metal tube having an arbitrary cross section and lying along the z-axis, as shown in Fig. 10–1. According to Eqs. (7–105) and (7–106), the electric and magnetic field intensities in the charge-free dielectric region inside satisfy the following homogeneous vector Helmholtz's equations:

$$\nabla^2\mathbf{E} + k^2\mathbf{E} = 0 \tag{10–3}$$

and

$$\nabla^2\mathbf{H} + k^2\mathbf{H} = 0, \tag{10–4}$$

where **E** and **H** are three-dimensional vector phasors, and k is the wavenumber:

$$k = \omega\sqrt{\mu\epsilon}. \tag{10–5}$$

The three-dimensional Laplacian operator ∇^2 may be broken into two parts: $\nabla^2_{u_1u_2}$ for the cross-sectional coordinates and ∇^2_z for the longitudinal coordinate. For waveguides with a rectangular cross section we use Cartesian coordinates:

$$\begin{aligned}\nabla^2\mathbf{E} &= (\nabla^2_{xy} + \nabla^2_z)\mathbf{E} = \left(\nabla^2_{xy} + \frac{\partial^2}{\partial z^2}\right)\mathbf{E} \\ &= \nabla^2_{xy}\mathbf{E} + \gamma^2\mathbf{E}.\end{aligned} \tag{10–6}$$

Combination of Eqs. (10–3) and (10–6) gives

$$\nabla^2_{xy}\mathbf{E} + (\gamma^2 + k^2)\mathbf{E} = 0. \tag{10–7}$$

Similarly, from Eq. (10–4) we have

$$\nabla_{xy}^2\mathbf{H} + (\gamma^2 + k^2)\mathbf{H} = 0. \tag{10–8}$$

We note that each of Eqs. (10–7) and (10–8) is really three second-order partial differential equations, one for each component of **E** and **H**. The exact solution of these component equations depends on the cross-sectional geometry and the boundary conditions that a particular field component must satisfy at conductor-dielectric interfaces. We note further that by writing $\nabla_{r\phi}^2$ for the transversal operator ∇_{xy}^2, Eqs. (10–7) and (10–8) become the governing equations for waveguides with a circular cross section.

Of course, the various components of **E** and **H** are not all independent, and it is not necessary to solve all six second-order partial differential equations for the six components of **E** and **H**. Let us examine the interrelationships among the six components in Cartesian coordinates by expanding the two source-free curl equations, Eqs. (7–104a) and (7–104b):

From $\nabla \times \mathbf{E} = -j\omega\mu\mathbf{H}$:		From $\nabla \times \mathbf{H} = j\omega\epsilon\mathbf{E}$:	
$\dfrac{\partial E_z^0}{\partial y} + \gamma E_y^0 = -j\omega\mu H_x^0$	(10–9a)	$\dfrac{\partial H_z^0}{\partial y} + \gamma H_y^0 = j\omega\epsilon E_x^0$	(10–10a)
$-\gamma E_x^0 - \dfrac{\partial E_z^0}{\partial x} = -j\omega\mu H_y^0$	(10–9b)	$-\gamma H_x^0 - \dfrac{\partial H_z^0}{\partial x} = j\omega\epsilon E_y^0$	(10–10b)
$\dfrac{\partial E_y^0}{\partial x} - \dfrac{\partial E_x^0}{\partial y} = -j\omega\mu H_z^0$	(10–9c)	$\dfrac{\partial H_y^0}{\partial x} - \dfrac{\partial H_x^0}{\partial y} = j\omega\epsilon E_z^0$	(10–10c)

Note that partial derivatives with respect to z have been replaced by multiplications by $(-\gamma)$. All the component field quantities in the equations above are phasors that depend only on x and y, the common $e^{-\gamma z}$ factor for z-dependence having been omitted. By manipulating these equations we can express the transverse field components H_x^0, H_y^0, and E_x^0, and E_y^0 in terms of the two longitudinal components E_z^0 and H_z^0. For instance, Eqs. (10–9a) and (10–10b) can be combined to eliminate E_y^0 and obtain H_x^0 in terms of E_z^0 and H_z^0. We have

$$H_x^0 = -\frac{1}{h^2}\left(\gamma\frac{\partial H_z^0}{\partial x} - j\omega\epsilon\frac{\partial E_z^0}{\partial y}\right), \tag{10–11}$$

$$H_y^0 = -\frac{1}{h^2}\left(\gamma\frac{\partial H_z^0}{\partial y} + j\omega\epsilon\frac{\partial E_z^0}{\partial x}\right), \tag{10–12}$$

$$E_x^0 = -\frac{1}{h^2}\left(\gamma\frac{\partial E_z^0}{\partial x} + j\omega\mu\frac{\partial H_z^0}{\partial y}\right), \tag{10–13}$$

$$E_y^0 = -\frac{1}{h^2}\left(\gamma\frac{\partial E_z^0}{\partial y} - j\omega\mu\frac{\partial H_z^0}{\partial x}\right), \tag{10–14}$$

where

$$h^2 = \gamma^2 + k^2. \tag{10-15}$$

The wave behavior in a waveguide can be analyzed by solving Eqs. (10–7) and (10–8) for the longitudinal components, E_z^0 and H_z^0, respectively, subject to the required boundary conditions, and then by using Eqs. (10–11) through (10–14) to determine the other components.

It is convenient to classify the propagating waves in a uniform waveguide into three types according to whether E_z or H_z exists.

1. *Transverse electromagnetic (TEM) waves.* These are waves that contain neither E_z nor H_z. We encountered TEM waves in Chapter 8 when we discussed plane waves and in Chapter 9 on waves along transmission lines.
2. *Transverse magnetic (TM) waves.* These are waves that contain a nonzero E_z but $H_z = 0$.
3. *Transverse electric (TE) waves.* These are waves that contain a nonzero H_z but $E_z = 0$.

The propagation characteristics of the various types of waves are different; they will be discussed in subsequent subsections.

10-2.1 TRANSVERSE ELECTROMAGNETIC WAVES

Since $E_z = 0$ and $H_z = 0$ for TEM waves within a guide, we see that Eqs. (10–11) through (10–14) constitute a set of trivial solutions (all field components vanish) unless the denominator h^2 also equals zero. In other words, TEM waves exist only when

$$\gamma_{\text{TEM}}^2 + k^2 = 0 \tag{10-16}$$

or

$$\gamma_{\text{TEM}} = jk = j\omega\sqrt{\mu\epsilon}, \tag{10-17}$$

which is exactly the same expression for the propagation constant of a uniform plane wave in an unbounded medium characterized by constitutive parameters ϵ and μ. We recall that Eq. (10–17) also holds for a TEM wave on a lossless transmission line. It follows that the velocity of propagation (phase velocity) for TEM waves is

$$\boxed{u_{p(\text{TEM})} = \frac{\omega}{k} = \frac{1}{\sqrt{\mu\epsilon}} \quad \text{(m/s)}.} \tag{10-18}$$

We can obtain the ratio between E_x^0 and H_y^0 from Eqs. (10–9b) and (10–10a) by setting E_z and H_z to zero. This ratio is called the ***wave impedance***. We have

$$Z_{\text{TEM}} = \frac{E_x^0}{H_y^0} = \frac{j\omega\mu}{\gamma_{\text{TEM}}} = \frac{\gamma_{\text{TEM}}}{j\omega\epsilon}, \tag{10-19}$$

which becomes, in view of Eq. (10–17),

$$\boxed{Z_{\text{TEM}} = \sqrt{\frac{\mu}{\epsilon}} = \eta \qquad (\Omega).} \tag{10–20}$$

We note that Z_{TEM} is the same as the intrinsic impedance of the dielectric medium, as given in Eq. (8–30). Equations (10–18) and (10–20) assert that ***the phase velocity and the wave impedance for TEM waves are independent of the frequency of the waves.***

Letting $E_z^0 = 0$ in Eq. (10–9a) and $H_z^0 = 0$ in Eq. (10–10b), we obtain

$$\frac{E_y^0}{H_x^0} = -Z_{\text{TEM}} = -\sqrt{\frac{\mu}{\epsilon}}. \tag{10–21}$$

Equations (10–19) and (10–21) can be combined to obtain the following formula for a TEM wave propagating in the $+z$-direction:

$$\boxed{\mathbf{H} = \frac{1}{Z_{\text{TEM}}}\,\mathbf{a}_z \times \mathbf{E} \qquad (\text{A/m}),} \tag{10–22}$$

which again reminds us of a similar relation for a uniform plane wave in an unbounded medium—see Eq. (8–29).

Single-conductor waveguides cannot support TEM waves. In Section 6–2 we pointed out that magnetic flux lines always close upon themselves. Hence if a TEM wave were to exist in a waveguide, the field lines of **B** and **H** would form closed loops in a transverse plane. However, the generalized Ampère's circuital law, Eq. (7–54b), requires that the line integral of the magnetic field (the magnetomotive force) around any closed loop in a transverse plane must equal the sum of the longitudinal conduction and displacement currents through the loop. Without an inner conductor there is no longitudinal conduction current inside the waveguide. By definition, a TEM wave does not have an E_z-component; consequently, there is no longitudinal displacement current. The total absence of a longitudinal current inside a waveguide leads to the conclusion that there can be no closed loops of magnetic field lines in any transverse plane. Therefore, we conclude that ***TEM waves cannot exist in a single-conductor hollow (or dielectric-filled) waveguide of any shape.*** On the other hand, *assuming perfect conductors*, a coaxial transmission line having an inner conductor *can* support TEM waves; so can a two-conductor stripline and a two-wire transmission line. When the conductors have losses, waves along transmission lines are strictly no longer TEM, as noted in Section 9–2.

10–2.2 TRANSVERSE MAGNETIC WAVES

Transverse magnetic (TM) waves do not have a component of the magnetic field in the direction of propagation, $H_z = 0$. The behavior of TM waves can be analyzed

by solving Eq. (10–7) for E_z subject to the boundary conditions of the guide and using Eqs. (10–11) through (10–14) to determine the other components. Writing Eq. (10–7) for E_z, we have

$$\nabla_{xy}^2 E_z^0 + (\gamma^2 + k^2)E_z^0 = 0 \tag{10–23}$$

or

$$\boxed{\nabla_{xy}^2 E_z^0 + h^2 E_z^0 = 0.} \tag{10–24}$$

Equation (10–24) is a second-order partial differential equation, which can be solved for E_z^0. In this section we wish to discuss only the general properties of the various wave types. The actual solution of Eq. (10–24) will wait until subsequent sections when we examine particular waveguides.

For TM waves we set $H_z = 0$ in Eqs. (10–11) through (10–14) to obtain

$$H_x^0 = \frac{j\omega\epsilon}{h^2}\frac{\partial E_z^0}{\partial y}, \tag{10–25}$$

$$H_y^0 = -\frac{j\omega\epsilon}{h^2}\frac{\partial E_z^0}{\partial x}, \tag{10–26}$$

$$E_x^0 = -\frac{\gamma}{h^2}\frac{\partial E_z^0}{\partial x}, \tag{10–27}$$

$$E_y^0 = -\frac{\gamma}{h^2}\frac{\partial E_z^0}{\partial y}. \tag{10–28}$$

It is convenient to combine Eqs. (10–27) and (10–28) and write

$$\boxed{(\mathbf{E}_T^0)_{\text{TM}} = \mathbf{a}_x E_x^0 + \mathbf{a}_y E_y^0 = -\frac{\gamma}{h^2}\nabla_T E_z^0 \quad \text{(V/m)},} \tag{10–29}$$

where

$$\nabla_T E_z^0 = \left(\mathbf{a}_x \frac{\partial}{\partial x} + \mathbf{a}_y \frac{\partial}{\partial y}\right)E_z^0 \tag{10–30}$$

denotes the gradient of E_z^0 in the transverse plane. Equation (10–29) is a concise formula for finding E_x^0 and E_y^0 from E_z^0.

The transverse components of magnetic field intensity, H_x^0 and H_y^0, can be determined simply from E_x^0 and E_y^0 on the introduction of the wave impedance for the TM mode. We have, from Eqs. (10–25) through (10–28),

$$\boxed{Z_{\text{TM}} = \frac{E_x^0}{H_y^0} = -\frac{E_y^0}{H_x^0} = \frac{\gamma}{j\omega\epsilon} \quad (\Omega).} \tag{10–31}$$

It is important to note that Z_{TM} is *not* equal to $j\omega\mu/\gamma$, because γ for TM waves, unlike γ_{TEM}, is *not* equal to $j\omega\sqrt{\mu\epsilon}$. The following relation between the electric and magnetic

field intensities holds for TM waves:

$$\boxed{\mathbf{H} = \frac{1}{Z_{TM}}(\mathbf{a}_z \times \mathbf{E}) \quad \text{(A/m)}.} \tag{10–32}$$

Equation (10–32) is seen to be of the same form as Eq. (10–22) for TEM waves.

When we undertake to solve the two-dimensional homogeneous Helmholtz equation, Eq. (10–24), subject to the boundary conditions of a given waveguide, we will discover that solutions are possible only for *discrete values of h*. There may be an infinity of these discrete values, but solutions are not possible for all values of h. The values of h for which a solution of Eq. (10–24) exists are called the ***characteristic values*** or ***eigenvalues*** of the boundary-value problem. Each of the eigenvalues determines the characteristic properties of a particular TM mode of the given waveguide.

In the following sections we will also discover that the eigenvalues of the various waveguide problems are real numbers. From Eq. (10–15) we have

$$\begin{aligned}\gamma &= \sqrt{h^2 - k^2} \\ &= \sqrt{h^2 - \omega^2\mu\epsilon}.\end{aligned} \tag{10–33}$$

Two distinct ranges of the values for the propagation constant are noted, the dividing point being $\gamma = 0$, where

$$\omega_c^2\mu\epsilon = h^2 \tag{10–34}$$

or

$$\boxed{f_c = \frac{h}{2\pi\sqrt{\mu\epsilon}} \quad \text{(Hz)}.} \tag{10–35}$$

The frequency, f_c, at which $\gamma = 0$ is called a ***cutoff frequency***. *The value of f_c for a particular mode in a waveguide depends on the eigenvalue of this mode.* Using Eq. (10–35), we can write Eq. (10–33) as

$$\gamma = h\sqrt{1 - \left(\frac{f}{f_c}\right)^2}. \tag{10–36}$$

The two distinct ranges of γ can be defined in terms of the ratio $(f/f_c)^2$ as compared to unity.

a) $\left(\dfrac{f}{f_c}\right)^2 > 1$, or $f > f_c$. In this range, $\omega^2\mu\epsilon > h^2$ and γ is imaginary. We have, from Eq. (10–33),

$$\gamma = j\beta = jk\sqrt{1 - \left(\frac{h}{k}\right)^2} = jk\sqrt{1 - \left(\frac{f_c}{f}\right)^2}. \tag{10–37}$$

It is a propagating mode with a phase constant β:

$$\boxed{\beta = k\sqrt{1-\left(\frac{f_c}{f}\right)^2} \quad \text{(rad/m)}.} \tag{10-38}$$

The corresponding wavelength in the guide is

$$\lambda_g = \frac{2\pi}{\beta} = \frac{\lambda}{\sqrt{1-(f_c/f)^2}} > \lambda, \tag{10-39}$$

where

$$\lambda = \frac{2\pi}{k} = \frac{1}{f\sqrt{\mu\epsilon}} = \frac{u}{f} \tag{10-40}$$

is the wavelength of a plane wave with a frequency f in an unbounded dielectric medium characterized by μ and ϵ, and $u = 1/\sqrt{\mu\epsilon}$ is the velocity of light in the medium. Equation (10–39) can be rearranged to give a simple relation connecting λ, the guide wavelength λ_g, and the cutoff wavelength $\lambda_c = u/f_c$:

$$\frac{1}{\lambda^2} = \frac{1}{\lambda_g^2} + \frac{1}{\lambda_c^2}. \tag{10-41}$$

The phase velocity of the propagating wave in the guide is

$$u_p = \frac{\omega}{\beta} = \frac{u}{\sqrt{1-(f_c/f)^2}} = \frac{\lambda_g}{\lambda}u > u. \tag{10-42}$$

We see from Eq. (10–42) that the phase velocity within a waveguide is always higher than that in an unbounded medium and is frequency-dependent. Hence ***single-conductor waveguides are dispersive transmission systems***, although an unbounded lossless dielectric medium is nondispersive. The group velocity for a propagating wave in a waveguide can be determined by using Eq. (8–72):

$$u_g = \frac{1}{d\beta/d\omega} = u\sqrt{1-\left(\frac{f_c}{f}\right)^2} = \frac{\lambda}{\lambda_g}u < u. \tag{10-43}$$

Thus,

$$u_g u_p = u^2. \tag{10-44}$$

For air dielectric, $u = c$, Eq. (10–44) becomes $u_g u_p = c^2$. In a lossless waveguide the velocity of signal propagation (the *velocity of energy transport*) is equal to the group velocity. An illustration of this statement can be found later, in Subsection 10–3.3.

Substitution of Eq. (10–37) in Eq. (10–31) yields

$$\boxed{Z_{\text{TM}} = \eta\sqrt{1-\left(\frac{f_c}{f}\right)^2} \quad (\Omega).} \tag{10-45}$$

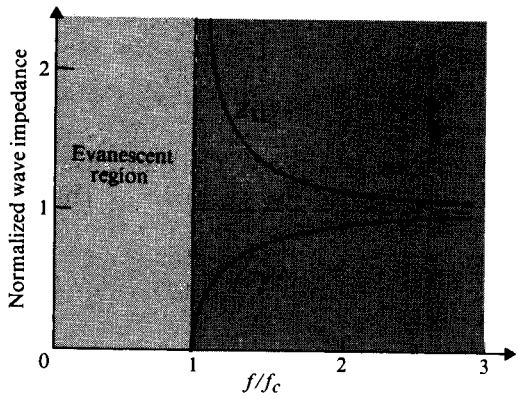

FIGURE 10–2
Normalized wave impedances for propagating TM and TE waves.

The wave impedance of propagating TM modes in a waveguide with a lossless dielectric is purely resistive and is always less than the intrinsic impedance of the dielectric medium. The variation of Z_{TM} versus f/f_c for $f > f_c$ is sketched in Fig. 10–2.

b) $\left(\frac{f}{f_c}\right)^2 < 1$, or $f < f_c$. When the operating frequency is lower than the cutoff frequency, γ is real and Eq. (10–36) can be written as

$$\gamma = \alpha = h\sqrt{1 - \left(\frac{f}{f_c}\right)^2}, \qquad f < f_c, \tag{10–46}$$

which is, in fact, an attenuation constant. Since all field components contain the propagation factor $e^{-\gamma z} = e^{-\alpha z}$, the wave diminishes rapidly with z and is said to be ***evanescent***. Therefore, ***a waveguide exhibits the property of a high-pass filter.*** *For a given mode, only waves with a frequency higher than the cutoff frequency of the mode can propagate in the guide.*

Substitution of Eq. (10–46) in Eq. (10–31) gives the wave impedance of TM modes for $f < f_c$:

$$Z_{TM} = -j\frac{h}{\omega\epsilon}\sqrt{1 - \left(\frac{f}{f_c}\right)^2}, \qquad f < f_c. \tag{10–47}$$

Thus, the wave impedance of evanescent TM modes at frequencies below cutoff is purely reactive, indicating that there is no power flow associated with evanescent waves.

10–2.3 TRANSVERSE ELECTRIC WAVES

Transverse electric (TE) waves do not have a component of the electric field in the direction of propagation, $E_z = 0$. The behavior of TE waves can be analyzed by first

solving Eq. (10–8) for H_z:

$$\boxed{\nabla_{xy}^2 H_z + h^2 H_z = 0.} \tag{10–48}$$

Proper boundary conditions at the guide walls must be satisfied. The transverse field components can then be found by substituting H_z into the reduced Eqs. (10–11) through (10–14) with E_z set to zero. We have

$$H_x^0 = -\frac{\gamma}{h^2}\frac{\partial H_z^0}{\partial x}, \tag{10–49}$$

$$H_y^0 = -\frac{\gamma}{h^2}\frac{\partial H_z^0}{\partial y}, \tag{10–50}$$

$$E_x^0 = -\frac{j\omega\mu}{h^2}\frac{\partial H_z^0}{\partial y}, \tag{10–51}$$

$$E_y^0 = \frac{j\omega\mu}{h^2}\frac{\partial H_z^0}{\partial x}. \tag{10–52}$$

Combining Eqs. (10–49) and (10–50), we obtain

$$\boxed{(\mathbf{H}_T^0)_{TE} = \mathbf{a}_x H_x^0 + \mathbf{a}_y H_y^0 = -\frac{\gamma}{h^2}\nabla_T H_z^0 \qquad \text{(A/m).}} \tag{10–53}$$

We note that Eq. (10–53) is entirely similar to Eq. (10–29) for TM modes.

The transverse components of electric field intensity, E_x^0 and E_y^0, are related to those of magnetic field intensity through the wave impedance. We have, from Eqs. (10–49) through (10–52),

$$\boxed{Z_{\text{TE}} = \frac{E_x^0}{H_y^0} = -\frac{E_y^0}{H_x^0} = \frac{j\omega\mu}{\gamma} \qquad (\Omega).} \tag{10–54}$$

Note that Z_{TE} in Eq. (10–54) is quite different from Z_{TM} in Eq. (10–31) because γ for TE waves, unlike γ_{TEM}, is *not* equal to $j\omega\sqrt{\mu\epsilon}$. Equations (10–51), (10–52), and (10–54) can now be combined to give the following vector formula:

$$\boxed{\mathbf{E} = -Z_{\text{TE}}(\mathbf{a}_z \times \mathbf{H}) \qquad \text{(V/m).}} \tag{10–55}$$

Inasmuch as we have not changed the relation between γ and h, Eqs. (10–33) through (10–44) pertaining to TM waves also apply to TE waves. There are also two distinct ranges of γ, depending on whether the operating frequency is higher or lower than the cutoff frequency, f_c, given in Eq. (10–35).

a) $\left(\frac{f}{f_c}\right)^2 > 1$, or $f > f_c$. In this range, γ is imaginary, and we have a propagating mode. The expression for γ is the same as that given in Eq. (10–37):

$$\gamma = j\beta = jk\sqrt{1 - \left(\frac{f_c}{f}\right)^2}. \tag{10–56}$$

Consequently, the formulas for β, λ_g, u_p, and u_g in Eqs. (10–38), (10–39), (10–42), and (10–43), respectively, also hold for TE waves. Using Eq. (10–56) in Eq. (10–54), we obtain

$$\boxed{Z_{TE} = \frac{\eta}{\sqrt{1 - (f_c/f)^2}} \quad (\Omega),} \tag{10–57}$$

which is obviously different from the expression for Z_{TM} in Eq. (10–45). Equation (10–57) indicates that ***the wave impedance of propagating TE modes in a waveguide with a lossless dielectric is purely resistive and is always larger than the intrinsic impedance of the dielectric medium.*** The variation of Z_{TE} versus f/f_c for $f > f_c$ is also sketched in Fig. 10–2.

b) $\left(\frac{f}{f_c}\right)^2 < 1$, or $f < f_c$. In this case, γ is real and we have an evanescent or nonpropagating mode:

$$\gamma = \alpha = h\sqrt{1 - \left(\frac{f}{f_c}\right)^2}, \qquad f < f_c. \tag{10–58}$$

Substitution of Eq. (10–58) in Eq. (10–54) gives the wave impedance of TE modes for $f < f_c$:

$$Z_{TE} = j\frac{\omega\mu}{h\sqrt{1 - (f/f_c)^2}}, \qquad f < f_c, \tag{10–59}$$

which is purely reactive, indicating again that there is no power flow for evanescent waves at $f < f_c$.

EXAMPLE 10–1 (a) Determine the wave impedance and guide wavelength at a frequency equal to twice the cutoff frequency in a waveguide for TM and TE modes. (b) Repeat part (a) for a frequency equal to one-half of the cutoff frequency. (c) What are the wave impedance and guide wavelength for the TEM mode?

Solution

a) At $f = 2f_c$, which is above the cutoff frequency, we have propagating modes. The appropriate formulas are Eqs. (10–45), (10–57), and (10–39).

For $f = 2f_c$, $(f_c/f)^2 = \frac{1}{4}$, $\sqrt{1 - (f_c/f)^2} = \sqrt{3}/2 = 0.866$. Thus,

$$Z_{TM} = 0.866\eta < \eta, \qquad \lambda_{TM} = 1.155\lambda > \lambda,$$
$$Z_{TE} = 1.155\eta > \eta, \qquad \lambda_{TE} = 1.155\lambda > \lambda,$$

TABLE 10–1
Wave Impedances and Guide Wavelengths for $f > f_c$

Mode	Wave Impedance, Z	Guide Wavelength, λ_g
TEM	$\eta = \sqrt{\frac{\mu}{\epsilon}}$	$\lambda = \frac{1}{f\sqrt{\mu\epsilon}}$
TM	$\eta\sqrt{1 - \left(\frac{f_c}{f}\right)^2}$	$\frac{\lambda}{\sqrt{1 - (f_c/f)^2}}$
TE	$\frac{\eta}{\sqrt{1 - (f_c/f)^2}}$	$\frac{\lambda}{\sqrt{1 - (f_c/f)^2}}$

where η is the intrinsic impedance of the guide medium. These results are summarized in Table 10–1.

b) At $f = f_c/2 < f_c$, the waveguide modes are evanescent, and guide wavelength has no significance. We now have

$$Z_{\text{TM}} = -j\frac{h}{\omega\epsilon}\sqrt{1 - \left(\frac{f}{f_c}\right)^2} = -j0.276h/f_c\epsilon,$$

$$Z_{\text{TE}} = j\frac{\omega\mu}{h\sqrt{1 - (f/f_c)^2}} = j3.63f_c\mu/h.$$

We note that both Z_{TM} and Z_{TE} become imaginary (reactive) for evanescent modes at $f < f_c$; their values depend on the eigenvalue h, which is a characteristic of the particular TM or TE mode.

c) The TEM mode does not exhibit a cutoff property and $h = 0$. The wave impedance and guide wavelength are independent of frequency. From Eqs. (10–20) and (10–18) we have

$$Z_{\text{TEM}} = \eta$$

and

$$\lambda_{\text{TEM}} = \lambda.$$

■

For propagating modes, $\gamma = j\beta$ and the variation of β versus frequency determines the characteristics of a wave along a guide. It is therefore useful to plot and examine an ω–β diagram.† Figure 10–3 is such a diagram in which the dashed line through the origin represents the ω–β relationship for TEM mode. The constant slope of this straight line is $\omega/\beta = u = 1/\sqrt{\mu\epsilon}$, which is the same as the velocity of light in an unbounded dielectric medium with constitutive parameters μ and ϵ.

† Also referred to as a ***Brillouin diagram.***

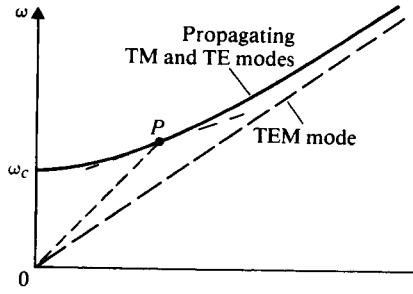

FIGURE 10–3
ω–β diagram for waveguide.

The solid curve above the dashed line depicts a typical ω–β relation for either a TM or a TE propagating mode, given by Eq. (10–38). We can write

$$\omega = \frac{\beta u}{\sqrt{1 - (\omega_c/\omega)^2}}. \tag{10–60}$$

The ω–β curve intersects the ω-axis ($\beta = 0$) at $\omega = \omega_c$. The slope of the line joining the origin and any point, such as P, on the curve is equal to the phase velocity, u_p, for a particular mode having a cutoff frequency f_c and operating at a particular frequency. The local slope of the ω–β curve at P is the group velocity, u_g. We note that, for propagating TM and TE waves in a waveguide, $u_p > u$, $u_g < u$, and Eq. (10–44) holds. As the operating frequency increases much above the cutoff frequency, both u_p and u_g approach u asymptotically. The exact value of ω_c depends on the eigenvalue h in Eq. (10–35)—that is, on the particular TM or TE mode in a waveguide of a given cross section. Methods for determining h will be discussed when we examine different types of waveguides. We recall that the ω–β graph for wave propagation in an ionized medium (Fig. 8–7) was quite similar to the ω–β diagram for a waveguide shown in Fig. 10–3.

EXAMPLE 10–2 Obtain a graph showing the relation between the attenuation constant α and the operating frequency f for evanescent modes in a waveguide.

Solution For evanescent TM or TE modes, $f < f_c$ and Eq. (10–46) or (10–58) applies. We have

$$\left(\frac{f_c}{h}\alpha\right)^2 + f^2 = f_c^2. \tag{10–61}$$

Hence the graph of $(f_c\alpha/h)$ plotted versus f is a circle centered at the origin and having a radius f_c. This is shown in Fig. 10–4. The value of α for any $f < f_c$ can be found from this quarter of a circle.

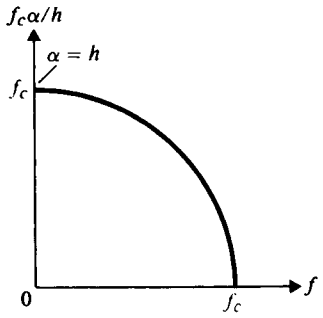

FIGURE 10–4
Relation between attenuation constant and operating frequency for evanescent modes (Example 10–2).

10–3 Parallel-Plate Waveguide

In Section 9–2 we discussed the characteristics of TEM waves propagating along a parallel-plate transmission line. It was then pointed out, and again emphasized in Subsection 10–2.1, that the field behavior for TEM modes bears a very close resemblance to that for uniform plane waves in an unbounded dielectric medium. However, TEM modes are not the only type of waves that can propagate along perfectly conducting parallel-plates separated by a dielectric. A parallel-plate waveguide can also support TM and TE waves. The characteristics of these waves are examined separately in following subsections.

10–3.1 TM WAVES BETWEEN PARALLEL PLATES

Consider the parallel-plate waveguide of two perfectly conducting plates separated by a dielectric medium with constitutive parameters ϵ and μ, as shown in Fig. 10–5. The plates are assumed to be infinite in extent in the x-direction. This is tantamount to assuming that the fields do not vary in the x-direction and that edge effects are negligible. Let us suppose that TM waves ($H_z = 0$) propagate in the $+z$-direction. For harmonic time dependence it is expedient to work with equations relating field

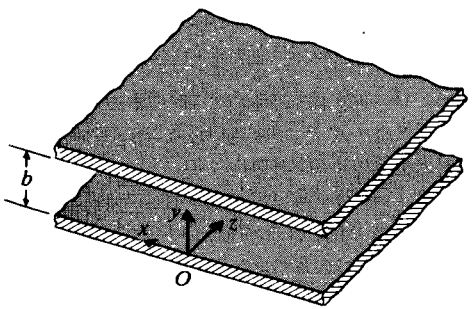

FIGURE 10–5
An infinite parallel-plate waveguide.

quantities with the common factor $e^{(j\omega t - \gamma z)}$ omitted. We write the phasor $E_z(y, z)$ as $E_z^0(y)e^{-\gamma z}$. Equation (10–24) then becomes

$$\frac{d^2E_z^0(y)}{dy^2} + h^2E_z^0(y) = 0. \tag{10–62}$$

The solution of Eq. (10–62) must satisfy the boundary conditions

$$E_z^0(y) = 0 \qquad \text{at } y = 0 \quad \text{and} \quad y = b.$$

From Section 4–5 we conclude that $E_z^0(y)$ must be of the following form ($h = n\pi/b$):

$$E_z^0(y) = A_n \sin\left(\frac{n\pi y}{b}\right), \tag{10–63}$$

where the amplitude A_n depends on the strength of excitation of the particular TM wave. The only other nonzero field components are obtained from Eqs. (10–25) and (10–28). Keeping in mind that $\partial E_z/\partial x = 0$ and omitting the $e^{-\gamma z}$ factor, we have

$$H_x^0(y) = \frac{j\omega\epsilon}{h} A_n \cos\left(\frac{n\pi y}{b}\right), \tag{10–64}$$

$$E_y^0(y) = -\frac{\gamma}{h} A_n \cos\left(\frac{n\pi y}{b}\right). \tag{10–65}$$

The γ in Eq. (10–65) is the propagation constant that can be determined from Eq. (10–33):

$$\gamma = \sqrt{\left(\frac{n\pi}{b}\right)^2 - \omega^2\mu\epsilon}. \tag{10–66}$$

The cutoff frequency is the frequency that makes $\gamma = 0$. We have

$$\boxed{f_c = \frac{n}{2b\sqrt{\mu\epsilon}} \quad \text{(Hz)},} \tag{10–67}$$

which, of course, checks with Eq. (10–35). Waves with $f > f_c$ propagate with a phase constant β, given in Eq. (10–38); and waves with $f \leq f_c$ are evanescent.

Depending on the values of n, there are different possible propagating TM modes (eigenmodes) corresponding to the different eigenvalues h. Thus there are the TM_1 mode ($n = 1$) with cutoff frequency $(f_c)_1 = 1/2b\sqrt{\mu\epsilon}$, the TM_2 mode ($n = 2$) with $(f_c)_2 = 1/b\sqrt{\mu\epsilon}$, and so on. Each mode has its own characteristic phase constant, guide wavelength, phase velocity, group velocity, and wave impedance; they can be determined from Eqs. (10–38), (10–39), (10–42), (10–43), and (10–45), respectively. When $n = 0$, $E_z = 0$ and only the transverse components H_x and E_y exist. Hence TM_0 mode is the TEM mode, for which $f_c = 0$. The mode having the lowest cutoff *frequency is called the* ***dominant mode*** of the waveguide. ***For parallel-plate waveguides the dominant mode is the TEM mode.***

EXAMPLE 10–3 (a) Write the instantaneous field expressions for TM_1 mode in a parallel-plate waveguide. (b) Sketch the electric and magnetic field lines in the yz-plane.

Solution

a) The instantaneous field expressions for the TM_1 mode are obtained by multiplying the phasor expressions in Eqs. (10–63), (10–64), and (10–65) with $e^{j(\omega t - \beta z)}$ and taking the real part of the product. We have, for $n = 1$,

$$E_z(y, z; t) = A_1 \sin\left(\frac{\pi y}{b}\right) \cos(\omega t - \beta z), \tag{10–68}$$

$$E_y(y, z; t) = \frac{\beta b}{\pi} A_1 \cos\left(\frac{\pi y}{b}\right) \sin(\omega t - \beta z), \tag{10–69}$$

$$H_x(y, z; t) = -\frac{\omega \epsilon b}{\pi} A_1 \cos\left(\frac{\pi y}{b}\right) \sin(\omega t - \beta z), \tag{10–70}$$

where

$$\beta = \sqrt{\omega^2 \mu \epsilon - \left(\frac{\pi}{b}\right)^2}. \tag{10–71}$$

b) In the yz-plane, **E** has both a y- and a z-component, and the equation of the electric field lines at a given t can be found from the relation

$$\frac{dy}{E_y} = \frac{dz}{E_z}. \tag{10–72}$$

For example, at $t = 0$, Eq. (10–72) can be written as

$$\frac{dy}{dz} = \frac{E_y(y, z; 0)}{E_z(y, x; 0)} = -\frac{\beta b}{\pi} \cot\left(\frac{\pi y}{b}\right) \tan \beta z, \tag{10–73}$$

which gives the slope of the electric field lines. Equation (10–73) can be integrated to give

$$\cos\left(\frac{\pi y}{b}\right) \cos \beta z = \text{Constant}, \qquad 0 \le y \le b. \tag{10–74}^{\dagger}$$

---

† Equation (10–73) can be rearranged as

$$\frac{dy}{dz} = -\left(\frac{\beta b}{\pi}\right) \frac{\cos(\pi y/b) \sin \beta z}{\sin(\pi y/b) \cos \beta z}$$

or

$$\frac{(\pi/b) \sin(\pi y/b)\, dy}{\cos(\pi y/b)} = \frac{-\beta \sin \beta z\, dz}{\cos \beta z}$$

or

$$-\frac{d[\cos(\pi y/b)]}{\cos(\pi y/b)} = \frac{d(\cos \beta z)}{\cos \beta z}.$$

Integration gives

$$-\ln[\cos(\pi y/b)] = \ln(\cos \beta z) + c_1$$

or

$$\cos(\pi y/b) \cos \beta z = c_2,$$

which is Eq. (10–74). c_1 and c_2 are constants.

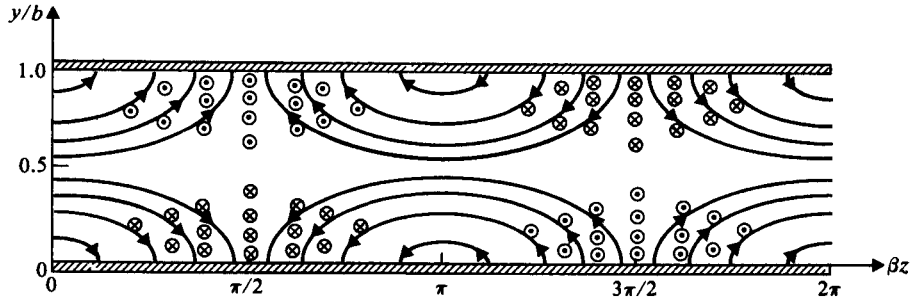

——— Electric field lines,

⊙ ⊗ Magnetic field lines (x-axis into the paper).

FIGURE 10–6
Field lines for TM_1 mode in parallel-plate waveguide.

Several such electric field lines are drawn in Fig. 10–6. The field lines repeat themselves for every change of 2π (rad) in βz and reverse their directions for every change of π (rad).

Since $\mathbf{H}$ has only an x-component, the magnetic field lines are everywhere perpendicular to the yz-plane. For the TM_1 mode at $t = 0$, Eq. (10–70) becomes

$$H_x(y, z; 0) = \frac{\omega\epsilon b}{\pi} A_1 \cos\left(\frac{\pi y}{b}\right) \sin \beta z. \tag{10–75}$$

The density of H_x lines varies as $\cos(\pi y/b)$ in the y-direction and as $\sin \beta z$ in the z-direction. This is also sketched in Fig. 10–6. At the conducting plates ($y = 0$ and $y = b$) there are surface currents because of a discontinuity in the tangential magnetic field, and surface charges because of the presence of a normal electric field. (Problem P.10–4). ▬

▬ **EXAMPLE 10–4** Show that the field solution of a propagating TM_1 wave in a parallel-plate waveguide can be interpreted as the superposition of two plane waves bouncing back and forth obliquely between the two conducting plates.

Solution This can be seen readily by writing the phasor expression of $E_z^0(y)$ from Eq. (10–63) for $n = 1$ and with the factor $e^{-j\beta z}$ restored. We have

$$\begin{aligned} E_z(y, z) &= A_1 \sin\left(\frac{\pi y}{b}\right) e^{-j\beta z} = \frac{A_1}{2j}(e^{j\pi y/b} - e^{-j\pi y/b})e^{-j\beta z} \\ &= \frac{A_1}{2j}[e^{-j(\beta z - \pi y/b)} - e^{-j(\beta z + \pi y/b)}]. \end{aligned} \tag{10–76}$$

From Chapter 8 we recognize that the first term on the right side of Eq. (10–76) represents a plane wave propagating obliquely in the $+z$ and $-y$ directions with phase constants β and π/b, respectively. Similarly, the second term represents a plane

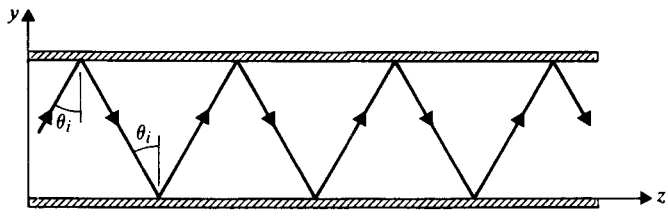

FIGURE 10–7
Propagating wave in parallel-plate waveguide as superposition of two plane waves.

wave propagating obliquely in the $+z$ and $+y$ directions with the same phase constants β and π/b as those of the first plane wave. Thus, a propagating TM_1 wave in a parallel-plate waveguide can be regarded as the superposition of two plane waves, as depicted in Fig. 10–7. ■

In Subsection 8–7.2 on reflection of a parallelly polarized (TM) plane wave incident obliquely at a conducting boundary plane, we obtained an expression for the longitudinal component of the total $\mathbf{E}_1$ field that is the sum of the longitudinal components of the incident $\mathbf{E}_i$ and the reflected $\mathbf{E}_r$. To adapt the coordinate designations of Fig. 8–13 to those of Fig. 10–5, x and z must be changed to z and $-y$, respectively. We rewrite E_x of Eq. (8–128) as

$$E_z(y, z) = E_{i0} \cos \theta_i (e^{j\beta_1 y \cos \theta_i} - e^{-j\beta_1 y \cos \theta_i}) e^{-j\beta_1 z \sin \theta_i}.$$

Comparing the exponents of the terms in this equation with those in Eq. (10–76), we obtain two equations:

$$\beta_1 \sin \theta_i = \beta, \tag{10–77}$$

$$\beta_1 \cos \theta_i = \frac{\pi}{b}. \tag{10–78}$$

(The field amplitudes involved in these equations are of no importance in the present consideration.) Solution of Eqs. (10–77) and (10–78) gives

$$\beta = \sqrt{\beta_1^2 - \left(\frac{\pi}{b}\right)^2} = \sqrt{\omega^2 \mu\epsilon - \left(\frac{\pi}{b}\right)^2},$$

which is the same as Eq. (10–71), and

$$\cos \theta_i = \frac{\pi}{\beta_1 b} = \frac{\lambda}{2b}, \tag{10–79}$$

where $\lambda = 2\pi/\beta_1$ is the wavelength in the unbounded dielectric medium.

We observe that a solution of Eq. (10–79) for θ_i exists only when $\lambda/2b \leq 1$. At $\lambda/2b = 1$, or $f = u/\lambda = 1/2b\sqrt{\mu\epsilon}$, which is the cutoff frequency in Eq. (10–67) for $n = 1$, $\cos \theta_i = 1$, and $\theta_i = 0$. This corresponds to the case in which the waves bounce back and forth in the y-direction, normal to the parallel plates, and there is no propagation in the z-direction ($\beta = \beta_1 \sin \theta_i = 0$). Propagation of TM_1 mode is possible only when $\lambda < \lambda_c = 2b$ or $f > f_c$. Both $\cos \theta_i$ and $\sin \theta_i$ can be expressed in terms of

cutoff frequency f_c. From Eqs. (10–79) and (10–77) we have

$$\cos \theta_i = \frac{\lambda}{\lambda_c} = \frac{f_c}{f} \tag{10–80}$$

and

$$\sin \theta_i = \frac{\lambda}{\lambda_g} = \frac{u}{u_p} = \sqrt{1 - \left(\frac{f_c}{f}\right)^2}. \tag{10–81}$$

Equation (10–81) is in agreement with Eqs. (10–39) and (10–42).

We studied traveling waves in a parallel-plate waveguide in terms of bouncing plane waves in Section 8–7 with the aid of Fig. 8–12. We note here that Eqs. (10–79) and (10–81) are consistent respectively with Eqs. (8–119) and (8–120), which hold for both perpendicular and parallel polarizations.

10–3.2 TE WAVES BETWEEN PARALLEL PLATES

For transverse electric waves, $E_z = 0$, we solve the following equation for $H_z^0(y)$, which is a simplified version of Eq. (10–48) with no x-dependence:

$$\frac{d^2 H_z^0(y)}{dy^2} + h^2 H_z^0(y) = 0. \tag{10–82}$$

We note that $H_z(y, z) = H_z^0(y)e^{-\gamma z}$. The boundary conditions to be satisfied by $H_z^0(y)$ are obtained from Eq. (10–51). Since E_x must vanish at the surfaces of the conducting plates, we require

$$\frac{dH_z^0(y)}{dy} = 0 \qquad \text{at } y = 0 \quad \text{and} \quad y = b.$$

Therefore the proper solution of Eq. (10–82) is of the form

$$H_z^0(y) = B_n \cos\left(\frac{n\pi y}{b}\right), \tag{10–83}$$

where the amplitude B_n depends on the strength of excitation of the particular TE wave. We obtain the only other nonzero field components from Eqs. (10–50) and (10–51), keeping in mind that $\partial H_z/\partial x = 0$:

$$H_y^0(y) = \frac{\gamma}{h} B_n \sin\left(\frac{n\pi y}{b}\right), \tag{10–84}$$

$$E_x^0(y) = \frac{j\omega\mu}{h} B_n \sin\left(\frac{n\pi y}{b}\right). \tag{10–85}$$

The propagation constant γ in Eq. (10–84) is the same as that for TM waves given in Eq. (10–66). Inasmuch as cutoff frequency is the frequency that makes $\gamma = 0$, ***the cutoff frequency for the TE_n mode in a parallel-plate waveguide is exactly the same as that for the TM_n mode given in Eq. (10–67).*** For $n = 0$, both H_y and E_x vanish; hence the TE_0 mode does not exist in a parallel-plate waveguide.

EXAMPLE 10–5 (a) Write the instantaneous field expressions for the TE_1 mode in a parallel-plate waveguide. (b) Sketch the electric and magnetic field lines in the yz-plane.

Solution

a) The instantaneous field expressions for the TE_1 mode are obtained by taking the real part of the products of the phasor expressions in Eqs. (10–83), (10–84), and (10–85) with $e^{j(\omega t - \beta z)}$. We have, for $n = 1$,

$$H_z(y, z; t) = B_1 \cos\left(\frac{\pi y}{b}\right) \cos(\omega t - \beta z), \tag{10–86}$$

$$H_y(y, z; t) = -\frac{\beta b}{\pi} B_1 \sin\left(\frac{\pi y}{b}\right) \sin(\omega t - \beta z), \tag{10–87}$$

$$E_x(y, z; t) = -\frac{\omega \mu b}{\pi} B_1 \sin\left(\frac{\pi y}{b}\right) \sin(\omega t - \beta z), \tag{10–88}$$

where the phase constant β is given by Eq. (10–71), same as that for the TM_1 mode.

b) The electric field has only an x-component. At $t = 0$, Eq. (10–88) becomes

$$E_x(y, z; 0) = \frac{\omega \mu b}{\pi} B_1 \sin\left(\frac{\pi y}{b}\right) \sin \beta z. \tag{10–89}$$

Thus the density of E_x lines varies as $\sin(\pi y/b)$ in the y direction and as $\sin \beta z$ in the z direction; E_x lines are sketched as dots and crosses in Fig. 10–8.

The magnetic field has both a y- and a z-component. The equation of the magnetic field lines at $t = 0$ can be found from the following relation:

$$\frac{dy}{dz} = \frac{H_y(y, z; 0)}{H_z(y, z; 0)} = \frac{\beta b}{\pi} \tan\left(\frac{\pi y}{b}\right) \tan \beta z. \tag{10–90}$$

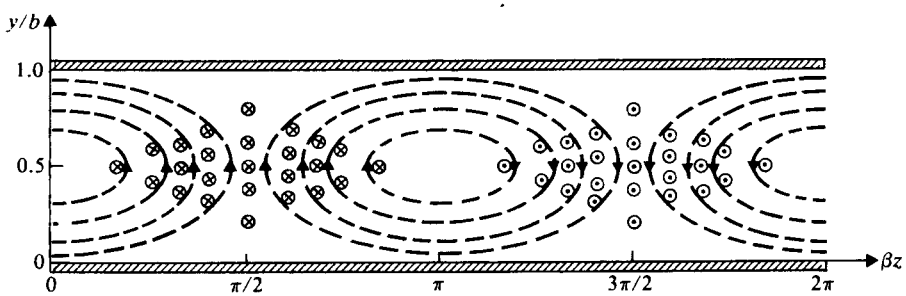

——— Magnetic field lines,

⊙ ⊗ Electric field lines (x-axis into the paper).

FIGURE 10–8
Field lines for TE_1 mode in parallel-plate waveguide.

Using the procedure illustrated in Example 10–3, we can integrate Eq. (10–90) to obtain

$$\sin\left(\frac{\pi y}{b}\right)\cos\beta z = \text{Constant}, \qquad 0 \le y \le b, \tag{10–91}$$

which is the equation for magnetic field lines in the yz-plane at $t = 0$. The constant in Eq. (10–91) lies between -1 and $+1$. According to Eq. (10–86), the density of the H_z line varies as $|\cos(\pi y/b)|$. Several magnetic field lines are drawn in Fig. 10–8. The lines repeat themselves for every change of 2π (rad) in βz. ■

10–3.3 ENERGY-TRANSPORT VELOCITY

In Subsections 10–2.2 and 10–2.3 we noted that signals having a frequency higher than the cutoff frequency will propagate in a waveguide with a phase velocity u_p given by Eq. (10–42) and a group velocity u_g given by Eq. (10–43). When the concept of group velocity was introduced in Section 8–4, it was defined as the velocity of the envelope of a narrow-band signal. For signals with a broad frequency spectrum, such as pulses of short durations, group velocity loses its significance because the low-frequency components may be below cutoff (therefore cannot propagate) and the high-frequency components will travel with widely different velocities. These wide-band signals will then be badly distorted, and no single group velocity can represent the signal-propagation velocity. In such cases we examine the velocity at which energy propagates along a waveguide, or ***energy-transport velocity***.

For signal transmission in a lossless waveguide we define energy-transport velocity, u_{en}, as the ratio of the time-average propagated power to the time-average stored energy per unit guide length:

$$\boxed{u_{en} = \frac{(P_z)_{av}}{W'_{av}} \quad \text{(m/s)},} \tag{10–92}$$

where the time-average power $(P_z)_{av}$ is equal to the time-average Poynting vector $\mathscr{P}_{av}$ integrated over the guide cross section:

$$(P_z)_{av} = \int_S \mathscr{P}_{av} \cdot d\mathbf{s}, \tag{10–93}$$

and the time-average stored energy per unit length W'_{av} is the sum of the time-average stored electric energy density $(w_e)_{av}$ and the time-average stored magnetic energy density $(w_m)_{av}$ integrated over the guide cross section:

$$W'_{av} = \int_S [(w_e)_{av} + (w_m)_{av}]\, ds. \tag{10–94}$$

For a particular mode of propagation in a waveguide we calculate $(P_z)_{av}$ and W'_{av} from Eqs. (10–93) and (10–94), respectively, and substitute into Eq. (10–92) to find energy-transport velocity.

EXAMPLE 10–6 Determine the energy-transport velocity of the TM_n mode in a lossless parallel-plate waveguide.

Solution We first obtain the time-average Poynting vector by using Eqs. (8–96), (10–63), (10–64), and (10–65):

$$\begin{aligned}\mathscr{P}_{av} &= \tfrac{1}{2}\mathscr{R}e(\mathbf{E} \times \mathbf{H}^*) \\ &= \tfrac{1}{2}\mathscr{R}e(-\mathbf{a}_z E_y^0 H_x^{0*} + \mathbf{a}_y E_z^0 H_x^{0*}).\end{aligned} \tag{10–95}$$

Thus,

$$\begin{aligned}\mathscr{P}_{av} \cdot \mathbf{a}_z &= -\tfrac{1}{2}\mathscr{R}e(E_y^0 H_x^{0*}) \\ &= \frac{\omega\epsilon\beta}{2h^2} A_n^2 \cos^2\left(\frac{n\pi y}{b}\right),\end{aligned} \tag{10–96}$$

where we have replaced γ by $j\beta$. For a unit width of the parallel-plate waveguide, substitution of Eq. (10–96) in Eq. (10–93) yields

$$\begin{aligned}(P_z)_{av} &= \int_0^b \mathscr{P}_{av} \cdot \mathbf{a}_z \, dy \\ &= \frac{\omega\epsilon\beta b}{4h^2} A_n^2.\end{aligned} \tag{10–97}$$

Following the procedure leading to Eq. (8–96) from Eq. (8–83), we can readily prove from Eqs. (8–85) and (8–86) that

$$(w_e)_{av} = \frac{\epsilon}{4}\mathscr{R}e(\mathbf{E} \cdot \mathbf{E}^*), \tag{10–98}$$

and

$$(w_m)_{av} = \frac{\mu}{4}\mathscr{R}e(\mathbf{H} \cdot \mathbf{H}^*). \tag{10–99}$$

Substituting Eqs. (10–63) and (10–65) in Eq. (10–98), we have

$$(w_e)_{av} = \frac{\epsilon}{4} A_n^2\left[\sin^2\left(\frac{n\pi y}{b}\right) + \frac{\beta^2}{h^2}\cos^2\left(\frac{n\pi y}{b}\right)\right] \tag{10–100}$$

and

$$\begin{aligned}\int_0^b (w_e)_{av}\, dy &= \frac{\epsilon b}{8} A_n^2\left[1 + \frac{\beta^2}{h^2}\right] \\ &= \frac{\epsilon b}{8h^2} k^2 A_n^2,\end{aligned} \tag{10–101}$$

where Eq. (10–15) has been used to replace $\beta^2 + h^2$ by k^2. Similarly, using Eq. (10–64) in Eq. (10–99), we obtain

$$(w_m)_{av} = \frac{\mu}{4}\left(\frac{\omega^2\epsilon^2}{h^2}\right) A_n^2 \cos^2\left(\frac{n\pi y}{b}\right) \tag{10–102}$$

and

$$\int_0^b (w_m)_{av}\, dy = \frac{\mu b}{8h^2}(\omega^2\epsilon^2) A_n^2 = \frac{\epsilon b}{8h^2} k^2 A_n^2, \tag{10–103}$$

which is seen to be equal to the time-average stored electric energy per unit guide width obtained in Eq. (10–101).

We are now ready to find u_{en} from Eq. (10–92) by dividing $(P_z)_{av}$ in Eq. (10–97) by the sum of the stored energies in Eqs. (10–101) and (10–103):

$$u_{en} = \frac{\omega\beta}{k^2} = \frac{\omega}{k}\left(\frac{\beta}{k}\right) = u\sqrt{1-\left(\frac{f_c}{f}\right)^2}, \tag{10–104}$$

where we have made use of Eqs. (10–5) and (10–38). We recognize that the energy-transport velocity in Eq. (10–104) is equal to the group velocity given in Eq. (10–43).

10–3.4 ATTENUATION IN PARALLEL-PLATE WAVEGUIDES

Attenuation in any waveguide (not just the parallel-plate waveguide) arises from two sources: lossy dielectric and imperfectly conducting walls. Losses modify the electric and magnetic fields within the guide, making exact solutions difficult to obtain. However, in practical waveguides the losses are usually very small, and we will assume that the transverse field patterns of the propagating modes are not affected by them. A real part of the propagation constant now appears as the attenuation constant, which accounts for power losses. The attenuation constant consists of two parts:

$$\alpha = \alpha_d + \alpha_c, \tag{10–105}$$

where α_d is the attenuation constant due to losses in the dielectric and α_c is that due to ohmic power loss in the imperfectly conducting walls.

We will now consider the attenuation constants for TEM, TM, and TE modes separately.

TEM Modes The attenuation constant for TEM modes on a parallel-plate transmission line has been discussed in Subsection 9–3.4. From Eq. (9–90) and Table 9–1 we have approximately

$$\alpha_d = \frac{G}{2}R_0 = \frac{\sigma}{2}\sqrt{\frac{\mu}{\epsilon}} = \frac{\sigma}{2}\eta \quad \text{(Np/m)}, \tag{10–106}$$

where ϵ, μ, and σ are the permittivity, permeability, and conductivity, respectively, of the dielectric medium. In Eq. (10–106), $\eta = \sqrt{\mu/\epsilon}$ is the intrinsic impedance of the dielectric if the dielectric is lossless. If the losses in the dielectric are represented by the imaginary part, $-\epsilon''$, of a complex permittivity as in Eq. (7–111), we may replace σ by $\omega\epsilon''$ and write Eq. (10–106) alternatively as

$$\alpha_d \cong \frac{\omega\epsilon''}{2}\eta \quad \text{(Np/m)}. \tag{10–107}$$

Also from Eq. (9–90) and Table 9–1 we have

$$\alpha_c = \frac{R}{2R_0} = \frac{1}{b}\sqrt{\frac{\pi f \epsilon}{\sigma_c}} \qquad \text{(Np/m)}, \tag{10–108}$$

where σ_c is the conductivity of the metal plates. We note that, for TEM modes, α_d is independent of frequency, and α_c is proportional to $\sqrt{f}$. We note further that $\alpha_d \to 0$ as $\sigma \to 0$ and that $\alpha_c \to 0$ as $\sigma_c \to \infty$, as expected.

TM Modes The attenuation constant due to losses in the dielectric at frequencies above f_c can be found from Eq. (10–66) by substituting $\epsilon_d = \epsilon + (\sigma/j\omega)$ for ϵ. We have

$$\begin{aligned}
\gamma &= j\left[\omega^2\mu\epsilon\left(1 - \frac{j\sigma}{\omega\epsilon}\right) - \left(\frac{n\pi}{b}\right)^2\right]^{1/2} \\
&= j\sqrt{\omega^2\mu\epsilon - \left(\frac{n\pi}{b}\right)^2}\left\{1 - j\omega\mu\sigma\left[\omega^2\mu\epsilon - \left(\frac{n\pi}{b}\right)^2\right]^{-1}\right\}^{1/2} \\
&\cong j\sqrt{\omega^2\mu\epsilon - \left(\frac{n\pi}{b}\right)^2}\left\{1 - \frac{j\omega\mu\sigma}{2}\left[\omega^2\mu\epsilon - \left(\frac{n\pi}{b}\right)^2\right]^{-1}\right\}.
\end{aligned} \tag{10–109}$$

Only the first two terms in the binomial expansion for the second line in Eq. (10–109) are retained in the third line under the assumption that

$$\omega\mu\sigma \ll \omega^2\mu\epsilon - \left(\frac{n\pi}{b}\right)^2.$$

From Eq. (10–67) we see that

$$\frac{n\pi}{b} = 2\pi f_c\sqrt{\mu\epsilon},$$

which enables us to write

$$\begin{aligned}
\sqrt{\omega^2\mu\epsilon - \left(\frac{n\pi}{b}\right)^2} &= \omega\sqrt{\mu\epsilon}\sqrt{1 - (\omega_c/\omega)^2} \\
&= \omega\sqrt{\mu\epsilon}\sqrt{1 - (f_c/f)^2}.
\end{aligned}$$

With the above relation, Eq. (10–109) becomes

$$\gamma = \alpha_d + j\beta = \frac{\sigma}{2}\sqrt{\frac{\mu}{\epsilon}}\frac{1}{\sqrt{1 - (f_c/f)^2}} + j\omega\sqrt{\mu\epsilon}\sqrt{1 - (f_c/f)^2},$$

from which we obtain

$$\alpha_d = \frac{\sigma\eta}{2\sqrt{1 - (f_c/f)^2}} \qquad \text{(Np/m)} \tag{10–110}$$

and

$$\beta = \omega\sqrt{\mu\epsilon}\sqrt{1 - (f_c/f)^2} \qquad \text{(rad/m)}. \tag{10–111}$$

Thus, α_d for TM modes decreases when frequency increases.

To find the attenuation constant due to losses in the imperfectly conducting plates, we use Eq. (9–88), which was derived from the law of conservation of energy. Thus,

$$\alpha_c = \frac{P_L(z)}{2P(z)}, \tag{10–112}$$

where $P(z)$ is the time-average power flowing through a cross section (say, of width w) of the waveguide, and $P_L(z)$ is the time-average power lost in the two plates per unit length. For TM modes we use Eqs. (10–64) and (10–65):

$$\begin{aligned} P(z) &= w\int_0^b -\tfrac{1}{2}(E_y^0)(H_x^0)^*\,dy \\ &= \frac{w\omega\epsilon\beta}{2}\left(\frac{bA_n}{n\pi}\right)^2\int_0^b \cos^2\left(\frac{n\pi y}{b}\right)dy \\ &= w\omega\epsilon\beta b\left(\frac{bA_n}{2n\pi}\right)^2. \end{aligned} \tag{10–113}$$

The surface current densities on the upper and lower plates have the same magnitude. On the lower plate where $y = 0$ we have

$$|J_{sz}^0| = |H_x^0(y=0)| = \frac{\omega\epsilon bA_n}{n\pi}.$$

The total power loss per unit length in two plates of width w is

$$P_L(z) = 2w\left(\frac{1}{2}|J_{sz}^0|^2R_s\right) = w\left(\frac{\omega\epsilon bA_n}{n\pi}\right)^2 R_s. \tag{10–114}$$

Substitution of Eqs. (10–113) and (10–114) in Eq. (10–112) yields

$$\alpha_c = \frac{2\omega\epsilon R_s}{\beta b} = \frac{2R_s}{\eta b\sqrt{1-(f_c/f)^2}} \quad \text{(Np/m)}, \tag{10–115}$$

where, from Eq. (9–26b),

$$R_s = \sqrt{\frac{\pi f\mu_c}{\sigma_c}} \quad (\Omega). \tag{10–116}$$

The use of Eq. (10–116) in Eq. (10–115) gives the explicit dependence of α_c on f for TM modes:

$$\alpha_c = \frac{2}{\eta b}\sqrt{\frac{\pi\mu_c f_c}{\sigma_c}}\frac{1}{\sqrt{(f_c/f)[1-(f_c/f)^2]}}. \tag{10–117}$$

A sketch of the normalized α_c is shown in Fig. 10–9, which reveals the existence of a minimum.

TE Modes In Subsection 10–3.2 we noted that the expression for the propagation constant for TE waves between parallel plates is the same as that for TM waves. It follows that the formula for α_d in Eq. (10–110) holds for TE modes as well.

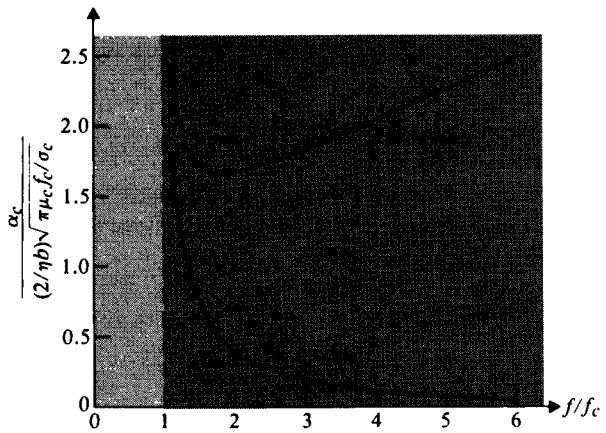

FIGURE 10–9
Normalized attenuation constant due to finite conductivity of the plates in parallel-plate waveguide.

In order to determine the attenuation constant α_c due to losses in the imperfectly conducting plates, we again apply Eq. (10–112). Of course, the field expressions in Eqs. (10–83), (10–84), and (10–85) for TE modes must now be used. We have

$$\begin{aligned} P(z) &= w\int_0^b \tfrac{1}{2}(E_x^0)(H_y^0)^*\,dy \\ &= \frac{w\omega\mu\beta}{2}\left(\frac{bB_n}{n\pi}\right)^2\int_0^b \sin^2\left(\frac{n\pi y}{b}\right)dy \\ &= w\omega\mu\beta b\left(\frac{bB_n}{2n\pi}\right)^2 \end{aligned} \tag{10–118}$$

and

$$\begin{aligned} P_L(z) &= 2w(\tfrac{1}{2}|J_{sx}^0|^2R_s) \\ &= w|H_z^0(y=0)|^2R_z = wB_n^2R_s. \end{aligned} \tag{10–119}$$

Consequently,

$$\begin{aligned} \alpha_c &= \frac{P_L(z)}{2P(z)} = \frac{2R_s}{\omega\mu\beta b}\left(\frac{n\pi}{b}\right)^2 \\ &= \frac{2R_sf_c^2}{\eta bf^2\sqrt{1-(f_c/f)^2}}. \end{aligned} \tag{10–120}$$

A normalized α_c curve based on Eq. (10–120) is also sketched in Fig. 10–9. Unlike α_c for TM modes, α_c for TE modes does not have a minimum but decreases monotonically as f increases.

10–4 Rectangular Waveguides

The analysis of parallel-plate waveguides in Section 10–3 assumed the plates to be of an infinite extent in the transverse x direction; that is, the fields do not vary with x. In practice, these plates are always finite in width, with fringing fields at the edges. Electromagnetic energy will leak through the sides of the guide and create undesirable stray couplings to other circuits and systems. Thus practical waveguides are usually uniform structures of a cross section of the enclosed variety. The simplest of such cross sections, in terms of ease both in analysis and in manufacture, are rectangular and circular. In this section we will analyze the wave behavior in hollow rectangular waveguides. Circular waveguides will be treated in the next section. Rectangular waveguides are more commonly used in practice than circular waveguides.

In the following discussion we draw on the material in Section 10–2 concerning general wave behaviors along uniform guiding structures. Propagation of time-harmonic waves in the $+z$ direction with a propagation constant γ is considered. TM and TE modes will be discussed separately. As we have noted previously, TEM waves cannot exist in a single-conductor hollow or dielectric-filled waveguide.

10–4.1 TM WAVES IN RECTANGULAR WAVEGUIDES

Consider the waveguide sketched in Fig. 10–10, with its rectangular cross section of sides a and b. The enclosed dielectric medium is assumed to have constitutive parameters ϵ and μ. For TM waves, $H_z = 0$ and E_z is to be solved from Eq. (10–24). Writing $E_z(x, y, z)$ as

$$E_z(x, y, z) = E_z^0(x, y)e^{-\gamma z}, \tag{10–121}$$

we solve the following second-order partial differential equation:

$$\left(\frac{\partial^2}{\partial x^2} + \frac{\partial^2}{\partial y^2} + h^2\right)E_z^0(x, y) = 0. \tag{10–122}$$

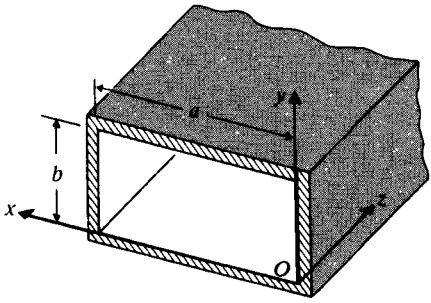

FIGURE 10–10
A rectangular waveguide.

Here we use the method of separation of variables discussed in Section 4–5 by letting

$$E_z^0(x, y) = X(x)Y(y). \tag{10–123}$$

Substituting Eq. (10–123) in Eq. (10–122) and dividing the resulting equation by $X(x)Y(y)$, we have

$$-\frac{1}{X(x)}\frac{d^2X(x)}{dx^2} = \frac{1}{Y(y)}\frac{d^2Y(y)}{dy^2} + h^2. \tag{10–124}$$

Now we argue that, since the left side of Eq. (10–124) is a function of x only and the right side is a function of y only, both sides must equal a constant in order for the equation to hold for all values of x and y. Calling this constant (separation constant) k_x^2, we obtain two separate ordinary differential equations:

$$\frac{d^2X(x)}{dx^2} + k_x^2X(x) = 0, \tag{10–125}$$

$$\frac{d^2Y(y)}{dy^2} + k_y^2Y(y) = 0, \tag{10–126}$$

where

$$k_y^2 = h^2 - k_x^2. \tag{10–127}$$

The possible solutions of Eqs. (10–125) and (10–126) are listed in Table 4–1, Section 4–5. The appropriate forms to be chosen must satisfy the following boundary conditions.

1. In the x-direction:

$$E_z^0(0, y) = 0, \tag{10–128}$$

$$E_z^0(a, y) = 0. \tag{10–129}$$

2. In the y-direction:

$$E_z^0(x, 0) = 0, \tag{10–130}$$

$$E_z^0(x, b) = 0. \tag{10–131}$$

Obviously, then, we must choose:

$X(x)$ in the form of $\sin k_x x$,

$$k_x = \frac{m\pi}{a}, \qquad m = 1, 2, 3, \ldots$$

$Y(y)$ in the form of $\sin k_y y$,

$$k_y = \frac{n\pi}{b}, \qquad n = 1, 2, 3, \ldots,$$

and the proper solution for $E_z^0(x, y)$ is

$$\boxed{E_z^0(x, y) = E_0 \sin\left(\frac{m\pi}{a}x\right)\sin\left(\frac{n\pi}{b}y\right) \quad \text{(V/m)}.} \tag{10–132}$$

From Eq. (10–127) we have

$$\boxed{h^2 = \left(\frac{m\pi}{a}\right)^2 + \left(\frac{n\pi}{b}\right)^2.} \tag{10–133}$$

The other field components are obtained from Eqs. (10–25) through (10–28):

$$E_x^0(x, y) = -\frac{\gamma}{h^2}\left(\frac{m\pi}{a}\right)E_0 \cos\left(\frac{m\pi}{a}x\right)\sin\left(\frac{n\pi}{b}y\right), \tag{10–134}$$

$$E_y^0(x, y) = -\frac{\gamma}{h^2}\left(\frac{n\pi}{b}\right)E_0 \sin\left(\frac{m\pi}{a}x\right)\cos\left(\frac{n\pi}{b}y\right), \tag{10–135}$$

$$H_x^0(x, y) = \frac{j\omega\epsilon}{h^2}\left(\frac{n\pi}{b}\right)E_0 \sin\left(\frac{m\pi}{a}x\right)\cos\left(\frac{n\pi}{b}y\right), \tag{10–136}$$

$$H_y^0(x, y) = -\frac{j\omega\epsilon}{h^2}\left(\frac{m\pi}{a}\right)E_0 \cos\left(\frac{m\pi}{a}x\right)\sin\left(\frac{n\pi}{b}y\right), \tag{10–137}$$

where

$$\gamma = j\beta = j\sqrt{\omega^2\mu\epsilon - \left(\frac{m\pi}{a}\right)^2 - \left(\frac{n\pi}{b}\right)^2}. \tag{10–138}$$

Every combination of the integers m and n defines a possible mode that may be designated as the TM_{mn} mode; thus there are a double infinite number of TM modes. The first subscript denotes the number of half-cycle variations of the fields in the x-direction, and the second subscript denotes the number of half-cycle variations of the fields in the y-direction. The cutoff of a particular mode is the condition that makes γ vanish. For the TM_{mn} mode the cutoff frequency is

$$\boxed{(f_c)_{mn} = \frac{1}{2\sqrt{\mu\epsilon}}\sqrt{\left(\frac{m}{a}\right)^2 + \left(\frac{n}{b}\right)^2} \quad \text{(Hz)},} \tag{10–139}$$

which checks with Eq. (10–35). Alternatively, we may write

$$\boxed{(\lambda_c)_{mn} = \frac{2}{\sqrt{\left(\frac{m}{a}\right)^2 + \left(\frac{n}{b}\right)^2}} \quad \text{(m)},} \tag{10–140}$$

where λ_c is the ***cutoff wavelength.***

For TM modes in rectangular waveguides, neither m nor n can be zero. (Do you know why?) Hence, the TM_{11} mode has the lowest cutoff frequency of all TM modes in a rectangular waveguide. The expressions for the phase constant β and the wave impedance Z_{TM} for propagating modes in Eqs. (10–38) and (10–45), respectively, apply here directly.

EXAMPLE 10–7 (a) Write the instantaneous field expressions for the TM_{11} mode in a rectangular waveguide of sides a and b. (b) Sketch the electric and magnetic field lines in a typical xy-plane and in a typical yz-plane.

Solution

a) The instantaneous field expressions for the TM_{11} mode are obtained by multiplying the phasor expressions in Eqs. (10–132) and (10–134) through (10–137) with $e^{j(\omega t - \beta z)}$ and then taking the real part of the product. We have, for $m = n = 1$,

$$E_x(x, y, z; t) = \frac{\beta}{h^2}\left(\frac{\pi}{a}\right)E_0 \cos\left(\frac{\pi}{a}x\right)\sin\left(\frac{\pi}{b}y\right)\sin(\omega t - \beta z), \tag{10–141}$$

$$E_y(x, y, z; t) = \frac{\beta}{h^2}\left(\frac{\pi}{b}\right)E_0 \sin\left(\frac{\pi}{a}x\right)\cos\left(\frac{\pi}{b}y\right)\sin(\omega t - \beta z), \tag{10–142}$$

$$E_z(x, y, z; t) = E_0 \sin\left(\frac{\pi}{a}x\right)\sin\left(\frac{\pi}{b}y\right)\cos(\omega t - \beta z), \tag{10–143}$$

$$H_x(x, y, z; t) = -\frac{\omega\epsilon}{h^2}\left(\frac{\pi}{b}\right)E_0 \sin\left(\frac{\pi}{a}x\right)\cos\left(\frac{\pi}{b}y\right)\sin(\omega t - \beta z), \tag{10–144}$$

$$H_y(x, y, z; t) = \frac{\omega\epsilon}{h^2}\left(\frac{\pi}{a}\right)E_0 \cos\left(\frac{\pi}{a}x\right)\sin\left(\frac{\pi}{b}y\right)\sin(\omega t - \beta z), \tag{10–145}$$

$$H_z(x, y, z; t) = 0, \tag{10–146}$$

where

$$\beta = \sqrt{k^2 - h^2} = \sqrt{\omega^2\mu\epsilon - \left(\frac{\pi}{a}\right)^2 - \left(\frac{\pi}{b}\right)^2}. \tag{10–147}$$

b) In a typical xy-plane, the slopes of the electric field and magnetic field lines are

$$\left(\frac{dy}{dx}\right)_E = \frac{a}{b}\tan\left(\frac{\pi}{a}x\right)\cot\left(\frac{\pi}{b}y\right), \tag{10–148}$$

$$\left(\frac{dy}{dx}\right)_H = -\frac{b}{a}\cot\left(\frac{\pi}{a}x\right)\tan\left(\frac{\pi}{b}y\right). \tag{10–149}$$

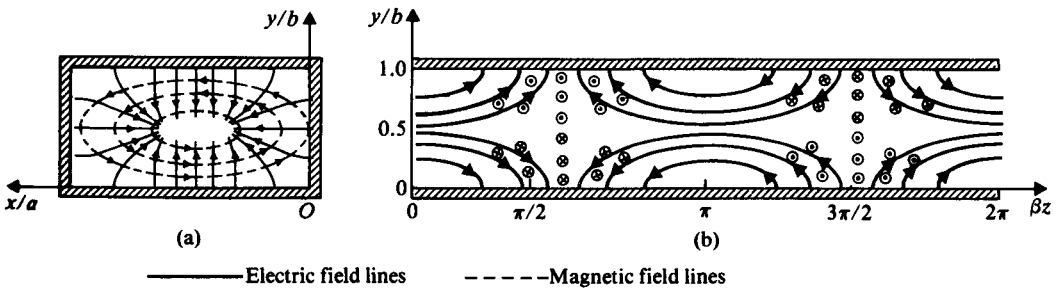

FIGURE 10–11
Field lines for TM_{11} mode in rectangular waveguide.

These equations are quite similar to Eq. (10–73) and can be used to sketch the **E** and **H** lines shown in Fig. 10–11(a). Note that from Eqs. (10–148) and (10–149),

$$\left(\frac{dy}{dx}\right)_E\left(\frac{dy}{dx}\right)_H = -1, \tag{10–150}$$

indicating that **E** and **H** lines are everywhere perpendicular to one another. Note also that **E** lines are normal and that **H** lines are parallel to conducting guide walls.

Similarly, in a typical yz-plane, say, for $x = a/2$ or $\sin(\pi x/a) = 1$ and $\cos(\pi x/a) = 0$, we have

$$\left(\frac{dy}{dz}\right)_E = \frac{\beta}{h^2}\left(\frac{\pi}{b}\right)\cot\left(\frac{\pi}{b}y\right)\tan(\omega t - \beta z), \tag{10–151}$$

and **H** has only an x-component. Some typical **E** and **H** lines are drawn in Fig. 10–11(b) for $t = 0$. ■

10–4.2 TE WAVES IN RECTANGULAR WAVEGUIDES

For transverse electric waves, $E_z = 0$, we solve Eq. (10–48) for H_z. We write

$$H_z(x, y, z) = H_z^0(x, y)e^{-\gamma z}, \tag{10–152}$$

where $H_z^0(x, z)$ satisfies the following second-order partial differential equation:

$$\left(\frac{\partial^2}{\partial x^2} + \frac{\partial^2}{\partial y^2} + h^2\right)H_z^0(x, y) = 0. \tag{10–153}$$

Equation (10–153) is seen to be of exactly the same form as Eq. (10–122). The solution for $H_z^0(x, y)$ must satisfy the following boundary conditions.

1. In the x-direction:

$$\frac{\partial H_z^0}{\partial x} = 0\ (E_y = 0) \quad \text{at} \quad x = 0, \tag{10–154}$$

$$\frac{\partial H_z^0}{\partial x} = 0\ (E_y = 0) \quad \text{at} \quad x = a. \tag{10–155}$$

2. In the y-direction:

$$\frac{\partial H_z^0}{\partial y} = 0\ (E_x = 0) \quad \text{at} \quad y = 0, \tag{10–156}$$

$$\frac{\partial H_z^0}{\partial y} = 0\ (E_x = 0) \quad \text{at} \quad y = b. \tag{10–157}$$

It is readily verified that the appropriate solution for $H_z^0(x, y)$ is

$$\boxed{H_z^0(x, y) = H_0 \cos\left(\frac{m\pi}{a}x\right)\cos\left(\frac{n\pi}{b}y\right) \quad \text{(A/m)}.} \tag{10–158}$$

The relation between the eigenvalue h and $(m\pi/a)$ and $(n\pi/b)$ is the same as that given in Eq. (10–133) for TM modes.

The other field components are obtained from Eqs. (10–49) through (10–52):

$$E_x^0(x, y) = \frac{j\omega\mu}{h^2}\left(\frac{n\pi}{b}\right)H_0 \cos\left(\frac{m\pi}{a}x\right)\sin\left(\frac{n\pi}{b}y\right), \tag{10–159}$$

$$E_y^0(x, y) = -\frac{j\omega\mu}{h^2}\left(\frac{m\pi}{a}\right)H_0 \sin\left(\frac{m\pi}{a}x\right)\cos\left(\frac{n\pi}{b}y\right), \tag{10–160}$$

$$H_x^0(x, y) = \frac{\gamma}{h^2}\left(\frac{m\pi}{a}\right)H_0 \sin\left(\frac{m\pi}{a}x\right)\cos\left(\frac{n\pi}{b}y\right), \tag{10–161}$$

$$H_y^0(x, y) = \frac{\gamma}{h^2}\left(\frac{n\pi}{b}\right)H_0 \cos\left(\frac{m\pi}{a}x\right)\sin\left(\frac{n\pi}{b}y\right), \tag{10–162}$$

where γ has the same expression as that given in Eq. (10–138) for TM modes.

Equation (10–139) for cutoff frequency also applies here. For TE modes, either m or n (but not both) can be zero. If $a > b$, the cutoff frequency is the *lowest* when $m = 1$ and $n = 0$:

$$\boxed{(f_c)_{\text{TE}_{10}} = \frac{1}{2a\sqrt{\mu\epsilon}} = \frac{u}{2a} \quad \text{(Hz)}.} \tag{10–163}$$

The corresponding cutoff wavelength is

$$\boxed{(\lambda_c)_{\text{TE}_{10}} = 2a \quad \text{(m)}.} \tag{10–164}$$

Hence ***the*** $\mathbf{TE_{10}}$ ***mode is the dominant mode of a rectangular waveguide with*** $\boldsymbol{a > b}$. Because the TE_{10} mode has the lowest attenuation of all modes in a rectangular waveguide and its electric field is definitely polarized in one direction everywhere, it is of particular practical importance (see Subsection 10–4.3).

EXAMPLE 10–8 (a) Write the instantaneous field expressions for the TE_{10} mode in a rectangular waveguide having sides a and b. (b) Sketch the electric and magnetic field lines in typical xy-, yz-, and xz-planes. (c) Sketch the surface currents on the guide walls.

Solution

a) The instantaneous field expressions for the dominant TE_{10} mode are obtained by multiplying the phasor expressions in Eqs. (10–158) through (10–162) with $e^{j(\omega t - \beta z)}$ and then taking the real part of the product. We have, for $m = 1$ and $n = 0$,

$$E_x(x, y, z; t) = 0, \tag{10–165}$$

$$E_y(x, y, z; t) = \frac{\omega\mu}{h^2}\left(\frac{\pi}{a}\right)H_0 \sin\left(\frac{\pi}{a}x\right)\sin(\omega t - \beta z), \tag{10–166}$$

$$E_z(x, y, z; t) = 0, \tag{10–167}$$

$$H_x(x, y, z; t) = -\frac{\beta}{h^2}\left(\frac{\pi}{a}\right)H_0 \sin\left(\frac{\pi}{a}x\right)\sin(\omega t - \beta z), \tag{10–168}$$

$$H_y(x, y, z; t) = 0, \tag{10–169}$$

$$H_z(x, y, z; t) = H_0 \cos\left(\frac{\pi}{a}x\right)\cos(\omega t - \beta z), \tag{10–170}$$

where

$$\beta = \sqrt{k^2 - h^2} = \sqrt{\omega^2\mu\epsilon - \left(\frac{\pi}{a}\right)^2}. \tag{10–171}$$

b) We see from Eqs. (10–165) through (10–170) that the TE_{10} mode has only three nonzero field components—namely, E_y, H_x, and H_z. In a typical xy-plane, say, when $\sin(\omega t - \beta z) = 1$, both E_y and H_x vary as $\sin(\pi x/a)$ and are independent of y, as shown in Fig. 10–12(a).

In a typical yz-plane, for example at $x = a/2$ or $\sin(\pi x/a) = 1$ and $\cos(\pi x/a) = 0$, we only have E_y and H_x, both of which vary sinusoidally with βz. A sketch of E_y and H_x at $t = 0$ is given in Fig. 10–12(b).

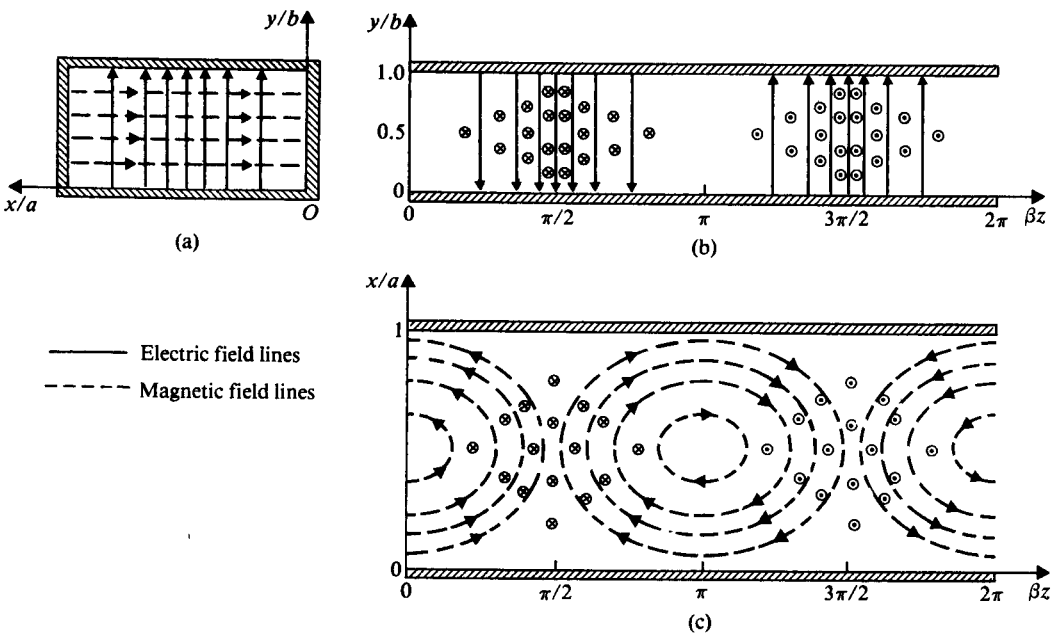

FIGURE 10–12
Field lines for TE_{10} mode in rectangular waveguide.

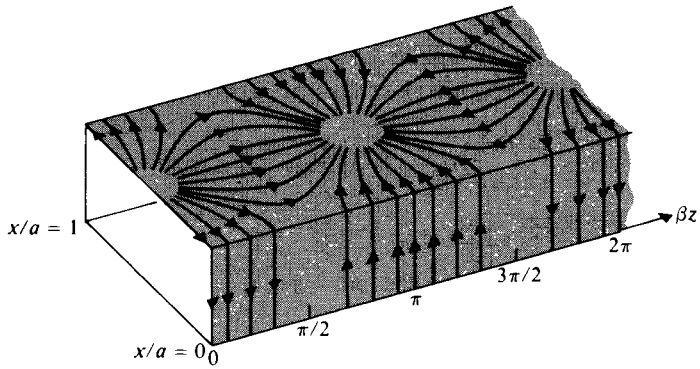

FIGURE 10–13
Surface currents on guide walls for TE_{10} mode in rectangular waveguide.

The sketch in an xz-plane will show all three nonzero field components—E_y, H_x, and H_z. The slope of the **H** lines at $t = 0$ is governed by the following equation:

$$\left(\frac{dx}{dz}\right)_{\mathrm{H}} = \frac{\beta}{h^2}\left(\frac{\pi}{a}\right)\tan\left(\frac{\pi}{a}x\right)\tan\beta z, \tag{10–172}$$

which can be used to draw the **H** lines in Fig. 10–12(c). These lines are independent of y.

c) The surface current density on guide walls, $\mathbf{J}_s$, is related to the magnetic field intensity by Eq. (7–66b):

$$\mathbf{J}_s = \mathbf{a}_n \times \mathbf{H}, \tag{10–173}$$

where $\mathbf{a}_n$ is the *outward* normal from the wall surface and **H** is the magnetic field intensity at the wall. We have, at $t = 0$,

$$\mathbf{J}_s(x = 0) = -\mathbf{a}_y H_z(0, y, z; 0) = -\mathbf{a}_y H_0 \cos\beta z, \tag{10–174}$$

$$\mathbf{J}_s(x = a) = \mathbf{a}_y H_z(a, y, z; 0) = \mathbf{J}_s(x = 0), \tag{10–175}$$

$$\begin{aligned}\mathbf{J}_s(y = 0) &= \mathbf{a}_x H_z(x, 0, z; 0) - \mathbf{a}_z H_x(x, 0, z; 0)\\ &= \mathbf{a}_x H_0 \cos\left(\frac{\pi}{a}x\right)\cos\beta z - \mathbf{a}_z \frac{\beta}{h^2}\left(\frac{\pi}{a}\right)H_0 \sin\left(\frac{\pi}{a}x\right)\sin\beta z,\end{aligned} \tag{10–176}$$

$$\mathbf{J}_s(y = b) = -\mathbf{J}_s(y = 0). \tag{10–177}$$

The surface currents on the inside walls at $x = 0$ and at $y = b$ are sketched in Fig. 10–13. ■

EXAMPLE 10–9 Standard air-filled waveguides have been designed for the radar bands listed in Subsection 7–7.4. One type, designated WG-16, is suitable for X-band applications. Its dimensions are: $a = 2.29$ cm (0.90 in.) and $b = 1.02$ cm (0.40 in.). If it is desired that a WG-16 waveguide operate only in the dominant TE_{10} mode and

that the operating frequency be at least 25% above the cutoff frequency of the TE_{10} mode but no higher than 95% of the next higher cutoff frequency, what is the allowable operating-frequency range?

Solution For $a = 2.29 \times 10^{-2}$ (m) and $b = 1.02 \times 10^{-2}$ (m), the two modes having the lowest cutoff frequencies are TE_{10} and TE_{20}. Using Eq. (10–139), we find

$$(f_c)_{10} = \frac{c}{2a} = \frac{3 \times 10^8}{2 \times 2.29 \times 10^{-2}} = 6.55 \times 10^9 \quad \text{(Hz)},$$

$$(f_c)_{20} = \frac{c}{a} = 13.10 \times 10^9 \quad \text{(Hz)}.^{\dagger}$$

Thus the allowable operating-frequency range under the specified conditions is

$$1.25(f_c)_{TE_{10}} \leq f \leq 0.95(f_c)_{TE_{20}}$$

or

$$8.19 \quad \text{(GHz)} \leq f \leq 12.45 \quad \text{(GHz)}. \qquad \blacksquare$$

10–4.3 ATTENUATION IN RECTANGULAR WAVEGUIDES

Attenuation for propagating modes results when there are losses in the dielectric and in the imperfectly conducting guide walls. Because these losses are usually very small, we will assume, as in the case of parallel-plate waveguides, that the transverse field patterns are not appreciably affected by the losses. The attenuation constant due to losses in the dielectric can be obtained by substituting $\epsilon_d = \epsilon + (\sigma/j\omega)$ for ϵ in Eq. (10–138). The result is exactly the same as that given in Eq. (10–110), which is repeated below:

$$\alpha_d = \frac{\sigma\eta}{2\sqrt{1 - (f_c/f)^2}}, \tag{10–178}$$

where σ and η are the equivalent conductivity (see Eq. 7–112) and intrinsic impedance of the dielectric medium, respectively, and f_c is given by Eq. (10–139). It is easy to see from Eq. (10–178) that the attenuation constant of propagating waves due to losses in the dielectric decreases monotonically from an infinitely large value toward the value $\sigma\eta/2$ as the frequency increases from the cutoff frequency.

To determine the attenuation constant due to wall losses, we make use of Eq. (10–112). The derivations of α_c for the general TM_{mn} and TE_{mn} modes tend to be tedious. Below we obtain the formula for the dominant TE_{10} mode, which is the most important of all propagating modes in a rectangular waveguide.

For the TE_{10} mode the only nonzero field components are E_y, H_x, and H_z. Letting $m = 1$, $n = 0$, and $h = (\pi/a)$ in Eqs. (10–160) and (10–161), we calculate the

---

† Note that $(f_c)_{01} = (c/2b) > (f_c)_{20}$ and $(f_c)_{11} = (c/2a)\sqrt{1 + (a/b)^2} > (f_c)_{20}$.

time-average power flowing through a cross section of the waveguide:

$$\begin{aligned} P(z) &= \int_0^b \int_0^a -\tfrac{1}{2}(E_y^0)(H_x^0)^* \, dx\, dy \\ &= \frac{1}{2}\omega\mu\beta\left(\frac{a}{\pi}\right)^2 H_0^2 \int_0^b \int_0^a \sin^2\left(\frac{\pi}{a}x\right) dx\, dy \\ &= \omega\mu\beta ab\left(\frac{aH_0}{2\pi}\right)^2. \end{aligned} \tag{10-179}$$

In order to calculate the time-average power lost in the conducting walls per unit length, we must consider all four walls. From Eqs. (10–173), (10–158), and (10–161) we see that

$$\mathbf{J}_s^0(x=0) = \mathbf{J}_s^0(x=a) = -\mathbf{a}_y H_z^0(x=0) = -\mathbf{a}_y H_0 \tag{10-180}$$

and

$$\begin{aligned} \mathbf{J}_s^0(y=0) = -\mathbf{J}_s^0(y=b) &= \mathbf{a}_x H_z^0(y=0) - \mathbf{a}_z H_x^0(y=0) \\ &= \mathbf{a}_x H_0 \cos\left(\frac{\pi}{a}x\right) - \mathbf{a}_z \frac{\beta a}{\pi} H_0 \sin\left(\frac{\pi}{a}x\right). \end{aligned} \tag{10-181}$$

The total power loss is then double the sum off the losses in the walls at $x = 0$ and at $y = 0$. We have

$$P_L(z) = 2[P_L(z)]_{x=0} + 2[P_L(z)]_{y=0}, \tag{10-182}$$

where

$$[P_L(z)]_{x=0} = \int_0^b \frac{1}{2}|J_s^0(x=0)|^2 R_s \, dy = \frac{b}{2} H_0^2 R_s \tag{10-183}$$

and

$$\begin{aligned} [P_L(z)]_{y=0} &= \int_0^a \frac{1}{2}\left[|J_{sx}^0(y=0)|^2 + |J_{sz}^0(y=0)|^2\right] R_s \, dx \\ &= \frac{a}{4}\left[1 + \left(\frac{\beta a}{\pi}\right)^2\right] H_0^2 R_s. \end{aligned} \tag{10-184}$$

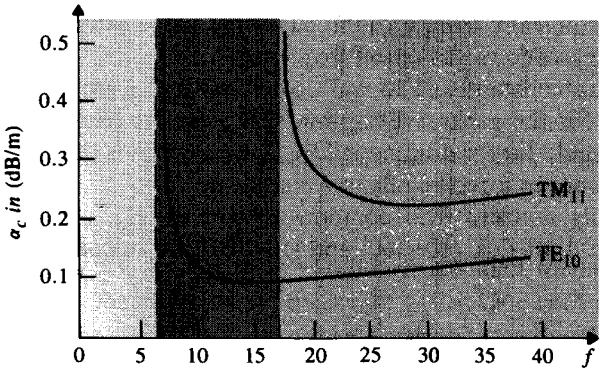

FIGURE 10–14
Attenuation due to wall losses in rectangular copper waveguide for TE_{10} and TM_{11} modes. $a = 2.29$ (cm), $b = 1.02$ (cm).

Substitution of Eqs. (10–183) and (10–184) in Eq. (10–182) yields

$$P_L(z) = \left\{ b + \frac{a}{2}\left[1 + \left(\frac{\beta a}{\pi}\right)^2 \right] \right\} H_0^2 R_s$$
$$= \left[b + \frac{a}{2}\left(\frac{f}{f_c}\right)^2 \right] H_0^2 R_s. \tag{10–185}$$

The last expression is the result of recognizing that

$$\beta = \sqrt{\omega^2 \mu\epsilon - \left(\frac{\pi}{a}\right)^2} = \omega\sqrt{\mu\epsilon}\sqrt{1 - \left(\frac{f_c}{f}\right)^2}. \tag{10–186}$$

Inserting Eqs. (10–179) and (10–185) in Eq. (10–112), we obtain

$$\boxed{(\alpha_c)_{\mathrm{TE}_{10}} = \frac{R_s[1 + (2b/a)(f_c/f)^2]}{\eta b\sqrt{1 - (f_c/f)^2}} = \frac{1}{\eta b}\sqrt{\frac{\pi f \mu_c}{\sigma_c[1 - (f_c/f)^2]}}\left[1 + \frac{2b}{a}\left(\frac{f_c}{f}\right)^2 \right] \quad \text{(Np/m)}.} \tag{10–187}$$

Equation (10–187) reveals a rather complicated dependence of $(\alpha_c)_{\mathrm{TE}_{10}}$ on the ratio (f_c/f). It tends to infinity when f is close to the cutoff frequency, decreases toward a minimum as f increases, and increases again steadily for further increases in f.

For a given guide width a, the attenuation decreases as b increases. However, increasing b also decreases the cutoff frequency of the next higher-order mode TE_{11} (or TM_{11}), with the consequence that the available bandwidth for the dominant TE_{10} mode (the range of frequencies over which TE_{10} is the only possible propagating mode) is reduced. The usual compromise is to choose the ratio b/a in the neighborhood of $\frac{1}{2}$.

If we follow a similar procedure that led to Eq. (10–187), the attenuation constant due to wall losses for TM modes can be derived. For the TM_{11} mode we obtain

$$(\alpha_c)_{\mathrm{TM}_{11}} = \frac{2R_s(b/a^2 + a/b^2)}{\eta ab\sqrt{1 - (f_c/f)^2}(1/a^2 + 1/b^2)}. \tag{10–188}$$

In Fig. 10–14 are plotted the graphs of $(\alpha_c)_{\mathrm{TE}_{10}}$ and $(\alpha_c)_{\mathrm{TM}_{11}}$ for a standard air-filled WR-16 rectangular copper waveguide with $a = 2.29$ (cm) and $b = 1.02$ (cm). From Eq. (10–139) we find $(f_c)_{10} = 6.55$ (GHz) and $(f_c)_{11} = 16.10$ (GHz). The curves show that the attenuation constant increases rapidly toward infinity as the operating frequency approaches the cutoff frequency. In the operating range ($f > f_c$), both curves possess a broad minimum. The attenuation constant of the TE_{10} mode is everywhere lower than that of the TM_{11} mode. These facts have direct relevance in the choice of operating modes and frequencies.

EXAMPLE 10–10 A TE_{10} wave at 10 (GHz) propagates in a brass—$\sigma_c = 1.57 \times 10^7$ (S/m)—rectangular waveguide with inner dimensions $a = 1.5$ (cm) and $b = 0.6$ (cm), which is filled with polyethylene—$\epsilon_r = 2.25$, $\mu_r = 1$, loss tangent $= 4 \times 10^{-4}$. Determine (a) the phase constant, (b) the guide wavelength, (c) the phase velocity, (d) the wave impedance, (e) the attenuation constant due to loss in the dielectric, and (f) the attenuation constant due to loss in the guide walls.

Solution At $f = 10^{10}$ (Hz) the wavelength in *unbounded* polyethylene is

$$\lambda = \frac{u}{f} = \frac{3 \times 10^8}{\sqrt{2.25} \times 10^{10}} = \frac{2 \times 10^8}{10^{10}} = 0.02 \quad \text{(m)}.$$

The cutoff frequency for the TE_{10} mode is, from Eq. (10–163),

$$f_c = \frac{u}{2a} = \frac{2 \times 10^8}{2 \times (1.5 \times 10^{-2})} = 0.667 \times 10^{10} \quad \text{(Hz)}.$$

a) The phase contant is, from Eq. (10–186),

$$\beta = \frac{\omega}{u}\sqrt{1 - \left(\frac{f_c}{f}\right)^2} = \frac{2\pi 10^{10}}{2 \times 10^8}\sqrt{1 - 0.667^2}$$
$$= 74.5\pi = 234 \quad \text{(rad/m)}.$$

b) The guide wavelength is, from Eq. (10–39),

$$\lambda_g = \frac{\lambda}{\sqrt{1 - (f_c/f)^2}} = \frac{0.02}{0.745} = 0.0268 \quad \text{(m)}.$$

c) The phase velocity is, from Eq. (10–42),

$$u_p = \frac{u}{\sqrt{1 - (f_c/f)^2}} = \frac{2 \times 10^8}{0.745} = 2.68 \times 10^8 \quad \text{(m/s)}.$$

d) The wave impedance is, from Eq. (10–57),

$$(Z_{TE})_{10} = \frac{\sqrt{\mu/\epsilon}}{\sqrt{1 - (f_c/f)^2}} = \frac{377/\sqrt{2.25}}{0.745} = 337.4 \quad (\Omega).$$

e) The attenuation constant due to loss in dielectric is obtained from Eq. (10–178). The effective conductivity for polyethylene at 10 (GHz) can be determined from the given loss tangent by using Eq. (7–115):

$$\sigma = 4 \times 10^{-4}\omega\epsilon = 4 \times 10^{-4} \times (2\pi \times 10^{10}) \times \left(\frac{2.25}{36\pi} \times 10^{-9}\right)$$
$$= 5 \times 10^{-4} \quad \text{(S/m)}.$$

Thus,

$$\alpha_d = \frac{\sigma}{2} Z_{TE} = \frac{5 \times 10^{-4}}{2} \times 337.4 = 0.084 \quad \text{(Np/m)}$$
$$= 0.73 \quad \text{(dB/m)}.$$

f) The attenuation constant due to loss in the guide walls is found from Eq. (10–187). We have, from Eq. (9–26b),

$$R_s = \sqrt{\frac{\pi f \mu_c}{\sigma_c}} = \sqrt{\frac{\pi 10^{10}(4\pi 10^{-7})}{1.57 \times 10^7}} = 0.0501 \quad (\Omega),$$

$$\alpha_c = \frac{R_s[1 + (2b/a)(f_c/f)^2]}{\eta b\sqrt{1 - (f_c/f)^2}} = \frac{0.0501[1 + (1.2/1.5)(0.667)^2]}{251 \times 0.006 \times 0.745} = 0.0605 \quad (\text{Np/m})$$

$$= 0.526 \quad (\text{dB/m}). \blacksquare$$

10–4.4 DISCONTINUITIES IN RECTANGULAR WAVEGUIDES

Just as in the case of transmission lines, it is desirable to have impedance match for wave propagation in waveguides in order to achieve maximum power transfer and to reduce local power loss due to a high standing-wave ratio. There is a need to introduce shunt susceptances at appropriate points along a waveguide. These shunt susceptances often take the form of a thin metal diaphragm with an iris such as those shown in Figs. 10–15(a) and 10–15(b). When a diaphragm with an iris is in place, the electric and magnetic fields must satisfy the additional boundary conditions on the metal surface. If the waveguide operates in the dominant TE_{10} mode, the additional boundary conditions require the presence of all higher-order modes, and the situation is vastly more complicated. However, the waveguide is usually designed so that only the dominant mode can propagate. The higher-order modes are then all cutoff modes; they are evanescent and are localized near the iris. An analytical determination of the effective shunt susceptance of an iris would necessitate the solution

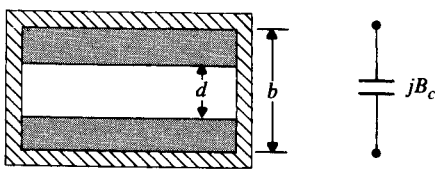

(a) Capacitive iris and equivalent susceptance

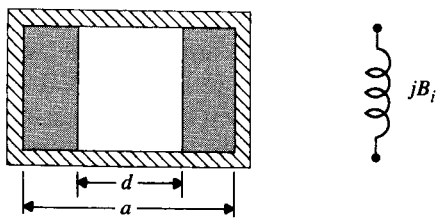

(b) Inductive iris and equivalent susceptance.

FIGURE 10–15
Irises in waveguide as susceptances.

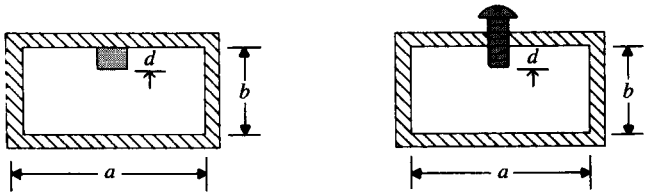

(a) A protruding post. (b) A tuning screw.

FIGURE 10–16
Post or screw in a waveguide.

of a difficult electromagnetics problem. We will offer only a qualitative discussion here and give the approximate formulas† for the irises in Figs. 10–15(a) and 10–15(b).

The iris in Fig. 10–15(a) is made of thin conducting diaphragms extending from one narrow wall to the other. As seen in Fig. 10–12(a), the electric field lines of the dominant TE_{10} mode in a cross section are in the y-direction, going across the narrow dimension. Reducing this dimension from b to d may be expected to have the effect of increasing this field as well as the stored electric energy locally. Consequently, the equivalent shunt susceptance is expected to be capacitive. An approximate expression for the normalized capacitive susceptance is

$$b_c = \frac{B_c}{Y_{10}} = \frac{4b}{\lambda_g} \ln\left[\csc\left(\frac{\pi d}{2b}\right)\right], \tag{10–189}$$

where Y_{10} is the reciprocal of $Z_{TE_{10}}$ from Eq. (10–57) and λ_g is the guide wavelength given in Eq. (10–39). As we have indicated before, the actual situation is much more complicated, owing to the presence of the evanescent higher-order modes near the iris. A more accurate analysis will show that b_c is not strictly proportional to (b/λ_g). The approximate formula in Eq. (10–189) is accurate to within 5% in the normal range of operating frequencies.

The iris in Fig. 10–15(b) provides additional current paths through the conducting diaphragms in the y-direction, causing new longitudinal magnetic field to exist in the iris opening and increasing the stored mangetic energy locally. Hence the equivalent shunt susceptance is expected to be inductive. An approximate expression for the normalized inductive susceptance of the iris is

$$b_i = \frac{B_i}{Y_{10}} = -\frac{\lambda_g}{a} \cot^2\left(\frac{\pi d}{2a}\right). \tag{10–190}$$

Another type of discontinuity that provides a shunt susceptance is a conducting post protruding into the waveguide on a broad face, as in Fig. 10–16(a). If the post length d is small, the shunt susceptance is capacitive. When d becomes an appreciable fraction of b, considerable current can flow along the post, causing an inductive effect. A resonance occurs when d is in the neighborhood of $(3/4)b$. Still longer d will result

† For more details, see R. E. Collin, *Field Theory of Guided Waves*, McGraw-Hill, New York, 1960, Chapter 8; C. C. Johnson, *Field and Wave Electrodynamics*, McGraw-Hill, New York, 1965, Chapter 5.

in an inductive susceptance. In practical usage the post usually takes the form of a metal screw, as shown in Fig. 10–16(b). The screw could be inserted in a slit cut axially in the center of the broad face. The center slit does not appreciably disturb the field pattern in the waveguide, and the sliding screw with a variable d can be used for tuning and matching a given load to the waveguide. This is a technique similar to the single-stub matching scheme discussed in Subsection 9–7.2.

EXAMPLE 10–11 Measurements on a WG-10 S-band waveguide ($a = 7.21$ cm, $b = 3.40$ cm) feeding a horn antenna show a standing-wave ratio (SWR) of 2.00 at the 3 (GHz) operating frequency, and the existence of a maximum electric field at 12 (cm) from the neck of the horn. Find the location and the dimensions of a symmetrical inductive iris necessary to achieve a perfect match. Assume the waveguide to be lossless.

Solution With $a = 7.21 \times 10^{-2}$ (m) and $b = 3.40 \times 10^{-2}$ (m), the cutoff frequency for the dominant TE_{10} mode is

$$f_c = \frac{c}{2a}$$

$$= \frac{3 \times 10^8}{2 \times 7.21 \times 10^{-2}} = 2.08 \times 10^9 \quad \text{(Hz)}.$$

The guide wavelength is, from Eq. (10–39),

$$\lambda_g = \frac{\lambda}{\sqrt{1 - (f_c/f)^2}} = \frac{c}{\sqrt{f^2 - f_c^2}}$$

$$= \frac{3 \times 10^8}{10^9\sqrt{3^2 - 2.08^2}} = 0.139 \text{ (m)} = 13.9 \quad \text{(cm)}.$$

Thus, the measured maximum of the electric field is at a distance $12/13.9 = 0.863\lambda_g$ from the neck of the horn. At that location the normalized effective load resistance is (see Eq. 9–145)

$$r_L = \frac{R_L}{R_0} = S.$$

The corresponding normalized conductance is

$$g_L = \frac{Y_L}{Y_0} = \frac{1}{S}$$

$$= \frac{1}{2.00} = 0.50.$$

The rest of the problem is that of single-stub matching discussed in Subsection 9–7.2. We use the Smith admittance chart and proceed as follows (see Fig. 10–17):

1. Enter $g_L = 0.50$ on an Smith admittance chart as P_M (point of maximum electric field).

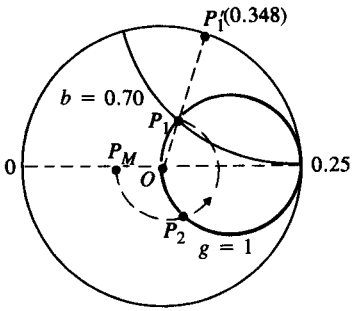

FIGURE 10–17
Construction on Smith admittance chart (Example 10–11).

2. Draw a $|\Gamma|$-circle centered at O with radius $\overline{OP}_M$, intersecting the $g = 1$ circle at two points, P_1 and P_2. Read

$$\text{at } P_1: \quad y_1 = 1 + j0.70,$$
$$\text{at } P_2: \quad y_2 = 1 - j0.70.$$

Point P_2 is not useful to us because it requires a capacitive (positive) susceptance to achieve matching.

3. Draw a straight line from O through P_1 to point P_1' on the perimeter. Read 0.348 on the "wavelength toward load" scale at P_1'. This is $(0.863 - 0.348)\lambda_g = 7.16$ (cm) from the neck of the horn and is where an inductive iris of a normalized susceptance -0.70 should be placed.

4. Using Eq. (10–190), we determine the distance d of the required inductive iris shown in Fig. 10–15(b):

$$-0.70 = -\frac{13.9}{7.21}\cot^2\left(\frac{\pi d}{2 \times 7.21}\right),$$

from which we find $d = 4.72$ (cm). ■

10–5 Circular Waveguides

Electromagnetic waves can also propagate inside round metal pipes. In this section we will study wave behaviors in circular waveguides—metal pipes having a uniform circular cross section and filled with a dielectric medium.

The basic equations to be satisfied by time-harmonic electric and magnetic field intensities in the charge-free dielectric region inside a waveguide are Eqs. (10–3) and (10–4), which are repeated below:

$$\nabla^2\mathbf{E} + k^2\mathbf{E} = 0 \tag{10–191}$$

and

$$\nabla^2\mathbf{H} + k^2\mathbf{H} = 0. \tag{10–192}$$

For a straight waveguide with a uniform circular cross section and having its axis in the z-direction, it is expedient to decompose the three-dimensional Laplacian op-

erator ∇^2 into two parts: $\nabla^2_{r\phi}$ for the transverse coordinates, and ∇^2_z for the longitudinal z-component. Similarly, both $\mathbf{E}$ and $\mathbf{H}$ vectors can be written as the sum of a transverse component and an axial component:

$$\mathbf{E} = \mathbf{E}_T + \mathbf{a}_z E_z \tag{10–193}$$

and

$$\mathbf{H} = \mathbf{H}_T + \mathbf{a}_z H_z, \tag{10–194}$$

where the subscript T denotes the two-dimensional transverse component. We already know from Subsection 10–2.1 that TEM waves cannot exist in such a waveguide without an inner conductor. The propagating waves can be classified into two groups, as in rectangular waveguides: transverse magnetic (TM) and transverse electric (TE). For TM waves, $H_z = 0$, $E_z \neq 0$, and all field components can be expressed in terms of $E_z = E_z^0 e^{-\gamma z}$, where E_z^0 satisfies the homogeneous Helmholtz's equation

$$\nabla^2_{r\phi} E_z^0 + (\gamma^2 + k^2) E_z^0 = 0 \tag{10–195}$$

or

$$\nabla^2_{r\phi} E_z^0 + h^2 E_z^0 = 0. \tag{10–196}$$

For TE waves, $E_z = 0$, $H_z \neq 0$, and all field components can be expressed in terms of $H_z = H_z^0 e^{-\gamma z}$, where H_z^0 satisfies exactly the same homogeneous Helmholtz's equation required of E_z^0 above.

Although Eq. (10–196) is similar in form to Eq. (10–24), their solutions are quite different. We will consider the solution of Eq. (10–196) in the following subsection.

10–5.1 BESSEL'S DIFFERENTIAL EQUATION AND BESSEL FUNCTIONS

In cylindrical coordinates the expansion of Eq. (10–196) gives (see Eq. 4–8)

$$\frac{1}{r}\frac{\partial}{\partial r}\left(r\frac{\partial E_z^0}{\partial r}\right) + \frac{1}{r^2}\frac{\partial^2 E_z^0}{\partial \phi^2} + h^2 E_z^0 = 0. \tag{10–197}$$

To solve Eq. (10–197), we apply the method of separation of variables by assuming a product solution.

$$E_z^0(r, \phi) = R(r)\Phi(\phi), \tag{10–198}$$

where $R(r)$ and $\Phi(\phi)$ are functions only of r and ϕ, respectively. Substituting solution (10–198) in Eq. (10–197) and dividing by the product $R(r)\Phi(\phi)$, we obtain

$$\frac{r}{R(r)}\frac{d}{dr}\left[r\frac{dR(r)}{dr}\right] + h^2 r^2 = -\frac{1}{\Phi(\phi)}\frac{d^2\Phi(\phi)}{d\phi^2}. \tag{10–199}$$

Now the left side of Eq. (10–199) is a function of r only, and the right side is a function of ϕ only. For Eq. (10–199) to hold for all values of r and ϕ, both sides must be equal to the same constant. Let this constant (separation constant) be n^2. We can separate Eq. (10–199) into two ordinary differential equations:

$$\frac{d^2\Phi(\phi)}{d\phi^2} + n^2\Phi(\phi) = 0 \tag{10–200}$$

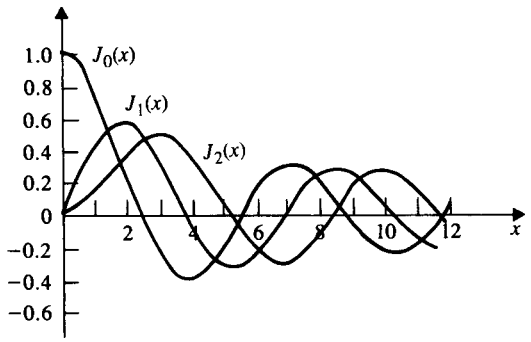

FIGURE 10–18
Bessel functions of the first kind.

and

$$\frac{r}{R(r)}\frac{d}{dr}\left[r\frac{dR(r)}{dr}\right] + h^2r^2 = n^2$$

or

$$\boxed{\frac{d^2R(r)}{dr^2} + \frac{1}{r}\frac{dR(r)}{dr} + \left(h^2 - \frac{n^2}{r^2}\right)R(r) = 0.} \tag{10–201}$$

Equation (10–201) is known as ***Bessel's differential equation.***

A solution of Eq. (10–201) can be obtained by assuming $R(r)$ to be a power series in r with unknown coefficients,

$$R(r) = \sum_{p=0}^{\infty} C_p(hr)^p, \tag{10–202}$$

substituting it into the equation, and equating the sum of the coefficients of each power of r to zero. The actual work is tedious.† The result is

$$R(r) = C_nJ_n(hr), \tag{10–203}$$

where C_n is an arbitrary constant, and

$$J_n(hr) = \sum_{m=0}^{\infty} \frac{(-1)^m(hr)^{n+2m}}{m!(n+m)!2^{n+2m}} \tag{10–204}$$

is called the ***Bessel function of the first kind*** of nth order with an argument hr. Equation (10–204) holds only for *integral values of n*, which is true for cases of our interest, as we shall see later. $J_n(x)$ versus x curves of the first few orders have been plotted in Fig. 10–18. Several things are worth noting. First, $J_n(0) = 0$ for all n except when $n = 0$; for the zeroth order, $J_0(0) = 1$. Second, $J_n(x)$ are alternating functions

† N. W. MaLachlan, *Bessel Functions for Engineers*, 2d ed, Oxford University Press, New York, 1946.

TABLE 10–2
Zeros of $J_n(x)$, x_{np}

p \ n	$n = 0$	$n = 1$	$n = 2$
1	2.405	3.832	5.136
2	5.520	7.016	8.417

of decreasing amplitudes that cross the zero level at progressively shorter intervals. As x becomes very large, all $J_n(x)$ approach a sinusoidal form. Table 10–2 lists the values of the first several x_{np}, which denotes the pth zero of $J_n(x)$: $J_n(x_{np}) = 0$. In the next subsection we will find that the values of x_{np} determine the eigenvalues of TM modes in a circular waveguide. The eigenvalues of TE modes, on the other hand, depend on the zeros of the derivative of Bessel functions of the first kind—that is, on the values of x'_{np}, which make $J'_n(x'_{np}) = 0$ (see Subsection 10–5.3). The values of the first several x'_{np} are tabulated in Table 10–3.

So far, we have obtained only one solution—Bessel function of the first kind, $J_n(hr)$—for the Bessel's differential equation (10–201). But Bessel's equation is a second-order equation; there should be two linearly independent solutions for each value of n. In other words, there should be another solution that is not linearly dependent on $J_n(hr)$. Such a solution exists. It is called ***Bessel function of the second kind*** or ***Neumann function*** and is usually denoted by $N_n(hr)$:

$$N_n(hr) = \frac{(\cos n\pi)J_n(hr) - J_{-n}(hr)}{\sin n\pi}. \tag{10–205}$$

The general solution of Eq. (10–201) can then be written as

$$R(r) = C_n J_n(hr) + D_n N_n(hr), \tag{10–206}$$

where C_n and D_n are arbitrary constants to be determined from boundary conditions.

A distinctive property of Bessel function of the second kind of all orders is that they become infinite when the argument is zero. When we study wave propagation in a circular waveguide, our region of interest includes the axis where $r = 0$. Since an infinite field is a physical impossibility, the solution $R(r)$ in Eq. (10–206) cannot contain a $N_n(hr)$ term. This means that the coefficient D_n must be zero for all n. Thus,

TABLE 10–3
Zeros of $J'_n(x)$, x'_{np}

p \ n	$n = 0$	$n = 1$	$n = 2$
1	3.832	1.841	3.054
2	7.016	5.331	6.706

for wave-mode problems inside a circular waveguide there is no need to be concerned with the $N_n(hr)$ term.

In the study of circular waveguides that follows, the preceding short summary of Bessel's differential equation and Bessel functions should suffice. The rest of this subsection discusses some additional aspects for completeness. It may be skipped if the material on dielectric-rod waveguides in Subsection 10–6.3 is to be omitted.

In case the region of interest of a problem in cylindrical coordinates does not include the axis where $r = 0$ (such as the problem of a coaxial waveguide with an inner conductor), the radial solution $R(r)$ in Eq. (10–206) must consist of both $J_n(hr)$ and $N_n(hr)$ terms, and the coefficients C_n and D_n are to be determined from boundary conditions. Furthermore, if a problem does not involve the entire 2π range of ϕ (such as the problem of a wedge-shaped waveguide), the constant n in Eq. (10–200) will not be an integer. Let it be denoted by ν. We write the solution of the Bessel's differential equation as

$$R(r) = CJ_\nu(hr) + DN_\nu(hr). \tag{10–207}^\dagger$$

In some wave problems it is convenient to define linear combinations of the Bessel functions:

$$H_\nu^{(1)}(hr) = J_\nu(hr) + jN_\nu(hr), \tag{10–208}$$

$$H_\nu^{(2)}(hr) = J_\nu(hr) - jN_\nu(hr), \tag{10–209}$$

where $H_\nu^{(1)}$ and $H_\nu^{(2)}$ are called ***Hankel functions*** of the first and second kind, respectively. When the argument hr is very large, the asymptotic expressions for $H_\nu^{(1)}$ and $H_\nu^{(2)}$ are

$$H_\nu^{(1)}(hr) \to \sqrt{\frac{2}{\pi hr}}\, e^{j(hr - \pi/4 - \nu\pi/2)}, \tag{10–210}$$

$$H_\nu^{(2)}(hr) \to \sqrt{\frac{2}{\pi hr}}\, e^{-j(hr - \pi/4 - \nu\pi/2)}. \tag{10–211}$$

These expressions with imaginary exponential coefficients and decreasing amplitudes place in evidence the wave character of the Hankel functions. They are useful in problems of radiation.

When h^2 is negative ($h = j\zeta$), two other functions $I_\nu(\zeta)$ and $K_\nu(\zeta)$, related to J_ν and $H_\nu^{(1)}$, respectively, are defined:

$$I_\nu(\zeta r) = j^{-\nu} J_\nu(j\zeta r), \tag{10–212}$$

$$K_\nu(\zeta r) = \frac{\pi}{2} j^{\nu+1} H_\nu^{(1)}(j\zeta r). \tag{10–213}$$

---

† The expression for $J_\nu(hr)$ for a nonintegral ν is that given in Eq. (10–204) with $(n + m)!$ replaced by the gamma function $\Gamma(\nu + m + 1)$.

I_ν and K_ν are called ***modified Bessel functions*** of the first and second kind, respectively. For large arguments the following asymptotic expressions are obtained:

$$I_\nu(\zeta r) \to \sqrt{\frac{1}{2\pi\zeta r}}\, e^{\zeta r}, \tag{10–214}$$

$$K_\nu(\zeta r) \to \sqrt{\frac{\pi}{2\zeta r}}\, e^{-\zeta r}. \tag{10–215}$$

It is seen that at large r, $K_\nu(\zeta r)$ shows an exponential decay with distance, characteristic of an evenescent wave. It is useful in surface-wave problems such as dielectric-rod waveguides and optical fibers. The choice of the appropriate form as a solution for the Bessel's differential equation depends on the type of the problem and on convenience.

10–5.2 TM WAVES IN CIRCULAR WAVEGUIDES

Figure 10–19 shows a circular waveguide of radius a. It consists of a metal pipe centered around the z-axis. The enclosed dielectric medium is assumed to have constitutive parameters ϵ and μ. For TM waves, $H_z = 0$. We write

$$E_z(r, \phi, z) = E_z^0(r, \phi)e^{-\gamma z}, \tag{10–216}$$

where $E_z^0(r, \phi)$ satisfies Eq. (10–196). The solution is written in the form of Eq. (10–198), in which

$$R(r) = C_n J_n(hr), \tag{10–217}$$

and $\Phi(\phi)$ is the solution of Eq. (10–200). Since all field components are periodic with respect to ϕ (period $= 2\pi$), the only admissible solution for Eq. (10–200) is $\sin n\phi$ or $\cos n\phi$, or a linear combination of the two (see Table 4–1). It is because of this requirement of periodicity that we demand n to be an integer, as indicated previously. Whether $\sin n\phi$ or $\cos n\phi$ is chosen is immaterial; it changes only the location of the

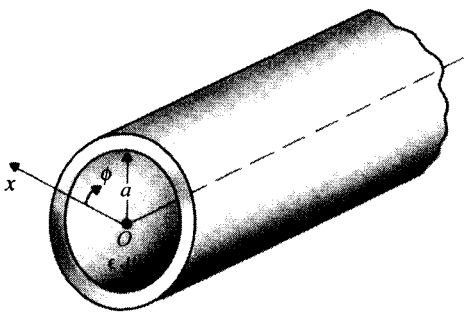

FIGURE 10–19
A circular waveguide.

reference $\phi = 0$ angle. Customarily, we write $E_z^0(r, \phi)$ for TM modes as

$$\boxed{E_z^0 = C_n J_n(hr) \cos n\phi. \qquad \text{(TM modes)}} \tag{10-218}$$

The transverse components E_r^0 and E_ϕ^0 can be found from an adaptation of Eq. (10–29) to the cross-sectional polar coordinates (Problem P.10–26):

$$(\mathbf{E}_T^0)_{\text{TM}} = \mathbf{a}_r E_r^0 + \mathbf{a}_\phi E_\phi^0 = -\frac{\gamma}{h^2} \nabla_T E_z^0, \tag{10-219}$$

where

$$\nabla_T E_z^0 = \left(\mathbf{a}_r \frac{\partial}{\partial r} + \mathbf{a}_\phi \frac{\partial}{r \partial \phi} \right) E_z^0. \tag{10-220}$$

The magnetic field components can then be obtained by using Eq. (10–32).

We have for TM modes, in addition to E_z^0 in Eq. (10–218),

$$E_r^0 = -\frac{j\beta}{h} C_n J_n'(hr) \cos n\phi, \tag{10-221}$$

$$E_\phi^0 = \frac{j\beta n}{h^2 r} C_n J_n(hr) \sin n\phi, \tag{10-222}$$

$$H_r^0 = -\frac{j\omega\epsilon n}{h^2 r} C_n J_n(hr) \sin n\phi, \tag{10-223}$$

$$H_\phi^0 = -\frac{j\omega\epsilon}{h} C_n J_n'(hr) \cos n\phi, \tag{10-224}$$

$$H_z^0 = 0, \tag{10-225}$$

where γ has been replaced by $j\beta$, J_n' is the derivative of J_n with respect to its argument (hr), and the coefficient C_n depends on the field strength of the excitation.

The eigenvalues of TM modes (the admissible values of h) are determined from the boundary condition that E_z^0 must vanish at $r = a$; that is,

$$\boxed{J_n(ha) = 0. \qquad \text{(TM modes)}} \tag{10-226}$$

There are infinitely many zeros of $J_n(x)$, the first several of which have been tabulated in Table 10–2. The cutoff frequency is given by Eq. (10–35) as before. Hence the eigenvalue for the TM_{01} mode that corresponds to the first zero ($x_{01} = 2.405$) of $J_0(x)$ is

$$(h)_{\text{TM}_{01}} = \frac{2.405}{a}, \tag{10-227}$$

which yields the lowest cutoff frequency for a TM mode:

$$(f_c)_{\text{TM}_{01}} = \frac{(h)_{\text{TM}_{01}}}{2\pi\sqrt{\mu\epsilon}} = \frac{0.383}{a\sqrt{\mu\epsilon}}. \tag{10-228}$$

The phase constant β and the guide wavelength λ_g can be found from Eqs. (10–38) and (10–39), respectively.

For the TM_{01} mode ($n = 0$), E_z^0, E_r^0, and H_ϕ^0 are the only nonzero field components. A sketch of the electric and magnetic field lines in a typical transverse plane is given in Fig. 10–20. According to Eq. (10–224), H_ϕ^0 varies with r as $J_0'(hr)$, which equals $-J_1(hr)$. Thus the density of the magnetic field lines increases from $r = 0$ to $r = a$.

Note that in rectangular waveguides the first and second numbers of the mode index denote the number of half-wave field variations in the x- and y-directions, respectively, in a transverse xy-plane. By convention *the first number of the mode index for circular waveguides always represents the number of half-wave field variations in the ϕ-direction*, and the second number represents the number of half-wave field variations in the r-direction. Hence the transverse field pattern of the TM_{01} mode in a circular waveguide is analogous to the TM_{11} mode (instead of the TM_{01} mode, which does not exist) in a rectangular waveguide.

10–5.3 TE WAVES IN CIRCULAR WAVEGUIDES

For TE modes, $E_z = 0$, and

$$H_z(r, \phi, z) = H_z^0(r, \phi)e^{-\gamma z}, \tag{10–229}$$

where H_z^0 satisfies the homogeneous Helmholtz's equation

$$\nabla_{r\phi}^2 H_z^0 + h^2 H_z^0 = 0. \tag{10–230}$$

Analogously to the TM case, we write the solution as

$$\boxed{H_z^0 = C_n' J_n(hr) \cos n\phi. \qquad \text{(TE modes)}} \tag{10–231}$$

From H_z^0 we find the transverse magnetic field components H_r^0 and H_ϕ^0 by using Eq. (10–53), and we find the electric field components E_r^0 and E_ϕ^0 by applying Eq. (10–55)—similar to Eq. (10–219).

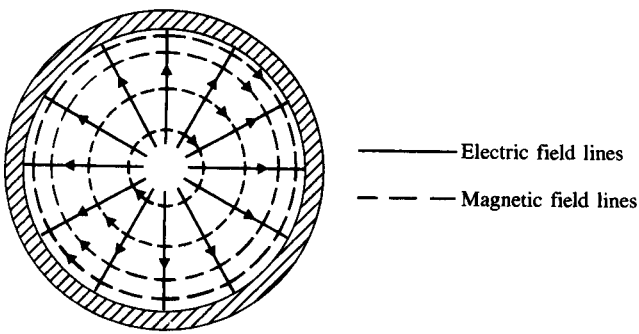

FIGURE 10–20
Field lines for TM_{01} mode in a transverse plane of circular waveguide.

We have for TE modes, in addition to H_z^0 in Eq. (10–229),

$$H_r^0 = -\frac{j\beta}{h} C_n' J_n'(hr) \cos n\phi, \tag{10–232}$$

$$H_\phi^0 = \frac{j\beta n}{h^2 r} C_n' J_n(hr) \sin n\phi, \tag{10–233}$$

$$E_r^0 = \frac{j\omega\mu n}{h^2 r} C_n' J_n(hr) \sin n\phi, \tag{10–234}$$

$$E_\phi^0 = \frac{j\omega\mu}{h} C_n' J_n'(hr) \cos n\phi, \tag{10–235}$$

$$E_z^0 = 0. \tag{10–236}$$

The required boundary condition for TE waves is that the normal derivative of H_z^0 must vanish at $r = a$; that is,

$$\boxed{J_n'(ha) = 0. \qquad \text{(TE modes)}} \tag{10–237}$$

The first several zeros of $J_n'(x)$ are listed in Table 10–3, from which we see that the smallest x_{np}' is $x_{11}' = 1.841$. This corresponds to the *smallest eigenvalue*

$$(h)_{\text{TE}_{11}} = \frac{1.841}{a}, \tag{10–238}$$

and the *lowest cutoff frequency*

$$\boxed{(f_c)_{\text{TE}_{11}} = \frac{h_{\text{TE}_{11}}}{2\pi\sqrt{\mu\epsilon}} = \frac{0.293}{a\sqrt{\mu\epsilon}} \qquad \text{(Hz)},} \tag{10–239}$$

which is lower than $(f_c)_{\text{TM}_{01}}$ given in Eq. (10–228). Hence ***the TE_{11} mode is the dominant mode in a circular waveguide.*** In an air-filled circular waveguide of radius a, the cutoff wavelength for the dominant mode is

$$\boxed{(\lambda_c)_{\text{TE}_{11}} = \frac{a}{0.293} = 3.41a \qquad \text{(m)}.} \tag{10–240}$$

It is interesting to compare Eq. (10–240) with Eq. (10–164) for a rectangular waveguide. A sketch of the electric and magnetic field lines for the TE_{11} mode in a typical transverse plane is shown in Fig. 10–21.

The attenuation constant due to losses in the imperfectly conducting wall of a circular waveguide can be calculated by following the same procedure used in Subsection 10–4.3 for a rectangular waveguide. However, integrals of Bessel's functions would be involved, and we shall not pursue this aspect further in this book. Suffice

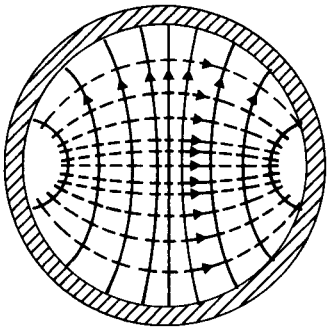

FIGURE 10–21
Field lines for TE_{11} mode in a transverse plane of a circular waveguide.

it to say that the attenuation constants of the dominant-mode propagating waves in circular and rectangular waveguides having comparable dimensions are of the same order of magnitude. A point of special interest for circular waveguides is that the attenuation constant of TE_{0p} waves decreases monotonically with frequency—the absence of a minimum point in $\alpha_c \sim f$ curves. No other waves in circular or rectangular waveguides have this property.

EXAMPLE 10–12 (a) A 10 (GHz) signal is to be transmitted inside a hollow circular conducting pipe. Determine the inside diameter of the pipe such that its lowest cutoff frequency is 20% below this signal frequency. (b) If the pipe is to operate at 15 (GHz), what waveguide modes can propagate in the pipe?

Solution

a) The cutoff frequency of the dominant mode in a circular waveguide of radius a is, from Eq. (10–239),

$$(f_c)_{TE_{11}} = \frac{0.293c}{a} = \frac{0.879}{a} \times 10^8 \quad \text{(Hz)}$$

$$= \frac{0.0879}{a} \quad \text{(GHz)}.$$

This is to be equated to $0.80 \times 10 = 8$ (GHz). Hence the required inside diameter of the pipe is $2a = 2 \times (0.0879/8) = 0.022$ (m), or 2.2 (cm).

b) Cutoff frequencies for waveguide modes in a hollow circular pipe of inner radius $a = 0.011$ (m) that are lower than 15 (GHz) are, from Tables 10–1 and 10–2,

$$(f_c)_{TE_{11}} = 8 \quad \text{(GHz)},$$

$$(f_c)_{TM_{01}} = 8 \times \left(\frac{x_{01}}{x'_{11}}\right) = 8 \times \left(\frac{2.405}{1.841}\right) = 10.45 \quad \text{(GHz)},$$

$$(f_c)_{TE_{21}} = 8 \times \left(\frac{x'_{21}}{x'_{11}}\right) = 8 \times \left(\frac{3.054}{1.841}\right) = 13.27 \quad \text{(GHz)}.$$

The f_c of all other modes are higher than 15 (GHz); hence only TE_{11}, TM_{01}, and TE_{21} modes can propagate in the pipe. ■

10–6 Dielectric Waveguides

In previous sections we discussed the behavior of electromagnetic waves propagating along waveguides with conducting walls. We now show that dielectric slabs and rods without conducting walls can also support guided-wave modes that are confined essentially within the dielectric medium.

Figure 10–22 shows a longitudinal cross section of a dielectric-slab waveguide of thickness d. For simplicity we consider this a problem with no dependence on the x-coordinate. Let ϵ_d and μ_d be the permittivity and permeability, respectively, of the dielectric slab, which is situated in free space (ϵ_0, μ_0). We assume that the dielectric is lossless and that waves propagate in the $+z$-direction. The behavior of TM and TE modes will now be analyzed separately.

10–6.1 TM WAVES ALONG A DIELECTRIC SLAB

For transverse magnetic waves, $H_z = 0$. Since there is no x-dependence, Eq. (10–62) applies. We have

$$\frac{d^2E_z^0(y)}{dy^2} + h^2E_z^0(y) = 0, \tag{10–241}$$

where

$$h^2 = \gamma^2 + \omega^2\mu\epsilon. \tag{10–242}$$

Solutions of Eq. (10–241) must be considered in both the slab and the free-space regions, and they must be matched at the boundaries.

In the slab region we assume that the waves propagate in the $+z$-direction without attenuation (lossless dielectric); that is, we assume

$$\gamma = j\beta. \tag{10–243}$$

The solution of Eq. (10–241) in the dielectric slab may contain both a sine term and a cosine term, which are an odd and an even function, respectively, of y:

$$E_z^0(y) = E_o \sin k_y y + E_e \cos k_y y, \qquad |y| \le \frac{d}{2}, \tag{10–244}$$

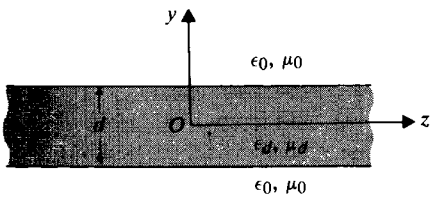

FIGURE 10–22
A longitudinal cross-section of a dielectric-slab waveguide.

where

$$\boxed{k_y^2 = \omega^2 \mu_d \epsilon_d - \beta^2 = h_d^2.} \tag{10–245}$$

In the free-space regions ($y > d/2$ and $y < -d/2$) the waves must decay exponentially so that they are guided along the slab and do not radiate away from it. We have

$$E_z^0(y) = \begin{cases} C_u e^{-\alpha(y-d/2)}, & y \geq \dfrac{d}{2}, \quad (10–246a) \\ C_l e^{\alpha(y+d/2)}, & y \leq -\dfrac{d}{2}, \quad (10–246b) \end{cases}$$

where

$$\boxed{\alpha^2 = \beta^2 - \omega^2 \mu_0 \epsilon_0 = -h_0^2.} \tag{10–247}$$

Equations (10–245) and (10–247) are called ***dispersion relations*** because they show the nonlinear dependence of the phase constant β on ω.

At this stage we have not yet determined the values of k_y and α; nor have we found the relationships among the amplitudes E_o, E_e, C_u, and C_l. In the following, we will consider the odd and even TM modes separately.

a) *Odd TM modes.* For odd TM modes, $E_z^0(y)$ is described by a sine function that is antisymmetric with respect to the $y = 0$ plane. The only other field components, $E_y^0(y)$ and $H_x^0(y)$, are obtained from Eqs. (10–28) and (10–25), respectively.

i) In the dielectric region, $|y| \leq d/2$:

$$E_z^0(y) = E_o \sin k_y y, \tag{10–248}$$

$$E_y^0(y) = -\frac{j\beta}{k_y} E_o \cos k_y y, \tag{10–249}$$

$$H_x^0(y) = \frac{j\omega\epsilon_d}{k_y} E_o \cos k_y y. \tag{10–250}$$

ii) In the upper free-space region, $y \geq d/2$:

$$E_z^0(y) = \left(E_o \sin \frac{k_y d}{2}\right) e^{-\alpha(y-d/2)}, \tag{10–251}$$

$$E_y^0(y) = -\frac{j\beta}{\alpha}\left(E_o \sin \frac{k_y d}{2}\right) e^{-\alpha(y-d/2)}, \tag{10–252}$$

$$H_x^0(y) = \frac{j\omega\epsilon_0}{\alpha}\left(E_o \sin \frac{k_y d}{2}\right) e^{-\alpha(y-d/2)}, \tag{10–253}$$

where C_u in Eq. (10–246a) has been set to equal $E_0 \sin (k_y d/2)$, which is the value of $E_z^0(y)$ in Eq. (10–248) at the upper interface, $y = d/2$.

iii) In the lower free-space region, $y \leq -d/2$:

$$E_z^0(y) = -\left(E_o \sin \frac{k_y d}{2}\right) e^{\alpha(y+d/2)}, \tag{10–254}$$

$$E_y^0(y) = -\frac{j\beta}{\alpha}\left(E_o \sin\frac{k_y d}{2}\right)e^{\alpha(y+d/2)}, \tag{10-255}$$

$$H_x^0(y) = \frac{j\omega\epsilon_0}{\alpha}\left(E_o \sin\frac{k_y d}{2}\right)e^{\alpha(y+d/2)}, \tag{10-256}$$

where C_l in Eq. (10–246b) has been set to equal $-E_o \sin(k_y d/2)$, which is the value of $E_z^0(y)$ in Eq. (10–248) at the lower interface $y = -d/2$.

Now we must determine k_y and α for a given angular frequency of excitation ω. The continuity of H_x at the dielectric surface requires that $H_x^0(d/2)$ computed from Eqs. (10–250) and (10–253) be the same. We have

$$\boxed{\frac{\alpha}{k_y} = \frac{\epsilon_0}{\epsilon_d}\tan\frac{k_y d}{2} \qquad \text{(Odd TM modes).}} \tag{10-257}$$

By adding dispersion relations Eqs. (10–245) and (10–247) we find

$$\alpha^2 + k_y^2 = \omega^2(\mu_d\epsilon_d - \mu_0\epsilon_0) \tag{10-258}$$

or

$$\boxed{\alpha = [\omega^2(\mu_d\epsilon_d - \mu_0\epsilon_0) - k_y^2]^{1/2}.} \tag{10-259}$$

Equations (10–257) and (10–259) can be combined to give an expression in which k_y is the only unknown:

$$[\omega^2(\mu_d\epsilon_d - \mu_0\epsilon_0) - k_y^2]^{1/2} = \frac{\epsilon_0}{\epsilon_d}k_y \tan\frac{k_y d}{2}. \tag{10-260}$$

Unfortunately, the transcendental equation, Eq. (10–260), cannot be solved analytically. But for a given ω and given values of ϵ_d, μ_d, and d of the dielectric slab, both the left and the right sides of Eq. (10–260) can be plotted versus k_y. The intersections of the two curves give the values of k_y for odd TM modes, of which there are only a finite number, indicating that there are only a finite number of possible modes. This is in contrast with the infinite number of modes possible in waveguides with conducting walls.

We note from Eq. (10–248) that $E_z^0 = 0$ for $y = 0$. Hence a perfectly conducting plane may be introduced to coincide with the $y = 0$ plane without affecting the existing fields. It follows that the characteristics of odd TM waves propagating along a dielectric-slab waveguide of thickness d are the same as those of the corresponding TM modes supported by a dielectric slab of a thickness $d/2$ that is backed by a perfectly conducting plane.

The ***surface impedance*** looking down from above on the surface of dielectric slab is

$$Z_s = -\frac{E_z^0}{H_x^0} = j\frac{\alpha}{\omega\epsilon_0} \qquad \text{(TM modes)}, \tag{10-261}$$

which is an inductive reactance. Thus *a TM surface wave can be supported by an inductive surface.*

b) *Even TM modes.* For even TM modes, $E_z^0(y)$ is described by a cosine function that is symmetric with respect to the $y = 0$ plane:

$$E_z^0(y) = E_e \cos k_y y, \qquad |y| \leq \frac{d}{2}. \tag{10–262}$$

The other nonzero field components, E_y^0 and H_x^0, both inside and outside the dielectric slab can be obtained in exactly the same manner as in the case of odd TM modes (see Problem P.10–33). Instead of Eq. (10–257), the characteristic relation between k_y and α now becomes

$$\boxed{\frac{\alpha}{k_y} = -\frac{\epsilon_0}{\epsilon_d} \cot \frac{k_y d}{2} \qquad \text{(Even TM modes),}} \tag{10–263}$$

which can be used in conjunction with Eq. (10–259) to determine the transverse wavenumber k_y and the transverse attenuation constant α. The several solutions correspond to the several even TM modes that can exist in the dielectric slab waveguide of thickness d. Of course, in this case a conducting plane *cannot* be placed at $y = 0$ without disturbing the whole field structure.

From Eqs. (10–245) and (10–247) it is easy to see that the phase constant, β, of propagating TM waves lies between the intrinsic phase constant of the free space, $k_0 = \omega\sqrt{\mu_0\epsilon_0}$, and that of the dielectric, $k_d = \omega\sqrt{\mu_d\epsilon_d}$; that is,

$$\omega\sqrt{\mu_0\epsilon_0} < \beta < \omega\sqrt{\mu_d\epsilon_d}.$$

As β approaches the value of $\omega\sqrt{\mu_0\epsilon_0}$, Eq. (10–247) indicates that α approaches zero. An absence of attenuation means that the waves are no longer bound to the slab. The limiting frequencies under this condition are called the ***cutoff frequencies*** of the dielectric waveguide. From Eq. (10–245) we have $k_y = \omega_c\sqrt{\mu_d\epsilon_d - \mu_0\epsilon_0}$ at cutoff. Substitution into Eqs. (10–257) and (10–263) with α set to zero yields the following relations for TM modes. At cutoff:

Odd TM Modes	Even TM Modes
$\tan\left(\frac{\omega_{co}d}{2}\sqrt{\mu_d\epsilon_d - \mu_0\epsilon_0}\right) = 0$	$\cot\left(\frac{\omega_{ce}d}{2}\sqrt{\mu_d\epsilon_d - \mu_0\epsilon_0}\right) = 0$
$\pi f_{co} d\sqrt{\mu_d\epsilon_d - \mu_0\epsilon_0} = (n-1)\pi,$ $n = 1, 2, 3, \ldots$	$\pi f_{ce} d\sqrt{\mu_d\epsilon_d - \mu_0\epsilon_0} = (n-\frac{1}{2})\pi,$ $n = 1, 2, 3, \ldots$
$\boxed{f_{co} = \frac{(n-1)}{d\sqrt{\mu_d\epsilon_d - \mu_0\epsilon_0}}}$ (10–264)	$\boxed{f_{ce} = \frac{(n-\frac{1}{2})}{d\sqrt{\mu_d\epsilon_d - \mu_0\epsilon_0}}}$ (10–265)

It is seen that $f_{co} = 0$ for $n = 1$. This means that *the lowest-order odd TM mode can propagate along a dielectric-slab waveguide regardless of the thickness of the slab.*

As the frequency of a given TM wave increases beyond the corresponding cutoff frequency, α increases and the wave clings more tightly to the slab.

10–6.2 TE WAVES ALONG A DIELECTRIC SLAB

For transverse electric waves, $E_z = 0$, and Eq. (10–82) applies

$$\frac{d^2H_z^0(y)}{dy^2} + h^2H_z^0(y) = 0, \tag{10–266}$$

where h^2 is the same as that given in Eq. (10–242). The solution for $H_z^0(y)$ may also contain both a sine term and a cosine term:

$$H_y^0(y) = H_o \sin k_y y + H_e \cos k_y y, \qquad |y| \leq \frac{d}{2}, \tag{10–267}$$

where k_y has been defined in Eq. (10–245). In the free-space regions ($y > d/2$ and $y < -d/2$) the waves must decay exponentially. We write

$$H_z^0(y) = \begin{cases} C_u' e^{-\alpha(y-d/2)}, & y \geq \dfrac{d}{2}, \quad \text{(10–268a)} \\ C_l' e^{\alpha(y+d/2)}, & y \leq -\dfrac{d}{2}, \quad \text{(10–268b)} \end{cases}$$

where α is defined in Eq. (10–247). Following the same procedure as used for TM waves, we consider the odd and even TE modes separately. Besides $H_z^0(y)$, the only other field components are $H_y^0(y)$ and $E_x^0(y)$, which can be obtained from Eqs. (10–50) and (10–51).

a) *Odd TE modes.*

i) In the dielectric region, $|y| \leq d/2$:

$$H_z^0(y) = H_o \sin k_y y, \tag{10–269}$$

$$H_y^0(y) = -\frac{j\beta}{k_y} H_o \cos k_y y, \tag{10–270}$$

$$E_x^0(y) = -\frac{j\omega\mu_d}{k_y} H_o \cos k_y y. \tag{10–271}$$

ii) In the upper free-space region, $y \geq d/2$:

$$H_z^0(y) = \left(H_o \sin \frac{k_y d}{2}\right) e^{-\alpha(y-d/2)}, \tag{10–272}$$

$$H_y^0(y) = -\frac{j\beta}{\alpha}\left(H_o \sin \frac{k_y d}{2}\right) e^{-\alpha(y-d/2)}, \tag{10–273}$$

$$E_x^0(y) = -\frac{j\omega\mu_0}{\alpha}\left(H_o \sin \frac{k_y d}{2}\right) e^{-\alpha(y-d/2)}. \tag{10–274}$$

iii) In the lower free-space region, $y \leq -d/2$:

$$H_z^0(y) = -\left(H_o \sin \frac{k_y d}{2}\right) e^{\alpha(y+d/2)}, \tag{10–275}$$

$$H_y^0(y) = -\frac{j\beta}{\alpha}\left(H_o \sin \frac{k_y d}{2}\right) e^{\alpha(y+d/2)}, \tag{10–276}$$

$$E_x^0(y) = -\frac{j\omega\mu_0}{\alpha}\left(H_o \sin \frac{k_y d}{2}\right) e^{\alpha(y+d/2)}. \tag{10–277}$$

A relation between k_y and α can be obtained by equating $E_x^0(y)$, given in Eqs. (10–271) and (10–274), at $y = d/2$. Thus,

$$\boxed{\frac{\alpha}{k_y} = \frac{\mu_0}{\mu_d} \tan \frac{k_y d}{2} \qquad \text{(Odd TE modes),}} \tag{10–278}$$

which is seen to be closely analogous to the characteristic equation, Eq. (10–257), for odd TM modes. Equations (10–259) and (10–278) can be combined in the manner of Eq. (10–260) to find k_y graphically. From k_y, α can be found from Eq. (10–259).

From a position of looking down from above, the surface impedance of the dielectric slab is

$$Z_s = \frac{E_x^0}{H_z^0} = -j\frac{\omega\mu_0}{\alpha} \qquad \text{(TE modes),} \tag{10–279}$$

which is a capacitive reactance. Hence *a TE surface wave can be supported by a capacitive surface.*

b) *Even TE modes.* For even TE modes, $H_z^0(y)$ is described by a cosine function that is symmetric with respect to the $y = 0$ plane.

$$H_z^0(y) = H_e \cos k_y y, \qquad |y| \leq d/2. \tag{10–280}$$

The other nonzero field components, H_y^0 and E_x^0, both inside and outside the dielectric slab can be obtained in the same manner as for odd TE modes (see Problem P.10–35). The characteristic relation between k_y and α is closely analogous to that for even TM modes as given in Eq. (10–263):

$$\boxed{\frac{\alpha}{k_y} = -\frac{\mu_0}{\mu_d} \cot \frac{k_y d}{2} \qquad \text{(Even TE modes).}} \tag{10–281}$$

It is easy to see that the expressions for the cutoff frequencies given in Eqs. (10–264) and (10–265) apply also to TE modes. Like the lowest-order ($n = 1$) TM mode, the lowest-order odd TE mode has no cutoff frequency. The characteristic relations for all the propagating modes along a dielectric-slab waveguide of a thickness d are listed in Table 10–4.

TABLE 10–4
Characteristic Relations for Dielectric-Slab Waveguide†

Mode		Characteristic Relation	Cutoff Frequency
TM	Odd	$(\alpha/k_y) = (\epsilon_0/\epsilon_d) \tan (k_y d/2)$	$f_{co} = (n-1)/d\sqrt{\mu_d\epsilon_d - \mu_0\epsilon_0}$
	Even	$(\alpha/k_y) = -(\epsilon_0/\epsilon_d) \cot (k_y d/2)$	$f_{ce} = (n-\frac{1}{2})/d\sqrt{\mu_d\epsilon_d - \mu_0\epsilon_0}$
TE	Odd	$(\alpha/k_y) = (\mu_0/\mu_d) \tan (k_y d/2)$	$f_{co} = (n-1)/d\sqrt{\mu_d\epsilon_d - \mu_0\epsilon_0}$
	Even	$(\alpha/k_y) = -(\mu_0/\mu_d) \cot (k_y d/2)$	$f_{ce} = (n-\frac{1}{2})/d\sqrt{\mu_d\epsilon_d - \mu_0\epsilon_0}$

† $\alpha = [\omega^2(\mu_d\epsilon_d - \mu_0\epsilon_0) - k_y^2]^{1/2}$.

EXAMPLE 10–13 A dielectric-slab waveguide with constitutive parameters $\mu_d = \mu_0$ and $\epsilon_d = 2.50\epsilon_0$ is situated in free space. Determine the minimum thickness of the slab so that a TM or TE wave of the even type at a frequency 20 GHz may propagate along the guide.

Solution The lowest TM and TE waves of the even type have the same cutoff frequency along a dielectric-slab waveguide:

$$f_c = \frac{n - \frac{1}{2}}{d\sqrt{\mu_d\epsilon_d - \mu_0\epsilon_0}}.$$

Letting $n = 1$, we have

$$f_c = \frac{c}{2d\sqrt{\dfrac{\mu_d\epsilon_d}{\mu_0\epsilon_0} - 1}}.$$

Therefore,

$$d_{\min} = \frac{c}{2f_c\sqrt{\dfrac{\mu_d\epsilon_d}{\mu_0\epsilon_0} - 1}}$$

$$= \frac{3 \times 10^8}{2 \times 20 \times 10^9\sqrt{2.5 - 1}} = 6.12 \times 10^{-3} \text{ (m) or } 6.12 \text{ (mm)}.$$

EXAMPLE 10–14 (a) Obtain an approximate expression for the decaying rate of the dominant TM surface wave outside of a very thin dielectric-slab waveguide. (b) Find the time-average power per unit slab width transmitted along the guide. (c) What is the time-average power transmitted in the transverse direction?

Solution

a) The dominant TM wave is the odd mode having a zero cutoff frequency—$f_{co} = 0$ for $n = 1$, independent of the slab thickness (see Table 10–4). With a slab that

is very thin in comparison to the operating wavelength, $k_y d/2 \ll 1$, $\tan(k_y d/2) \cong k_y d/2$, and Eq. (10–257) becomes

$$\alpha \cong \frac{\epsilon_0}{2\epsilon_d} k_y^2 d. \tag{10–282}$$

Using Eq. (10–258), Eq. (10–282) can be written approximately as

$$\alpha \cong \frac{\epsilon_0}{2\epsilon_d} \omega^2(\mu_d\epsilon_d - \mu_0\epsilon_0)d \qquad \text{(Np/m)}. \tag{10–283}$$

In Eq. (10–283) it has been assumed that $\alpha d/2 \ll \epsilon_d/\epsilon_0$.

b) The time-average Poynting vector in the $+z$-direction in the dielectric slab is

$$\mathscr{P}_{av} = \tfrac{1}{2}\mathscr{R}e(-\mathbf{a}_y E_y \times \mathbf{a}_x H_x).$$

Using Eqs. (10–249) and (10–250), we have $\mathbf{P}_{av} = \mathbf{a}_z P_{av}$ and

$$P_{av} = 2\int_0^{d/2} \mathscr{P}_{av}\, dy = \frac{\omega\epsilon_d\beta}{k_y^2} E_o^2 \int_0^{d/2} \cos^2(k_y y)\, dy$$

$$= \frac{\omega\epsilon_d\beta}{4k_y^2} E_o^2 \left[d + \frac{1}{k_y}\sin(k_y d) \right] \qquad \text{(W/m)}, \tag{10–284}$$

where

$$k_y \cong \omega\sqrt{\mu_d\epsilon_d - \mu_0\epsilon_0} \tag{10–284a}$$

and

$$\beta \cong \omega\sqrt{\mu_0\epsilon_0}. \tag{10–284b}$$

c) The time-average Poynting vector in the transverse direction is calculated from

$$\mathscr{P}_{av} = \tfrac{1}{2}\mathscr{R}e(\mathbf{a}_z E_z \times \mathbf{a}_x H_x).$$

From Subsection 10–6.1 we see that the expressions of E_z^0 and H_x^0 are 90° out of time phase. Their product has no real part, yielding a zero $\mathscr{P}_{av}$. Hence no average power is transmitted in the transverse direction normal to the reactive surface. ■

10–6.3 ADDITIONAL COMMENTS ON DIELECTRIC WAVEGUIDES

In the preceding subsection we studied the characteristics of electromagnetic waves guided by dielectric slabs with an analysis based on Maxwell's equations and the associated boundary conditions. We can gain some physical insight from the concept of total reflection in plane-wave theory that we discussed in Section 8–10.

Consider the dielectric slab in Fig. 10–23. From Section 8–10 we know that if a plane wave in the slab with a permittivity $\epsilon_d > \epsilon_0$ is incident obliquely on the lower

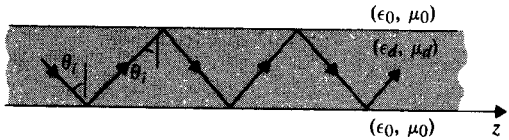

FIGURE 10–23
Bouncing-wave interpretation of propagating waves along a dielectric waveguide.

boundary at an angle of incidence θ_i greater than the critical angle (see Eq. 8–188)

$$\theta_c = \sin^{-1} \sqrt{\frac{\epsilon_0}{\epsilon_d}}, \tag{10–285}$$

it will be totally reflected toward the upper boundary. Moreover, an evanescent wave exists along the interface (in z-direction) that is attenuated exponentially in the transverse direction outside of the boundary. The reflected wave from the lower boundary will be incident on the upper boundary at the same angle of incidence $\theta_i > \theta_c$ and will be similarly totally reflected. This process will continue so that there will be two sets of multiply reflected waves: one set going from the upper boundary toward the lower boundary, and the other set from the lower boundary toward the upper boundary. Under the condition that the points on the same wavefront have the same phase, each set of reflected waves forms a single uniform plane wave. We then have two interfering uniform plane waves, giving rise to an interference pattern, which is the mode pattern of the propagating wave. It is clear that the phase requirements at both reflecting boundaries depend on the angle of incidence θ_i, since θ_i determines the phase shifts caused by total internal reflections. Analysis shows that the required phase conditions correspond precisely to the dispersion and characteristic relations obtained in the preceding section.† Thus the results based on Maxwell's equations and boundary conditions can be interpreted by bouncing waves due to total internal reflections.

So far our attention has been directed toward the wave behavior in dielectric-slab waveguides. Similar analyses apply to round dielectric-rod waveguides. In particular, they can be used to study the transmission of light waves along quartz or glass fibers that form optical waveguides. Optical fiber waveguides are of great importance as transmission media for communication or control systems because of their low-attenuation and large-bandwidth properties. They also are extremely compact and flexible. A study of circular dielectric waveguides necessitates the use of cylindrical coordinates that lead to Bessel's differential equation and Bessel functions. The study is complicated by the fact that pure TM or TE modes are possible only if the fields are circularly symmetrical; that is, if the fields are independent of the angle coordinate ϕ. When the fields are dependent on ϕ, separation into TM and TE modes is no longer possible, and it is necessary to assume the existence of both E_z and H_z components simultaneously and study the so-called ***hybrid modes***.

As a simple example, consider the circularly symmetrical TM modes for a round dielectric rod of radius a and permittivity ϵ_d, situated in air. The transverse distribution of the axial component of electric field intensity, E_z^0, in the dielectric rod ($r \leq a$) is, from Eq. (10–218) by setting $n = 0$,

$$E_{zi}^0 = C_0 J_0(hr), \qquad r \leq a, \tag{10–286}$$

where

$$h^2 = \gamma^2 + k_d^2 = \omega^2 \mu_0 \epsilon_d - \beta^2. \tag{10–287}$$

† S. R. Seshadri, *Fundamentals of Transmission Lines and Electromagnetic Fields*, Addison-Wesley, Reading, Mass., 1971, Chapter 8.

The corresponding $H_{\phi i}^0$ is, from Eq. (10–224),

$$H_{\phi i}^0 = -\frac{j\omega\epsilon_d}{h} C_0 J_0'(hr), \qquad r \leq a. \tag{10–288}$$

Outside the dielectric rod, the fields are required to be evanescent and must decrease exponentially with distance. An appropriate choice for E_{zo}^0 is $K_0(\zeta r)$, the modified Bessel function of the second kind of order zero, whose asymptotic expansion for large arguments is given in Eq. (10–215). We write

$$E_{zo}^0 = D_0 K_0(\zeta r), \qquad r \geq a, \tag{10–289}$$

where

$$\zeta^2 = \beta^2 - k_0^2 = \beta^2 - \omega^2\mu_0\epsilon_0, \tag{10–290}$$

and D_0 is a constant. The corresponding $H_{\phi o}^0$ is

$$H_{\phi o}^0 = \frac{j\omega\epsilon_0}{\zeta} D_0 K_0'(\zeta r), \qquad r \geq a. \tag{10–291}$$

The field components E_z^0 and H_ϕ^0 must be continuous at $r = a$, which requires

$$C_0 J_0(ha) = D_0 K_0(\zeta a) \tag{10–291}$$

and

$$\frac{\epsilon_d}{h} C_0 J_0'(ha) = -\frac{\epsilon_0}{\zeta} D_0 K_0'(\zeta a). \tag{10–292}$$

Combination of Eqs. (10–291) and (10–292) gives the following characteristic equation for circularly symmetrical TM modes:

$$\frac{J_0(ha)}{J_0'(ha)} = -\frac{\epsilon_d \zeta}{\epsilon_0 h} \frac{K_0(\zeta a)}{K_0'(\zeta a)}, \tag{10–293}$$

where ζ and h are related through Eqs. (10–287) and (10–290):

$$h^2 + \zeta^2 = \omega^2\mu_0(\epsilon_d - \epsilon_0). \tag{10–294}$$

Equations (10–293) and (10–294) can be solved for h and ξ either graphically or on a computer. Once the eigenvalues have been found, the cutoff frequencies and other properties of the corresponding circularly symmetrical TM modes can be determined.

In the above example we discussed only the analysis procedure for circularly symmetrical TM modes in an unclad homogeneous optical fiber. In practice, commercially available optical fibers are mainly of two types: step-index fibers that consist of a central homogeneous dielectric core and an outer sheath of a material having a lower refractive index and graded-index fibers whose center core has a nonhomogeneous refractive-index profile. Detailed studies of these types do not fall into the scope of this book.†

† See, for instance, D. Marcuse, *Theory of Dielectric Waveguides*, Academic Press, New York, 1974; A. W. Snyder and J. D. Love, *Optical Waveguide Theory*, Methuen Inc., New York, 1984.

10–7 Cavity Resonators

We have previously pointed out that at UHF (300 MHz to 3 GHz) and higher frequencies, ordinary lumped-circuit elements such as R, L, and C are difficult to make, and stray fields become important. Circuits with dimensions comparable to the operating wavelength become efficient radiators and will interfere with other circuits and systems. Furthermore, conventional wire circuits tend to have a high effective resistance both because of energy loss through radiation and as a result of skin effect. To provide a resonant circuit at UHF and higher frequencies, we look to an enclosure (a cavity) completely surrounded by conducting walls. Such a shielded enclosure confines electromagnetic fields inside and furnishes large areas for current flow, thus eliminating radiation and high-resistance effects. These enclosures have natural resonant frequencies and a very high Q (quality factor), and are called ***cavity resonators***. In this section we will study the properties of rectangular and circular cylindrical cavity resonators.

10–7.1 RECTANGULAR CAVITY RESONATORS

Consider a rectangular waveguide with both ends closed by a conducting wall. The interior dimensions of the cavity are a, b, and d, as shown in Fig. 10–24. Let us disregard for the moment the probe-excitation part of the figure. Since both TM and TE modes can exist in a rectangular guide, we expect TM and TE modes in a rectangular resonator too. However, the designation of TM and TE modes in a resonator is *not unique* because we are free to choose x or y or z as the "direction of propagation"; that is, there is no unique "longitudinal direction." For example, a TE mode with respect to the z-axis could be a TM mode with respect to the y-axis.

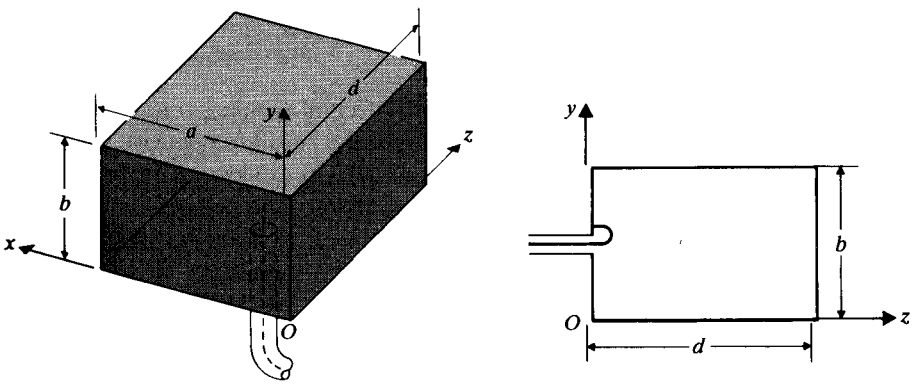

(a) Probe excitation. (b) Loop excitation.

FIGURE 10–24
Excitation of cavity modes by a coaxial line.

For our purposes *we choose the z-axis as the reference* "direction of propagation." In actuality the existence of conducting end walls at $z = 0$ and $z = d$ gives rise to multiple reflections and sets up standing waves; no wave propagates in an enclosed cavity. A three-symbol (***mnp***) subscript is needed to designate a TM or TE standing wave pattern in a cavity resonator.

TM_{mnp} Modes The expressions for the transverse variations of the field components for TM_{mn} modes in a waveguide have been given in Eqs. (10–132) and (10–134) through (10–137). Note that the longitudinal variation for a wave traveling in the $+z$-direction is described by the factor $e^{-\gamma z}$ or $e^{-j\beta z}$, as indicated in Eq. (10–121). This wave will be reflected by the end wall at $z = d$; and the reflected wave, going in the $-z$-direction, is described by a factor $e^{j\beta z}$. The superposition of a term with $e^{-j\beta z}$ and another of the same amplitude† with $e^{j\beta z}$ results in a standing wave of the sin βz or cos βz type. Which should it be? The answer to this question depends on the particular field component.

Consider the transverse component $E_y(x, y, z)$. Boundary conditions at the conducting surfaces require that it be zero at $z = 0$ and $z = d$. This means that (1) its z-dependence must be of the sin βz type, and that (2) $\beta = p\pi/d$. The same argument applies to the other transverse electric field component $E_x(x, y, z)$.

Recalling that the appearance of the factor $(-\gamma)$ in Eqs. (10–134) and (10–135) is the result of a differentiation with respect to z, we conclude that the other components $E_z(x, y, z)$, $H_x(x, y, z)$, and $H_y(x, y, z)$, which do not contain the factor $(-\gamma)$, must vary according to cos βz. We have then, from Eqs. (10–132) and (10–134) through (10–137), the following *phasors* of the field components for TM_{mnp} modes in a rectangular cavity resonator:

$$E_z(x, y, z) = E_0 \sin\left(\frac{m\pi}{a}x\right)\sin\left(\frac{n\pi}{b}y\right)\cos\left(\frac{p\pi}{d}z\right), \tag{10–295}$$

$$E_x(x, y, z) = -\frac{1}{h^2}\left(\frac{m\pi}{a}\right)\left(\frac{p\pi}{d}\right)E_0 \cos\left(\frac{m\pi}{a}x\right)\sin\left(\frac{n\pi}{b}y\right)\sin\left(\frac{p\pi}{d}z\right), \tag{10–296}$$

$$E_y(x, y, z) = -\frac{1}{h^2}\left(\frac{n\pi}{b}\right)\left(\frac{p\pi}{d}\right)E_0 \sin\left(\frac{m\pi}{a}x\right)\cos\left(\frac{n\pi}{b}y\right)\sin\left(\frac{p\pi}{d}z\right), \tag{10–297}$$

$$H_x(x, y, z) = \frac{j\omega\epsilon}{h^2}\left(\frac{n\pi}{b}\right)E_0 \sin\left(\frac{m\pi}{a}x\right)\cos\left(\frac{n\pi}{b}y\right)\cos\left(\frac{p\pi}{d}z\right), \tag{10–298}$$

$$H_y(x, y, z) = -\frac{j\omega\epsilon}{h^2}\left(\frac{m\pi}{a}\right)E_0 \cos\left(\frac{m\pi}{a}x\right)\sin\left(\frac{n\pi}{b}y\right)\cos\left(\frac{p\pi}{d}z\right), \tag{10–299}$$

where

$$h^2 = \left(\frac{m\pi}{a}\right)^2 + \left(\frac{n\pi}{b}\right)^2. \tag{10–300}$$

† The reflection coefficient at a perfect conductor is -1.

It is clear that the integers m, n, and p denote the number of half-wave variations in the x-, y-, and z-direction, respectively.

From Eq. (10–138) we obtain the following expression for the resonant frequency:

$$\omega_{mnp} = \frac{1}{\sqrt{\mu\epsilon}} \sqrt{\left(\frac{m\pi}{a}\right)^2 + \left(\frac{n\pi}{b}\right)^2 + \left(\frac{p\pi}{d}\right)^2}$$

or

$$\boxed{f_{mnp} = \frac{u}{2} \sqrt{\left(\frac{m}{a}\right)^2 + \left(\frac{n}{b}\right)^2 + \left(\frac{p}{d}\right)^2} \quad \text{(Hz)}.} \tag{10–301}$$

Equation (10–301) states the obvious fact that the resonant frequency increases as the order of a mode becomes higher.

TE_{mnp} Modes For TE_{mnp} modes ($E_z = 0$) the phasor expressions for the standing-wave field components can be written from Eqs. (10–158) and (10–159) through (10–162). We follow the same rules as those we used for TM_{mnp} modes; namely, (1) the transverse (tangential) electric field components must vanish at $z = 0$ and $z = d$, and (2) the factor γ indicates a negative partial differentiation with respect to z. The first rule requires a $\sin(p\pi z/d)$ factor in $E_x(x, y, z)$ and $E_y(x, y, z)$, as well as in $H_z(x, y, z)$; and the second rule indicates a $\cos(p\pi z/d)$ factor in $H_x(x, y, z)$ and $H_y(x, y, z)$, and the replacement of γ by $-(p\pi/d)$. Thus,

$$H_z(x, y, z) = H_0 \cos\left(\frac{m\pi}{a} x\right) \cos\left(\frac{n\pi}{b} y\right) \sin\left(\frac{p\pi}{d} z\right), \tag{10–302}$$

$$E_x(x, y, z) = \frac{j\omega\mu}{h^2}\left(\frac{n\pi}{b}\right) H_0 \cos\left(\frac{m\pi}{a} x\right) \sin\left(\frac{n\pi}{b} y\right) \sin\left(\frac{p\pi}{d} z\right), \tag{10–303}$$

$$E_y(x, y, z) = -\frac{j\omega\mu}{h^2}\left(\frac{m\pi}{a}\right) H_0 \sin\left(\frac{m\pi}{a} x\right) \cos\left(\frac{n\pi}{b} y\right) \sin\left(\frac{p\pi}{d} z\right), \tag{10–304}$$

$$H_x(x, y, z) = -\frac{1}{h^2}\left(\frac{m\pi}{a}\right)\left(\frac{p\pi}{d}\right) H_0 \sin\left(\frac{m\pi}{a} x\right) \cos\left(\frac{n\pi}{b} y\right) \cos\left(\frac{p\pi}{d} z\right), \tag{10–305}$$

$$H_y(x, y, z) = -\frac{1}{h^2}\left(\frac{n\pi}{b}\right)\left(\frac{p\pi}{d}\right) H_0 \cos\left(\frac{m\pi}{a} x\right) \sin\left(\frac{n\pi}{b} y\right) \cos\left(\frac{p\pi}{d} z\right), \tag{10–306}$$

The value of h^2 has been given in Eq. (10–300). The expression for resonant frequency, f_{mnp}, remains the same as that obtained for TM_{mnp} modes in Eq. (10–301). Different modes having the same resonant frequency are called ***degenerate modes***. Thus TM_{mnp} and TE_{mnp} modes are always degenerate if none of the mode indices is zero. The mode with the lowest resonant frequency for a given cavity size is referred to as the ***dominant mode*** (see Example 10–15).

Examination of the field expressions, Eqs. (10–295) through (10–299), for TM modes in a cavity reveals that the longitudinal and transverse electric field compo-

nents are in time phase with one another and in time quadrature with the magnetic field components. Hence the time-average Poynting vector and time-average power transmitted in any direction are zero, as they should be in a lossless cavity. This is in contrast to the field expressions Eqs. (10–132) and (10–134) through (10–137) for TM modes in a waveguide, where the transverse electric field components are in time phase with the transverse magnetic field components, resulting in a time-average power flow in the direction of wave propagation. The same contrasting phase relationships between electric and magnetic field components for TE modes in a cavity resonator (Eqs. 10–302 through 10–306) and those in a waveguide (Eqs. 10–158 through 10–162) are also in evidence.

A particular mode in a cavity resonator (or a waveguide) may be excited from a coaxial line by means of a small probe or loop antenna. In Fig. 10–24(a) a probe is shown that is the tip of the inner conductor of a coaxial cable and protrudes into a cavity at a location where the electric field is a maximum for the desired mode. The probe is, in fact, an antenna that couples electromagnetic energy into the resonator. Alternatively, a cavity resonator may be excited through the introduction of a small loop at a place where the magnetic flux of the desired mode linking the loop is a maximum. Figure 10–24(b) illustrates such an arrangement. Of course, the source frequency from the coaxial line must be the same as the resonant frequency of the desired mode in the cavity.

As an example, for the TE_{101} mode in an $a \times b \times d$ rectangular cavity, there are only three nonzero field components:

$$E_y = -\frac{j\omega\mu a}{\pi} H_0 \sin\left(\frac{\pi}{a}x\right) \sin\left(\frac{\pi}{d}z\right), \tag{10–307}$$

$$H_x = -\frac{a}{d} H_0 \sin\left(\frac{\pi}{a}x\right) \cos\left(\frac{\pi}{d}z\right), \tag{10–308}$$

$$H_z = H_0 \cos\left(\frac{\pi}{a}x\right) \sin\left(\frac{\pi}{d}z\right). \tag{10–309}$$

This mode may be excited by a probe inserted in the center region of the top or bottom face where E_y is maximum, as shown in Fig. 10–24(a), or by a loop to couple a maximum H_x placed inside the front or back face, as shown in Fig. 10–24(b). The best location of a probe or a loop is affected by the impedance-matching requirements of the microwave circuit of which the resonator is a part.

A commonly used method for coupling energy from a waveguide to a cavity resonator is the introduction of a hole or iris at an appropriate location in the cavity wall. The field in the waveguide at the hole must have a component that is favorable in exciting the desired mode in the resonator.

EXAMPLE 10–15 Determine the dominant modes and their frequencies in an air-filled rectangular cavity resonator for (a) $a > b > d$, (b) $a > d > b$, and (c) $a = b = d$, where a, b, and d are the dimensions in the x-, y-, and z-directions, respectively.

Solution With the z-axis chosen as the reference "direction of propagation": First, for TM_{mnp} modes, Eqs. (10–295) through (10–299) show that neither m nor n can be zero, but that p can be zero; second, for TE_{mnp} modes, Eqs. (10–302) through (10–306) show that either m or n (but not both m and n) can be zero, but that p cannot be zero. Thus the modes of the lowest orders are

$$TM_{110}, \quad TE_{011}, \quad \text{and } TE_{101}.$$

The resonant frequency for both TM and TE modes is given by Eq. (10–301).

a) For $a > b > d$: The lowest resonant frequency is

$$f_{110} = \frac{c}{2}\sqrt{\frac{1}{a^2} + \frac{1}{b^2}}, \tag{10–310}$$

where c is the velocity of light in free space. Therefore TM_{110} is the dominant mode.

b) For $a > d > b$: The lowest resonant frequency is

$$f_{101} = \frac{c}{2}\sqrt{\frac{1}{a^2} + \frac{1}{d^2}}, \tag{10–311}$$

and TE_{101} is the dominant mode.

c) For $a = b = d$, all three of the lowest-order modes (namely, TM_{110}, TE_{011}, and TE_{101}) have the same field patterns. The resonant frequency of these degenerate modes is

$$f_{110} = \frac{c}{\sqrt{2}a}. \tag{10–312}$$

■

10–7.2 QUALITY FACTOR OF CAVITY RESONATOR

A cavity resonator stores energy in the electric and magnetic fields for any particular mode pattern. In any practical cavity the walls have a finite conductivity; that is, a nonzero surface resistance, and the resulting power loss causes a decay of the stored energy. The ***quality factor***, or Q, of a resonator, like that of any resonant circuit, is a measure of the bandwidth of the resonator and is defined as

$$Q = 2\pi \frac{\text{Time-average energy stored at a resonant frequency}}{\text{Energy dissipated in one period of this frequency}}. \tag{10–313}$$

(Dimensionless)

Let W be the total time-average energy in a cavity resonator. We write

$$W = W_e + W_m, \tag{10–314}$$

where W_e and W_m denote the energies stored in the electric and magnetic fields, respectively. If P_L is the time-average power dissipated in the cavity, then the energy

dissipated in one period is P_L divided by frequency, and Eq. (10–313) can be written as

$$\boxed{Q = \frac{\omega W}{P_L} \qquad \text{(Dimensionless).}} \tag{10–315}$$

In determining the Q of a cavity at a resonant frequency, it is customary to assume that the loss is small enough to allow the use of the field patterns without loss.

We will now find the Q of an $a \times b \times d$ cavity for the TE_{101} mode that has three nonzero field components given in Eqs. (10–307), (10–308), and (10–309). The time-average stored electric energy is

$$\begin{aligned} W_e &= \frac{\epsilon_0}{4}\int |E_y|^2\, dv \\ &= \frac{\epsilon_0\omega^2\mu_0^2\pi^2}{4h^4a^2} H_0^2 \int_0^d\int_0^b\int_0^a \sin^2\left(\frac{\pi}{a}x\right)\sin^2\left(\frac{\pi}{d}z\right) dx\, dy\, dz \\ &= \frac{\epsilon_0\omega_{101}^2\mu_0^2a^2}{4\pi^2} H_0^2\left(\frac{a}{2}\right)b\left(\frac{d}{2}\right) = \frac{1}{4}\epsilon_0\mu_0^2a^3bdf_{101}^2H_0^2, \end{aligned} \tag{10–316}$$

where we have used $h^2 = (\pi/a)^2$ from Eq. (10–300). The total time-average stored magnetic energy is

$$\begin{aligned} W_m &= \frac{\mu_0}{4}\int \{|H_x|^2 + |H_z|^2\}\, dv \\ &= \frac{\mu_0}{4} H_0^2 \int_0^d\int_0^b\int_0^a \left\{\frac{\pi^4}{h^4a^2d^2}\sin^2\left(\frac{\pi}{a}x\right)\cos^2\left(\frac{\pi}{d}z\right)\right. \\ &\quad \left. + \cos^2\left(\frac{\pi}{a}x\right)\sin^2\left(\frac{\pi}{d}z\right)\right\} dx\, dy\, dz \\ &= \frac{\mu_0}{4} H_0^2\left\{\frac{a^2}{d^2}\left(\frac{a}{2}\right)b\left(\frac{d}{2}\right) + \left(\frac{a}{2}\right)b\left(\frac{d}{2}\right)\right\} = \frac{\mu_0}{16}abd\left(\frac{a^2}{d^2}+1\right)H_0^2. \end{aligned} \tag{10–317}$$

From Eq. (10–311) the resonant frequency for the TE_{101} mode is

$$f_{101} = \frac{1}{2\sqrt{\mu_0\epsilon_0}}\sqrt{\frac{1}{a^2}+\frac{1}{d^2}}. \tag{10–318}$$

Substitution of f_{101} from Eq. (10–318) in Eq. (10–316) proves that, *at the resonant frequency*, $W_e = W_m$. Thus,

$$W = 2W_e = 2W_m = \frac{\mu_0 H_0^2}{8}abd\left(\frac{a^2}{d^2}+1\right). \tag{10–319}$$

To find P_L, we note that the power loss per unit area is

$$\mathscr{P}_{av} = \tfrac{1}{2}|J_s|^2R_s = \tfrac{1}{2}|H_t|^2R_s, \tag{10–320}$$

where $|H_t|$ denotes the magnitude of the tangential component of the magnetic field at the cavity walls. The power loss in the $z = d$ (back) wall is the same as that in the $z = 0$ (front) wall. Similarly, the power loss in the $x = a$ (left) wall is the same as that in the $x = 0$ (right) wall; and the power loss in the $y = b$ (upper) wall is the same as that in the $y = 0$ (lower) wall. We have

$$\begin{aligned} P_L = \oint \mathscr{P}_{av} ds &= R_s \left\{ \int_0^b \int_0^a |H_x(z=0)|^2 \, dx\, dy + \int_0^d \int_0^b |H_z(x=0)|^2 \, dy\, dz \right. \\ &\left. + \int_0^d \int_0^a |H_x|^2 \, dx\, dz + \int_0^d \int_0^a |H_z|^2 \, dx\, dz \right\} \qquad (10\text{–}321) \\ &= \frac{R_s H_0^2 a}{2} \left\{ \frac{a^2}{d}\left(\frac{b}{d} + \frac{1}{2}\right) + d\left(\frac{b}{a} + \frac{1}{2}\right) \right\}. \end{aligned}$$

Using Eqs. (10–319) and (10–321) in Eq. (10–315), we obtain

$$Q_{101} = \frac{\pi f_{101} \mu_0 abd(a^2 + d^2)}{R_s[2b(a^3 + d^3) + ad(a^2 + d^2)]} \qquad (\text{TE}_{101} \text{ mode}), \qquad (10\text{–}322)$$

where f_{101} has been given in Eq. (10–318).

EXAMPLE 10–16 (a) What should be the size of a hollow cubic cavity made of copper in order for it to have a dominant resonant frequency of 10 (GHz)? (b) Find the Q at that frequency.

Solution

a) For a cubic cavity, $a = b = d$: From Example 10–15 we know that TM_{110}, TE_{011}, and TE_{101} are degenerate dominant modes having the same field patterns and that

$$f_{101} = \frac{3 \times 10^8}{\sqrt{2}a} = 10^{10} \quad (\text{Hz}).$$

Therefore,

$$a = \frac{3 \times 10^8}{\sqrt{2} \times 10^{10}} = 2.12 \times 10^{-2} \quad (\text{m})$$
$$= 21.2 \quad (\text{mm}).$$

b) The expression of Q in Eq. (10–322) for a cubic cavity reduces to

$$Q_{101} = \frac{\pi f_{101} \mu_0 a}{3R_s} = \frac{a}{3}\sqrt{\pi f_{101} \mu_0 \sigma}. \qquad (10\text{–}323)$$

For copper, $\sigma = 5.80 \times 10^7$ (S/m), we have

$$Q_{101} = \left(\frac{2.12}{3} \times 10^{-2}\right)\sqrt{\pi 10^{10}(4\pi 10^{-7})(5.80 \times 10^7)} = 10{,}700.$$

The Q of a cavity resonator is thus extremely high in comparison with that obtainable from lumped L–C resonant circuits. In practice, the preceding value is somewhat lower owing to losses through feed connections and surface irregularities.

10–7.3 CIRCULAR CAVITY RESONATOR

In a manner similar to the construction of a rectangular cavity resonator from a rectangular waveguide, a circular cylindrical resonator can be formed by placing conducting walls at both ends of a cylindrical waveguide. For simplicity, let us consider the TM_{01} mode in a circular waveguide of radius a at cutoff so that there is no variation in the z-direction. The ends of the waveguide are shorted by conducting plates at a distance d ($< 2a$) apart, forming a circular cylindrical cavity. The field components inside the cavity are, from Eqs. (10–218) and (10–224) by setting $n = 0$ and recalling Eq. (10–227),

$$E_z = C_0 J_0(hr) = C_0 J_0\left(\frac{2.405}{a} r\right), \tag{10–324}$$

$$H_\phi = -\frac{jC_0}{\eta_0} J_0'(hr) = \frac{jC_0}{\eta_0} J_1\left(\frac{2.405}{a} r\right), \tag{10–325}$$

where the relation $J_0'(hr) = -J_1(hr)$ has been used. The electric and magnetic field patterns for the TM_{010} mode in the circular cavity in both transverse and longitudinal sections are sketched in Fig. 10–25. Note from Eqs. (10–324) and (10–325) again that

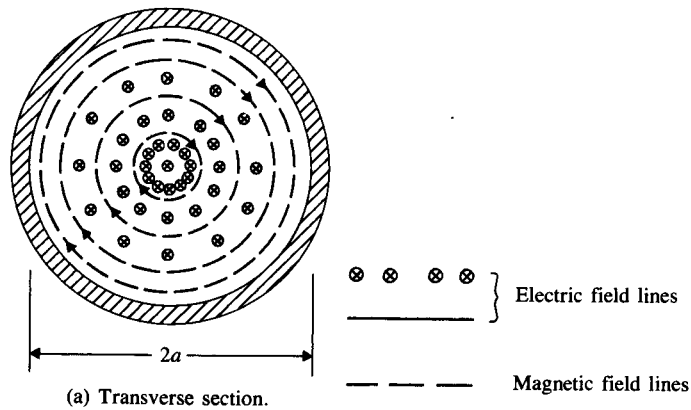

(a) Transverse section.

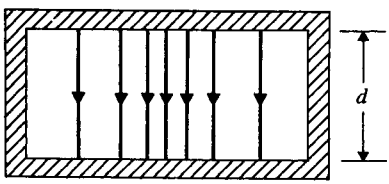

(b) Longitudinal section.

FIGURE 10–25
TM_{010} field patterns in a circular cylindrical cavity resonator.

the electric and magnetic fields are in time quadrature, resulting in no power loss in the cavity walls.

In actuality the cavity walls do have a finite conductivity and a nonzero surface resistance. There will be power loss in the walls, and the cavity Q is not infinite. To calculate the cavity Q, we apply Eq. (10–315) and follow the same procedure as that used in the preceding subsection for the rectangular resonator. We will assume that the field intensities inside a low-loss cavity remain approximately the same as those for a lossless cavity.

Let us find the Q of a circular cylindrical cavity of radius a and length d for the TM_{010} mode. The field components have been given in Eqs. (10–324) and (10–325). The time-average stored energy is

$$\begin{aligned} W = 2W_e &= \frac{\epsilon_0}{2}\int_V |E_z|^2\,dv \\ &= \frac{\epsilon_0 C_0^2}{2}(2\pi d)\int_0^a J_0^2\left(\frac{2.405}{a}r\right)r\,dr \\ &= (\pi\epsilon_0 d)C_0^2\left[\frac{a^2}{2}J_1^2(2.405)\right]. \end{aligned} \tag{10–326}$$

The average power loss per unit area is given by Eq. (10–320). Here $H_t = H_\phi$, and there are radial surface currents $\mathbf{J}_r$ on the flat end faces and uniform longitudinal surface currents $\mathbf{J}_z$ on the inside of the cylindrical walls. We have

$$\begin{aligned} P_L &= \frac{R_s}{2}\left\{2\int_0^a |J_r|^2 2\pi r\,dr + (2\pi ad)|J_z|^2\right\} \\ &= \pi R_s\left\{2\int_0^a |H_\phi|^2 r\,dr + (ad)|H_\phi(r=a)|^2\right\} \\ &= \frac{\pi R_s C_0^2}{\eta_0^2}\left\{2\int_0^a rJ_1^2\left(\frac{2.405}{a}r\right)dr + (ad)J_1^2(2.405)\right\} \\ &= \frac{\pi a R_s C_0^2}{\eta_0^2}(a+d)J_1^2(2.405). \end{aligned} \tag{10–327}$$

Substituting Eqs. (10–326) and (10–327) in Eq. (10–315), we obtain

$$Q = \left(\frac{\eta_0}{R_s}\right)\frac{2.405}{2(1+a/d)} \qquad (TM_{010}\text{ mode}), \tag{10–328}$$

---

† The following relations have been used:

$$\int J_n^2(hr)r\,dr = \frac{r^2}{2}\left[J_n'^2(hr) + \left(1 - \frac{n^2}{h^2r^2}\right)J_n^2(hr)\right],\quad J_1'(hr) = J_0(hr) - \frac{1}{hr}J_1(hr),\text{ and } J_0(ha) = 0.$$

where $R_s = \sqrt{\pi f \mu_0/\sigma}$ is to be calculated at the resonant frequency for the TM_{010} mode, which is, from Eqs. (10–227) and (10–228),

$$(f)_{TM_{010}} = \frac{2.405}{2\pi a\sqrt{\mu_0\epsilon_0}} = \frac{0.115}{a} \quad \text{(GHz)}. \tag{10–329}$$

EXAMPLE 10–17 A hollow circular cylindrical cavity resonator is to be constructed of copper such that its length d equals its diameter $2a$. (a) Determine a and d for a resonant frequency of 10 (GHz) at the TM_{010} mode. (b) Find the Q of the cavity at resonance.

Solution

a) From Eq. (10–329) we have

$$\frac{0.115}{a} = 10,$$

or

$$a = 1.15 \times 10^{-2}\,(\text{m}) = 1.15 \quad \text{(cm)}.$$

Thus,

$$d = 2a = 2.30 \quad \text{(cm)}.$$

b)

$$R_s = \sqrt{\frac{\pi f \mu_0}{\sigma}}$$

$$= \sqrt{\frac{\pi \times 10^{10} \times (4\pi 10^{-7})}{5.80 \times 10^7}} = 2.61 \times 10^{-2} \quad (\Omega).$$

From Eq. (10–328) we obtain

$$Q = \left(\frac{377}{2.61 \times 10^{-2}}\right)\frac{2.405}{2(1 + 1/2)} = 11{,}580.$$

It is interesting to compare the results of this example with those obtained in Example 10–16 for a rectangular cavity resonator of a comparable size that resonates at the same frequency.

	Circular Cavity	Rectangular Cavity
Resonant mode at frequency	TM_{010} 10 (GHz)	TE_{101} 10 (GHz)
Dimensions	Diameter $2a = 2.30$ (cm) Length $d = 2.30$ (cm)	$a = b = d = 2.12$ (cm)
Volume	$\pi a^2 d = 9.56$ (cm^3)	$a \times b \times d = 9.53$ (cm^3)
Total area	$2(\pi a^2) + (2\pi ad) = 24.93$ (cm^2)	$6a^2 = 26.97$ (cm^2)
Q	11,580	10,700

We see that these two cavities have approximately the same volume, but the total surface area of the rectangular cavity is about 8.2% larger. The larger surface area leads to a higher power loss and a lower Q. The Q of the circular cavity is approximately 8.2% higher. ■

Review Questions

R.10–1 Why are the common types of transmission lines not useful for the long-distance signal transmission at microwave frequencies in the TEM mode?

R.10–2 What is meant by a *cutoff frequency* of a waveguide?

R.10–3 Why are lumped-parameter elements connected by wires not useful as resonant circuits at microwave frequencies?

R.10–4 What is the governing equation for electric and magnetic field intensity phasors in the dielectric region of a straight waveguide with a uniform cross section?

R.10–5 What are the three basic types of propagating waves in a uniform waveguide?

R.10–6 Define *wave impedance.*

R.10–7 Explain why single-conductor hollow or dielectric-filled waveguides cannot support TEM waves.

R.10–8 Discuss the analytical procedure for studying the characteristics of TM waves in a waveguide.

R.10–9 Discuss the analytical procedure for studying the characteristics of TE waves in a waveguide.

R.10–10 What are *eigenvalues* of a boundary-value problem?

R.10–11 Can a waveguide have more than one cutoff frequency? On what factors does the cutoff frequency of a waveguide depend.

R.10–12 What is an *evanescent mode*?

R.10–13 Is the guide wavelength of a propagating wave in a waveguide longer or shorter than the wavelength in the corresponding unbounded dielectric medium?

R.10–14 In what way does the wave impedance in a waveguide depend on frequency:

a) For a propagating TEM wave?
b) For a propagating TM wave?
c) For a propagating TE wave?

R.10–15 What is the significance of a purely reactive wave impedance?

R.10–16 Can one tell from an ω–β diagram whether a certain propagating mode in a waveguide is dispersive? Explain.

R.10–17 Explain how one determines the phase velocity and the group velocity of a propagating mode from its ω–β diagram.

R.10–18 What is meant by an *eigenmode*?

R.10–19 On what factors does the cutoff frequency of a parallel-plate waveguide depend?

R.10–20 What is meant by the *dominant mode* of a waveguide? What is the dominant mode of a parallel-plate waveguide?

R.10–21 Can a TM or TE wave with a wavelength 3 (cm) propagate in a parallel-plate waveguide whose plate separation is 1 (cm)? 2 (cm)? Explain.

R.10–22 Compare the cutoff frequencies of TM_0, TM_n, TM_m ($m > n$), and TE_n modes in a parallel-plate waveguide.

R.10–23 Define *energy-transport velocity.*

R.10–24 Does the attenuation constant due to dielectric losses increase or decrease with frequency for TM and TE modes in a parallel-plate waveguide?

R.10–25 Discuss the essential differences in the frequency behavior of the attenuation caused by finite plate conductivity in a parallel-plate waveguide for TEM, TM, and TE modes.

R.10–26 State the boundary conditions to be satisfied by E_z for TM waves in a rectangular waveguide.

R.10–27 Which TM mode has the lowest cutoff frequency of all the TM modes in a rectangular waveguide?

R.10–28 State the boundary conditions to be satisfied by H_z for TE waves in a rectangular waveguide.

R.10–29 Which mode is the dominant mode in a rectangular waveguide if (a) $a > b$, (b) $a < b$, and (c) $a = b$?

R.10–30 What is the cutoff wavelength of the TE_{10} mode in a rectangular waveguide?

R.10–31 Which are the nonzero field components for the TE_{10} mode in a rectangular waveguide?

R.10–32 Discuss the frequency-dependence of the attenuation constant caused by losses in the dielectric medium in a waveguide.

R.10–33 Discuss the general attenuation behavior caused by wall losses as a function of frequency for the TE_{10} mode in a rectangular waveguide.

R.10–34 Discuss the general attenuation behavior caused by wall losses as a function of frequency for the TM_{11} mode in a rectangular waveguide.

R.10–35 Discuss the factors that affect the choice of the linear dimensions a and b for the cross section of a rectangular waveguide.

R.10–36 What type of conducting diaphragm with an iris in a waveguide can provide a shunt capacitive susceptance? A shunt inductive susceptance? Explain.

R.10–37 Under what circumstances does a Bessel's differential equation arise?

R.10–38 Describe some general properties of Bessel functions of the first kind.

R.10–39 Why are Bessel functions of the second kind not useful in the analysis of wave propagation in a hollow circular waveguide?

R.10–40 Which mode is the dominant mode in a circular waveguide?

R.10–41 It is claimed that the TE_{11} wave of a given frequency will propagate in a circular cylindrical pipe having a diameter only 76.5% of that required to support a TM_{01} wave of the same frequency. Explain.

R.10–42 What is the distinctive characteristic of the attenuation constant of TE_{0n} modes in a circular waveguide?

R.10–43 Why is it necessary that the permittivity of the dielectric slab in a dielectric waveguide be larger than that of the surrounding medium?

R.10–44 What are dispersion relations?

R.10–45 Can a dielectric-slab waveguide support an infinite number of discrete TM and TE modes? Explain.

R.10–46 What kind of surface can support a TM surface wave? A TE surface wave?

R.10–47 What is the dominant mode in a dielectric-slab waveguide? What is its cutoff frequency?

R.10–48 Does the attenuation of the waves outside a dielectric slab waveguide increase or decrease with slab thickness?

R.10–49 How does the time-average power transmitted in the transverse direction of a dielectric waveguide depend on the propagating mode in the guide?

R.10–50 What kinds of Bessel functions are appropriate in the analysis of wave behavior in and around optical fibers? Explain.

R.10–51 What are cavity resonators? What are their most desirable properties?

R.10–52 Are the field patterns in a cavity resonator traveling waves or standing waves? How do they differ from those in a waveguide?

R.10–53 In terms of field patterns, what does the TM_{110} mode signify? The TE_{123} mode?

R.10–54 What is the expression for the resonant frequency of TM_{mnp} modes in a rectangular cavity resonator of dimensions $a \times b \times d$? Of TE_{mnp} modes?

R.10–55 What is meant by *degenerate modes*?

R.10–56 What are the modes of the lowest orders in a rectangular cavity resonator?

R.10–57 Define the quality factor, Q, of a resonator.

R.10–58 What fundamental assumption is made in the derivation of the formulas for the Q of cavity resonators?

R.10–59 What field components exist in a circular cylindrical cavity operating in the TM_{010} mode?

R.10–60 Will the Q of a circular cylindrical cavity resonator be higher or lower by increasing its length? Explain by physical reasoning.

R.10–61 Explain why the measured Q of a cavity resonator is lower than the calculated value.

Problems

P.10–1 In studying the wave behavior in a straight waveguide having a uniform but arbitrary cross section it is expedient to find general formulas expressing the transverse field components in terms of their longitudinal components. We write

$$\mathbf{E} = \mathbf{E}_T + \mathbf{a}_z E_z,$$

$$\mathbf{H} = \mathbf{H}_T + \mathbf{a}_z H_z;$$

$$\nabla = \nabla_T + \mathbf{a}_z \frac{\partial}{\partial z},$$

where the subscript T denotes "transverse." Prove the following relations for time-harmonic excitation:

a) $\mathbf{E}_T = -\frac{1}{h^2}(\gamma \nabla_T E_z - \mathbf{a}_z j\omega\mu \times \nabla_T H_z)$ (10–330)

b) $\mathbf{H}_T = -\frac{1}{h^2}(\gamma \nabla_T H_z + \mathbf{a}_z j\omega\epsilon \times \nabla_T E_z)$, (10–331)

where h^2 is that given in Eq. (10–15).

P.10–2 For rectangular waveguides, use appropriate relations in Section 10–2 to:
- **a)** plot the universal circle diagrams relating u_g/u and β/k versus f_c/f,
- **b)** plot the universal graphs of u/u_p, β/k, and λ_g/λ versus f/f_c,
- **c)** find u_p/u, u_g/u, β/k, and λ_g/λ at $f = 1.25f_c$.

P.10–3 Sketch the ω–β diagrams of a parallel-plate waveguide separated by a dielectric slab of thickness b and constitutive parameters (ϵ, μ) for TM_1, TM_2, and TM_3 modes. Discuss
- **a)** how b and the constitutive parameters affect the diagrams,
- **b)** whether the same curves apply to TE modes.

P.10–4 Obtain the expressions for the surface charge density and the surface current density for TM_n modes on the conducting plates of a parallel-plate waveguide. Do the currents on the two plates flow in the same direction or in opposite directions?

P.10–5 Obtain the expressions for the surface current density for TE_n modes on the conducting plates of a parallel-plate waveguide. Do the currents on the two plates flow in the same direction or in opposite directions?

P.10–6 Sketch the electric and magnetic field lines for (a) the TM_2 mode and (b) the TE_2 mode in a parallel-plate waveguide.

P.10–7 Determine the energy-transport velocity of the TE_n mode in a lossless parallel-plate waveguide in terms of its cutoff frequency.

P.10–8 A waveguide is formed by two parallel copper sheets—$\sigma_c = 5.80 \times 10^7$ (S/m)—separated by a 5 (cm) thick lossy dielectric—$\epsilon_r = 2.25$, $\mu_r = 1$, $\sigma = 10^{-10}$ (S/m). For an operating frequency of 10 (GHz), find β, α_d, α_c, u_p, u_g, and λ_g for (a) the TEM mode, (b) the TM_1 mode, and (c) the TM_2 mode.

P.10–9 Repeat Problem P.10–8 for (a) the TE_1 mode and (b) the TE_2 mode.

P.10–10 For a parallel-plate waveguide,
- **a)** find the frequency (in terms of the cutoff frequency f_c) at which the attenuation constant due to conductor losses for the TM_n mode is a minimum,
- **b)** obtain the formula for this minimum attenuation constant,
- **c)** calculate this minimum α_c for the TM_1 mode if the parallel plates are made of copper and spaced 5 (cm) apart in air.

P.10–11 A parallel-plate waveguide made of two perfectly conducting infinite planes spaced 3 (cm) apart in air operates at a frequency 10 (GHz). Find the maximum time-average power that can be propagated per unit width of the guide without a voltage breakdown for **a)** the TEM mode, **b)** the TM_1 mode, **c)** the TE_1 mode.

P.10–12 Without deriving any new equations, roughly sketch the electric and magnetic field lines in a typical xy-plane of a rectangular waveguide for
- **a)** TM_{21} mode by an extension of Fig. 10–11(a).
- **b)** TE_{11} mode by an extension of Fig. 10–12(a).

The densities of the field lines should show the proper sine or cosine variations.

P.10–13 For an $a \times b$ rectangular waveguide operating at the TM_{11} mode,

a) derive the expressions for the surface current densities on the conducting walls,

b) sketch the surface currents on the walls at $x = 0$ and at $y = b$.

P.10–14 A standard air-filled S-band rectangular waveguide has dimensions $a = 7.21$ (cm) and $b = 3.40$ (cm). What mode types can be used to transmit electromagnetic waves having the following wavelengths?

a) $\lambda = 10$ (cm) **b)** $\lambda = 5$ (cm)

P.10–15 Determine the energy-transport velocity of the TE_{10} mode in a lossless $a \times b$ rectangular waveguide in terms of its cutoff frequency.

P.10–16 Calculate and list in ascending order the cutoff frequencies (in terms of the cutoff frequency of the dominant mode) of an $a \times b$ rectangular waveguide for the following modes: TE_{01}, TE_{10}, TE_{11}, TE_{02}, TE_{20}, TM_{11}, TM_{12}, and TM_{22} (a) if $a = 2b$ and (b) if $a = b$.

P.10–17 An air-filled $a \times b$ ($b < a < 2b$) rectangular waveguide is to be constructed to operate at 3 (GHz) in the dominant mode. We desire the operating frequency to be at least 20% higher than the cutoff frequency of the dominant mode and also at least 20% below the cutoff frequency of the next higher-order mode.

a) Give a typical design for the dimensions a and b.

b) Calculate for your design β, u_p, λ_g, and the wave impedance at the operating frequency.

P.10–18 Calculate and compare the values of β, u_p, u_g, λ_g, and $Z_{TE_{10}}$ for a 2.5 (cm) × 1.5 (cm) rectangular waveguide operating at 7.5 (GHz)

a) if the waveguide is hollow,

b) if the waveguide is filled with a dielectric medium characterized by $\epsilon_r = 2$, $\mu_r = 1$ and $\sigma = 0$.

P.10–19 An air-filled rectangular waveguide made of copper and having transverse dimensions $a = 7.20$ (cm) and $b = 3.40$ (cm) operates at a frequency 3 (GHz) in the dominant mode. Find (a) f_c, (b) λ_g, (c) α_c, and (d) the distance over which the field intensities of the propagating wave will be attenuated by 50%.

P.10–20 An average power of 1 (kW) at 10 (GHz) is to be *delivered to* an antenna at the TE_{10} mode by an air-filled rectangular copper waveguide 1 (m) long and having sides $a = 2.25$ (cm) and $b = 1.00$ (cm). Find

a) the attenuation constant due to conductor losses,

b) the maximum values of the electric and magnetic field intensities within the waveguide,

c) the maximum value of the surface current density on the conducting walls,

d) the total amount of average power dissipated in the waveguide.

P.10–21 Find the maximum amount of 10 (GHz) average power that can be transmitted through an air-filled rectangular waveguide—$a = 2.25$ (cm), $b = 1.00$ (cm)—at the TE_{10} mode without a breakdown.

P.10–22 Determine the value of (f/f_c) at which the attenuation constant due to conductor losses in an $a \times b$ rectangular waveguide for the TE_{10} mode is a minimum. What is the minimum obtainable α_c in a 2 (cm) × 1 (cm) guide? At what frequency?

P.10–23 Derive Eq. (10–188), the formula for the attenuation constant due to conductor losses in an $a \times b$ rectangular waveguide for the TM_{11} mode. Determine the value of (f/f_c) at which this attenuation constant is a minimum.

P.10–24 Measurements at 10 (GHz) on an X-band air-filled rectangular waveguide ($a = 2.29$ cm, $b = 1.02$ cm) connected to an unknown load indicate a minimum electric field at 6 (cm) from the load and a standing-wave ratio (SWR) of 1.80. Find the location and the dimensions of a symmetrical capacitive iris required to bring the SWR to unity.

P.10–25 A solution of the Bessel's differential equation

$$\frac{d^2R(r)}{dr^2} + \frac{1}{r}\frac{dR(r)}{dr} + R(r) = 0 \tag{10–332}$$

can be obtained by assuming $R(r)$ to be a power series in r as in Eq. (10–202), substituting it in the equation, and equating the sum of the coefficients of each power of r to zero. Find the solution and verify that it is consistent with $J_0(r)$ given in Eq. (10–204).

P.10–26 Starting from Maxwell's curl equations in simple media, verify Eq. (10–219) for TM modes in a circular waveguide.

P.10–27 Without deriving any new equations, roughly sketch the electric and magnetic field lines in a typical transverse plane of a circular waveguide

a) for TM_{11} mode by an extension of Fig. 10–20, and

b) for TE_{01} mode.

c) Determine the cutoff frequencies for TM_{11} and TE_{01} modes in an air-filled circular waveguide of radius a.

P.10–28 Sketch the ω–β diagrams for TE_{11} and TM_{01} modes in a hollow circular waveguide of radius a. Discuss how the diagrams will be affected

a) if a is doubled,

b) if the waveguide is filled with a nonmagnetic medium having a dielectric constant ϵ_r.

P.10–29 For a straight waveguide with a semicircular cross section shown in Fig. 10–26,

a) write the appropriate expression of E_z^0 for TM modes,

b) write the appropriate expression of H_z^0 for TE modes.

c) Explain how the eigenvalues of the respective modes can be determined.

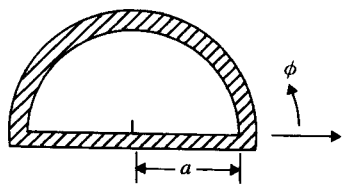

FIGURE 10–26
Cross section of a semicircular waveguide (Problem P.10–29).

P.10–30 Show that electromagnetic waves propagate along a dielectric waveguide with a velocity between that of plane-wave propagation in the dielectric medium and that in the medium outside.

P.10–31 Find the solutions of Eq. (10–260) for k_y by plotting Eqs. (10–257) and (10–258) with $\alpha d/2$ versus $k_y d/2$ for $d = 1$ (cm) and $\epsilon_r = 3.25$ if (a) $f = 200$ (MHz), and (b) $f = 500$ (MHz). Determine β and α for the lowest-order odd TM modes at the two frequencies.

P.10–32 Repeat problem P.10–31 using Eq. (10–263). What can you conclude about the even TM modes?

P.10–33 For an infinite dielectric-slab waveguide of thickness d situated in air, obtain the instantaneous expressions of all the nonzero field components for even TM modes in the slab, as well as in the upper and lower free-space regions.

P.10–34 When the slab thickness of a dielectric-slab waveguide is very small in terms of the operating wavelength, the field intensities decay very slowly away from the slab surface, and the propagation constant is nearly equal to that of the surrounding medium.

a) Show that if $k_y d \ll 1$, the following relations hold approximately for the dominant TE mode:

$$\beta \cong k_0,$$

$$\alpha \cong \frac{\mu_0 d}{2\mu_d}(k_d^2 - k_0^2),$$

where $k_d = \omega\sqrt{\mu_d \epsilon_d}$ and $k_0 = \omega\sqrt{\mu_0 \epsilon_0}$.

b) For a slab of thickness 5 (mm) and dielectric constant 3, estimate the distance from the slab surface at which the field intensities have decayed to 36.8% of their values at the surface for an operating frequency of 300 (MHz).

P.10–35 For an infinite dielectric-slab waveguide of thickness d situated in free space, obtain the instantaneous expressions of all the nonzero field components for even TE modes in the slab, as well as in the upper and lower free-space regions. Derive Eq. (10–281).

P.10–36 A waveguide consists of an infinite dielectric slab (ϵ_d, μ_d) of thickness d that is sitting on a perfect conductor.

a) What are the propagating modes and what are their cutoff frequencies?

b) Obtain the phasor expressions for the surface current and surface charge densities on the conducting base for the propagating modes.

P.10–37 A round dielectric-rod waveguide of radius a, permittivity ϵ_1, and permeability μ_1 is enveloped in a homogeneous medium characterized by permittivity ϵ_2 and permeability μ_2.

a) Write the expressions of all the field amplitudes for circularly symmetrical TE modes.

b) Obtain the characteristic equation for these modes.

P.10–38 Given an air-filled lossless rectangular cavity resonator with dimensions 8 (cm) × 6 (cm) × 5 (cm), find the first twelve lowest-order modes and their resonant frequencies.

P.10–39 An air-filled rectangular cavity with brass walls—ϵ_0, μ_0, $\sigma = 1.57 \times 10^7$ (S/m)—has the following dimensions: $a = 4$ (cm), $b = 3$ (cm), and $d = 5$ (cm).

a) Determine the dominant mode and its resonant frequency for this cavity.

b) Find the Q and the time-average stored electric and magnetic energies at the resonant frequency, assuming H_0 to be 0.1 (A/m).

P.10–40 If the rectangular cavity in Problem P.10–39 is filled with a lossless dielectric material having a dielectric constant 2.5, find

a) the resonant frequency of the dominant mode,

b) the Q,

c) the time-average stored electric and magnetic energies at the resonant frequency, assuming H_0 to be 0.1 (A/m).

P.10–41 A rectangular cavity resonator of length d is constructed from an $a \times b$ rectangular waveguide. It is to be operated at the TE_{101} mode.

a) For a fixed b, determine the relative magnitudes of a and d such that the cavity Q is maximized.

b) Obtain an expression for Q as a function of a/b under the above conditions.

P.10–42 For an air-filled rectangular copper cavity resonator,

a) calculate its Q for the TE_{101} mode if its dimensions are $a = d = 1.8b = 3.6$ (cm),

b) determine how much b should be increased in order to make Q 20% higher.

P.10–43 Derive an expression for the Q of an air-filled $a \times b \times d$ rectangular resonator for the TM_{110} mode.

P.10–44 For an air-filled circular cylindrical cavity resonator of radius a and length d:

a) Write the general expressions for the resonant frequencies and the corresponding wavelengths for TM_{mnp} and TE_{mnp} modes.

b) For $d = a$, list the first seven modes that have the lowest resonant frequencies.

P.10–45 In some microwave applications, ring-shaped cavity resonators with a very narrow center part are used. A cross section of such a resonator is shown in Fig. 10–27, in which d is very small in comparison with the resonant wavelength. Assuming that this resonator can be represented approximately by a parallel combination of the capacitance of the narrow center part and the inductance of the rest of the structure, find

a) the approximate resonant frequency,

b) the approximate resonant wavelength.

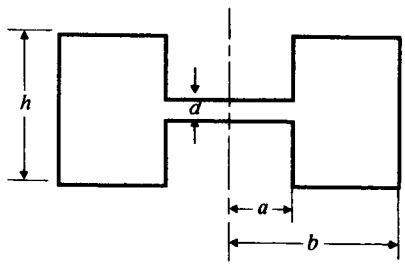

FIGURE 10–27
A ring-shaped resonator with a narrow center part (Problem P.10–45).

11

Antennas and Radiating Systems

11–1 Introduction

In Chapter 8 we studied the propagation characteristics of plane electromagnetic waves in source-free media without considering how the waves were generated. Of course, the waves must originate from sources, which in electromagnetic terms are time-varying charges and currents. In order to radiate electromagnetic energy efficiently in prescribed directions, the charges and currents must be distributed in specific ways. ***Antennas*** are structures designed for radiating electromagnetic energy effectively in a prescribed manner. Without an efficient antenna, electromagnetic energy would be localized, and wireless transmission of information over long distances would be impossible.

An antenna may be a single straight wire or a conducting loop excited by a voltage source, an aperture at the end of a waveguide, or a complex array of these properly arranged radiating elements. Reflectors and lenses may be used to accentuate certain radiation characteristics. Among radiation characteristics of importance are field pattern, directivity, impedance, and bandwidth. These parameters will be examined when particular antenna types are studied in this chapter.

To study electromagnetic radiation, we must call upon our knowledge of Maxwell's equations and relate electric and magnetic fields to time-varying charge and current distributions. A primary difficulty of this task is that the charge and current distributions on antenna structures resulting from given excitations are generally unknown and very difficult to determine. In fact, the geometrically simple case of a straight conducting wire (linear antenna) excited by a voltage source in the middle[†] has been a subject of extensive research for many years, and the exact charge and current distributions on a wire of a finite radius are extremely complicated even when the wire is assumed to be perfectly conducting. Fortunately, the radiation field

[†] This arrangement is called a ***dipole antenna.***

of such an antenna is relatively insensitive to slight deviations in the current distribution, and a physically plausible approximate current on the wire yields useful results for nearly all practical purposes. We will examine the radiation properties of linear antennas with assumed currents.

By combining Maxwell's equations we can derive nonhomogeneous wave equations in **E** and in **H** (see Problem P.11–1). However, these equations tend to involve the charge and current densities in a complicated way. It is generally simpler to solve for the auxiliary potential functions **A** and V first. Using **A** and V in Eqs. (7–55) and (7–57), we can determine **H** and **E**. For harmonic time variation in a simple medium we have

$$\mathbf{H} = \frac{1}{\mu} \nabla \times \mathbf{A} \tag{11–1}$$

and

$$\mathbf{E} = -\nabla V - j\omega \mathbf{A}. \tag{11–2}$$

The potential functions **A** and V are themselves solutions of nonhomogeneous wave equations, Eqs. (7–63) and (7–65), and the solutions are given in Eqs. (7–78) and (7–77), respectively. For harmonic time dependence the ***phasor retarded potentials*** are, from Eqs. (7–100) and (7–99),

$$\mathbf{A} = \frac{\mu}{4\pi} \int_{V'} \frac{\mathbf{J} e^{-jkR}}{R} \, dv', \tag{11–3}$$

$$V = \frac{1}{4\pi\epsilon} \int_{V'} \frac{\rho e^{-jkR}}{R} \, dv', \tag{11–4}$$

where $k = \omega\sqrt{\mu\epsilon} = 2\pi/\lambda$ is the wavenumber. Of course, **A** and V are related by the Lorentz condition, Eq. (7–98), for potentials, just as **J** and ρ are related by the equation of continuity Eq. (7–48), or

$$\nabla \cdot \mathbf{J} = -j\omega\rho. \tag{11–5}$$

Hence there is no need for evaluating the integrals in both Eqs. (11–3) and (11–4). As a matter of fact, since **E** and **H** are related by Eq. (7–104b),

$$\mathbf{E} = \frac{1}{-j\omega\epsilon} \nabla \times \mathbf{H}. \tag{11–6}$$

We follow three steps in the determination of electromagnetic fields from a current distribution: (1) determine **A** from **J** using Eq. (11–3); (2) find **H** from **A** using Eq. (11–1); and (3) find **E** from **H** using Eq. (11–6). Note that only Step 1 requires an integration and that Steps 2 and 3 involve only straightforward differentiation. This is the procedure we will use in finding the radiation pattern of antennas.

We will first study the radiation fields and characteristic properties of an elemental electric dipole and of a small current loop (or magnetic dipole). We then consider finite-length thin linear antennas, of which the half-wavelength dipole is an important special case. The radiation characteristics of a linear antenna are largely determined by its length and the manner in which it is excited. To obtain more

directivity and other desirable properties, a number of such antennas may be arranged together to form an ***antenna array***. The geometrical configuration, the spacings between the array elements, as well as the relative amplitudes and phases of the excitations in the elements all affect the field pattern of the array. Some basic properties of simple arrays will be considered.

When an antenna is used as a receiving device, its function is to collect energy from an incoming electromagnetic wave and deliver it to a receiver. Any antenna that is useful for radiation is also useful for reception. We will use the reciprocity theorem to show that the pattern, directivity, input impedance, effective height, and effective aperture of an antenna are the same for transmitting as for receiving. We will define backscatter cross section and study the radar equation and the effect of wave propagation near the earth's surface. Finally, we will discuss such antenna types as traveling-wave antennas, Yagi-Uda antennas, helical antennas, broadband antennas and arrays, and aperture antennas.

11–2 Radiation Fields of Elemental Dipoles

In this section we study the radiation fields of the simplest types of all radiating systems—namely, elemental oscillating electric and magnetic dipoles. We will find that the field solutions for electric and magnetic dipoles are duals of each other. As a consequence, the radiation properties of one can be deduced from those of the other without recalculation.

11-2.1 THE ELEMENTAL ELECTRIC DIPOLE

Consider the elemental oscillating electric dipole (in free space), as shown in Fig. 11–1, which consists of a short conducting wire of length $d\ell$ terminated in two small conductive spheres or disks (capacitive loading). We assume the current in the wire to be uniform and to vary sinusoidally with time:

$$i(t) = I \cos \omega t = \mathscr{R}e[Ie^{j\omega t}]. \tag{11-7}$$

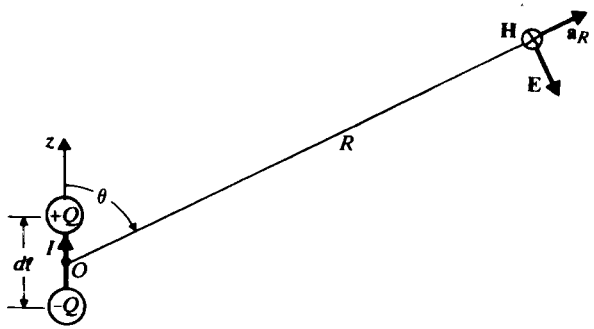

FIGURE 11–1
A Hertzian dipole.

Since the current vanishes at the ends of the wire, charge must be deposited there. The relation between the charge and the current is

$$i(t) = \pm\frac{dq(t)}{dt}. \tag{11–8}$$

In phasor notation, $q(t) = \mathcal{R}e[Qe^{j\omega t}]$, we have

$$I = \pm j\omega Q \tag{11–9}$$

or

$$Q = \pm\frac{I}{j\omega}, \tag{11–10}$$

where, for the indicated current direction in Fig. 11–1, the positive sign is for the charge on the upper end and the negative sign for the charge on the lower end. The pair of equal and opposite charges separated by a short distance effectively form an electric dipole with a vector phasor electric moment

$$\mathbf{p} = \mathbf{a}_z Q\, d\ell \qquad (\text{C·m}). \tag{11–11}$$

Such an oscillating dipole is called a ***Hertzian dipole.***

To determine the electromagnetic field of a Hertzian dipole, we follow the three steps outlined in Section 11–1. The phasor representation of the retarded vector potential is, from Eq. (11–3),

$$\mathbf{A} = \mathbf{a}_z \frac{\mu_0 I\, d\ell}{4\pi}\left(\frac{e^{-j\beta R}}{R}\right), \tag{11–12}$$

where $\beta = k_0 = \omega/c = 2\pi/\lambda$. Since

$$\mathbf{a}_z = \mathbf{a}_R \cos\theta - \mathbf{a}_\theta \sin\theta, \tag{11–13}$$

the spherical components of $\mathbf{A} = \mathbf{a}_R A_R + \mathbf{a}_\theta A_\theta + \mathbf{a}_\phi A_\phi$ are

$$A_R = A_z \cos\theta = \frac{\mu_0 I\, d\ell}{4\pi}\left(\frac{e^{-j\beta R}}{R}\right)\cos\theta, \tag{11–14a}$$

$$A_\theta = -A_z \sin\theta = -\frac{\mu_0 I\, d\ell}{4\pi}\left(\frac{e^{-j\beta R}}{R}\right)\sin\theta, \tag{11–14b}$$

$$A_\phi = 0. \tag{11–14c}$$

From the geometry of Fig. 11–1 we expect no variation with respect to the coordinate ϕ. We have, from Eq. (2–139)

$$\begin{aligned}\mathbf{H} &= \frac{1}{\mu_0}\nabla \times \mathbf{A} = \mathbf{a}_\phi \frac{1}{\mu_0 R}\left[\frac{\partial}{\partial R}(RA_\theta) - \frac{\partial A_R}{\partial \theta}\right] \\ &= -\mathbf{a}_\phi \frac{I\, d\ell}{4\pi}\beta^2 \sin\theta\left[\frac{1}{j\beta R} + \frac{1}{(j\beta R)^2}\right]e^{-j\beta R}.\end{aligned} \tag{11–15}$$

The electric field intensity can be obtained from Eq. (11–6):

$$\mathbf{E} = \frac{1}{j\omega\epsilon_0}\nabla \times \mathbf{H}$$
$$= \frac{1}{j\omega\epsilon_0}\left[\mathbf{a}_R \frac{1}{R\sin\theta}\frac{\partial}{\partial\theta}(H_\phi \sin\theta) - \mathbf{a}_\theta \frac{1}{R}\frac{\partial}{\partial R}(RH_\phi)\right], \tag{11–16}$$

which gives

$$E_R = -\frac{I\,d\ell}{4\pi}\eta_0\beta^2 2\cos\theta\left[\frac{1}{(j\beta R)^2} + \frac{1}{(j\beta R)^3}\right]e^{-j\beta R}, \tag{11–16a}$$

$$E_\theta = -\frac{I\,d\ell}{4\pi}\eta_0\beta^2 \sin\theta\left[\frac{1}{j\beta R} + \frac{1}{(j\beta R)^2} + \frac{1}{(j\beta R)^3}\right]e^{-j\beta R}, \tag{11–16b}$$

$$E_\phi = 0, \tag{11–16c}$$

where $\eta_0 = \sqrt{\mu_0/\epsilon_0} \cong 120\pi\ (\Omega)$.

Equations (11–15) and (11–16) constitute the electromagnetic field of a Hertzian dipole. Note that in deriving these expressions we used only the current in the dipole to find the vector potential **A**; the charges at the ends of the dipole did not enter into the calculations. We could, however, take an alternative approach by finding both **A** from $I\,d\ell$, as in Eq. (11–12), and the scalar potential V from the pair of equal and opposite charges using Eq. (11–4). The electric field intensity could then be determined from Eq. (11–2), instead of from Eq. (11–6). The result would be exactly the same as that obtained above (see Problem P.11–2).

The complete field expressions in Eqs. (10–15) and (10–16) are fairly complicated. It is advantageous to examine their behavior in regions near to and far from the dipole separately.

Near Field In the region near to the Hertzian dipole (in the ***near zone***), $\beta R = 2\pi R/\lambda \ll 1$, the leading term in Eq. (11–15) is

$$H_\phi = \frac{I\,d\ell}{4\pi R^2}\sin\theta, \tag{11–17}$$

where we have approximated the factor $e^{-j\beta R} = 1 - j\beta R - (\beta R)^2/2 + \cdots$ by unity. Equation (11–17) is exactly what would be obtained for the magnetic field intensity due to a current element $I\,d\ell$ by applying the Biot-Savart law in magnetostatics as given in Eq. (6–33b).

The leading near-zone terms for the electric field intensity are, from Eqs. (11–16a) and (11–16b),

$$E_R = \frac{p}{4\pi\epsilon_0 R^3}2\cos\theta \tag{11–18a}$$

and

$$E_\theta = \frac{p}{4\pi\epsilon_0 R^3}\sin\theta, \tag{11–18b}$$

where the phasor relations (11–10) and (11–11) have been used. These expressions are identical to those of the electric field intensity due to an elemental electric dipole of a moment p in the z-direction, as given in Eq. (3–31), obtained by an application of the laws of electrostatics. The ***near-zone fields*** of an oscillating time-varying dipole are then ***quasi-static fields***.

Far Field The region where $\beta R = 2\pi R/\lambda \gg 1$ is the ***far zone***. The far-zone leading terms in Eqs. (11–15) and (11–16) are

$$H_\phi = j\frac{I\,d\ell}{4\pi}\left(\frac{e^{-j\beta R}}{R}\right)\beta \sin\theta \qquad \text{(A/m)}, \tag{11–19a}$$

$$E_\theta = j\frac{I\,d\ell}{4\pi}\left(\frac{e^{-j\beta R}}{R}\right)\eta_0\beta \sin\theta \qquad \text{(V/m)}. \tag{11–19b}$$

Several important observations can be made on these ***far-zone fields***. First, E_θ and H_ϕ are in space quadrature and in time phase. Second, their ratio $E_\theta/H_\phi = \eta_0$ is a constant equal to the intrinsic impedance of the medium (which is, in the present case, free space). The far-zone fields, then, have the same properties as those of a plane wave. This is not unexpected, since at very large distances from the dipole a spherical wavefront closely resembles a plane wavefront.

A third observation from Eqs. (11–19a, b) is that the magnitude of the far-zone fields varies inversely with the distance from the source. The phase of both E_θ and H_ϕ is a periodic function of R with a period that is the wavelength:

$$\lambda = \frac{2\pi}{\beta} = \frac{c}{f}. \tag{11–20}$$

Note that the far-zone condition $\beta R \gg 1$ translates into $R \gg \lambda/2\pi$; hence one has to be farther away from the dipole at lower frequencies in order to be in the far zone. (Other characteristics of far-zone fields will be discussed in Section 11–3.)

11–2.2 THE ELEMENTAL MAGNETIC DIPOLE

Let us now consider a small filamentary loop of radius b carrying a uniform time-harmonic current $i(t) = I\cos\omega t$ around its circumference, as shown in Fig. 11–2. This is an elemental magnetic dipole with a vector phasor magnetic moment

$$\mathbf{m} = \mathbf{a}_z I\pi b^2 = \mathbf{a}_z m \qquad (\text{A}\cdot\text{m}^2). \tag{11–21}$$

To determine the electromagnetic field, we first find the vector potential. The procedure is the same as that used in Section 6–5, except for the time-dependent nature of the current. Instead of starting from Eq. (6–39), we have

$$\mathbf{A} = \frac{\mu_0 I}{4\pi}\oint \frac{e^{-j\beta R_1}}{R_1}\,d\ell'. \tag{11–22}$$

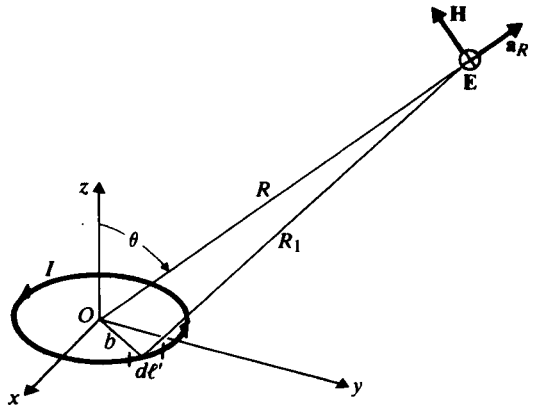

FIGURE 11–2
A magnetic dipole.

The integral in Eq. (11–22) is relatively difficult to carry out exactly because R_1 changes with the location of $d\ell'$ on the loop. For a small loop the exponential factor in the numerator can be written as

$$\begin{aligned} e^{-j\beta R_1} &= e^{-j\beta R} e^{-j\beta(R_1 - R)} \\ &\cong e^{-j\beta R}[1 - j\beta(R_1 - R)]. \end{aligned} \tag{11–23}$$

Substitution of Eq. (11–23) in Eq. (11–22) yields approximately

$$\mathbf{A} = \frac{\mu_0 I}{4\pi} e^{-j\beta R}\left[(1 + j\beta R)\oint \frac{d\ell'}{R_1} - j\beta \oint d\ell'\right]. \tag{11–24}$$

The second integral in Eq. (11–24) obviously vanishes. The first integral is the same as that in Eq. (6–39), except for the multiplying factor $(1 + j\beta R)e^{-j\beta R}$. In view of the result in Eq. (6–43) we have

$$\mathbf{A} = \mathbf{a}_\phi \frac{\mu_0 m}{4\pi R^2}(1 + j\beta R)e^{-j\beta R} \sin\theta. \tag{11–25}$$

The electric and magnetic field intensities can be determined by straightforward differentiation using Eqs. (11–6) and (11–1), respectively:

$$E_\phi = \frac{j\omega\mu_0 m}{4\pi}\beta^2 \sin\theta\left[\frac{1}{j\beta R} + \frac{1}{(j\beta R)^2}\right]e^{-j\beta R}, \tag{11–26a}$$

$$H_R = -\frac{j\omega\mu_0 m}{4\pi\eta_0}\beta^2 2\cos\theta\left[\frac{1}{(j\beta R)^2} + \frac{1}{(j\beta R)^3}\right]e^{-j\beta R}, \tag{11–26b}$$

$$H_\theta = -\frac{j\omega\mu_0 m}{4\pi\eta_0}\beta^2 \sin\theta\left[\frac{1}{j\beta R} + \frac{1}{(j\beta R)^2} + \frac{1}{(j\beta R)^3}\right]e^{-j\beta R}. \tag{11–26c}$$

Comparison of Eqs. (11–26a, b, c) with Eqs. (11–15) and (11–16a, b) reveals immediately the dual nature of the electromagnetic fields of electric and magnetic dipoles.

Let $(\mathbf{E}_e, \mathbf{H}_e)$ denote the electric and magnetic fields of the electric dipole and $(\mathbf{E}_m, \mathbf{H}_m)$ the electric and magnetic fields of the magnetic dipole. We have

$$\mathbf{E}_e = \eta_0 \mathbf{H}_m \tag{11–27}$$

and

$$\mathbf{H}_e = -\frac{\mathbf{E}_m}{\eta_0} \tag{11–28}$$

if the electric and magnetic dipole moments are related as follows:

$$I\,d\ell = j\beta m, \tag{11–29}$$

where $\beta = \omega\mu_0/\eta_0 = \omega\sqrt{\mu_0\epsilon_0}$. Equations (11–27) and (11–28) are results expected from the principle of duality, which was introduced in connection with Example 7–7. Thus Hertzian electric dipole and elemental magnetic dipole are dual devices, and their electromagnetic fields are dual solutions of source-free Maxwell's equations. As a consequence of this duality, the discussions about the nature of the near and far fields of an electric dipole apply to the dual quantities of a magnetic dipole. In particular, the far-zone ($\beta R \gg 1$) fields of a magnetic dipole are

$$\boxed{E_\phi = \frac{\omega\mu_0 m}{4\pi}\left(\frac{e^{-j\beta R}}{R}\right)\beta \sin\theta \quad \text{(V/m)},} \tag{11–30a}$$

$$\boxed{H_\theta = -\frac{\omega\mu_0 m}{4\pi\eta_0}\left(\frac{e^{-j\beta R}}{R}\right)\beta \sin\theta \quad \text{(A/m)}.} \tag{11–30b}$$

We can see that the far-field intensities vary inversely as R and their ratio E_ϕ/H_θ equals the intrinsic impedance η_0 of free space.

Examination of the far-field E_θ in Eq. (11–19b) of the electric dipole and E_ϕ in Eq. (11–30a) of the magnetic dipole reveals that they have the same pattern function $|\sin\theta|$ and are in both space and time quadrature. Thus it is possible to combine electric and magnetic dipoles to form an antenna that produces circular polarization (see Problem P.11–4).

11–3 Antenna Patterns and Antenna Parameters

In antenna problems we are primarily interested in the far-zone fields. These are also called ***radiation fields***. No physical antennas radiate uniformly in all directions in space. The graph that describes the relative far-zone field strength versus direction at a fixed distance from an antenna is called the ***radiation pattern*** of the antenna, or

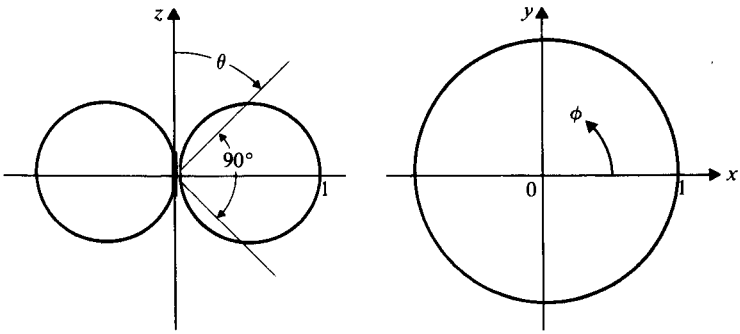

(a) E-plane pattern. (b) H-plane pattern.

FIGURE 11–3
Radiation patterns of a Hertzian dipole.

simply the ***antenna pattern***. In general, an antenna pattern is three-dimensional, varying with both θ and ϕ in a spherical coordinate system. The difficulties of making three-dimensional plots can be avoided—as is the usual practice—by plotting separately the magnitude of the normalized field strength (with respect to the peak value) versus θ for a constant ϕ (an ***E-plane pattern***) and the magnitude of the normalized field strength versus ϕ for $\theta = \pi/2$ (the ***H-plane pattern***).

EXAMPLE 11–1 Plot the E-plane and H-plane radiation patterns of a Hertzian dipole.

Solution Since E_θ and H_ϕ in the far zone are proportional to each other, we need only consider the normalized magnitude of E_θ.

a) *E-plane pattern.* At a given R, E_θ is independent of ϕ; and from Eq. (11–19b) the normalized magnitude of E_θ is

$$\text{Normalized } |E_\theta| = |\sin\theta|. \tag{11–31}$$

This is the E-plane ***pattern function*** of a Hertzian dipole. For any given ϕ, Eq. (11–31) represents a pair of circles, as shown in Fig. 11–3(a).

b) *H-plane pattern.* At a given R and for $\theta = \pi/2$ the normalized magnitude of E_θ is $|\sin\theta| = 1$. The H-plane pattern is then simply a circle of unity radius centered at the z-directed dipole, as shown in Fig. 11–3(b).

The radiation pattern of practical antennas are usually more complicated than those shown in Fig. 11–3. A typical H-plane pattern might look like the one illustrated in Fig. 11–4(a), which is plotted in polar coordinates with normalized $|E_\theta|$ versus ϕ. It generally has a major maximum and several minor maxima. The region of maximum

radiation between the first null points around it is the ***main beam***, and the regions of minor maxima are ***sidelobes***.

Sometimes it is convenient to plot antenna patterns in rectangular coordinates. The polar plot in Fig. 11–4(a) will appear as Fig. 11–4(b) in rectangular coordinates. Since the field intensities in the main-beam and sidelobe directions may differ by many orders of magnitude, antenna patterns are frequently plotted in a logarithmic scale measured in decibels down from the main-beam level. The pattern in Fig. 11–4(b) converted to a decibel scale will have the shape shown in Fig. 11–4(c).

In the comparison of various antenna patterns the following characteristic parameters are of importance: (1) width of main beam, (2) sidelobe levels, and (3) directivity.

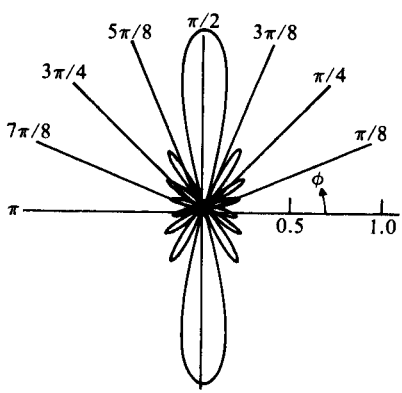

(a) A typical radiation pattern in polar coordinates.

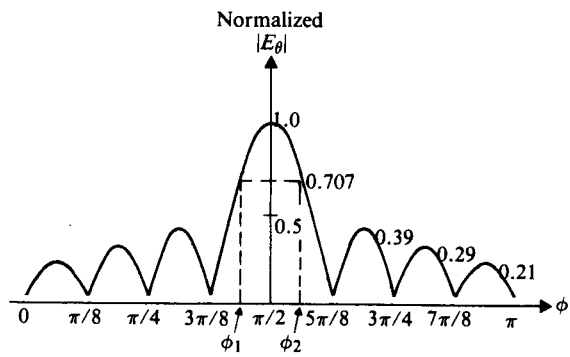

(b) Radiation pattern in rectangular coordinates.

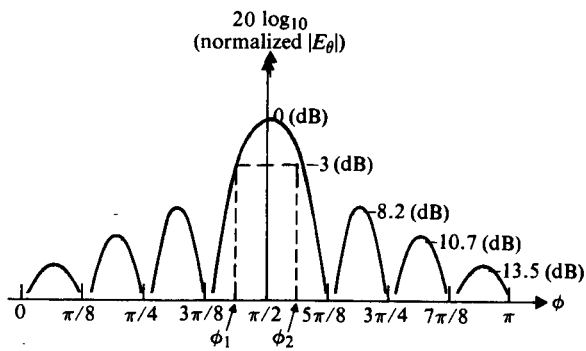

(c) Radiation pattern in rectangular coordinates plotted in dB scale.

FIGURE 11–4
Typical *H*-plane radiation patterns.

The significance of each of these parameters is explained below.

1. *Width of main beam* (or simply ***beamwidth***). The main-beam beamwidth describes the sharpness of the main radiation region. It is generally taken to be the angular width of a pattern between the half-power, or -3 (dB), points. In electric-intensity plots it is the angular width between points that are $1/\sqrt{2}$ or 0.707 times the maximum intensity. Thus, the H-plane pattern in Fig. 11–4 has a 3 (dB) beamwidth equal to $(\phi_2 - \phi_1)$, and the E-plane pattern of the Hertzian dipole in Fig. 11–3(a) has a 3 (dB) beamwidth of 90°. Occasionally the angular width of the main beam between -10 (dB) points or between the first nulls is also of interest. Of course, the main beam must point in the direction where the antenna is designed to have its maximum radiation.
2. *Sidelobe levels.* Sidelobes of a directive (nonisotropic) pattern represent regions of unwanted radiation; they should have levels as low as possible. Generally, the levels of distant sidelobes are lower than the levels of those near the main beam. Hence, when one talks about the sidelobe level of an antenna pattern, one usually refers to the first (the nearest and highest) sidelobe. In modern radar applications, sidelobe levels of the order of minus 40 or more decibels are required. In practical applications the locations of the sidelobes are also of importance.
3. *Directivity.* The beamwidth of an antenna pattern specifies the sharpness of the main beam, but it does not provide us with any information about the rest of the pattern. For example, the sidelobes may be very high—an undesirable feature. A commonly used parameter to measure the overall ability of an antenna to direct radiated power in a given direction is ***directive gain***, which may be defined in terms of radiation intensity. ***Radiation intensity*** is the time-average power per unit solid angle. The SI unit for radiation intensity is watt per steradian (W/sr). Since there are R^2 square meters of spherical surface area for each unit solid angle, radiation intensity, U, equals R^2 times the time-average power per unit area or R^2 times the magnitude of the time-average Poynting vector, $\mathscr{P}_{av}$:

$$U = R^2 \mathscr{P}_{av} \qquad \text{(W/sr)}. \tag{11–32}$$

The total time-average power radiated is

$$P_r = \oint \mathscr{P}_{av} \cdot d\mathbf{s} = \oint U \, d\Omega \qquad \text{(W)}, \tag{11–33}$$

where $d\Omega$ is the differential solid angle, $d\Omega = \sin\theta \, d\theta \, d\phi$.

The ***directive gain***, $G_D(\theta, \phi)$, of an antenna pattern is the ratio of the radiation intensity in the direction (θ, ϕ) to the average radiation intensity:

$$G_D(\theta, \phi) = \frac{U(\theta, \phi)}{P_r/4\pi} = \frac{4\pi U(\theta, \phi)}{\oint U \, d\Omega}. \tag{11–34}$$

Obviously, the directive gain of an isotropic or omnidirectional antenna (an antenna that radiates uniformly in all directions) is unity. However, an isotropic antenna does not exist in practice.

The maximum directive gain of an antenna is called the ***directivity*** of the antenna. It is the ratio of the maximum radiation intensity to the average radiation intensity and is usually denoted by D:

$$D = \frac{U_{\max}}{U_{av}} = \frac{4\pi U_{\max}}{P_r} \quad \text{(Dimensionless).} \tag{11–35}$$

In terms of electric field intensity, D can be expressed as

$$D = \frac{4\pi |E_{\max}|^2}{\int_0^{2\pi} \int_0^{\pi} |E(\theta, \phi)|^2 \sin\theta \, d\theta \, d\phi} \quad \text{(Dimensionless).} \tag{11–36}$$

Directivity is frequently expressed in decibels, referring to unity.

EXAMPLE 11–2 Find the directive gain and the directivity of a Hertzian dipole.

Solution For a Hertzian dipole the magnitude of the time-average Poynting vector is

$$\mathscr{P}_{av} = \tfrac{1}{2}\mathscr{R}e|\mathbf{E} \times \mathbf{H}^*| = \tfrac{1}{2}|E_\theta|\,|H_\phi|. \tag{11–37}$$

Hence from Eqs. (11–19a, b) and (11–32),

$$U = \frac{(I\,d\ell)^2}{32\pi^2} \eta_0 \beta^2 \sin^2\theta. \tag{11–38}$$

The directive gain can be obtained from Eq. (11–34):

$$G_D(\theta, \phi) = \frac{4\pi \sin^2\theta}{\int_0^{2\pi} \int_0^{\pi} (\sin^2\theta) \sin\theta \, d\theta \, d\phi}$$

$$= \tfrac{3}{2} \sin^2\theta.$$

The directivity is the maximum value of $G_D(\theta, \phi)$:

$$D = G_D\left(\frac{\pi}{2}, \phi\right) = 1.5,$$

which corresponds to $10 \log_{10} 1.5$ or 1.76 (dB).

We note that beamwidth, sidelobe levels, and directive gain are parameters of an antenna pattern; they do not convey information about the efficiency or the input impedance of the antenna. A measure of antenna efficiency is the power gain. The ***power gain***, or simply the ***gain***, G_P, of an antenna referred to an isotropic source is the ratio of its maximum radiation intensity to the radiation intensity of a lossless isotropic source with the same power input. The directive gain as defined in Eq. (11–34) is based on radiated power P_r. Because of ohmic power loss, P_ℓ, in the

antenna itself as well as in nearby lossy structures including the ground, P_r is less than the total input power P_i. We have

$$P_i = P_r + P_\ell. \tag{11-39}$$

The power gain of an antenna is then

$$\boxed{G_P = \frac{4\pi U_{\max}}{P_i} \quad \text{(Dimensionless).}} \tag{11-40}$$

The ratio of the gain to the directivity of an antenna is the ***radiation efficiency***, η_r:

$$\boxed{\eta_r = \frac{G_P}{D} = \frac{P_r}{P_i} \quad \text{(Dimensionless).}} \tag{11-41}$$

Normally, the efficiency of well-constructed antennas is very close to 100%.

A useful measure of the amount of power radiated by an antenna is radiation resistance. The ***radiation resistance*** of an antenna is the value of a hypothetical resistance that would dissipate an amount of power equal to the radiated power P_r when the current in the resistance is equal to the maximum current along the antenna. Naturally, a high radiation resistance is a desirable property for an antenna.

EXAMPLE 11–3 Find the radiation resistance of a Hertzian dipole.

Solution If we assume no ohmic losses, the time-average power radiated by a Hertzian dipole for an input time-harmonic current with an amplitude I is

$$P_r = \tfrac{1}{2}\int_0^{2\pi}\int_0^{\pi} E_\theta H_\phi^* R^2 \sin\theta \, d\theta \, d\phi. \tag{11-42}$$

Using the far-zone fields in Eqs. (11–19a, b), we find

$$\begin{aligned} P_r &= \frac{I^2(d\ell)^2}{32\pi^2}\eta_0\beta^2 \int_0^{2\pi}\int_0^{\pi} \sin^3\theta \, d\theta \, d\phi \\ &= \frac{I^2(d\ell)^2}{12\pi}\eta_0\beta^2 = \frac{I^2}{2}\left[80\pi^2\left(\frac{d\ell}{\lambda}\right)^2\right]. \end{aligned} \tag{11-43}$$

In this last expression we have used 120π for the intrinsic impedance of free space, η_0, and substituted $2\pi/\lambda$ for β.

Since the current along the short Hertzian dipole is uniform, we refer the power dissipated in the radiation resistance R_r to I. Equating $I^2R_r/2$ to P_r, we obtain

$$\boxed{R_r = 80\pi^2\left(\frac{d\ell}{\lambda}\right)^2 \quad (\Omega).} \tag{11-44}$$

As an example, if $d\ell = 0.01\lambda$, R_r is only about 0.08 (Ω), an extremely small value. Hence a short dipole antenna is a poor radiator of electromagnetic power. However, it is erroneous to say without qualification that the radiation resistance of a dipole antenna increases as the square of its length because Eq. (11–44) holds only if $d\ell \ll \lambda$.

Radiation resistance may be quite different from the real part of the input impedance because the latter includes ohmic losses in the antenna structure itself as well as losses in the ground. The input impedance of a short dipole antenna has a large capacitive reactance, which makes it difficult to match and therefore difficult to feed power to the antenna efficiently.

EXAMPLE 11–4 Find the radiation efficiency of an isolated Hertzian dipole made of a metal wire of radius a, length d, and conductivity σ.

Solution Let I be the amplitude of the current in the wire dipole having a loss resistance R_ℓ. Then the ohmic power loss is

$$P_\ell = \tfrac{1}{2} I^2 R_\ell. \tag{11–45}$$

In terms of radiation resistance R_r the radiated power is

$$P_r = \tfrac{1}{2} I^2 R_r. \tag{11–46}$$

From Eqs. (11–39) and (11–41) we have

$$\begin{aligned} \eta_r &= \frac{P_r}{P_r + P_\ell} = \frac{R_r}{R_r + R_\ell} \\ &= \frac{1}{1 + (R_\ell / R_r)}, \end{aligned} \tag{11–47}$$

where R_r has been found in Eq. (11–44). The loss resistance R_ℓ of the metal wire can be expressed in terms of the surface resistance R_s:

$$R_\ell = R_s \left(\frac{d\ell}{2\pi a} \right), \tag{11–48}$$

where

$$R_s = \sqrt{\frac{\pi f \mu_0}{\sigma}} \tag{11–49}$$

as given in Eq. (9–26b). Using Eqs. (11–44) and (11–48) in Eq. (11–47), we obtain the radiation efficiency of an isolated Hertzian dipole:

$$\eta_r = \frac{1}{1 + \dfrac{R_s}{160\pi^3} \left(\dfrac{\lambda}{a} \right) \left(\dfrac{\lambda}{d\ell} \right)}. \tag{11–50}$$

Assume that $a = 1.8$ (mm), $d\ell = 2$ (m), operating frequency $f = 1.5$ (MHz), and σ (for copper) $= 5.80 \times 10^7$ (S/m). We find that

$$\lambda = \frac{c}{f} = \frac{3 \times 10^8}{1.5 \times 10^6} = 200 \quad \text{(m)},$$

$$R_s = \sqrt{\frac{\pi \times (1.50 \times 10^6) \times (4\pi 10^{-7})}{5.80 \times 10^7}} = 3.20 \times 10^{-4} \quad (\Omega),$$

$$R_\ell = 3.20 \times 10^{-4} \times \left(\frac{2}{2\pi 1.8 \times 10^{-3}}\right) = 0.057 \quad (\Omega),$$

$$R_r = 80\pi^2 \left(\frac{2}{200}\right)^2 = 0.079 \quad (\Omega),$$

and

$$\eta_r = \frac{0.079}{0.079 + 0.057} = 58\%,$$

which is very low. Equation (11–50) shows that smaller values of (a/λ) and $(d\ell/\lambda)$ lower the radiation efficiency. ■

11–4 Thin Linear Antennas

We have just indicated that a short dipole antenna is not a good radiator of electromagnetic power because of its low radiation resistance and low radiation efficiency. We now examine the radiation characteristics of a center-fed thin straight antenna having a length comparable to a wavelength, as shown in Fig. 11–5. Such an antenna is a ***linear dipole antenna.*** If the current distribution along the antenna is known, we can find its radiation field by integrating over the entire length of the antenna the radiation field due to an elemental dipole. The determination of the exact current distribution on such a seemingly simple geometrical configuration (a straight wire

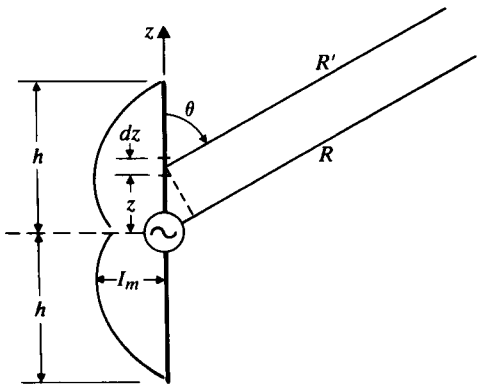

FIGURE 11–5
A center-fed linear dipole with sinusoidal current distribution.

of a finite radius) is, however, a very difficult boundary-value problem even if the wire is assumed to be perfectly conducting. The current must be zero at the ends of the wire where charges are deposited, and the tangential electric field due to all currents and charges must vanish at every point on the wire surface. An analytical formulation of the problem leads to an integral equation in which the current distribution along the antenna is the unknown function under the integral. Unfortunately, an exact solution of the integral equation does not exist. Various approximate solutions have been attempted. With the advent of high-speed digital computers, numerical solutions for current distributions and input impedances can be obtained for linear antennas of specific lengths and thicknesses. The ratio of the voltage and the current at the feed points is the input impedance. Both the solution procedure and the numerical results are quite involved, and we shall not delve into them in this book. For our purposes the knowledge of the exact current distribution on the linear antenna is not of prime importance; a good estimate will give us considerable useful information on the radiation characteristics of the antenna. We assume a sinusoidal current distribution on a very thin, straight dipole. Such a current distribution constitutes a kind of standing wave over the dipole and represents a good approximation.

Since the dipole is center-driven, the currents on the two halves of the dipole are symmetrical and go to zero at the ends. We write the current phasor as

$$\begin{aligned} I(z) &= I_m \sin \beta(h - |z|), \\ &= \begin{cases} I_m \sin \beta(h - z), & z > 0, \\ I_m \sin \beta(h + z), & z < 0. \end{cases} \end{aligned} \tag{11–51}$$

We are interested only in the far-zone fields. The far-field contribution from the differential current element $I\,dz$ is, from Eqs. (11–19a, b),

$$dE_\theta = \eta_0\, dH_\phi = j \frac{I\,dz}{4\pi} \left(\frac{e^{-j\beta R'}}{R'} \right) \eta_0 \beta \sin \theta. \tag{11–52}$$

Now R' in Eq. (11–52) is slightly different from R measured to the origin of the spherical coordinates, which coincides with the center of the dipole. In the far zone, $R \gg h$,

$$R' = (R^2 + z^2 - 2Rz \cos \theta)^{1/2} \cong R - z \cos \theta. \tag{11–53}$$

The magnitude difference between $1/R'$ and $1/R$ is insignificant, but the approximate relation in Eq. (11–53) must be retained in the phase term. Using Eqs. (11–51) and (11–53) in Eq. (11–52) and integrating, we have

$$\begin{aligned} E_\theta &= \eta_0 H_\phi \\ &= j \frac{I_m \eta_0 \beta \sin \theta}{4\pi R} e^{-j\beta R} \int_{-h}^{h} \sin \beta(h - |z|) e^{j\beta z \cos \theta}\, dz. \end{aligned} \tag{11–54}$$

The integrand in Eq. (11–54) is the product of an even function of z, $\sin \beta(h - |z|)$, and

$$e^{j\beta z \cos \theta} = \cos (\beta z \cos \theta) + j \sin (\beta z \cos \theta),$$

where $\sin(\beta z \cos\theta)$ is an odd function of z. Integrating between symmetrical limits $-h$ and h, we find that only the part of the integrand containing the product $\sin\beta(h-|z|)\cos(\beta z\cos\theta)$ does not vanish. Equation (11–54) then reduces to

$$E_\theta = \eta_0 H_\phi = j\frac{I_m\eta_0\beta\sin\theta}{2\pi R}e^{-j\beta R}\int_0^h \sin\beta(h-z)\cos(\beta z\cos\theta)\,dz$$
$$= \frac{j60I_m}{R}e^{-j\beta R}F(\theta), \tag{11–55}$$

where

$$F(\theta) = \frac{\cos(\beta h\cos\theta) - \cos\beta h}{\sin\theta}. \tag{11–56}$$

The factor $|F(\theta)|$ is the E-plane ***pattern function*** of a linear dipole antenna. It describes the radiation pattern or the variation of the normalized far field, $|E_\theta|$, versus the angle θ. The exact shape of the radiation pattern represented by $|F(\theta)|$ in Eq. (11–56) depends on the value of $\beta h = 2\pi h/\lambda$ and can be quite different for different antenna lengths. The radiation pattern, however, is always symmetrical with respect to the $\theta = \pi/2$ plane. Figure 11–6 shows the E-plane patterns for four different dipole lengths measured in terms of wavelength: $2h/\lambda = \frac{1}{2}, 1, \frac{3}{2}$ and 2. The H-plane patterns are circles inasmuch as $F(\theta)$ is independent of ϕ. From the patterns in Fig. 11–6 we see that the direction of maximum radiation tends to shift away from the $\theta = 90°$ plane when the dipole length approaches $3\lambda/2$. For $2h = 2\lambda$ there is no radiation in the $\theta = 90°$ plane.

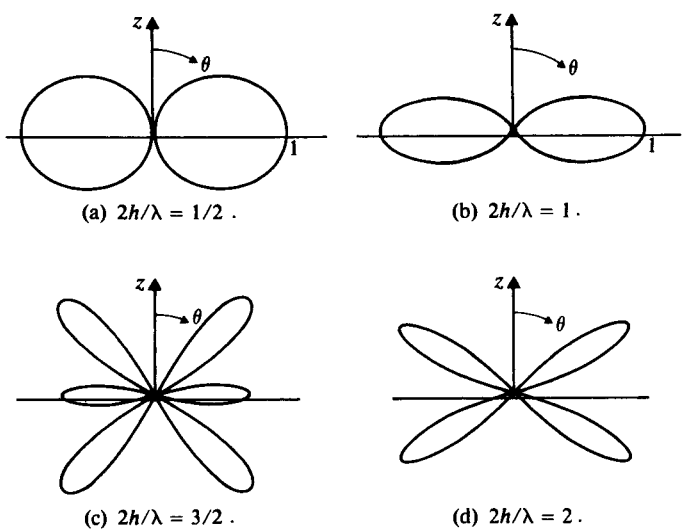

(a) $2h/\lambda = 1/2$. (b) $2h/\lambda = 1$.

(c) $2h/\lambda = 3/2$. (d) $2h/\lambda = 2$.

FIGURE 11–6
E-plane radiation patterns for center-fed dipole antennas.

11–4.1 THE HALF-WAVE DIPOLE

The half-wave dipole having a length $2h = \lambda/2$ is of particular practical importance because of its desirable pattern and impedance characteristics. We shall now examine its properties in more detail.

For a half-wave dipole, $\beta h = 2\pi h/\lambda = \pi/2$, the pattern function in Eq. (11–56) becomes

$$F(\theta) = \frac{\cos\left[(\pi/2)\cos\theta\right]}{\sin\theta}. \tag{11–57}$$

This function has a maximum equal to unity at $\theta = 90°$ and has nulls at $\theta = 0°$ and 180°. The corresponding E-plane radiation pattern is sketched in Fig. 11–6(a). The far-zone field phasors are, from Eq. (11–55),

$$E_\theta = \frac{j60I_m}{R} e^{-j\beta R}\left\{\frac{\cos\left[(\pi/2)\cos\theta\right]}{\sin\theta}\right\} \tag{11–58}$$

and

$$H_\phi = \frac{jI_m}{2\pi R} e^{-j\beta R}\left\{\frac{\cos\left[(\pi/2)\cos\theta\right]}{\sin\theta}\right\}. \tag{11–59}$$

The magnitude of the time-average Poynting vector is

$$\mathscr{P}_{av} = \frac{1}{2} E_\theta H_\phi^* = \frac{15I_m^2}{\pi R^2}\left\{\frac{\cos\left[(\pi/2)\cos\theta\right]}{\sin\theta}\right\}^2. \tag{11–60}$$

The total power radiated by a half-wave dipole is obtained by integrating $\mathscr{P}_{av}$ over the surface of a great sphere:

$$\begin{aligned} P_r &= \int_0^{2\pi}\int_0^{\pi} \mathscr{P}_{av} R^2 \sin\theta\, d\theta\, d\phi \\ &= 30I_m^2 \int_0^{\pi} \frac{\cos^2\left[(\pi/2)\cos\theta\right]}{\sin\theta}\, d\theta. \end{aligned} \tag{11–61}$$

The integral in Eq. (11–61) can be evaluated numerically to give a value 1.218. Hence

$$P_r = 36.54I_m^2 \quad \text{(W)}, \tag{11–62}$$

from which we obtain the radiation resistance of a free-standing half-wave dipole:

$$R_r = \frac{2P_r}{I_m^2} = 73.1 \quad (\Omega). \tag{11–63}$$

Neglecting losses, we find that the input resistance of a thin half-wave dipole equals 73.1 (Ω) and that the input reactance is a small positive number that can be made to vanish when the dipole length is adjusted to be slightly shorter than $\lambda/2$. (As we have indicated before, the actual calculation of the input impedance is tedious and is beyond the scope of this book.)

The directivity of a half-wave dipole can be found by using Eq. (11–35). We have, from Eqs. (11–32) and (11–60),

$$U_{\max} = R^2 \mathscr{P}_{av}(90°) = \frac{15}{\pi} I_m^2 \tag{11–64}$$

and

$$D = \frac{4\pi U_{\max}}{P_r} = \frac{60}{36.54} = 1.64, \tag{11–65}$$

which corresponds to $10 \log_{10} 1.64$ or 2.15 (dB) referring to an omnidirectional radiator.

The half-power beamwidth of the radiation pattern is the angle between the two solutions of the equation

$$\frac{\cos[(\pi/2)\cos\theta]}{\sin\theta} = \frac{1}{\sqrt{2}}, \qquad 0 < \theta < \pi,$$

which can be solved either numerically or graphically to give a beamwidth of 78°. Thus a half-wave dipole is only slightly more directive than a short Hertzian dipole that has a directivity of 1.76 (dB) and a beamwidth of 90°.

EXAMPLE 11–5 A thin quarter-wavelength vertical antenna over a perfectly conducting ground is excited by a sinusoidal source at its base. Find its radiation pattern, radiation resistance, and directivity.

Solution Since current is charge in motion, we can use the method of images discussed in Section 4–4 and replace the conducting ground by the image of the vertical antenna. A little thought will convince us that the image of a vertical antenna carrying a current I is another vertical antenna. The image antenna has the same length, is equidistant from the ground, and carries the same current in the *same direction* as

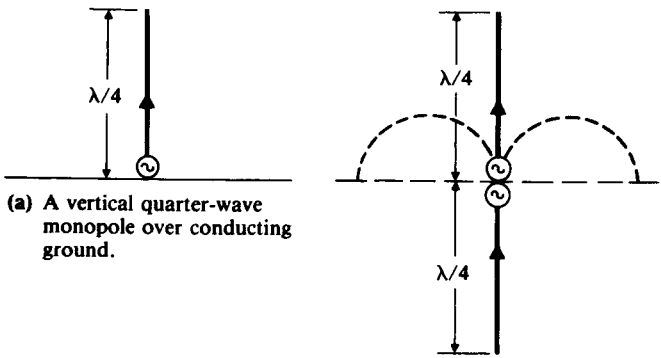

(a) A vertical quarter-wave monopole over conducting ground.

(b) Equivalent half-wave dipole radiating into upper half-space.

FIGURE 11–7
Quarter-wave monopole over a conducting ground and its equivalent half-wave dipole.

the original antenna. The electromagnetic field *in the upper half-space* due to the quarter-wave vertical antenna in Fig. 11–7(a) is, then, the same as that of the half-wave antenna in Fig. 11–7(b). The pattern function in Eq. (11–57) applies here for $0 \leq \theta \leq \pi/2$, and the radiation pattern drawn in dashed lines in Fig. 11–7(b) is the upper half of that in Fig. 11–6(a).

The magnitude of the time-average Poynting vector, $\mathscr{P}_{av}$, in Eq. (11–60), holds for $0 \leq \theta \leq \pi/2$. Inasmuch as the quarter-wave antenna (a ***monopole***) radiates only into the upper half-space, its total radiated power is only one-half that given in Eq. (11–62):

$$P_r = 18.27 I_m^2 \quad \text{(W)}.$$

Consequently, the radiation resistance is

$$R_r = \frac{2P_r}{I_m^2} = 36.54 \quad (\Omega), \tag{11–66}$$

which is one-half of the radiation resistance of a half-wave antenna in free-space.

To calculate directivity, we note that although the maximum radiation intensity $U_{\max}$ remains the same as that given in Eq. (11–64), the average radiation intensity is now $P_r/2\pi$. Thus,

$$D = \frac{U_{\max}}{U_{av}} = \frac{U_{\max}}{P_r/2\pi} = 1.64, \tag{11–67}$$

which is the same as the directivity of a half-wave antenna. ■

11–4.2 EFFECTIVE ANTENNA LENGTH

For thin linear antennas with a given current distribution it is sometimes convenient to define a quantity called the ***effective length***, to which the far-zone field is proportional. Let us refer to the dipole antenna in Fig. 11–5 and assume a general phasor current distribution $I(z)$. The far-zone field is then, from Eq. (11–54),

$$E_\theta = \eta_0 H_\phi = \frac{j30}{R} \beta e^{-j\beta R} \left\{ \sin\theta \int_{-h}^{h} I(z) e^{j\beta z \cos\theta} dz \right\}. \tag{11–68}$$

Let $I(0)$ be the input current at the feed point of the antenna. We write Eq. (11–68) as

$$E_\theta = \eta_0 H_\phi = \frac{j30 I(0)}{R} \beta e^{-j\beta R} \ell_e(\theta), \tag{11–69}$$

where

$$\ell_e(\theta) = \frac{\sin\theta}{I(0)} \int_{-h}^{h} I(z) e^{j\beta z \cos\theta} dz \tag{11–70}$$

is the ***effective length*** of the transmitting antenna. (We will discuss the effective length of a receiving antenna presently.) As we see from Eq. (11–69), ℓ_e measures the effectiveness of the antenna as a radiator, and for a given current distribution the far-zone field is proportional to ℓ_e, which contains all the information about the directional properties of the antenna. In most practical situations the important value of the

effective length is that at $\theta = \pi/2$, where

$$\boxed{\ell_e = \frac{1}{I(0)} \int_{-h}^{h} I(z)\, dz \qquad \text{(m)}.} \tag{11-71}$$

Equation (11–71) indicates that ℓ_e is the length of an equivalent linear antenna with a uniform current $I(0)$ such that it radiates the same far-zone field in the $\theta = \pi/2$ plane.

EXAMPLE 11–6 Assume a sinusoidal current distribution on a center-fed, thin, straight half-wave dipole. Find its effective length. What is its maximum value?

Solution For the assumed sinusoidal current distribution we use Eq. (11–51) for $I(z)$ and substitute it in Eq. (11–70), where $I(0) = I_m$ and $h = \lambda/4$. We have

$$\ell_e(\theta) = \sin\theta \int_{-\lambda/4}^{\lambda/4} \sin\beta\left(\frac{\lambda}{4} - |z|\right) e^{j\beta z \cos\theta}\, dz. \tag{11-72}$$

The above integral has been evaluated in Eq. (11–56). Thus,

$$\ell_e(\theta) = \frac{2}{\beta}\left[\frac{\cos\left(\frac{\pi}{2}\cos\theta\right)}{\sin\theta}\right]. \tag{11-73}$$

The maximum value of $\ell_e(\theta)$ is at $\theta = \pi/2$, where the effective length is

$$\ell_e\left(\frac{\pi}{2}\right) = \frac{2}{\beta} = \frac{\lambda}{\pi}. \tag{11-74}$$

We note from Eq. (11–74) that the maximum effective length of a half-wave dipole is less than its physical length, $\lambda/2$. ■

A careful examination of Eq. (11–71) reveals a potential anomaly in the appearance of $I(0)$ in the denominator. When the half-length of a dipole is greater than $\lambda/4$ and approaches $\lambda/2$, $I(0)$ would be progressively less than I_m, which would not occur at $z = 0$. This could make ℓ_e much greater than $2h$. Thus the definition of effective length as given in Eqs. (11–70) and (11–71) is meaningful only for relatively short antennas that have a current maximum at the feed point.

The effective length of a receiving linear antenna is defined as the ratio of the open-circuit voltage V_{oc} induced at the antenna terminals and the electric field intensity $E_i = |\mathbf{E}_i|$ at the antenna that induces it:

$$\boxed{\ell_e(\theta) = -\frac{V_{oc}}{E_i},} \tag{11-75}$$

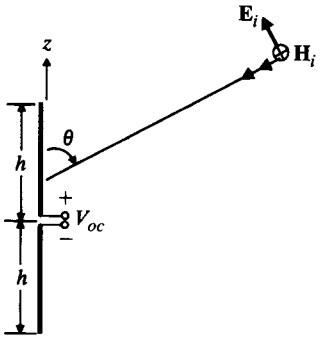

FIGURE 11–8
A linear antenna in the receiving mode.

where the negative sign is to conform with the convention that the electric potential increases in a direction opposite to that of the electric field. The situation is illustrated in Fig. 11–8. We will assume that $\mathbf{E}_i$ lies in the plane of incidence, since the component of $\mathbf{E}_i$ normal to the antenna does not induce a voltage across the antenna terminals. Obviously, the open-circuit voltage V_{oc} depends on E_i, θ, and βh in a complicated way. It is possible to use a reciprocity theorem to prove formally that ***the effective length of an antenna for receiving is the same as that for transmitting*** [14].† In Section 11–6 we shall prove that both the impedance and the directional pattern of an isolated antenna in the receiving mode are the same as those of the antenna in the transmitting mode. We may also conclude the equality of the effective lengths operating under these two modes.

If the incoming electric field $\mathbf{E}_i$ is not parallel to the dipole, there is a polarization mismatch, and the magnitude of the open-circuit voltage will be

$$|V_{oc}| = |\ell_e \cdot \mathbf{E}_i|, \tag{11–76}$$

where ℓ_e denotes the vector effective length. Obviously, $|V_{oc}|$ will be maximum when $\mathbf{E}_i$ is parallel to the dipole and will be zero if $\mathbf{E}_i$ is perpendicular to the dipole.

11–5 Antenna Arrays

Antenna arrays are groups of similar antennas arranged in various configurations (straight lines, circles, triangles, and so on) with proper amplitude and phase relations to give certain desired radiation characteristics. Frequently, the radiation characteristics of importance are the direction and width of the main beam, sidelobe levels, and/or directivity. In this section we examine the basic theories and characteristics of linear antenna arrays (radiating elements arranged along a straight line). The electromagnetic field of an array is the vector superposition of the fields produced by

† Bracketed numbers refer to the literature listed in the reference section at the end of this chapter.

the individual antenna elements. We first consider the simplest case of two-element arrays. After some experience has been gained with them, we consider the basic properties of uniform linear arrays made up of many identical elements.

11–5.1 TWO-ELEMENT ARRAYS

The simplest array is one consisting of two identical radiating elements (antennas) spaced a distance apart. This is illustrated in Fig. 11–9. For simplicity, let us assume that the far-zone electric field of the individual antennas be in the θ-direction and that the antennas are lined along the x-axis. The antennas are excited with a current of the same magnitude, but the phase in antenna 1 leads that in antenna 0 by an angle ξ. We have

$$E_0 = E_m F(\theta, \phi) \frac{e^{-j\beta R_0}}{R_0}, \tag{11–77}$$

$$E_1 = E_m F(\theta, \phi) \frac{e^{j\xi} e^{-j\beta R_1}}{R_1}, \tag{11–78}$$

where $F(\theta, \phi)$ is the pattern function of the individual antennas, and E_m is an amplitude function. The electric field of the two-element array is the sum of E_0 and E_1. Hence,

$$E = E_0 + E_1 = E_m F(\theta, \phi) \left[\frac{e^{-j\beta R_0}}{R_0} + \frac{e^{j\xi} e^{-j\beta R_1}}{R_1} \right]. \tag{11–79}$$

In the far zone, $R_0 \gg d/2$, and the factor $1/R_1$ in the magnitude may be replaced approximately by $1/R_0$. However, a small difference between R_0 and R_1 in the exponents may lead to a significant phase difference, and a better approximation must be used. Because the lines joining the field point P and the two antennas are nearly parallel, we may write

$$R_1 \cong R_0 - d \sin\theta \cos\phi. \tag{11–80}$$

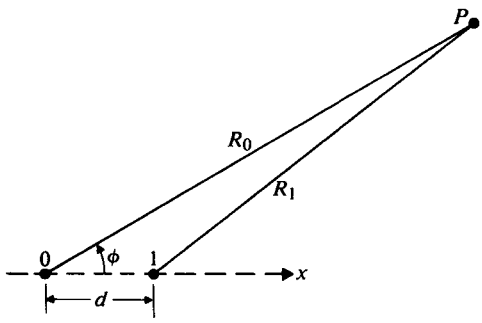

FIGURE 11–9
A two-element array.

Substitution of Eq. (11–80) in Eq. (11–79) yields

$$E = E_m \frac{F(\theta, \phi)}{R_0} e^{-j\beta R_0}[1 + e^{j\beta d \sin\theta \cos\phi} e^{j\xi}]$$
$$= E_m \frac{F(\theta, \phi)}{R_0} e^{-j\beta R_0} e^{j\psi/2}\left(2 \cos\frac{\psi}{2}\right), \tag{11–81}$$

where

$$\psi = \beta d \sin\theta \cos\phi + \xi. \tag{11–82}$$

The magnitude of the electric field of the array is

$$|E| = \frac{2E_m}{R_0} |F(\theta, \phi)| \left|\cos\frac{\psi}{2}\right|, \tag{11–83}$$

where $|F(\theta, \phi)|$ may be called the ***element factor***, and $|\cos(\psi/2)|$ the normalized ***array factor***. The element factor is the magnitude of the pattern function of the individual radiating elements, and the array factor depends on array geometry as well as on the relative amplitudes and phases of the excitations in the elements. (In this particular case the excitation amplitudes are equal.) The array factor is that of an array of *isotropic* elements, the directional property of the elements having been accounted for by the element factor. From Eq. (11–83) we may conclude that ***the pattern function of an array of identical elements is described by the product of the element factor and the array factor***. This property is called the ***principle of pattern multiplication.***

For an array of two parallel z-directed half-wave dipoles the magnitude of the total electric field is, from Eqs. (11–57) and (11–83),

$$|E| = \frac{2E_m}{R_0} \left|\frac{\cos[(\pi/2)\cos\theta]}{\sin\theta}\right| \left|\cos\frac{\psi}{2}\right|. \tag{11–84}$$

Since ψ is also a function of θ, we see that the pattern in an E-plane is not the same as that of a single dipole, except when $\phi = \pm\pi/2$. In the H-plane, $\theta = \pi/2$, and the pattern is determined entirely by the array factor $|\cos(\psi/2)|$.

EXAMPLE 11–7 Plot the H-plane radiation patterns of two parallel dipoles for the following two cases: (a) $d = \lambda/2$, $\xi = 0$; (b) $d = \lambda/4$, $\xi = -\pi/2$.

Solution Let the dipoles be z-directed and placed along the x-axis, as shown in Fig. 11–9. In the H-plane ($\theta = \pi/2$), each dipole is omnidirectional, and the normalized pattern function is equal to the normalized array factor $|A(\phi)|$. Thus

$$|A(\phi)| = \left|\cos\frac{\psi}{2}\right| = \left|\cos\frac{1}{2}(\beta d \cos\phi + \xi)\right|.$$

a) $d = \lambda/2$ ($\beta d = \pi$), $\xi = 0$:

$$|A(\phi)| = \left|\cos\left(\frac{\pi}{2}\cos\phi\right)\right|. \tag{11–85a}$$

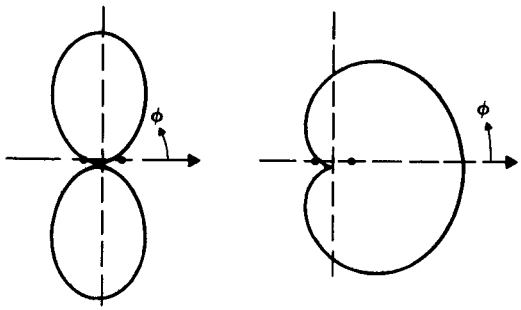

(a) $d = \lambda/2$, $\xi = 0$. (b) $d = \lambda/4$, $\xi = -\pi/2$.

FIGURE 11–10
H-plane radiation patterns of two-element parallel dipole array.

The pattern has its maximum at $\phi_0 = \pm\pi/2$—that is, in the broadside direction. This is a type of ***broadside array***. Figure 11–10(a) shows this broadside pattern. Since the excitations in the two dipoles are in phase, their electric fields add in the broadside directions, $\phi = \pm\pi/2$. At $\phi = 0$ and π the electric fields cancel each other because the $\lambda/2$ separation leads to a phase difference of 180°.

b) $d = \lambda/4$ ($\beta d = \pi/2$), $\xi = -\pi/2$:

$$|A(\phi)| = \left|\cos\frac{\pi}{4}(\cos\phi - 1)\right|, \tag{11–85b}$$

which has a maximum at $\phi_0 = 0$ and vanishes at $\phi = \pi$. The pattern maximum is now in a direction *along* the line of the array, and the two dipoles constitute an ***endfire array***. Figure 11–10(b) shows this endfire pattern. In this case the phase in the right-hand dipole *lags* by $\pi/2$, which exactly compensates for the fact that its electric field arrives in the $\phi = 0$ direction a quarter of a cycle *earlier* than the electric field of the left-hand dipole. As a consequence, the electric fields add in the $\phi = 0$ direction. In the $\phi = \pi$ direction, the $\pi/2$ phase lag in the right-hand dipole plus the quarter-cycle delay results in a complete cancellation of the fields.

EXAMPLE 11–8 Discuss the radiation pattern of a linear array of the three isotropic sources spaced $\lambda/2$ apart. The excitations in the sources are in-phase and have amplitude ratios 1:2:1.

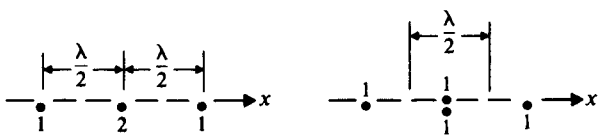

(a) Three-element binomial array. (b) Two displaced two-element arrays.

FIGURE 11–11
A three-element array and its equivalent pair of displaced two-element arrays.

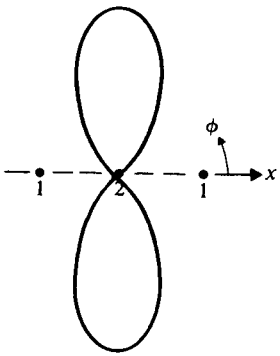

FIGURE 11–12
Radiation pattern of three-element broadside binomial array.

Solution This three-source array is equivalent to two two-element arrays displaced $\lambda/2$ from each other as depicted in Fig. 11–11. Each two-element array can be considered as as a radiating source with an element factor as given by Eq. (11–85a) and an array factor, which is also given by the same equation. By the principle of pattern multiplication we obtain

$$|E| = \frac{4E_m}{R_0}\left|\cos\left(\frac{\pi}{2}\cos\phi\right)\right|^2. \tag{11–86}$$

The radiation pattern represented by the pattern function $|\cos[(\pi/2)\cos\phi]|^2$ is sketched in Fig. 11–12. Compared to the pattern of the uniform two-element array in Fig. 11–10(a), this three-element broadside pattern is sharper (more directive). Both patterns have no sidelobes. ■

The three-element broadside array is a special case of a class of *sidelobeless* arrays called ***binomial arrays***. In a binomial array of N elements the excitation amplitudes vary according to the coefficients of a binomial expansion $\binom{N-1}{n}$, $n = 0, 1, 2, \ldots, N-1$. For $N = 3$ the relative excitation amplitudes are $\binom{2}{0} = 1$, $\binom{2}{1} = 2$ and $\binom{2}{2} = 1$, as in Example 11–8. To obtain a directive pattern without sidelobes, d in a binomial array is normally restricted to be $\lambda/2$. The feature of no sidelobes in the array pattern of a binomial array is accompanied by a wider beamwidth and a lower directivity compared to those of a uniform array with the same number of elements.

11–5.2 GENERAL UNIFORM LINEAR ARRAYS

We now consider an array of identical antennas equally spaced along a straight line. The antennas are fed with currents of equal magnitude and have a uniform progressive phase shift along the line. Such an array is called a ***uniform linear array.*** An example is shown in Fig. 11–13, where N antenna elements are aligned along the x-axis. Since the antenna elements are identical, the array pattern function is the product of the element factor and the array factor. Our attention here will be concentrated on the

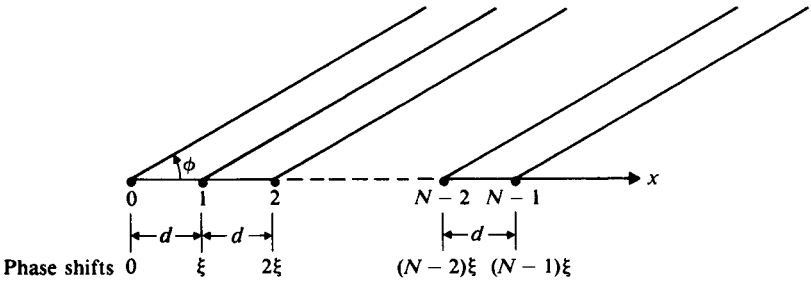

FIGURE 11–13
A general uniform linear array.

manner in which the array factor depends on the parameter βd $(=2\pi d/\lambda)$ and the progressive phase shift ξ between neighboring elements. The normalized array factor in the xy-plane is

$$|A(\psi)| = \frac{1}{N}|1 + e^{j\psi} + e^{j2\psi} + \cdots + e^{j(N-1)\psi}|, \tag{11–87}$$

where

$$\psi = \beta d \cos\phi + \xi. \tag{11–88}$$

The polynomial on the right side of Eq. (11–87) is a geometric progression and can be summed up in a closed form:

$$|A(\psi)| = \frac{1}{N}\left|\frac{1 - e^{jN\psi}}{1 - e^{j\psi}}\right|$$

or

$$\boxed{|A(\psi)| = \frac{1}{N}\left|\frac{\sin(N\psi/2)}{\sin(\psi/2)}\right| \qquad \text{(Dimensionless).}} \tag{11–89}$$

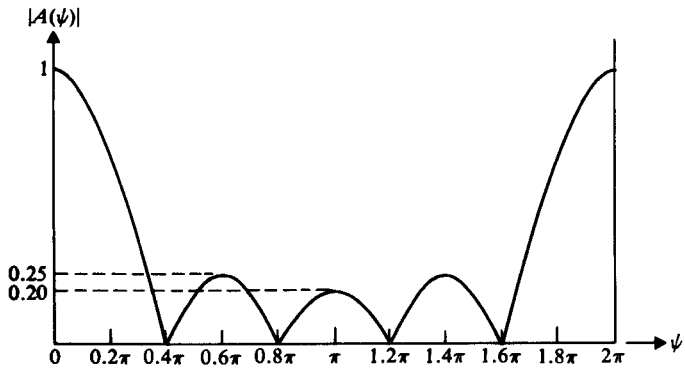

FIGURE 11–14
Normalized array factor of a five-element uniform linear array.

This is the general expression of the normalized array factor for a uniform linear array. Figure 11–14 is a sketch of the normalized array factor for a five-element array. The actual radiation pattern as a function of ϕ depends on the values of βd and ξ (see Problem P.11–17). As ϕ varies from 0 to 2π, the value of ψ changes from $\beta d + \xi$ to $-\beta d + \xi$, covering a range of $2\beta d$ or $4\pi d/\lambda$. This defines the ***visible range*** of the radiation pattern.

We may derive several significant properties from $|A(\psi)|$ as given in Eq. (11–89).

1. *Main-beam direction.* The maximum value occurs when $\psi = 0$ or when

$$\beta d \cos \phi_0 + \xi = 0,$$

which leads to

$$\cos \phi_0 = -\frac{\xi}{\beta d}. \tag{11–90}$$

Two special cases are of particular importance.

a) *Broadside array.* For a broadside array, maximum radiation occurs at a direction perpendicular to the line of the array—that is, at $\phi_0 = \pm\pi/2$. This requires $\xi = 0$, which means that all the elements in a linear broadside array should be excited in phase, as was the case in Example 11–7(a).

b) *Endfire array.* For an endfire array, maximum radiation occurs at $\phi_0 = 0$. Equation (11–90) gives

$$\xi = -\beta d \cos \phi_0 = -\beta d.$$

We note that this condition is satisfied by the two-element array in Example 11–7(b).

2. *Null locations.* The array pattern has nulls when $|A(\phi)| = 0$ or when

$$\frac{N\psi}{2} = \pm k\pi, \qquad k = 1, 2, 3, \ldots. \tag{11–91}$$

It is obvious that the corresponding null locations in ϕ are different for broadside and endfire arrays because of the different values of ξ implicit in ψ.

3. *Width of main beam.* The angular width of the main beam between the first nulls can be determined approximately for large N. Let ψ_{01} denote the values of ψ at the first nulls:

$$\frac{N\psi_{01}}{2} = \pm\pi \qquad \text{or} \qquad \psi_{01} = \pm\frac{2\pi}{N}.$$

In order to see how ψ_{01} converts to an angle between the first nulls in ϕ, we need to know the direction of the main beam.

a) *Broadside array* ($\xi = 0$, $\phi_0 = \pi/2$). For a broadside array, $\psi = \beta d \cos \phi$. If the first null occurs at ϕ_{01}, then the width of the main beam between the first nulls is $2\Delta\phi = 2(\phi_{01} - \phi_0)$. At ϕ_{01} we have

$$\cos \phi_{01} = \cos (\phi_0 + \Delta\phi) = \frac{\psi_{01}}{\beta d},$$

which, for $\phi_0 = \pi/2$, gives

$$\cos\left(\frac{\pi}{2} + \Delta\phi\right) = -\sin\Delta\phi = -\frac{2\pi}{N\beta d}$$

or

$$\Delta\phi = \sin^{-1}\left(\frac{\lambda}{Nd}\right) \cong \frac{\lambda}{Nd}. \tag{11-92}$$

The last approximation is obtained when $Nd \gg \lambda$. Equation (11-92) leads to a useful rule of thumb that the width of the main beam (in radians) of a long uniform broadside array is approximately *twice* the reciprocal of the array length in wavelengths.

b) *Endfire array* ($\xi = -\beta d$, $\phi_0 = 0$). For an endfire array, $\psi = \beta d(\cos\phi - 1)$, and

$$\cos\phi_{01} - 1 = \frac{\psi_{01}}{\beta d} = -\frac{2\pi}{N\beta d} = -\frac{\lambda}{Nd}.$$

But $\cos\phi_{01} = \cos\Delta\phi \cong 1 - (\Delta\phi)^2/2$ for small $\Delta\phi$. Thus,

$$\frac{(\Delta\phi)^2}{2} \cong \frac{\lambda}{Nd}$$

or

$$\Delta\phi \cong \sqrt{\frac{2\lambda}{Nd}}. \tag{11-93}$$

Comparing Eq. (11-93) with Eq. (11-92), we may conclude that the width of the main beam of a uniform endfire array is greater than that of a uniform broadside array of the same length (because $Nd > \lambda/2$).

4. *Sidelobe locations.* Sidelobes are minor maxima that occur approximately when the numerator on the right side of Eq. (11-89) is a maximum—that is, when $|\sin(N\psi/2)| = 1$ or when

$$\frac{N\psi}{2} = \pm(2m+1)\frac{\pi}{2}, \qquad m = 1, 2, 3, \ldots. \tag{11-94}$$

The first sidelobes occur when

$$\frac{N\psi}{2} = \pm\frac{3}{2}\pi, \qquad (m = 1). \tag{11-95}$$

Note that $N\psi/2 = \pm\pi/2$ ($m = 0$) does not represent locations of sidelobes because they are still within the main-lobe region.

5. *First sidelobe level.* An important characteristic of the radiation pattern of an array is the level of the first sidelobes compared to that of the main beam, since the former is usually the highest of all sidelobes. All sidelobes should be kept as low as possible in order that most of the radiated power be concentrated in the main-beam direction and not be diverted to sidelobe regions. Substituting Eq.

(11–95) in Eq. (11–89), we find the amplitude of the first sidelobes to be

$$\frac{1}{N}\left|\frac{1}{\sin(3\pi/2N)}\right| \cong \frac{1}{N}\left|\frac{1}{3\pi/2N}\right| = \frac{2}{3\pi} = 0.212$$

for large N. In logarithmic terms the first sidelobes of a uniform linear antenna array of many elements are $20 \log_{10}(1/0.212)$ or 13.5 (dB) down from the principal maximum. This number is almost independent of N as long as N is large.

One way to reduce the sidelobe level in the radiation pattern of a linear array is to taper the current distribution in the array elements—that is, to make the excitation amplitudes in the elements in the center portion of an array higher than those in the end elements. This method is illustrated in the following example.

EXAMPLE 11–9 Find the array factor and plot the normalized radiation pattern of a broadside array of five isotropic elements spaced $\lambda/2$ apart and having excitation amplitude ratios 1:2:3:2:1. Compare the first sidelobe level with that of a five-element uniform array.

Solution The normalized array factor of the five-element tapered array is

$$\begin{aligned} |A(\psi)| &= \tfrac{1}{9}|1 + 2e^{j\psi} + 3e^{j2\psi} + 2e^{j3\psi} + e^{j4\psi}| \\ &= \tfrac{1}{9}|e^{j2\psi}[3 + 2(e^{j\psi} + e^{-j\psi}) + (e^{j2\psi} + e^{-j2\psi})]| \\ &= \tfrac{1}{9}|3 + 4\cos\psi + 2\cos 2\psi|. \end{aligned} \tag{11–96}$$

The graph of $|A(\psi)|$ versus ψ is shown in Fig. 11–15(a). Note that this figure holds for a general $\psi = \beta d \cos\phi + \xi$; the values of βd and ξ have not yet been specified.

In order to plot the desired radiation pattern we use the following additional information:

$$\text{Broadside radiation, } \zeta = 0: \quad \psi = \beta d \cos\phi;$$

$$\text{Element spacing, } d = \frac{\lambda}{2}: \quad \psi = \pi \cos\phi.$$

The normalized radiation pattern can be plotted from

$$|A(\phi)| = \tfrac{1}{9}|3 + 4\cos(\pi\cos\phi) + 2\cos(2\pi\cos\phi)|.$$

However, having calculated and plotted $|A(\psi)|$, we do not need to recalculate the array factor as a function of ϕ. This conversion can be effected graphically as follows (see Fig. 11–15):

1. Extend the vertical axis of the array-factor graph downward, and let it intersect with a horizontal line (which represents the line for $\phi = 0$ and $\phi = \pi$). The point of intersection is the point for $\xi = 0$.
2. Locate the point, P_0, on the horizontal line that is ξ radians to the right or left of the point of intersection, depending on whether ξ is positive or negative. (In the present case, $\xi = 0$ and P_0 is at the point of intersection.)

3. Using P_0 as the center, draw a circle with βd as the radius.
4. For any angle ϕ_1, draw the radius vector P_0P_1. (The projection P_0P_1' is equal to $\psi_1 = \beta d \cos \phi_1$.)
5. At ψ_1, measure the magnitude of $|A(\psi_1)|$, which is marked as P_2 on the radius vector P_0P_1. (P_2 is a point on the normalized radiation pattern.)

Repeat this process until the entire radiation pattern is obtained.

Figure 11–15(b) shows the normalized radiation pattern of this five-element broadside array with tapered excitation. The first sidelobe level is found to be 0.11

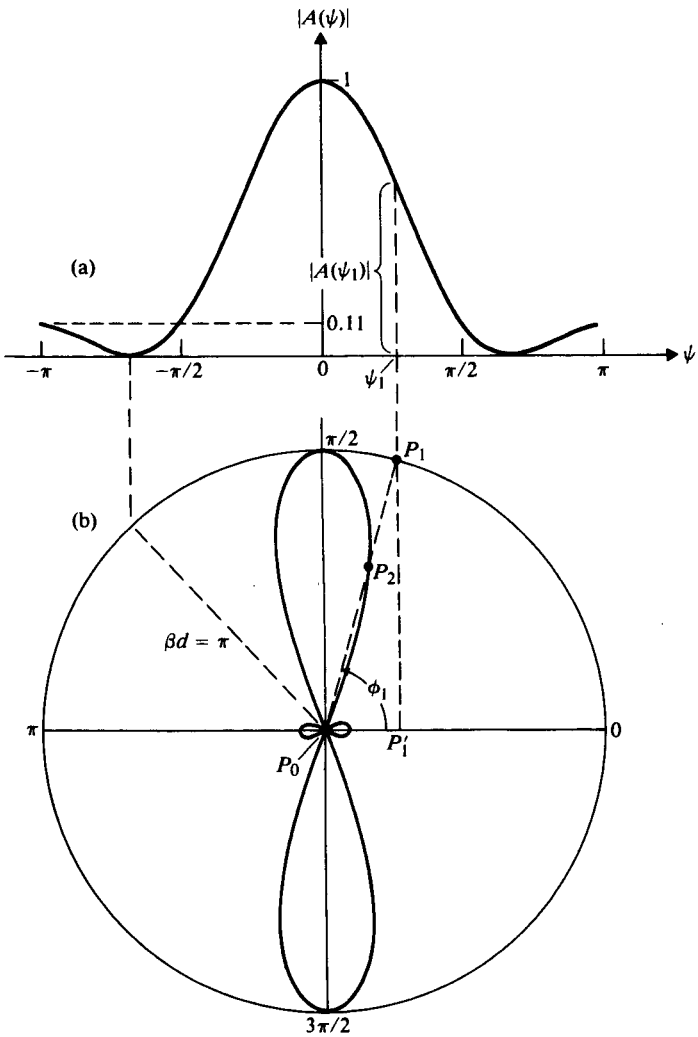

FIGURE 11–15
(a) Graph for normalized array factor as a function of ψ, and (b) normalized polar radiation pattern of a five-element broadside array with $d = \lambda/2$ and tapered excitation amplitude ratios 1:2:3:2:1 (Example 11–9).

or $20 \log_{10} (1/0.11) = 19.2$ (dB) down from the main-beam radiation. This compares with 0.25 or 12 (dB) down for the five-element uniform broadside array shown in Fig. 11–14. ■

In the discussion of uniform linear arrays we started out with the assumptions of equal spacing, equal excitation amplitude, and constant progressive phase shifts. The main reason for making these assumptions is mathematical simplicity in analyzing radiation characteristics. The preceding example shows that a tapered nonuniform amplitude distribution in the array elements produces the desirable result of a reduction in the sidelobe level. In a similar manner the spacings between neighboring elements may be made unequal [1]–[4], and the phase shifts do not have to be constant [5]. In two-dimensional arrays the elements need not be arranged in a rectangular lattice [6], [7]. We have, then, many additional parameters that can be adjusted to achieve desirable results. Adjustments in these parameters, however, destroy the simplicity of the analysis. There are techniques for synthesizing an antenna array to approximate a specified radiation pattern closely. It is not possible to examine all the various possible array designs in this book, but they do exist and present themselves as interesting problems [8]–[12].

Our discussions on linear arrays can be extended to two-dimensional rectangular arrays. A rectangular array can be studied as an array of linear arrays, to which the principle of pattern multiplication applies. From Eq. (11–90) we note that the direction of the main beam of a uniform linear array can be changed by simply changing the amount of progressive phase shift ξ. In fact, the radiation pattern can be changed from broadside ($\xi = 0$) to endfire ($\xi = -\beta d$) or to somewhere in between. We see here a possibility of *scanning* the main beam by simply varying ξ. This can be achieved in practice by using electronically controlled phase shifters. Antenna arrays equipped with phase shifters to steer the main beam electronically are called ***phased arrays***. The main beam of a two-dimensional array can be made to scan in both θ (elevation) and ϕ (azimuth) directions. Scanning phased arrays are of great practical importance in radar and radioastronomy work, in which the antenna system may be arrays of many thousands of elements that are not amenable to rapid mechanical motion for beam steering. Time-delay circuits may also be used to furnish the required phase shifts to the various array elements. By changing the frequency the time-delays are translated into varying phase shifts. This scheme is called ***frequency scanning***.

11–6 Receiving Antennas

In the discussion of antennas and antenna arrays so far we have implied that they operate in a transmitting mode. In the transmitting mode a voltage source is applied to the input terminals of an antenna, setting up currents and charges on the antenna structure. The time-varying currents and charges, in turn, radiate electromagnetic waves, which carry energy and/or information. A transmitting antenna can then be regarded as a device that transforms energy from a source (a generator) to energy

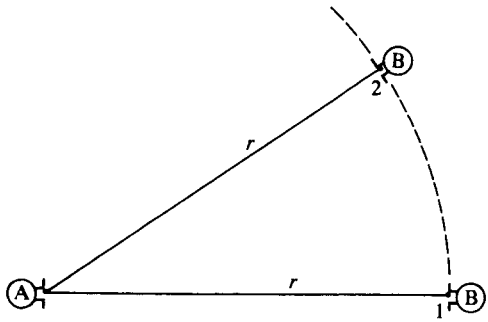

FIGURE 11–16
Two coupled antennas.

associated with an electromagnetic wave. A receiving antenna, on the other hand, extracts energy from an incident electromagnetic wave and delivers it to a load. In the receiving mode the external electromagnetic field that causes currents and charges to flow is incident on the entire antenna structure, not just at the input terminals. Moreover, the induced currents and charges, which depend on the direction of arrival of the incident electromagnetic wave, will produce reradiation or scattering of electromagnetic energy, making the situation very complicated. We may reasonably expect that the current and charge distributions on an antenna in the receiving mode are different from those in the transmitting mode. Nevertheless, despite these differences, reciprocity relations enable us to conclude that (1) the equivalent generator impedance of an antenna in the receiving mode is equal to the input impedance of the antenna in the transmitting mode, and (2) the directional pattern of an antenna for reception is identical with that for transmission. We will justify these two important conclusions by using equivalent network representations. Also in this section we will discuss the concepts of effective area and backscatter cross section.

11–6.1 INTERNAL IMPEDANCE AND DIRECTIONAL PATTERN

Let us assume that a transmitter with antenna A radiates electromagnetic energy, which is absorbed by a distant receiver with antenna B. Antenna B moves about antenna A at a constant distance r[†] and is always oriented in such a way as to receive maximum power, as illustrated in Fig. 11–16. The two coupled antennas and the space between can be represented as a two-port T-network shown in Fig. 11–17. The terminal characteristics, (V_1, I_1) and (V_2, I_2) of antennas A and B, respectively, are linearly related by the following equations:

$$V_1 = Z_{11}I_1 + Z_{12}I_2, \tag{11–97}$$

$$V_2 = Z_{21}I_1 + Z_{22}I_2, \tag{11–98}$$

where Z_{11}, Z_{12}, Z_{21}, and Z_{22} are open-circuit impedance coefficients.

[†] The symbol r, instead of R, is used here to denote distance in order to avoid possible confusion of the latter with the symbol for resistance used later in this chapter.

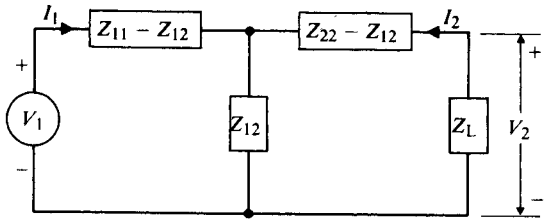

FIGURE 11–17
Equivalent two-port network of coupled transmitting and receiving antennas.

When the medium in the transmission path between antennas A and B is bilateral such that reciprocity relations hold, the transfer or coupling impedances Z_{12} and Z_{21} are equal.† Under normal circumstances, transmitting and receiving antennas are separated by very large distances, and the coupling impedances are negligibly small as far as *the reaction on the transmitting antenna* owing to scattering by the receiving antenna is concerned. In the limit $r \to \infty$,

$$\lim_{r \to \infty} Z_{12} = 0. \tag{11–99}$$

The parallel arm of the T-network in Fig. 11–17 is almost a short-circuit, and the impedance coefficients Z_{11} and Z_{22} are nearly equal to the input impedances Z_A and Z_B, respectively, of isolated antennas A and B in the transmitting mode. Equation (11–97) can be written approximately as

$$V_1 \cong Z_{11} I_1 \cong Z_A I_1. \tag{11–100}$$

An equivalent circuit representing Eq. (11–100) is drawn in Fig. 11–18(a).

The coupling *from* the transmitting antenna *to* the receiving antenna, however, cannot be neglected inasmuch as it is through this coupling that the latter extracts energy from the electromagnetic wave originated from the former. Thévenin's theorem can be applied to the left of the load impedance Z_L in the network in Fig. 11–17 to determine an open-circuit voltage V_{oc} and an internal impedance Z_g. An equivalent circuit at the receiving end is shown in Fig. 11–18(b). We have

$$V_{oc} = \frac{Z_{12}}{Z_{11}} V_1, \tag{11–101}$$

$$Z_g = (Z_{22} - Z_{12}) + \frac{Z_{12}}{Z_{11}}(Z_{11} - Z_{12}) = Z_{22} - \frac{Z_{12}^2}{Z_{11}}. \tag{11–102}$$

Because of the weak coupling, we conclude that *the equivalent generator internal impedance Z_g for antenna B in the receiving mode is approximately equal to its input impedance when it is transmitting*; that is,

$$Z_g \cong Z_{22} \cong Z_B. \tag{11–103}$$

† An example of a nonbilateral medium for which $Z_{12} \neq Z_{21}$ is the ionosphere under the influence of the earth's magnetic field.

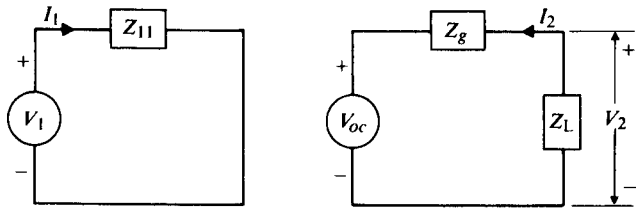

(a) Circuit at transmitting end. (b) Circuit at receiving end.

FIGURE 11–18
Approximate equivalent circuits for weakly coupled antennas.

When antenna B is receiving, $V_2 = -I_2 Z_L$, and Eq. (11–98) becomes

$$I_2 = -\frac{Z_{21}}{Z_{22} + Z_L} I_1. \tag{11–104}$$

The time-average power absorbed in Z_L is

$$P_L = \frac{1}{2}\mathscr{R}e[-V_2 I_2^*] = \frac{|I_1|^2}{2}\left|\frac{Z_{21}}{Z_{22} + Z_L}\right|^2 \mathscr{R}e(Z_L). \tag{11–105}$$

For two successive positions of antenna B as indicated in Fig. 11–16 the ratio of the absorbed powers in Z_L is

$$\frac{P_L(\theta_1, \phi_1)}{P_L(\theta_2, \phi_2)} = \left|\frac{Z_{21}(\theta_1, \phi_1)}{Z_{21}(\theta_2, \phi_2)}\right|^2. \tag{11–106}$$

Thus the absorbed power is proportional to the square of the transfer impedance coefficient.

If we consider the situation in which antenna B is transmitting and antenna A is receiving, then the ratio of the absorbed powers in Z_L connected to antenna A for the two successive locations of antenna B would be the same as that given in Eq. (11–106), except that Z_{21} would be replaced by Z_{12}. Because of the reciprocity relation $Z_{12} = Z_{21}$, we conclude that ***the directional pattern of an antenna for reception is identical with that for transmission.***

11–6.2 EFFECTIVE AREA

In discussing receiving antennas it is convenient to define a quantity called the ***effective area.***† The effective area, A_e, of a receiving antenna is the ratio of the average power delivered to a *matched load* to the time-average power density (time-average Poynting vector) of the incident electromagnetic wave at the antenna. We write

$$P_L = A_e \mathscr{P}_{av}, \tag{11–107}$$

where P_L is the maximum average power transferred to the load (under matched conditions) with the receiving antenna properly oriented with respect to the polariza-

† Also called ***effective aperture*** or ***receiving cross section.***

tion of the incident wave. We will now show that the effective area bears a definite relationship with the directive gain of an antenna.

When the load impedance is matched to the internal impedance,

$$Z_L = Z_g^* \cong R_B - jX_B, \tag{11–108}$$

the maximum power delivered to the load is, from Eq. (11–105),

$$P_L = \frac{|I_1 Z_{21}|^2}{8R_B}. \tag{11–109}$$

Let R_A be the input resistance of transmitting antenna A. The transmitted power is then

$$P_t = \tfrac{1}{2}|I_1|^2 R_A. \tag{11–110}$$

Combining Eqs. (11–109) and (11–110), we have

$$\frac{P_L}{P_t} = \frac{|Z_{21}|^2}{4R_A R_B}. \tag{11–111}$$

When antenna B is receiving, the time-average power density at B depends on the directive gain of transmitting antenna A in that direction:

$$\mathscr{P}_{av} = \frac{P_t}{4\pi r^2} G_{DA}. \tag{11–112}$$

Using Eq. (11–112) in Eq. (11–107), we obtain

$$\frac{P_L}{P_t} = \frac{A_{eB} G_{DA}}{4\pi r^2}. \tag{11–113}$$

Comparison of Eqs. (11–111) and (11–113) yields

$$|Z_{21}|^2 = \frac{R_A R_B A_{eB} G_{DA}}{\pi r^2}. \tag{11–114}$$

If antenna B is transmitting and antenna A is receiving, a similar derivation leads to

$$|Z_{12}|^2 = \frac{R_B R_A A_{eA} G_{DB}}{\pi r^2}. \tag{11–115}$$

Since $Z_{12} = Z_{21}$, Eqs. (11–114) and (11–115) lead to the following important relation:

$$\frac{G_{DA}}{A_{eA}} = \frac{G_{DB}}{A_{eB}}. \tag{11–116}$$

Inasmuch as we have not specified the types of transmitting and receiving antennas in obtaining Eq. (11–116), we conclude that ***the ratio of the directive gain and the effective area of an antenna is a universal constant.*** This constant can be found by determining the directive gain and effective area of any antenna—for instance, those of an elemental dipole as illustrated in the following example.

EXAMPLE 11–10 Determine the effective area, $A_e(\theta)$, of an elemental electric dipole of a length $d\ell$ ($\ll\lambda$) used to receive an incident plane electromagnetic wave of wavelength λ that is polarized in a direction shown in Fig. 11–8.

Solution Let E_i be the amplitude of the electric field intensity at an elemental dipole of length $d\ell$. Then the time-average power density is

$$\mathscr{P}_{av} = \frac{E_i^2}{2\eta_0}. \tag{11–117}$$

The average power delivered to a matched load ($Z_L = Z_g^*$) is

$$P_L = \frac{1}{2}\left|\frac{E_i\, d\ell \sin\theta}{Z_g + Z_g^*}\right|^2 R_r = \frac{(E_i\, d\ell)^2 \sin^2\theta}{8R_r}, \tag{11–118}$$

where $R_r = 80(\pi\, d\ell/\lambda)^2$ has been given in Eq. (11–44). The ratio $P_L/\mathscr{P}_{av}$ gives the effective area of the elemental dipole:

$$\begin{aligned} A_e(\theta) &= \frac{P_L}{\mathscr{P}_{av}} = \frac{\eta_0}{4R_r}(d\ell)^2 \sin^2\theta \\ &= \frac{3}{8\pi}(\lambda \sin\theta)^2 \qquad (\text{m}^2). \end{aligned} \tag{11–119}$$

It is interesting to note that the effective area of an elemental electric dipole is independent of its length. ■

From Example 11–2 we have $G_D(\theta) = \frac{3}{2}\sin^2\theta$ for an elemental electric dipole. Thus,

$$\begin{aligned} G_D(\theta) &= \frac{3}{2}\sin^2\theta = \frac{4\pi}{\lambda^2}\frac{3}{8\pi}(\lambda \sin\theta)^2 \\ &= \frac{4\pi}{\lambda^2} A_e(\theta), \end{aligned} \tag{11–120}$$

which indicates that the universal constant for Eq. (11–116) is $4\pi/\lambda^2$, and we may write the following relation for an antenna under matched impedance conditions:

$$\boxed{G_D(\theta, \phi) = \frac{4\pi}{\lambda^2} A_e(\theta, \phi) \qquad \text{(Dimensionless).}} \tag{11–121}$$

In the case of thin linear antennas the concept of effective area may seem arbitrary. Nevertheless, its definition is useful in measuring the power available to a particular antenna. Of course, we expect the effective area $A_e(\theta)$ to be related to the effective length $\ell_e(\theta)$. The available power to the antenna load under matched conditions is

$$P_L = \frac{V_{oc}^2}{8R_r} = \frac{(-\ell_e E_i)^2}{8R_r}, \tag{11–122}$$

where the relation in Eq. (11–75) has been used. Substitution of Eqs. (11–117) and (11–122) into Eq. (11–107) yields

$$\boxed{A_e(\theta) = \frac{30\pi}{R_r}\ell_e^2(\theta).} \tag{11–123}$$

11–6.3 BACKSCATTER CROSS SECTION

As we saw in the preceding subsection, the concept of effective area pertains to the power available to the matched load of a receiving antenna for a given incident power density. In cases in which the incident wave impinges on a passive object whose purpose is not to extract energy from the incident wave but whose presence creates a scattered field, it is appropriate to define a quantity called the ***backscatter cross section***, or ***radar cross section***. The backscatter cross section of an object is the equivalent area that would intercept that amount of incident power in order to produce the same scattered power density at the receiver site if the object scattered uniformly (isotropically) in all directions. Let

$\mathscr{P}_i$ = Time-average incident power density at the object (W/m^2),
$\mathscr{P}_s$ = Time-average scattered power density at the receiver site (W/m^2),
σ_{bs} = Backscatter cross section (m^2),
r = Distance between scatterer and receiver (m).

Then,

$$\frac{\sigma_{bs}\mathscr{P}_i}{4\pi r^2} = \mathscr{P}_s$$

or

$$\boxed{\sigma_{bs} = 4\pi r^2 \frac{\mathscr{P}_s}{\mathscr{P}_i} \quad \text{(m)}.} \tag{11–124}$$

Note that $\mathscr{P}_s$ is inversely proportional to r^2 for large r and that σ_{bs} does not change with r.

The backscatter cross section is a measure of the detectability of the object (target) by ***radar*** (***ra***dio ***d***etection ***a***nd ***r***anging); hence the term radar cross section. It is a composite measure, depending on the geometry, orientation, and constitutive parameters of the object, and on the frequency and polarization of the incident wave in a complicated way.

EXAMPLE 11–11 A uniform plane wave with electric field intensity $\mathbf{E}_i = \mathbf{a}_z E_i$ impinges on a small dielectric sphere of radius $b\,(\ll\lambda)$ and dielectric constant ϵ_r, as shown in Fig. 11–19. Assume the polarization produced in the sphere to be the same

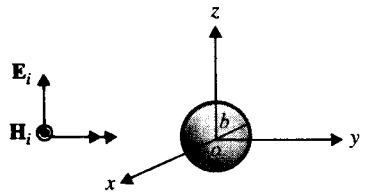

FIGURE 11–19
Plane wave incident on a small dielectric sphere.

as that produced in a uniform static electric field $\mathbf{E}_i$ and to be given by (see Problem P.4–29)

$$\begin{aligned}\mathbf{P} &= \epsilon_0(\epsilon_r - 1)\mathbf{E} \\ &= \mathbf{a}_z 3\epsilon_0\left(\frac{\epsilon_r - 1}{\epsilon_r + 2}\right)E_i \qquad (\text{C/m}^2).\end{aligned} \tag{11–125}$$

a) Find the backscatter cross section σ_{bs}.
b) Determine σ_{bs} for a spherical raindrop of diameter 3 (mm) at 15 (GHz), assuming the dielectric constant of water to be 55 at that frequency.

Solution

a) Since the induced polarization vector (the volume density of electric dipole moment) **P** is constant within the dielectric sphere, the total electric dipole moment induced in the sphere of radius b ($\ll \lambda$) is

$$\begin{aligned}\mathbf{p} &= \tfrac{4}{3}\pi b^3\mathbf{P} \\ &= \mathbf{a}_z 4\pi b^3\epsilon_0\left(\frac{\epsilon_r - 1}{\epsilon_r + 2}\right)E_i \qquad (\text{C}\cdot\text{m}).\end{aligned} \tag{11–126}$$

Thus the dielectric sphere acts electromagnetically like an elemental electric dipole of moment **p** given in Eq. (11–126). The scattered electric field intensity in the far-zone is then, from Eq. (11–19b) and using Eqs. (11–10) and (11–11),

$$\begin{aligned}\mathbf{E}_s = \mathbf{a}_\theta E_s &= -\mathbf{a}_\theta \frac{\omega p}{4\pi}\left(\frac{e^{-j\beta r}}{r}\right)\eta_0\beta\sin\theta \\ &= -\mathbf{a}_\theta\beta^2 b^3\left(\frac{e^{-j\beta r}}{r}\right)\left(\frac{\epsilon_r - 1}{\epsilon_r + 2}\right)E_i\sin\theta \qquad (\text{V/m}).\end{aligned} \tag{11–127}$$

The time-average backscattered power density is

$$\mathscr{P}_s = \frac{1}{2\eta_0}|E_s|^2_{\theta=\pi/2} = \frac{b^2(\beta b)^4}{2\eta_0 r^2}\left(\frac{\epsilon_r - 1}{\epsilon_r + 2}\right)^2 E_i^2 \qquad (\text{W/m}^2). \tag{11–128}$$

The time-average incident power density is

$$\mathscr{P}_i = \frac{1}{2\eta_0}E_i^2 \qquad (\text{W/m}^2). \tag{11–129}$$

Substitution of Eqs. (11–128) and (11–129) in Eq. (11–124) yields the backscatter cross section:

$$\sigma_{bs} = 4\pi b^2(\beta b)^4\left(\frac{\epsilon_r - 1}{\epsilon_r + 2}\right)^2 \quad (\text{m}^2). \tag{11–130}$$

b) For $f = 15$ (GHz), $\lambda = 20$ (mm), the radius of the raindrop $b = \frac{3}{2}$ (mm) $\ll \lambda$. We obtain

$$\sigma_{bs} = 1.25 \times 10^{-6} \quad (\text{m}^2)$$
$$= 1.25 \quad (\text{mm}^2),$$

which is a fraction of the geometrical cross section πb^2 of the sphere:

$$\frac{\sigma_{bs}}{\pi b^2} = \frac{1.25}{1.5^2\pi} = 0.177.$$

■

Of course, raindrops do not exist singly; nor is their shape strictly spherical. Meaningful calculations of backscatter from rain require a knowledge of the rainfall rate and the distribution of the drop size, which are mutually dependent. The assumption of an equivalent spherical drop for nonspherical droplets has been found to be acceptable as long as their sizes are much smaller than the wavelength. Of equal importance to the calculation of backscatter from rainfall is the estimation of the attenuation suffered by an electromagnetic wave propagating through rain due to an imaginary part of the permittivity of raindrops. Interested readers should refer to the literature for details. [13]

11–7 Transmit-Receive Systems

In the preceding section we discussed the concepts of effective area for receiving antennas and backscatter cross section for scattering objects. We shall now examine the power transmission relation between transmitting and receiving antennas. When the same antenna is used for transmitting short pulses of radiation and for receiving them after they have been reflected (scattered) back by a target, the transmit-receive system is a ***radar***; it is a special case. Measurement of the time elapsed Δt between the transmitted pulse and the received pulse determines the distance r of the target to the antenna site through the relation $\Delta t = 2r/c$, where c is the velocity of light.

If the transmission path between the transmitting and receiving antennas is near the earth's surface, the effect of the conducting earth must be considered. We shall also discuss the transmit-receive arrangement over a flat earth in this section.

11–7.1 FRIIS TRANSMISSION FORMULA AND RADAR EQUATION

Consider a communication circuit between stations 1 and 2 with antennas having effective areas A_{e1} and A_{e2}, respectively. The antennas are separated by a distance r. We wish to find a relation between the transmitted and the received powers.

Let P_L and P_t be the received and transmitted powers, respectively. Combining Eqs. (11–113) and (11–121), we obtain

$$\frac{P_L}{P_t} = \left(\frac{A_{e2}}{4\pi r^2}\right) G_{D1} = \left(\frac{A_{e2}}{4\pi r^2}\right)\left(\frac{4\pi A_{e1}}{\lambda^2}\right)$$

or

$$\boxed{\frac{P_L}{P_t} = \frac{A_{e1}A_{e2}}{r^2\lambda^2}.} \tag{11–131}$$

The relation in Eq. (11–131) is referred to as the ***Friis transmission formula.*** For a given transmitted power the received power is directly proportional to the product of the effective areas of the transmitting and receiving antennas and is inversely proportional to the square of the product of the distance of separation and wavelength.

Noting Eq. (11–121), we may write the Friis transmission formula in the following alternative form:

$$\boxed{\frac{P_L}{P_t} = \frac{G_{D1}G_{D2}\lambda^2}{(4\pi r)^2}.} \tag{11–132}$$

The received power P_L in Eqs. (11–131) and (11–132) assumes a matched condition and disregards the power dissipated in the antenna itself. From Eq. (11–131) we see that for a given transmitted power the received power increases as the square of the operating frequency (decreases as the inverse square of wavelength). But, at progressively increasing frequencies, P_t is limited by available technology, and the minimum detectable power over electromagnetic noise also increases. It is incorrect to conclude from Eq. (11–132) that P_L increases as the square of the wavelength because the directive gains usually decrease as the wavelength increases.

Now consider a radar system that uses the same antenna for transmitting short pulses of time-harmonic radiation and for receiving the energy scattered back from a target. For a transmitted power P_t the power density at a target at a distance r away is (see Eq. 11–112)

$$\mathscr{P}_T = \frac{P_t}{4\pi r^2} G_D(\theta, \phi), \tag{11–133}$$

where $G_D(\theta, \phi)$ is the directive gain of the antenna in the direction of the target. If σ_{bs} denotes the backscatter or radar cross section of the target, then the equivalent power that is scattered isotropically is $\sigma_{bs}\mathscr{P}_T$, which results in a power density at the antenna $\sigma_{bs}\mathscr{P}_T/4\pi r^2$. Let A_e be the effective area of the antenna. We have the following expression for the received power:

$$\begin{aligned} P_L &= A_e \sigma_{bs} \frac{\mathscr{P}_T}{4\pi r^2} \\ &= A_e \sigma_{bs} \frac{P_t}{(4\pi r^2)^2} G_D(\theta, \phi). \end{aligned} \tag{11–134}$$

By using Eq. (11–121), Eq. (11–134) becomes

$$\boxed{\frac{P_L}{P_t} = \frac{\sigma_{bs}\lambda^2}{(4\pi)^3 r^4} G_D^2(\theta, \phi),} \tag{11–135}$$

which is called the ***radar equation***. In terms of the antenna effective area A_e instead of the directive gain $G_D(\theta, \phi)$, the radar equation can be written as

$$\boxed{\frac{P_L}{P_t} = \frac{\sigma_{bs}}{4\pi}\left(\frac{A_e}{\lambda r^2}\right)^2.} \tag{11–136}$$

Because radar signals have to make round trips from the antenna to the target and then back to the antenna, the received power is inversely proportional to the fourth power of the distance r of the target from the antenna.

EXAMPLE 11–12 Assume that 50 (kW) is fed into the antenna of a radar system operating at 3 (GHz). The antenna has an effective area of 4 (m^2) and a radiation efficiency of 90%. The minimum detectable signal power (over noise inherent in the receiving system and from the environment) is 1.5 (pW), and the power reflection coefficient for the antenna on receiving is 0.05. Determine the maximum usable range of the radar for detecting a target with a backscatter cross section of 1 (m^2).

Solution At $f = 3 \times 10^9$ (Hz), $\lambda = 0.1$ (m):

$$A_e = 4 \quad (m^2),$$
$$P_t = 0.90 \times 5 \times 10^4 = 4.5 \times 10^4 \quad (W),$$
$$P_L = 1.5 \times 10^{-12}\left(\frac{1}{1 - 0.05}\right) = 1.58 \times 10^{-12} \quad (W),$$
$$\sigma_{bs} = 1 \quad (m^2).$$

From Eq. (11–136),

$$r^4 = \frac{\sigma_{bs} A_e^2}{4\pi\lambda^2}\left(\frac{P_t}{P_L}\right),$$

and

$$r = 4.36 \times 10^4 \text{ (m)} = 43.6 \quad \text{(km)}.$$

A satellite communication system makes use of satellites traveling in orbits in the earth's equatorial plane. The speed of the satellites and the radius of their orbits are such that the period of rotation of the satellites around the earth is the same as that of the earth. Thus the satellites appear to be stationary with respect to the earth's surface, and they are said to be geostationary. The radius of the geosynchronous orbit is 42,300 (km). With an earth radius of 6380 (km) the satellites are about 36,000 (km) from the earth's surface.

Signals are transmitted from a high-gain antenna at an earth station toward a satellite, which receives the signals, amplifies them, and retransmits them back toward the earth station at a different frequency. Three satellites equally spaced around the geosynchronous orbit would cover almost the entire earth's surface except the polar regions (see Problem P.11–27). A quantitative analysis of the power and antenna gain relations for a satellite communication circuit requires the application of the Friis transmission formula twice, once for the uplink (earth station to satellite) and once for the downlink (satellite to earth station).

11–7.2 WAVE PROPAGATION NEAR EARTH'S SURFACE

Consider a transmitting antenna A at a height h_1 and a receiving antenna B at a height h_2 above the flat earth's surface with a distance of separation d, as shown in Fig. 11–20. If antenna A is an elemental electric dipole, then the electric field intensity at B is the sum of the direct contribution $\mathbf{E}_{\theta 1}$ from A and the indirect contribution $\mathbf{E}_{\theta 2}$ after reflection at point C. We write

$$\mathbf{E} = \mathbf{E}_{\theta 1} + \mathbf{E}_{\theta 2}, \tag{11–137}$$

where the magnitudes of $\mathbf{E}_{\theta 1}$ and $\mathbf{E}_{\theta 2}$ are

$$E_{\theta 1} = K\left(\frac{e^{-j\beta R}}{R}\right)\sin\theta, \tag{11–137a}$$

$$E_{\theta 2} = K\left(\frac{e^{-j\beta R'}}{R'}\right)\sin\theta'. \tag{11–137b}$$

The constant K equals $jI\,d\ell\eta_0\beta/4\pi$ (see Eq. 11–19b), and the distance $R' = \overline{AC} + \overline{CB} = \overline{A'B}$. The effect of the perfectly conducting (assumed) earth's surface is replaced by an image antenna at A'. In the general case, $\mathbf{E}_{\theta 1}$ and $\mathbf{E}_{\theta 2}$ are not parallel; but if $d \gg h_1, h_2$, then $\theta \cong \theta'$, and Eqs. (11–137a) and (11–137b) may be combined to give

$$E_\theta \cong \mathbf{a}_\theta K\left(\frac{e^{-j\beta R}}{R}\right)(\sin\theta)F, \tag{11–138}$$

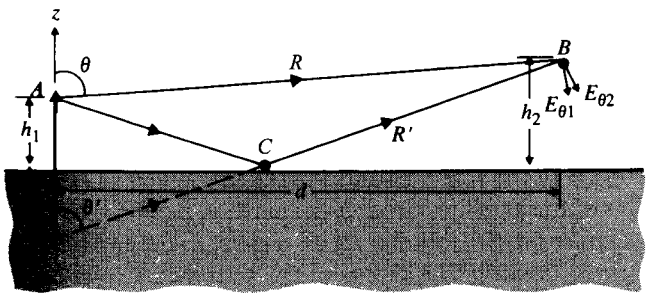

FIGURE 11–20
Transmit-receive system near the earth's surface.

where

$$F = 1 + e^{-j\beta(R'-R)}. \tag{11–139}$$

The distances

$$R = [d^2 + (h_2 - h_1)^2]^{1/2}$$
$$= d\left[1 + \frac{(h_2 - h_1)^2}{d^2}\right]^{1/2} \cong d + \frac{(h_2 - h_1)^2}{2d} \tag{11–140a}$$

and

$$R' = [d^2 + (h_2 + h_1)^2]^{1/2} \cong d + \frac{(h_2 + h_1)^2}{2d} \tag{11–140b}$$

yield approximately

$$R' - R \cong \frac{(h_2 + h_1)^2}{2d} - \frac{(h_2 - h_1)^2}{2d}$$
$$= \frac{2h_1h_2}{d}. \tag{11–141}$$

Substituting Eq. (11–141) in Eq. (11–139), we obtain

$$|F| = |1 + e^{-j\beta 2h_1h_2/d}|, \tag{11–142}$$

which is like the array factor of a two-element array.

Equation (11–142) may be written as

$$|F| = |e^{-j\beta h_1h_2/d}(e^{j\beta h_1h_2/d} + e^{-j\beta h_1h_2/d})| = 2\left|\cos\left(\frac{2\pi h_1h_2}{\lambda d}\right)\right|. \tag{11–143}$$

Equation (11–143) shows that for fixed values of h_1 and λ the electric field intensity E_θ at the receiving site B will have nulls and maximum values as the ratio h_2/d is changed. The quantity $|F|$ varies from 0 to 2 and is called the ***path-gain factor***. Calculation of the path-gain factor for a spherical earth is a much more involved task.

11–8 Some Other Antenna Types

Practical antennas take many different shapes and sizes, each designed to fulfill certain desired performance characteristics. Our attention so far has been focused on the radiation properties of linear antennas having a current distribution in the form of a standing wave. In this section we shall discuss several other types of antennas of practical importance.

11–8.1 TRAVELING-WAVE ANTENNAS

In the analysis of thin linear antennas in Section 11–4 we assumed that the center-driven dipole antennas were not terminated and that the currents from the excitation

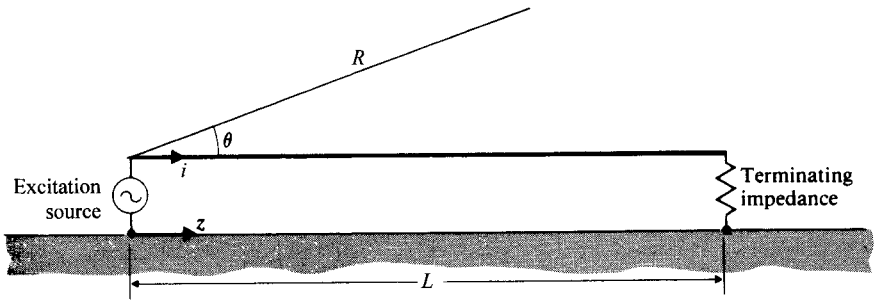

FIGURE 11–21
A traveling-wave antenna with termination.

sources were reflected at the ends, resulting in a standing-wave distribution as given in Eq. (11–51). If an antenna is several wavelengths long and properly terminated, as illustrated in Fig. 11–21, we have a situation similar to that of a transmission line terminated in its characteristic impedance. No reflection results, and the current distribution along the antenna is in the form of a traveling wave:

$$I(z) = I_0 e^{-j\beta z}. \tag{11–144}$$

Disregarding for the moment the effect of the nearby ground, we can find the far-zone electric field of an isolated antenna by using Eq. (11–144) in Eq. (11–19b) and integrating:

$$\begin{aligned} E_\theta &= \frac{j\eta_0 \beta \sin\theta}{4\pi r} e^{-j\beta R} \int_0^L I(z) e^{j\beta z \cos\theta}\, dz \\ &= \frac{j\eta_0 \beta I_0 \sin\theta}{4\pi R} e^{-j\beta R} \int_0^L e^{-j\beta z(1-\cos\theta)}\, dz \\ &= \frac{j60 I_0}{R} e^{-j\beta[R + (L/2)(1-\cos\theta)]} F(\theta), \end{aligned} \tag{11–145}$$

where

$$F(\theta) = \frac{\sin\theta \sin[\beta L(1-\cos\theta)/2]}{1-\cos\theta} \tag{11–146}$$

is the pattern function of an isolated traveling-wave antenna of length L. Comparison of Eqs. (11–146) and (11–56) shows that the pattern functions of traveling-wave and standing-wave antennas have quite different characteristics. One especially notable difference is that the pattern represented by Eq. (11–146) is no longer symmetrical with respect to the $\theta = \pi/2$ plane.

A typical radiation pattern of an isolated traveling-wave antenna that is several wavelengths long may look like that shown in Fig. 11–22. In general, the main beams tilt toward the direction of the traveling current wave: The longer the antenna, the more the tilt. The sidelobes are generally only a few decibels down from the main beam level.

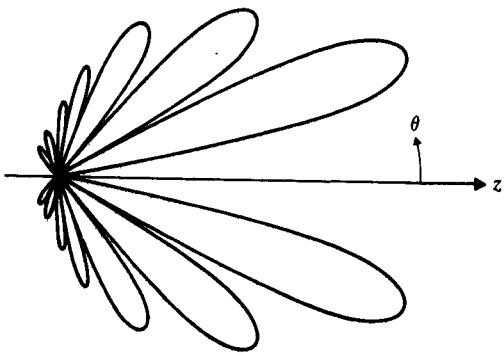

FIGURE 11–22
A typical radiation pattern of a traveling-wave antenna.

We can examine the effect of the ground by applying the method of images. The flat, perfectly conducting ground may be replaced by an image antenna carrying a current $I(z)$ given by Eq. (11–144) in the *opposite* direction, as shown in Fig. 11–23. We have, in effect, an array of two traveling-wave antennas separated by a distance $2h$ and carrying equal and opposite currents. By the principle of pattern multiplication the resultant pattern function is then the product of $F(\theta)$ in Eq. (11–146) and the array factor $|\cos(\psi/2)|$ of two elements given in Eq. (11–83). In this case, $d = 2h$ and $\xi = \pi$. We have

$$\left|\cos\frac{\psi}{2}\right| = \left|\cos\left(\beta h \sin\theta\cos\phi + \frac{\pi}{2}\right)\right| = |\sin(\beta h \sin\theta\cos\phi)|. \tag{11–147}$$

The long linear antenna excited by a progressive current wave is only one of many traveling-wave antennas.

11–8.2 HELICAL ANTENNAS

We have seen that the far-zone electromagnetic field produced by linear antennas and small loop antennas are linearly polarized; that is, the electric field at a given

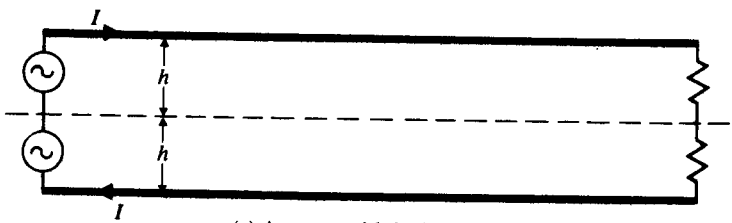

(a) Antenna with its image.

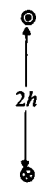

(b) End view
(a two-element array).

FIGURE 11–23
Method of images applied to traveling-wave antenna above perfectly conducting ground.

location has a fixed direction that does not change with time. For instance, the electric field in the far zone of a vertical dipole is $\mathbf{E} = \mathbf{a}_\theta E_\theta$, and that of a horizontal loop is $\mathbf{E} = \mathbf{a}_\phi E_\phi$. The signals radiated from these antennas can be received efficiently by a linear antenna oriented in the direction of the electric field. There are circumstances, however, in which the direction of polarization of the incoming radiation is unknown or the orientation of the receiving antenna changes (such as the antennas on satellites or space vehicles). No reception will occur when the receiving antenna happens to be perpendicular to the direction of polarization of the signal. Earth communication with satellites and space vehicles is complicated by the fact that radiations from the earth must propagate through the ionosphere, which, under the influence of the earth magnetic field, becomes anisotropic and causes the electric field to change direction, the extent of this change being dependent on the electron density of the ionosphere, the strength of the earth magnetic field, and the propagation path. In these circumstances the use of antennas with circular polarization is advantageous because they are able to intercept waves polarized in any direction not normal to the plane of circular polarization.

Since the superposition of two equal-magnitude linearly polarized waves in both space and time quadrature yields a circularly polarized wave (see Subsection 8–2.3), we can obviously construct an antenna radiating (and receiving, by virtue of reciprocity) circularly polarized waves by feeding two perpendicularly oriented dipoles with currents that are equal in magnitude but 90° out of phase. This type of composite crossed-dipole arrangement is called a ***turnstile antenna.*** If the currents are of different magnitudes, an elliptically polarized wave is radiated. A circularly or elliptically polarized wave can also be generated by combining electric and magnetic dipoles (see Problem P.11–4).

A ***helical antenna*** is a wire antenna wound in the form of a helix. It is usually installed over a flat grounded conducting plane and fed by a coaxial transmission line, as shown in Fig. 11–24. Depending on the dimensions of the helix, the helical antenna has two quite different modes of operation. When the dimensions are very small in comparison to the operating wavelength, its radiation pattern is like that of an elemental electric dipole, given in Fig. 11–3. Maximum radiation occurs in the

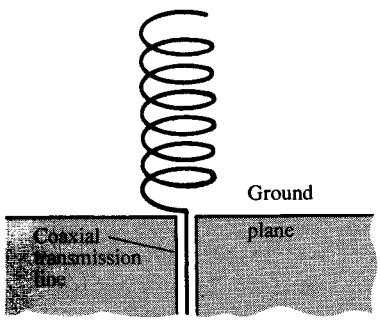

FIGURE 11–24
A helical antenna.

plane perpendicular to the helix axis. The helical antenna is said to be in the ***normal mode.*** An approximate analysis of the helical antenna radiating in the normal mode can be made with two assumptions. First, it is assumed that the helix can be replaced by a combination of elemental electric and magnetic dipoles, as illustrated in Fig. 11–25(a). Second, the current along the helix is assumed to be uniform both in amplitude and in phase. (Some kind of top loading would then be necessary.) The far-zone electric field for an N-turn helical antenna is then a combination of Eqs. (11–19b) and (11–30a):

$$\begin{aligned}\mathbf{E} &= \mathbf{a}_\theta E_\theta + \mathbf{a}_\phi E_\phi \\ &= \frac{N\omega\mu_0 I}{4\pi}\left(\frac{e^{-j\beta R}}{R}\right)[\mathbf{a}_\theta js + \mathbf{a}_\phi \beta\pi b^2]\sin\theta.\end{aligned} \tag{11–148}$$

Thus, the θ- and ϕ-components are in both space and time quadrature, resulting in elliptical polarization—circular polarization if

$$s = \beta\pi b^2 \tag{11–148a}$$

or

$$b = \frac{1}{\pi}\sqrt{\frac{s\lambda}{2}}. \tag{11–148b}$$

The maximum radiation is in the broadside direction, and the radiation pattern has the shape of a doughnut with zero inner diameter. Fig. 11–25(b) shows a section in the E-plane. Normal-mode helical antennas are seldomly used in practice on account of their low radiation efficiency and low directive gain.

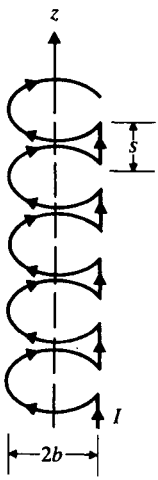

(a) Combination of elemental electric and magnetic dipoles.

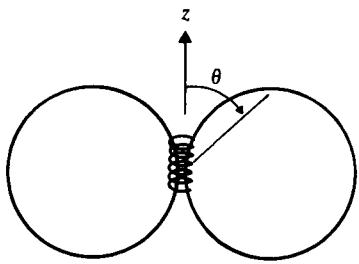

(b) E-plane radiation pattern.

FIGURE 11–25
Analysis of a normal-mode helical antenna.

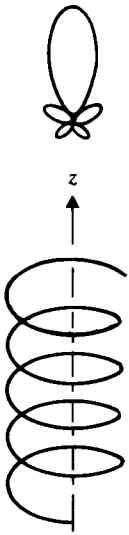

FIGURE 11–26
Axial-mode helical antenna and radiation pattern.

When both the turn circumference and the spacing between turns of a helix are comparable to a wavelength, the antenna behaves in an entirely different manner. The main beam of radiation will be in the end-fire direction, operating in the ***axial mode***. A theoretical analysis of an axial-mode helical antenna is very difficult because of its geometry. The boundary-value problem of determining the current distribution along the helix can only be solved numerically in a limited way. The usual approach is to use some experimentally observed results for an assumed traveling-wave current and find the radiation pattern [14]. We will simply assert that the radiation pattern of an axial-mode helical antenna takes the form of a main beam in the end-fire direction together with some sidelobes, as indicated in Fig. 11–26. The radiation in the main beam is elliptically polarized, the axial ratio of the polarization ellipse being dependent on the frequency and the various dimensions of the helix. Helical antennas operating in the axial mode have been installed on communication satellites and space vehicles as well as on earth stations. Arrays of helical antennas have been used at radio telescope sites.

11–8.3 YAGI-UDA ANTENNAS

One type of antenna that is of particular practical importance is the ubiquitous Yagi-Uda antenna [15], [16], which one sees on the rooftops of many households for reception of television signals. A ***Yagi-Uda antenna*** in the transmitting mode is an array of parallel linear antennas, of which only one is driven by an excitation source and the rest are parasitic (not directly connected to the source). In the receiving mode an electromagnetic wave impinges on all elements of the array, but the received signal is collected from one "active element." The simplicity in the feed structure is a major advantage of Yagi-Uda antennas over other linear arrays.

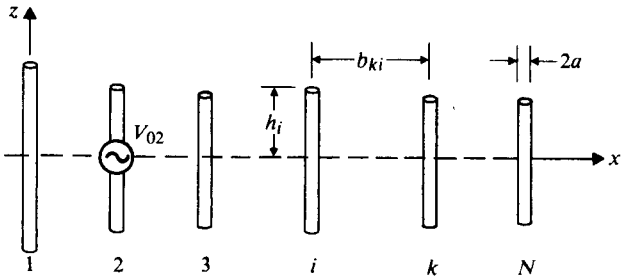

FIGURE 11–27
A typical Yagi-Uda array.

Figure 11–27 is a sketch of a typical Yagi-Uda antenna, which is actually an array. Element 2 is the dirven or active element and is normally a dipole of approximately (slightly less than) a half-wavelength long tuned to resonance. All other elements are parasitic. Element 1 is a ***reflector*** that is usually slightly longer than the driven element, whereas elements 3 to N are ***directors*** and are shorter than the driven element. Because all the elements are coupled, the current distribution in each element depends on the length and spacing of all the other elements. Consequently, a Yagi-Uda antenna of many elements presents a formidable analytical problem.

Experience has shown that little advantage is gained by using more than one reflector, but directivity can be improved by increasing the number of directors. A Yagi-Uda antenna is an endfire array with its main beam pointing away from the reflector. A good Yagi-Uda antenna should have a high directivity, a narrow beamwidth, low sidelobes, and a high front-to-back ratio. With the dipole radius assumed to be $a = 0.003369\lambda$ ($\ln \lambda/2a = 5$) a typical well-designed six-element Yagi-Uda array with four uniformly spaced directors of equal length may have the following data:

Antenna Dimensions

Element lengths	$2h_1$ 0.510λ	$2h_2$ 0.490λ	$2h_3 = 2h_4 = 2h_5 = 2h_6$ 0.430λ
Element spacings	b_{12} 0.250λ		$b_{23} = b_{34} = b_{45} = b_{56}$ 0.310λ

Pattern Characteristics

Directivity (Referring to $\lambda/2$ Dipole)	Half-power Beamwidth	First Sidelobes	Front-to-back Ratio
7.54 (8.77 dB)	45°	−7.2 (dB)	9.52 (dB)

The directivity of a half-wave dipole is 1.64 or 2.15 (dB)—see Eq. (11–65).

It has been found that uniformly spaced directors of equal lengths do not make an optimum array. Analytical methods have been developed for the maximization of the directivity of a Yagi-Uda array by adjusting both the interelement spacings and the lengths of all the array elements [17], [18]. The effects of a finite element radius and the mutual coupling between the array elements are taken into consideration. An application of these methods to the foregoing six-element array leads to the following optimized array (for dipole radius $a = 0.003369\lambda$):

Antenna Dimensions

Element lengths	$2h_1$ 0.476λ	$2h_2$ 0.452λ	$2h_3$ 0.436λ	$2h_4$ 0.430λ	$2h_5$ 0.434λ	$2h_6$ 0.430λ
Element spacings	b_{12} 0.250λ	b_{23} 0.289λ	b_{34} 0.406λ	b_{45} 0.323λ	b_{56} 0.422λ	

Pattern Characteristics

Directivity (Referring to $\lambda/2$-Dipole)	Half-power Beamwidth	First Sidelobes	Front-to-back Ratio
13.36 (12.58 dB)	37°	−10.9 (dB)	10.04 (dB)

The pattern characteristics of the optimized array are better in all aspects than those of the array with uniformly spaced directors of equal length. The optimized array sustains a predominantly traveling wave in the sense that the amplitudes of the currents in the driven and director elements decrease smoothly and the phases change progressively.

11-8.4 BROADBAND ANTENNAS

To provide flexibility and versatility, antennas are often required to operate over a wide frequency range with satisfactory pattern, impedance, and polarization characteristics. It is difficult to define the useful bandwidth of an antenna in general terms because what is useful depends critically on applications. Normally, one refers to the characteristics of the radiation pattern—namely, the directivity, the main-lobe beamwidth, and/or the sidelobe levels. However, for antennas of relatively small dimensions in terms of wavelength, the impedance characteristics become very important. For antennas with circular polarization the polarization characteristics may be the limiting factor on useful bandwidth. The bandwidth of linear dipoles is very narrow. Increasing the thickness of the dipoles improves the bandwidth slightly, but the latter can seldom be more than a few percent of the designed center frequency. In this subsection we discuss briefly two types of broadband antennas that have come

to be known as ***frequency-independent antennas*** and ***log-periodic antennas***. The design concepts of log-periodic dipole arrays will also be introduced.

The concept of frequency-independent antennas evolved from the observation that the pattern and impedance characteristics of an antenna depend critically on its dimensions measured in wavelengths. An examination of the pattern function in Eq. (11–56) and the radiation patterns in Fig. 11–6 will confirm this observation.† Antennas having similar geometric structures will then retain the same radiation characteristics if a frequency change does not change the ratio of antenna dimensions to wavelength—that is, if the dimensions of the antenna structures are scaled in wavelengths. This observation led to the suggestion that, if an antenna structure could be described entirely by *angles* without specifying any characteristic length dimensions, its pattern and impedance characteristics would be frequency-independent [19]. The ***equiangular spiral*** defined by the equation

$$r = r_0 e^{a(\phi - \delta)} \tag{11–149a}$$

is such a structure. In Eq. (11–149a), r and ϕ are the usual polar coordinates (cylindrical coordinates for a constant z); and r_0, a, and δ are design constants. The spiral is equiangular in the sense that it makes a constant angle with the radius vector at all points on the curve.

The structure defined by Eq. (11–149a) is also called a ***logarithmic spiral*** because the angle change is proportional to $\ln (r/r_0)$:

$$\phi - \delta = \frac{1}{a} \ln \left(\frac{r}{r_0} \right). \tag{11–149b}$$

The three constants r_0, a, and δ in Eqs. (11–149a) and (11–149b) determine the size of the terminal region, the reciprocal of the rate of spiral, and the arm width, respectively. Figure 11–28 shows a planar equiangular spiral antenna consisting of two symmetrical arms. The four edges of the two spirals are defined by the relations $r = r_0 \exp(a\phi)$, $r = r_0 \exp[a(\phi - \delta)]$, $r = r_0 \exp[a(\phi - \pi)]$, and $r = r_0 \exp[a(\phi - \pi - \delta)]$.

The antenna is excited at the terminals by a voltage source that causes currents to flow. One viewpoint is that the currents flow outward along the spiral arms until they reach a region where most of the radiation occurs. Another viewpoint is that the electric field vector between the spiral arms travels outward until the space between the arms is approximately a half-wavelength at the operating frequency. In this region, resonance occurs and strong radiation takes place. Beyond this region, currents and fields diminish rapidly, and the truncation of the infinite spiral at a finite boundary is of little consequence. An increase or a decrease in the operating frequency simply moves the radiating region inward or outward along the spiral, but the effective radiating aperture in terms of wavelength does not change. As a result, an automatic scaling process takes place, and the pattern and impedance characteristics

† We have not studied the method for calculating the input impedance of antennas. The impedance characteristics depend on the current distribution on an antenna, which, in turn, depends critically on antenna dimensions measured in wavelengths.

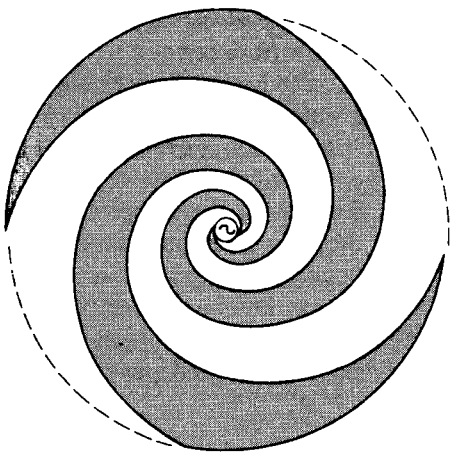

FIGURE 11–28
A planar two-arm equiangular spiral antenna.

remain almost indepedent of frequency [20]. The two-arm equiangular spiral antenna is circularly polarized. As the frequency is changed, the radiation pattern rotates about the axis normal to the spirals. Strictly speaking, the spirals must extend to infinity in order to be truly frequency-independent.

The planar equiangular spiral antenna of Fig. 11–28 is bidirectional in that it radiates a broadside main beam on both sides of the plane. This is sometimes undesirable. By wrapping a balanced two-arm equiangular spiral on the surface of a cone of revolution we can obtain a unidirectional radiation pattern with a single main beam in the direction of the cone apex. The pattern is still broadband and substantially circularly polarized. Both planar and conical equiangular spiral antennas can be designed to cover a 30-to-1 frequency range or more.

Can a broadband antenna be designed with linear (instead of circular) polarization? The search for an answer to this question led to a distinctive class of broadband linearly polarized antennas called ***log-periodic antennas*** [21], [22]. The basic log-periodic antenna has a toothed design cut out of sheet metal as shown in Fig. 11–29. The teeth are discontinuities that tend to localize the region of maximum radiation and cause the current to diminish rapidly beyond this region. The lengths of the teeth (the distances between the tips and the triangular support section) are determined by the angles between the lines from the origin. The region of strongest radiation is where the teeth are approximately a quarter-wavelength long.

The spacings between the successive edges of the teeth follow the rule that governs the distance between neighboring conductors in an equiangular spiral. From Eq. (11–149a),

$$\frac{r_{n+1}}{r_n} = \frac{r_0 e^{a(\phi-\delta)}}{r_0 e^{a(\phi+2\pi-\delta)}} = e^{-2\pi a} \qquad (11\text{–}150)$$
$$= \tau \qquad \text{(a constant)}.$$

This constant ratio is used as a design parameter for log-periodic antennas. Changing the operating frequency changes the tooth, whose length corresponds to a definite fraction of a wavelength. In terms of wavelength a scaling scheme is in effect that does not rely on a specification of length dimensions. This is the basis of the broadband nature of these antennas.

For an infinite structure, antenna characteristics would be identical at a discrete number of frequencies that are related by the parameter τ:

$$f_n = \tau f_{n+1} \tag{11–151a}$$

or

$$\ln (f_{n+1}) = \ln (f_n) + \ln \left(\frac{1}{\tau}\right). \tag{11–151b}$$

Antenna characteristics will vary somewhat between the discrete frequencies f_n and f_{n+1}; but, plotted versus the logarithm of frequency, they are periodic with a period equal to $\ln (1/\tau)$. Thus the name ***log-periodic antennas.***

It has been found that, instead of the basic sheet metal structure, a log-periodic antenna can be made with wires or tubes that outline the cut-out design. Theoretically, the sheet thickness and the wire diameter should increase linearly with the distance from the feed point in accordance with Eq. (11–150). This consideration becomes important when the demand on bandwidth is severe. Bandwidths covering a 30-to-1 frequency range or more are achievable.

The planar log-periodic antenna of Fig. 11–29 is bidirectional as was the planar equiangular spiral antenna. It can be made unidirectional if the two halves of the antenna are folded to form a wedge-like structure. The main beam will point off the

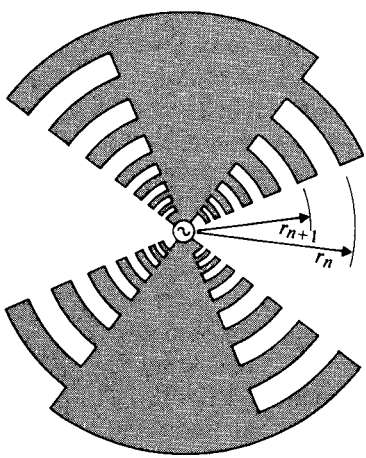

FIGURE 11–29
A planar log-periodic antenna.

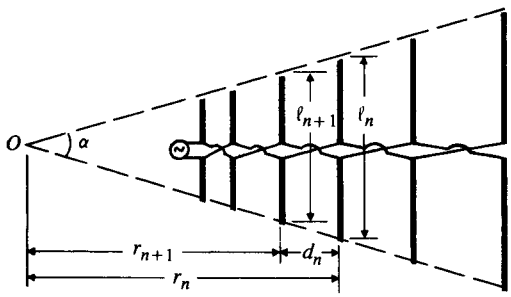

FIGURE 11–30
A log-periodic dipole array.

direction of the apex. It is interesting to note here that the planar log-periodic antenna in Fig. 11–29 without the teeth becomes a bow-tie antenna, which can be described entirely by the apex angle and is therefore expected to have broadband properties. This is true to a limited degree and explains the appearance of the bow-tie antenna as a form of commercially available UHF television antennas; but its finite length and lack of distinct resonance regions limit the bandwidth.

Broadband characteristics can also be achieved by a class of linear dipole arrays called ***log-periodic dipole arrays*** [23], [24], an example of which is shown in Fig. 11–30. The dipoles are of unequal lengths and are nonuniformly spaced according to the following relations:

$$\frac{\ell_{n+1}}{\ell_n} = \frac{r_{n+1}}{r_n} = \tau, \tag{11–152}$$

where τ is a design parameter, as in Eq. (11–150). Since the element spacings are related to the distances to the imaginary apex point O,

$$d_n = r_n - r_{n+1} = r_n(1 - \tau), \tag{11–153}$$

we also have

$$\frac{d_{n+1}}{d_n} = \tau. \tag{11–154}$$

Besides τ, only one other design parameter is required, which may be the angle α or the spacing factor κ:

$$\kappa = \frac{d_n}{2\ell_n}. \tag{11–155}$$

The relation among τ, α, and κ is as follows:

$$\begin{aligned} \tan\frac{\alpha}{2} &= \frac{\ell_n}{2r_n} = \frac{\ell_n(1-\tau)}{2d_n} \\ &= \frac{1-\tau}{4\kappa}. \end{aligned} \tag{11–156}$$

Hence only two of the three parameters are independent. Because of the scaling relations in Eqs. (11–152) and (11–154), a change in the operating frequency changes only the particular dipole whose length is a certain fraction of a wavelength.† The remarks pertaining to Eqs. (11–150), (11–151a), and (11–151b) apply, and we have a log-periodic dipole array.

The array is usually fed by a source connected to a transmission line. An important discovery is that neighboring elements must be fed at opposite phases. This is accomplished by transposing the wires of the transmission line leading to alternate dipoles, as illustrated in Fig. 11–30. At the operating frequency the active region of the array consists mainly of the several dipoles whose lengths are approximately a half-wavelength and where the dipole currents are large. The currents in the dipoles outside this region are relatively very small. The array operates in an end-fire fashion with its main beam of radiation in the direction of short dipoles.

11–9 Aperture Radiators

Our analysis of the radiation characteristics of antennas has generally proceeded from a current distribution on the antenna structure. From the current distribution the retarded vector potential is determined by using Eq. (11–3). The magnetic and electric field intensities can then be found from Eqs. (11–1) and (11–6), respectively. In many cases, electromagnetic radiation may be viewed as emanating from an opening or an aperture in a conducting enclosure. To be sure, the source of radiation can always be traced to some time-varying currents somewhere; but the current distributions are often unknown and difficult to determine or approximate. Such radiating systems are quite unlike dipole antennas and must be analyzed in a different way. They are aperture radiators or aperture antennas. Examples are slots, horns, reflectors, and lenses, some of which are illustrated in Fig. 11–31.

In our analysis we will use an approximate aperture-field method, assuming that electric and magnetic fields exist only in the aperture area and that the field elsewhere in an infinite screen containing the aperture is zero. In the case of the slot radiator shown in Fig. 11–31(a), the field for dominant TE_{10}-mode excitation is usually assumed to be a half-sine having a maximum at the center of the slot and tapering to zero at the edges. For the horn in Fig. 11–31(b) the aperture field is derived from the waveguide mode propagating into a horn of infinite extent. The aperture fields of the reflector in Fig. 11–31(c) and the lens in Fig. 11–31(d) are found by methods of geometrical optics from the reflection and refraction of rays emanating from the primary feed.

For TE_{10}-mode excitation the field in a plane aperture is approximately linearly polarized, and deviations from the results obtained by geometrical optics are small.

† Strictly speaking, it is also necessary to scale the radius a_n of the dipoles according to $a_{n+1}/a_n = \tau$.

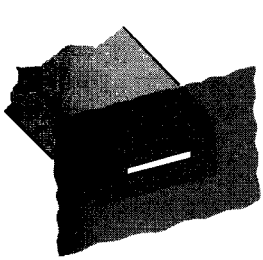

(a) Slot.

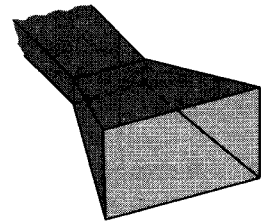

(b) Horn.

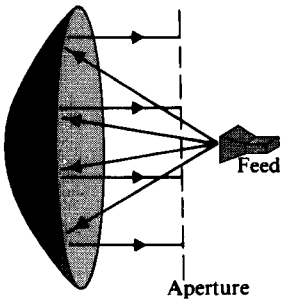

(c) Reflector.

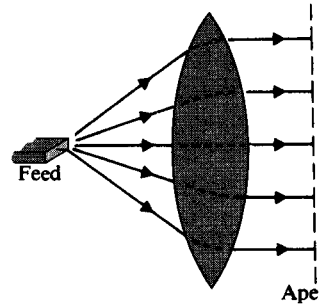

(d) Lens.

FIGURE 11–31
Aperture antennas.

With a nearly uniform phase over the aperture, the far-zone field is a two-dimensional Fourier integral of the field distribution in the aperture. Let the electric field distribution in the aperture outlined in Fig. 11–32 be linearly polarized, say in the x-direction, with no phase variation:

$$\mathbf{E}_a = \mathbf{a}_x E_a. \tag{11–157}$$

If the aperture dimensions are large in comparison to the operating wavelength, then almost all the energy of the radiated field will be contained in a small angular region around the z-axis, and the far-zone electric field at a distant point $P(R_0, \theta, \phi)$ can be written as $\mathbf{E}_P = \mathbf{a}_x E_P$, where [13], [25]

$$E_P = \frac{j}{\lambda R_0} \iint_{\text{aper.}} E_a(x', y') e^{-j\beta R}\, dx'\, dy'. \tag{11–158}$$

For $\beta R \gg 1$ we have

$$\begin{aligned} R &\cong R_0 - (\mathbf{a}_x x' + \mathbf{a}_y y') \cdot (\mathbf{a}_x \sin\theta \cos\phi + \mathbf{a}_y \sin\theta \sin\phi) \\ &= R_0 - (x' \sin\theta \cos\phi + y' \sin\theta \sin\phi). \end{aligned} \tag{11–159}$$

Substitution of Eq. (11–159) in Eq. (11–158) yields

$$E_P = \frac{j}{\lambda R_0} e^{-j\beta R_0} F(\theta, \phi), \tag{11–160}$$

where

$$\boxed{F(\theta, \phi) = \iint_{\text{aper.}} E_a(x', y') e^{j\beta \sin\theta(x' \cos\phi + y' \sin\phi)} \, dx' \, dy'} \tag{11–161}$$

is the pattern function of the aperture antenna. Equation (11–161) expresses the rather simple relation between the aperture distribution and the pattern function; namely, they are the Fourier transform of each other. The inverse relation, expressing $E_a(x', y')$ in terms of $F(\theta, \phi)$ enables us to determine the aperture field required for a specified pattern function. This is a synthesis problem.

For a rectangular aperture with dimensions $a \times b$ and separable field distributions:

$$E_a(x', y') = f_1(x') f_2(y'), \tag{11–162}$$

the pattern function in Eq. (11–161) is also separable:

$$F(\theta, \phi) = \int_{-a/2}^{a/2} f_1(x') e^{j\beta x' \sin\theta \cos\phi} \, dx' \int_{-b/2}^{b/2} f_2(y') e^{j\beta y' \sin\theta \sin\phi} \, dy'. \tag{11–163}$$

If we are interested only in the patterns in the principal planes, Eq. (11–163) can be further simplified.

1. *In the xz-plane,* $\phi = 0$:

$$\begin{aligned} F_{xz}(\theta) &= \left[\int_{-b/2}^{b/2} f_2(y') \, dy' \right] \int_{-a/2}^{a/2} f_1(x') e^{j\beta x' \sin\theta} \, dx' \\ &= C_1 \int_{-a/2}^{a/2} f_1(x') e^{j\beta x' \sin\theta} \, dx', \end{aligned} \tag{11–164}$$

   where C_1 is a constant. We see that the radiation pattern in the xz-plane depends only on the aperture field distribution in the x'-direction.

2. *In the yz-plane,* $\phi = \pi/2$:

$$\begin{aligned} F_{yz}(\theta) &= \left[\int_{-a/2}^{a/2} f_1(x') \, dx' \right] \int_{-b/2}^{b/2} f_2(y') e^{j\beta y' \sin\theta} \, dy' \\ &= C_2 \int_{-b/2}^{b/2} f_2(y') e^{j\beta y' \sin\theta} \, dy', \end{aligned} \tag{11–165}$$

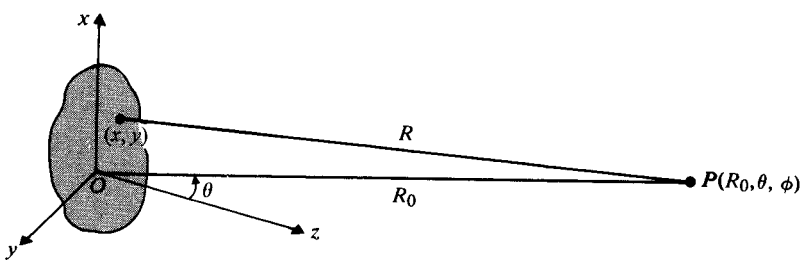

FIGURE 11–32
Pattern calculation from aperture-field distribution.

where C_2 is a constant. The radiation pattern in the yz-plane depends only on the aperture-field distribution in the y'-direction.

The directivity of an aperture radiator is obtained by using Eq. (11–35), which for convenience, is repeated below:

$$D = \frac{4\pi U_{\max}}{P_r}, \tag{11–166}$$

where

$$\begin{aligned} U_{\max} &= \frac{1}{2\eta_0} R_0^2 |E_p|^2_{\max} \\ &= \frac{1}{2\eta_0 \lambda^2} \left| \iint_{\text{aper.}} E_a(x', y')\, dx'\, dy' \right|^2 \end{aligned} \tag{11–167}$$

and

$$\begin{aligned} P_r &= \text{Total power radiated} \\ &= \frac{1}{2\eta_0} \iint_{\text{aper.}} |E_a(x', y')|^2\, dx'\, dy'. \end{aligned} \tag{11–168}$$

Combining Eqs. (11–166), (11–167), and (11–168), we have

$$\boxed{D = \frac{4\pi}{\lambda^2} \frac{\left| \iint_{\text{aper.}} E_a(x', y')\, dx'\, dy' \right|^2}{\iint_{\text{aper.}} |E_a(x', y')|^2\, dx'\, dy'} \qquad \text{(Dimensionless).}} \tag{11–169}$$

It is interesting to note that, when $E_a(x', y')$ = a constant (uniform aperture-field distribution), D is a maximum and equals $4\pi/\lambda^2$ times the area of the aperture. This is in agreement with Eq. (11–121).

EXAMPLE 11–13 For an $a \times b$ rectangular aperture with a uniform field distribution, find (a) the pattern function in a principal plane, (b) the half-power beamwidth, (c) the location of the first nulls, and (d) the level of the first sidelobes.

Solution For simplicity we set $E_a(x', y') = 1$.

a) The pattern function in a principal plane can be found from either Eq. (11–164) or Eq. (11–165). In the xz-plane ($\phi = 0$) we have, from Eq. (11–164),

$$\begin{aligned} F_{xz}(\theta) &= b \int_{-a/2}^{a/2} e^{j\beta x' \sin\theta}\, dx' \\ &= ab\left(\frac{\sin\psi}{\psi}\right), \end{aligned} \tag{11–170}$$

where

$$\psi = \frac{\pi a}{\lambda} \sin\theta. \tag{11–171}$$

Exactly the same pattern function is obtained for $F_{yz}(\theta)$ in the other principal plane ($\phi = \pi/2$) except that b will replace a in Eq. (11–171). Note that the pattern function in Eq. (11–170) is similar to the array factor of a uniform linear array given in Eq. (11–89) when ψ is small.

b) The half-power points are determined by setting

$$\frac{\sin \psi_{1/2}}{\psi_{1/2}} = \frac{1}{\sqrt{2}},$$

from which we find

$$\psi_{1/2} = \frac{\pi a}{\lambda} \sin \theta_{1/2} = 1.39$$

or

$$\sin \theta_{1/2} = 0.442 \frac{\lambda}{a}. \tag{11–172}$$

For sufficiently large apertures, $\sin \theta_{1/2}$ is nearly equal to $\theta_{1/2}$,† and the half-power beamwidth is approximately

$$2\theta_{1/2} \cong 0.88 \frac{\lambda}{a} \quad \text{(rad)}$$

$$\cong 50 \frac{\lambda}{a} \quad \text{(deg)}.$$

c) The first null occurs at

$$\psi_{n1} = \frac{\pi a}{\lambda} \sin \theta_{n1} = \pi$$

or

$$\theta_{n1} \cong \sin \theta_{n1} = \frac{\lambda}{a} \quad \text{(rad)}. \tag{11–173}$$

d) The location of the first sidelobes is found by setting

$$\frac{\partial}{\partial \psi}\left(\frac{\sin \psi}{\psi}\right) = 0,$$

which requires $\tan \psi_1 = \psi_1$ or $\psi_1 = \pm 1.43\pi$. Thus,

$$\left|\frac{\sin \psi_1}{\psi_1}\right| = \left|\frac{\sin 1.43\pi}{1.43\pi}\right| = 0.217.$$

Referring to unity at $\psi = 0$, we find that the first sidelobes are $20 \log_{10} (1/0.217) = 13.3$ (dB) down from the level of maximum radiation. ■

† For example, when $a = 5\lambda$, $\sin \theta_{1/2} = 0.442/5 = 0.0884$ and $\theta_{1/2} = \sin^{-1}(0.0884) = 0.0885$, an error of only 0.11%. The narrow beamwidth of the main lobe confirms our previous statement that almost all of the radiated energy is confined in a small angular region around the z-axis.

EXAMPLE 11–14 A linearly polarized uniform electric field $\mathbf{E}_a = \mathbf{a}_x E_0$ exists in a circular aperture of radius b in a conducting plane at $z = 0$. Assuming b to be large in comparison to wavelength, (a) find an expression for the far-zone electric field, and (b) determine the width of the main beam between first nulls.

Solution

a) For a circular aperture we use polar coordinates $x' = \rho' \cos \phi'$, $y' = \rho' \sin \phi'$, and $x' \cos \phi + y' \sin \phi = \rho'(\cos \phi \cos \phi' + \sin \phi \sin \phi') = \rho'(\cos (\phi - \phi')$. The integrand in Eq. (11–161) is to be integrated over the circular aperture. We have

$$\begin{aligned} F(\theta, \phi) &= E_0 \int_0^b \int_0^{2\pi} e^{j\beta\rho' \sin\theta \cos(\phi - \phi')} \rho' \, d\phi' \, d\rho' \\ &= E_0 \int_0^b 2\pi J_0(\beta\rho' \sin\theta) \rho' \, d\rho' \\ &= E_0 2\pi b^2 \left[\frac{J_1(\beta b \sin\theta)}{\beta b \sin\theta} \right], \end{aligned} \tag{11–174}^{\dagger}$$

where $J_1(u)$ is the Bessel function of the first kind of the first order. The far-zone electric field is then, from Eq. (11–160),

$$\mathbf{E}_P = \mathbf{a}_x j E_0 \frac{2\pi b^2}{\lambda R_0} e^{-j\beta R_0} \left[\frac{J_1(u)}{u} \right], \tag{11–175}$$

where

$$u = \beta b \sin\theta = \frac{2\pi b}{\lambda} \sin\theta. \tag{11–176}$$

b) The first null of the radiation pattern occurs at the first zero, u_{11}, of $J_1(u)$. From Table 10–2 we find $u_{11} = 3.832$, which corresponds to an angle

$$\begin{aligned} \theta_1 &= \sin^{-1}\left(\frac{3.832\lambda}{2\pi b}\right) \cong \frac{3.832\lambda}{2\pi b} \\ &= 1.22 \frac{\lambda}{D} \quad \text{(rad)}, \end{aligned} \tag{11–177}$$

where $D = 2b$ is the diameter of the circular aperture. Hence the width of the main beam between the first nulls is $2\theta_1 = 2.44\lambda/D$ (rad). Comparing θ_1 in Eq. (11–177) with θ_{n1} in Eq. (11–173) for a rectangular aperture with width a equaling the diameter D of the circular aperture, we find that the main-lobe beamwidth for the circular aperture is wider. On the other hand, the first sidelobe level for the circular aperture is found to be 0.13, which is $20 \log_{10}(1/0.13) = 17.7$ (dB) down from the maximum radiation. This is lower than the 13.3 (dB) first sidelobes for the rectangular aperture with $a = D$. ■

---

† We have made use of the following two integral relations:

$\int_0^{2\pi} e^{jw\cos\phi'} \, d\phi' = 2\pi J_0(w)$ and $\int w J_0(w) \, dw = w J_1(w)$.

In this section we have considered the radiation properties of only relatively simple cases of rectangular and circular apertures in conducting planes. The analysis of other aperture-type antennas such as horns, reflectors, and lenses is more difficult and requires the use of more advanced concepts. Slots cut in the walls of a waveguide that interrupt current flow will radiate. Suitably arranged, they will form antenna arrays in a manner analogous to dipole arrays. These and other radiation problems are topics for more specialized books on antennas [9], [11]–[13].

References

[1] H. Unz, "Linear arrays with arbitrarily distributed elements," *IRE Transactions on Antennas and Propagation*, vol. AP-8, pp. 222–223, March 1960.

[2] R. F. Harrington, "Sidelobe reduction by nonuniform element spacing," *IRE Transactions on Antennas and Propagation*, vol. AP-9, pp. 187–192, March 1961.

[3] A. Ishimaru and Y. S. Chen, "Thinning and broadbanding antenna arrays by unequal spacings," *IEEE Transactions on Antennas and Propagation*, vol. AP-13, pp. 34–42, January 1965.

[4] F. I. Tseng and D. K. Cheng, "Spacing perturbation techniques for array optimization," *Radio Science*, vol. 3 (New Series), pp. 451–457, May 1968.

[5] D. K. Cheng and P. D. Raymond, Jr., "Optimization of array directivity by phase adjustments," *Electronics Letters*, vol. 7, pp. 552–553, September 9, 1971.

[6] E. D. Sharp, "A triangular arrangement of planar array elements that reduces the number needed," *IRE Transactions on Antennas and Propagation*, vol. AP-9, pp. 126–129, March 1961.

[7] N. Goto, "Pattern synthesis of hexagonal planar array," *IEEE Transactions on Antennas and Propagation*, vol. AP-20, pp. 104–106, January 1972.

[8] D. K. Cheng, "Optimization techniques for antenna arrays," *Proceedings of the IEEE*, vol. 59, pp. 1664–1674, December 1971.

[9] E. C. Jordan and K. G. Balmain, *Electromagnetic Waves and Radiating Systems*, Prentice-Hall, Englewood Cliffs, N.J., 1968.

[10] M. T. Ma, *Theory and Application of Antenna Arrays*, Wiley, New York, 1974.

[11] R. S. Elliott, *Antenna Theory and Design*, Prentice-Hall, Englewood Cliffs, N.J., 1981.

[12] W. L. Stutzman and G. A. Thiele, *Antenna Theory and Design*, Wiley, New York, 1981.

[13] R. E. Collin, *Antennas and Radiowave Propagation*, McGraw-Hill, New York, 1985.

[14] K. F. Lee, *Principles of Antenna Theory*, Wiley, New York, 1984.

[15] H. Yagi, "Beam transmission of ultra short waves," *Proceedings of the IEEE*, vol. 16, pp. 715–741, June 1928.

[16] S. Uda and Y. Mushiaki, *Yagi-Uda Antenna*, Maruzan, Tokyo, 1954.

[17] D. K. Cheng and C. A. Chen, "Optimum element spacings for Yagi-Uda arrays," *IEEE Transactions on Antennas and Propagation*, vol. AP-21, pp. 615–623, September 1973.

[18] C. A. Chen and D. K. Cheng, "Optimum element lengths for Yagi-Uda arrays," *IEEE Transactions on Antennas and Propagation*, vol. AP-23, pp. 8–15, January 1975.

[19] V. H. Rumsey, *Frequency-Independent Antennas*, Academic Press, New York, 1966.

[20] J. D. Dyson, "The equiangular spiral," *IRE Transactions on Antennas and Propagation*, vol. AP-7, pp. 181–187, April 1959.

[21] R. H. DuHamel and D. E. Isbell, "Broadband logarithmically periodic antenna structures," *IRE National Convention Record,* Part I, pp. 119–128, 1957.
[22] R. H. DuHamel and F. R. Ore, "Logarithmically periodic antenna design," *IRE National Convention Record,* Part I, pp. 139–151, 1958.
[23] R. Carrel, "The design of log-periodic dipole antennas," *IRE International Convention Record,* Part I, pp. 61–75, 1961.
[24] E. C. Jordan et al., "Developments in broadband antennas," *IEEE Spectrum,* vol. 1, pp. 58–71, April 1964.
[25] S. Silver (ed.), *Microwave Antenna Theory and Design,* M.I.T. Radiation Laboratory Series, vol. 12, Chapters 5 and 6, McGraw-Hill, New York, 1949.

Review Questions

R.11–1 Give a general definition for *antenna.*

R.11–2 Why are antennas important for wireless communication over long distances?

R.11–3 State the procedure for finding the electromagnetic field due to an assumed time-harmonic current distribution on an antenna structure.

R.11–4 What is a *Hertzian dipole*?

R.11–5 What constitutes an elemental magnetic dipole?

R.11–6 Define the *near zone* and the *far zone* of an antenna.

R.11–7 Why are the near-zone fields called quasi-static fields?

R.11–8. Explain how the magnitude of far fields varies with distance.

R.11–9 In what ways does the electromagnetic field of a radiating magnetic dipole differ from that of a Hertzian dipole?

R.11–10 What are *radiation fields*?

R.11–11 Define *antenna pattern.*

R.11–12 Describe the E-plane and H-plane patterns of a Hertzian dipole.

R.11–13 Define *beamwidth* of an antenna pattern.

R.11–14 Define *sidelobe level* of an antenna pattern.

R.11–15 Define *radiation intensity.*

R.11–16 Define *directive gain* and *directivity* of an antenna.

R.11–17 Define *power gain* and *radiation efficiency* of an antenna.

R.11–18 Define *radiation resistance* of an antenna.

R.11–19 Discuss how the ratios (a/λ) and $(d\ell/\lambda)$ of a Hertzian dipole affect its radiation resistance and radiation efficiency.

R.11–20 Describe the radiation pattern of a half-wave dipole antenna.

R.11–21 What are the radiation resistance and directivity of a half-wave dipole antenna?

R.11–22 What is the image of a horizontal dipole over a conducting ground?

R.11–23 What are the radiation resistance and directivity of a vertical quarter-wave monopole over a conducting ground?

R.11–24 Define the *effective length* of a linear antenna for transmitting. Upon what factors does it depend?

R.11–25 Define the *effective length* of a linear antenna for receiving.

R.11–26 What is meant by the *normalized array factor* of an antenna array? How is it different from the pattern function of the individual antennas?

R.11–27 State the *principle of pattern multiplication.*

R.11–28 State the difference between a *broadside array* and an *endfire array.*

R.11–29 What is a *binomial array*? What are the relative excitation amplitudes of a six-element binomial array?

R.11–30 Is the radiation pattern of all linear binomial arrrays sidelobeless? Explain.

R.11–31 In the radiation pattern of a uniform linear array of many elements, how many decibels down from the principal maximum are the first sidelobes?

R.11–32 How can the sidelobes of an equally spaced linear array be made lower than those of a uniform linear array?

R.11–33 What is a *phased array*?

R.11–34 What is a *frequency-scanning array*?

R.11–35 What are the important consequences of reciprocity relations concerning antennas that operate in the transmitting and receiving modes?

R.11–36 Define *effective area* of an antenna.

R.11–37 What is the universal constant that is the ratio of the directive gain and the effective area of an antenna?

R.11–38 Define *backscatter cross section* of an object.

R.11–39 Explain the principle of *radar.*

R.11–40 What does the *Friis transmission formula* say?

R.11–41 Define *path gain factor* concerning wave propagation near the earth's surface.

R.11–42 In what essential ways does the radiation pattern of a long traveling-wave antenna differ from that of an unterminated dipole antenna?

R.11–43 What is the essential difference between the radiation characteristics of a helical antenna and a dipole antenna?

R.11–44 What are the two different operating modes of a helical antenna? Explain.

R.11–45 What is a *Yagi-Uda antenna*?

R.11–46 How should the lengths of the reflector and director elements in a Yagi-Uda array compare with the length of the driven element?

R.11–47 What is the principle of *frequency-independent antennas*?

R.11–48 What is an *equiangular spiral*? Why does it have broadband properties?

R.11–49 What is a *log-periodic antenna*?

R.11–50 Explain the principle of operation of log-periodic dipole arrays.

R.11–51 Give three examples of aperture radiators.

R.11–52 For a linearly polarized aperture field with uniform phase, what is the relation between the aperture's field distribution and the pattern function?

R.11–53 What is the directivity of an aperture having an area A and a linearly polarized uniform field distribution at frequency f?

R.11–54 Describe the manner in which the beamwidth in a principal plane of a rectangular aperture with a uniform field distribution depends on its dimensions.

R.11–55 Assume that a linearly polarized constant excitation field exists in a rectangular aperture with width b and a circular aperture with diameter $D = b$. Compare the main-lobe beamwidths and the first sidelobe levels of their radiation patterns.

Problems

P.11–1 Starting from Maxwell's equations, derive the nonhomogeneous wave equations (a) for **E**, and (b) for **H** in a simple medium.

P.11–2 Obtain the electric field intensity of a Hertzian dipole by finding both **A** and V and using Eq. (11–2). Check your result with Eqs. (11–16a, b, c).

P.11–3 A small filamentary rectangular loop of dimensions L_x and L_y lies in the xy-plane with its center at the origin and sides parallel to the x- and y-axes. The loop carries a current $i(t) = I_0 \cos \omega t$. Assuming L_x and L_y to be much less than the wavelength, find the instantaneous expressions for the following quantities at a point in the far zone:

a) vector magnetic potential **A**,
b) electric field intensity **E**,
c) magnetic field intensity **H**.

Compare the results in parts (b) and (c) with Eqs. (11–30a) and (11–30b), respectively.

P.11–4 A composite antenna consists of an elemental Hertzian electric dipole of length L along the z-axis and an elemental magnetic dipole of area S lying in the xy-plane. Equal time-harmonic currents of amplitude I_0 and angular frequency ω flow in the dipoles.

a) Verify that the far field of the composite antenna is elliptically polarized.
b) Determine the condition for circular polarization.

P.11–5 (a) Assume the spatial distribution of the current on a very thin center-fed half-wave dipole lying along the z-axis to be $I_0 \cos \beta z$, where $\beta = \omega/c = 2\pi/\lambda$. Find the charge distribution on the dipole. (b) Repeat part (a), assuming the current distribution along the dipole to be a triangular function described by

$$I(z) = I_0\left(1 - \frac{4}{\lambda}|z|\right).$$

P.11–6 A 1 (MHz) uniform current flows in a vertical antenna of length 15 (m). The antenna is a center-fed copper rod having a radius of 2 (cm). Find:

a) the radiation resistance,
b) the radiation efficiency,
c) the maximum electric field intensity at a distance of 20 (km) if the radiated power of the antenna is 1.6 (kW).

P.11–7 The amplitude of the time-harmonic current distribution on a center-fed short dipole antenna of length $2h (h \ll \lambda)$ can be approximated by a triangular function

$$I(z) = I_0\left(1 - \frac{|z|}{h}\right).$$

Find (a) the far-zone electric and magnetic field intensities, (b) the radiation resistance, and (c) the directivity.

P.11–8 The transmitting antenna of a radio navigation system is a vertical metal mast 40 (m) in height insulated from the earth. A 180 (kHz) source sends a current having an amplitude of 100 (A) into the base of the mast. Assuming the current amplitude in the antenna to decrease linearly toward zero at the top of the mast and the earth to be a perfectly conducting plane, determine:

a) the effective length of the antenna,
b) the maximum field intensity at a distance 160 (km) from the antenna,
c) the time-average radiated power,
d) the radiation resistance.

P.11–9 A time-harmonic uniform current $I_0 \cos \omega t$ flows in a small circular loop of radius b ($\ll \lambda$) lying in the xy-plane.

a) Find the radiation resistance R_r of the magnetic dipole.
b) Obtain an expression for its radiation efficiency η_r if the loop is made of copper wire of radius a,
c) Calculate R_r and η_r for $f = 1$ (MHz), $b = 50$ (cm), and $a = 3$ (mm).
d) Rework part (c) if the loop has ten closely wound insulated turns.

P.11–10 Repeat parts (a) and (b) of Problem P.11–9 for a small rectangular loop of sides L_x and L_y. Repeat part (c) for $f = 1$ (MHz), $L_x = L_y = 2b = 1$ (m), a = 3 (mm), and compare results.

P.11–11 Use the total field expressions in Eqs. (11–15) and (11–16) to find the time-average power radiated by a Hertzian dipole, and compare it with the result in Eq. (11–43) using only the far-zone fields.

P.11–12 Sketch the polar radiation pattern versus θ for a thin dipole antenna of total length $2h = 1.25\lambda$. Determine the width of the main beam between the first nulls.

P.11–13 Assuming a triangular current distribution on a center-fed $\lambda/6$ dipole ($h = \lambda/12$), find an expression for its effective length. What is its maximum value?

P.11–14 A 1.5 (MHz) uniform plane wave having a peak electric field intensity E_0 is incident on a half-wave dipole at an angle θ.

a) Find the expression for the open-circuit voltage V_{oc} at the terminals of the dipole.
b) If the dipole is connected to a matched load, what is the maximum power P_L delivered to the load?
c) Calculate V_{oc} and P_L for $E_0 = 50$ (mV/m) and for $\theta = \pi/2$ and $\pi/4$.

P.11–15 Two elemental dipole antennas, each of length $2h \ll \lambda$, are aligned colinearly along the z-axis with their centers spaced a distance d ($d > 2h$) apart. The excitations in the two antennas are of equal amplitude and equal phase.

a) Write the general expression for the far-zone electric field of this two-element colinear array.
b) Plot the normalized E-plane pattern for $d = \lambda/2$.
c) Repeat part (b) for $d = \lambda$.

P.11–16 A horizontal elemental electric dipole of length $d\ell$ and carrying a time-harmonic current of amplitude I_0 in the $+y$-direction is situated at a distance d above a perfectly conducting ground. Find its pattern functions (a) in the xy-plane, (b) in the xz-plane, and (c) in the yz-plane. (d) Sketch the patterns for parts (a), (b), and (c) for $d = \lambda/4$.

P.11–17 Plot the H-plane polar radiation pattern of two parallel dipoles for
a) $d = \lambda/4$, $\xi = \pi/2$; **b)** $d = 3\lambda/4$, $\xi = \pi/2$.

P.11–18 For a five-element broadside binomial array:
a) Determine the relative excitation amplitudes in the array elements.
b) Plot the array factor for $d = \lambda/2$.
c) Determine the half-power beamwidth and compare it with that of a five-element uniform array having the same element spacings.

P.11–19 For a uniform linear array of 12 elements spaced $\lambda/2$ apart:
a) Sketch the normalized array pattern $|A(\psi)|$ in Eq. (11–89) versus ψ.
b) Find the widths of the main beam at half-power points and between the first nulls when the array is operated in the broadside mode.
c) Repeat part (b) for an endfire operation.

P.11–20 For a uniform linear array with a large number of elements the denominator $\sin(\psi/2)$ in Eq. (11–89) remains small over a large portion of the normalized array pattern near the main beam and can be approximated by $(\psi/2)$. Use this approximation to determine the directivity of the array of a large uniform array with many elements.

P.11–21 Using the graph in Fig. 11–15(a) for the normalized array factor of a five-element broadside linear array with $d = \lambda/2$ and amplitude ratios 1:2:3:2:1, plot the polar radiation pattern for $d = \lambda/4$ and $\xi = -\pi/2$.

P.11–22 Letting $\zeta = \exp(j\psi)$, we can write the array factor of an equally spaced array as a polynomial, $A(\psi)$, in ψ, and many characteristics of the array pattern can be estimated by examining the distribution of the zeros of the array polynomial on a unit circle. In general, an N-element linear array has $N - 1$ zeros, ψ_{0m} $(m = 1, 2, \ldots, N - 1)$, distributed around the unit circle. Find $A(\psi)$ and locate all ψ_{0m} on a unit circle for the following linear arrays:
a) a two-element array,
b) a three-element binomial array,
c) a five-element uniform array,
d) a five-element array having amplitude ratios 1:2:3:2:1 (as in Example 11–9).
e) Based on the locations of ψ_{0m} for the two arrays in parts (c) and (d), explain why the pattern for the array in part (d) has lower sidelobes but a wider beamwidth.

P.11–23 Obtain the pattern function of a uniformly excited rectangular array of $N_1 \times N_2$ parallel half-wave dipoles. Assume that the dipoles are parallel to the z-axis and their centers are spaced d_1 and d_2 apart in the x- and y-directions, respectively.

P.11–24 Assume that a linearly polarized plane electromagnetic wave is incident on a half-wave dipole, as in Fig. 11–8.
a) Obtain an expression for the effective area, $A_e(\theta)$.
b) Calculate the maximum value of A_e for 100 (MHz).

P.11–25 A uniform plane wave with electric field intensity $\mathbf{E}_i = \mathbf{a}_z E_i$ impinges on a small dielectric sphere of radius b ($\ll \lambda$) and dielectric constant ϵ_r.
a) Find the total time-average power scattered by the sphere.
b) Obtain the expression for the *total scattering cross section* σ_s, which is the ratio of the total scattered power to the incident power density. Compare σ_s with the back-scatter cross section σ_{bs}.

P.11–26 Communication is to be established between two stations 1.5 (km) apart that operate at 300 (MHz). Each is equipped with a half-wave dipole.

a) If 100 (W) is transmitted from one station, how much power is received by a matched load at the other station?

b) Repeat part (a) assuming that both antennas are Hertzian dipoles.

P.11–27 (a) Show that three satellites equally spaced around the geosynchronous orbit in the equatorial plane would cover almost the entire earth's surface. Explain why the polar regions are not covered. (b) Assuming the main beam of the radiation pattern of the satellite antenna to have the shape of a circular cone that just covers the earth with no spillover, find a relation between the main-lobe beamwidth and the directive gain of the antenna.

P.11–28 The antenna at the earth station of a satellite communication link having a gain of 55 (dB) at 14 (GHz) is aimed at a geostationary satellite 36,500 (km) away. Assume that the antenna on the satellite has a gain of 35 (dB) in transmitting the signal back toward the earth station at 12 (GHz). The minimum usable signal is 8 (pW).

a) Neglecting antenna ohmic and mismatch losses, find the minimum satellite transmitting power required.

b) Find the peak transmitting pulse power needed at the earth station in order to detect the satellite as a passive object, assuming the backscatter cross section of the satellite including its solar panels as 25 (m^2) and the minimum detectable return pulse power to be 0.5 (pW).

P.11–29 A transmitting vertical half-wave dipole 60 (m) above the ground radiates 400 (W) at 100 (MHz). Assume the ground to be perfectly conducting.

a) Calculate the power available at a vertical half-wave receiving antenna 50 (km) away at a height 30 (m) above the ground.

b) At a distance 50 (km) from the transmitting antenna, where (at what altitudes) would there be a null field?

P.11–30 The current along an isolated and terminated traveling-wave antenna of length L is given as

$$I(z) = I_0 e^{-j\beta z}.$$

a) Find the far-zone vector potential, $\mathbf{A}(R, \theta)$.

b) Determine $\mathbf{H}(R, \theta)$ and $\mathbf{E}(R, \theta)$ from $\mathbf{A}(R, \theta)$.

c) Sketch the radiation pattern for $L = \lambda/2$.

P.11–31 A turnstile antenna consists of two perpendicular half-wave dipoles, one (antenna A) lying along the x-axis and the other (antenna B) along the y-axis. The output of antenna B, after a 90° phase retardation, is combined with that of antenna A. A right-hand elliptically polarized plane wave $\mathbf{E}_i = E_0(\mathbf{a}_x + \mathbf{a}_y jp) \exp(jkz)$ is incident on the antennas.

a) Determine the open-circuit voltage at the output terminals of the turnstile antenna. What is its value if $p = 1$?

b) Repeat part (a) for a left-hand elliptically polarized incident wave $\mathbf{E}_i = E_0(\mathbf{a}_x - \mathbf{a}_y jp) \exp(jkz)$.

c) Repeat part (a) for a linearly polarized incident wave $\mathbf{E}_i = \mathbf{a}_x E_0 \exp(jkz)$.

(*Hint:* Find the complex effective length of the turnstile antenna and use Eq. 11–76.)

P.11–32 A helical antenna operating in the normal mode has N turns with diameter $2b$ and interturn spacing s. Both $2b$ and s are very small in comparison to λ/N and are adjusted to radiate circularly polarized waves. Find:

a) its directive gain and directivity,

b) its radiation resistance.

P.11–33 For the problem in Example 11–13, write the expression for the far-zone electric field $\mathbf{E}_P(\theta, \phi)$ at a point $P(\theta, \phi)$ located near the z-axis ($\cos\theta \cong 1$) but not in either of the principal planes.

P.11–34 Assume that the field in an $a \times b$ rectangular aperture in an xy-plane is linearly polarized in the y-direction and that the aperture excitation has a uniform phase and a triangular amplitude distribution

$$f(x) = 1 - \left|\frac{2}{a}x\right|, \qquad |x| \leq \frac{a}{2}.$$

Find (a) the pattern function in the xz-plane, (b) the half-power beamwidth, (c) the location of the first nulls, and (d) the level of the first sidelobes. Compare the results with those obtained in Example 11–13 for uniform field distribution.

P.11–35 Do Problem P.11–34 for a uniform-phased cosinusoidal amplitude distribution

$$f(x) = \cos\left(\frac{\pi x}{a}\right), \qquad |x| \leq \frac{a}{2},$$

and compare your results with those obtained in Example 11–13 for a uniform field distribution.

Appendixes

A

Symbols and Units

A–1 Fundamental SI (Rationalized MKSA) Units†

Quantity	Symbol	Unit	Abbreviation
Length	ℓ	meter	m
Mass	m	kilogram	kg
Time	t	second	s
Current	I, i	ampere	A

† Besides the MKSA system for the units of length, mass, time, and current, the SI adopted by the International Committee on Weights and Measures consists of two other fundamental units. They are Kelvin degree (K) for thermodynamic temperature and candela (cd) for luminous intensity.

A–2 Derived Quantities

Quantity	Symbol	Unit	Abbreviation
Admittance	Y	siemens	S
Angular frequency	ω	radian/second	rad/s
Attenuation constant	α	neper/meter	Np/m
Capacitance	C	farad	F
Charge	Q, q	coulomb	C
Charge density (linear)	ρ_ℓ	coulomb/meter	C/m
Charge density (surface)	ρ_s	coulomb/meter^2	C/m^2
Charge density (volume)	ρ	coulomb/meter^3	C/m^3

(continued)

A–2 Derived Quantities (continued)

Quantity	Symbol	Unit	Abbreviation
Conductance	G	siemens	S
Conductivity	σ	siemens/meter	S/m
Current density (surface)	$\mathbf{J}_s$	ampere/meter	A/m
Current density (volume)	$\mathbf{J}$	ampere/meter^2	A/m^2
Dielectric constant (relative permittivity)	ϵ_r	(dimensionless)	—
Directivity	D	(dimensionless)	—
Electric dipole moment	$\mathbf{p}$	coulomb-meter	C·m
Electric displacement (Electric flux density)	$\mathbf{D}$	coulomb/meter^2	C/m^2
Electric field intensity	$\mathbf{E}$	volt/meter	V/m
Electric potential	V	volt	V
Electric susceptibility	χ_e	(dimensionless)	—
Electromotive force	$\mathscr{V}$	volt	V
Energy (work)	W	joule	J
Energy density	w	joule/meter^3	J/m^3
Force	$\mathbf{F}$	newton	N
Frequency	f	hertz	Hz
Impedance	Z, η	ohm	Ω
Inductance	L	henry	H
Magnetic dipole moment	$\mathbf{m}$	ampere-meter^2	A·m^2
Magnetic field intensity	$\mathbf{H}$	ampere/meter	A/m
Magnetic flux	Φ	weber	Wb
Magnetic flux density	$\mathbf{B}$	tesla	T
Magnetic potential (vector)	$\mathbf{A}$	weber/meter	Wb/m
Magnetic susceptibility	χ_m	(dimensionless)	—
Magnetization	$\mathbf{M}$	ampere/meter	A/m
Magnetomotive force	$\mathscr{V}_m$	ampere	A
Permeability	μ, μ_0	henry/meter	H/m
Permittivity	ϵ, ϵ_0	farad/meter	F/m
Phase	ϕ	radian	rad
Phase constant	β	radian/meter	rad/m
Polarization vector	$\mathbf{P}$	coulomb/meter^2	C/m^2
Power	P	watt	W
Poynting vector (power density)	$\mathscr{P}$	watt/meter^2	W/m^2
Propagation constant	γ	meter^{-1}	m^{-1}

(continued)

A–2 Derived Quantities (continued)

Quantity	Symbol	Unit	Abbreviation
Radiation intensity	U	watt/steradian	W/sr
Reactance	X	ohm	Ω
Relative permeability	μ_r	(dimensionless)	—
Relative permittivity (dielectric constant)	ϵ_r	(dimensionless)	—
Reluctance	$\mathscr{R}$	henry^{-1}	H^{-1}
Resistance	R	ohm	Ω
Susceptance	B	siemens	S
Torque	T	newton-meter	N·m
Velocity	u	meter/second	m/s
Voltage	V	volt	V
Wavelength	λ	meter	m
Wavenumber	k	radian/meter	rad/m
Work (energy)	W	joule	J

A–3 Multiples and Submultiples of Units

Factor by Which Unit Is Multiplied	Prefix	Symbol
$1\,000\,000\,000\,000\,000\,000 = 10^{18}$	exa	E
$1\,000\,000\,000\,000\,000 = 10^{15}$	peta	P
$1\,000\,000\,000\,000 = 10^{12}$	tera	T
$1\,000\,000\,000 = 10^{9}$	giga	G
$1\,000\,000 = 10^{6}$	mega	M
$1\,000 = 10^{3}$	kilo	k
$100 = 10^{2}$	hecto†	h
$10 = 10^{1}$	deka†	da
$0.1 = 10^{-1}$	deci†	d
$0.01 = 10^{-2}$	centi†	c
$0.001 = 10^{-3}$	milli	m
$0.000\,001 = 10^{-6}$	micro	μ
$0.000\,000\,001 = 10^{-9}$	nano	n
$0.000\,000\,000\,001 = 10^{-12}$	pico	p
$0.000\,000\,000\,000\,001 = 10^{-15}$	femto	f
$0.000\,000\,000\,000\,000\,001 = 10^{-18}$	atto	a

† These prefixes are generally not used except for measurements of length, area, and volume.

B

Some Useful Material Constants

B–1 Constants of Free Space

Constant	Symbol	Value
Velocity of light	c	$\sim 3 \times 10^8$ (m/s)
Permittivity	ϵ_0	$\sim \frac{1}{36\pi} \times 10^{-9}$ (F/m)
Permeability	μ_0	$4\pi \times 10^{-7}$ (H/m)
Intrinsic impedance	η_0	$\sim 120\pi$ or 377 (Ω)

B–2 Physical Constants of Electron and Proton

Constant	Symbol	Value
Rest mass of electron	m_e	9.107×10^{-31} (kg)
Charge of electron	$-e$	-1.602×10^{-19} (C)
Charge-to-mass ratio of electron	$-e/m_e$	-1.759×10^{11} (C/kg)
Radius of electron	R_e	2.81×10^{-15} (m)
Rest mass of proton	m_p	1.673×10^{-27} (kg)

B–3 Relative Permittivities (Dielectric Constants)†

Material	Relative Permittivity, ϵ_r
Air	1.0
Bakelite	5.0
Glass	4–10
Mica	6.0
Oil	2.3
Paper	2–4
Parafin wax	2.2
Plexiglass	3.4
Polyethylene	2.3
Polystyrene	2.6
Porcelain	5.7
Rubber	2.3–4.0
Soil (dry)	3–4
Teflon	2.1
Water (distilled)	80
Seawater	72

B–4 Conductivities†

Material	Conductivity, σ(S/m)	Material	Conductivity, σ(S/m)
Silver	6.17×10^7	Fresh water	10^{-3}
Copper	5.80×10^7	Distilled water	2×10^{-4}
Gold	4.10×10^7	Dry soil	10^{-5}
Aluminum	3.54×10^7	Transformer oil	10^{-11}
Brass	1.57×10^7	Glass	10^{-12}
Bronze	10^7	Porcelain	2×10^{-13}
Iron	10^7	Rubber	10^{-15}
Seawater	4	Fused quartz	10^{-17}

† Note that the constitutive parameters of some of the materials are frequency and temperature dependent. The listed constants are average low-frequency values at room temperature.

B–5 Relative Permeabilities†

Material	Relative Permeability, μ_r
Ferromagnetic (nonlinear)	
Nickel	250
Cobalt	600
Iron (pure)	4,000
Mumetal	100,000
Paramagnetic	
Aluminum	1.000021
Magnesium	1.000012
Palladium	1.00082
Titanium	1.00018
Diamagnetic	
Bismuth	0.99983
Gold	0.99996
Silver	0.99998
Copper	0.99999

† Note that the constitutive parameters of some of the materials are frequency and temperature dependent. The listed constants are average low-frequency values at room temperature.

C

Index of Tables

General Bibliography

In addition to the references included in the footnotes throughout the book and at the end of Chapter 11, the following books on electromagnetic fields and waves at a comparable level have been found to be useful.

Bewley, L. V., *Two Dimensional Fields in Electrical Engineering*, Dover Publications, New York, 1963.

Collin, R. E., *Antennas and Radiowave Propagation*, McGraw-Hill, New York, 1985.

Crowley, J. M., *Fundamentals of Applied Electrostatics*, Wiley, New York, 1986.

Feynman, R. P.; Leighton, R. O.; and Sands, M., *Lectures on Physics*, vol. 2, Addison-Wesley, Reading, Mass., 1964.

Javid, M., and Brown, P. M., *Field Analysis and Electromagnetics*, McGraw-Hill, New York, 1963.

Jordan, E. C., and Balmain, K. G., *Electromagnetic Waves and Radiating Systems*, 2nd ed., Prentice-Hall, Englewood Cliffs, N.J., 1968.

Kraus, J. D., *Electromagnetics*, 3rd ed., McGraw-Hill, New York, 1984.

Lorrain, P., and Corson, D., *Electromagnetic Fields and Waves*, 2nd ed., Freeman, San Franscisco, Calif., 1970.

Paris, D. T., and Hurd, F. K., *Basic Electromagnetic Theory*, McGraw-Hill, New York, 1969.

Parton, J. E.; Owen, S. J. T.; and Raven, M. S., *Applied Electromagnetics*, 2nd ed., Macmillan, London, 1986.

Plonsey, R., and Collin, R. E., *Principles and Applications of Electromagnetic Fields*, 2nd ed., McGraw-Hill, New York, 1982.

Popović B. D. *Introductory Engineering Electromagnetics*, Addison-Wesley, Reading, Mass., 1971.

Ramo, S.; Whinnery, J. R.; and Van Duzer, T., *Fields and Waves in Communication Electronics*, 2nd ed., Wiley, New York, 1984.

Sander K. F., and Reed, G. A. L., *Transmission and Propagation of Electromagnetic Waves*, 2nd ed., Cambridge University Press, Cambridge, England, 1986.

Seshadri, S. R., *Fundamentals of Transmission Lines and Electromagnetic Fields*, Addison-Wesley, Reading, Mass., 1971.

Shen, L. C., and Kong, J. A., *Applied Electromagnetism*, 2nd ed., PWS Engineering, Boston, Mass., 1987.

Zahn, M., *Electromagnetic Field Theory*, Wiley, New York, 1979.

Answers to Selected Problems

Chapter 2

P.2-1 a) $(\mathbf{a}_x + \mathbf{a}_y 2 - \mathbf{a}_z 3)/\sqrt{14}$. b) $\sqrt{53}$. c) -11. d) 135.5°.
e) $11/\sqrt{29}$. f) $-(\mathbf{a}_x 4 + \mathbf{a}_y 13 + \mathbf{a}_z 10)$. g) -42.
h) $\mathbf{a}_x 2 - \mathbf{a}_y 40 + \mathbf{a}_z 5$ and $\mathbf{a}_x 55 - \mathbf{a}_y 44 - \mathbf{a}_z 11$.

P.2-5 $\mathbf{X} = (p\mathbf{A} + \mathbf{B} \times \mathbf{A})/A^2$.

P.2-9 a) $\cos(\alpha - \beta) = \cos\alpha\cos\beta + \sin\alpha\sin\beta$.

P.2-15 1.12.

P.2-17 a) $|\mathbf{E}| = 1/2, E_x = -0.212$. b) $\theta = 154°$.

P.2-21 a) 14. b) 14.

P.2-23 a) $(\nabla V)_P = -(\mathbf{a}_y 0.026 + \mathbf{a}_z 0.043)$. b) 0.0485.

P.2-25 $\ell = 0, m = p = 1/\sqrt{2}$; $\int_S \mathbf{F} \cdot d\mathbf{s} = 20$.

P.2-29 $\oint_S \mathbf{A} \cdot d\mathbf{s} = \int_V \nabla \cdot \mathbf{A}\, dv = 1{,}200\pi$.

P.2-31 See Eq. (2–114).

P.2-35 $\dfrac{1}{R\sin\theta}\left[\dfrac{\partial}{\partial\theta}(A_\phi \sin\theta) - \dfrac{\partial A_\theta}{\partial\phi}\right]$.

P.2-39 a) $c_1 = 1, c_2 = 0, c_3 = -3$. b) $c_4 = -1$. c) $V = -\dfrac{x^2}{2} - xz + 3yz + \dfrac{z^2}{2}$.

Chapter 3

P.3-1 a) $\alpha = \tan^{-1}(mu_0^2/ewE_d)$. b) $L/w = 10.5$.

P.3-5 a) $Q_1/Q_2 = -3/4\sqrt{2}$. b) $Q_1/Q_2 = 1/2\sqrt{2}$.

P.3-7 $|\mathbf{F}| = Q\rho_\ell bh/2\epsilon(b^2 + h^2)^{3/2}$.

P.3-9 $\mathbf{a}_y 3\rho_{\ell 1}/4\pi\epsilon_0 L$.

P.3–11 (1) $0 \le R \le b$: $E_{R1} = \dfrac{\rho_0 R}{\epsilon_0}\left(\dfrac{1}{3} - \dfrac{R^2}{5b^2}\right)$. (2) $b \le R < R_i$: $E_{R2} = \dfrac{2\rho_0 b^3}{15\epsilon_0 R^2}$.

(3) $R_i < R < R_o$: $E_{R3} = 0$. (4) $R > R_o$: $E_{R4} = \dfrac{2\rho_0 b^3}{15\epsilon_0 R^2}$.

P.3–13 a) $28(\mu J)$. b) $28(\mu J)$.

P.3–15 a) $V = \dfrac{qd^2}{16\pi\epsilon_0 R^3}(3\cos^2\theta - 1)$, $\mathbf{E} = \dfrac{3qd^2}{16\pi\epsilon_0 R^4}[\mathbf{a}_R(3\cos^2\theta - 1) + \mathbf{a}_\theta \sin 2\theta]$.

b) $R^3 = C_V(3\cos^2\theta - 1)$.

c) $R^2 = C_E \sin^2\theta\cos\theta$.

P.3–17 $V_P = \dfrac{\rho_\ell}{4\pi\epsilon}\left[\sinh^{-1}\left(\dfrac{L-x}{b}\right) + \sinh^{-1}\left(\dfrac{x}{b}\right)\right]$.

P.3–19 If origin is chosen at the center of the base of the circular tube:

a) $z \ge h$, $V_o = \dfrac{b\rho_s}{2\epsilon_0}\ln\dfrac{z + \sqrt{b^2 + z^2}}{(z-h) + \sqrt{b^2 + (z-h)^2}}$.

b) $z \le h$, $V_i = \dfrac{b\rho_s}{2\epsilon_0}\ln\dfrac{1}{b^2}(z + \sqrt{b^2 + z^2})[(h - z) + \sqrt{b^2 + (h-z)^2}]$,

where $\rho_s = Q/2\pi bh$.

P.3–21 $r_o = \dfrac{4\pi\epsilon_0 b^3}{Ne}E_o$.

P.3–23 $\mathbf{P}/3\epsilon_0$.

P.3–25 $\mathbf{E}_2(z=0) = \mathbf{a}_x 2y - \mathbf{a}_y 3x + \mathbf{a}_z(10/3)$.

P.3–29 a) 19.3 (kV). b) 1.82 (kV).

P.3–31 a) $\mathbf{E}(a) = \mathbf{a}_r \dfrac{V_0}{a\ln(b/a)}$. b) $b/a = e = 2.718$. c) $\min E(a) = eV_0/b$.

d) $C = 2\pi\epsilon$ (F/m).

P.3–33 $C = \dfrac{\pi\epsilon_0(\epsilon_{r1} + \epsilon_{r2})L}{\ln(r_o/r_i)}$.

P.3–35 a) 0.708 (mF). b) 1.35×10^{10} (C).

P.3–37 a) $\mathbf{D} = \begin{cases} \mathbf{a}_R \dfrac{\epsilon_0\epsilon_r V}{R^2\left(\dfrac{1}{R_i} - \dfrac{1}{2b} - \dfrac{1}{2R_o}\right)}, & \text{for } R_i < R < R_o; \\ 0, \text{ for } R < R_i \text{ and } R > R_o. \end{cases}$

b) $C = \dfrac{4\pi\epsilon_0\epsilon_r}{\dfrac{1}{R_i} - \dfrac{1}{2b} - \dfrac{1}{2R_o}}$.

P.3–39 Designate the wires as conductors 0, 1, and 2 with wire 1 in the center. $C_{10} = C_{12} = 3.36$ (pF/m), $C_{20} = 2.35$ (pF/m).

P.3–41 1.69×10^{-15} (m).

P.3–47 $F_\ell = \dfrac{\pi\epsilon_0 V_0^2}{2D[\ln(D/b)]^2}$.

Chapter 4

P.4–1 a) $V_d = \dfrac{5yV_0}{(4+\epsilon_r)d}$, $\mathbf{E}_d = -\mathbf{a}_y \dfrac{5V_0}{(4+\epsilon_r)d}$.

b) $V_a = \dfrac{5\epsilon_r y - 4(\epsilon_r - 1)d}{(4+\epsilon_r)d} V_0$, $\mathbf{E}_a = -\mathbf{a}_y \dfrac{5\epsilon_r V_0}{(4+\epsilon_r)d}$.

c) $(\rho_s)_{y=d} = \dfrac{5\epsilon_0\epsilon_r V_0}{(4+\epsilon_r)d} = -(\rho_s)_{y=0}$.

P.4–7 a) $\rho_s = -\dfrac{Qd}{2\pi(d^2+r^2)^{3/2}}$.

b) $-Q$.

P.4–11 $C = \dfrac{\pi\epsilon_0}{\ln\{d/[a\sqrt{1+(d/2h)^2}]\}}$.

P.4–13 $C = \dfrac{2\pi\epsilon_0}{\ln\left[\frac{1}{2}\left(\frac{D^2}{a_1a_2} - \frac{a_1}{a_2} - \frac{a_2}{a_1}\right) - \sqrt{\frac{1}{4}\left(\frac{D^2}{a_1a_2} - \frac{a_1}{a_2} - \frac{a_2}{a_1}\right)^2 - 1}\right]}$

$= \dfrac{2\pi\epsilon_0}{\cosh^{-1}\left[\frac{1}{2}\left(\frac{D^2}{a_1a_2} - \frac{a_1}{a_2} - \frac{a_2}{a_1}\right)\right]}$.

P.4–15 b) $\rho_s = -\dfrac{Q(b^2-d^2)}{4\pi b(b^2+d^2-2bd\cos\theta)^{3/2}}$.

P.4–17 $Q_1 = Q_2 = \dfrac{\epsilon_2 - \epsilon_1}{\epsilon_2 + \epsilon_1} Q$.

P.4–19 $V_n(x,y) = C_n \cosh\dfrac{n\pi}{b}(x-a)\cos\dfrac{n\pi}{b}y$.

P.4–21 $V_n(x,y) = \sin\dfrac{n\pi}{a}x\left[A_n \sinh\dfrac{n\pi}{a}y + B_n\cosh\dfrac{n\pi}{a}y\right]$.

P.4–23 a) $V(\phi) = \dfrac{V_0}{\alpha}\phi$. b) $V(\phi) = \dfrac{V_0}{2\pi-\alpha}(2\pi - \phi)$.

P.4–25 $V(r,\phi) = -E_0 r\left(1 - \dfrac{b^2}{r^2}\right)\cos\phi$.

$\mathbf{E}(r,\phi) = \mathbf{a}_r E_0\left(1 + \dfrac{b^2}{r^2}\right)\cos\phi - \mathbf{a}_\phi E_0\left(1 - \dfrac{b^2}{r^2}\right)\sin\phi$.

P.4–27 a) $V(\theta) = V_0 \dfrac{\ln\left(\tan\frac{\theta}{2}\right)}{\ln\left(\tan\frac{\alpha}{2}\right)}$.

b) $\mathbf{E}(\theta) = -\mathbf{a}_\theta \dfrac{V_0}{R\ln[\tan(\alpha/2)]\sin\theta}$.

P.4–29 $V_i(R,\theta) = -\dfrac{3E_0}{\epsilon_r + 2}R\cos\theta, \quad V_o(R,\theta) = -\left[R - \dfrac{(\epsilon_r - 1)\,b^3}{(\epsilon_r + 2)\,R^2}\right]E_0\cos\theta.$

$$\mathbf{E}_i(R,\theta) = (\mathbf{a}_R\cos\theta - \mathbf{a}_\theta\sin\theta)\frac{3E_0}{\epsilon_r + 2} = \mathbf{a}_z\frac{3E_0}{\epsilon_r + 2}.$$

$$\mathbf{E}_o(R,\theta) = \mathbf{a}_R\left[1 + \frac{2(\epsilon_r - 1)b^3}{(\epsilon_r + 2)R^3}\right]E_0\cos\theta - \mathbf{a}_\theta\left[1 - \frac{(\epsilon_r - 1)b^3}{(\epsilon_r + 2)R^3}\right]E_0\sin\theta.$$

Chapter 5

P.5–1 **a)** $V(y) = V_0(y/d)^{4/3}, \quad E(y) = -(4V_0/3d)(y/d)^{1/3}.$

b) $Q = -(4V_0/3d)\epsilon_0 S.$

c) Charge on cathode = 0; charge on anode = $-Q$.

d) 3.58 (ns).

P.5–3 **a)** $2.32\,a$.

b) $E_1 = E_2 = I/2\pi a^2\sigma.$

P.5–5 $I_1 = 0.7\,(\text{A}), \quad P_{R1} = 0.163\,(\text{W}); \quad I_2 = 0.140\,(\text{A}), P_{R2} = 0.392\,(\text{W});$
$I_3 = 0.093\,(\text{A}), P_{R3} = 0.261\,(\text{W}); \quad I_4 = 0.233\,(\text{A}), P_{R4} = 0.436\,(\text{W});$
$I_5 = 0.467\,(\text{A}), P_{R5} = 2.178\,(\text{W}).$

P.5–7 **a)** 4.88 (ps). **b)** $W_i/(W_i)_0 = 10^{-4}$; heat loss.

c) $W_o = 45\,(\text{kJ}).$

P.5–9 **a)** $E_2 = \left[\sin^2\alpha_1 + \left(\dfrac{\sigma_1}{\sigma_2}\cos\alpha_1\right)^2\right]^{1/2}, \quad \alpha_2 = \tan^{-1}\left[\dfrac{\sigma_2}{\sigma_1}\tan\alpha_1\right].$

b) $\rho_s = \left(\dfrac{\sigma_1}{\sigma_2}\epsilon_2 - \epsilon_1\right)E_1\sin\alpha_1.$

P.5–11 **b)** $P = \mathcal{V}^2 S\,\sigma_1\sigma_2/(\sigma_1 d_2 + \sigma_2 d_1).$

P.5–13 **a)** $J = \dfrac{\sigma_1\sigma_2 V_0}{r[\sigma_1\ln(b/c) + \sigma_2\ln(c/a)]}.$

b) $\rho_{sa} = \dfrac{\epsilon_1\sigma_2 V_0}{a[\sigma_1\ln(b/c) + \sigma_2\ln(c/a)]}, \quad \rho_{sb} = -\dfrac{\epsilon_2\sigma_1 V_0}{b[\sigma_1\ln(b/c) + \sigma_2\ln(c/a)]},$

$$\rho_{sc} = \frac{(\epsilon_2\sigma_1 - \epsilon_1\sigma_2)V_0}{c[\sigma_1\ln(b/c) + \sigma_2\ln(c/a)]}.$$

P.5–15 $\dfrac{1}{4\pi\sigma}\left(\dfrac{1}{R_1} - \dfrac{1}{R_2}\right).$

P.5–17 $\dfrac{R_2 - R_1}{2\pi\sigma R_1 R_2(1 - \cos\theta_0)}.$

P.5–19 $\dfrac{1}{4\pi\sigma}\left(\dfrac{1}{b_1} + \dfrac{1}{b_2} - \dfrac{2}{d}\right).$

P.5–21 6.36 (MΩ).

P.5–23 $\mathbf{J} = \mathbf{a}_x J_0 - \dfrac{J_0 b^2}{r^2}(\mathbf{a}_r\cos\phi + \mathbf{a}_\phi\sin\phi).$

Chapter 6

P.6–1 $y^2 + \left(z + \frac{u_0}{\omega_0}\right)^2 = \left(\frac{u_0}{\omega_0}\right)^2$, $\omega_0 = \frac{qB_0}{m}$.
Path of motion of q in magnetic field is a semicircle.

P.6–3 $B_\phi = \frac{\mu_0 I r}{2\pi a^2}$, $r \le a$; $B_\phi = \frac{\mu_0 I}{2\pi r}$, $a \le r \le b$;
$B_\phi = \frac{\mu_0 I(c^2 - r^2)}{2\pi(c^2 - b^2)r}$, $b \le r \le c$; $B_\phi = 0$, $r \ge c$.

P.6–5 $\mathbf{a}_z 1.38 I/w$.

P.6–7 $B = \frac{\mu_0 NI}{2L}\left[\frac{L - z}{\sqrt{(L - z)^2 + b^2}} + \frac{z}{\sqrt{z^2 + b^2}}\right]$.

P.6–9 $\mathbf{F}_{12} = \frac{\mu_0 q_1 q_2}{4\pi R^2}\mathbf{u}_2 \times (\mathbf{u}_1 \times \mathbf{a}_{12})$.

P.6–11 $\frac{\mu_0 I}{2b}\left(\frac{1}{\pi} + \frac{1}{2}\right)$.

P.6–15 $\mathbf{a}_z \mu_0 J d/2$.

P.6–17 $\mathbf{A}_1 = \mathbf{a}_z\left[-\frac{\mu_0 I}{4\pi}\left(\frac{r_1}{b}\right)^2 + c\right]$, $r_1 \le b$; $\mathbf{A}_2 = \mathbf{a}_z\left\{-\frac{\mu_0 I}{4\pi}\left[\ln\left(\frac{r_2}{b}\right)^2 + 1\right] + c\right\}$, $r_2 \ge b$.

P.6–21 a) $\mathbf{a}_z \mu_0 H_0/\mu$. b) $\mathbf{a}_z(H_0 - M_i)$.

P.6–27 a) $\mathcal{R}_g = 1.21 \times 10^6\,(\mathrm{H}^{-1})$, $\mathcal{R}_c = 6.75 \times 10^4\,(\mathrm{H}^{-1})$.
b) $\mathbf{B}_g = \mathbf{B}_c = \mathbf{a}_\phi 5.09 \times 10^{-3}\,(\mathrm{T})$.
$\mathbf{H}_g = \mathbf{a}_\phi 4.05 \times 10^3\,(\mathrm{A/m})$, $\mathbf{H}_c = \mathbf{a}_\phi 1.35\,(\mathrm{A/m})$.
c) $I = 25.6\,(\mathrm{mA})$.

P.6–33 b) $\mathbf{B} = -\mathbf{a}_x \frac{\mu_0 I}{2\pi}\left[\frac{y - d}{(y - d)^2 + x^2} + \frac{y + d}{(y + d)^2 + x^2}\right]$
$+ \mathbf{a}_y \frac{\mu_0 I}{2\pi} x\left[\frac{1}{(y - d)^2 + x^2} + \frac{1}{(y + d)^2 + x^2}\right]$.

P.6–35 $L = \mu_0 N^2(r_o - \sqrt{r_o^2 - b^2})$.

P.6–37 $L'_{AA'/BB'} = \frac{\mu_0}{2\pi}\ln\left(1 + \frac{d^2}{D^2}\right)$.

P.6–39 $L_{12} = \mu_0(d - \sqrt{d^2 - b^2})$.

P.6–41 $I_1/I_2 = -M/L_1$.

P.6–43 $\mathbf{f} = \mathbf{a}_x \frac{\mu_0 I^2}{\pi w}\tan^{-1}\left(\frac{w}{2D}\right)$.

P.6–45 $\mathbf{F} = \mathbf{a}_x \mu_0 I_1 I_2\left[\frac{1}{\sqrt{1 - (b/d)^2}} - 1\right]$, repulsive.

P.6–47 $\mathbf{T} = -\mathbf{a}_x 0.1\,(\mathrm{N \cdot m})$.

P.6–51 Maximum deviation from north-south direction: 55.8°.

P.6–53 $\mathbf{F} = \mathbf{a}_x \frac{\mu_0}{2}(\mu_r - 1)n^2 I^2 S$.

Chapter 7

P.7–3 a) $i_2(t) = -\dfrac{L_{12}}{L} I_1 e^{-(R/L)t}$, $0 < t < T$; $L_{12} = \dfrac{\mu_0 h}{2\pi} \ln\left(1 + \dfrac{w}{d}\right)$.

$$i_2(t) = \frac{L_{12}}{L} I_1 [e^{-(R/L)(t-T)} - e^{-(R/L)T}], \quad t > T.$$

P.7–5 a) 0.234 (A) b) 48.2°.

P.7–7 a) $0.0472\mu_0 I\omega b$. b) $0.0469\mu_0 I\omega b$.

P.7–13 a) $V' = V - \dfrac{\partial \psi}{\partial t}$. b) $\nabla^2\psi - \mu\epsilon \dfrac{\partial^2 \psi}{\partial t^2} = 0$.

P.7–23 $E_0 = 0.068, \theta = -72.8°$.

P.7–25 $\beta = 54.4$ (rad/m).

$$\mathbf{H}(x, z; t) = -\mathbf{a}_x 2.30 \times 10^{-4} \sin(10\pi x) \cos(6\pi 10^9 t - 54.4z) - \mathbf{a}_z 1.33 \times 10^{-4} \cos(10\pi x) \sin(6\pi 10^9 t - 54.4z) \text{(A/m)}.$$

P.7–27 $k = \omega\sqrt{\mu_0\epsilon_0}$. $\mathbf{H} = \mathbf{a}_\phi \dfrac{E_0}{R} \sqrt{\dfrac{\epsilon_0}{\mu_0}} \sin\theta \cos\omega(t - \sqrt{\mu_0\epsilon_0} R)$.

Chapter 8

P.8–3 a) $\Delta f = -(2u/c)f$, assuming the vehicle to be moving in the same direction as the direction of the incident wave.

b) 120 (km/hr), or 74.6 (miles/hr).

P.8–5 a) $k_0 = 0.1047$ (rad/m), $y = 22.5 \pm n\lambda/2$ (m).

b) $\mathbf{E}(y, t) = -\mathbf{a}_x 1.508 \times 10^{-3} \cos\left(10^7\pi t - \dfrac{\pi}{30} y + \dfrac{\pi}{4}\right)$ (V/m).

P.8–7 $\left(\dfrac{E_y}{E_{20} \sin\psi}\right)^2 + \left(\dfrac{E_x}{E_{10} \sin\psi}\right)^2 - 2\dfrac{E_x E_y \cos\psi}{E_{10} E_{20} \sin^2\psi} = 1$, where $E_x = E_{10} \sin(wt - kz)$, and $E_y = E_{20} \sin(wt - kz + \psi)$.

P.8–11 a) 1.395 (m).

b) $\eta_c = 238(1 + j0.005)\,(\Omega)$, $\lambda = 6.3$ (cm), $u_p = 1.8973 \times 10^8$ (m/s), $u_g = 1.8975 \times 10^8$ (m/s).

c) $\mathbf{H} = \mathbf{a}_x 0.21\, e^{-0.497x} \sin(6\pi 10^9 t - 31.6\pi x + 1.042)$(A/m).

P.8–13 a) 0.99×10^5 (S/m). b) 0.175 (mm).

P.8–21 a) Left-hand circularly polarized wave in $-z$ direction.

b) $\dfrac{2E_0}{\eta_0}(\mathbf{a}_x - j\mathbf{a}_y)$. c) $2E_0 \sin\beta z(\mathbf{a}_x \sin\omega t - \mathbf{a}_y \cos\omega t)$.

P.8–23 a) $f = 5.73$ (MHz), $\lambda = 0.524$ (m).

b) $\mathbf{E}_i(y, z; t) = 5(\mathbf{a}_y + \mathbf{a}_z\sqrt{3}) \cos(3.6 \times 10^9 t + 6\sqrt{3}y - 6z)$ (V/m),

$$\mathbf{H}_i(y, z; t) = -\mathbf{a}_x \frac{1}{12\pi} \cos(3.6 \times 10^9 t + 6\sqrt{3}y - 6z) \text{(A/m)}.$$

c) $\theta_i = 60°$.

d) $\mathbf{E}_r(y, z) = 5(-\mathbf{a}_y + \mathbf{a}_z\sqrt{3})e^{j6(\sqrt{3}y+z)}$ (V/m),

$\mathbf{H}_r(y, z) = -\mathbf{a}_x\dfrac{1}{12\pi}e^{j6(\sqrt{3}y+z)}$ (A/m).

e) $\mathbf{E}_t(y, z) = (-\mathbf{a}_y j10\sin 6z + \mathbf{a}_z 10\sqrt{3}\cos 6z)e^{j6\sqrt{3}y}$ (V/m),

$\mathbf{H}_t(y, z) = -\mathbf{a}_x\dfrac{1}{6\pi}(\cos 6z)e^{j6\sqrt{3}y}$ (A/m).

P.8–25 $\mathbf{H}_1(x, z; t) = \mathbf{a}_y\dfrac{2E_{i0}}{\eta_1}\cos(\beta_1 z\cos\theta_i)\sin(\omega t - \beta_1 x\sin\theta_i)$

$\mathscr{P}_{av} = \mathbf{a}_x\dfrac{2E_{i0}^2}{\eta_1}\sin\theta_i\sin^2(\beta_1 z\cos\theta_i).$

P.8–27 **a)** $\mathbf{E}_r(z, t) = \mathbf{a}_x 2.77\cos(1.8\times10^9 t + 6z + 157°)$ (V/m),

$\mathbf{E}_t(z, t) = \mathbf{a}_x 7.53\,e^{-2.3z}\cos(1.8\times10^9 t - 9.76z - 172°)$ (V/m).

b) $\mathscr{P}_{av} = \mathbf{a}_z 0.122e^{-4.61z}$ (W/m^2).

P.8–29 **a)** $E_{r0} = -\dfrac{j(\eta_0^2 - \eta_2^2)\tan\beta_2 d}{\eta_0\eta_2 + j(\eta_0^2 + \eta_2^2)\tan\beta_2 d}E_{i0},$

$E_2^+ = \dfrac{\eta_2(\eta_0 + \eta_2)e^{j\beta_2 d}}{\eta_0\eta_2\cos\beta_2 d + j(\eta_0^2 + \eta_2^2)\sin\beta_2 d}\mathrm{E}_{i0},$

$E_2^- = \dfrac{\eta_2(\eta_0 - \eta_2)e^{-j\beta_2 d}}{\eta_0\eta_2\cos\beta_2 d + j(\eta_0^2 + \eta_2^2)\sin\beta_2 d}\mathrm{E}_{i0},$

$E_{t0} = \dfrac{2\eta_0\eta_2 e^{j\beta_0 d}}{\eta_0\eta_2\cos\beta_2 d + j(\eta_0^2 + \eta_2^2)\sin\beta_2 d}\mathrm{E}_{i0}.$

P.8–31 $\Gamma_0 = \dfrac{(\Gamma_{12} + \Gamma_{23}) + j(\Gamma_{12} - \Gamma_{23})\tan\beta_2 d}{(1 + \Gamma_{12}\Gamma_{23}) + j(1 - \Gamma_{12}\Gamma_{23})\tan\beta_2 d}.$

P.8–33 Assume $|\eta_2| \ll \eta_0$.

a) $E_2^+ = -j\left(\dfrac{\eta_2}{\eta_0}\right)\dfrac{e^{\alpha_2 d}e^{j\beta_2 d}E_{i0}}{\sin(\beta_2 - j\alpha_2)d}.$ **b)** $E_2^- = -j\left(\dfrac{\eta_2}{\eta_0}\right)\dfrac{e^{-\alpha_2 d}e^{-j\beta_2 d}E_{i0}}{\sin(\beta_2 - j\alpha_2)d}.$

c) $E_{30} = -j\left(\dfrac{\eta_2}{\eta_0}\right)\dfrac{2e^{j\beta_0 d}E_{i0}}{\sin(\beta_2 - j\alpha_2)d}.$ **d)** $(\mathscr{P}_{av})_3/(\mathscr{P}_{av})_i = 1.839\times10^{-11}.$

P.8–35 **a)** $\theta_i = 0.03°$ **b)** $\Gamma_{\|} = 0.0214e^{j\pi/4}$

c) $(\mathscr{P}_{av})_t/(\mathscr{P}_{av})_i = 1.054\times10^{-3}e^{-0.795z}.$ **d)** 8.69 (m).

P.8–37 **a)** $\mathbf{E}_t(x, z) = \mathbf{a}_y E_{t0}\,e^{-\alpha_2 z}e^{-j\beta_{2x}x},$

$\mathbf{H}_t(x, z) = \dfrac{E_{t0}}{\eta_2}\left(\mathbf{a}_x j\alpha_2 + \mathbf{a}_z\sqrt{\dfrac{\epsilon_1}{\epsilon_2}}\sin\theta_i\right)e^{-\alpha_2 z}e^{-j\beta_{2x}x},$

where $\beta_{2x} = \beta_2\sqrt{\dfrac{\epsilon_1}{\epsilon_2}}\sin\theta_i,\ \alpha_2 = \beta_2\sqrt{\left(\dfrac{\epsilon_1}{\epsilon_2}\right)\sin^2\theta_i - 1},$

and $E_{t0} = \dfrac{2\eta_2\cos\theta_i E_{i0}}{\eta_2\cos\theta_i - j\eta_1\sqrt{\left(\dfrac{\epsilon_1}{\epsilon_2}\right)\sin^2\theta_i - 1}}.$

P.8–39 **a)** 6.38°. **b)** $e^{j0.66}$. **c)** $1.89e^{j0.33}$. **d)** 159 (dB).

P.8–41 **a)** $\theta_a = \sin^{-1}\left(\dfrac{1}{n_0}\sqrt{n_1^2 - n_2^2}\right).$ **b)** 80.4°.

P.8–45 a) $\Gamma_\perp = \dfrac{1.5\cos\theta_i - \sqrt{1-(1.5\sin\theta_i)^2}}{1.5\cos\theta_i + \sqrt{1-(1.5\sin\theta_i)^2}}$.

$$\Gamma_\parallel = \frac{1.5\sqrt{1-(1.5\sin\theta_i)^2} - \cos\theta_i}{1.5\sqrt{1-(1.5\sin\theta_i)^2} + \cos\theta_i}.$$

P.8–47 a) $\Gamma'_\parallel = \dfrac{\eta_2\cos\theta_t - \eta_1\cos\theta_i}{\eta_2\cos\theta_t + \eta_1\cos\theta_i} = \Gamma_\parallel$,

$$\tau'_\parallel = \frac{2\eta_2\cos\theta_t}{\eta_2\cos\theta_t + \eta_1\cos\theta_i} = \tau_\parallel\left(\frac{\cos\theta_t}{\cos\theta_i}\right).$$

Chapter 9

P.9–3 a) $d' = \sqrt{2}d$, $u'_p = u_p/\sqrt{2}$.

P.9–7 $\alpha = \sqrt{\dfrac{LC}{2}}\left(\dfrac{R}{L}+\dfrac{G}{C}\right)\left[1-\dfrac{1}{8\omega^2}\left(\dfrac{R}{L}-\dfrac{G}{C}\right)^2\right]$, $\beta = \omega\sqrt{LC}\left[1+\dfrac{1}{8\omega^2}\left(\dfrac{R}{L}-\dfrac{G}{C}\right)^2\right]$,

$$R_0 = \sqrt{\frac{L}{C}}\left[1+\frac{1}{8\omega^2}\left(\frac{R}{L}-\frac{G}{C}\right)\left(\frac{R}{L}+\frac{3G}{C}\right)\right],\quad X_0 = -\frac{1}{2\omega}\sqrt{\frac{L}{C}}\left(\frac{R}{L}-\frac{G}{C}\right).$$

P.9–9 $R = 0.058\,(\Omega/\text{m})$, $L = 0.20\,(\mu\text{H/m})$, $C = 80\,(\text{pF/m})$, $G = 24\,(\mu\text{S/m})$.

P.9–11 Maximum power-transfer efficiency = 50%.

P.9–13 a) $A = D = \dfrac{1}{Z_0}\cosh\gamma\ell$,

$$B = Z_0\sinh\gamma\ell,\quad C = \frac{1}{Z_0}\sinh\gamma\ell.$$

P.9–15 a) $V(z,t) = 5.27\,e^{-0.01z}\sin(8000\pi t - 5.55z - 0.322)\,(\text{V})$.

b) $V(50,t) = 3.20\sin(8000\pi t - 0.432\pi)\,(\text{V})$.

c) 0.102 (W).

P.9–17 a) $4Z_0/\alpha\lambda$. b) $Z_0\alpha\lambda/4$.

P.9–19 a) $Z_0 = 289.8 - j77.6\,(\Omega)$, $\alpha = 0.139\,(\text{Np/m})$, $\beta = 0.235\,(\text{rad/m})$.

b) $R = 58.6\,(\Omega/\text{m})$, $L = 0.812\,(\mu\text{H/m})$, $G = 0.246\,(\text{mS/m})$, $C = 12.4\,(\text{pF/m})$.

P.9–21 $\Delta f = \dfrac{\alpha}{\pi\sqrt{LC}} = \dfrac{1}{2\pi}\left(\dfrac{R}{L}+\dfrac{G}{C}\right)$; $\quad Q = \dfrac{\beta}{2\alpha} = \dfrac{1}{[(R/\omega L)+(G/\omega c)]}$.

P.9–27 a) $\Gamma = \frac{1}{3}e^{j0.2\pi}$. b) $Z_L = 466 + j206\,(\Omega)$. c) $R_m = 150\,(\Omega)$, $\ell_m = 0.2\lambda$.

P.9–29 $Z_L = Z_0\left[\dfrac{1 - jS\tan(2\pi z'_m/\lambda)}{S - j\tan(2\pi z'_m/\lambda)}\right]$.

P.9–31 a) $P_{\text{inc}} = V_g^2/8R_0$. b) $P_L = \dfrac{V_g^2}{8R_0}(1-|\Gamma|^2)$. c) $\dfrac{P_L}{P_{\text{inc}}} = \dfrac{4S}{(S+1)^2}$.

d) $P_{\text{inc}} = 25\,(\text{W})$, $\Gamma = 0.243\underline{/-76°}$, $S = 1.64$,

$P_L = 23.5\,(\text{W})$, $|V_L| = 54.2\,(\text{V})$, $|I_L| = 0.97\,(\text{A})$.

P.9–33 At $t = 4T$, the voltage and current distributions along the line revert to the conditions at $t = 0$, and the cycle repeats itself.

P.9–35 $\Gamma_g = -1/3,\ \Gamma_L = 1.$

P.9–43 **a)** $S = 1.77.$ **b)** $\Gamma = 0.28e^{j146°}.$ **c)** $Z_i = 50 + j29\,(\Omega).$
d) $Y_i = 0.015 - j0.009\,(\mathrm{S}).$

P.9–45 **a)** $Z_L = 33.75 - j23.75\,(\Omega).$ **b)** $\Gamma = \frac{1}{3}e^{j252.5°}.$ **c)** $z'_m = 25\,(\mathrm{cm}).$

P.9–47 Line length = 0.375 (m), Wire radius = 5.4 (mm).

P.9–49 $d_1/\lambda = 0.074, \ell_1/\lambda = 0.347;\ d_2/\lambda = 0.250, \ell_2/\lambda = 0.153.$

P.9–51 **a)** $d_L/\lambda = 0.0113.$ **b)** $\ell_A/\lambda = 0.304, \ell_B/\lambda = 0.125.$

Chapter 10

P.10–5 From Eqs. (10–83a, b, & c): $\mathbf{J}_{s\ell} = \mathbf{a}_x B_n,\ \mathbf{J}_{su} = \mathbf{a}_x(-1)^{n+1}B_n.$

P.10–7 $u_{en} = \dfrac{1}{\sqrt{\mu\epsilon}}\sqrt{1 - (f_c/f)^2}.$

P.10–9 **a)** $\beta = 308\,(\mathrm{rad/m}), \alpha_d = 1.28 \times 10^{-8}\,(\mathrm{Np/m}), \alpha_c = 1.69 \times 10^{-4}\,(\mathrm{Np/m}),$
$u_p = 2.04 \times 10^8\,(\mathrm{m/s}), u_g = 1.96 \times 10^8\,(\mathrm{m/s}), \lambda_g = 2.04\,(\mathrm{cm}).$
b) $\beta = 288\,(\mathrm{rad/m}), \alpha_d = 1.37 \times 10^{-8}\,(\mathrm{Np/m}), \alpha_c = 7.25 \times 10^{-4}\,(\mathrm{Np/m}),$
$u_p = 2.18 \times 10^8\,(\mathrm{m/s}), u_g = 1.83 \times 10^8\,(\mathrm{m/s}), \lambda_g = 2.18\,(\mathrm{cm}).$

P.10–11 **a)** 358 (MW/m). **b)** 207 (MW/m). **c)** 155 (MW/m).

P.10–13 **a)** $\mathbf{J}_s(y = 0) = -\mathbf{a}_z \dfrac{j\omega\epsilon}{h^2}\left(\dfrac{\pi}{b}\right) E_0 \sin\left(\dfrac{\pi x}{a}\right) e^{-j\beta_{11}z} = \mathbf{J}_s(y = b).$

$$\mathbf{J}_s(x = 0) = -\mathbf{a}_z \frac{j\omega\epsilon}{h^2}\left(\frac{\pi}{a}\right) E_0 \sin\left(\frac{\pi y}{b}\right) e^{-j\beta_{11}z} = \mathbf{J}_s(x = a).$$

P.10–15 $u_{en} = u\sqrt{1 - (u/2af)^2}, u = 1/\sqrt{\mu\epsilon}.$

P.10–17 **a)** $a > 6\,(\mathrm{cm}), b < 4\,(\mathrm{cm}).$ Choose $a = 6.5\,(\mathrm{cm})$ and $b = 3.5\,(\mathrm{cm}).$
b) $\beta = 40.1\,(\mathrm{rad/m}), u_p = 4.70 \times 10^8\,(\mathrm{m/s}), \lambda_g = 15.7\,(\mathrm{cm}),$
$(Z_{TE})_{10} = 590\,(\Omega).$

P.10–19 **a)** $f_c = 2.08 \times 10^9\,(\mathrm{Hz}).$ **b)** $\lambda_g = 0.139\,(\mathrm{m}).$
c) $\alpha_c = 2.26 \times 10^{-3}\,(\mathrm{Np/m}).$ **d)** 307 (m).

P.10–21 1 (MW).

P.10–23 $\alpha_c = \dfrac{2R_s(b/a^2 + a/b^2)}{\eta ab\sqrt{1 - (f_c/f)^2}\,(1/a^2 + 1/b^2)}.$

P.10–29 **a)** $E_z^0 = C_n J_n(hr)\sin n\phi.$
c) Eigenvalues of TM modes are determined by requiring $J_n(ha) = 0$. The lowest TM mode is TM_{11}.

P.10–31 **a)** $\alpha = 0.061\,(\mathrm{Np/m}), \beta = 4.19\,(\mathrm{rad/m}).$
b) $\alpha = 0.380\,(\mathrm{Np/m}), \beta = 10.48\,(\mathrm{rad/m}).$

P.10–33 Even TM modes in the slab: $E_z(y, z; t) = E_e \cos k_y y \cos(\omega t - \beta z)$,

$$E_y(y, z; t) = -\frac{\beta}{k_y} E_e \sin k_y y \sin(\omega t - \beta z), H_x(y, z; t) = \frac{\omega \epsilon_d}{k_y} E_e \sin k_y y \sin(\omega t - \beta z).$$

P.10–37 a) $H_{zi}^0 = C_0 J_0(hr), r \le a$; $H_{zo}^0 = D_0 K_0(\zeta r), r \le a$.

b) $$\frac{J_0(ha)}{J_0'(ha)} = -\frac{\mu_1 \zeta}{\mu_2 h} \frac{K_0(\zeta a)}{K_0'(\zeta a)}.$$

P.10–39 a) Dominant mode: TE_{101}. $f_{101} = 4.802$ (GHz).
b) $Q = 6869$, $W_e = W_m = 0.07728$ (pJ).

P.10–41 a) $a = d$. b) $1.11\eta/R_s(1 + a/2b)$.

P10–43 $$Q_{110} = \frac{\sqrt{\pi f_{110} \mu_0 \sigma}\, abd(a^2 + b^2)}{2d(a^3 + b^3) + ab(a^2 + b^2)}.$$

P.10–45 $$f = \frac{1}{\pi a \sqrt{\frac{2h}{d} \mu \epsilon \ln\left(\frac{b}{a}\right)}}.$$

Chapter 11

P.11–1 $$\nabla^2 \mathbf{E} - \mu\epsilon \frac{\partial^2 \mathbf{E}}{\partial t^2} = \frac{1}{\epsilon} \nabla \rho + \mu \frac{\partial \mathbf{J}}{\partial t}.$$

P.11–3 a) $$\mathbf{A} = \mathbf{a}_\phi \frac{\mu_0 m}{4\pi R^2} e^{-j\beta R}(1 + j\beta R) \sin\theta.$$

P.11–5 a) $\rho_\ell = -j(I_0/c) \sin \beta z$. b) $$\rho_\ell = \begin{cases} -j2I_0/\pi c, & 0 < z \le \lambda/4; \\ +j2I_0/\pi c, & -\lambda/4 \le z < 0. \end{cases}$$

P.11–7 a) $$\mathbf{E} = \mathbf{a}_\theta \frac{j30\beta h}{R} I_0 e^{-j\beta R} \sin\theta.$$ b) $$R_r = 20\pi^2 \left(\frac{2h}{\lambda}\right)^2.$$ c) 1.76 (dB).

P.11–9 a) $R_r = 320\pi^6 (b/\lambda)^4$. b) $$\eta_r = \frac{R_r}{R_r + (bR_s/a)}.$$

P.11–13 $$\ell_e(\theta) = \frac{2 \sin\theta [1 - \cos(\beta h \cos\theta)]}{\beta^2 h \cos^2\theta}$$; Max. $\ell_e = h = \frac{\lambda}{12}$.

P.11–15 a) $$E_\theta = \frac{j120I\beta h}{R} e^{-j\beta(R - \frac{d}{2}\cos\theta)} F(\theta)$$, where $$F(\theta) = \sin\theta \cos\left(\frac{\beta d}{2} \cos\theta\right).$$

P.11–19 b) $(2\Delta\phi)_{1/2} = 4.23\,(\lambda/d)$ (deg.) c) $(2\Delta\phi)_0 = 46.8\sqrt{\lambda/d}$ (deg.)

P.11–23 $$|F(\theta, \phi)| = \frac{1}{N_1 N_2} \left| \left[\frac{\cos\left(\frac{\pi}{2}\cos\theta\right)}{\sin\theta}\right] \frac{\sin\left(\frac{N_1 \psi_x}{2}\right) \sin\left(\frac{N_2 \psi_y}{2}\right)}{\sin\left(\frac{\psi_x}{2}\right) \sin\left(\frac{\psi_y}{2}\right)} \right|,$$

where $$\psi_x = \frac{\beta d_1}{2} \sin\theta \cos\phi \quad \text{and} \quad \psi_y = \frac{\beta d_2}{2} \sin\theta \cos\phi.$$

P.11–25 **a)** $W_s = \dfrac{8\pi}{3}\beta^4 b^6 \left(\dfrac{\epsilon_r - 1}{\epsilon_r + 2}\right)^2 \left(\dfrac{E_i^2}{2\eta_0}\right)$. **b)** $\sigma_s = 1.5\sigma_{bs}$.

P.11–27 **b)** Main-lobe beamwidth $= 4/\sqrt{G_D}$.

P.11–29 **a)** 0.55 (nW). **b)** 1.25 n (km), n $= 1, 2, \cdots$.

P.11–31 **a)** $|V_{oc}| = 2\lambda E_0/\pi$ if $p = 1$. **b)** $V_{oc} = 0$ if $p = 1$. **c)** $|V_{oc}| = \lambda E_0/\pi$.

P.11–33 $\mathbf{E}_P(\theta, \phi) = \dfrac{jab}{\lambda R_0} e^{-j\beta R_0} \left[\left(\dfrac{\sin u}{u}\right)\left(\dfrac{\sin v}{v}\right)\right] (\mathbf{a}_\theta \cos\phi - \mathbf{a}_\phi \sin\phi)$;

$u = \left(\dfrac{\pi a}{\lambda}\right) \sin\theta\cos\phi, \; v = \left(\dfrac{\pi b}{\lambda}\right) \sin\theta \sin\phi.$

P.11–35 **a)** $F_{xz}(\theta) = \dfrac{(\pi/2)^2 \cos\psi}{(\pi/2)^2 - \psi^2}, \; \psi = \dfrac{\beta a}{2} \sin\theta.$

b) $68\lambda/a$ (degrees). **c)** $86\lambda/a$ (degrees). **d)** -23.5 (dB).

Index

Some Useful Vector Identities

$$\mathbf{A}\cdot\mathbf{B}\times\mathbf{C}=\mathbf{B}\cdot\mathbf{C}\times\mathbf{A}=\mathbf{C}\cdot\mathbf{A}\times\mathbf{B}$$

$$\mathbf{A}\times(\mathbf{B}\times\mathbf{C})=\mathbf{B}(\mathbf{A}\cdot\mathbf{C})-\mathbf{C}(\mathbf{A}\cdot\mathbf{B})$$

$$\nabla(\psi V)=\psi\nabla V+V\nabla\psi$$

$$\nabla\cdot(\psi\mathbf{A})=\psi\nabla\cdot\mathbf{A}+\mathbf{A}\cdot\nabla\psi$$

$$\nabla\times(\psi\mathbf{A})=\psi\nabla\times\mathbf{A}+\nabla\psi\times\mathbf{A}$$

$$\nabla\cdot(\mathbf{A}\times\mathbf{B})=\mathbf{B}\cdot(\nabla\times\mathbf{A})-\mathbf{A}\cdot(\nabla\times\mathbf{B})$$

$$\nabla\cdot\nabla V=\nabla^2V$$

$$\nabla\times\nabla\times\mathbf{A}=\nabla(\nabla\cdot\mathbf{A})-\nabla^2\mathbf{A}$$

$$\nabla\times\nabla V=0$$

$$\nabla\cdot(\nabla\times\mathbf{A})=0$$

$$\int_V\nabla\cdot\mathbf{A}\,dv=\oint_S\mathbf{A}\cdot d\mathbf{s}\qquad\text{(Divergence theorem)}$$

$$\int_S\nabla\times\mathbf{A}\cdot d\mathbf{s}=\oint_C\mathbf{A}\cdot d\ell\qquad\text{(Stokes's theorem)}$$

Gradient, Divergence, Curl, and Laplacian Operations

Cartesian Coordinates (x, y, z)

$$\nabla V=\mathbf{a}_x\frac{\partial V}{\partial x}+\mathbf{a}_y\frac{\partial V}{\partial y}+\mathbf{a}_z\frac{\partial V}{\partial z}$$

$$\nabla\cdot\mathbf{A}=\frac{\partial A_x}{\partial x}+\frac{\partial A_y}{\partial y}+\frac{\partial A_z}{\partial z}$$

$$\nabla\times\mathbf{A}=\begin{vmatrix}\mathbf{a}_x & \mathbf{a}_y & \mathbf{a}_z\\ \dfrac{\partial}{\partial x} & \dfrac{\partial}{\partial y} & \dfrac{\partial}{\partial z}\\ A_x & A_y & A_z\end{vmatrix}=\mathbf{a}_x\left(\frac{\partial A_z}{\partial y}-\frac{\partial A_y}{\partial z}\right)+\mathbf{a}_y\left(\frac{\partial A_x}{\partial z}-\frac{\partial A_z}{\partial x}\right)+\mathbf{a}_z\left(\frac{\partial A_y}{\partial x}-\frac{\partial A_x}{\partial y}\right)$$

$$\nabla^2V=\frac{\partial^2V}{\partial x^2}+\frac{\partial^2V}{\partial y^2}+\frac{\partial^2V}{\partial z^2}$$

Cylindrical Coordinates (r, ϕ, z)

$$\nabla V = \mathbf{a}_r \frac{\partial V}{\partial r} + \mathbf{a}_\phi \frac{\partial V}{r\partial \phi} + \mathbf{a}_z \frac{\partial V}{\partial z}$$

$$\nabla \cdot \mathbf{A} = \frac{1}{r}\frac{\partial}{\partial r}(rA_r) + \frac{\partial A_\phi}{r\partial \phi} + \frac{\partial A_z}{\partial z}$$

$$\nabla \times \mathbf{A} = \frac{1}{r}\begin{vmatrix} \mathbf{a}_r & \mathbf{a}_\phi r & \mathbf{a}_z \\ \dfrac{\partial}{\partial r} & \dfrac{\partial}{\partial \phi} & \dfrac{\partial}{\partial z} \\ A_r & rA_\phi & A_z \end{vmatrix} = \mathbf{a}_r\left(\frac{\partial A_z}{r\partial \phi} - \frac{\partial A_\phi}{\partial z}\right) + \mathbf{a}_\phi\left(\frac{\partial A_r}{\partial z} - \frac{\partial A_z}{\partial r}\right) + \mathbf{a}_z \frac{1}{r}\left[\frac{\partial}{\partial r}(rA_\phi) - \frac{\partial A_r}{\partial \phi}\right]$$

$$\nabla^2 V = \frac{1}{r}\frac{\partial}{\partial r}\left(r\frac{\partial V}{\partial r}\right) + \frac{1}{r^2}\frac{\partial^2 V}{\partial \phi^2} + \frac{\partial^2 V}{\partial z^2}$$

Spherical Coordinates (R, θ, ϕ)

$$\nabla V = \mathbf{a}_R \frac{\partial V}{\partial R} + \mathbf{a}_\theta \frac{\partial V}{R\partial \theta} + \mathbf{a}_\phi \frac{1}{R\sin\theta}\frac{\partial V}{\partial \phi}$$

$$\nabla \cdot \mathbf{A} = \frac{1}{R^2}\frac{\partial}{\partial R}(R^2 A_R) + \frac{1}{R\sin\theta}\frac{\partial}{\partial \theta}(A_\theta \sin\theta) + \frac{1}{R\sin\theta}\frac{\partial A_\phi}{\partial \phi}$$

$$\nabla \times \mathbf{A} = \frac{1}{R^2\sin\theta}\begin{vmatrix} \mathbf{a}_R & \mathbf{a}_\theta R & \mathbf{a}_\phi R\sin\theta \\ \dfrac{\partial}{\partial R} & \dfrac{\partial}{\partial \theta} & \dfrac{\partial}{\partial \phi} \\ A_R & RA_\theta & (R\sin\theta)A_\phi \end{vmatrix} = \mathbf{a}_R \frac{1}{R\sin\theta}\left[\frac{\partial}{\partial \theta}(A_\phi \sin\theta) - \frac{\partial A_\theta}{\partial \phi}\right] + \mathbf{a}_\theta \frac{1}{R}\left[\frac{1}{\sin\theta}\frac{\partial A_R}{\partial \phi} - \frac{\partial}{\partial R}(RA_\phi)\right] + \mathbf{a}_\phi \frac{1}{R}\left[\frac{\partial}{\partial R}(RA_\theta) - \frac{\partial A_R}{\partial \theta}\right]$$

$$\nabla^2 V = \frac{1}{R^2}\frac{\partial}{\partial R}\left(R^2\frac{\partial V}{\partial R}\right) + \frac{1}{R^2\sin\theta}\frac{\partial}{\partial \theta}\left(\sin\theta\frac{\partial V}{\partial \theta}\right) + \frac{1}{R^2\sin^2\theta}\frac{\partial^2 V}{\partial \phi^2}$$